

Editor-in-Chief: Bruce LEYBOURNE (leybourneb@iascc.org)



ISSN 2202-0039

WWW.ncgtjournal.com



“The Yarlung Tsangpo Canyon [evidenced by a red ellipse] is located at the great bend of the river before entering the Indian State of Arunachal Pradesh.” Figure (modified) and captions after Wikipedia with CC BY-SA 3.0 Wikimedia Commons kind permission.

**Special Issue on
Air-Earth Currents**

– *An international journal for New Concepts in Global Tectonics* –

NCGT



JOURNAL

Volume 13, Number 8, October 2025. ISSN 2202-0039.

EDITORIAL BOARD

Editor-in-Chief: Bruce LEYBOURNE, USA (leybourneb@iascc.org)

Co-Editor-in-Chief: Masahiro SHIBA, Japan (shiba@dino.or.jp)

Giovanni P. GREGORI, Italy (giovannipgregori38@gmail.com)

Louis HISSINK Australia (louis.hissink@outlook.com)

Per MICHAELSEN, Mongolia (perm@must.edu.mn)

Biju LONGHINOS, India (biju.longhinos@gmail.com)

Vladimir ANOKHIN, Russia (vladanokhin@yandex.ru)

CONTENTS

Articles

Part 2

| | |
|--|------|
| Palæo- and archæo-climate in the Chinese subcontinent: Giovanni Pietro Gregori, Bruce Allen Leybourne, Dong Wenjie, Gao Xiaoqing..... | 1170 |
| Topics in palæoclimatology - The role of the biosphere for air-earth currents: Giovanni Pietro Gregori, Bruce Allen Leybourne, Dong Wenjie, Gao Xiaoqing..... | 1234 |
| About the NCGT Journal | 1332 |

For donations, please feel free to contact the Research Director of the Geoplasma Research Institute, Mr. Bruce Leybourne, at leybourneb@iascc.org. For contact, correspondence, or inclusion of material in the NCGT Journal please use the following methods: *NEW CONCEPTS IN GLOBAL TECTONICS*. 1. E-mail: leybourneb@iascc.org (files in MS Word or ODT format, and figures in gif, bmp or tif format) as separate files; 3. Telephone, +61 402 509 420. *DISCLAIMER:* The opinions, observations and ideas published in this journal are the responsibility of the contributors and do not necessarily reflect those of the Editor and the Editorial Board. *NCGT Journal* is a refereed quarterly international online journal and appears in March, June, September and December. *ISSN number;* ISSN 2202-0039.

Palæo- and archæo-climate in the Chinese subcontinent

Giovanni Pietro Gregori¹, Bruce Allen Leybourne², Dong Wenjie³, Gao Xiaoqing⁴

¹ Former Senior Researcher at *IDASC-Institute of Acoustics and Sensors O. M. Corbino (CNR), Rome*, now merged with the *INM-Institute of Marine Engineering "Section of Acoustics and Sensors O.M. Corbino"- (CNR Rome)*; and *ISSO-International Seismic Safety Organization, Italy*

² *GeoPlasma Research Institute-(GeoPlasmaResearchInstitute.org)*, Aurora, CO 80014, USA

³ *Professor and Dean, School of Atmospheric Science, Sun Yat-sen University, Zhuhai, Guangdong, (PRC), Director of Future Earth Global Secretariat Hub China and Secretary-General of FE Chinese National Committee*

⁴ *Northwest Institute of Eco-Environment and Resources, Chinese Academy of Sciences, 730000, Lanzhou, (PRC)*

Corresponding Author: G. P. Gregori, IDASC-Istituto di Acustica e Sensoristica O. M. Corbino (CNR), Roma, now merged into IMM-Istituto per la Microelettronica e Microsistemi (CNR);
Email:
giovannipgregori38@gmail.com
leybourneb@iascc.org
dongwj3@mail.sysu.edu.cn
xqgao@lzb.ac.cn

Abstract: We concisely review the huge literature related to the studies of the Tang Maocang school concerned with climate and palæo- and archæo-climate of the Chinese subcontinent. We add no critical exhaustive treatment. Rather, we give a reminder about papers that are poorly known in the western community. We give no updating according to the more recent available literature. The key scientific novelty of these papers deals with the leading focus of the Tang Maocang school on the variations of endogenous heat flow. They infer seismic precursors, middle-range meteorological forecast, and climate control, both at present and in the past. In contrast, the western literature considers the change of temperature in the atmosphere as the leading driver of climate change. We discuss the mechanisms for climate control, and the evidences inferred from ice cores, loess, and stalagmites concerning climate and palæo- and archæo-climate in China, including some related items discussed in the western literature.

Keywords: Tang Maocang school - climate and palæo- and archæo-climate of the Chinese subcontinent - change of endogenous heat flow - mechanisms for climate control - atmospheric heat engine - ice cores and loess - stalagmites and ice cores – related studies in the western literature

Background – The present set of papers includes the coauthors Dong Wenjie and Gao Xiaoqing, who in the 1990s spent one sabbatical year each, at the *Istituto di Fisica dell'Atmosfera (CNR)* in Rome for cooperation with G.P. Gregori. Dong Wenjie and Gao Xiaoqing had a scholarship provided by of *World Laboratory*, with President Prof. Antonino Zichichi, who is warmly thanked for providing this opportunity. *World Laboratory*, with the support of the Italian government, strongly promoted cooperation between different countries. The content of the present papers strictly and exclusively relies on information that was exchanged during those two sabbatical years. The full responsibility is by G.P. Gregori and B.A. Leybourne, while Dong Wenjie and Gao Xiaoqing agreed to be included as coauthors. Dong Wenjie and Gao Xiaoqing - two really brilliant scientists and gentlemen - greatly contributed to the implementation of the present study, and we feel sincerely very grateful to them. We hope this is also a way to honor the recent passing away of Professor Tang Maocang.

Introduction

The present paper addresses items dealing with climate and palæo- and archæo-climate of the Chinese subcontinent, according to several inferences related to the Chinese network of shallow geotherms. A previous paper (Gregori et al., 2025g) deals with the timing of the uplift of the Tibet Plateau (TP). A second paper (Gregori et al., 2025h) deals with an extensive illustration of the shallow geotherm network and with application to middle-range meteorological forecast and to seismic precursors. A

subsequent paper (Gregori et al., 2025j) deals with an indicative reminder of related items that deal with the climate perspective in other regions of the world - and also with the crucial role of the biosphere in the control of air-earth currents. Instead, we only mention, with no extensive report, several discussions carried out by the Tang Maocang school on the relationship between climate and the development of civilization in China – as we focus on air-earth currents *per se*.

In any case, the aim of the present set of papers is devoted to the illustration of the achievement of the Tang

Maocang school, concerning only an illustration – as far as possible – of their several studies, with no attempt to give any topical review.

A subsequent set of papers (Gregori et al., 2025k, 2025l, 2025m, 2025n, 2025o, and 2025q) illustrates an investigation carried out in Rome during the sabbatical year spent by Dong Wenjie and by Gao Xiaoqing, independent of the achievements of the Tang Maocang school. The leading topic is the origin of the endogenous heat, which is closely related to the primary mechanism that is here envisaged for the control of climate, and to the topics discussed by the Tang's school.

In the present paper we begin by discussing the mechanisms for climate control. Then, we discuss ice cores and loess, stalagmites and ice cores, and finally climate in China according to the western literature. In general, we report the arguments and conclusions by the authors, adding at most some comments, although we carry out no critical review. We did not attempt to update the discussion according to the more recent available papers. We cannot read Chinese character, and sometimes we can rely only on English abstracts. *In addition, for a matter of respect for the authors – and as far as permitted by copyright constraints – we want to report original statements borrowed from the original papers.* In case of copyright limitation, we attempt to synthesize the original text, or to describe the original figures.

The key scientific novelty is that the western literature is focused on the change of temperature in the atmosphere, and on how heat propagates underground. The Tang Maocang school looks rather at the change of endogenous heat flow, on how this is indicative of seismic precursors, and on how it affects meteorology, middle-range forecast, and climate, both at present and in the past.

As a general premise, the peculiarity must be stressed of the Chinese subcontinent, as it includes the Tibet Plateau (*TP*), the Loess Plateau, extended river systems, deserts, an intense tectonic activity, a large variety of space- and time-variation of endogenous heat flow, intense atmospheric phenomena (various kinds of monsoons), etc. The Chinese subcontinent is therefore a unique natural laboratory where several mechanisms can be investigated and their role considered during the geological history of the Earth. In this respect, the achievements of the Tang Maocang school deserve a great attention by the scientific community.

The mechanisms for climate control - The role of the timing of the uplift of the Tibet Plateau - Palæo-geophysical evidences

Let us focus on palæo-geophysical evidences in the *TP* that support some expected palæoclimatic trends – and let us consider how far these evidences support the role of a time variation of geothermal flow. The literature is very large, and we report only some excerpts. We first summarize some items that are more extensively illustrated in Gregori et al. (2025g). The Tang and Dong (1997a) and of Dong and Tang (1997) innovative approach (Gregori et al., 2025g) led to an actual model of the history of the uplift of the *TP*, and of its crucial role as a trigger for the planetary

Great Ice Age (*GIA*). The focus is here on the palæoclimatic implications. Refer to Fig. 1.

Tang and Dong (1997a) and of Dong and Tang (1997) systematically discussed in detail their 7 guessed periods that characterized the history of the uplift of the *TP*. The needed assumptions are explained in Gregori et al. (2025g and 2025h), and also the observational support provided by sedimentological data, which were collected in the Indo-Ganges basin and in the Bengal fan. Tang and Dong (1997a) contains a specific discussion of the correlation between tectonic and climatic evidence, according to standard meteorological processes.

The *TP* began its uplift ~ 45 Ma ago. Although there is some disagreement between different authors on the exact timing, Tang and Dong (1997a) referred to 7 relatively long periods when uplift occurred: $\sim 41 - 37$ Ma, $\sim 28 - 25$ Ma, $\sim 20 - 18$ Ma, $\sim 15-14$ Ma, $\sim 10 - 7$ Ma, $\sim 3.4 - 1.7$ Ma and ~ 0.73 Ma – *present*. Everyone of these uplift episodes had a different impact on climate, although the relevant influence of every given period did not immediately occur at the beginning of every tectonic uplift. Rather, it was delayed by a time lag, because either topographic height and/or the plateau horizontal extension had to reach a suitable critical threshold. The threshold must respond to specific requirements in order to cause a relevant readjustment of the general circulation of the atmosphere.

A large global change in the Earth system occurred ~ 40 Ma ago (more precisely, ~ 41.8 Ma, which is the age of Kammu Seamount, i.e. at the time when the direction bent northward - from older to younger seamounts - of the Hawai'i-Emperor Seamounts chain. At that time, the Tethys Sea disappeared and the *TP* began to uplift. Tang and Dong (1997a) stress that the consequent relevant change of the climate pattern seemingly occurred only later, ~ 37 Ma ago, when the size of the plateau reached ~ 800 km (Tang and Liu, 1995). The age-difference between the two events was ~ 3 Ma, or more precisely ~ 4.81 Ma. Note that, in general, such a time lag can be different in different case histories, depending on the altitude a.s.l. and surface extension of the *TP*, and on the speed of the uplift. All these crucial parameters can vary between case histories, thus implying different time delays.

Another case history occurred ~ 3.4 Ma BP, when the plateau began to raise quickly, at the time of the beginning of the Gauss normal geomagnetic period. However, the relevant change of climate seemingly occurred ~ 900 ka BP when the plateau altitude reached ~ 2000 m (Tang, 1993). Therefore, in every case the beginning of the tectonic uplift is not to be expected to coincide with the time of the climate change.

The 1st and 7th uplift episodes caused a relevant impact on global climate - unlike the others, which seem to have caused only regional effects. The cause of these different behaviors has to be clarified, being perhaps a consequence of the assumptions chosen for the derivation of the uplift model. Refer to the aforementioned discussion. Tang and Dong (1997a) discuss in detail some episodes.

During the Palæogene Period (i.e. during the Lower Tertiary) - and before the start of the uplift process - climate was like during the Cretaceous Period, which is believed to

have been the driest and hottest climate of the entire Phanerozoic (Frakes, 1979).

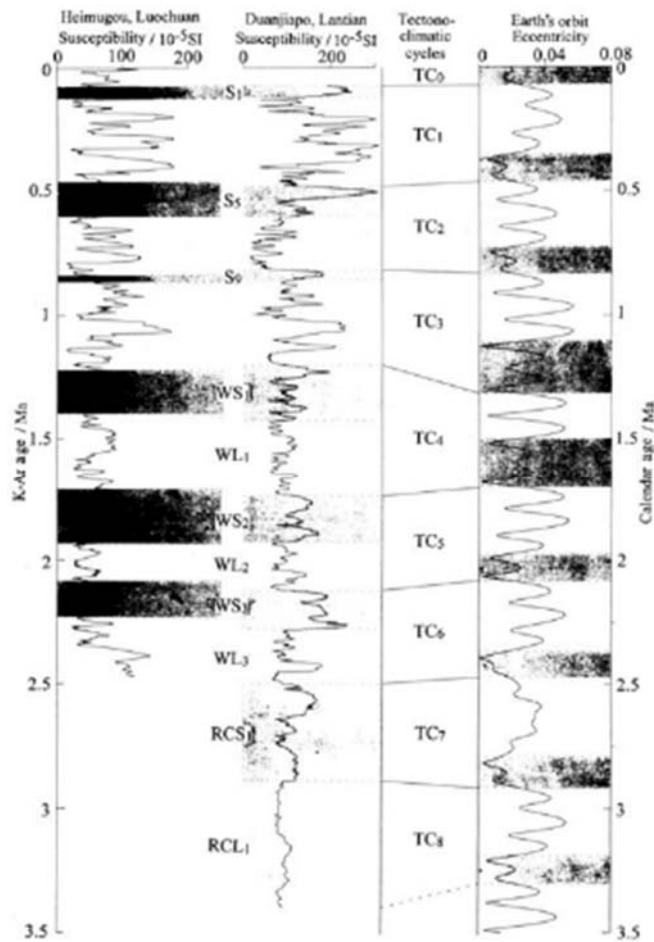


Fig. 1. “Chronologic susceptibility curves and orbital eccentricity curve (Berger and Loutre, 1991).” Figure and captions after Wu and An (1996). With kind permission of *Science in China, Series D*.

Compared to present time, the polar temperature was higher by at least $\sim 15^\circ\text{C}$, while the temperature difference between equator and poles was lower by a factor $\sim 1/2 - 1/3$. The space pattern of climate was seemingly very regular, or much close to the trend implied by a simple astronomical dependence. Southeastern Asia was

controlled by the subtropical high, thus being somewhat drier compared to present time. The signature of this is found in the red soil developed at that time in the Changjiang River¹ basin (see Shi et al., 1999). This simple “astronomical” climatic pattern, which is guessed to have preceded the TP uplift, was in fact confirmed by Jiang et al. (2001), who express it by Fig. 2.

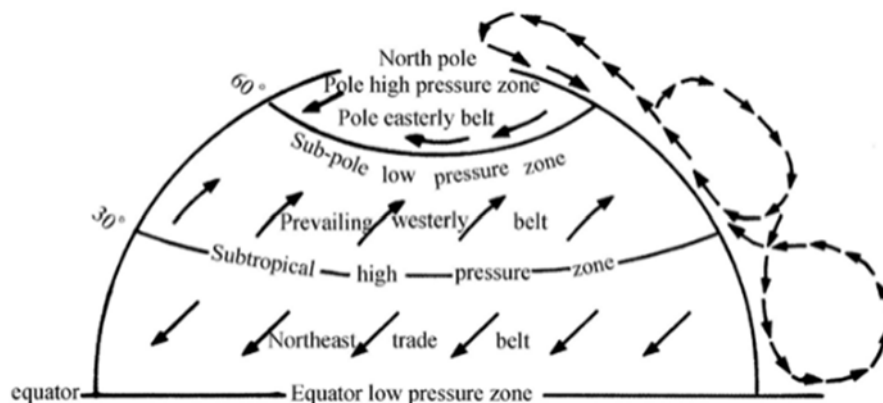


Fig. 2. “Ideal pattern of planetary wind circulation (after Gao and Lu, 1988).” Figure and captions after Jiang et al. (2001). With kind permission of *Science in China, Series D*.

¹ Concerning toponyms refer to Gregori et al. (2025f).

Jiang et al. (2001) investigated the general circulation of the atmosphere (*GCA*) in eastern Asia by considering also the records of palæo-wind directions in desert areas during the Cretaceous. They confirm that, before the uplift of the plateau, the *GCA* in eastern Asia was really controlled by the planetary circulation, i.e. westerlies in the north, and northeast trades in the south. They stress that previous studies were only based on scalar geological indicators. In contrast, they consider also directional geological indicators, which are suited to give evidence of planetary wind circulation.

The best-known general view considers the Cretaceous as a time of uniform climate, while more recent studies envisage some non-uniformity, including seasonal variability. Therefore, based on palæoclimate, also monsoon² circulation possibly existed. Jiang et al. (2001) also envisage that the same conclusion is consistent with the guessed geographical distribution of lands and oceans at that time.

Some previous authors in general claimed that atmospheric warming was caused by an increased density of atmospheric CO_2 . This explanation is, however, considered oversimplifying by Tang and Dong (1997a), who claim that this phenomenon “should have nothing to do with CO_2 ”. They consider rather a change of performance of the “atmospheric engine” according to the model computed under some simplifying assumption by Tang (1981), where by “atmospheric engine” they mean the general circulation pattern associated with a thermal process. This is indeed a key item in the astute Tang’s analysis. The definition of “heat engine” is a classical concept,³ which is explained e.g. by Tang and Guo (2000) as follows.

Different atmospheric heat engines are found in the atmosphere, e.g. mountain-valley winds, land-sea breezes, monsoons, and Hadley’s circulation. Their common characteristic is that air is warmed at a lower level, it converges and ascends until it reaches the upper level where it diverges. These are “positive heat engines” where the available potential energy (*APE*) keeps increasing, due to the work spent to overcome friction. Correspondingly, the other kind of heat engine, or “negative heat engine” (such as the circumpolar vortex), converts *APE* into work during its cooling process. The global atmospheric heat engine efficiency (*AHEE*) is the sum of the effects of both positive and negative heat engines. At present, it is ~ 2%, but it varied on the geological time scale, mainly as a response to the variation of efficiency of the “positive heat engine”, while its counterpart was passive. In fact, the increase of endogenous heat release produces an increase the efficiency of the positive heat engine.

Fig. 3 is a cartoon showing a typical “positive heat engine”. A cold high is generated on top of it, where air diverges. The work spent by the pressure-gradient force is required to overcome the friction during air convergence and divergence, thus maintaining wind rotation. In addition, consider that, according to the rationale extensively discussed Gregori et al. (2025d), owing to the ions that exist inside every air mass, the Cowling dynamo enters into play, by which an increased convection implies a higher activity of atmospheric electricity, a higher water condensation and precipitation rate, and also a supplementary contribution to the electric charging of the ionosphere.

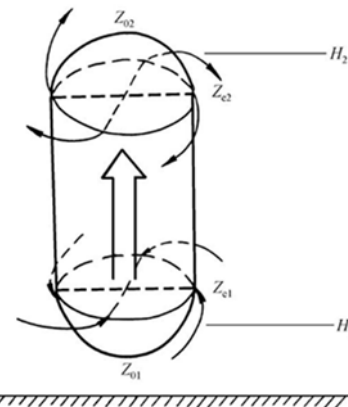


Fig. 3. Scheme of a typical positive atmospheric heat engine. The rotation direction refers to the Northern Hemisphere. After Tang and Guo (2000). With kind permission of *Science in China, Series D*.

For a positive heat engine, its efficiency η_g is defined (Lorenz, 1967)⁴ as the ratio of the work spent by the pressure-gradient force and the amount of input heat

$$\eta_g = \frac{\Gamma_D (\Delta Z_2 - \Delta Z_1)}{(n + 2)(\Gamma_D - \Gamma)(H_2 - H_1)} \quad (1)$$

where Γ_D is the dry adiabatic lapse rate ($= g/c_p$, where g is the mean acceleration of gravity, and c_p is the specific heat of air at constant pressure); Γ is the vertical lapse rate of temperature ($= -\partial T/\partial r$), and r is radial distance from the Earth’s center; n is a coefficient related to the horizontal distribution of wind, usually $n = 1$; ΔZ_1 and ΔZ_2 indicate the height differences between the isobaric surfaces at the center and the edge, namely (see Fig. 3), $\Delta Z_1 = Z_{01} - Z_{e1}$ and $\Delta Z_2 = Z_{02} - Z_{e2}$, respectively; H_1 and H_2 are the average heights of lower (convergence) and upper (divergence) regions. Upon substituting into (1) the parameters for the present *TP*, it is found $\eta_g = 1.6\%$.

For comparison purpose, for the Hadley circulation it is $\eta_g = 0.3\%$ (Tang, 1981); for the present plateau monsoon in the western United States $\eta_g = 0.7\%$, upon assuming $\Gamma = 6.5 \text{ }^\circ\text{C km}^{-1}$, $H_2 = 12.5 \text{ km}$, $H_1 = 1.5 \text{ km}$, $\Delta Z_2 =$

instance, the role of a varying atmospheric concentration of CO_2 implies substantial changes in its energy balance (e.g. Qiu, 2008; Deckers, 2011). The details of these items are not directly pertinent for the present discussion.

⁴ Edward Norton Lorenz (1917-2008).

² The term *monsoon* derives from the Arabic "mausim", meaning "seasonal reversal of winds". Generally it is defined as a system of winds characterized by a seasonal reversal of direction, but a detailed definition seems lacking.

³ Compared to the few mentions that are here considered, the concern involves a much wider perspective. For

67 m, and $\Delta Z_1 = 13$ m; for a typical mountain-valley system $\eta_g = 0.25\%$, if $H_2 - H_1 = 4$ km and $\Delta Z_2 - \Delta Z_1 \approx 10$ m.⁵

By means of these estimates Tang and Guo (2000) discuss the variation of efficiency of global atmospheric heat engines at different stages of intense orogenesis during the geological history. On the basis of present observational data, and owing to the present *TP* morphology - compared to an ocean area - the *TP* has an efficiency that is ~ 5 times higher. From the Cretaceous through the Old Tertiary, the global landform was smoother, and in addition the temperature difference between poles and equator was lower. According to Tang (1997), compared to present time, the efficiency of the “atmospheric engine” was ~ 1/2. This implied a significant weakening of the planetary wind system, smaller atmospheric disturbances, less clouds and a smaller amount of precipitations. This entire scenario ought thus to have produced a hotter and drier climate.

Tang and Dong (1997a) claim that a ~ 1/10 decrease of cloud cover causes the same effect on the radiation balance that is obtained by doubling the CO_2 concentration.

Hence, it is possible - or maybe even likely - that several other periods of Earth’s history occurred, similar to the Cretaceous, when the surface landform was smooth, and climate was hot-dry. This specifically may have occurred during the entire Phanerozoic, such as during the Cambrian Period, during the Devonian Period, and from the Late Triassic Period through the Jurassic Period (Tang et al., 1995).

Tang and Dong (1997a) summarize therefore the entire picture. They emphasize that from the Cretaceous through the Old Tertiary the temperature was almost the same all over the world. This small thermal gradient implied that the atmosphere was just transforming short wave into long wave radiation, and only a small amount of it into kinetic energy. The speed of biological evolution correspondingly slowed down, while by the onset of a new cold age several living beings became extinct (Tang et al., 1995).

Tang and Dong (1997a) firstly focus their concern on the great climate change occurred at the beginning of the Oligocene Epoch. They envisage a trigger by the *TP* orogenesis. This ought to correspond to the first of their aforementioned 7 uplift periods. The *TP*, the Zagros plateau, the Alps, etc. almost simultaneously started to uplift, and this violent global event had a dramatic impact on climate: the efficiency of the atmospheric engine began to improve. That is, according to warm-mud tectonics (*WMT*), this corresponded to an intense thrust phenomenon inside the huge Pyrenean - Himalayan megasyncline (Gregori, 2002, Gregori and Leybourne, 2021).

At the beginning, the planetary atmospheric circulation was characterized by two huge cells, extending from either pole until the equator. Only ~ 37 Ma ago the uplift of the *TP* and its horizontal extension reached the critical scale for

geostrophic readjustment of baroclinic atmosphere (Tang and Liu, 1995). Subsequently, the thermal action of the plateau was sufficient to maintain a new pressure field and a new atmospheric dynamics.

Note that, according to the rationale of the present study, this phenomenon was determined by a threefold effect.

A first effect was caused by the heat island identified with the plateau as a consequence of its elevation: the greater elevation implied a greater insolation and a different air temperature where the *TP* resulted to be embedded.

A second identical effect was caused by the larger geothermal flow, associated to the friction heat due to overthrust inside the megasyncline.

A third effect was originated by Joule heat released on the *ALB*, due to the increased electrical conductivity σ (Gregori, 2002, and Gregori et al., 2025a, or Fig. 1 of Gregori and Leybourne, 2025k). In addition, this effect was amplified by the channeling of the telluric currents induced on the planetary scale (see Gregori et al., 2025q).

In every case, a by-product was the generation of a stronger Cowling dynamo (Gregori et al., 2025d), hence enhanced precipitation on the *TP*, with additional release of latent heat. That is, a warmer *TP* was comparatively wet while the surrounding region enjoyed a reduced amount of atmospheric precipitations. The result was thus the onset of the monsoon regime, in terms of a three-cell global atmospheric circulation, associated with the role of the *TP*, which acted (like it is still acting) like a “Third Pole” (*TrP*). The Asian monsoons - which include plateau monsoons, southwest monsoons, and southeast monsoons - were thus born, including their associated precipitations. Therefore, climate no more had an approximately “astronomical” pattern. The estimated plateau height was roughly ~ 1000 m (see Fig. 4), and its effect was comparable to the present plateau monsoons in North America (Tang and Reiter, 1984). However, the whole system was going to be later dramatically changed by the subsequent uplift of the *TP*.

The next uplift episode, considered by Tang and Dong (1997a), deals with the 6th case of their 7 uplifts. It started ~ 3.4 Ma BP. By ~ 2.5 Ma BP the *TP* height rapidly raised from the original ~ 1200 m to ~ 2000 m.

Note that, according to the rationale of the present study, these abrupt changes of uplift speed must be explained in terms of corresponding changes of the elevation of the height of superswells, i.e. of the primary energy supply to the planetary array of sea-urchin spikes. This implied a change of the convergence speed of lithospheric slabs - and overthrust inside megasynclines. That is, the entire phenomenon was controlled by the efficiency of the *TD* (tide-driven) dynamo that responded to the encounters of the Solar System with interstellar matter (Gregori, 2002; Gregori and Leybourne, 2021).

⁵Note the comparatively limited spatial extension of these convection cells, i.e. in the case of plateau monsoon a few tens of meters in lateral size for the whole

tropospheric height, and for a mountain-valley system a few meters for a few kilometers height.

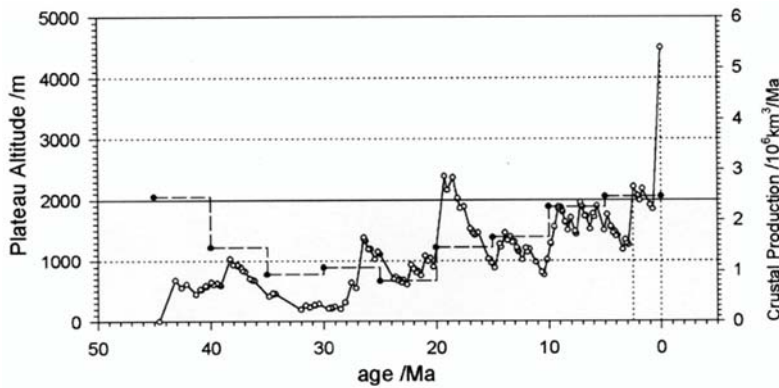


Fig. 4. Computed model for the history of the uplift of the TP (solid line), and crustal production (dashed line) according to Larson and Olson (1991). See details in Gregori et al. (2025g). After Dong and Tang (1997). With kind permission of Science in China, Series D: Earth Sciences.

In any case, the ~ 2000 m elevation of the TP was critical in two respects (Liu and Tang, 1997). When the altitude reached this value, a greater amount of vapor condensation occurred implying a release of latent heat, which strengthened the heating action of the plateau. This immediately changed the shallow plateau monsoons into deep plateau monsoons. The other effect was related to the increased horizontal extension of the plateau. These effects implied some relevant consequences (Tang and Liu, 1995).

- a) - The planetary westerlies intensified. High latitude regions greatly cooled. The GIA of the Quaternary Period was started (see below).
- b) - The so-called “Qinghai-Xizang High” in the stratosphere implied that the southwest upper level of the plateau became an area of convergence of descending wind. Climate became dry. In Africa the forest climate changed to prairie, and “Homo” appeared.
- c) - The plateau winter monsoons intensified, with a “maximum wind level” at ~ 2000 m a.s.l., which generated the loess plateau (Liu et al., 1985).

The subsequent planation period during ~ 2.4 – 0.73 Ma was also characterized by a short uplift period during ~ 1.8 – 1.6 Ma. At that time, the systems were formed of the present Changjiang and Huanghe Rivers (Li et al., 1995).

Tang and Dong (1997a) finally refer to the very last uplift periods, begun ~ 730 ka BP, when the height of the TP raised from the original ~ 2000 m up to the present ~ 4500 m. We point out that this event occurred some comparably short-time ago seems to be related to the present ongoing “Iceland” heartbeat of the Earth electrocardiogram (see Gregori, 2002, and Gregori et al., 2025a, or Fig. 1 of Gregori and Leybourne, 2025k). This was a real climate catastrophe: when the plateau elevation reached the cryosphere level, rainfall changed into snow and ice, the plateau albedo rapidly increased, and climate violently changed. This was the trigger of the planetary GIA. Some ~ 0.5 Ma ago the ice extension of the plateau reached its maximum, being ~ 18 times larger compared to present time, according to an estimate by Shi and Zheng (1997) who computed Table 6 1, which shows the comparison of the albedo of the plateau between the GIA and present time.

During the GIA, the plateau was a strong cooling source, except in May through August. Cold weather increased over the winter plateau, its winter winds were intensified, the northern part of the plateau was dry, hence loess accumulation increased (Shi and Zheng, 1997).

Table 1. Comparison between the GIA and present time of the albedo energy balance in the Earth-atmosphere system

| month | present ($W m^{-2}$) | Great Ice Age ($W m^{-2}$) |
|-------------|---------------------------|---------------------------------|
| January | -71 | -128 |
| February | -43 | -100 |
| March | 21 | -50 |
| April | 58 | -20 |
| May | 88 | 2 |
| June | 100 | 58 |
| July | 98 | 58 |
| August | 75 | 36 |
| September | 49 | -6 |
| October | -4 | -71 |
| November | -47 | -99 |
| December | -74 | -123 |
| annual mean | 21 | -37 |

A specific meteorological feature of East Asia is the so-called *Meiyu*, from the Chinese term for “plum rain”. The term *Meiyu* is Chinese, pronounced *Baiu* in Japanese. In Japan its season is sometimes called *Samidare* (“rains of May”). It is the precipitation that is caused by a front, associated to a persistent E-W zone of disturbed weather, which is typically observed during spring. It is quasi-stationary. It is located over the east coast of China and Taiwan at its western end, and over the Pacific Ocean into the southern peninsula of South Korea, south of Japan at its eastern end. In Japan and Korea the rainy season usually lasts roughly ~ 50 days from June through July. In contrast, in Eastern China (especially in the Changjiang and Huaihe regions) and in Taiwan, it typically lasts from July through August. The phenomenon occurs when moist air over the Pacific meets cooler continental air mass. The front can move back and forth with the changing strength of cool and warm air masses, often causing prolonged precipitation in eastern China, and sometimes floods. However, if it does

⁶ Reproduced with kind permission.

not rain as much as usual, a drought can occur.⁷ The rainy season ends when the warm air mass associated with the subtropical ridge affords to push the front northward and away. Mudslides and floods also occur. In addition, a high air humidity leads to the formation of mold and rot, which are found both on food and on fabrics. Hence, the name of “mold rain”.

At present, the southern branch of the west jet withdraws northward at the middle of July, and this corresponds to the disappearance of the mold rain in the Changjian River basin, where typically it lasts from mid-June through mid-July. In contrast, in the past, due to the amplification of the cooling source by the plateau, the south branch of the west jet could not withdraw. Hence, precipitations in the SE of the plateau were amplified, and the mold rain in the Changjian River basin persisted during whole summer.

Differently stated, the greater the thermal gradient - which is experienced by air masses and which is caused by the cooling action of the plateau - the more intense are the associated Cowling dynamos, the greater the atmospheric storminess and amount of precipitation, hence the devastating consequences. Consider the critical role played by the Cowling dynamo that determines the activity of atmospheric electricity, and also water condensation and precipitation, and the electrostatic charging of the ionosphere (Gregori and Leybourne, 2025a).

Therefore, during the Pleistocene Epoch, the Changjian River basin was characterized by frequent storms, rainfall, and mudslide. The signature of these occurrences is represented by the deposits (in Chinese “*xalsonte*”) of coarse-grain sand and gravel.

Thus, the *TP* elevation played a crucial role. Tang and Dong (1997a) discuss therefore the reliability of the available estimates, and complain that different opinions exist about the height the *TP* reached ~ 0.5 Ma ago. According to the model of Fig. 4 and by applying linear interpolation, it is found that before ~ 0.5 Ma BP the height was $h = 2753$ m, or, say, $h \approx 2800$ m a.s.l.

Tang and Dong (1997a) make a check also by means of air temperature. They first neglect the role of the annual and daily variations of air temperature over the *TP*. Under this assumption, temperature varies only vs. altitude: at the altitude line of 0°C rain transforms into snow and ice. When the *TP* reaches this height, a *GIA* is started, because - after an additional uplift - the available water vapor is reduced, hence also snowfall. Upon adding also the effect of the annual variation of temperature, the *GIA* had thus to start when the *TP* reached a height where the temperature t_a was still slightly higher than 0° . Suppose that this occurred for $t_a \approx 1^\circ\text{C}$. The present plateau temperature is $t_a \sim -4^\circ\text{C}$. Dong and Tang (1997) recall the station Tuotuohe, 4533 m a.s.l., where the mean annual temperature has been $t_a = -4.3^\circ\text{C}$ during 1961-1990.

The next step by Tang and Dong (1997a) is to consider the temperature variation during the last ~ 0.5 Ma that was caused by the Milanković astronomical modulation. The

estimated amplitude is $\sim 10^\circ\text{C}$. The lowest minimum is believed to have occurred ~ 18 ka ago, being $\sim 5^\circ\text{C}$ lower than at present.

If a temperature decrease is assumed vs. height of $\sim 0.6^\circ\text{C} (100\text{ m})^{-1}$, it is found that, at the time of the lowest Milanković temperature, the level of $t_a \approx 1^\circ\text{C}$ was attained at ~ 2800 m, which was thus the height to be expected in order to trigger the *GIA*. Therefore, they concluded that before ~ 0.5 Ma ago the elevation of the *TP* was slightly lower than ~ 3000 m. Afterwards, and particularly after ~ 200 ka, the plateau temperature was mainly controlled by Milanković, as this effect implied a temperature variation by $\sim 10^\circ\text{C}$ during a time interval of ~ 100 ka. This should be compared with the temperature variation caused by the uplift, i.e. ~ 350 m during ~ 100 ka. Therefore, compared to Milanković, during the last $\sim 100 - 200$ ka the influence of plateau uplift can be ignored.

Tang and Guo (2000) reconsider the same model, with some improvement. They deal with every *GIA*, which occurred sometimes during the entire Earth's history, and they associate it with a strong orogenic process (see Fig. 5). They claim that the whole evidence seems to be consistent with their proposed causality chain: strong orogenic process \Rightarrow great topographic differences at Earth's surface \Rightarrow relevant changes of atmospheric circulation system (plateau monsoon) \Rightarrow greater efficiency of the global atmospheric heat engine \Rightarrow generation of a greater amount of atmospheric kinetic energy \Rightarrow enhancement of planetary westerly (under the condition that the huge relief has a mainly longitudinal trend) \Rightarrow increase of the temperature gap between equatorial and polar regions (constrained by thermal wind law) \Rightarrow sharp cooling in high latitudes and in polar regions (upon supposing approximate constancy of solar radiation) \Rightarrow development of a *GIA* event.

Just note that, as mentioned above, the starting strong orogenic process was triggered by the intensification of the *TD* dynamo etc. (“Iceland” heartbeat). In addition, note that the greater energy and dynamics of the atmosphere is closely related to - or identified with - a greater role of the Cowling dynamo that determines atmospheric precipitations and strengthens atmospheric electricity processes (Gregori et al., 2025d).

More specifically Tang and Guo (2000) focus on three remarkable cooling processes that finally determined a *GIA* in the Cenozoic Era. These cooling processes occurred, respectively, at the beginning of the Oligocene (~ 37 Ma BP), at the middle of the Miocene (~ 18 Ma BP), and at the beginning of the early Pleistocene (~ 2.4 Ma BP).

The time interval during the late Eocene Epoch spanning $\sim 44.57 - 37$ Ma BP is named “no plateau monsoon era”, because $L_t < L_0$ (defined in Fig. 6, see Gregori et al., 2025g). Hence, no adjustment was required by the *TP* for

“prediction” method of the Tang MaoCang school (see Gregori et al., 2025h).

⁷ The spacetime variations of geothermal heat flux modulates the details of this phenomenon, according to the rationale of the present study, and according to the

atmospheric pressure and winds. No stable cold high or heat low, i.e. plateau monsoon, could be formed, although the

process of the uplift had already started and it eventually acted as a heat/cold source on its surrounding atmosphere.

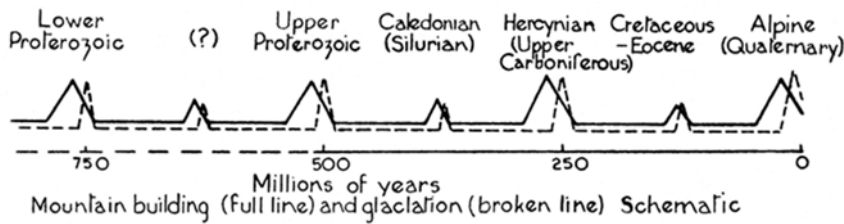


Fig. 5. “Mountain building and glaciation.” Figure and captions after Brooks (1926, p. 178, II ed.). With kind permission of Dover Publications.

The consequent atmospheric system over the plateau was therefore only a small or intermediate-scale mountain-valley wind, with quite low *AHEE* only $\sim 0.25\%$, i.e. lower by 5 – 6 times compared to present plateau monsoon ($\eta_g \approx 1.6\%$). Therefore, compared to today, the planetary

westerlies were several times weaker. The temperature difference between the equatorial and polar regions was much smaller. No real steep relief existed at Earth’s surface. Climatic regions were essentially longitudinal, determined by the astronomical position of the Sun, or the climate can be said to have been “quasi-solar”.

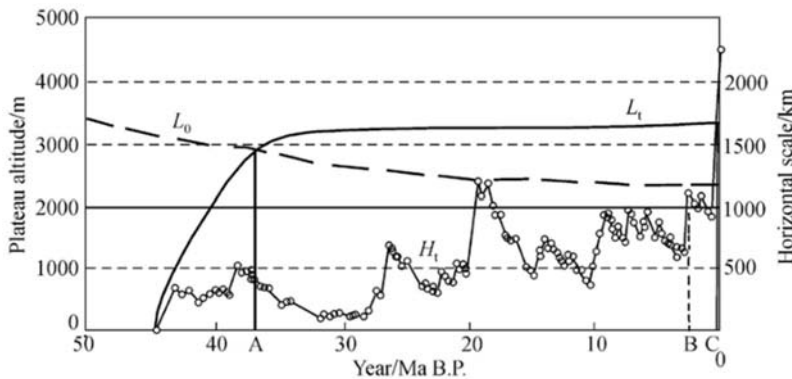


Fig. 6. The same as Fig. 4, with the addition of the trend vs. time of the horizontal scale L_t of the *TP*, and of the critical scale L_0 of the geostrophic adjustment in the baroclinic atmosphere. After Tang and Guo (2000). With kind permission of *Science in China, Series D*.

The intersection of the curves for L_0 and L_t in Fig. 6 occur exactly at the Holocene start (~ 37 Ma BP), which is the beginning of a new epoch, in terms of change of global climate. The essential reason is that the pressure systems became steady, which were caused by the thermodynamic effect of the plateau (such as heat low in summer and cold high in winter). The wind field was readjusted to the new pressure field, and the plateau monsoon emerged. The effect on global climate was twofold.

- (i) The basic pattern of the global atmospheric circulation shifted from “two polar vortices” to “three vortices”. These vortices could exist independent of one another, as it has already been proved theoretically (Zeng, 1979). The atmospheric circulation was thus characterized by “monsoon climate” compared to the previous “quasi-solar climate”.
- (ii) At that time the *AHEE* of plateau monsoon was $\sim 0.7\%$, i.e. 2 – 3 times larger than for mountain-valley winds, although it was still a shallow system, similar to the present plateau monsoon in western United States (Tang and Reiter, 1984). Correspondingly, the planetary winds had to increase, originating an increase of westerlies. According to the theory of thermal-wind, the inevitable consequence was the widening of temperature difference between equator and poles. This led to a cooling trend in high latitude regions,

upon supposing that the variation of solar radiation was negligible. Indeed, the first global cooling in the Cenozoic Era happened at this time (Frakes, 1979). “Some people believe” the formation of the Antarctic sea ice was caused by this cooling event.

Another abrupt change of global *AHEE*, hence of climate, occurred when the plateau reached the dynamic critical height (H_d) and the condensation height (H_c). Concerning the values of H_d and H_c , it is generally accepted that H_d is nearly equal to H_c , at $\sim 1.5 - 2$ km (Trenberth⁸ and Chen, 1988; Liu and Tang, 1996). Tang and Guo (2000) choose 2 km. According to Fig. 6, during the middle Miocene the plateau had experienced an intense uplift. The highest elevation (H_t) occurred ~ 18 Ma ago, being > 2.0 km, i.e. $H_t > H_d$ and $H_t > H_c$. This originated another intensification of the plateau monsoon, and its efficiency increased up to $\sim 1.6\%$, which is almost the same as for the present plateau monsoon. Meanwhile, the planetary westerlies were strengthened anew, and another cooling process involved the Antarctic region, where a perpetual ice sheet appeared. This was the so-called global cooling of the middle Miocene.

Subsequently, owing to planation or denudation, the plateau height was reduced to an altitude < 2000 m. In fact, when the uplift-speed is reduced, erosion and denudation prevail due to weathering.⁹ Some ~ 15 Ma ago

⁸ Kevin Edward Trenberth (1944-).

⁹ In this respect, as a historical curiosity, Leonardo da Vinci was well aware of a comparative fast present erosion

it was even $< 2000\text{ m}$ (Fig. 6). Thus, the plateau monsoon had to change into a “shallow plateau monsoon” regime with $AHEE$ of $\sim 0.7\%$. At the same time, the planetary westerlies began to decline and the temperature in polar regions raised up. On the other hand, the ice cap could survive, due to its self-protection deriving from an increase in albedo, which limited the temperature recovery.

By $\sim 2.5\text{ Ma}$ ago, H_t reached $\sim 2\text{ km}$, and since that time it has been basically $H_t > 2\text{ km}$. This originated another abrupt change of global climate. The plateau horizontal size increased by several times. The latent heat absorbed by the plateau increased suddenly, the depth of the plateau monsoon deepened, and high monsoons reached the bottom of the stratosphere. The shallow plateau monsoons were transformed into deep monsoons. The present monsoon pattern was thus established.

The heat engine efficiency was $\sim 1.6\%$ for deep monsoons, and more than twice for shallow monsoons. However, some global climatic and environmental impact occurred.

- (i) The whole Northern Hemisphere (NH) was involved in the GIA , due to the doubling of the $AHEE$ that strengthened the planetary westerlies.
- (ii) Following the establishment of the deep plateau monsoon, the descending compensation current became stronger on the northern slope of the plateau. The desert was formed, which prepared the formation of the Loess Plateau. In addition, an obvious characteristic of the vertical structure of the plateau winter monsoon was a maximum thickness of the wind layer, reaching at most $\sim 2\text{ km}$. This constrained below $\sim 2\text{ km}$ the height of the loess transported by the winter monsoon. Therefore, loess fell in the divergence region of the northern plateau, and it finally shaped the Loess Plateau (Liu et al., 1985).

Note that, according to the general rationale of the present whole study, in general it can be stated that all palaeoclimatic changes were always originated by a variation of the TD efficiency that modulates the input of endogenous energy into the ocean/atmosphere system, i.e. in the “climate” system. This is a correct general statement, although - if it is taken in its literal sense - it can be misleading. In fact, the injection of endogenous energy in the climate system occurs differently in different regions, depending on the pattern - at every given epoch - of the sea-urchin spikes that - on their part - evolve according to the Earth’s electrocardiogram process. Large bunches of sea-urchin spikes determine the uplift of superswells. Superswells determine the overthrust of lithospheric slabs inside megasynclines. Orogenic processes occur. They are comparatively rapidly destroyed by weathering, erosion and planation. On the other hand, they are continuously uplifted, as long as the overthrust phenomenon is in progress. This newly generated orogeny - through mountain elevation -

process. It appears that this was quite a serious nightmare for him. He was concerned with the possibility that the Earth was going to become soon a unique huge swamp. Several Leonardo’s sentences - generally denoted as “prophecies” that in the 1950s

and through friction heat plus eventual Joule heat from the ALB such as it happens for the TP - has a very complicated interaction with the atmosphere. Mountains eventually play the dramatic role of a “Third Pole”, or eventually of a “Fourth Pole”, etc.

That is, the planetary dynamics of the atmosphere, including precipitation, wet or dry periods, warm or cold air temperature in different regions of the world, are all phenomena that are severely affected by this very complicated ensemble of feedback, compensation, amplification, generation of enhanced gradients in both space and/or time. Also note that, in general, every larger gradient implies a stronger Cowling dynamo. That is, this very intricate and eventually violent dynamic scenario is transformed into e.m. energy, which also affects the electrification of the ionosphere, and in general enters into the magnetosphere and in the interaction with the solar wind. This entire process implies, as a by-product, also seismic and volcanic activity, according to WMT .

Therefore, it is naïve to hope that one phenomenon alone can be “the correct” reliable precursor suited to forecast either an earthquake or any other kind of natural catastrophe. The unique realistic approach is to consider the kind of phenomenon of concern. Then, one must carry out a diagnosis of the state of the natural system by means of different multidisciplinary parameters. Then, one can envisage whether the natural system is more or less rapidly approaching a threshold for the occurrence of a possible “catastrophe” (in the mathematical sense). In this case, one can release an alert for a possible occurrence of an unwanted event. However, in a strict sense the certainty is *per se* always impossible.

In this same respect, the present ongoing climate change is associated to the present “Iceland” heartbeat of the electrocardiogram of the Earth, and it is impossible - with the present observational information - to make any forecast on its evolution (see Gregori and Leybourne, 2025k).

Tang and Liu (2001)¹⁰ improved their model by new computations. For three times during three typical monsoon climate periods the condensation level was above 2000 m .

According to the assumption by Tang and co-workers, the endogenous energy release, which caused the plateau uplift, occurred only during normal geomagnetic field and not during reversed field. Note that this assumption cannot be shared by the present study. In any case, according to this assumption, the strong positive geomagnetic polarity ought to have implied a response into the strong uplift of the plateau and into a low sea-level. Correspondingly, the long reverse polarity period had a response as a denudation period of the plateau and a high sea-level. However, compared to geomagnetic field reversals (FRs), the sea-level effect occurred $\sim 0.8 - 1.0\text{ Ma}$ later.

seemed to be mysterious - reveal his profound psychological depression, which was evidently a great concern for him. He missed that, in some way, new mountains are steadily regenerated somewhere.

¹⁰ Not available to us.

Cui et al. (1998) studied the Kunlun Mountains Pass area. A violent tectonic movement occurred during $\sim 1.1 - 0.7 Ma$ ago, i.e. the time-range can be inside the “Iceland” heartbeat. They envisage the first occurrence of a large-scale uplift, followed by a fault-block rising and a simultaneous fault depression, which suddenly interested the northern plateau. This sudden and tremendous uplift raised this area over the critical elevation of $\sim 3000 m$ and they guess that this event caused the appearance of the maximum glaciation of the Quaternary. Perhaps this was the driving force of the huge environmental change of tectonic-climatic circulation at the break of the early and middle Pleistocene in China.

Shi et al. (1999) carried out a detailed investigation of the second uplift of the *TP*, which occurred $\sim 25 - 17 Ma$ ago - and that was the initiation of the Asian monsoon system, and this occurred much earlier than the “Iceland” heartbeat. The rationale is just the same as the Tang and Dong model. They considered, however, the set of evidences provided by geology, by flora and fauna, etc. focusing on the uncertainties etc. When the elevation of the plateau reached a height such as to change the general

atmospheric circulation, a warming was observed in the tropical oceans, altogether with an enhancement of the cross-equatorial current, the enlargement of the marginal sea basins in east-southeastern Asia, a westward extension of the Asian continent and the regression of the Paratethys Sea. This caused a general increase of thermal gradients. Consequently, air currents enhanced between continents and oceans. At the same time, the Asian monsoon system, mainly the summer monsoon, began. This caused important environmental changes, such as the large shrinkage of the dry steppe in Central Asia, and the extension of the humid forest zone in East Asia. These changes occurred $\sim 21.8 Ma$ ago, according to measurements carried out along the Lingxia profile on the northeastern border of the *TP*. At that time, the savanna changed into forest. Concerning the evidence of changes in marine environment, they report Fig. 7, which is the water temperature in the tropical Pacific Ocean, inferred from $\delta^{18}O$ records in benthic foraminifera (Douglas and Woodruff, 1981).

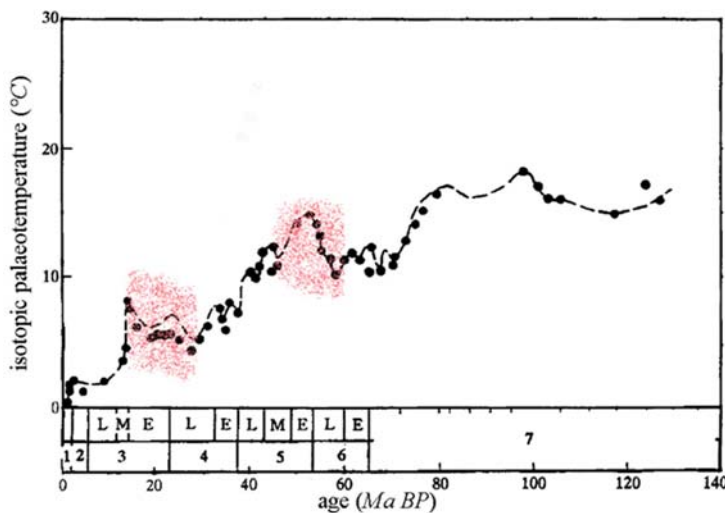


Fig. 7. Palaeo-temperature of the tropical Pacific Ocean from the Cretaceous Period through the Cenozoic Era based on $\delta^{18}O$ records in benthic foraminifera (Douglas and Woodruff, 1981). Legend: 1 - Quaternary; 2 - Pliocene; 3 - Miocene; 4 - Oligocene; 5 - Eocene; 6 - Palaeocene; 7 - Cretaceous. The two major warming events mentioned in the text are evidenced in color. Adapted after Shi et al. (1999). With kind permission of *Science in China, Series D*.

Shi et al. (1999) note the general long-time cooling trend since $\sim 100 Ma$ ago, from Cretaceous through Cenozoic. Several temperature fluctuations are observed superposed on this long-period trend. They emphasize the two prominent warming events (evidenced in color in Fig. 7). One implied a $\sim 5^\circ C$ increase during the Late Palaeocene ($\sim 60 - 55 Ma$). The other was by $\sim 3^\circ C$ from Middle/Late Oligocene through the end of the Early Miocene ($\sim 27 - 14 Ma$) (Douglas and Woodruff, 1981). The record of this second event was found also in the South Pacific, less clearly in the Atlantic. The second *TP* uplift occurred during this warming event.

Shi et al. (1999) recall that, according to Zubakov and Borzenkova (1990), “during the warming event at $\sim 21 - 25 Ma$ ago, the temperature had an increase of $\sim 3 - 5^\circ C$ at the surface of the equatorial ocean and had an increase of $\sim 2 - 3^\circ C$ at the bottom of the Antarctic ocean”. Shi et al. (1999) comment that “the warming of the tropical water enhanced the evaporation of the ocean, while the existence

of the Antarctic Ice Sheet and the Circum-Antarctic ocean current increased the longitudinal temperature gradient and strengthened the cold wind of the Southern Hemisphere (SH) in winter. It crossed the equator as the energetic source of the summer monsoon in the NH and brought a large amount of the vapor from the tropical ocean to the Asian Continent.”

Also the sea basins, from the Late Oligocene through the Miocene ($\sim 32 - 15 Ma$), experienced great changes along the east and southeast margin of Asia (Jin et al., 1995), such as e.g. the Kuril basin ($\sim 30 - 15 Ma$ ago), the Japan Sea basin ($\sim 28 - 15 Ma$ ago), the Shikoku Sea basin ($\sim 27 - 13 Ma$ ago), and the South China Sea basin ($32 - 17 Ma$ ago). The widening of these basins provided more water vapor, which was also closer to the main continent. At the same time, also the continental area considerably expanded. Africa and Arabia moved northward, approaching Asia. The eastern end of the Mediterranean Sea had closed $\sim 23 Ma$ ago after the

closure of the Turgai strait, which crossed through Asia and Europe to the Arctic. The Eurasian supercontinent formed. In addition, the Paratethys Sea, in central-western Asia, shrank.

The Paratethys Sea had occupied a vast area in the latitude span $40^{\circ} - 60^{\circ}N$ and west of $90^{\circ}E$ with a southeast branch (named the Kashi Bay) that extended until the present Tarim Basin. This configuration resulted $\sim 30 Ma$ ago in a humid and temperate climate in the surrounding area. Afterwards, the Paratethys Sea rapidly withered. During Mid-Miocene it could occupy only an area equivalent to the present Aral Sea, Caspian Sea and Black Sea and their surrounding regions. Central Asia became drier, and a strong continental climate appeared.

According to the simulation by Ramstein et al. (1997) by means of an atmospheric general circulation model (AGCM), when the Paratethys Sea existed during the Oligocene, the annual range of air temperature was $\leq 17^{\circ}C$, and the annual precipitation was at most $\sim 900 mm$. The Kazakhstan was partly covered by broad-leaved trees and bogs. After the westward regression of the Paratethys Sea, the annual range of the temperature increased to $\geq 30^{\circ}C$, the mean winter temperature had a decrease of $\sim 10^{\circ}C$ and the summer temperature an increase of $\sim 4^{\circ}C$, while precipitation decreased, and the desertification widened. In addition, the greater thermal gradient between Asian continent and Pacific-Indian Ocean enhanced also the monsoon system.

Other Chinese palaeoclimatologists

The rationale, based on the evidence that the Himalaya region is the site of an anomalous release of endogenous energy, was also applied by other Chinese palaeoclimatologists to several studies on the TP. A clear effect on climate is observed over a reasonably wider area and during a suitable time lag. A partial list of papers on this item is given here below, with no presumption for completeness. The literature is very large. The topics here mentioned give a perspective of the amount of understanding provided by different proxies (ice cores, permafrost, loess, sediments, stalagmites, pollen, tree rings, archaeology, ...) in a very peculiar area of the Earth that - as a climate driver - can be likened to a "Third Pole" (TrP) of the Earth. In addition, we stress the great variety of phenomena in the Chinese subcontinent that looks like a unique natural laboratory suited to check several different mechanisms that control global climate. These papers are often written in Chinese, and we could rely only on their English abstract.¹¹

Yang and Chiu (1965) gave a seemingly classical and detailed report about the glacier history in the region of the upper Urumqi valley, Sinkiang, related to the evidences of Pleistocene and recent climatic fluctuations. Most of the 55 present glaciers owe their existence to an exceptionally favorable exposition. Upon analyzing moraines and deposits, Yang and Chiu (1965) envisage that some of the

present glaciers considerably shrunk, and are believed not to endure the warm period of the Climatic Optimum. Hence, they cannot be considered as the direct survivor of the last glacial period.

Note that, according to the recent evidence, an increase of endogenous heat flow activates Cowling dynamo and atmospheric precipitation (Gregori et al., 2025d). The increased endogenous heat flow causes ice melt, although it determines an increase of air temperature and of humidity, hence of greenhouse effect. Thus, thermal excursions are damped, climate gets wet and milder with vegetation development occurring in formerly desert areas. In contrast, fresh moraines - which overly unconformably and overthrust on older glacial deposits - were the products of regeneration and expansion of glaciers during the Little Ice Age. The present glaciers are the direct survivors of the Little Ice Age that, after the Climatic Optimum, was a dominant cold phase in eastern Tienshan. That is, the climate change seems to be controlled by a time variation of the availability of endogenous energy.

Yang and Chiu (1965) recognized the re-advances of three main phases of glacier during the general retreat of the last glacial period. Large quantities of Pleistocene melting water were flowing from the mountain gaps of northern Tienshan. The resulting outwash plains provide the basis of Pleistocene chronology - and also the ground for geomorphological hypotheses concerning the mechanics of river deposition and erosion and the origin of the formation of depositional terraces beyond the glacial borders.

Owing to tectonic movements and/or to climatic conditions, the outwashes display a large scale and thickness. The oldest outwash plain, $> 400 m$ thick, was uplifted to $\sim 2200 m$ a.s.l. Repeated glaciations of the mountain regions resulted in the building of successive outwash fans and valley trains. The available evidences indicate that the oldest glaciation built the largest outwash plain while the younger glaciations built smaller plains. That is, according to the interpretation that is here given, this whole evidence denotes a large time-varying amount of release of endogenous heat.

Qin (1981) studied the glaciations and glacial changes in the Suzhulian Feng occurred since the Würm glaciation. The results show that the snow line - during the Würm glaciation, the Neoglaciacion and the Little Ice Ages - was, respectively, $\sim 590 - 630$, $\sim 230 - 360$, $\sim 140 - 150 m$ below present altitude, while the temperature near the snow line was lower than at present by $\sim 4^{\circ}C$, $\sim 1.5^{\circ} - 2.5^{\circ}C$, and $\sim 1^{\circ}$, respectively.

Guo and Li (1981) studied the changes of cold- and warm-climate that, since the beginning of Quaternary, occurred in northeastern China following the world climatic fluctuation. That is, in general the time variation of endogenous heat release inside a given region is other than in other regions. Guo and Li (1981) relied on palaeo-vegetation evolution, palaeo-periglacial remains and palaeontological facies. Owing to palaeoclimatic changes -

¹¹ In addition, one author (GPG) had the privilege of having long discussions with Dong Wenjie and Gao Xiaoqing, and they deserve a sincere and deep appreciation.

since the beginning of Quaternary - the formation, development and disappearance of palæo-permafrost have been in progress in this region. Several times palæo-permafrost appeared and disappeared in this area due to the alternation of cold- and warm palæoclimate. Note that permafrost is a particularly sensible local sensor for endogenous energy release. Indeed, climate is a very complicated phenomenon. A map of present permafrost in China is shown in Fig. 3 of Gregori et al. (2025f).

On the basis of palæo-periglacial remains, of palæo-air temperature determined by spore-pollens, and of palæo-environmental proxies derived from mineral composition, Guo and Li (1981) divided the history of palæo-permafrost in Northeastern China into three stages, and for every stage they inferred the southern boundary of the palæo-permafrost and the general pattern of its development.

- (a) *Late Pleistocene stage.* Guo and Li (1981) assumed that permafrost can be conserved and developed depending on the annual ground-surface mean-temperature at $0^{\circ} C$. Based on the inferred palæo-air temperature, they concluded that, during the Guxiang-tun periglacial epoch of late Pleistocene, the $0^{\circ} C$ isotherm of annual mean ground-surface temperature roughly stretched along Ouhan-qi, Ganqika, Changtu within the Xialiaohu plain area. In addition, this inference approximately agrees with the present $7 - 8^{\circ} C$ isotherm of annual mean air temperature. It also agrees with the southern boundary of palæo-permafrost in this area, determined by the palæo-periglacial remains of cold climate periods.
- (b) *Stage from post-glacial period to Hypsithermal interval of Holocene.*¹² At this stage, most of the permafrost in the area developed at the former stage, as it thawed due to the global air temperature increase. Hence, the southern permafrost boundary retreated northward. Guo and Li (1981) claim that, owing to the inferred palæo-air temperature and environment, a palæo-periglacial environment persisted in the northern part of the existing permafrost of this area, i.e. a part of permafrost survived during late Pleistocene.
- (c) *Stage from Hypsithermal interval to late Holocene.* After the Hypsithermal interval, the palæo-permafrost, which had disappeared, developed anew when air temperature lowered. As a result, the ground temperature of the old permafrost, which had been formed during late Pleistocene, extended downward and its thickness was thus enlarged through the previously existing permafrost area. Consequently, the permafrost gradually stretched southward, and finally reached the farthest southern boundary during the 17th-18th century. According to the palæo-periglacial remains - which were discovered in the black shale of $\sim 7,500 - 2,500$ years ago at places beyond the southern boundary of the existing permafrost - Guo and Li (1981) inferred that permafrost had extended beyond its previous southern boundary that had been attained at the time of its maximum extension.

Fan and Yao (1982) investigated the perennial frost in the southern Qinghai Northern Xizang area, which belongs to low-to-middle latitude and high elevation type. This feature resulted from numerous factors that were operative over a long period of time. The leading driver was a new tectonic movement, and a second driver was the variation of Quaternary climate. The observed trend is therefore the result of the competing trend of a warmer climate and of tectonic uplift. However, different evidence and ^{14}C data indicate that the general trend during the last $\sim 10,000$ years is regression of perennial frost. This is consistent with the fact that at present the Earth is close to the top-point of the "Iceland" heartbeat, i.e. a steady general increase is in progress of endogenous energy release. Since the duration of a heartbeat is of the order of a few million years, this steady increase is likely to be ongoing since a few million years.

Concerning future perspectives, fast uplift alone of the plateau ought to cause a progressively drier and colder climate, with an increasing periglacial area. That is, at this high altitude, the glacier extension is also significantly controlled by tectonic uplift - altogether with water precipitation, thawing and evaporation, and geothermal flow. This conclusion, however, was later contended by the model of Tang and Dong (see below), who claim that at the present time, which is characterized by a slow uplift speed, the climate control ought to be mostly controlled by Milanković rather than by tectonic uplift.

Li et al. (1982) reported about a discovery made in May 1980 close to the little town of Zhalianuoer ($49^{\circ} 20' N$, $117^{\circ} 35' E$). Two fossil mammoth skeletons were discovered in an old river bed, $\sim 35 - 40$ m below soil surface, at the eastern open-cut of a coal mine. The ^{14}C age of the coprolites was found $\sim 33,760 \pm 1,700$ years BP. Mammoths are representative of the fauna of the late Pleistocene in northeastern China, being associated with a cold climatic environment. Therefore, Li et al. (1982) divided the periglacial phenomena of the Zhalianuoer stage into three substages: (1) the Lingquan Periglacial substage ($\sim 33,700$ years BP); (2) the Huangshan Interperiglacial substage, which is a relatively warmer period of glacial retreat ($\sim 33,000 - 23,000$ years BP); (3) the Zhalianuoer New Glacial substage, for which the ^{14}C determination of the silt (black clay) is $\sim 3,080 \pm 80$ years BP, and this substage occurred $\sim 3,000 - 5,000$ years BP, with present layer ~ 0.5 m below ground surface.

An accurate report was published by Huang et al. (1982), with main concern, however, just being glaciological, rather than palæontological. In any case, let us insert here their discussion, because glaciers are an important component in the interpretation of past climate. The entire discussion by Huang et al. (1982) is closely pertinent for the present treatment, concerning the evidence of an anomalous endogenous heat release underneath the whole Himalaya orogen. Concerning toponomy, Huang et

¹² "The Hypsithermal followed the cool climate of earliest Holocene time (pollen zone IV=Preboreal) and

preceded an interval of cool late Holocene climate (pollen zone IX=Subatlantic)." (Porter, 2007).

al. (1982) refer to Fig. 1 of Gregori et al. (2025f). They investigated the temperature profiles inside several different glaciers by means of a database beginning in 1959. They focus on “continental-type” glaciers. They suggest empirical formulas for the temperature stratification of the active layer and for annual mean temperature profiles. Concerning their entire rationale and conclusions, refer to the final Fig. 8.

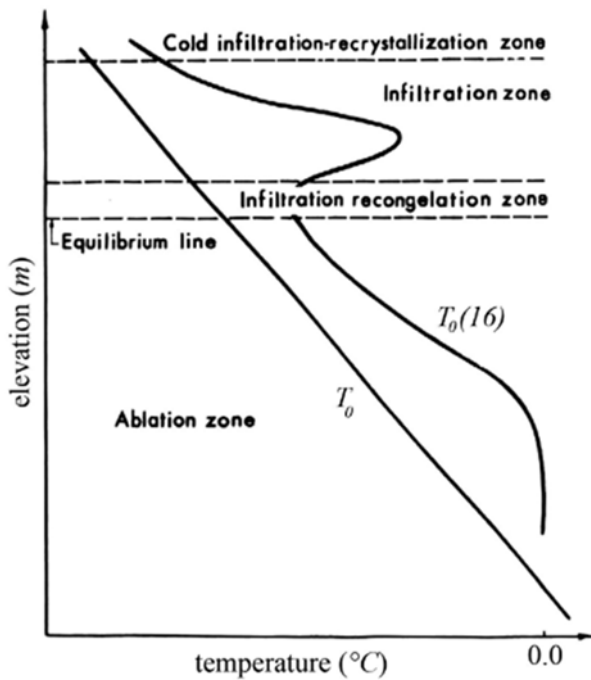


Fig. 8. “Diagram showing how the lower-bound temperature in the active layer changes with glacial zones.” See text. Note that ‘re congelation’ means “refreezing.” Figure and captions after Huang et al. (1982). Reprinted from the *Journal of Glaciology* with kind permission of the International Glaciological Society and of Cambridge University Press (CC-BY 4.0).

Huang et al. (1982) conclude that “the temperature in continental-type glaciers in China is quite low, rising rapidly with depth. A major part of the bottom of most glaciers reaches the pressure-melting point, with basal sliding. The extreme huge valley glacier will change from a cold glacier into a temperate one when it descends to the district where the climate is temperate. The ice temperature of the lower bound of the active layer at the altitude of the equilibrium line is 1.8° – 3.7 °C higher than the annual mean air temperature at the same level. The western section of Ch’i-li en Shan (Qili an Shan) may be the place where the temperature of alpine glaciers is the lowest of the middle and low latitudes. The infiltration zone is warmed significantly by the infiltration and conglobulation process ...”

They stress that “early in the 1960s the glaciers in West China were classified into continental type and maritime type according to their main properties and geographical environments. To the former belong those in most parts of

Ch’ing-hai - Hsitsang kao-y uan (Qinghai-Xizang gao-yuan - TP) from the middle Himalaya Shan to Ch’i-lien Shan (Qilian Shan) and T’ien Shan (Tian Shan) with low precipitation and low temperature, while to the latter those in south-eastern parts of the Plateau with high monsoon precipitation ...”

Huang et al. (1982) refer to continental-type glaciers, and they could rely on measurements carried out at 24 sites in 12 glaciers (see Fig. 1 of Gregori et al., 2025f), including measurements of the snow cover. “Furthermore, Chinese glaciologists have taken temperature measurements on Batura Glacier (36° 35’N, 74° 23’E) ... and Bait Bare glacier (36° 20’N, 74° 52’E) ... in Karakoram mountains ... The ice temperature is usually measured using a copper resistance thermometer measured by a Wheatstone’s bridge. For laying the thermometer, a hand drill and a steam drill are used to make holes, the maximum depth of which reaches 18 m. Most drill holes are located in the ablation zone, while a few are in the accumulation zone.”

Let us recall that evaporation and melting together are called ablation. Two glaciers in Fig. 1 of Gregori et al. (2025f) [Ku-hsiang ping-ch’uan (Gu-xiang bing-chuan) and A-cha ping-ch’uan (A-zha bing-chuan)] are of maritime type (“they have temperatures equal to 0 °C”) and are not considered. All others are of continental type.

Fig. 9 shows the temperature stratification in glacier No. 1, Urumchi River, measured weekly during June-September 1962. Fig. 10 shows the same, monthly during 1964-1966. Fig. 11 refers to glacier No. 5, Yang-lung he (Yang-long he), weekly during 1977.¹³

Ren and Huang (1981) derived a semi-empirical formula by fitting the glacier No. 5 records and concerning the yearly wave, i.e. with $\omega/2\pi = 1 \text{ year}$

$$T(y, t) = T_s \exp \left[-\beta y \left(\frac{\omega}{2k} \right)^{\frac{1}{2}} \right] \cdot \sin \left[\omega t - y \left(\frac{\omega}{2k} \right)^{\frac{1}{2}} \right] + T_0(y) \quad (\text{for } y > 3\text{m}) \quad (2)$$

where y is the depth coordinate, positive downward with respect to the glacier’s surface; t is time; $T(y, t)$ is the temperature at (y, t) ; T_s is an apparent wave amplitude at the surface; $\omega/2\pi$ is the frequency; k is the thermal diffusivity; β a factor for correcting the amplitude, being roughly ~ 1.0 ; $T_0(y)$ is the equilibrium temperature at depth y , i.e. the annual mean temperature. They chose 30 April as time origin $t = 0$ in order to optimize the fit with observations. In addition, they empirically found

$$T_0(y) = \alpha + \gamma y \quad (\text{for } y > 3\text{m}) \quad (3)$$

$$T(y, t) = T_s \exp \left[-\beta y \left(\frac{\omega}{2k} \right)^{\frac{1}{2}} \right] \cdot \sin \left[\omega t - y \left(\frac{\omega}{2k} \right)^{\frac{1}{2}} \right] + T_0(y)T_0(y) = \alpha + \gamma y$$

where α is a constant, and γ is the vertical temperature gradient.

Huang et al. (1982) warn, however, that these formulas can be applied to the glacier-level close to its equilibrium line, and that it is not sure that conduction is the dominant

¹³ See also Fig. 1 of Gregori et al. (2025f) and Fig. 8.

factor for heat exchange when $y < 3 \text{ m}$, where, compared to a simple heat-conduction equation, heat exchange is

more complicated. By this, they can distinguish three layers in their temperature measurements:

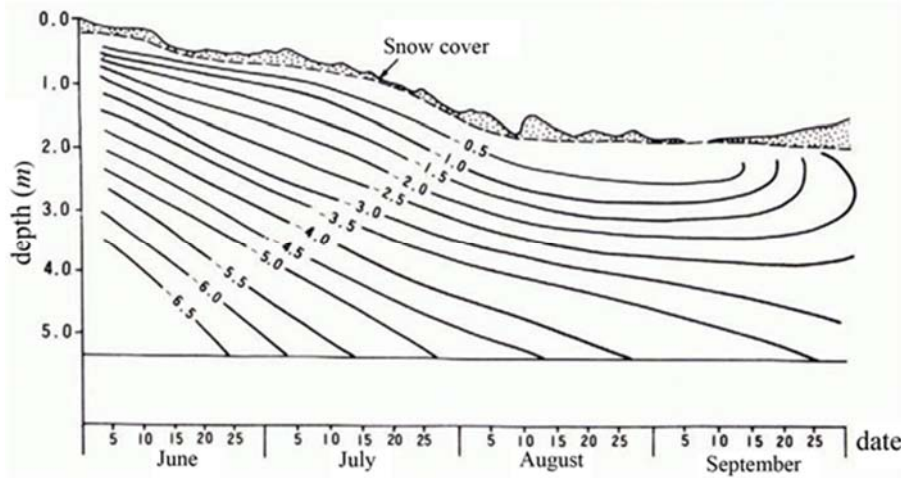


Fig. 9. "The summer temperature stratification of the upper layer in No. 1 glacier, Urumchi River measured in 1962 at an altitude of 3825 m (ablation zone) (from Huang and Yuan, 1965)." Figure and captions after Huang et al. (1982). Reprinted from the *Journal of Glaciology* with kind permission of the International Glaciological Society and of Cambridge University Press (CC-BY 4.0).

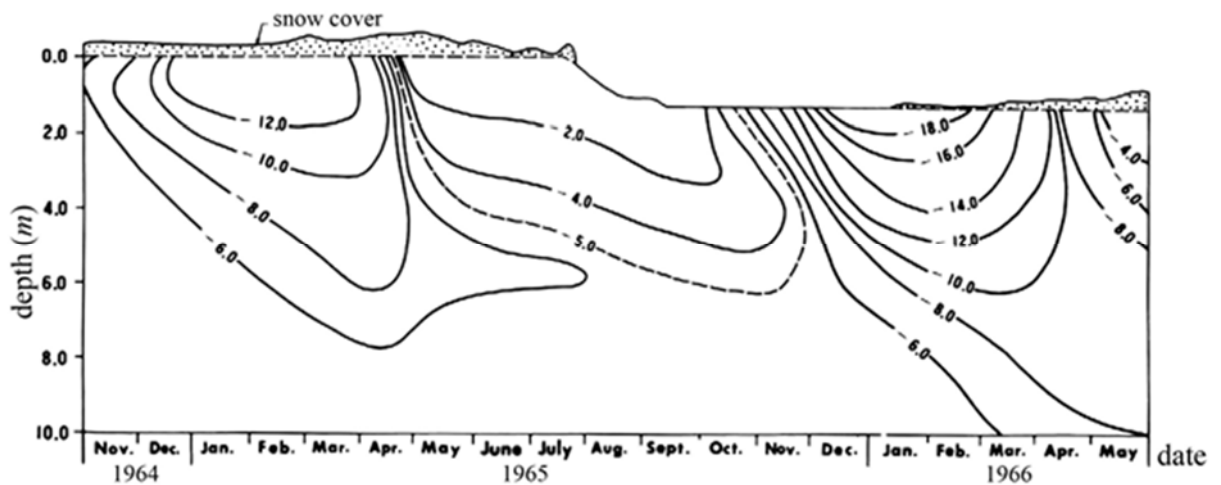


Fig. 10. "The temperature stratification of active layer in No. 1 glacier, Urumchi River, measured from October 1964 to May 1966 at the altitude of 3845 m (ablation zone)." Figure and captions after Huang et al. (1982). Reprinted from the *Journal of Glaciology* with kind permission of the International Glaciological Society and of Cambridge University Press (CC-BY 4.0).

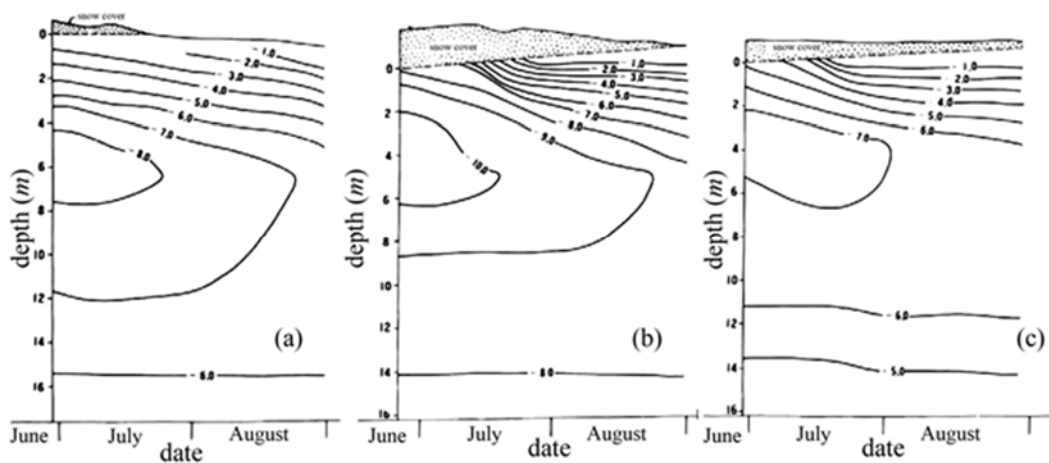


Fig. 11. "The summer temperature stratification of the active layer in No. 5 glacier, Yang-lung he (Yang-long he), measured from June 10 to August 1977. (a) at an altitude of 4513 m in ablation zone, (b) at an altitude of 4648 m near equilibrium line, (c) at an altitude of 4835 m in infiltration zone." Figure and captions after Huang et al. (1982). Reprinted from the *Journal of Glaciology* with kind permission of the International Glaciological Society and of Cambridge University Press (CC-BY 4.0).

- “a surface layer, where an obvious temperature change occurs during all seasons of the year with a large amplitude and a variable sign of temperature gradient, so that the heat conducts sometimes upwards and sometimes downwards in this layer;
- a middle layer, where the temperature change becomes less and less during the year and the temperature gradient does not change sign, so the heat conduction always occurs in one direction in this layer;
- a deep layer, at the upper bound of which the yearly temperature change is $< 0.2\text{ }^{\circ}\text{C}$, so this layer can be considered to be lacking in yearly temperature change and the heat always conducts upwards [i.e. this is endogenous heat, of any origin].”

Let us stress the last statement: “the heat always conducts upwards.” In fact, the Himalaya region is a true great geothermal “stove”. This feature, altogether with its large elevation, makes it act like a real “Third Pole” of the Earth.

Huang et al. (1982) also claim that the surface layer plus the middle layer is sometimes called the “active layer”, and that the boundary between surface and middle layer is typically $\sim 6\text{ m}$ deep. The lower boundary of the active layer is at $15 - 20\text{ m}$ depth. In reality, they measured temperatures only down to $16 - 18\text{ m}$, and therefore they chose 16 m as the indicative depth for the lower boundary of the active layer. They show that $T_0(16)$ can be considered an important characteristic of the regime of the glacial temperature.

Since they had no measurement at any deeper layer, they inferred these missing measurements by means of some approximation. They assumed that roughly all heat generated by friction is concentrated at the bottom of the glacier. Thus, the heat input to the glacier at its bottom is the sum of geothermal flux plus friction heat (Budd, 1969). Hence, for a cold glacier in a thermal steady state, it can be assumed

$$G = \frac{Q}{\lambda} \quad (4)$$

where Q is the total heat input per unit time at the glacier’s bottom, G is the temperature gradient, and λ is the thermal conductivity. Huang et al. (1982) distinguish three kinds of temperature boundary condition at the glacier bottom:

- (a) - “the temperature of the interface between ice and bedrock is below $0\text{ }^{\circ}\text{C}$,
- (b) ice and bedrock freeze together, namely $T_b < \theta$ and $(\partial T/\partial y)_b = G$ [where T_b and $(\partial T/\partial y)_b$ are the ice temperature and temperature gradient at the interface respectively, and θ pressure-melting point];
- (c) - the interface is at the pressure-melting point, but the bottom ice layer is below pressure-melting point, namely $T_b = \theta$ and $0 < (\partial T/\partial y)_b < G$, a part of the heat input transmits upwards and another part is expended by melting the bottom ice;
- (d) - there is a temperate layer at the bottom; i.e. $T_b = \theta$ and $(\partial T/\partial y)_b = 0$, all the input is expended by melting without transmitting upwards.”

They approximately estimate the depth L at which the pressure-melting point occurs by

$$L = -\frac{T_0(16)}{\gamma} + 16 \quad (m) \quad (5)$$

where γ and L are assumed to be the same as in the active layer. They also note that the following relations hold between L and glacier thickness H , and between G and γ , corresponding to the aforementioned three boundary conditions:

$L > H$ and $G = \gamma$ for condition (a);

$L = H$ for condition (b);

$L < H$ and $G > \gamma$ for condition (c).

They stress that, as already mentioned, (3) and (5) hold only close to the equilibrium line. They consider, however, the relation between mass balance and altitude, because the mass balance gradient represents the climatic sensitivity of a glacier, and - at the same time - the mass balance gradient is the main forcing function of the glacier flow over long time intervals. The mass balance gradient near the equilibrium line is often called the activity index of the glacier. They claim that “*fortunately the annual surface accumulation/ablation rate of the continental-type glaciers in China is quite low, the gradient of mass balance (activity index) ranges from 2.9 to 6.2 mm/m in T’ien Shan (Tian Shan) and Ch’i-lien Shan (Qilian Shan) for instance (Xie, 1980), so we can apply these equations approximately to some several hundred meters below equilibrium line.*”

Tables 2 and 3 report¹⁴ their findings. When observations did not extend below 16 m , the values are extrapolated by means of (2), (3) and (5).

Huang et al. (1982) consider a few different case histories. In the glacier Hsi-ch’iung-t’ai-lan ping-ch’uan (Xi-qiong-tai-lan bing-chuan), at an average altitude 3850 m , the observed H is 229 m with maximum 302 m . “*It will rise at the altitude shown in Table 2 and so be much greater than L as in condition (c) above mentioned.*”

In Jung-pu ping-ch’uan (Rong-bu bing-chuan) the maximum observed H is 146 m at the altitude 5350 m . Thus $H > L$ as in aforementioned condition (c).

In the glacier No. 5, i.e. Yang-lung he (Yang-long he), no data for H are available. However, data are available for an adjacent glacier, which is a little bigger than glacier No. 5, i.e., for the Ch’i yi’ping-ch’uan (Qi Yi’bing-chuan), where H is tens of meters with a maximum $H = 93\text{ m}$. Then glacier No. 5, Yang-lung he (Yang-long he), seems to partake to condition (c) or (b).

Therefore, Huang et al. (1982) state that it is possible to infer the temperature features through deep layers of continental-type glaciers in China depending on the following features:

- (1) when the temperature at the upper-boundary of the deep layer is quite low - i.e. when the glacier is excessively thin - ice at the bottom, and the glacier bed, freeze altogether with the underlying permafrost;
- (2) the interface between ice and bed is at the pressure-melting point, while the ice layer at the bottom is still

¹⁴ Reproduced with kind permission of Cambridge University Press (CC-BY 4.0).

below the pressure-melting point; this happens when the upper-boundary temperature is quite low, but either the glacier is very thick or the glacier thickness is not very large, but the upper-boundary temperature is rather high;

(3) when the upper-boundary temperature is rather high and the glacier thickness is sufficiently large, there is a temperate ice layer in the lower part of the glacier on a thawed ground (rock).

Table 2. The values of $T_0(16)$ and L for glaciers in China where the temperature has been either measured or estimated vs. depth

| glacier | year of record | elevation (m) | depth (m) | $T_0(16)$ ($^{\circ}C$) | γ ($^{\circ}C/m$) | L (m) |
|----------------------------------|----------------|---------------|-----------|---------------------------|----------------------------|---------|
| Hsi-ch'iung-t'ai-lan ping-ch'uan | 1978 | 4050 | 18 | -1.8 | 0.104 | 33 |
| | | 4300 | 16 | -3.0 | 0.124 | 40 |
| No. 5, Yang-lung he | 1977 | 4513 | 16.1 | -6.2 | 0.083 | 91 |
| | | 4648 | 15.8 | -7.9 | 0.134 | 75 |
| | | 4835 | 15.2 | -4.9 | 0.196 | 41 |
| Jung-pu ping-ch'uan | 1966 | 5400 | 10 | -1.0 | 0.11 | 25 |
| Ye-po-k'ang-chia-le ping-ch'uan | 1964 | 5650 | 10 | -3.3 | 0.14 | 40 |

(The altitude of the equilibrium line of every glacier is shown in Table 3)

Table 3. Ice temperature at the lower boundary of the active layer, compared with the annual mean air temperature, at the altitude of the equilibrium line

| Glacier | Year | Altitude of equilibrium line (m) | $T_0(16)_E$ ($^{\circ}C$) | T_E ($^{\circ}C$) | $T_0(16)_E - T_E$ ($^{\circ}C$) |
|----------------------------------|------|----------------------------------|-----------------------------|-----------------------|-----------------------------------|
| Hsi-ch'iung-t'ai-lan ping-ch'uan | 1978 | 4500 | -5.5 | -8.8 | 3.3 |
| No. 5, Yang-lung he | 1977 | 4600 | -7.3 | -11.0 | 3.7 |
| Jung-pu ping-ch'uan | 1966 | 5800 | -6.0 | -8.5 | 2.5 |
| Ye-po-k'ang-chia-le ping-ch'uan | 1964 | 6000 | -7.7 | -9.5 | 1.8 |

Usually, the cases (2) and (3) are a more frequent occurrence. The γ values in Table 2 seem to display a regular trend vs. height through the same glacier. In addition, as Huang et al. (1982) stress, they are 3.5 – 8.2 times the gradient needed for the geothermal heat flux to cross upward the entire glacier thickness. They compare their results with previous analogous measurements from the literature referring to glaciers from regions other than China. They mention one case history with $0.08 \text{ }^{\circ}C \text{ m}^{-1}$ near the bottom of a glacier characterized by a substantial basal sliding on most of the glacier bed.

Another case history gives $0.14 \text{ }^{\circ}C \text{ m}^{-1}$, between 19 – 23 m depth, corresponding to 7.5 times the amount needed for ensuring geothermal outflow from the glacier surface. However, in one glacier, “which is similar to the continental-type glaciers in China”, a gradient was measured of $0.11 \text{ }^{\circ}C \text{ m}^{-1}$ between 10 – 20 m depth, 600 m from the front, “but the gradient decreased downwards, and a temperature of (-0.10°) – ($-0.7 \text{ }^{\circ}C$) appeared at the bottom, 52 m in depth.” They guess, therefore, “that in cold glaciers γ should be greater, several times more than the gradient needed for the geothermal flux. The problem is to extrapolate γ from the active layer to the deep layer.” That is, there is no clear relation between their parametrization of the continental type glaciers in China and the glacial flow. They claim that “the basic fact that basal sliding takes place extensively in glaciers in China cannot be changed in any case.”

Huang et al. (1982) also claim that “the surface flow velocity observed in the middle and lower parts of glaciers in China shows that without exception the summer velocity is faster than the winter velocity, or than the annual mean

velocity.” They quote several specific case histories referring to different glaciers in China: (i) a factor 1.6 observed during 1960-1961; (ii) a factor 1.05 – 1.90 during 1959-1962; (iii) a factor 1.06 during August 1976-September 1977; (iv) a factor 1.22 during 10 July-28 July 1977, faster than the value 1.43 observed during July 1977-July 1978. “This phenomenon indicates that the pressure melting point appears at the glacier bed, where basal sliding exists, while the melt water percolates to the bed during the ablation period, lubricating and promoting basal sliding.”

From the viewpoint of the present study, let us point out that, according to Fig. 1 of Gregori et al. (2025q), one should expect some substantially different endogenous heat flow underneath seemingly similar glaciers located in different geothermal flux environment. Hence, the basal sliding of a glacier ought to be largely controlled by the local geothermal flow. In contrast, the control by its structural features in a suitable upper layer are largely influenced by atmospheric climate.

Huang et al. (1982) discuss the temperature at the lower-boundary of the active layer at the elevation of the equilibrium line. According to the evidence reported by several papers, an inference is found dealing with “the regional variation of glacier temperatures in China, giving an impression that the lowest ice temperatures arise in the western section of Ch'i-lien Shan (Qilian Shan) - the place where glacier temperatures may be the lowest of all alpine glaciers located in the middle and low latitudes. From there eastwards to middle and eastern section of Ch'i-lien Shan (Qilian Shan), westwards to the middle and western sections of T'ien Shan (Tian Shan) and southwards to the

middle Himalaya Shan, the glacial temperature will rise gradually, reflecting the increase of continentality towards the western section of Ch'i-lien Shan (Qilian Shan) from the east, west, and south."

Therefore, they consider in Table 2 the $T_0(16)$ values, and extrapolate them to the equilibrium level. However, for such a purpose there is need for an estimate of both gradient $dT_0(16)/dz$ and its variation with altitude z . Glacier No. 5, Yang-lung he (Yang-long he), extends across the equilibrium line and can be used to carry out this estimate. It is thus found $dT_0(16)/dz = -1.26 \text{ }^\circ\text{C} (100 \text{ m})^{-1}$ between 4513 – 4648 m. This absolute value is greater than the estimated annual mean vertical air temperature gradient, $-0.74 \text{ }^\circ\text{C} (100 \text{ m})^{-1}$. This difference, which amounts to $0.52 \text{ }^\circ\text{C} (100 \text{ m})^{-1}$, can result from upward advection and strain heating.

Hence, Huang et al. (1982) choose $dT_0(16)/dz = -1.25 \text{ }^\circ\text{C} (100 \text{ m})^{-1}$. They extrapolate the values of Table 2, and compute Table 3, where also the annual mean air temperature T_E at the altitude of the equilibrium line is shown for comparison. They focus mainly on the last column in Table 3, and report that according to the literature it is always $T_0(16)_E - T_E > 0$, and for the Russian Tyan'-Shan' it is $2 \text{ }^\circ\text{C}$. Therefore, they conclude their analysis by inferring the pattern sketched in Fig. 8.¹⁵ They emphasize that "most temperature measurements we have taken are in the ablation zone, where a temperature below zero is always measured. The temperature regime of the active layer in the ablation zone can be described by (2) except in the first 3 m ...". That is, they distinguish what occurs below and above $\sim 3 \text{ m}$ depth.

Concerning the lower layer where (2) holds, they state that "the lower-bound temperature of the active layer is generally higher than the annual mean air temperature at the same height, e.g., $3.7 \text{ }^\circ\text{C}$ higher at an altitude of 4513 m in No. 5 glacier, Yang-lung he (Yang-long he). The pressure-melting point usually appears at the bottom layer of the glacier, at least at the interface between ice and bedrock. Basal sliding exists except at some termini of small glaciers and their margins or some extremely small glaciers like hanging glaciers, which may be entirely below zero and freeze onto bedrock. [In fact, in this case the ice cohesion force represents some kind of containing belt, according to the rationale that determines the "sac effect" behavior of Greenland or Antarctica outlet glaciers that generate huge icebergs. See Gregori and Leybourne (2025k).]

The extremely large valley glaciers descend to a region where the climate is warm. The temperature in the active layer of its ablation zone will rise as elevation decreases. The rising rate will be greater than the vertical air-temperature gradient, so that the difference between the annual air temperature and the lower-bound temperature of the active layer gradually increases (of course the pressure-melting point is a limit for the rise of the lower-bound temperature). Finally, the ablation zone changes into a temperate glacier The pressure-melting point

generally occurs at the bottom except in some glaciers with extremely small thickness."

This is consistent with the rationale of the present study. As mentioned above, the boundary between surface and middle layer is typically $\sim 6 \text{ m}$ deep. The lower boundary of the active layer is at 15 – 20 m depth. However, the glacier is largely insulated - with respect to its atmospheric environment – by its first 3 m layer. Underneath this layer, the thermal balance is controlled by geothermal heat plus by friction heat, which is a consequence of basal sliding. This phenomenon is enhanced by the pressure-melting point, where ice transforms into water and lubricate the glacier motion while it slides by gravity. This thermal balance is a function of the local geothermal flux, and seemingly also of altitude, although - concerning altitude - a focus ought to be (maybe) more on the steepness of the bedrock than on atmospheric temperature.

Very different phenomena occur in the shallowest 3 m layer, and Fig. 8 is a sketch showing this complicated structure. "The heat exchange in the surface layer is complicated by accumulation, ablation, and the infiltration and refreezing of melt water Accumulation, ablation, and the infiltration and refreezing of melt water play a leading role in the surface layer, profoundly affecting the temperature regime in the active layer. The temperature of the entire active layer in this zone is higher than that in the other zones below it. For example, in No. 5 glacier, Yang-lung he (Yang-long he), $T_0(16)$ at the altitude of 4835 m is higher than that at the other two sites [see Gregori et al. (2025f)], hence the difference between $T_0(16)$ and the annual mean air temperature at the same height grows to $7.3 \text{ }^\circ\text{C}$ During the main melting season at between 20 – 40 cm depth the snow temperature is near $0 \text{ }^\circ\text{C}$ all day long, with a minimum of $-0.03 \text{ }^\circ\text{C}$ before dawn and a maximum over $0.00 \text{ }^\circ\text{C}$ at noon, resulting from the thermometer absorbing transmitted radiation ..."

Huang et al. (1982) stress that "a complicated heat exchange exists and a zero temperature casing arises in the warmest months. In many small-scale glaciers such as No. 1 glacier, Urumchi River, and No. 5 glacier, Yang-lung he (Yang-long he), a zero temperature casing of $< 0.5 \text{ m}$ was found." This is the first layer where ice thaws below the glacier's surface.

"A temperature of $0 \text{ }^\circ\text{C}$ will appear and remain in the upper snow layer in summer. In the snow layer nearest the surface, the temperature will lower quickly in winter, with an extreme temperature lower than that in other zones below, but in inner snow layers, the temperature will not lower so much, because there is liquid water within it, which releases latent heat as a result of refreezing. Thus a special temperature regime is formed: a quite low surface temperature followed by a quite high inner temperature; a large surface temperature amplitude accompanies a small inner temperature amplitude

One can see a rapid temperature rise before the melting season and a slow lowering after it, the latter, of course, results from the melt-water store and its refreezing. During

¹⁵ See also Fig. 1 of Gregori et al. (2025q) and Figs 9, 10 and 11.

the days of intense melting and infiltration there is a snow and ice layer of at least 4 m falling to the melting point. It is to be expected that infiltration and refreezing would weaken and disappear with increasing height, and that the primary influence of climatic factors on ice temperature would then again be given full play."

This ends the discussion here considered about glaciology. This careful discussion by Huang et al. (1982) shows how intricate is the study of the balance of a glacier. We can say that we poorly understand this whole phenomenon. In any case, glacier retirement or expansion is an unreliable proxy for "global climate change". The main concern is here rather about the climate impact of glaciers and ice sheets that are found on the two polar caps or on the "Third Pole". An authoritative updating is reported relying on Raina (2009).

Shi et al. (1984) dealt with a specific area, which is rich of present glaciers and remnants of ancient glaciers. They recognized four stages during the Pleistocene, according to mineral, chemical and spore/pollen evidence.

Xie (1985) analyzed the palæo-evolution of permafrost. According to fauna and flora evidence and extensive periglacial sediments and their relief, they inferred that a cold climate existed in the vast plain and mountain area of northeastern China, with an annual mean temperature $\sim 6^\circ - 10^\circ \text{C}$ lower than at present. Therefore, permafrost was formed in this area during the periglacial period of late Pleistocene. However, the permafrost that was formed at that time could not completely melt after the Pleistocene due to the gradual change of climate. In fact, the fluctuation of annual mean temperature in China was only $\sim 2^\circ - 3^\circ \text{C}$ and no marked climate warming occurred before the postglacial period $\sim 11,000$ years BP. In addition to the old permafrost - which was formed during late Pleistocene - new permafrost was formed during the Holocene. Even permafrost exists that was formed during the historical period, mainly during the cold period of the 17th-18th century.

Three periods can be recognized of permafrost formation: (1) $\sim 35,000 - 26,000$ years BP ; (2) $\sim 23,000 - 12,000$ years BP ; (3) $\sim 3,000$ years BP . From the distribution of palæo-periglacial phenomena, it appears that the southern limit of permafrost was located at $\sim 42^\circ \text{N}$, to be compared with the present limit at $\sim 48^\circ \text{N}$, i.e. the present permafrost limit moved northward by $\sim 6^\circ$.

Concerning altitude, the palæo-periglacial signature (e.g. the stony sea) during the late Pleistocene was (in the Changbaishan area) up to $\sim 760 - 1000$ m a.s.l., while at present it is > 2000 m . Hence, a rise of permafrost occurred by ~ 1000 m since the late Pleistocene. As already stressed, this is consistent with the present ongoing increase of endogenous energy release that is associated with the top point of the "Iceland" heartbeat.

Chen (1987) investigated the Holocene moraines that at present are found at the headwater of the Urumqi River and in the Bulate Valley on the northern slope near Tianger Peak II (4486 m) in the Tianshan Mountains, and also the moraines on its southern slope. Large-scale glacio-geomorphological maps were drawn, and moraine ages were estimated by ^{14}C dating, by lichenometric dating, etc.

It was thus found that, during the general retreat processes occurred during the Holocene, the glaciers in these regions experienced at least four periods of glacial advance, which occurred ~ 5700 , ~ 4100 , ~ 2800 and $\sim 403-74$ years BP, respectively. The first advance was comparatively more extensive, and it lasted for a longer period of time.

The Little Ice Age includes three stages of glacial advance, occurred respectively ~ 403 , ~ 208 and ~ 74 years BP, with the second advance being more extensive. In addition, concerning the glacial fluctuations in the thousand-year range, during the Holocene a $\sim 2300 - 3000$ year cycle might have occurred during which there was a longer period of glacial retreat, and a brief period of glacial advance. That is, the trend reminds about a "saw-tooth" pattern (see below).

The cold climate of the last ice-age ended $\sim 10,000 - 9,500$ years BP and during this cold period the average temperature was $\sim 4^\circ \text{C}$ lower than the present. At least four cold periods occurred during the Holocene, which ended ~ 5700 , ~ 4100 , ~ 2800 and $\sim 420 - 91$ years BP, respectively, displaying warm periods in between them. The temperature of these cold periods were, respectively, $\sim 1.5^\circ \text{C}$, $\sim 1.25^\circ \text{C}$, $\sim 0.9^\circ \text{C}$ and $\sim 0.65^\circ \text{C}$ lower than at present. The amplitude of temperature variation during the Holocene was $\sim 2.5^\circ \text{C}$.

Note that these alternating periods of warm/cold climate ought to occur according to a saw-tooth trend. Even though these authors mention no observational evidence, this expectation is consistent with the observed evidence of "terminations" and also of all shorter period fluctuations (see Gregori and Leybourne, 2025k). In fact, this is the basic rationale of the endogenous energy release, whether it is originated by a sea-urchin spike, or by friction heat deriving from geodynamics. On the other hand, according to *WMT*, friction heat is originated by Joule heat of the sea-urchin spikes. In fact, the phenomenon ought always to be manifested beginning with a slow temperature decrease, which is the "long segment" of the saw-tooth. In the meantime, the endogenous heat affords to open a "channel" through which energy reaches Earth's surface. When this "channel" opens, abruptly the capability is increased to release the endogenous energy that, thus, rapidly exhausts its availability. This is the "short segment" of the saw-tooth. Then, the "channel" closes anew, and a new slow cooling begins. Therefore, the detection of the saw-tooth trend requires the availability of some proxy that permits the time-resolution needed for the detection of thermal phenomena.

Moraine dating, soil and vegetation data, and lichenometry resulted significant for relative age dating, and also for moraine correlation and investigation over large regions, and for dating mid- and late-Holocene deposits in high mountainous and cold regions.

Wang (1990) investigated the evidence in China about a short low-temperature event that is commonly reported from many sites of the world during the middle Holocene - in contrast with the evidence that the climate of Holocene was generally warm. In China this short duration event began ~ 5500 years BP in the north and ~ 4500 years BP in the south. Ages appear older while moving

northward. Note that this is a “transmigration” of the endogenous heat source. In some respect, this “transmigration” reminds about the transmigration of seismic and/or volcanic activity (see references in Gregori et al., 2025h), although these palæoclimatic phenomena display a comparatively much smoother trend, spread over some large region, and spanning a much longer time span.

That is, a slow climate change occurred through China. It lasted ~ 1000 years and displayed a progressive cooling that moved northward. This low-temperature event during the Holocene is therefore believed to play an important role in the study of the distribution and structure of Holocene sediments, of environmental changes, of the development of lakes and swamps, of sea-level fluctuation, of the formation of beach places, of the division of ground water beds, of glacial advance and recession in western China, and in general of the whole climatic sequence during Holocene in China.

Bi et al. (1991) addressed the problem (i) of climate during historic times and (ii) of the Holocene sea-level change, which is somewhat disputed. They investigated the Holocene beach-rocks of China, and found that the formation and depositional break periods of beach-rocks, the warming and cooling periods of climate, the rise and fall periods of sea-level, and so on, are characterized by asynchronous periods, every one lasting ~ 500 years. Note that the lack of synchronism is likely to denote that a unique primary driver (e.g. endogenous heat release) has been responsible for all kinds of phenomena. However, the maxima and minima of every phenomenon depended on the relative phase or time-delay with respect to one another, caused by the complex behavior of the natural system.

Therefore, Bi et al. (1991) proposed what they call a “dynastic” sequence of the Holocene climatic strata. By this, they could organize periods of climatic changes in historic times, periods of Holocene climatic changes and sea-level changes, and other related natural phenomena. Beach-rocks were formed on the coast of tropical zones with an annual average temperature > 26.5 °C. At present, they are formed in the tropical area south of Xisha Islands. The latitudinal extension of the Chinese subcontinent is such that it is possible to recognize this “dynastic” sequential model of Holocene beach-rocks, and the rock-forming regularities that Bi et al. (1991) call “northward advance” and “southward movement”. The beach-rocks that have been so far discovered are mostly the relic bodies formed at different stages since ~ 6850 years BP, and their sequence can be used to test climate and sea-level changes. Two major stages can thus be recognized: one is dominated by the rise before ~ 6500 years BP, the other is characterized by fluctuations around the present sea-level.

Bi et al. (1991) quote a study by Bloom (1983), who envisaged an average long period of $\sim 2 \times 10^4$ years of sea-level changes during the past $\sim 14 \times 10^4$ years BP. In China, during Holocene the temperature began to rise $\sim 13,000$ years BP, and after $\sim 10,000$ years it has been cooling during the last ~ 3100 years. In addition, a cold climate seems to move southward at a speed of $\sim 7^\circ$ latitudes every 1000 years, while the amplitude of sea-

level fluctuation also gradually decreases. Therefore, after $\sim 6000 - 7000$ years the sea-level ought to fall by “some dozens of meters”.

They conclude that, since the “greenhouse effect” can be partly offset by the aforementioned cooling trend, it appears impossible that sea-level is going to experience a large rise during the forthcoming $\sim 50 - 100$ years. Rather, it can remain similar to its present state, or maybe it can even decrease. That is, is it impossible to issue any reasonable and objectively sound forecast about the real future climatic trend in every given region. It is even more difficult to define a “mean planetary” climatic trend. In addition, one must consider that - at present - we cannot estimate the interannual change of the total amount of water underground, consequent to serpentinization (see Gregori and Hovland, 2025, and Gregori and Leybourne, 2025k).

Qiu and Cai (1992) carried out ^{14}C dating on 16 samples of sediments and found a lowest boundary for Holocene around $\sim 11,000$ years BP, except concerning some samples from Yunnan Province, which are older. Perhaps, this could be the result of a latitude dependence.

Liu et al. (1996b) (see Fig. 12) investigated the correlation between SH and NH during the last 0.6 Ma. They found evidence for a strengthening of the Asia summer monsoon during $\sim 35 - 25$ ka BP and $\sim 4 - 2.5$ ka BP correlated with a strengthening of aridity or desertification in Australia. They envisage that the Australian high led to desertification while it strengthened the Asia summer monsoon.

On the other hand, the Holocene Optimum seems synchronous in Asia and Australia. Therefore, it appears that the Mongolia high has a relationship with the Australia summer monsoon. In addition, consider that Australia seems to be located close a vertex of the tetrahedron, which is a particularly intense source of endogenous heat (Gregori and Leybourne, 2021).

Zhou et al. (1997) found a correlation of climatic events between East Asia and Norwegian Sea during the last deglaciation. They used ^{14}C , $\delta^{13}\text{C}$, and organic carbon content to investigate loess palæosol and peat profiles in China. On the century scale, during the last deglaciation they found evidence of the palæoclimatic fluctuations of the East Asian monsoon, and a significant variability of precipitations.

The major recognized climatic events were the Bølling ($\sim 1.3 - 12.5$ ka BP), Older Dryas ($\sim 12.5 - 11.750$ ka BP), Allerød ($\sim 11.75 - 11.2$ ka BP) and Younger Dryas (YD) ($\sim 11.2 - 10.0$ ka BP). They also found evidence of frequent changes in sedimentation phases reflecting climatic instability.

The SST in the Norwegian Sea looks correlated with these fluctuations, envisaging a palæoclimate teleconnection between polar, high latitude areas and East Asian monsoon areas, through westerlies and the planetary atmospheric dynamics (see Fig. 13). However, according to Chen et al. (2000), this correlation does not hold for the entire Loess Plateau, envisaging a more complicated relation.

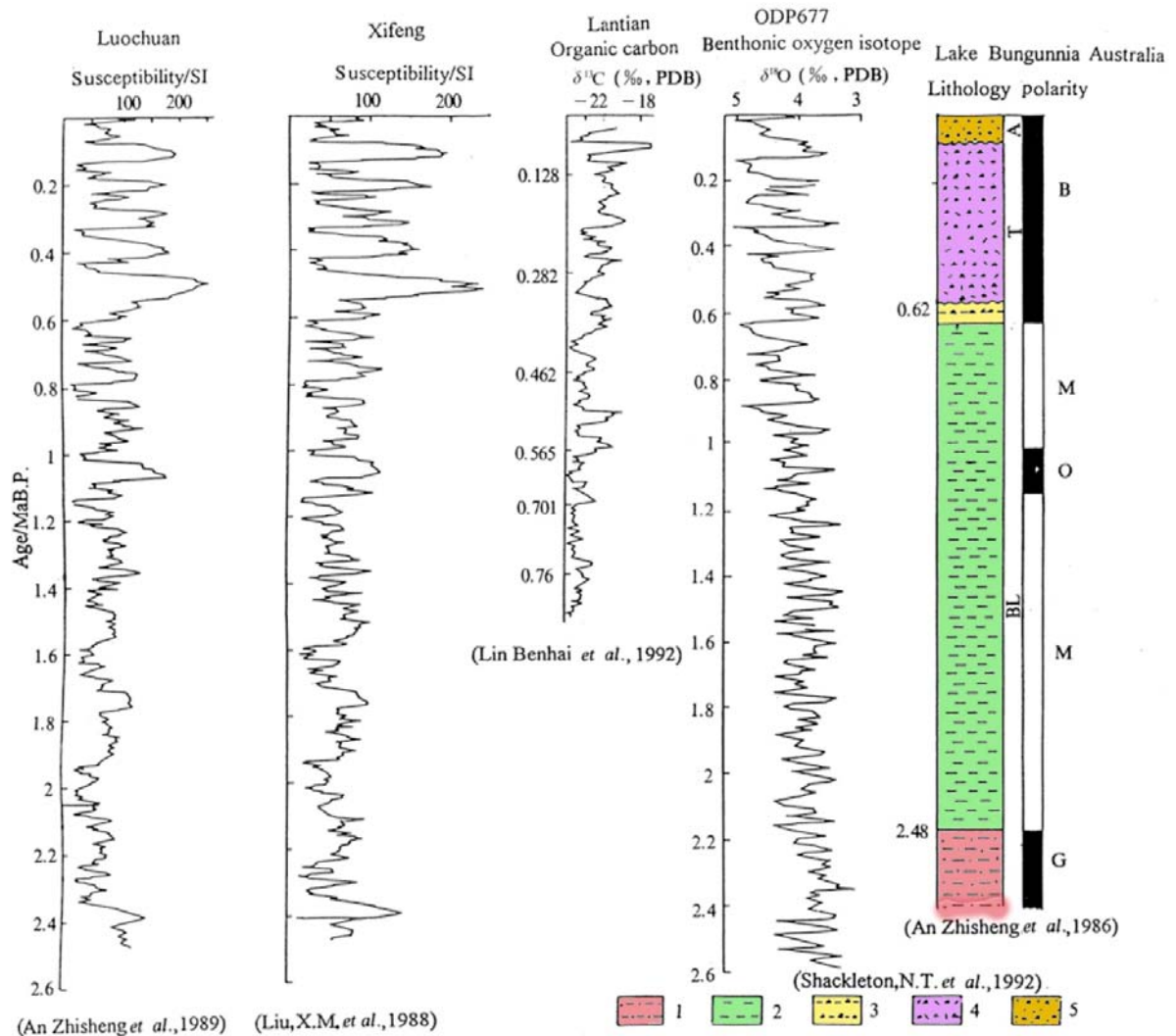


Fig. 12. "Correlation of Asia and Australia palaeoclimate reflected by deep-sea oxygen isotope. 1, Sandy clay; 2, clay; 3 gypsum-bearing clay; 4, gypsum slat-bearing (dry salt lake facies); 5, gypsum-bearing æolian sand." Figure and captions after Liu et al. (1996b). With kind permission of *Sci. in China, Ser. D*.

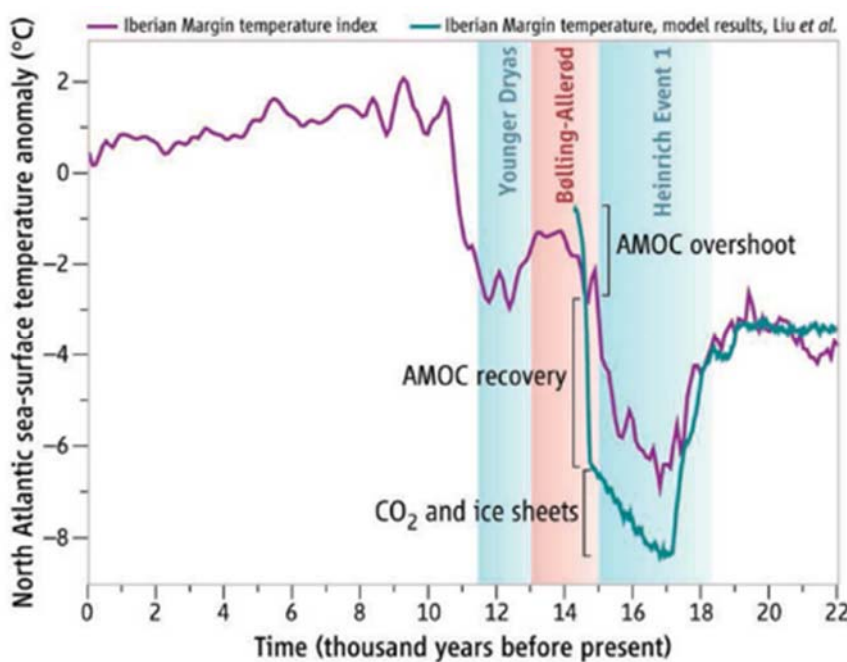


Fig. 13. "North Atlantic SST evolution. The simulated North Atlantic temperature in the Iberian margin region agrees well with a reconstructed temperature index obtained by averaging different alkenone-based SST reconstructions from cores SU-8118 and MD01-2443. The Bolling-Allerød warming can be decomposed into contributions that originate from the recovery of the Atlantic meridional overturning circulation (AMOC), an overshooting effect, and the climate response to increasing greenhouse gas concentration and shrinking glacial ice sheets." Figure and captions after Timmermann and Menviel (2009), who give some information about modeling, including the related references. Reproduced with kind permission of *Science*.

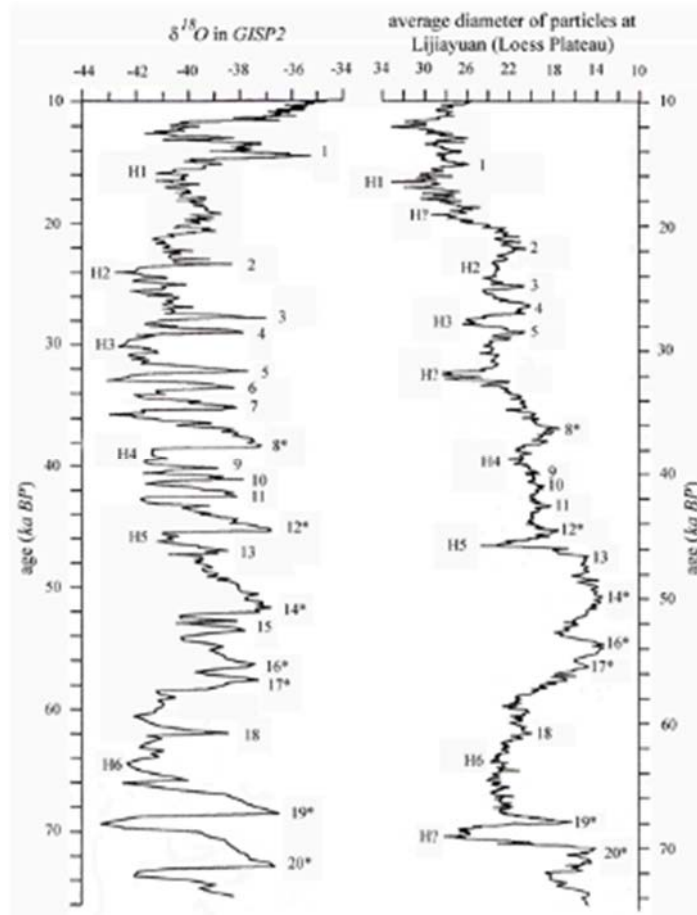


Fig. 14. Average diameter of loess particles at Lijiayuan (Loess Plateau), and its correlation with $\delta^{18}O$ in the GISP2 core (Greenland Ice Sheet Project). Adapted after Ding et al. (1996). With kind permission of *Science in China, Series D*.

Zhao et al. (1997) studied the evidence of desertification on the ocean shelves, at the time when sea-level was low, and defined the concept of “shelf desertification”.

Ice cores and loess

Ice cores and loess are particularly important proxies in the Chinese subcontinent. There is a large Chinese literature, and only some partial information is available to us.¹⁸ Some information is here given, which can give at least the feeling of the relevance of this palaeoclimatic information. In any case, the amount of literature is very large, and the picture here presented is certainly incomplete.

The average grain size of loess is a climatic proxy, as it is shown e.g. by Fig. 14, where the¹⁹ $\delta^{18}O$ clearly envisages several episodes that display a saw-tooth trend.

Yao et al. (1997) published the results of the analysis of the upper 268 m of the 309 m long Guliya ice core (Figs 15, 16, and 17). By means of $\delta^{18}O$ records - that display some clear features of saw-tooth trend - they distinguished 5 stages during the Last Interglaciation: (1) deglaciation, (2) the late stadial of the Last Glacial Age or the Last Glacial Maximum (LGM), (3) interstadial of the Last Glacial Age, (4) early stadial of the Last Glacial Age, and (5) the Last Interglaciation. In addition, they divided Stage (5) into 5 substages, (a), (b), (c), (d), and (e), respectively.

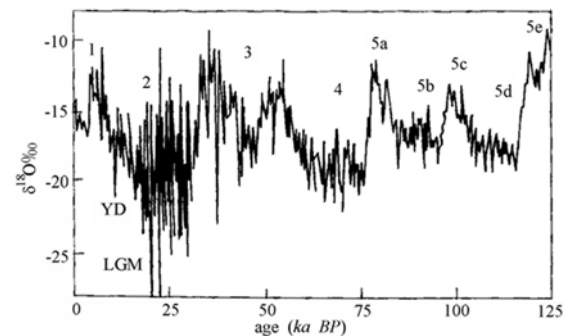


Fig. 15. Temperature variation since ~ 125 ka BP according to $\delta^{18}O$ records from the Guliya ice core, plotted every 0.1 ka. YD denotes the Younger Dryas. After Yao et al. (1997). With kind permission of *Science in China, Series D*.

The temperatures during substages (5a), (5b), (5c) were 3 °C, 0.9 °C, and 5 °C higher than at present. All transitions (5e) → (5d), (5c) → (5b), and (5a) → (4) were characterized by dramatic cooling, unlike the warming during (5d) → (5c) and (5b) → (5a), which were gradual. These trends are consistent with “saw-tooth” mechanism.

The start of the Last Glacial Stage [(5a) → (4)] was abrupt: the temperature decreased by ~ 12 °C during ~ 3000 years. The two cold periods (4) (75 – 58 ka ago)

¹⁸ Relying also on private information and discussion with Gao Xiaoqing, to whom we are very grateful.

¹⁹ $\delta^{18}O$ refers to the deviation from the standard of the ratio $^{18}O/^{16}O$.

and (2) had roughly the same duration, but the average temperature decrease of (4) was larger than that of (2), and the lowest temperature occurred during (2), ~ 23 ka ago. During the cold period 23 – 30 ka ago, the temperature was ~ 10 °C less than at present.

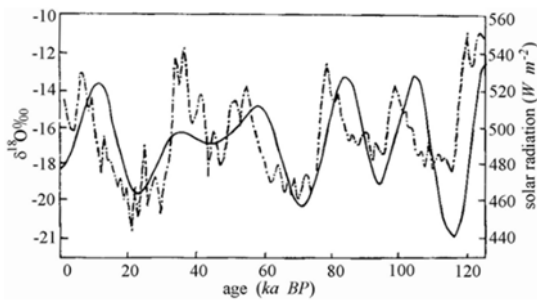


Fig. 16. Comparison between the $\delta^{18}O$ records in the Guliya ice core and solar radiation at high North Hemisphere latitudes (60°N), plotted every 0.1 ka. After Yao et al. (1997). With kind permission of *Science in China, Series D*.

Substage (3) is usually called an interstadial, i.e. a weak warm period found both in deep-sea $\delta^{18}O$ records and in the Vostok ice core. Its temperature is compared to (2) and (4), but it is lower than during the Holocene and (1), i.e. during the Last Interglaciation. However, in the Guliya ice core record, the temperature during (3) (58 – 31 ka ago) was found higher than today. Hence, during (3) the climate warming is comparable with the Last Interglaciation. This abnormal warm period was confirmed by studies on the palæo-lakes and palæo-vegetation of the plateau.

An unprecedented finding of the Guliya's ice core was that there are at least 4 cold events during (3). During the two cold periods that occurred ~ 47 ka ago and ~ 43 ka ago, respectively, the temperature decreased as much as during (2) and (4). Fig. 16 shows that the variation of solar radiation always leads the temperature variation in the Guliya ice core record, showing that it appears to be a leading climate driver on the Qinghai-Xizang TP.

Note that, according to the general aforementioned rationale based on the model by Dong and Tang (1997) and Tang and Dong (1997a) - which is in close agreement with the whole rationale of the present study - the changes in solar radiation are an index that is somewhat related to changes in the solar wind, hence to the efficiency of the TD dynamo and endogenous energy production and supply, hence to time-delayed gas exhalation and endogenous energy transfer into the atmosphere, altogether with WMT activity, uplift of superswells and to overthrust (such as underneath the TP), etc. This entire scenario finally ends into a variation of climate temperature, although with different effects in different regions, depending on atmospheric circulation and precipitation, etc.

Concerning the comparison with the records from the Vostok and Greenland ice core (Fig. 18), the Guliya record displays comparatively larger relative deviations. That is, the Qinghai-Xizang TP where the Guliya ice core was drilled seems comparatively more sensible to climate change than Greenland. Yao et al. (1997) interpreted this discrepancy in terms of two effects.

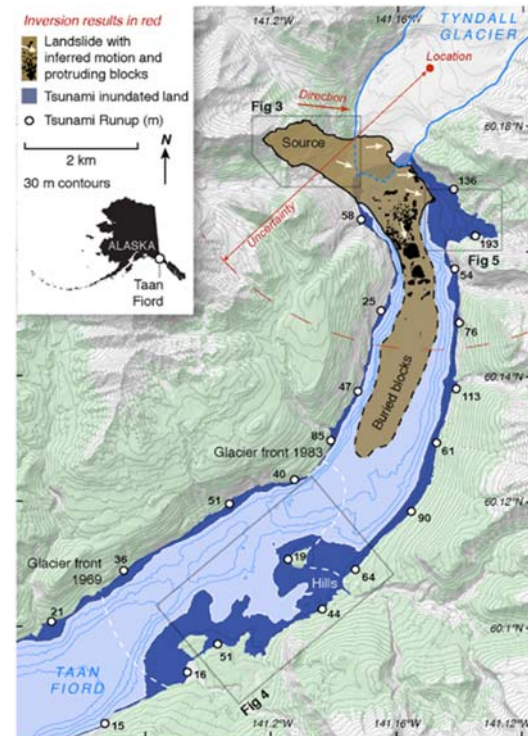


Fig. 17. “Changes in Taan Fjord. Tyndall Glacier retreated at an increasing pace through the late 20th century until it stabilized in 1991, at approximately the location of the current terminus. The slope failure in October 2015 entered the recently deglaciated fjord at the calving front, generating a tsunami that swept the coast to a height of 193 m. [This is consistent with the several indirect evidences of an ongoing large increase of endogenous heat release beneath the Arctic cap, located on top of the vertex of the tetrahedron right at the North Pole (see Gregori and Leybourne, 2021). An increase of soil temperature causes a detachment of ice sheets from the rocky bedrock.] Seismic inversion completed within hours of the event produced an accurate picture of initial motion and a rough location, but could not determine whether the landslide had set off a tsunami. In 2016, marine surveys revealed tens of meters thick blocky submarine runout extending several kilometers ... Only the more proximal blocks form submarine hillocks, while more distant ones are buried beneath one or possibly two post-landslide turbidites ... Field surveys mapped run-up, selected examples of which are presented here. Map created with QGIS 2.18 (<http://www.qgis.org/en/site/>).” Figure and captions after Higman et al. (2018). Reproduced with kind permission of *Scientific Reports*, (CC BY 4.0).

On the one hand, a colder climate results in a thicker, larger and longer-lasting snow cover on the Qinghai-Xizang TP, and this can amplify a cool stage. In comparison, in Greenland the surface is permanently covered by snow and ice all the time. Hence, climate change is less likely to be amplified. On the other, the top of the Guliya ice core is located at the height of mid-upper troposphere. Hence, it directly records atmospheric process, thus resulting more sensitive to changes. In addition, compared to Vostok and Greenland, also the high scatter of time-resolution looks

much more pronounced in Guliya's denoting a higher sensitivity..

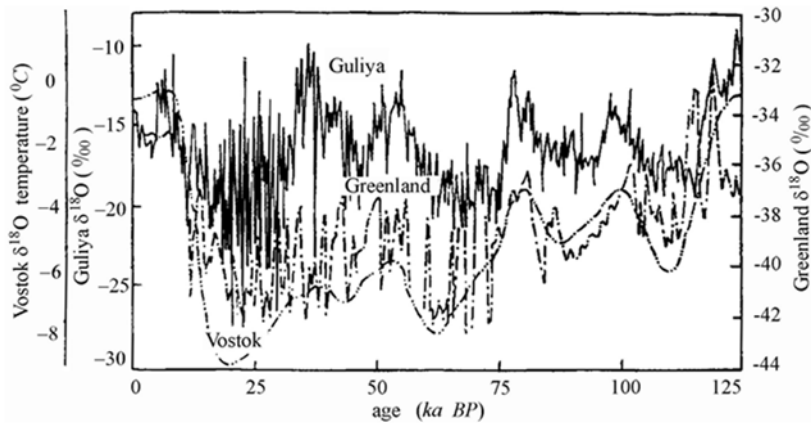


Fig. 18 - Comparing the $\delta^{18}O$ records in the Guliya, Vostok, and Greenland ice cores. After Yao et al. (1997). With kind permission of *Science in China, Series D*.

An et al. (1999) made an extensive study on the magnetic susceptibility and on the depositional rate change of $\delta^{18}O$ from the equatorial East Pacific Ocean and also from flux variations of $\delta^{18}O$ from the equatorial East Pacific Ocean and also from flux variations of $\delta^{18}O$ from the North Pacific Ocean. Thus, they could recognize that the Great Glaciation of Late C $\delta^{18}O$ in the NH can be divided into three stages: (i) the arrival stage $\sim 7.2 - 3.4 Ma$ ago, (ii) the initial stage $\sim 3.4 - 2.6 Ma$ ago, and the Great Ice Age (GIA) since $\sim 2.6 Ma$ ago. They also envisaged a crucial role played by the timing of the TP uplift.

Zhang and Zhu (2000) studied climate proxies on the northern bank of the Yangtse River. An expansion of swamps occurred $\sim 14,000$ years ago. Then, owing to aridity, the swamp area began to shrink, until it even disappeared. An immediate flooding period followed. After the Younger Dryas (YD) cooling event (108.0 – 10.2 ka) this region experienced the Holocene warming period ($7,562 \pm 90$ years - 3,800 years), and climate experienced the associated fluctuations. Then, during the Little Ice Age the temperature decreased. The soil on the top of this layer - which reminds about loess - was the result of winds blowing during the Holocene after the main cooling period ($\sim 3,000 - 2,850$ years ago). Floods seemingly usually occurred during the climate transition period - and this envisages that, perhaps, floods occur when climate experiences some abrupt change. Indeed, it is reasonable to expect that, in general, on the occasion of a climate transition, more intense atmospheric dynamics occur. A greater kinetic energy implies a greater role for the Cowling dynamo process (Gregori et al., 2025d), greater atmospheric electricity activity, greater electric charge in the ionosphere, larger number of wildfires in dry areas, more intense atmospheric precipitation and floods, etc.

Sun and An (2002a) investigated the history and the variability of aridity in the interior of Asia, on the basis of $\delta^{18}O$ from the equatorial East Pacific Ocean and also from flux variations of $\delta^{18}O$ from the North Pacific Ocean. Thus, they could recognize that the Great Glaciation of Late C $\delta^{18}O$ in the NH can be divided into three stages: (i) the arrival stage $\sim 7.2 - 3.4 Ma$ ago, (ii) the initial stage $\sim 3.4 - 2.6 Ma$ ago, and the Great Ice Age (GIA) since $\sim 2.6 Ma$ ago. They also envisaged a crucial role played by the timing of the TP uplift.

and the $CaCO_3$ content of the late C $\delta^{18}O$ in the NH can be divided into three stages: (i) the arrival stage $\sim 7.2 - 3.4 Ma$ ago, (ii) the initial stage $\sim 3.4 - 2.6 Ma$ ago, and the Great Ice Age (GIA) since $\sim 2.6 Ma$ ago. They also envisaged a crucial role played by the timing of the TP uplift.

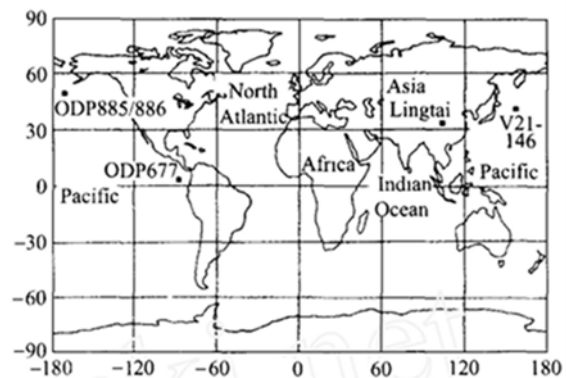


Fig. 19. Map showing the sites (black squares), considered by Sun and An (2002a), of $\delta^{18}O$ from the equatorial East Pacific Ocean and also from flux variations of $\delta^{18}O$ from the North Pacific Ocean. Thus, they could recognize that the Great Glaciation of Late C $\delta^{18}O$ in the NH can be divided into three stages: (i) the arrival stage $\sim 7.2 - 3.4 Ma$ ago, (ii) the initial stage $\sim 3.4 - 2.6 Ma$ ago, and the Great Ice Age (GIA) since $\sim 2.6 Ma$ ago. They also envisaged a crucial role played by the timing of the TP uplift.

Sun and An (2002a) compared their records (Fig. 20) with the records from ODP sites 885/886 and V21-146.²⁰ Their location is also shown in Fig. 19. They found a gradual drying trend in the dust source regions in the Asia's interior, superposed over a significant wet-dry variability. A sharp drying of the dust sources occurred $\sim 3.6 - 2.6 Ma$ ago that they interpret as a possible effect of the TP uplift. Compared to previous times, after $\sim 2.6 Ma$ the average value and variability of the $\delta^{18}O$ from the equatorial East Pacific Ocean and also from flux variations of $\delta^{18}O$ from the North Pacific Ocean. Thus, they could recognize that the Great Glaciation of Late C $\delta^{18}O$ in the NH can be divided into three stages: (i) the arrival stage $\sim 7.2 - 3.4 Ma$ ago, (ii) the initial stage $\sim 3.4 - 2.6 Ma$ ago, and the Great Ice Age (GIA) since $\sim 2.6 Ma$ ago. They also envisaged a crucial role played by the timing of the TP uplift.

²⁰ V21-146 is a sediment core in the North Pacific. See Liu et al. (1985), An et al. (1990, 1991), Chen (1991), Guo

et al. (1999), Hovan et al. (1989), Rea (1994), Rea et al. (1998).

The occurrence of aeolian deposits depends on several and complicated climate factors, ranging from the level of snow and vegetation cover, to differences in soil moisture and salt levels. Kurosaki et al. (2011) investigated these difficult issues. “A decadal change in the frequency of dust outbreaks for April over East Asia using WMO synoptic data was identified. [They used data back to 1970.] The causes of the decadal change can be defined in terms of aeolian erosivity (i.e., ability of wind to cause erosion represented by wind speed) and erodibility (i.e., susceptibility of soil and land surface to wind erosion represented by the threshold wind speed for dust outbreak) ... The change in erodibility is linked, in part, to the effect of dead leaves of grasses in spring, which are the residue of

vegetation in summer from the previous year, which can cause an increase in the threshold wind speed.” They considered that during the past two decades a dramatic increase occurred of dust storms over East Asia. Their analysis showed that the rise in dust storms in desert regions can be attributed largely to an increase in the frequency of strong winds. However, for crops and grasslands, the increase in storms seemingly depended on a change in erodibility, indicating that the soil had somehow changed. They concluded that monitoring plant growth and precipitation during the summer are the correct premises for the evaluation of the probable frequency of dust storms during the subsequent year.

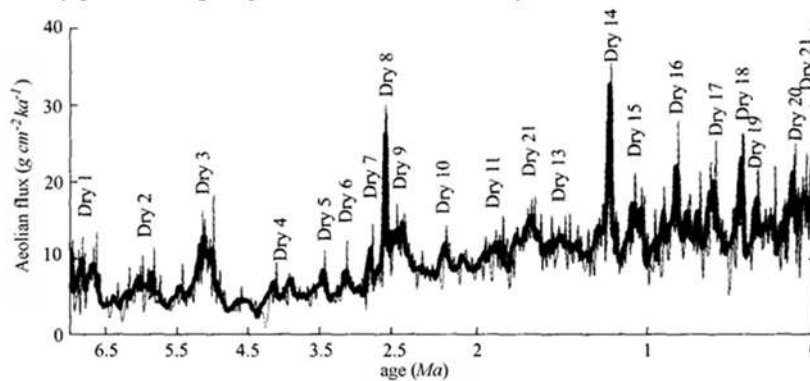


Fig. 20. Aeolian flux variation in the Lingtai profile during the past 7 Ma. Figure and captions after Sun and An (2002a). With kind permission of *Science in China, Series D*.

Yu et al. (2002) found climatic oscillations, manifested as a series of high-frequency, large-amplitude and abrupt cold events occurred during the Holocene Hypsithermal. These oscillations are recorded in a Holocene coral reef close to Leizhou Peninsula, in front of the Hainan Island, in the South China Sea. This period corresponds to ¹⁴C age of ~ 6.2 – 6.7 ka or calendar age of ~ 6.7 – 7.2 ka BP, when the climatic conditions were ideal for coral reefs to develop. They could recognize at least nine stages. Every stage, which they called a “climate optimum”, lasted ~ 20 – 50 years, was terminated by an abrupt cold interval and/or a sea-level lowering event in winter, which caused a widespread emergence and death of the corals, and growth discontinuities on the coral surface. In fact, this is a saw-tooth trend. The monthly mean temperature in winter was ~ 7.9 °C lower than during warm periods. During this period, the crust subsided periodically totaling up to > 3.42 m while the sea-level was rising.

Chen et al. (2004b) reconstructed the distribution of desert and sandy land in China since the last interglacial period, during the last glacial maximum (LGM), and during the Holocene Megathermal. At present, they look correlated with the following conditions: (i) arid and hyper-arid desert zones, at isohyet of < 200 mm, are dominated by mobile dunes; (ii) semi-arid steppe and arid desert steppe, with the precipitation between 200 – 400 mm, are dominated by semi-fixed and fixed sand dunes; (iii) the precipitation of sub-humid forest grassland and humid forest zones, with scattered fixed sand land, is characterized by precipitations > 400 mm.

Compared to present environment, the results show that the distribution of desert and sandy land in China was

greatly dwindled during the last interglacial period. The mobile dune area was ~ 2/3 today’s area, but it greatly expanded during the LGM. However, the reduced area of desert and sandy land during the Holocene Megathermal was smaller than the area during the last interglacial period.

Stalagmites and ice cores

Consider first the information provided by stalagmites. The first efforts were concerned with the assessment of their calibration (e.g. see Li et al., 2000 and references therein). Stalagmites are reliable indicators only when considering mean data averaged over time lags of the order of one century, as the signal-to-noise ratio allows for no better time resolution.

Let us mention first Shi et al. (1993), who carried out a careful multiparametric analysis dealing with climate and environmental variations during ~ 8.5 – 3 ka BP with particular reference to the stable warmer and wetter millennium ~ 7.2 – 6 ka BP. They evidenced some large-scale centennial warming, characterized by an increase in precipitation, following the expansion of monsoon circulation, e.g. during ~ 8.5 – 8.3 ka BP, also correlated with high level of some inland lakes and the sudden expansion of vegetation. They stress that the growth of the Neolithic culture, i.e. agriculture and settlement in the present semi-arid area of northwestern China, was undoubtedly related to the dramatic warming and wetting before ~ 8 ka BP. According to palynological studies, compared to today, ~ 7 – 6 ka BP ago the mean annual temperature was higher ~ 1°C in southern China, ~ 2°C in the Changjiang (Yangtze) Valley, ~ 3°C in northern and in

northeastern China, and $\sim 4 - 5^\circ\text{C}$, which was the highest warming, in Qinghai-Xizang TP. Compared to today, during winter the differences were much larger.

Shi et al. (1993) also investigated, through the entire Chinese subcontinent, the corresponding variations of vegetation. In addition, $\sim 6 - 5 \text{ ka BP}$ sea-level was $\sim 1 - 3 \text{ m}$ higher than at present. Large coastal lowlands were submerged by sea-water, while the frequency of occurrence of storm surges increased during the high sea-level periods. Fig. 42 shows the variations of lake water-

levels, and Fig. 40 the $\delta^{18}\text{O}$ trend (which is related to temperature) derived from the Dundee ice core.

Yao et al. (2001) studied the Guliya ice core. See Figs 21 through 24. See below concerning the discussion of this ice core.

Zhang et al. (2004) investigated the time sequence of high-resolution palaeoclimatic changes since the last glacial period $\sim 60,500 \text{ years BP}$. They analyzed, in the Q4 and Q6 stalagmites of the Qixin cave in southern Guizhou, the oxygen isotopes, and compared their results with the $\delta^{18}\text{O}$ from the GISP2 ice core.

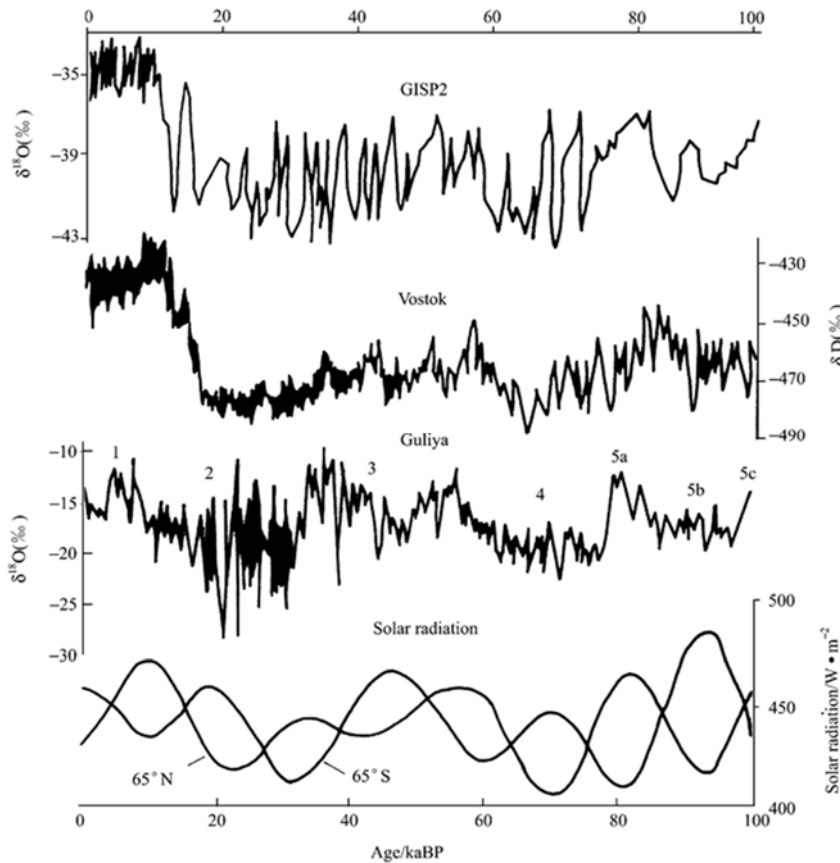


Fig. 21. "A comparison of climate record in the Guliya ice core with those in GISP2 ice core and Vostok ice core." Figure and captions after Yao et al. (2001). With kind permission of Science in China, Series D.

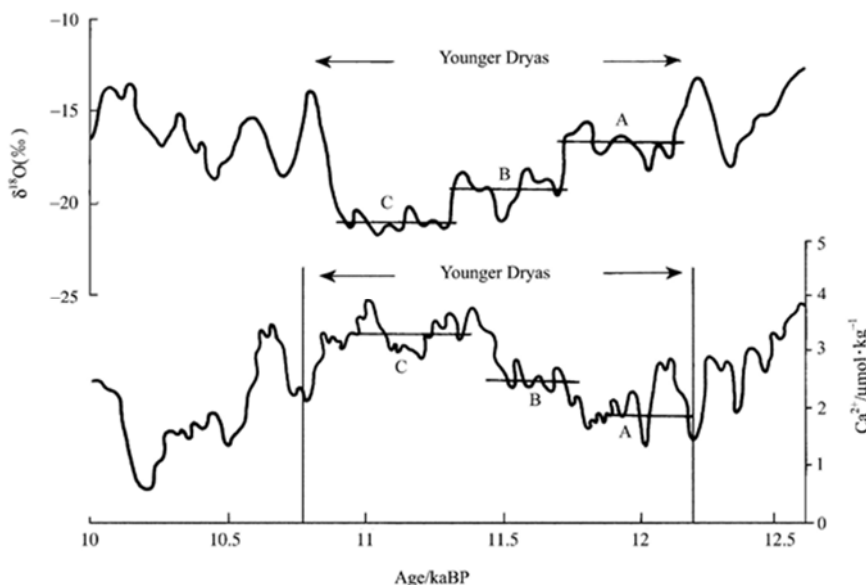


Fig. 22. "A high-resolution record of Younger Dryas (YD) event by Guliya ice core." Figure and captions after Yao et al. (2001). With kind permission of Science in China, Series D.

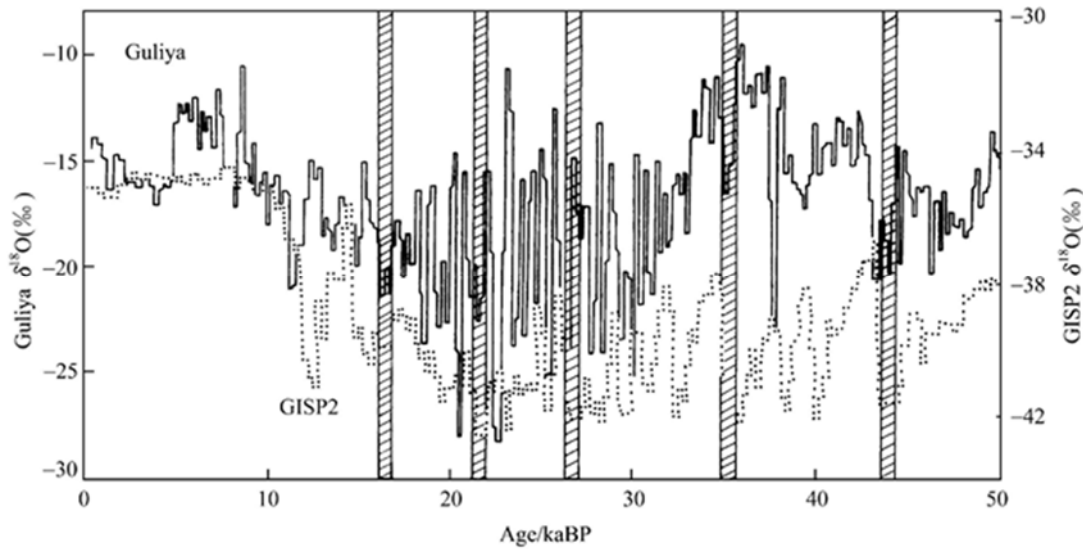


Fig. 23. "Heinrich event recorded by Guliya ice core." Figure and captions after Yao et al. (2001). With kind permission of Science in China, Series D.

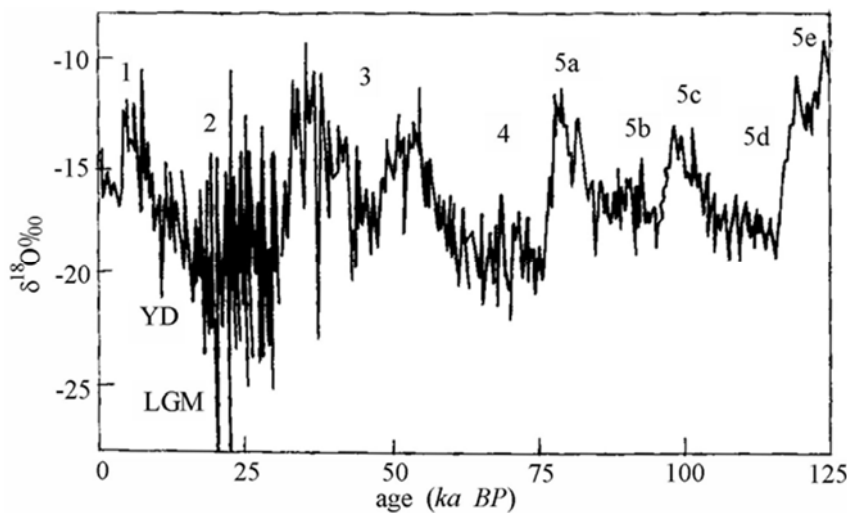


Fig. 24. "A comparison of Guliya ice core record with Greenland ice core record on glacial-interglacial time scale." Figure and captions after Yao et al. (2001). With kind permission of Science in China, Series D.

They found that the depositional records in the two stalagmites - corresponding to the Dansgaard-Oeschger (DO) cycle events 1-18 and Heinrich's events H1-H5 - display rapid climate changes during a short time scale since the last glacial stage. In fact, the recorded cold and warm events since ~ 60,500 years BP reflect the palaeo-monsoon circulation. These changes are clearly correlated to climate oscillation associated to the North Atlantic Ocean (NAO). This is clearly suggestive of a strong teleconnection with the palaeoclimate variations occurred in the North Polar region.

During the period that they studied ~ 60,590 – 11,290 years BP they envisage a weakening of the Asian summer monsoon, while climate generally became drier and cooler. Concerning the Dansgaard-Oeschger (DO) and Heinrich events see below.

Wang et al. (2008a) improved the stalagmite analysis and searched for the millennial- and orbital-scale changes in the East Asian monsoon over the past 224,000 years.

"High-resolution speleothem records from China have provided insights into the factors that control the strength of the East Asian monsoon ... Our understanding of these

factors remains incomplete, however, owing to gaps in the record of monsoon history over the past two interglacial-glacial cycles. In particular, missing sections have hampered our ability to test ideas about orbital-scale controls on the monsoon ..., the causes of millennial-scale events ... and relationships between changes in the monsoon and climate in other regions.

Here we present an absolute-dated oxygen isotope record from Sanbao cave (SB), central China, that completes a Chinese-cave-based record of the strength of the East Asian monsoon that covers the past 224,000 years. The record is dominated by 23,000 year-long cycles that are synchronous within dating errors with summer insolation at 65° N ... supporting the idea that tropical/subtropical monsoons respond dominantly and directly to changes in NH summer insolation on orbital timescales ...

The cycles are punctuated by millennial-scale strong-summer monsoon events (Chinese interstadials ...), and the new record allows us to identify the complete series of these events over the past two interglacial-glacial cycles. Their duration decreases and their frequency increases during

glacial build-up in both the last and penultimate glacial periods, indicating that ice sheet size affects their character and pacing. The ages of the events are exceptionally well constrained and may thus serve as benchmarks for correlating and calibrating climate records.”

This evidence is also emphasized by Overpeck and Cole (2008). They show a figure (not here shown) and comment that “*like many proxies, they [i.e. speleothems] record the ratios of different oxygen isotopes in material laid down over time. These ratios are sensitively linked to the composition of precipitation, and thus to the prevailing climate. There are valuable examples of speleothem records from most continents, from mid-latitudes into the tropics, but few regions have proved to be as fertile as eastern China. Among the exciting records stored here are several from the Dongge Cave that span the Holocene, the interglacial period from 11,550 years ago to the present (Dykoski, 2005; Wang, 2005). These complementary records elegantly confirm the orbital theory of monsoon variability, but also reveal decade to century-scale variability that differs between geological formations ...*”

In the figure not here shown, Overpeck and Cole (2008) compare the oxygen isotope ratios ($\delta^{18}\text{O}$) from two records of the Sanbao (Wang, 2008a) cave and the Dongge (Dykoski, 2005; Wang, 2005) cave in eastern China during the Holocene period. The plots support a clear trend in agreement with millennial scale decline in insolation (Berger, 1978) due to variations in Earth’s orbit – considering the July at 30°N insolation. They apply an offset between the two caves due to different elevation and temperature (Wang, 2008a). “*Century-scale variance is not always consistent among the records, highlighting the need for replication to isolate climate signals that are uniform over whole regions.”*

Chen et al. (2006b) studied two stalagmites from two high-altitude caves in Shennongjia area, Hubei Province, with a decadal time resolution. The $\delta^{18}\text{O}$ records from Swan cave (1600 m a.s.l.) reflect large spatial changes in the circulation strength and precipitation of the Asian monsoon. The evidence derives from a great similarity between the stalagmite $\delta^{18}\text{O}$ records from Nanjing (Jiangsu Province), Libo (Guizhou Province), and the Chen et al. (2006b) stalagmites, and they referred to the time of the last deglaciation, including a part interval of the YD event and Bølling-Allerød.

A 30 year resolution $\delta^{18}\text{O}$ record from a stalagmite from the Yongxing cave (1400 m a.s.l., Baokang County, Hubei Province), 70 km away from the Swan cave reveals a rapid transition of Asian monsoon climate during Termination 3, 245 ± 5 ka BP. It shows a millennial dry episode during the Asian monsoonal Termination 3.

Upon considering structure, duration and transition, the dry reversal generally agrees with the pattern of the YD event, which is clear in the $\delta^{18}\text{O}$ records of the Chinese stalagmites. This YD-type event is characterized by a large decrease in $\delta^{18}\text{O}$, i.e. as large as 2.30‰, which is more than half of the $\delta^{18}\text{O}$ excursion between glacial/interglacial

periods. It lasted 1371 ± 59 years. After this event and within 74 ± 4 years, the monsoon climate abruptly shifted into the interglacial period. Chen et al. (2006b) conclude and claim that their findings support the view that the repeated occurrence of YD-type events was not accidental, rather resulting, maybe, from the coupling of ice-sheets and oceanic/atmospheric circulation. They emphasize that no general agreement exists on the mechanism that triggers a YD-type event.

“*A recent study suggested that the discharge of Arctic freshwater flux into the Greenland-Iceland-Norwegian seas via the Fram Strait may cause the North Atlantic meridional overturning circulation to decrease, and trigger YD (Peltier and Tarasov, 2005). Because there is no evidence that a similar millennium-long cold episode punctuated earlier glacial terminations, so the YD appears to be a one-time event (Broecker, 2003).*

A key issue is whether the YD-type event occurred only during Termination 1 (T1) ... Existing high-resolution multi-proxies have shown no occurrence of YD-type event during the Termination 2 (T2) (Yuan et al., 2004; Zhao et al., 2001; Bischoff et al., 1997). Previous studies have scarcely involved variations of high-resolution climate during Termination 3 (T3), due to timing and/or resolution limitations. The detailed deuterium and $\delta^{40}\text{Ar}$ Vostok profiles firmly identified the existence of a cold reversal at the start of T3 (Caillon et al., 2003), without interpretation of its magnitude and duration. Many records from ice core (Petit et al., 1999; Fischer et al., 1999), deep sea sediment (Pahnke et al., 2003), speleothems (Winograd et al., 1992), continental deposits of flora (Abrantes, 2003) and loess (Sun and An, 2002) have showed similar climate changes during the last four terminations.” It has been guessed that “*YD-type events seem to be an intrinsic feature of climate change during glacial-interglacial cycles.”*

Chen et al. (2006b) studied the Yongxing cave stalagmite, which is a high-resolution Asian monsoon climate record during T3. Their analysis relied on U/Th dating, on annual band counting, and on $\delta^{18}\text{O}$ measurements. This U/Th and $\delta^{18}\text{O}$ analysis is briefly explained as follows by Wilson (2016c). “*Earth’s naturally occurring ^{234}U steadily decays into ^{230}Th with a half-life of 245,000 years. When water passes through soil and bedrock to reach the cave, it carries U with it. But as the ^{230}Th grows, it also radioactively decays, with a half-life of 76,000 years; the concentration of $^{230}\text{Th}/^{234}\text{U}$ in a stalagmite layer determines the layer’s age.*

Oxygen isotopes in rainwater are also preserved in the stalagmites, and the variation in $^{18}\text{O}/^{16}\text{O}$ over time is a proxy of both local and regional climate conditions, such as the amount of rainwater falling on the cave.”

Chen et al. (2006b) found a feature that looks much similar to a YD-event, consistently with the evidence during the last deglaciation from various sites in China. Their results are synthesized in Figs 25 and 26.

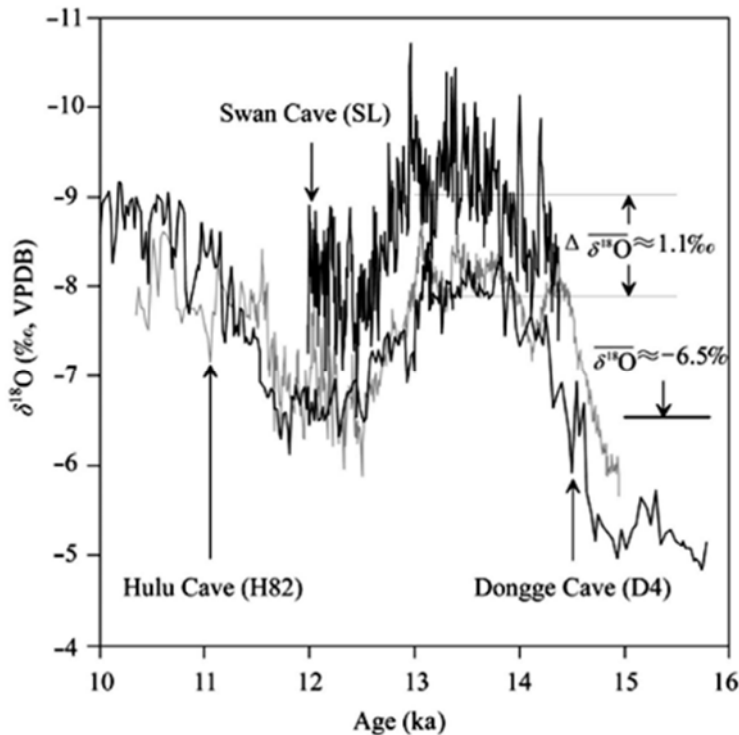


Fig. 25. Comparison of the $\delta^{18}O$ records from Swan, Hulu and Dongge caves during the last deglacial period. The $\delta^{18}O$ curve of stalagmite H82, D4 is from Wang et al. (2001b) and Yuan et al. (2004), respectively. The $\delta^{18}O$ trend varies within a magnitude of $\sim 10.7 - 6.5\text{‰}$, with two distinct climatic episodes: warm/humid (BA) and dry/cold (YD). Between 14.3 – 13 ka BP, $\delta^{18}O$ scatters around a mean -9.0‰ , then ~ 13 ka BP it shifts from -10.7‰ to -8.6‰ and, after that, it fluctuates around an average of -8.1‰ . The boundary between BA and YD resembles the age estimates by other stalagmites in Southern China (Wang et al., 2001a, Yuan et al., 2004). $\Delta\delta^{18}O \approx 1.1\text{‰}$ is the difference of the average $\delta^{18}O$ values between the stalagmites SL and D4 during the BA episode; $\delta^{18}O \approx -6.5\text{‰}$ is the average during the LGM recorded in the stalagmite SL. After Chen et al. (2006b). With kind permission of *Science China Ser. D*.

Wu et al. (2006) studied the grain size of microparticles in the Muztagata ice core (see Fig. 27) and found substantial differences that reflect the dust deposit process in high mountain glaciers at mid-low latitudes compared to polar ice sheets.

Let us remind about Xia et al. (2007). They studied the records provided by two speleothems (BS22 and SB25) in the Sanbao (SB) cave (Shennongjia, central China). They compared their data with the data from the stalagmite from the Hulu cave (near Nanjing). The locations of different sites is shown in Fig. 28.

Xia et al. (2007) used 23 U/Th analyses and 532 $\delta^{18}O$ data, with data averaged over 80 years spanning the time interval $\sim 95 - 56$ ka BP. Thus, they could investigate the characteristics of millennial oscillations in the East-Asian-Summer monsoon (EASM). The trend of the SB record seems to be generally correlated with the mid-July solar insolation at $\sim 65^\circ N$. This is suggestive, as a first order approximation, of a control of EASM intensity by insolation in mid-high northern latitudes. In addition, the millennial EASM oscillations appear to be well related to the Greenland interstadials DO events numbered 1-22. This is a clear indication of the permanent teleconnection between China and rapid ocean-atmosphere reorganization in the North Atlantic (Fig. 29).

This finding is further confirmed, by means of the same SB record, and improved by Cheng et al. (2009) who show that it is possible to correlate the Asian monsoon records of the past four glacial Terminations with the records from ice cores and marine sediments. In the NH, observations are consistent, in all four cases, with the classic summer insolation trigger for a starting retreat of ice sheets. The oceanic and atmospheric circulation in the North Atlantic

are affected by meltwater and icebergs. This implies fluxes of heat and carbon that cause increases in atmospheric CO_2 , and changes in the Antarctic temperatures that drive the Termination in the Southern Hemisphere (SH). In addition, “probable positive feedbacks between sea-level and CO_2 ” are caused by the CO_2 increase and by summer insolation that drive recession of northern ice sheets. That is, the DO events, which are well-dated by means of stalagmites, probably provide a reliable absolute calibration for chronologies of the Greenland ice cores. Compared to the available Greenland ice cores, the SB dates for DOs are somewhat different and they differ in a seemingly irregular way. The age offsets are particularly significant for DO19 and 20, and are larger than the uncertainties of the U-series dating. These two events appear younger by $\sim 1 - 2$ ka in the SB compared to the North GRIP (Greenland Ice Core Project) record, and older by $\sim 3 - 4$ ka compared to the GISP2 ice core (Fig. 30).

Cheng et al. (2016) extended the analysis on these stalagmites, and carried out a skillful analysis. Their target is to prove the Milanković effect. Maybe, this is the most accurate and precise investigation on palæoclimatic records that successfully proves the astronomical modulation. Hence, it is worthwhile to illustrate their analysis and finding in some detail. However, only a few highlights are here reported and a few original figures. The interested reader ought to refer to the original paper for an extensive and exhaustive discussion of several details that are here omitted. These figures have detailed captions and - as far as the present purpose is concerned - they are self-explanatory. A few basic comments are to be specified like a needed premise for their interpretation.

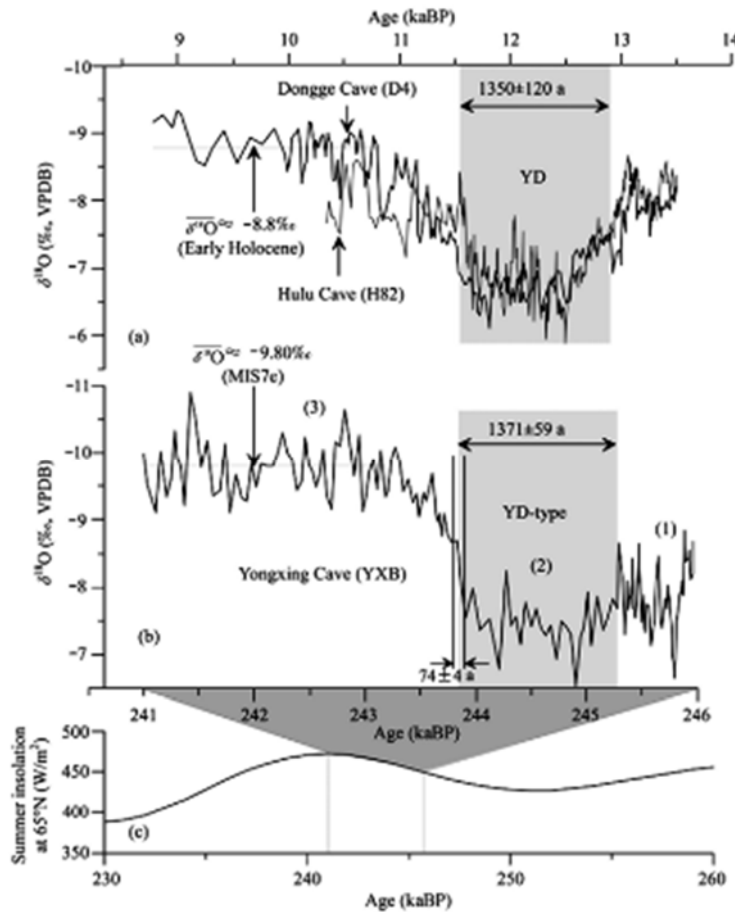


Fig. 26. Comparison of the $\delta^{18}O$ records in stalagmites showing millennial scale reversals in Asian monsoon climates during *T3* and *T1*. (a) $\delta^{18}O$ curves of the stalagmites *H82* and *D4*, from Wang et al. (2001a, 2001b) and Yuan et al. (2004), respectively ($\delta^{18}O \approx -8.8\text{‰}$ is the $\delta^{18}O$ mean during early Holocene recorded in stalagmite *D4*, 1350 ± 120 years is the duration of the *YD* event recorded in the stalagmite *H82*); (b) $\delta^{18}O$ curve of the stalagmite *YXB* ($\delta^{18}O \approx -9.8\text{‰}$ is the $\delta^{18}O$ mean during 1890 *MIS7* recorded²¹ in the stalagmite *YXB*, 1371 ± 59 years is the duration of *YD*-type event during *T3* recorded in the stalagmite *YXB*, 74 ± 4 years is the duration at the ending of the *YD*-type event); (c) the growth interval of stalagmite *YXB* corresponds to the summer insolation curve at $65^\circ N$. After Chen et al. (2006b). With kind permission of *Science China Ser. D*.

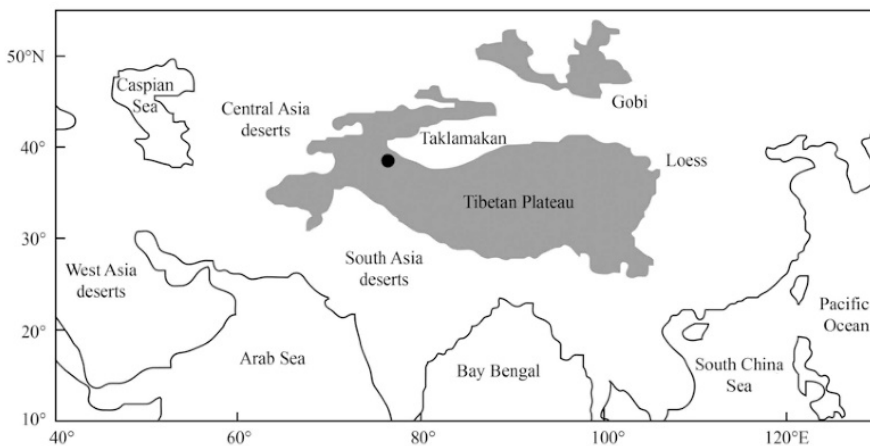


Fig. 27. "Location of Muztagata ice core (black dot) and dust source areas around the TP." Figure and captions after Wu et al. (2006). With kind permission of *Science in China, Series D*.

The climate system is complex. No phenomenon, of any kind, can give any quantity or index that, according to the standards of bivariate correlation analysis, can result formally correlated to some given climatic parameter. Therefore, also the astronomical parameters are to be found eventually partially correlated with some climatic quantity, due to the large set of drivers that enter into play. Every driver has a specific impact on the natural system, and this impact depends on the constraints eventually imposed by other drivers. In addition, the response of the natural system to every different driver occurs according to a suitable time-

delay. Hence, the final observed climate is a sum of several effects. Every effect responds to a different driver or set of drivers, everyone with a specific time delay.

Thus, it is difficult to interpret observations and the role of every original driver. The algorithms are therefore to be chosen in order to assess a physical hierarchy of effects in decreasing order of amplitude. Subtract the larger effect and carry out the analysis of the residuals. Thus, get evidence of the next comparably stronger effect in the hierarchy etc. Note, however, that this procedure is a formal phenomenological analysis of observations, with no

²¹ *MIS* means Marine Isotope Stage.

presumption of any physical rationale and/or explanation behind the procedure. Hence, whenever we can prove the Milanković effect by means of this procedure, the concern remains about the mechanism by which the astronomical modulation operates and controls a given natural system. This mechanism is the target of the rationale of the present whole study. In fact, the orbit of the Earth is such that the e.m. induction by the solar wind inside the Earth is correspondingly modulated. Whenever suitable long period e.m. variations influence the TD dynamo, a corresponding change occurs in the recharge of the Earth's battery. This changes the energy balance of the Earth and of the climate system, although with suitable time-delays etc.

As far as the history is concerned of the definition of this time scale, no mention is here given and only the result is mentioned. The reference paper is Lisiecki and Raymo (2005) where the interested reader can find detailed information. The abstract, and Figs 31 and 32, are here reported, where the aforementioned saw-tooth trend is clearly shown.

"We present a 5.3 Ma stack (the 'LR04' stack)²² of benthic $\delta^{18}O$ records from 57 globally distributed sites aligned by an automated graphic correlation algorithm. This is the first benthic $\delta^{18}O$ stack composed of more than three records to extend beyond 850 ka, and we use its improved signal quality to identify 24 new marine isotope stages in the early Pliocene. We also present a new LR04 age model for the Pliocene-Pleistocene derived from tuning the $\delta^{18}O$ stack to a simple ice model based on 21 June insolation at 65°N. Stacked sedimentation rates provide additional age model constraints to prevent overtuning. Despite a conservative tuning strategy, the LR04 benthic

stack exhibits significant coherency with insolation in the obliquity band throughout the entire 5.3 Ma and in the precession band for more than half of the record

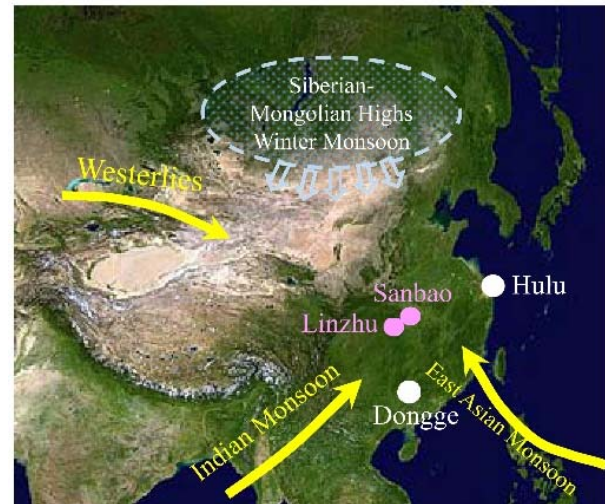


Fig. 28. Cave locations and monsoons in China. Two pink circles indicate Sanbao (110° 26' E, 31° 40' N) and Linzhu (110° 19' E, 31° 31' N) caves, central China. White circles denote Hulu (119° 10' E, 32° 30' N) and Dongge (108° 5' E, 21° 17' N) caves. Arrows show wind directions of the Asian Monsoons (yellow, i.e. the East Asian Monsoon and the Indian Monsoon), the Westerlies and the winter monsoon (light yellow). Figure redrawn after Cheng et al. (2009; Supplement). Unpublished figure. Background image after satellite observations, with kind permission of Wikipedia.

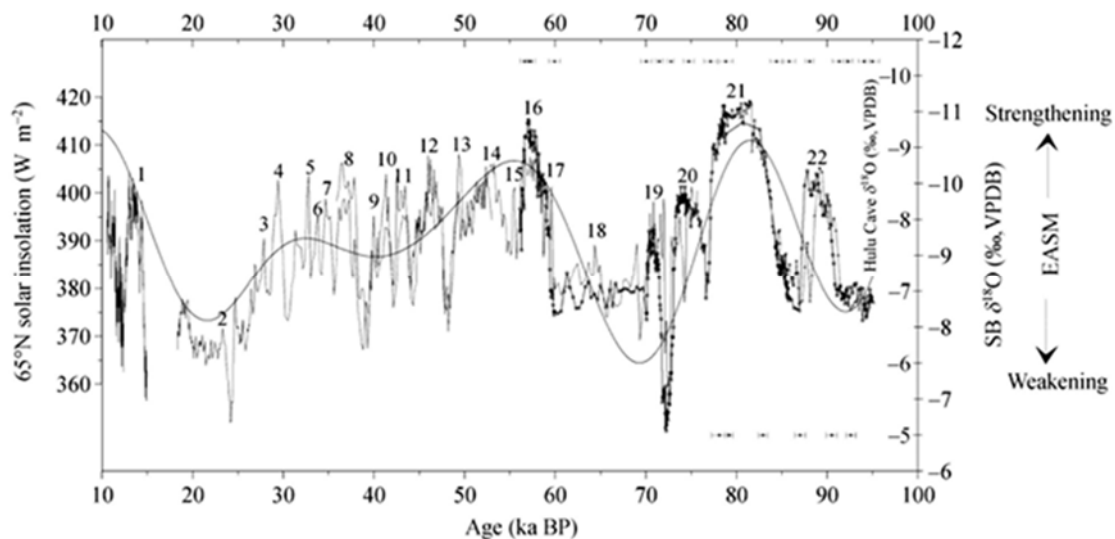


Fig. 29. Comparison of Sanbao and Hulu $\delta^{18}O$ records, and with mid-July insolation at 65°N. Xia et al. (2007) claim that the SB22 record is displayed in this figure as dark symbol-line curve, the SB25 record as light symbol-line curve, the Hulu cave stalagmite record (Wang et al., 2001b) as light line, and the solar insolation profile of mid-July from 65°N (Berger and Loutre, 1991) as dark line, respectively. Error bars on the top and on the bottom of the plot refer to SB22 and SB25, respectively. DO events are marked with numbers (Dansgaard et al., 1993). After Xia et al. (2007). With kind permission of Science China Ser. D.

²² The LR04 stack (Lisiecki and Raymo, 2005) spans 5.3 Ma and is an average of 57 globally distributed

benthic $\delta^{18}O$ records reported in the scientific literature.

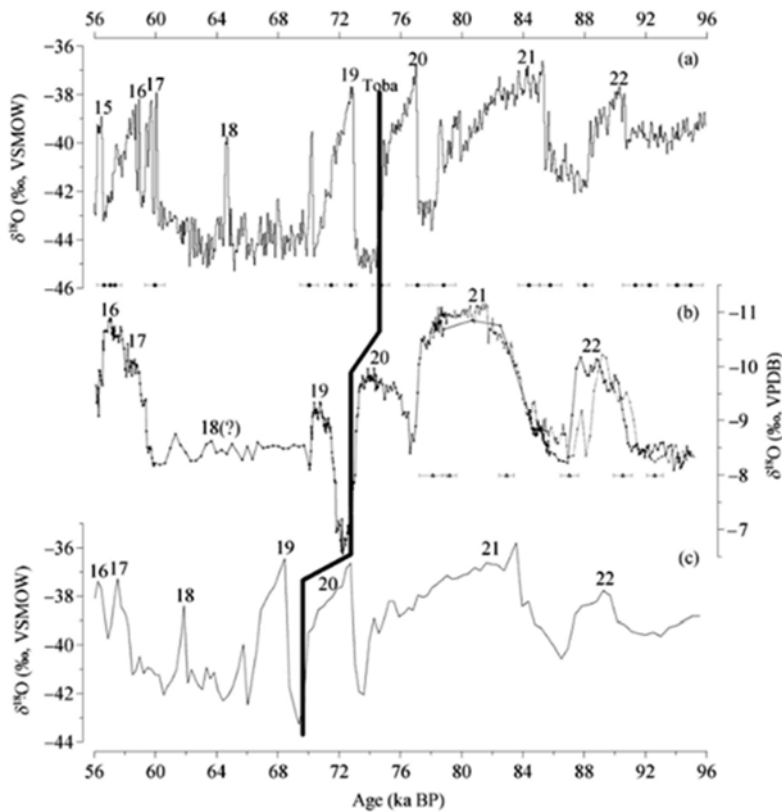


Fig. 30. “Comparison of $\delta^{18}O$ profiles from Shennongjia stalagmites and Greenland ice cores. (a) North GRIP $\delta^{18}O$ record (North Greenland Ice Core Project members, 2004); (b) SB record; (c) GISP2 $\delta^{18}O$ record (Grootes et al., 1993). $\delta^{18}O$ record in (a) and (c) are used in the same unit interval for better comparison. Numbers indicate the corresponding DO events (Dansgaard et al., 1993). The chronologies of the latest eruption of Toba related to the same isotopic event in three records are marked with gray heavy line. Ages and its error bars are the same as in Fig. 29.” Figure and captions after Xia et al. (2007). With kind permission of Science China Ser. D.

The LR04 stack contains significantly more variance in benthic $\delta^{18}O$ than previously published stacks of the late Pleistocene as the result of higher-resolution records, a better alignment technique, and a greater percentage of records from the Atlantic. Finally, the relative phases of the stack’s 41 ka and 23 ka components suggest that the precession component of $\delta^{18}O$ from 2.7 – 1.6 Ma is primarily a deep-water temperature signal and that the phase of $\delta^{18}O$ precession response changed suddenly at 1.6 Ma.”

The acronym MIS is the conventional name given to different stages. Some stage is also subdivided into substages. MIS means “marine isotope stage” or “marine oxygen-isotope stage”, sometimes also called “marine interglacial stage” or “oxygen isotope stage” (OIS). Some stages have some conventional, more or less informal names. These names are specified, wherever needed, *passim* in the present study.

Therefore, the entire skillful empirical findings by Cheng et al. (2016) fit very well into the general logical framework of the present study. Cheng et al. (2016) first briefly summarize the state-of-the-art and define several acronyms. They begin and report about a datum from China that spans – altogether with previous records - the full period from 640 ka ago to present, based on U/Th dating. The existing cave investigations in Chinese caves showed a close relation between variations on orbital timescales of the Asian monsoon (AM) and shifts in NH summer insolation (NHSI). They also showed a close correlation, on millennial scales, between the AM and climate in the North Atlantic. The correlated data are monsoons, and, for North

Atlantic, the Heinrich stadials (HSs) and the ice rafted debris (IRD) events. A few of these phenomena coincide with Weak Monsoon Intervals (WMIs) in China. The cave chronology and the marine oxygen isotope record were therefore used to improve the timing of ice age Terminations. This is the criterion used also by Cheng et al. (2016).

In this way, Cheng et al. (2016) use their analysis of new $\delta^{18}O$ records from Sanbao Cave, China, to improve the determination of Terminations (T) IV through VII. They stress four relevant results.

First, they checked the guessed ~100 ka spacing of late Pleistocene ice age cycles, and how the Termination timing can correlate with a forcing by Earth’s orbit obliquity and/or precession.

Second, they removed the AM part that correlates with insolation, and could thus analyze the residual, showing some variability on the millennial-scale that is correlated to orbital geometry.

Third, they noted that their records cross the Mid-Brunhes Event (MBE). At that time, the character changed of CO_2 and of ice volume cycles (see below for details). Cheng et al. (2016) could thus focus on how these changes affected the AM.

Fourth, they could estimate the maximal AM intensity (timing and duration) during the MIS 11, which is a period that can be considered analogue to the Holocene, concerning the analysis of future climate due to similar orbital geometry. That is, this is also important for understanding the present ongoing climate change.

They explain in some detail their data source.

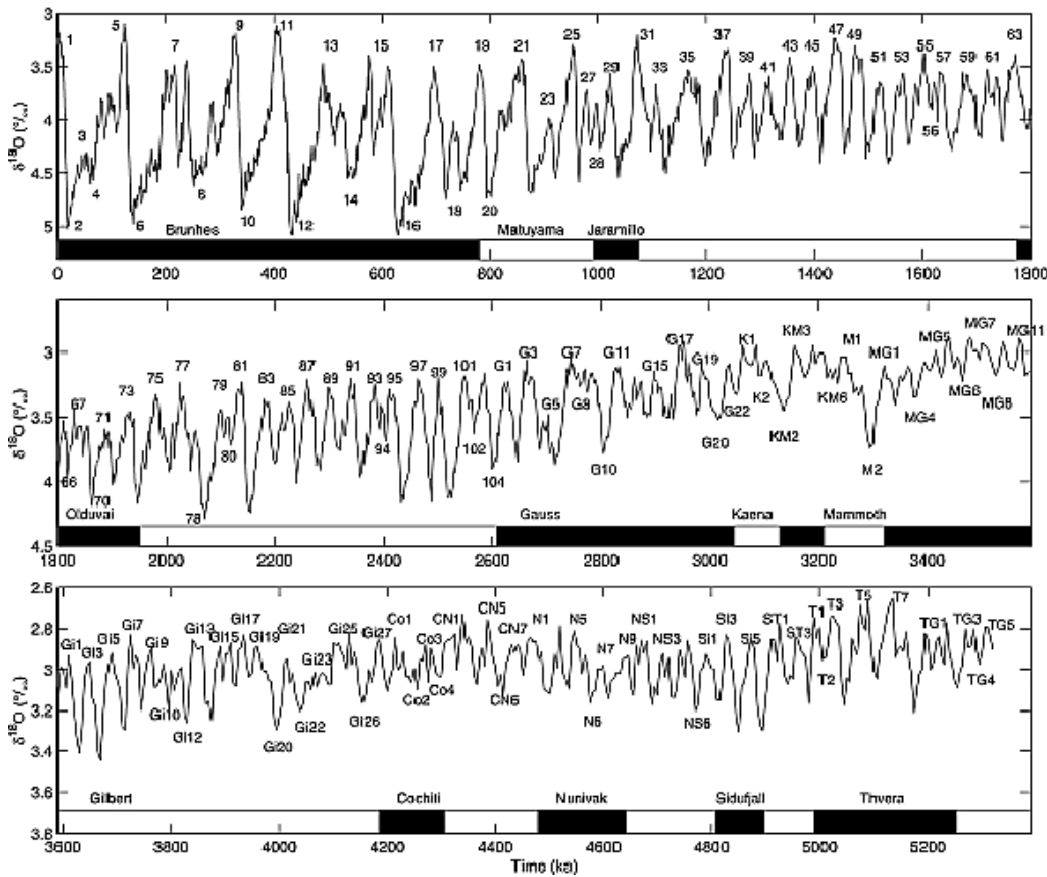


Fig. 31. “The LR04 benthic $\delta^{18}O$ stack constructed by the graphic correlation of 57 globally distributed benthic $\delta^{18}O$ records. The stack is plotted using the LR04 age model ... and with new MIS labels for the early Pliocene ... Note that the scale of the vertical axis changes across panels.” Figure and captions after Lisiecki and Raymo (2005). AGU copyright free policy.

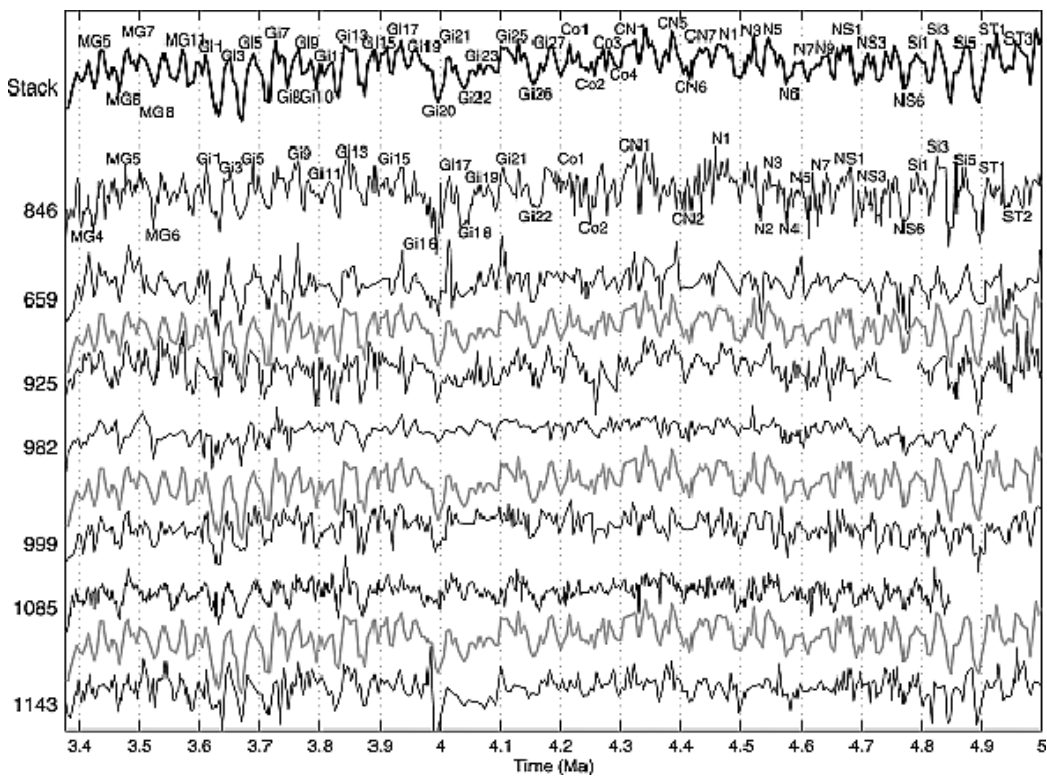


Fig. 32. “New Pliocene marine isotope stages. The LR04 stack (top and repeated as shaded line) and seven of the highest resolution records aligned to the stack. Site 846 is labeled with SHP95 stage identifications.” Figure and captions after Lisiecki and Raymo (2005). AGU copyright free policy.

The Sanbao Cave (SB) (110° 26'E, 31° 40'N, elevation 1,900 m a.s.l.) is in central China on the northern slope of

Mt Shennongjia, where the mean annual temperature is 8°C, and the mean annual precipitation is 1,950 mm. The

main part of precipitation (80%) occurs during June-August. They analyzed four new stalagmites located ~1,500 m from the cave entrance. They applied a recently improved ^{230}Th dating technique attaining a precise age determination (e.g., ± 1.5 ka for *T-V*), achieving, by means of the new $\delta^{18}\text{O}$ measurements, a time resolution of ~200 – 70 years (with average ~120 years).

Some “*intense debate*” deals with the changes of climate interpretation according to the records inside the cave $\delta^{18}\text{O}$ determinations. Most studies support either one of two interpretations. Yuan et al. (2004) appealed to Rayleigh fractionation, which is the conventional name for fractional distillation of mixed liquids, used also to describe isotopic enrichment or depletion as material moves between gaseous and liquid reservoirs. By this, they showed the observed variability in the cave records was explained by variations in the fraction of water vapor that rained out, comparing tropical sources and the cave site. The largest part of modelling agrees with this hypothesis, even though most papers refer to the process calling it “upstream depletion”.

In contrast, Cheng et al. (2016) proposed that variations of the fraction of low $\delta^{18}\text{O}$ monsoon rainfall - with respect to annual totals - could also justify the record. Cheng et al. (2016) claim that recent theoretical and empirical studies (see the original paper for references) support this inference. Both processes can affect the Chinese cave $\delta^{18}\text{O}$ records.

Both models imply that a lower $\delta^{18}\text{O}$ is correlated with a larger spatially integrated monsoon rainfall, comparing tropical monsoon data with the cave site and/or the increased summer monsoon rainfall in the cave region. Therefore, Cheng et al. (2016) call “*strong monsoon*” and “*weak monsoon*” the periods of low and high cave $\delta^{18}\text{O}$, respectively.

The new Cheng et al. (2016) data range during 640 – 330 ka BP (present time is AD 1950). Thus, combined with previous records, they give a composite *AM* $\delta^{18}\text{O}$ record spanning the past 640 ka. They find a millennial scale variation that is superposed on a quasi-sinusoidal wave-like orbital-scale variability that broadly tracks the *NH* summer insolation (*NHSI*) on 21 July. The plot (not here shown) shows the correlation between different parameters related to Asian monsoon associated to changes of the Earth’s orbital elements. In particular, they plot variations of obliquity, eccentricity and precession, the composite *AM* $\delta^{18}\text{O}$ record in the cave, the 21 July insolation at 65°N. They show the *Termination* timing and duration, and the timing of *WMIs* correlated to glacial terminations and two similar events (*MIS* 4/3 and 5.2/5.1 transitions). The timing of *T-IIIa-WMI* in their results study differs from a previous estimate by Cheng et al. (2009), although they consider the new datum more plausible. Finally, they plot the composite sea-level trend. Note that *MBE* is the Mid-Brunhes climatic event, which is contemporaneous with *T-V* (Jansen et al., 1986). “*Removal of orbital-scale variations yields a record of the suborbital variability of the AM (the $\Delta\delta^{18}\text{O}$ record) ... Detrending methods (e.g., choice of insolation curve) could introduce artefacts in the $\Delta\delta^{18}\text{O}$ record ... Similar $\Delta\delta^{18}\text{O}$ power*

spectra independent of detrending curve suggest that this artefact is not significant.” (Cheng et al., 2016)

The next focus of Cheng et al. (2016) deals with the timing and character of *Terminations*. They recall that a ~100 ka cycle is well-known to characterize the past ~650 ka. This agrees with a gradual build-up and rapid termination of every ice age, consistently with what we call the “saw-tooth” trend. Cheng et al. (2016) stress that both glacial cycles and variations of Earth’s orbit eccentricity share a common spectral power. However, the eccentricity is associated with negligible changes in insolation. This is “*an enduring climate puzzle*”, which is usually called the “100 ka problem”. Several hypotheses were proposed to explain this mystery. One hypothesis envisages an average of 4 to 5 discrete precession cycles, with missed beats in between. Another hypothesis appeals to 2 to 3 obliquity cycles with missed beats. A third hypothesis appeals to a combination of effects related to both obliquity and precession. Other hypotheses speculate interactions related to internal oscillations in the Earth system (see Cheng et al., 2016 for references).

Let us remark that - according to the rationale of the present study - the “saw-tooth” trend is explained by a slow variation of climate while the endogenous heat progressively increases the efficiency of heat release through Earth’s surface. When the “channel” is fully opened, the Earth’s battery rapidly releases a large fraction of the available endogenous heat. Then, the “channel” closes, as the mantle cools. Thus, the endogenous heat release shortly attains a minimum. That is, the asymmetric trend of a *Termination* is explained by an energy balance, i.e. by a “calorimetric” rationale, analogously to the balance of a pressure cooker and to the steam release from the security valve.

According to Cheng et al. (2009), every one of the last four *Terminations* is associated to one or two *WMIs* that coincide with *HSs* observed in the cores of North Atlantic. In addition, abrupt *WMI* endings are found in Antarctic ice cores, to be synchronous with abrupt increases in atmospheric CH_4 . Thus, Cheng et al. (2009) afforded to construct a common chronology putting altogether the evidence from cave stalagmites, marine cores, and ice cores. The *WMIs* look correlated with a relevant portion of every marine *Termination*. The *WMIs* and the marine *Terminations* occurred in coincidence with rising *NHSI*. The largest of the CO_2 rise related to every *Termination* occurred during the *WMIs*. Cheng et al. (2009) suggested therefore that, on the occasion of every *Termination*, a rise in insolation started the initial melting of the ice sheets. The input of ice and meltwater determined a cold anomaly in the North Atlantic that affected the ocean/atmosphere system. That is, the effect is a slowdown in Atlantic Meridional Overturning Circulation (*AMOC*) that originates a cold anomaly over the North Atlantic, which causes a weaker *AM*, recorded as a high $\delta^{18}\text{O}$ anomaly. This caused the *WMIs* and the rise in atmospheric CO_2 , altogether with the increase of insolation drove the *Termination*. This explanation – based on a change of insolation - is other than the mechanism that is here proposed that appeals to a change of endogenous heat exhalation.

Cheng et al. (2016) use the improved chronology relying on the cave records to tackle the “100 ka problem”. They report (not here shown) a detailed analysis and plot of several *Terminations*. They claim that the new data series support the former hypothesis by Cheng et al. (2009) relying on a supposed increase of *NHSI*, which starts ice-sheet disintegration, perturbing the ocean/atmosphere system, the carbon cycles, resulting in a CO_2 increase, etc.

They comment that all seven *Terminations* (*T*) occurred at as time of rising *NHSI*, separated by 4, 5, 5, 4, 5, and 5 precession cycles. The durations between successive *Terminations* (*T-VII* to *T-I*) are found to be ~93, ~105, ~92, ~92, ~113 and ~115 ka, respectively, which are other than a precise ~100 ka cycle. The stress, however, that the average duration is ~100 ka. They note two “extra *Terminations*” recorded in marine data series. They call them, respectively, *T-IIIa* observed one precession cycle after *T-III* (i.e. between *MIS* 7.4 and 7.3), and *T-VIIa* observed two precession cycles after *T-VII* (i.e. between *MIS* 15.2 and 15.1). These extra *Terminations* display features analogous to the seven main events, including comparable marine $\delta^{18}\text{O}$ or sea-level changes.

We note that, according to our interpretation (Gregori, 2002; Gregori and Leybourne, 2021), the timing of the variations of endogenous heat production and (time-delayed) release is controlled by the encounters of the Solar System with interstellar matter. The mean duration of ~100 ka is justified by internal mechanism of sea-urchin propagation through the mantle, much like the duration of an Earth’s heartbeat is ~27.4 *Ma*. That is, the ~100 ka depends on a layer, which is shallower than the mantle, posed between the source of endogenous heat and Earth’s surface. The timing of closing and opening of the “channel” for endogenous energy exhalation depends on the amount of recharging of the Earth battery during every *Termination* or extra *Termination*. All other effects observed in marine records, and in general in other climate proxies, are related either simultaneous or time-delayed phenomena. On the other hand, this entire mechanism can experience, superposed, an additional trigger related to solar insolation. In fact, the Sun is unique system, and it may prove impossible to separate the roles of solar radiation and of e.m. induction by the solar wind.

Cheng et al. (2016) note that an integral number of precession cycles separate adjacent *Terminations* (for all nine case histories), while no clear dependence is evidenced on the obliquity or eccentricity cycles that seem thus uninfluential on *Terminations*. “However, as none of the nine events takes place when obliquity is substantially below average, obliquity may play some causal role ...”

In this respect, let us remind (Gregori, 2002)²³ that the output of the Hawai’ian hotspot clearly displays a modulation²⁴ of ~0.41 *Ma*, which seems to find a correspondence only in the orbit eccentricity, which ought thus to modulate the efficiency of the *TD* dynamo that recharges the Earth’s battery.

Concerning the “*pacemaker of millennial-scale events*”, Cheng et al. (2016) review several morphological dissimilarities of different events. They appeal to an interplay and feedbacks “among factors internal to the climate system, such as ice volume dynamics, in addition to orbital forcing ...” On the other hand, all *Terminations*, including some small-scale *Terminations*, seem to be related with millennial-scale intervals of unusually weak monsoon. Therefore, Cheng et al. (2016) investigate a possible correlation with orbital geometry. They first subtract orbital-scale frequencies and get a residual $\Delta\delta^{18}\text{O}$ record that displays a clear suborbital variability (figure not here shown). They plot suborbital composite *AM* $\delta^{18}\text{O}$ records, Antarctic $\Delta\delta\text{D}$ (a temperature proxy) records detrended by subtracting the 21 July insolation at 65°N, and the 21 June insolation at 65°N on a reversed scale (for comparison). They find a remarkable similarity between suborbital variations in *AM* $\delta^{18}\text{O}$ records and Antarctic $\Delta\delta\text{D}$ records.

They observe relevant effects associated to the aforementioned *WMIs*, and also millennial-scale features related to large positive anomalies in $\delta^{18}\text{O}$ correlated with *Terminations*. In addition, upon a closer inspection, they detect several smaller amplitude, millennial-scale, high- $\delta^{18}\text{O}$ events, i.e. phenomena that seems associated to some kind of small-scale *Terminations*. In fact, these smaller events seemingly share a common display of trends of the same proxies that characterize the large *Terminations*. That is, the pattern is invariant with respect to time-scale, similarly to the “saw-tooth” trend that depends on an energy balance on every time-scale. The duration of the “tooth” depends on the depth of the endogenous heat reservoir that determines the “calorimetric” effect.

Cheng et al. (2016) guess that the smaller events are related to the decay of the northern ice sheets - indeed, this happens, e.g., whenever an anomalous increase occurs of endogenous heat that is released beneath the ice sheet.

By means of an analysis of the frequency spectra of $\Delta\delta^{18}\text{O}$ and of obliquity, Cheng et al. (2016) conclude that there are indications that favor the rupture of the northern ice sheets, with release of ice and meltwater in the North Atlantic. This seems correlated with, or favored by, high *NHSI*. That is, according to our interpretation, the e.m. induction in the Earth’s mantle, which is consequent to the orbital modulation of the solar wind interaction, originates a control on the *TD* dynamo, hence on the endogenous energy balance of the Earth. The effect further develops until the weakening of the monsoon.

As already mentioned, Cheng et al. (2016) carried out an analogous investigation on Antarctica records, in order to seek the seesaw trend that, however, is not shared by the interpretation that is here proposed, although the seesaw could be an optional addition whenever a suitable mechanism is envisaged that can explain it. We point out that “seesaw” implies some kind of oscillation, while a

²³ See also the entire discussion reported in the set of papers Gregori et al. (2025k, 2025l, 2025m, 2025n, 2025o, 2025p, 2025q).

²⁴ Formerly discovered by Dong Wenjie.

“saw-tooth” trend has a well-defined asymmetric behavior, associated with a “calorimetric” – i.e., energy balance - physical interpretation. They refer to the Antarctic δD (a temperature proxy) record. They removed the low frequency, orbital-scale variability. Then, they computed the power spectrum of the residual suborbital variability. They found that the suborbital scale Antarctic temperature and the *AM* records look quite similar, where, however, an anti-correlation is found between suborbital *AM* components and the Antarctic temperature. They envisage therefore a “*bi-polar seesaw mechanism*”.

They detect the aforementioned scale invariance, as a similar correlation is observed between the different proxies, although with different amplitude. They are therefore concerned why a discrete number of precession cycles characterizes the sequence of events even though a “full” *Termination* is eventually not completed. According to our interpretation, this depends on the erratic sequence of the arrival times of sea-urchin spikes at Earth’s surface.

They guess a dependence on the “*climate system at that time - e.g., favorable internal interplays / feedbacks of ice-sheet dynamics and size, insolation, and ocean and CO₂ feedbacks*”. However, note that a primary driver is in any case related to the amount of energy that is released by a sea-urchin spike when it arrives at Earth’s surface.

Cheng et al. (2016) also discuss the evidence related to the so-called Mid-Brunhes event (*MBE*). They claim that their records contain the so-called Mid-Pleistocene revolution, including the *MBE*, which occurs at the same time as *T-V*, and a portion of this event is correlated with a *WMI* in their record. They find that several proxies increased after the *MBE*, i.e. the amplitude of glacial-interglacial cycles in CO₂, Antarctic temperature, and global ice volume (or sea-level). Conversely, interglacial CH₄, $\delta^{18}O_{atm}$, and *AM* intensity display only a slight enhancement across the *MBE* (figure not here shown). Cheng et al. (2016) claim that the same trend has been previously reported in other low latitude hydrological records. The plotted Antarctic temperature relies on *EDC* ice core records (*EDC3* chronology), i.e. the *European Project for Ice Coring in Antarctica (EPICA)* has provided two records in East Antarctica, one at Dome C (*EDC*), and one in the Dronning Maud Land area (*EDML*).

In any case, Cheng et al. (2016) remark that across the *MBE* they observe changes in the *AM* behavior that are not as intense as variations at high latitudes and in CO₂. In addition, they remind about several examples of large *AM* intensity when ice volume was large and CO₂ was low. Moreover, they stress that the starting *AM* increase tends to occur at every respective insolation minimum, although, in some cases, it does not seem to be associated with any ice volume and/or CO₂ changes. We note that this variety of events is consistent with our interpretation that envisages a common driver for every proxy, rather than a cause-and-effect sequence between different proxies.

Cheng et al. (2016) conclude therefore that, at the orbital scale, the *AM* - and related climate and atmospheric chemistry effects - are largely controlled by *NHSI*. On the other hand, the post-*MBE* *WMIs* effects, related to *Terminations* look much stronger. In this respect, they

envisage a possible time-shift in the response of the *AM* to *NHSI*. They claim, however, that - according to their feeling - the observed shift to higher maximum ice volume is a more likely cause, as this implies a larger ice and meltwater flux during *Terminations* and stronger perturbations of “climate”, including more extreme *WMIs*. However, we stress that also the possibility ought to be taken into account of a variation vs. time of the energy release from the sea-urchin spike after its arrival at Earth’s surface.

Cheng et al. (2016) give some additional details. The first of the intense post-*MBE*-style *WMIs* is displayed by *T-V*. Their data series contains also a well-dated measurement of *AM* changes during *MIS 11*. The *MIS 11* orbital parameters appear closer to those of the Holocene, better than other recent interglacial periods. This is helpful, being an analogue for the Holocene, hence for future climate. On the other hand, they stress that timing and duration of events are still uncertain.

They estimate that the beginning of *AM MIS 11* occurred 26 ± 1 ka BP, close to the abrupt end of the *T-V* *WMI*. Suppose that the end of *AM MIS 11* coincided with the end at the *AM* minimum at 396 ± 3 ka BP. This is about the time of the half-height of the benthic $\delta^{18}O$ *MIS 11/10* shift. Hence, the duration of *AM MIS 11* was 30 ± 4 ka. If we suppose that the end was (399 ± 3 ka BP) the time of the half-height of the *AM* shift after the *AM* peak, the duration was 27 ± 4 ka. Both these estimates are consistent within the previous age uncertainties based on less precise records.

Particularly interesting is the study of the last 2 ka, as this directly fits into the present trend of climate change. Cheng et al. (2016) call it “*the 2 ka shift*”, as the *AM* displays an anomalous increase with respect to the downward trend in *NHSI*. This climate change anomaly looks much like the millennial-scale shifts over the past 640 ka. This anomaly of late Holocene is the “*the 2 ka shift*”. The plot (figure not here shown) contains: (i) the 21 July insolation at 65°N, (ii) the composite *AM* $\delta^{18}O$ records, (iii) the terrestrial $^{18}O/^{16}O$ fractionation variation, (iv) the mean grain size of sortable silt (10 – 63 μ m) for North Atlantic sediment cores *MD2251* and *MD2024*, which is a proxy of North Atlantic Deep Water formation, (v) a proxy of North Atlantic deep-flow dynamics (low field magnetic susceptibility, *k*) recorded in the cores *CH77-02* and *MD08-3182Cq*, (vi) the South American monsoon record, (vii) the $\delta^{18}O$ record (*WAIS*, a temperature proxy) from western Antarctica. During the last 2 ka the plots of (i), (vi) and (vii) show a decreasing trend, while all others show an increasing trend.

Cheng et al. (2016) comment that this 2 ka shift is not a simple regional trend in the *AM*, due to the in phase, positively-correlated shift in the $\delta^{18}O$ of atmospheric O₂, as this datum is an integration over broad regions of the world and, in large part, can respond to changes of *AM* intensity.

In addition, the *AM* shift is anti-correlated with the South American monsoon and with temperature records in some parts of Antarctica. This looks similar to the trend observed for millennial-scale events during much of the past several hundred ka. An explanation of these

millennial-scale changes was proposed in terms of a change in *AMOC*. Two studies (see references in Cheng et al., 2016) envisage a generally decreasing *AMOC* during several millennia, followed by constant or perhaps slight increase of *AMOC* before ~2 ka, during the last 2 ka (as shown in the aforementioned figure not here shown). That is, we can speculate that the origin of the “2 ka shift” is a progressive *AMOC* increase during the past 2 ka, even though harder thinking, new observations, and model studies are required.

Every guessed interpretation - that in some way ought to refer to continental or hemispherical or global scale sizes - can be supported by observations carried out on stalagmites from other continents. Cross et al. (2015) report about an investigation referring to Nevada that they summarize as follows. They refer to variations of stable isotopes ($\delta^{18}\text{O}$, $\delta^{13}\text{C}$) and trace element (Mg/Ca, Sr/Ca) in a speleothem from Lehman Caves, Nevada concerning the time interval 139 – 128 ka. The record includes the penultimate *Termination (T-II)*. Subsequent growth phases refer to records from ~123 ka, i.e., a time related to *MIS 5e* through ~84 ka and between ~82 – 81 ka (*MIS 5a*).

The chronologies were computed for two new stalagmites by means of 36 U/Th dates. Cross et al. (2015) also provide new trace element data from a previously published stalagmite *LC-2* (Shakun et al., 2011) that was measured with U/Th dating and with a stable isotope record of *T-II*. The new T-II $\delta^{18}\text{O}$ records broadly agree with the Shakun et al. (2011) and Lachniet et al. (2014) records for that period of time. The records show low values from 139 – 135 ka followed by a ~3.5‰ increase during a long interval 134 – 129 ka. This rise in $\delta^{18}\text{O}$ values is observed during Heinrich Stadial 11 and the related Weak Monsoon Interval (*WMI*) that is recorded in the Chinese caves. The Cross et al. (2015) records broadly follow the marine *Termination*, and the increase of boreal summer insolation, and of atmospheric CO_2 .

In contrast with every possible explanation in terms of changes of endogenous heat release on the planetary scale, Cross et al. (2015) appeal to “increasing atmospheric CO_2 and potentially a change in moisture source or precipitation seasonality from greater influence of the North American Monsoon accompanying summer insolation increase.” They also guess that the melting of the ice sheet is a plausible cause for the seasonal changes of both temperature and precipitation. “Trace element ratios and $\delta^{13}\text{C}$ values are largely decoupled from $\delta^{18}\text{O}$ values, showing minimal variation between 139 – 130 ka, for the duration of the Chinese *WMI*. However, these values increase sharply between 130 – 128 ka, which we interpret as increased prior calcite precipitation (*PCP*)²⁵ driven by a transition from wet to dry conditions. This abrupt drying event coincides within dating uncertainties with the abrupt strengthening of the East Asian summer monsoon, which marks the end of both the *WMI* and Heinrich Stadial 11.”

Cross et al. (2015) also show a relationship during this time between North Atlantic climate and Great Basin moisture. This is consistent with the interpretation given for the last glacial period. The prime driver can rely on abrupt shifts in *AMOC* that affects the strength of the Aleutian Low. In this respect, we note, however, that an anomalous endogenous heat release in the Baikal Rift, along the less exposed edge of the tetrahedron (Gregori and Leybourne, 2021), can be the trigger of the Aleutian Low anomaly, which affects a shift in *AMOC* etc.

The same speleothems are investigated by Steponaitis et al. (2015) referring to a more recent time, from latest Pleistocene to mid-Holocene. They refer to the same two Lehman Caves, NV speleothems, and comment that the two stalagmites together span the time-lag 16.4 – 3.8 ka, with a hiatus from 15.0 – 12.7 ka. They claim that Mg/Ca and $\delta^{13}\text{C}$ covary in the whole set of records, in agreement with a control by degassing and prior calcite precipitation (*PCP*). In fact, they stress that modern measurements of cave and soil waters support *PCP* as the primary control on trace-element composition of drip-water.

Therefore, they interpret Mg/Ca and $\delta^{13}\text{C}$ records as reflecting infiltration rates, where higher rates denote drier periods. According to both Mg/Ca and $\delta^{13}\text{C}$, a wet period occurred at the beginning of the record (12.7 – 8.2 ka), and a pronounced drying after 8.2 ka. They stress that this mid-Holocene drying agrees with records from around the western United States, and also with a new compilation of Great Basin lake-level records. In fact, Steponaitis et al. (2015) want to seek evidence correlated with lake level records in Great Basin that are indicative of dramatic changes water balance over the last 25 ka, while the timing and pace of Holocene drying is poorly documented. “*The strong temporal correspondence with the collapse of the Laurentide ice sheet over Hudson Bay suggests that this drying may have been triggered by northward movement of the winter storm track as a result of ice sheet retreat. However, we cannot rule out an alternative hypothesis that wet early Holocene conditions are related to equatorial Pacific SST. Regardless, our results suggest that Great Basin water balance in the early Holocene was driven by factors other than orbital changes.*” In fact, according to the interpretation that is here proposed, the primary driver is a change of the planetary release of endogenous energy, due to the modulation of the energy production by the *TD* dynamo inside the Earth.

Concerning the prior calcite precipitation (*PCP*) definition, it is “carbonate precipitation from infiltrating water before the water drips on a stalagmite”, according to Hori et al. (2013) who report about an investigation on stalagmites in Japan. They refer to a similar recent time interval. Their abstract can be interesting in order to envisage the information that they afford to get from this kind of analysis.

They focus on Sr/Ca, Ba/Ca, $^{87}\text{Sr}/^{86}\text{Sr}$ ratios, and on $\delta^{18}\text{O}$ and $\delta^{13}\text{C}$ values measured in a stalagmite in southwestern Japan, and spanning the interval 18.0 –

²⁵ Concerning *PCP* see below.

4.5 ka. They observe a covariance among Sr/Ca, Ba/Ca, and $\delta^{13}\text{C}$ profiles, and this is suggestive of a significant role played by PCP.

They studied also dripwater and limestone and andesite at the locality. They found relatively homogeneous data of $^{87}\text{Sr}/^{86}\text{Sr}$ ratios of the stalagmite (0.706852 – 0.706921), and they comment that this suggests a steady source mixing ratio of ~ 40% from high- $^{87}\text{Sr}/^{86}\text{Sr}$ limestone and ~ 60% from low- $^{87}\text{Sr}/^{86}\text{Sr}$ andesite. However, the Sr/Ca and Ba/Ca ratios measured in the stalagmite were higher than expected from the dissolved fraction of limestone and andesite.

The observed relations between Sr/Ca, Ba/Ca ratios and $\delta^{13}\text{C}$ values recorded in the stalagmite are consistent with the Rayleigh-type fractionation model. They support that PCP derives from successive enrichment of Sr, Ba and ^{13}C in the aqueous phase that later leads to the formation of the stalagmite.

“The degree of PCP calculated for the stalagmite is highly variable from 0 to 85%, and generally decreased from the last glacial period to the middle Holocene. The large degree of PCP observed during 18 – 15 ka implies a relatively dry climate during this period, which is consistent with weak monsoon intensity inferred by the $\delta^{18}\text{O}$ values. The $^{87}\text{Sr}/^{86}\text{Sr}$ ratios of the stalagmite show a slight decrease through the entire period. The increase in the andesite-derived fraction with relatively high $^{87}\text{Sr}/^{86}\text{Sr}$ may result from accelerated silicate weathering in the epikarst with increasing temperature, humidity, and soil $p\text{CO}_2$.”

No additional details are here given about these chemical investigations, which are outside the general perspective of the present paper. In addition, these investigations refer to a comparatively recent time.

As a general perspective, large time variations of endogenous heat release simultaneously occur through wide regions, although eventually not on the whole planetary scale. The circulation of the ocean/atmosphere system is correspondingly more or less largely changed in different regions, with suitable time delays. Large variations vs. time are therefore observed in the data series of different proxies monitored at different locations. These variations will appear correlated, although every datum with an eventual different signature and time delay. This scant information, which can be available from different locations on the globe, can help to test physical hypotheses.

Upon referring to the Xia et al. (2007) investigation, a comparison between the SB and a Brazil stalagmite shows an anti-phase relation on the millennial time-scale monsoon precipitation between the two sites (Fig. 33).

Concerning the previous available information, Xia et al. (2007) recall that *“based on high precision U/Th ages of the growth phases of speleothems and travertine deposits in northern Brazil over the past ~ 210 ka, Wang et al. (2004a) suggested that the wet periods in north-eastern Brazil correlated well to the weak EASM events (Wang et*

al., 2001b), cold periods in Greenland (Grootes and Stuiver, 1997), Heinrich events in the North Atlantic (Bond et al., 1993), and periods of decreased river runoff to the Cariaco basin (Peterson et al., 2000).”

Xia et al. (2007) also remind about the concern for climate connections, on the millennial time scale, between the two hemispheres. They shortly review this item as follows, reminding about the “seesaw” mode between the two hemispheres, envisaged by Broecker (1998).

The observational evidence shows that during the Younger Dryas (YD) the climate conditions in the northern Atlantic basin remained cold, and a simultaneous cooling has been documented in many places around the world, including New Zealand. However, $\delta^{18}\text{O}$ correlation between the ice core ^{18}O in ice records for Antarctica and Greenland, have demonstrated that in Antarctica the YD was a time of maximum warming. Broecker (1998) envisages that *“the steep rise in ^{18}O rise in Antarctic ice which commenced close to the onset of the YD might have been caused by heat released to the atmosphere in response to an increase in deep-sea ventilation in the Southern Ocean.”* Xia et al. (2007) recall that *“using the isotopic composition of O_2 as a correlation tool, Bender et al. (1994) put Greenland and Antarctic ice core records on a common time scale and suggested that the climate events were coupled between two hemispheres.”*

Blunier et al. (1998) and Blunier and Brook (2001) used the CH_4 concentration records in bipolar ice cores as a reference, and confirmed that the bipolar temperature ‘seesaw’ mode (Broecker, 1998) occurred on DO event time scale. The ‘seesaw’ mode could also account for global climate link as supported by various terrestrial and marine climate records (Broecker, 1998; Ninnemann et al., 1999; Vidal et al., 1999; Stocker, 2000; Indermühle et al., 2000). Unfortunately, the ‘seesaw’ on the millennial time scale cannot be directly identified from frequency domain analyses for the bipolar ice core records (Wunsch, 2003). In addition, the bipolar ‘seesaw’ mode may be problematic because of uncertainties induced by Δ age between the age of ice-bubble and of surrounding solid ice (Schwander et al., 1997) ... “Xia et al. (2007) conclude that their findings appear consistent with a “seesaw” mode for ocean-atmosphere coupling.

For completeness sake, however, note that - according to the rationale envisaged in the present study - the asynchronism between the two hemispheres is to be most simply explained in terms of a different amount of release of endogenous heat through different large regions of the globe - similarly e.g. to the larger present heat release that is in progress underneath the northern polar cap due to the tetrahedron pattern (Gregori and Leybourne, 2021). In contrast, a “seesaw” trend implies the concept of an oscillation. On the other hand, according to our present understanding, no physical driver or mechanism seems to justify and support from a “top-down” viewpoint such a “bottom-up” assumption.

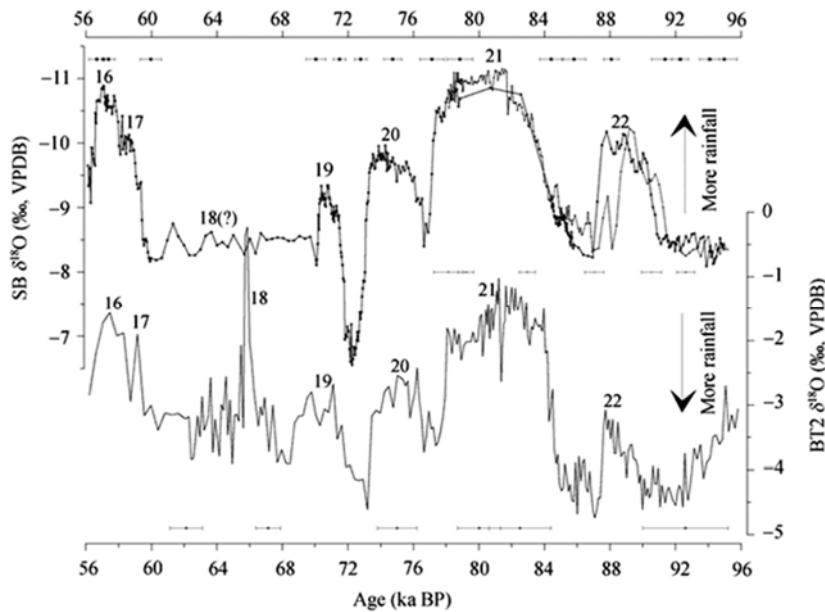


Fig. 33. “A comparison of stalagmite records between Shennongjia and southeastern Brazil. Upper is SB record with the same notes as in Fig. 30, lower is $\delta^{18}\text{O}$ record of Brazil stalagmite BT2 (Cruz et al., 2005). Error bars, from the top to the bottom, are successively for SB22, SB25 and BT2.” Figure and captions after Xia et al. (2007). With kind permission of Science China Ser. D.

Wu et al. (2009) studied a stalagmite (No. *H82*) from the Nanjing Hulu cave, spanning $\sim 22.1 - 10.3$ ka BP, with a decadal resolution. They found a detailed, complete Last Glacial Maximum (*LGM*)/deglacial history of the *EASM*. They found two centennial-scale weak monsoon events within the analogue *H1* event, and they can be correlated with corresponding records of the Greenland temperature. They stress that this is suggestive of a rapid re-organization of atmospheric and oceanic circulations during the ice-rafted debris (*IRD*) event in North Atlantic (Bond et al., 2001).

A strengthened *EASM* event, which spans $\sim 19.9 - 17.1$ ka BP and which – as they claim - they report for the first time, reaches on average a half of the monsoon intensity of Bølling warming²⁶ with its peak close to full level. Their results are synthesized in Figs 34, 35, and 36.

Shortly before the Holocene, during the Last Glacial Maximum (*LGM*), i.e. between $\sim 26,500$ and $\sim 19,000 - 20,000$ years BP (Clark et al., 2009) – and according to the geological evidence provided by lakes in western China (Yu et al., 2003) - compared to today, the lake levels were

much higher and with much fresher water. In eastern China the *LGM* conditions were much drier than today, while in western China they were somewhat wetter. This E-W asymmetric pattern of climate was completely different from the present dry-wet conditions, which display a N-S asymmetry.

According to an atmospheric global circulation model (*AGCM*) implemented by Yu et al. (2003), the dry conditions in eastern China resulted from a reduced summer precipitation due to the Pacific Subtropical High, which overlies eastern China while the summer monsoon declines. The wet conditions in western China were a consequence of the decreased evaporation due to a low temperature on land surface at the time of the *LGM* and to an increase in precipitation. They suggest that the feedback within the climate system from the Asian land surface seems to amplify and modify the external forcing.

According to Clark et al. (2009), the ice sheets attained their maximum positions between $\sim 33.0 - 26.5$ ka due to climate forcing derived from a decrease of insolation in the northern summer, of *SST* in tropical Pacific, and of atmospheric CO_2 . From 26.5 ka to $\sim 19 - 20$ ka nearly all

²⁶ Bølling oscillation is called a warm interstadial period between the Oldest Dryas and Older Dryas stadials, at the end of the last glacial period. In regions where the Older Dryas is not detected in climatological evidence, the Bølling-Allerød is considered a single interstadial period. At the beginning of the Bølling a sharp temperature rise occurred, which marked the end of the Oldest Dryas $\sim 14,670$ years BP (but, most of the recent estimated dates are slightly different, scattered within a few hundred years). The Bølling-Allerød interstadial was warm and moist during $\sim 14,700 - 12,700$ years BP. It ended abruptly with the onset of the *YD*. During *YD*, climate cooled, reaching within a decade temperatures back to near-glacial levels. In some regions, the Older Dryas, which is a cold period, can be

detected in the middle of the Bølling- Allerød interstadial, and the period is further divided into the Bølling oscillation, peaked around $\sim 14,500$ BC, and the Allerød oscillation, peaked closer to $\sim 13,000$ BC. Note that the closer the observed phenomena are to our epoch, the greater is the available information and detail. Hence, a larger number is reported of small-duration sub-events. According to the interpretation that is here proposed, these details reflect the different arrival times of sea-urchin spikes at Earth’s surface. Every spike thus affects at a different time the planetary ocean/atmosphere circulation, triggering time-delayed effects on the climate of other regions. Therefore, in principle, every minor event of this kind, in general, ought to be expected to display a “saw-tooth” trend, due to the “calorimetric” principle.

ice sheets were located at their *LGM* positions, corresponding to minima in these forcings. An increase in northern summer insolation $\sim 19 - 20$ ka triggered the onset of *NH* deglaciation, being the source for an abrupt rise in sea-level. The deglaciation of the West Antarctic Ice Sheet began between $\sim 14 - 15$ ka, and this is consistent

with an abrupt rise in sea-level ~ 14.5 ka BP. Let just remark that no role is considered to be associated to a time variation of endogenous heat release.

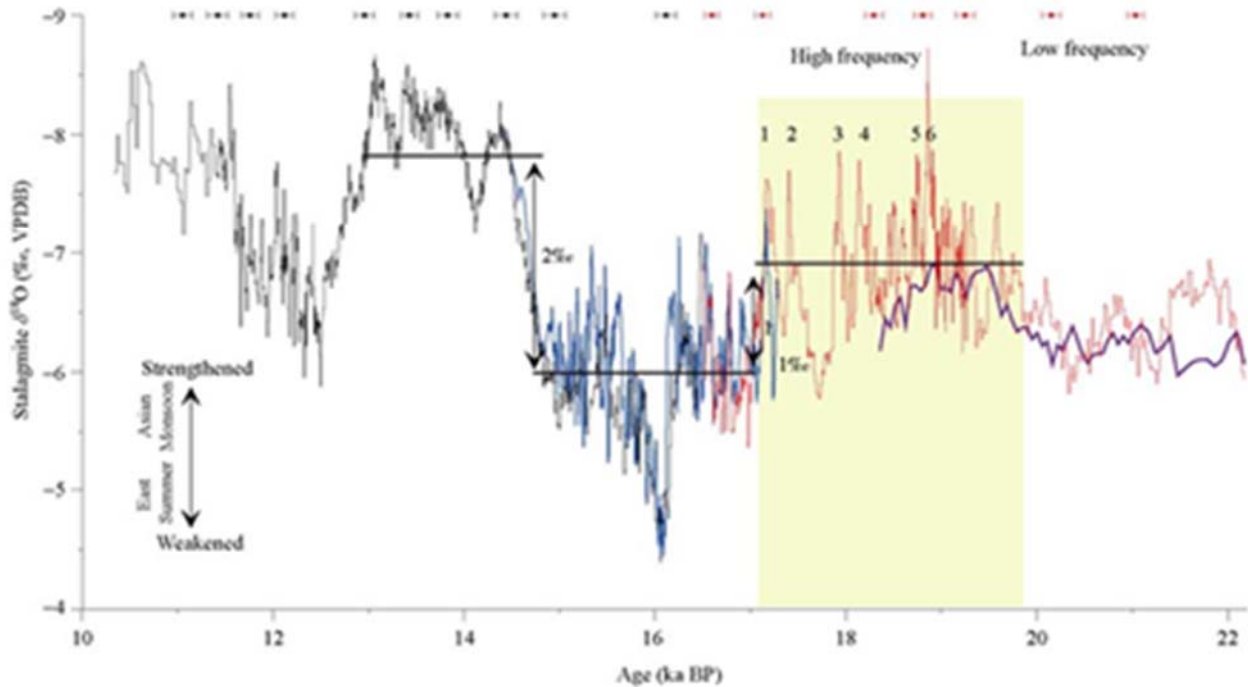


Fig. 34. $\delta^{18}O$ time series from the stalagmites from Hulu cave. Blue and purple lines represent the $\delta^{18}O$ curves of other two contemporaneous stalagmites (*YT* and *MSD*; see Wang et al., 2001b). Gray and red lines represent the $\delta^{18}O$ curve of *H82* during $\sim 16.5 - 10$ ka BP and $\sim 22 - 16.5$ ka BP, respectively. ^{230}Th ages are plotted with black and red $\pm 2\sigma$ error bars. Numbers 1 to 6 denote the six peaks of $\delta^{18}O$ record during $\sim 19.9 - 17.1$ ka BP. After Wu et al. (2009). With kind permission of *Science China Ser. D*.

Li and Kang (2006) and Ge et al. (2007) synthesize into a short review the more recent achievements in the study of Holocene in the Himalaya region. Li and Kang (2006) claim that, in general, the Holocene was warm, and a gradual rise of temperature occurred during the last 2000 years, and the increase was more rapid in recent decades. On the Tibetan Plateau (*TP*) climate changes occurred earlier, on different time scales, and the amplitude of climate change was more pronounced than in other parts of China. We note that this is consistent with an increase of soil exhalation due to an increased friction heat derived from tectonic activity.

Li and Kang (2006) introduce their review and remark that the SE monsoon from the Pacific Ocean and the SW monsoon from the Indian Ocean directly influence, respectively, the eastern and southern parts of the *TP*. In addition, the *TP* in winter and spring divides the westerlies into two branches. In general, Li and Kang (2006) distinguish the *TP* into three areas, according to atmospheric phenomena (Feng et al., 2001). Climate change in the north of the plateau seems to have always been influenced by the westerlies in every season.

The Guliya ice core is located in the northern part of the plateau (e.g. Yao et al., 1995). They note that the associated high resolution records extend to the last inter-glacial

period. In addition, since the coring is at high altitude, i.e. close to the stratosphere, the records are particularly significant of the impact of the *TP* on the atmosphere. The records should therefore show a great coherence with the data from the Greenland ice core since the last inter-glacial period. That is, the Guliya ice core can be considered as particularly significant to represent long term climate change.

Li and Kang (2006) give the map shown in Fig. 37, which is very helpful for localizing the sites where records were collected. Also a figure (not here shown) is helpful shown by Harrison et al. (1992).

Li and Kang (2006) divide climate change - which occurred since the last inter-glacial period - into three general stages, referring mostly to temperature fluctuation, i.e. (i) the last inter-glacial and the last glacial period ($\sim 125 - 10$ ka BP), (ii) the abrupt climate change known as *YD* ($\sim 12.2 - 10.9$ ka BP), and (iii) the Holocene after *YD*.

The most useful index is $\delta^{18}O$. The major climatic events are displayed in Fig. 38. "Since ~ 125 ka BP, the *TP* has entered into the last inter-glacial period, which is corresponding to the deep sea oxygen isotope stage 5 (Fig. 38). Guliya ice core records showed that the climate of the *TP* fluctuated intensely and several warm-cold cycles

occurred in the time scale of thousand years during the last interglacial period. The temperatures of three warmest periods (5a, 5c, 5e) are ~ 3°C, ~ 0.9°C and ~ 5°C higher than the present, respectively, and the change amplitude of temperature during the 5e is even higher than the recent

world average value, while in the two cold stages the temperature of 5b and 5e dropped by ~ 3°C and ~ 4°C from 5e and 5c, respectively, also there are many hundred year scale warm-cold fluctuations at each stage.”

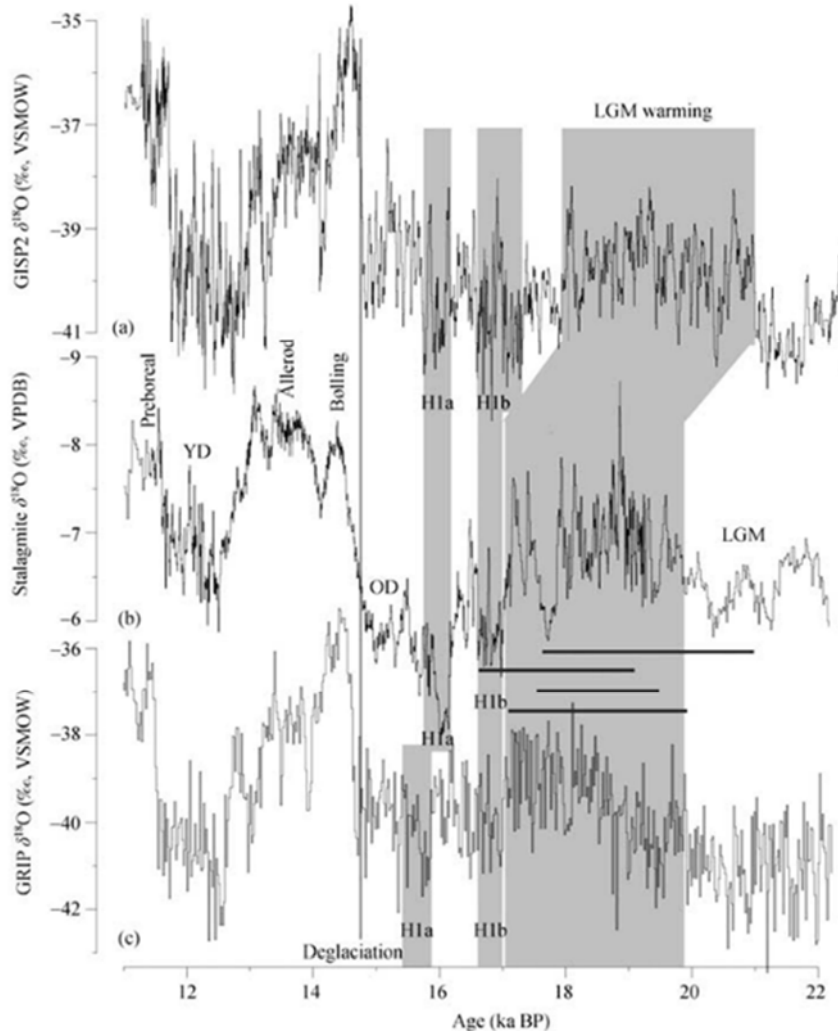


Fig. 35. “Comparison between $\delta^{18}O$ records from Hulu stalagmite and Greenland ice cores. (a) GISP2 ice core $\delta^{18}O$ record (Stuiver and Grootes, 2000); (b) stalagmite H82 $\delta^{18}O$ record; (c) GRIP ice core $\delta^{18}O$ record (Johnsen et al., 2001). H1a and H1b represent the cooling events at Greenland and weakened monsoon events at low-latitude in H1 event, respectively. Shadow parts indicate the strengthened EASM event recorded in stalagmite and the LGM warming recorded in Greenland ice cores. The black vertical line indicates the isochrone of the last deglaciation. The gray horizontal lines represent the warming time intervals of different oceans, from the above to the bottom are: record of SST in Santa Barbara basin from North Pacific (Hendy et al., 2002); records of SST in two sub-polar North Pacific cores ODP883 and MD01-2416 (Kiefer et al., 2006) and record of SST in California offshore site (Seki et al., 2002); record of SST derived from alkenones measured in Indian ocean (Bard et al., 1997a); record of SST in equatorial Pacific core V21-30 (Koutavas et al., 2002).” Figure and captions after Wu et al. (2009). With kind permission of Science China Ser. D.

Li and Kang (2006) remark that the Guliya ice core displays a remarkable correlation with the records of the GRIP and GRIP2 ice cores, but the Guliya $\delta^{18}O$ displays larger amplitude variations, and its changes always precede the GRIP ice core’s trend. For instance, when the subinterglacial period changed into the subglacial period, compared to the GRIP ice core’s, Guliya’s changed more dramatically. In addition, on the short time scale, it displayed comparatively larger climatic fluctuations.

Li and Kang (2006) also mention the Ruergai (RM) hole (see Fig. 37) in eastern TP (Wu and Wang, 1996), where the last inter-glacial period, ~ 140 – 80 ka BP, is evidenced by $\delta^{18}O$ and ^{14}C in lake sediments. Compared to Guliya, this period occurred a little earlier, but the general trend of fluctuations was almost the same.

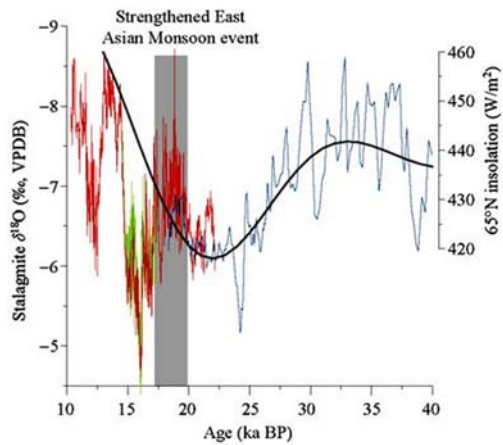


Fig. 36. “Comparison between stalagmite $\delta^{18}O$ record from Hulu cave and summer insolation. Red, green and blue lines represent the $\delta^{18}O$ records from samples H82, YT and MSD, respectively. Gray line represents the average summer insolation at $65^{\circ}N$; shadowed area indicates the

strengthened EASM event.” Figure and captions after Wu et al. (2009). With kind permission of *Science China Ser. D*.

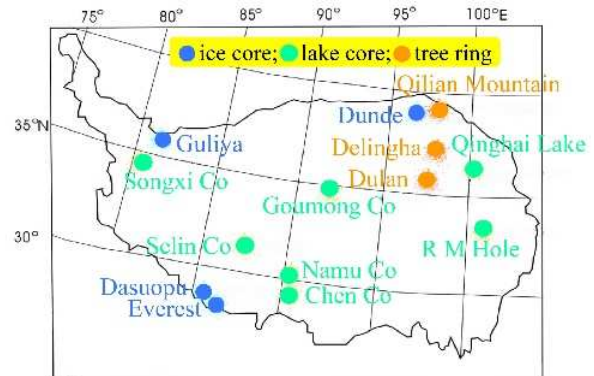


Fig. 37. “Main sites relating to the reconstruction of the past climate on the Tibetan Plateau.” Figure redrawn and captions after Li and Kang (2006). Unpublished figure.

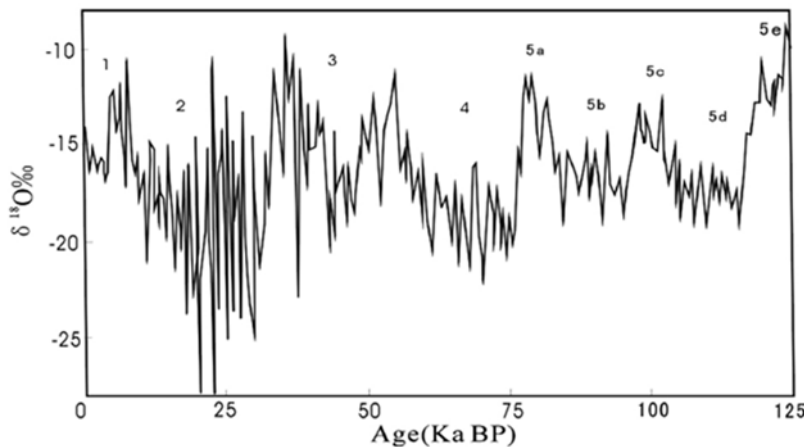


Fig. 38. The main climate change events on the TP occurred since the last inter-glacial period. Figure after Yao et al. (1997a) (also in Li and Kang, 2006). With kind permission of *Science in China, Series D*.

“In general, the temperature drop was fast and abrupt while temperature rise was slow. The switch from the last inter-glacial period to the last glacial period (according to deep sea isotope stage 4) took place abruptly over the TP. From the records of the Guliya ice core, the temperature had dropped by $\sim 12^{\circ}C$ during the 3000 years from 5a warm summit to stage 4.

The last glacial period can be divided into three stages: early ice stage (75 – 58 ka BP), inter ice stage (58 – 32 ka BP) and late ice stage (32 – 10 ka BP). In the SE of the TP this period ended ~ 18.5 ka BP (Xu et al., 2004), a little earlier than the Guliya ice core.”

The coldest temperature of this period recorded by the Guliya ice core occurred ~ 23 ka BP. Tang et al. (1998a), based on pollen records in lake sediment, found that TP entered into the Last Glacial Maximum $\sim 25 - 15$ ka BP. The warmest time of this period was 58 – 32 ka BP.

Tang et al. (2000a) state that “high-resolution pollen records from 6 small lakes in the TP provided the details of evolution of South Asian monsoon since the Last Glacial Maximum. Prior to 16 ka BP, the region was a desert-steppe characterized by cold and dry climates, the January temperature was $7 - 10^{\circ}C$ lower than that of present and

the annual precipitation only accounted for 40% of the present.

The temperature and precipitation increased gradually and trees began to live in the region after 12 ka BP, but during the interval 9.2 – 6.3 ka BP, forest and forest-meadow appeared occasionally. From 8 to 5 ka BP, both January and July temperature was $2 - 3^{\circ}C$ higher and annual precipitation was also about 200 mm higher than that of the present. After 5 ka BP, temperature and precipitation decreased linearly and steppe vegetation began to degenerate.”

Shi et al. (1999a) - based on ice core records of high levels of lakes, and vegetation changes - found that TP experienced an abnormal warm and humid period during $\sim 40 - 30$ ka BP. The temperature was $\sim 2 - 4^{\circ}C$ higher than at present and precipitation $\sim 40\%$ or even several times larger, being suggestive of “an unusual strong summer monsoon which corresponded with high solar radiation stage of the ~ 20 ka precessional cycle.”

Concerning the YD event of ~ 12 ka BP, i.e. during the transition from the last glacial period to the Holocene, its first evidence is found in the records from the Atlantic coasts (Pettet, 1995). Then, it triggered climate and

environmental changes in other continents, including an “*extensive and profound effect on the TP*”. In general, the *YD* records are better evident in north-western than in southern *TP* (Yao and Yang, 1994). The Guliya ice core gives the best evidence in the *TP*, dating ~ 12.2 – 10.9 *ka BP*. Three stages of temperature decrease occurred (Fig. 39): (A) ~ 12.2 – 11.8 *ka BP*, (B) ~ 11.8 – 11.4 *ka BP*, and (C) ~ 11.4 – 10.9 *ka BP*, displaying a temperature drop of, respectively, ~ 5°C, ~ 6°C, and ~ 2°C. The minimum temperature occurred ~ 11.05 *ka BP*. Then, it gradually increased, until the dramatic increase occurred ~ 10.9 *ka BP*, which marked the end of *YD* and the start of Holocene.

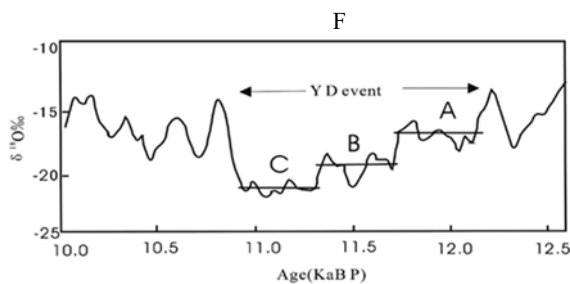


Fig. 39. The *YD* evidence, in *TP* according the Guliya ice core. Figure after Yang and Yao (1997), also in Li and Kang (2006). With kind permission of *Chinese Science Bull.*

The *YD* began and ended at different times in different regions of the *TP*. For instance, Gasse et al. (1991) found a remarkably cold-dry climate during ~ 11 – 10 *ka BP* in the records of the Songxi Co lake sediment, which are similar to the records from the Qinghai Lake (Liu et al., 2002) and Selin Co Lake (Lin and Wu, 1981; Hou et al., 2021), while the Gounong Co records dating is ~ 4 *ka* earlier (~ 11.5 – 10.4 *ka BP*).

Compared to the Guliya’s dates, all records from lake sediments occurred later, and the duration of every event was shorter. In general, the date of *YD* is mainly ~ 11 – 10 *ka BP* in most areas of the *TP*. Only at few sites it is found at ~ 12 *ka BP*. The coldest time appears, however, consistent and centered at ~ 10.5 – 10.7 *ka BP*, being similar to the records from the Atlantic coasts. Therefore, the records of the *YD* event collected on the *TP* appear to have a global significance (Broecker et al., 1988; Zhu et al., 2004).

Concerning the cause of the whole *YD* event, Li and Kang (2006) mention that – even though there are some disagreements about the reason and original trigger site (Smith, 2000) - many authors agree on the fact that it ought to have been caused by a stagnation in the production of North Atlantic deep water, which originated the great temperature drop that finally affected other regions of the world. See, however, some comments in Gregori et al. (2025h), as nobody seems to be aware of the possible spacetime variations of endogenous heat release. In fact, a different time variation of the release of endogenous energy in different regions is the simplest possible explanation of this very intricate trend of the spacetime distribution of climate temperature over the globe.

After the *YD* event, the global temperature quickly

raised into the Holocene, which has been the last glacier-melting period. However, Kutzbach and Guetter (1986) considered it as another inter-glacial period. Solar radiation increased during this period. During this period both the Guliya’s and the Dunde’s (Fig. 40) ice cores, from the north and east of *TP*, display clear warm records. After *YD* the temperature began to increase and it entered the Holocene Megathermal until ~ 7 *ka BP*, when a sudden temperature drop occurred. This was the end of the Holocene Megathermal.

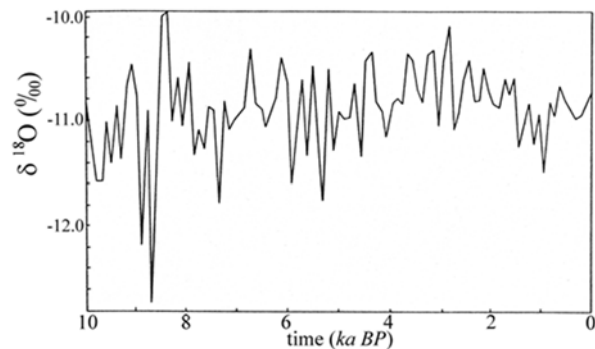


Fig. 40. Variation of $\delta^{18}O$ in the Dunde ice core during the last 10 *ka*. Every plotted point is an average over 100 years. Adapted after Shi et al. (1992). Reproduced with kind permission.

A relative cold period occurred during ~ 7.2 – 5.0 *ka BP*, and temperature finally steadily increased after ~ 5.0 *ka BP*. These results are also supported by the investigations by Li et al. (1994a) and Wu et al. (2004), shown in Fig. 41. Some differences were found, however, between these two ice cores. The starting time was found earlier in Guliya’s than in Dunde’s, the amplitude of the temperature larger, and the change rate slower. Maybe - they comment - the difference depended on the atmospheric systems that controlled the two sites.

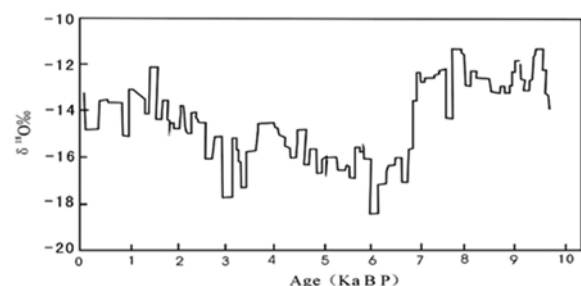


Fig. 41. Temperature records during the Holocene on the *TP*. Fig. after He et al. (2003a), also in Li and Kang (2006). With kind permission of *J. Glaciol. Geocryol.*

Concerning the evidence from Arctic Norwegian peatland, Nichols et al. (2009a) state that the middle Holocene, 7.5 – 5.5 *ka*, was characterized by a warm and dry climate, which from the mid-Holocene to the present later progressively changed towards cooler and wetter conditions. In fact, the seasonal precipitation during the Holocene displayed changes that look coherent with changes in *SST* in the Norwegian Sea, and with higher *SST* correlated with a larger percent of winter precipitation. The

high SST in the Norwegian Sea, and also a greater moisture in northern Europe during winter, look correlated with a large gradient between the subpolar low and subtropical high over the North Atlantic, i.e. with a positive North Atlantic Oscillation (NAO).

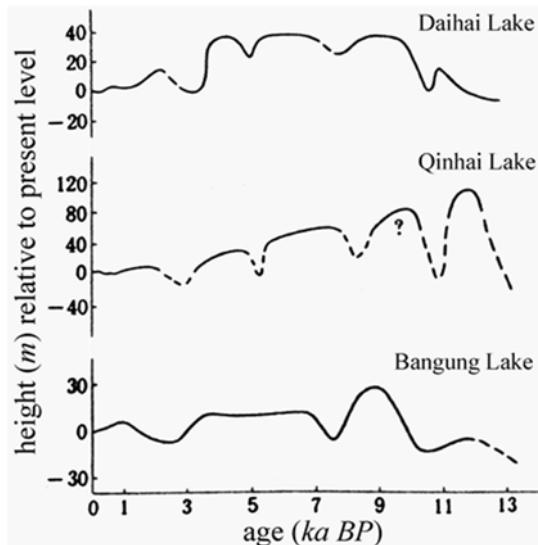


Fig. 42. Some lake level variations in China, relative to present. After Shi et al. (1992a). Reproduced with kind permission granted from *Science in China Series B, Chemistry*. The Managing Director of *Science China Press*, Zhixin Wang, very kindly provided a high-quality copy of the paper.

Li and Kang (2006) claim that, in general, during the Holocene the climate change appears more pronounced in the northern TP, and claim that this is the likely consequence of the changes occurred in the Southwest Monsoon, which mainly affected the southern TP. Hong et al. (2004) found several consistencies between the history of Southwest Monsoon during the Holocene and the reconstruction of climate change on the TP, especially on the southern TP. Fig. 42 shows some results from a few lake cores.

That is, whether the primary energy source is heat transport by a change of oceanic circulation - or rather an effect of ocean water warming by an increase of endogenous heat release - a stronger gradient between the subpolar low and subtropical high over the North Atlantic (or positive NAO) implies an increase of SST temperature and also of winter precipitation, i.e., a comparatively greater atmospheric dynamics. In either case, the North Pole area is a comparatively larger heat source for atmospheric dynamics, reminding about a somewhat analogous role played – both in the geological past and at present - by the Himalaya (the “Third Pole”). This reminds also about the ongoing climatic anomaly over the northern polar cap associated with the North Pole vertex of the tetrahedron (Gregori and Leybourne, 2021; see Gregori et al., 2025g and 2025h).

Similarly, the regional difference during the Holocene Megathermal showed the effect of monsoon on different TP areas. Liu et al. (1997) summarized the results of the Holocene Megathermal, which first appeared in northeastern and southern TP, and later spread through the

whole TP. However, the retreat began from the central TP, in correspondence with a precipitation decrease, observed in the same period, from south, east, and north towards central TP. These phenomena are indicative that monsoon intensity is closely related to the change of temperature and precipitation during the Holocene.

A stable warm and wet period followed during ~ 7.2 – 6 ka BP, being the Megathermal maximum. According to Guan et al. (2010), the maximum warming occurred during 72 – 71.4 ka BP. A significant increase occurred of summer monsoon precipitation in eastern China, in Xinjiang, in the Inner Mongolia, and in northern China. Vegetation was exuberant. It was the most prosperous and powerful time of the Yangshao culture of the Neolithic period (Fig. 44). In contrast, the millennium between ~ 6 – 5 ka BP was characterized by strong climatic fluctuations, resulting into the comparably worst environmental conditions. A sharp decrease of temperature influenced the development of culture.

Climate in China

Shi et al. (1992a) state that the Holocene Megathermal in China spanned the time lag ~ 8.5 – 3 ka BP (see Figs 40, 42, and 43). During this ~ 5.5 ka period large climate fluctuations occurred, including severe cold periods. A particularly unstable period occurred during ~ 8.5 – 7.2 ka BP, with alternating warm and cold events. Precipitations increased, the botanic belt moved northward and westward, the culture of the Neolithic Age (New Stone age) rapidly developed.

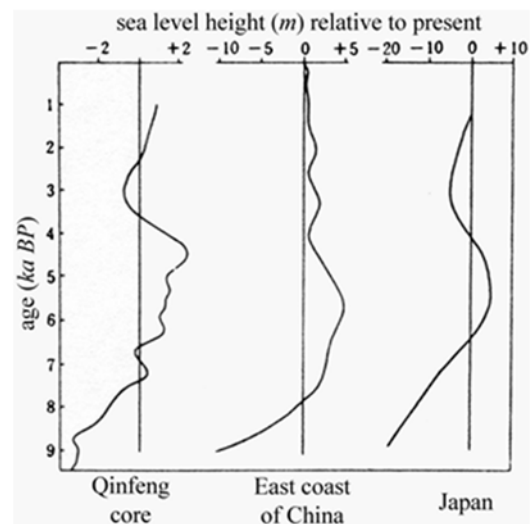


Fig. 43. Sea-level variations relative to present in the Eastern China Sea. After Shi et al. (1992a). Reproduced with kind permission granted from *Science in China Series B, Chemistry*. The Managing Director of *Science China Press*, Zhixin Wang, very kindly provided a high-quality copy of the paper.

Note that, natural climate change always occurred and severely influenced the humans and their culture

E.g., a recent study (Carolin et al., 2019) by means of a speleothem geochemical record from northern Iran envisages an “enhanced dust activity, indicating a threshold

behavior in response to aridity. Coincident gradual peaks in $\delta^{18}O$ support the interpretation of regional drying. The precise chronology shows the later event, 4.26 ka – 3.97 ka, is coincident within decades of the period of abandonment of advanced urban settlements in northern Mesopotamia”. That is, maybe, the Akkadian Empire fell by dust. Was this a natural phenomenon, or was it related to an improper management of environment?

In contrast, the humans always believed (and presently often believe) that the environment is an invariant condition vs. time. This is certainly a utopia, an illusion. On the other hand, on several occasions the humans certainly had a more or less great responsibility in the determination of the fate of their “cultures”.

E.g., let us quote a few recent studies. Defleura (2019) investigated how the last interglacial climate change impacted the ecosystems and the Neanderthals behavior as

observed at Baume Moula-Guercy, Ardèche, France. He comments that a major warming occurred during the last interglacial period (Eemian, MIS 5e, LIG 128 – 114 ka). Flora and fauna experienced a geographical redistribution due to the rapid climate change. Owing to the scarcity of archaeological sites that are representative of this period, the behavior of Neanderthal hunter-gatherers in Western Europe due to these events is poorly understood. According to new evidence, the challenges can be investigated that the Neanderthals had to face when new ecosystems and ecological communities formed. Defleura (2019) argues that, on the European continent, a collapse of human population occurred, although it could survive only in a few regions. In addition, Defleura (2019) suggests that at the beginning of the Upper Pleistocene these environmental changes caused a depletion of prey biomass, and contributed to the rise of cannibalistic behavior in Neanderthals.

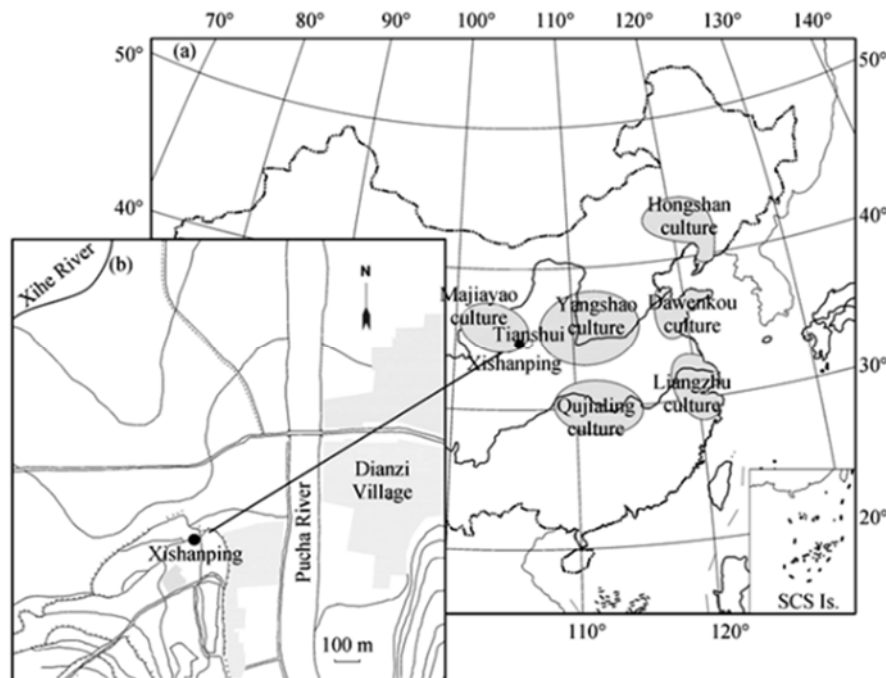


Fig. 44. “(a) The main culture regions in mid-Late Neolithic China; (b) the map of Xishanping archaeological site.” Figure and captions after Li et al. (2007). With kind permission of Science in China, Series D.

The causes of the fall of the Byzantine Empire were investigated by Bar-Oz et al. (2019). “Historians have long debated the role of climate in the rise and fall of empires of the 1st millennium AD. Drastic territorial contraction of the Byzantine Empire, societal decline, and beginning of the European Middle Ages have generally been linked to the Islamic conquests of the 7th century. This multidisciplinary archaeological investigation of trash mounds in the Negev Desert establishes the end date of organized trash management in the Byzantine-period city of Elusa and demonstrates urban collapse a century before the Islamic transition. Our findings, taken together with other evidence for Byzantine urban dysfunction, the Justinianic Plague, and recent research on the Late Antique Little Ice Age, flesh out the impact of the 6th century on broad historical trajectories.” Weisberger (2019b), while announcing the aforementioned investigation claims that “at that time, a climate event known as the Late Antique Little Ice Age was

taking hold in the NH, and an epidemic known as the Justinian plague raged through the Roman Empire, eventually killing over 100 million people.” The impact of the Little Ice Age certainly had implications that contributed to shape present world (Blom, 2019). Kocha et al. (2019) report about a study on “whether the decline in global atmospheric CO₂ concentration by 7 – 10 ppm in the late 1500s and early 1600s which globally lowered surface air temperatures by 0.15°C, were generated by natural forcing or were a result of the large-scale depopulation of the Americas after European arrival, subsequent land use change and secondary succession.” They conclude that, maybe, “the Great Dying of the indigenous peoples of the Americas resulted in a human-driven global impact on the Earth System in the two centuries prior to the Industrial Revolution.” The active role (“pollution”) caused by the humans dates back to several ten thousand years ago, as shown by Schreuder et

al. (2019). Their study is explained by Cook (2019), who claims that “Schreuder *et al.* present a continuous, 192,000 year long record of fire history in sub-Saharan northwest Africa. The team reconstructed the rate of accumulation of levoglucosan, a fire biomarker, from a marine sediment core extracted offshore of Guinea and sampled for organic geochemical analyses at 5 cm intervals. The results indicate that after remaining relatively steady for > 100,000 years, the rate of levoglucosan accumulation nearly doubled about 80,000 years ago. However, because the sedimentation rate and the rate of accumulation of other organic compounds increased at the same time, the authors attribute this change to an overall increase in sediment accumulation rather than increased biomass burning. [That is, this was natural climate change.] The new record also contains two significant spikes in the rate of levoglucosan accumulation, at about 57,000 and 55,000 years ago, a period that roughly corresponds to the onset of marine isotope stage 3. Because the peaks don’t correlate with any observed changes in sedimentation rate, the authors ascribe them to increased biomass burning in sub-Saharan northwest Africa. These findings suggest that changes in vegetation and regional climate did not exert a major long-term influence on the region’s fire history. The researchers attribute the two fire events to a greater abundance of C3 vegetation, combined with increased human settlement, and a resulting uptick in fire use at a time when other lines of evidence suggest the savanna became wetter and thus more hospitable to humans. Collectively, these results suggest there is a tantalizing connection between changes in climate, vegetation, and human fire history that coincide with a major period of hominin dispersal out of Africa. According to genetic and archaeological evidence, this wave of migration occurred between about 60,000 – 40,000 years ago and set the stage for the colonization of the other continents.”

This is the so-called Cycle of Climate and Civilization (see e.g. Gregori *et al.*, 2000, and Gregori, 2002a). A huge disciplines ought to be developed, with an astute analysis of uncertainties and critical assumptions, in cooperation between Earth’s scientists and also humanistic specialists (historians, archaeologists, linguists, geneticists, etc.) in order to exploit “environmental anthropology”, but this enormous topic is outside the general framework of the present study.

Subsequently, after ~ 5 ka BP climate and environmental conditions improved and archaeological sites correspondingly increased (Fig. 45). Climate worsened again close to ~ 4 ka BP, with catastrophic floods and spates. Then, climate became anew warm and wet until ~ 3 ka BP.

Ge *et al.* (2007) state that “the Megathermal was the warmest period of the Holocene in China, but a series of

cold events occurred in ~ 8.7 – 8.5 ka BP, ~ 7.3 ka BP, ~ 5.5 ka BP and ~ 4.4 ka BP.”

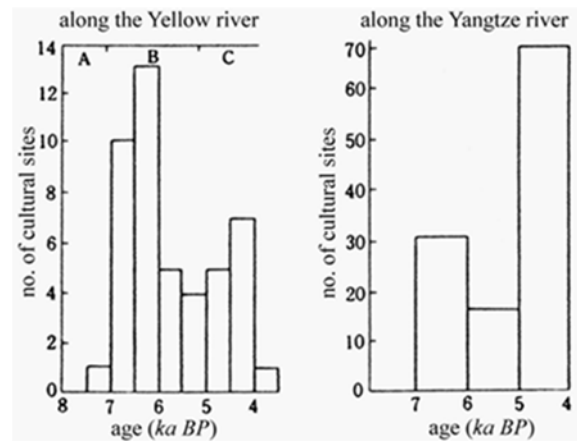


Fig. 45. Number of Neolithic sites along the Yellow River and Yangtze (or Yangzi, or Cháng Jiāng) river during the last ~ 8 ka. (A)-Pre-Yangshao culture; (B)-Yangshao culture; (C)-Longshan culture. After Shi *et al.* (1992a). Reproduced with kind permission granted from *Science in China Series B, Chemistry*. The Managing Director of *Science China Press*, Zhixin Wang, very kindly provided a high-quality copy of the paper.

Li and Kang (2006) specifically address the climate change observed during the last ~ 2000 years, when, owing to a better database, climate reconstruction is more reliable. The historical information from other studies is reviewed by Ge *et al.* (2007) (Figs 46 and 47). Additional analysis on tree rings (not here reported) are described by Yao *et al.* (2001a), Shao *et al.* (2005), and Liu *et al.* (2006g). Let us only mention some results by Liu *et al.* (2009b) dealing with the annual temperatures estimated by tree rings during the last 2485 years in the mid-eastern TP. They carried out a suitable discussion on error bars, calibration, etc. Only Fig. 48 is here reported, and their brief summary.

Liu *et al.* (2009b) comment that “the climate variations ... indicate that there were four periods to have average temperatures similar to or even higher than that mean of AD 1970 to AD 2000. A particularly notable rapid shift from cold to warm, we call it the ‘Eastern Jin Event’, occurred from AD 348 to AD 413.” They also carried out a careful comparison with the temperature variation in other areas and found the “the temperature variations over the mid-eastern TP are not only representative for large parts of north-central China, but also closely correspond to those of the entire NH over long time scales.”

[This is consistent with the interpretation that is here proposed, in terms of a synchronous planetary change of endogenous heat release, although with eventual relevant space gradients.] They also note that “during the last 2485 years, the downfall of most major dynasties in China coincides with intervals of low temperature.”

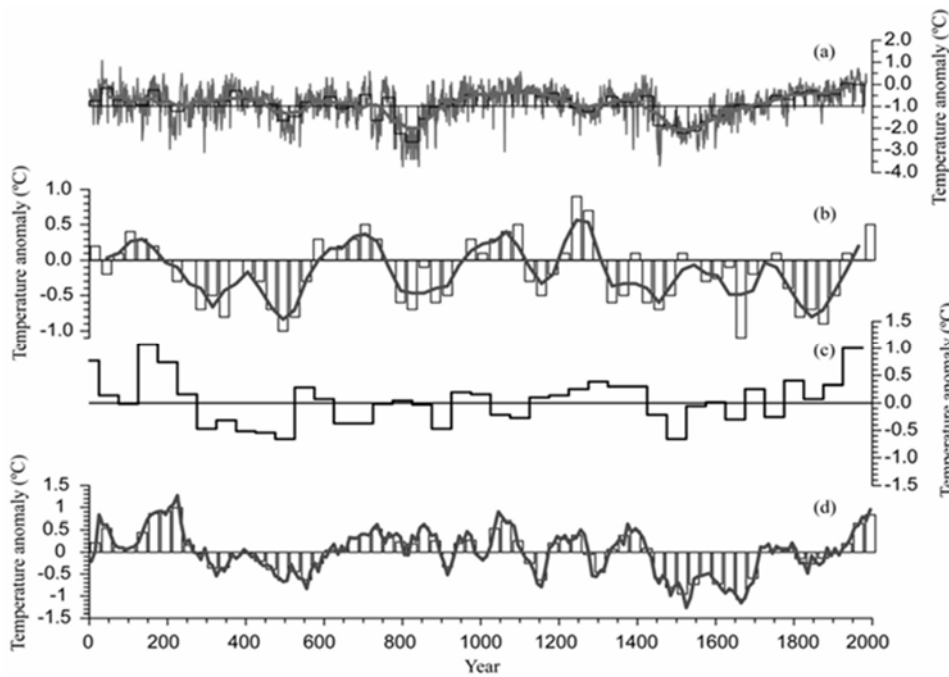


Fig. 46. “The reconstructed temperature series during the last 2000 years in China derived from various historical climate proxy data. (a) summer temperature (May-August) in Beijing by Tan et al.(2003), line: annual temperature, bar: temperature change with 30 year resolution; (b) Winter half year temperature in Eastern China at 30 year time resolution by Ge et al.(2003); (c) temperature change at 50 year resolution in whole TP by Yang et al. (2003); (d) Weighted temperature reconstruction over China by Yang et al. (2002, 2002a), line: 10 year resolution, bar: 30 year resolution.” Figure and captions after Ge et al. (2007). Reproduced with kind permission after *China Nat. Rep. Met. Atmos. Sci.* (2003-2006).

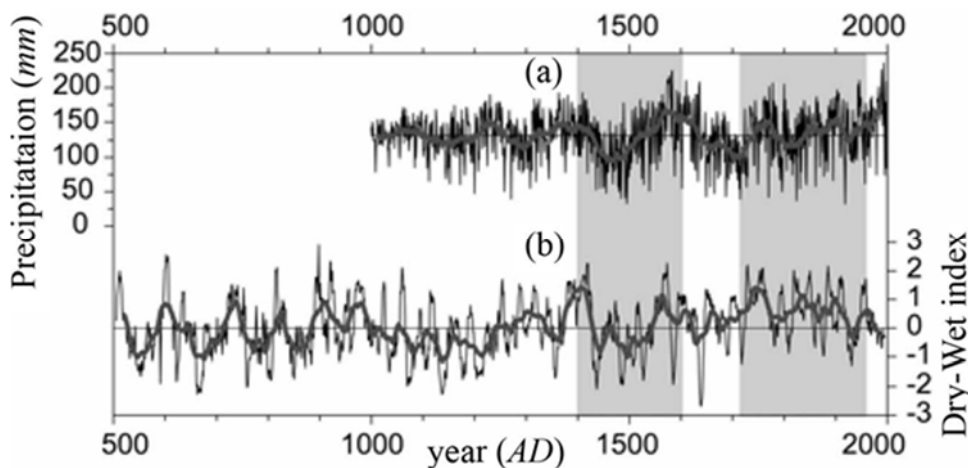


Fig. 47. “The reconstructed precipitation (dry/wet) series from the tree ring in western China during the last 1000 years (a) (Shao et al., 2004), and historical document in eastern China during the last 1500 years (b), (Zheng et al., 2006a). The consistent increasing or decreasing change trend is marked with shaded area. The heavy line is 31 year running average smoothing.” Figure and captions after Ge et al. (2007). Reproduced with kind permission after *China Nat. Rep. Met. Atmos. Sci.* (2003-2006).

In any case, they stress that “compared with the temperature records in other regions of China during the last 1000 years, this reconstruction from the TP shows a significant warming trend after the 1950s.” This last statement is in agreement with the general evidence of an ongoing increase of the planetary release of endogenous energy, associated with the current “Iceland” heartbeat of the Earth’s electrocardiogram (see Gregori et al., 2025a).

Reporting the analysis by Li and Kang (2006), Fig. 49 shows a synthesis by Yang (2003) that includes temperature records from ice core (Yao, 1995; Yao et al., 1995), from tree rings (Kang et al., 2000), from lake sediments (Zhang et al., 1994), and glacier fluctuations.

Remarkable warm periods are observed on the TP, on ~AD 1000, ~AD 1150-1400 (the Medieval Warm Period), and ~AD 1700. The 3rd-5th century AD were cold periods.

Some difference occurred of temperature variation in different regions. The Medieval Warm Period lasted a little longer, but the temperature was lower, in southern compared to northeastern TP. In addition, the temperature decreased in northwestern TP.

The warm period that occurred in the eastern China was only found in northeastern TP, while southern and northern TP experienced the general cold period. The Little Ice Age appeared earlier in northeastern than in southern TP, in contrast to what occurred in northwestern TP. The Guliya ice core temperature not only increased, but it also became warmer than during Middle Ages, although colder than the Little Ice Age during 7th-9th centuries. Summarizing, during the last ~ 2000 years the temperature variation displayed no regular trend, and the change in western TP was opposite to the changed occurred in southern TP.

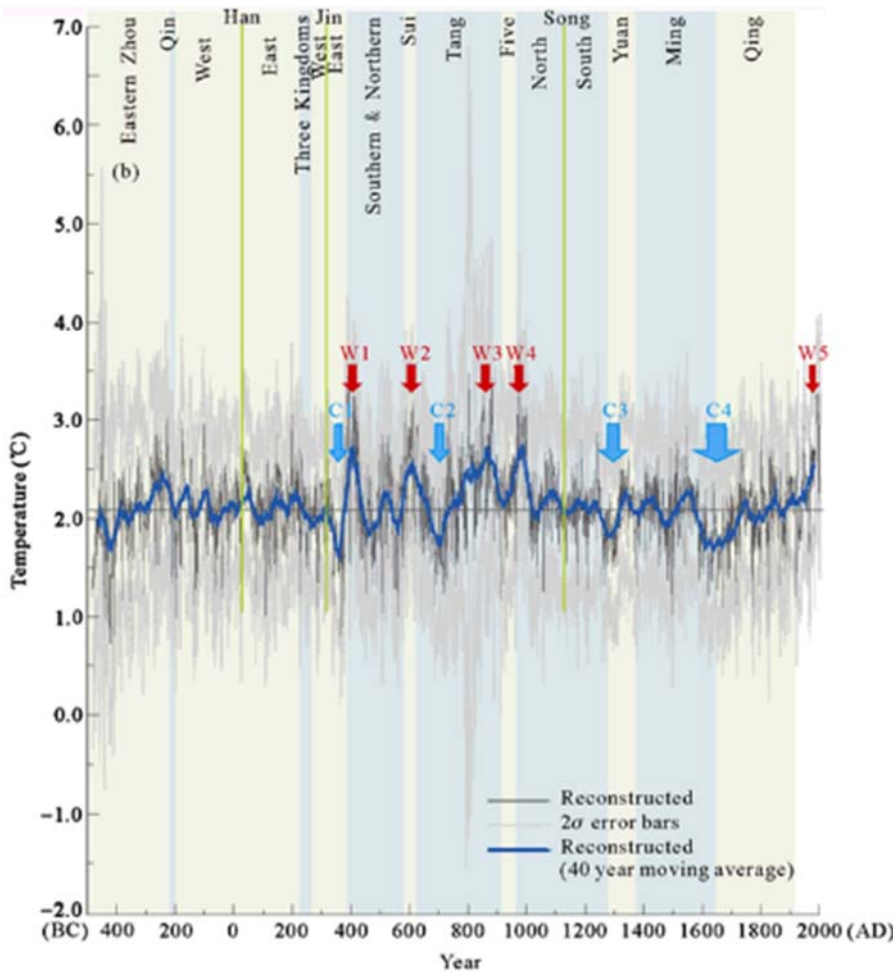


Fig. 48. “The reconstructed temperature over the mid-eastern TP from 484 BC to AD 2000 (thin lines) with 2σ error bars (dashed lines). The horizontal line is the mean of 484 BC-AD 2000, and the thick line is the 40 year moving average. The colored areas indicate periods covered by different Dynasties. W1 to W5 are the warm periods, and C1 to C4 are the cold intervals.” Figure (simplified) and captions after Liu et al. (2009b). With kind permission of *Science in China, Series D*.

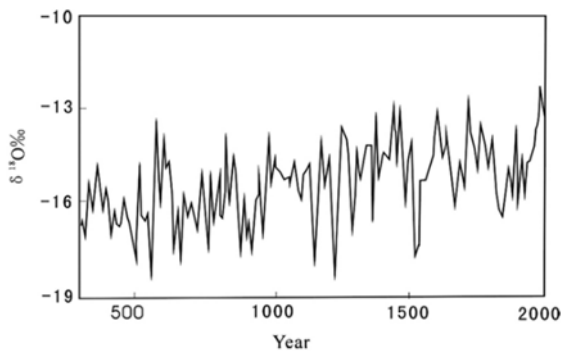


Fig. 49. Temperature variation on the TP during the last 2000 years. Figure after Yao et al. (1997b), also in Li and Kang (2006). Reproduced with kind permission from the Editorial Division, of the *Institute of Atmospheric Physics (IAP) of the Chinese Academy of Sciences (CAS)*.

The pattern of precipitation during the last ~ 2000 years was more complicated than temperature's. Guliya's ice core gives evidence of 5 high and 4 low precipitation periods. Cycles are found of ~ 200 year, ~ 15 year, ~ 14 year, and ~ 6 year. Li and Kang (2006) claim that all of them can be related to the solar cycle, except the ~ 6 year cycle, which may reflect the ENSO cycle.

Shao et al. (2004) also found different rates of precipitation variation rate during different periods.

Precipitation change was smaller before AD 1430 and after AD 1850, while it was larger during AD 1430-1850, and high precipitation experienced a larger excursion compared to low precipitation.

In general, the features of precipitation changes during the last ~ 2000 years were as follows. Precipitation was large at the beginning of the Christian era. It decreased from the late 5th century through the 15th century. It increased during the 16th-17th century, it decreased again during the 19th century. In addition, upon comparing changes of temperature and of precipitation, on the long-time scale there appears to be more low frequency fluctuations of temperature compared to precipitation's. In addition, the variations of precipitation always lagged temperature's by ~ 50 – 100 years, and the variations in northern TP were synchronous, of precipitation and temperature (Yao et al., 2001; Gong and Hameed, 1993), but reversed in southern TP (Yao et al., 2000, 2000a).

Li and Kang (2006) also discuss the most recent evidence, dealing with the last 50 years, but this is not here of direct concern (see Fig. 3 of Gregori et al., 2025f). The great space and time variability is impressive. No reasonable explanation seems to justify these seemingly erratic phenomena, which occur on much different time scales, and in terms of a great variety of observed amplitudes, impact, and geomorphology. A tentative

explanation is here proposed in terms of a spacetime change of endogenous heat release.

As an anticipation, note that solar activity enters into play in a twofold way. On the short time range, an increase of the induced telluric currents strengthens their intensity, when they are channeled underneath Himalaya. Thus, they originate a more intense generation of Joule heat on the *ALB* (see Fig. 1 of Gregori et al., 2025q). On the longer (secular variation, i.e., *SV*, and/or geological) time range, a modulation of the *TD* geodynamo causes a large production of endogenous Joule heat, which supplies sea-urchin spikes and superswells. This causes a faster uplift of superswells and geotumors, hence a greater geodynamic activity. Therefore, the overthrust is comparatively faster, which causes the Himalaya orogenesis. This originates a larger amount of kinetic pressure, hence, at a subsequent time, a larger amount of friction heat. Both processes produce an increase of geothermal flux underneath the *TP*, and this “Third Pole” of the Earth is thus comparably more anomalous, while it effectively plays the role of driver in the global climate system. Consider that the two aforementioned processes occur on comparably much different spacetime scales, and the result - of both these time-varying primary effects associated with solar activity - is therefore to be expected to look an almost erratic phenomenon.

In any case, whatever is the explanation of this entire set of phenomena, the anthropic influence on climate cannot be reduced to a simple concern about greenhouse gases injection.

Li and Kang (2006), as a conclusion of their review, comment as follows. “*With the average level of ~ 4500 m, the TP is a ‘sensitive area’ of climate change, which has the quick reaction ability and also produces great feedback to the world climate change. Generally, the climate change over the TP has the characteristics of great amplitude, high frequency and always ahead of other regions due to its high altitude and sensitive snow/ice environment.* [Remind about the well assessed – and already emphasized - important role of the albedo change of an ice sheet following the eventual deposition of dust. This can dramatically change the amount of solar radiation - that is absorbed by soil in order to melt ice or snow, and that is complementary to the remaining amount of radiation, which is reflected in space. This process has a relevant impact on the energy balance of the climate system.]

Liu and Ma (1996) found that the increase of the TP surface reflectivity is an important controlling factor for the short term climate change of China. Feng et al. (1998) found that temperature fluctuation over the TP is ~ 30 years ahead of the Qilian Mountains and ~ 10 – 60 years ahead of the eastern China on a scale of hundred years. Hence, it is possible to forecast the climate change of other regions of China according to the analysis of climate change of the TP.” This effect is clearly consistent with a possible consequence of a modulation by spacetime variation of endogenous heat release.

Therefore, they conclude that climate changes on the *TP* can be used as a gauge to forecast climate on the planetary scale. In general, cold events seem to originate from

northwestern *TP* and warm events from southeastern *TP*. Li and Kang (2006) claim that this can be due to the connections with the North Atlantic deep water that is located in a NW direction relative to *TP*, and that triggers cold events and also the monsoon, which blows from SE in the Pacific and Indian oceans.

However, also few other drivers have been investigated, such as solar radiation and other Earth’s cycles (Bond et al., 2001). The cycle of temperature and precipitation in the Guliya ice core was thus found to be correlated with solar activity: the temperature change always lags the solar activity, consistently with the spacetime modulation by endogenous heat release, as proposed in the present study.

An active - although baleful - experiment was carried out by the Gulf War Kuwait oil fires of January-November 1991 (Fig. 50). The effect was investigated quantitatively by Zhou et al. (2018a) by means of models of atmospheric circulation and radiative balance.



Fig. 50. “Satellite imagery of oil fires spreading westwards (Source: NASA Earth Observatory).” Figure and captions after Islam (2019) (also in Zhou et al., 2018a). NASA copyright free policy.

“*The black carbon (BC) deposition on the ice core at Muztagh Ata Mountain, northern TP, was analyzed. Two sets of measurements were used in this study, which included the air samplings of BC particles during 2004-2006 and the ice core drillings of BC deposition during 1986-1994. Two numerical models were used to analyze the measured data ... The results show that, during 1991-1992, there was a strong spike in the BC deposition at Muztagh Ata, suggesting that there was an unusual emission in the upward region during this period ... The analysis indicated that the emissions from large Kuwait fires at the end of the first Gulf War in 1991 caused this high peak of the BC concentrations and deposition (about 3-4 times higher than other years) at Muztagh Ata Mountain, suggesting that the upward BC emissions had important impacts on this remote site located on the northern TP.*

Thus, there is a need to quantitatively estimate the effect of surrounding emissions on the BC concentrations on the northern TP. In this study, a sensitivity study with four individual BC emission regions (Central Asia, Europe, the Persian Gulf, and South Asia) was conducted ... The result suggests that during the ‘normal period’ (non-Kuwait fires), the largest effect was due to the Central Asia source (44%) during the Indian monsoon period, while during the non-monsoon period, the largest effect was due to the South Asia source (34%).

The increase in radiative forcing increase (RFI) due to the deposition of BC on snow was estimated ... The results show that under the fresh snow assumption, the estimated increase in RFI ranged from 0.2 to 2.5 W m⁻², while under the aged snow assumption, the estimated increase in RFI ranged from 0.9 to 5.7 W m⁻². During the Kuwait fires period, the RFI values increased about 2-5 times higher than in the 'normal period', suggesting a significant increase for the snow melting on the northern TP due to this fire event. This result suggests that the variability of BC deposition at Muztagh Ata Mountain provides useful information to study the effect of the upward BC emissions on environmental and climate issues in the northern TP. The radiative effect of BC deposition on the snow melting provides important information regarding the water resources in the region."

Active experiments are an important (though generally unwanted) opportunity to check the performance of model computation. Some concern deals with the impact on the water reservoir of the TP by the ongoing climate change (Gao et al., 2019). *"The region hosts the world's 14 highest mountains and about 100,000 km² of glaciers ... Meltwater feeds 10 great rivers, including the Indus, Brahmaputra, Ganges, Yellow and Yangtze, on which almost one-fifth of the world's population depends."* Therefore, the TP and its ice sheet is one of the leading components of the global water balance and availability for societal needs. The TP is a leading contributor to the global water balance related to ice sheets. This is the target focused by Farinotti et al. (2019) also illustrated by Kornei (2019a).

Farinotti et al. (2019) claim that *"knowledge of the ice thickness distribution of the world's glaciers is a fundamental prerequisite for a range of studies ... Previous estimates of global glacier volumes are mostly based on scaling relations between glacier area and volume, and only one study provides global-scale information on the ice thickness distribution of individual glaciers. Here we use an ensemble of up to five models to provide a consensus estimate for the ice thickness distribution of all the about 215,000 glaciers outside the Greenland and Antarctic Ice Sheets. The models use principles of ice flow dynamics to invert for ice thickness from surface characteristics. We find a total volume of $158 \pm 41 \times 10^3$ km³, which is equivalent to 0.32 ± 0.08 m of sea-level change when the fraction of ice located below present-day sea-level (roughly 15%) is subtracted. Our results indicate that High Mountain Asia hosts ~27% less glacier ice than previously suggested, and imply that the timing by which the region is expected to lose half of its present-day glacier area has to be moved forward by about one decade."*

The uncertainties ought to be stressed of these difficult estimates. Multi-parametric comparisons are needed, e.g. through GRACE records (although referring to regional estimates and on a short time-range), while the unknown role ought to be guessed of serpentinization (see Gregori and Hovland, 2025) including its long-term SV that depends on the geological scale changes of the global release of endogenous heat. The entire scenario is a great challenge that still requires some long hard-thinking.

Climate in China according to the western literature

Let us list, more or less disorderly, a few additional observational evidences that we found in the literature available in the western world. The climate in China during the Holocene was generally warm, consistently with the main climatic features during the inter-glacial period. Shi et al. (1992) (already mentioned for Fig. 40) indicated that the Megathermal (i.e., the tropical period, ~ 8.5 – 3.0 ka BP) was the warmest period of the Holocene in China, with a temperature ~ 1 – 5°C higher than at present. The temperature difference between Megathermal and present time was ~ 3 – 4°C in northern China and ~ 1 – 2°C in southeastern China. They also stress the important resulting influence on the development of culture.

Wang et al. (2001a) reconstructed the mean temperature series of China during the last ~ 10 ka with 250 years time resolution, using averages of 10 regional series, weighted depending on area coverage. During ~ 7.5 – 7.0 ka BP and ~ 6.0 ka BP the temperature was ~ 2°C higher than at present.

The results by Shi et al. (1992) and Wang et al. (2001a), however, were mainly obtained from pollen data. Hence, the chronology was constructed using ¹⁴C years with no correction with tree ring data. Therefore, the real timing (Cal years), compared to ¹⁴C years, should be anticipated, e.g., in early Holocene from 0.5 ka to 1.0 ka. In addition, the end of the Megathermal, which was estimated by Shi et al. (1992), does not fully agree with ice core data in western China that indicate for the warmest period a date before ~ 7.0 ka BP (Cal) (Thompson et al., 1997). Shi et al. (1992), on the basis of pollen, lake level, and loess data, envisaged a generally wet climate during the Holocene. This conclusion was, however, challenged by subsequent high-resolution palaeoclimate records that showed a reduction, during the mid-Holocene, of effective wetness over the Inner-Mongolian Plateau.

According to An (2000), the maximum increment of precipitation occurred, respectively, ~ 9 ka BP, ~ 6 ka BP, and ~ 3 ka BP in northern China, in the Changjiang River valley, and in the Zhujiang River valley. An et al. (2000) later gave better details, during the mid-Holocene over mainland China. The maximum increment of precipitation was observed during ~ 10 – 7 ka BP over northern China, and ~ 7 – 5 ka BP in the Changjiang River valley. They also envisaged a reduction of wetness in central northern China – where precipitations are usually low when the summer monsoon is weak - while precipitations are often concentrated in the Changjiang River valley. However, wetness reduction does not necessarily imply a precipitation decrease. Persistent warming significantly increases the evaporation over the arid and semi-arid zones, and then reduces wetness by a great extent.

Hong et al. (2000) plotted a ~ 6000 years high-resolution δ¹⁸O record from peat plant cellulose referring to northeastern China. Their data agree well with archaeological and historical evidence, and with

atmospheric radiocarbon in tree rings. The spectral analysis of their records gave periodicities of ~ 86, ~ 93, ~ 101, ~ 110, ~ 127, ~ 132, ~ 140, ~ 155, ~ 207, ~ 245, ~ 311, ~ 590, ~ 820 and ~ 1046 years. Table 4, borrowed with kind permission after Ge et al. (2007), shows a classification of cold events during the Holocene. Bond et al. (1997) constructed a typical chronology over the North Atlantic, numbering the cold events as 0 to 8. The Little Ice Age was referred as event 0 and the event at the very beginning of the Holocene as event 8.

Shi et al. (1992) indicated that the climate of China in the Holocene was unstable, and a series of cold events occurred, respectively, ~ 8.7 – 8.5 ka BP, ~ 7.3 ka BP, ~ 5.5 ka BP and ~ 4.0 ka BP, which appear to be almost

identical to the 6th-3rd cold events (¹⁴C) found by Bond et al. (1997). There appears to be a general agreement in Table 4 among all cold period determinations in different regions and by different authors. Cold events at many sites were correlated with a failure of the summer monsoon, apart the exception of northeastern China where monsoon rainfall increases when a cold event occurs. Note, however, that the periodicities are technically useful and indicative, even though phenomena are cyclic, although not strictly periodical, due to the modulation by the irregular encounters of the Solar System with interstellar clouds of matter (Gregori, 2002, and Gregori et al., 2025a).

Table 4. Cold events over the North Atlantic and monsoon failures in China [ka BP (Cal)]

| region | climate | 0 | 1 | 2 | 3 | 4 | 5 | 6 | 7 | 8 | Ref. |
|-----------------|---------|-----|-----|-----|-----|-----|-----|-----|------|------|------|
| North Atlantic | Cold | 0.4 | 1.4 | 2.8 | 4.3 | 5.9 | 8.2 | 9.5 | 10.3 | 11.1 | (a) |
| Qinghai-TP | Cold | 0.9 | 1.7 | 3.4 | 4.0 | 5.5 | 8.3 | 9.0 | 10.1 | 11.2 | (b) |
| Qilian Mountain | Cold | 0.4 | 1.5 | 3.0 | 4.0 | 5.2 | 8.8 | 9.7 | | | (c) |
| Inner-Mongolia | Dry | 0.4 | 1.7 | 3.0 | 4.2 | 6.0 | 8.6 | 9.3 | 10.5 | 11.4 | (d) |
| Zoigê | Dry | 0.3 | 1.5 | 2.8 | 4.4 | 5.9 | 8.2 | 9.5 | 10.2 | 11.3 | (e) |
| Hongyuan | Dry | 0.3 | 1.5 | 2.8 | 4.1 | 5.9 | 8.3 | 9.5 | 10.4 | 11.2 | (f) |
| South China Sea | Dry | 0.3 | 1.2 | 3.1 | 4.3 | 6.0 | 8.3 | 9.5 | | | (g) |
| Northeast China | Wet | 0.3 | 1.5 | 2.8 | 4.3 | 5.9 | 8.4 | 9.7 | 10.4 | 11.4 | (h) |

References: (a)-Bond et al. (1997); (b)-Thompson et al.(1997); (c)-Yao and Shi (1992); (d)-Chen et al. (2003); (e)-Zhou et al. (2002); (f)-Hong et al. (2005); (g)-Wang et al. (1999a); (h)-Hong et al. (2005).

Wei and Wang (2004) implemented a model, based on a coupling between an atmospheric general circulation model and an oceanic general circulation model. They simulated the mid-Holocene East Asian monsoon climate. They found more intense precipitation, a stronger monsoon during summer, and a corresponding increase of winter temperature in China.

Qin et al. (2005) studied the isotope records inside a stalagmite (named *D4*, and found in the Dongge cave in Libo, Guizhou, China). They analyzed its length in the range 45 cm – 193.6 cm of its upper part, spanning the time lag ~ 3.9 – 15.7 ka BP with an average resolution of ~ 90 years. Fig. 51 shows their results, which are compared with the records from the Greenland ice core *GISP2* (see above). Their study indicates that the last cold event of the last glacial period, the *YD*, occurred - according to the *D4* record - between ~ 12.80 ka BP and ~ 11.58 ka BP, displaying a conspicuous temperature decrease. The end of the last glacial period (~ 11.3 ka BP) is consistent with the so-called *Termination I* found in oceanic isotope records.

The three most distinct cold events of early and middle Holocene occurred, respectively, at times ~ 10.91 ka BP, ~ 8.27 ka BP and ~ 4.75 ka BP, with a temperature decrease in the range ~ 2 – 5°C. The sudden climate changes - that occurred on the time scale of thousands or hundreds of years - can be correlated upon comparing the stalagmite and *GISP2* records. There is, however, some disagreement. Consider, e.g., the “a” to “c” sections in the *D4* record. However, the Hulu cave stalagmite in Nanjing (Wang et al., 2001b) shows results that have the same trend as *D4*, which is opposite to the *GISP2* trend.

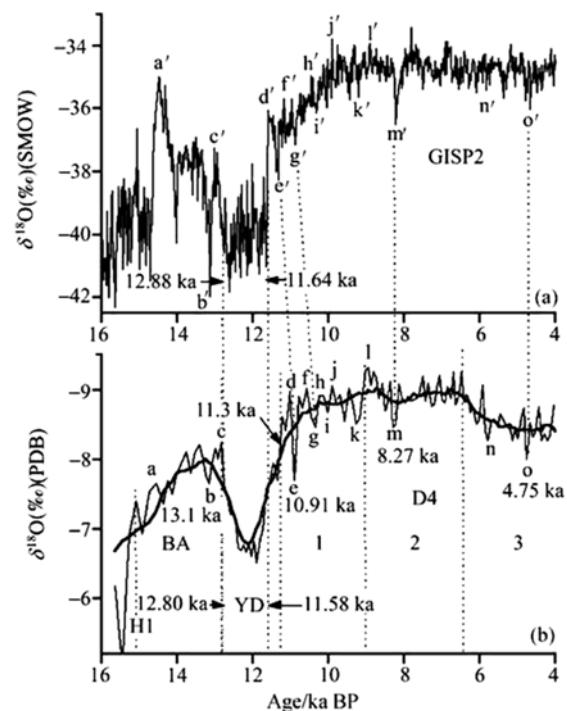


Fig. 51. Comparison of the records of the *D4* stalagmite and *GISP2* during ~ 4 – 15.5 ka BP. [top diagram] $\delta^{18}O$ records of *GISP2*; [bottom diagram] $\delta^{18}O$ records of the *D4* stalagmite, where the gray thick line is a 10 points running mean; *BA* is the Bølling Allerød period, and *YD* is the Younger Dryas period; 1, 2 and 3 are transition periods during Holocene, i.e. special warm-moisture age and relatively warm-moisture age. After Qin et al. (2005). With kind permission of *Science in China, Series D*.

Hence, probably the *D4* records reflect an ongoing increase of temperature. That is, the change of temperature in the monsoon regions at middle latitude was opposite to Greenland's.

Qin et al. (2005) compared the dating of the *YD* event, according to the evidence of different sources, and they are here synthesized in Table 5 (reproduced with kind permission of *Science in China, Series D*).

Table 5. Comparative determinations of the Younger Dryas

| source | beginning | end | duration | Ref. |
|-------------------------------------|----------------------|----------------------|----------|----------------------------|
| <i>GISP2</i> (Greenland) | 12.88 ± 0.26 ka BP | 11.64 ± 0.25 ka BP | 1.24 ka | Stuiver et al. (1995,1997) |
| <i>GRIP</i> (Greenland) | 12.70 ka BP | 11.55 ka BP | 1.15 ka | Dansgaard et al. (1993) |
| Guliya ice core Qinghai--TP) | 12.2 ka BP | 10.9 ka BP | 1.3 ka | |
| stalagmite in Hulu cave, Nanjing | 12.823 ± 0.060 ka BP | 11.473 ± 0.100 ka BP | 1.35 ka | Wang et al. (2001) |
| <i>D4</i> stalagmite in Dongge cave | 12.80 ± 0.14 ka BP | 11.58 ± 0.09 ka BP | 1.22 ka | Qin et al. (2005) |

Yao et al. (1997a) and Yao (1999) suggested that the time of the *YD* event in the Guliya ice cores lagged that in Greenland. The time difference between the Qinghai-TP datum and the Nanjing stalagmite may be caused by different techniques used for time determination.

In addition, the cold events that occurred ~ 8.27 ka BP and ~ 4.75 ka BP can also be compared with the *CC3* stalagmite records in Ireland (McDermott et al., 2001). The ~ 8.27 ka BP was recorded also in other areas, giving 8.30 ± 0.06 ka BP in rock cores from the Norway Strait (Klitgaard-Kristensen et al., 1998), 8.32 ± 0.12 ka BP in the *CC3* stalagmite from southwestern Ireland (McDermott et al., 2001), 8.21 ka in the *GISP2* ice cores, and 8.27 ± 0.5 ka BP in the *D4* stalagmite. All dates agree one another within an error bar ~ 1 – 2%.

Therefore, the short-range climate changes, which occurred in the monsoon areas in China, have the same driving factor in western Europe, and in the Arctic regions — likely a synchronous time-variation of the release of endogenous energy. On the other hand, the timing appears sometimes different, which reflects probably some difference of the environment in the monsoon areas compared to the environment of polar regions.

However, in general, Qin et al. (2005) claim that these phenomena appear to be mostly global. On the other hand, this is what has to be expected upon considering the role of teleconnection of atmospheric/oceanic phenomena on the planetary scale. Qin et al. (2005) finally suggest a division of climate into five main periods (these three most recent periods are part of the Holocene):

- the *BA* warm period (~ 14.7 – 12.8 ka BP); during the early times of this period the summer monsoon in Eastern Asia probably started to strengthen;
- the *YD* period (~ 12.8 – 11.58 ka BP);
- the transition period (~ 11.3 – 9.0 ka BP); the summer monsoon in Eastern Asia seemingly largely fade away roughly in ~ 9000 BP;
- a particularly warm-humid period (~ 9.0 – 6.45 ka BP); the summer monsoon in Eastern Asia resumed and began to decline in ~ 6.45 ka BP.
- a relatively warm-humid period (~ 6.45 – 4.0 ka BP).

An et al. (2006) reconstructed the spacetime variation of effective moisture during the mid-Holocene. They used palaeoclimate records, ice cores, lake levels, pollens, and loess-palaeosol records. In desert areas, climate was dry,

although the timing seems different at different sites. Deserts with higher aridity remained dry for a longer time. In arid and semi-arid areas, dry intervals appeared to be more asynchronous than synchronous. In the Xinjiang region, except at sites located in deserts, climate was generally wet during ~ 7000 – 5000 years BP. In the northern Qinghai-TP, effective moisture at most sites began to decrease after ~ 5000 years BP. Climate became dry after ~ 4000 years BP except in the deserts, in the Loess Plateau and in the Inner Mongolia Plateau.

Jin and Liu (2002) reconstructed the palaeoclimatic history, by means of pollen and $\delta^{18}O$ in 160 peat cores 2.7 m deep, from Taishizhuang, Huailai County, Hebei Province. Upon considering the historical and archaeological information from this area, they found a close relation between cultural development and the environment changes occurred during the mid-Holocene (~ 6000 – 3000 Cal years BP).

During ~ 5678 – 5400 Cal years BP the climate was unstable and in general colder and drier than today. During ~ 5400 – 4800 Cal years BP the climate was much warmer and wetter than before. The climate during ~ 4800 – 4300 Cal years BP was persistently cold, with an exceptional cold event occurring during ~ 4600 – 4300 Cal years BP. This cold event was recorded at several other localities in northern China even in the whole NH. It played an important role in the cultural development. After this cold event, a return occurred to warmer conditions, during ~ 4200 – 3300 Cal years BP

Tarasov et al. (2006) studied pollen record from the Taishizhuang site (40° 21.5' N, 115° 49.5' E) located in the transitional forest-steppe zone, near the present limit of the summer monsoon. They found that:

- during the mid-Holocene, the annual precipitation was ~ 550 – 750 mm, i.e. ~ 100 – 300 mm higher than at present; it was the so-called “forest phase”; during the following “forest-steppe phase” the annual precipitation decreased to ~ 450 – 650 mm;
- during the prehistoric and early historic periods from ~ 8200 Cal years BP the archaeological records from 100 sites prove the habitation of northeastern China, but give no evidence of a use of wood resources that is sufficient to influence the regional vegetation development and to leave traces in the pollen assemblages;

- between $\sim 5700 - 2100$ Cal years BP both archaeological and palaeoenvironmental data support the conclusion that changes in pollen composition reflect natural variations in precipitation and no major deforestation caused by the humans;
- between $\sim 5700 - 4400$ Cal years BP, according to quantitative biome, the reconstruction suggests that temperate deciduous forest dominated the vegetation cover; after that time the landscape became more open and the scores of the steppe biome were always higher than those of the temperate deciduous forest;
- two oscillations occurred dated ~ 4000 Cal years BP and ~ 3500 Cal years BP;
- since ~ 3400 Cal years BP, during the so-called “steppe phase” the annual precipitation was similar to modern values ($\sim 300 - 500$ mm);
- however, during $\sim 3400 - 2100$ Cal years BP the common vegetation became steppe, and the landscape was more open in comparison with previous time.

Herzschuh et al. (2009) investigated the mechanism and the causes of a broad-scale vegetation change and of the associated loss of biomass that occurred during the aforementioned transition from the forest phase to the steppe phase during the second half of the Holocene. They studied pollen records from the northeastern Tibet-Qinghai Plateau (TQP) (Fig. 52). They found a dramatic and extensive forest decline beginning ~ 6000 Cal years BP.

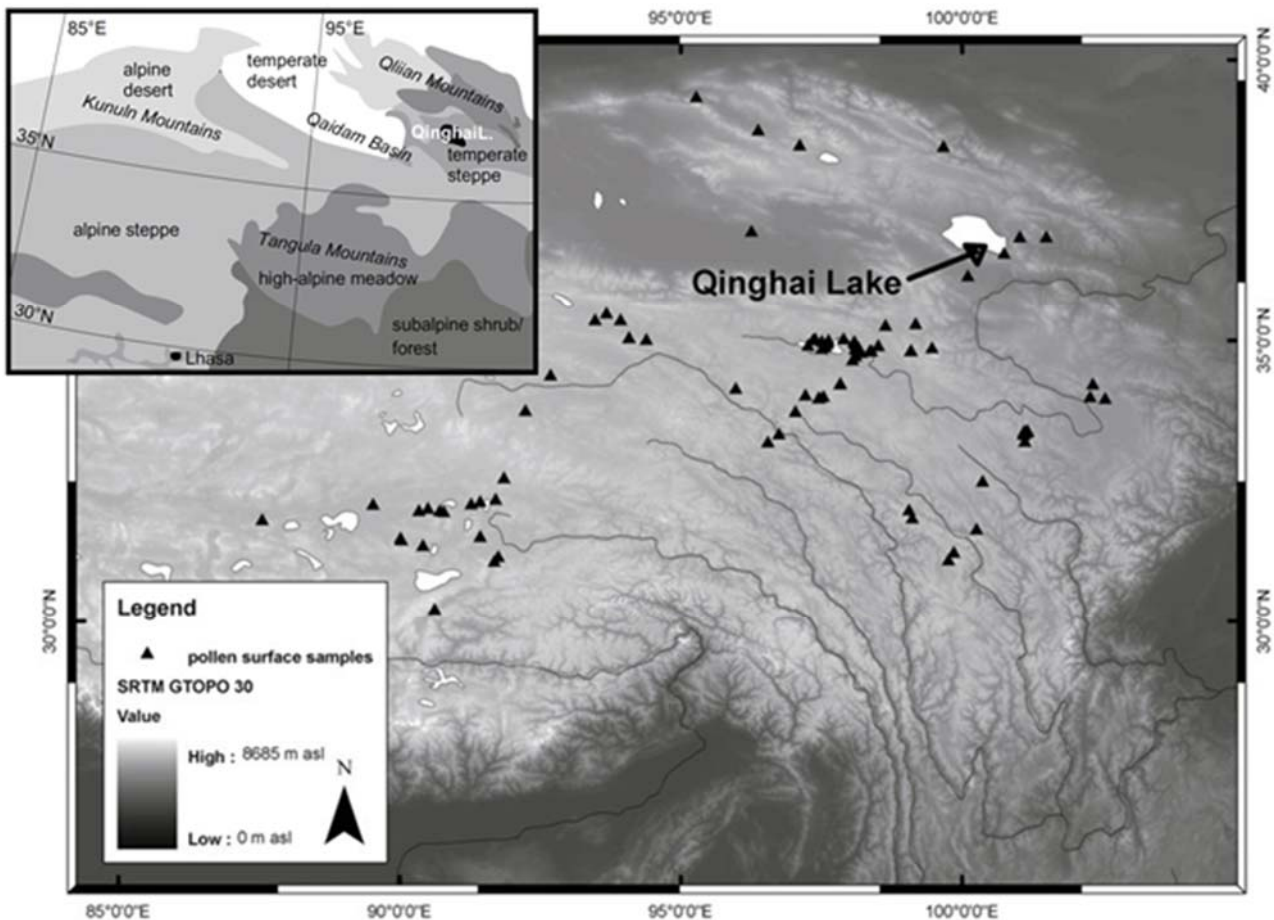


Fig. 52. “Sketch map showing the location of Qinghai Lake and the 108 lakes on the eastern Tibet-Qinghai Plateau (TQP) used to develop the modern pollen-precipitation transfer function. The rough distribution of the main vegetation types on the eastern TQP are shown in the inset map.” Figure and captions after Herzschuh et al. (2009). AGU copyright free policy.

They used stratigraphical data from Qinghai Lake (3200 m a.s.l., $36^{\circ} 32' - 37^{\circ} 15' N$, $99^{\circ} 36' - 100^{\circ} 47' E$). The results of the pollen-based precipitation reconstruction during the Holocene agrees both with the moisture changes inferred from the stable oxygen-isotope record, and with models based on past annual precipitation changes. Their main conclusion was that “it is not necessary to attribute the broad-scale forest decline to human activity. Climate change as a result of changes in the intensity of the East Asian Summer Monsoon in the mid-Holocene is the most parsimonious explanation for the widespread forest

decline ... Moreover, climate feedback from a reduced forest cover accentuates increasingly drier conditions in the area, indicating complex vegetation-climate interactions during this major ecological change.” That is, also in this case the feedback by vegetation on precipitation and climate looks much effective.

There appears to be a global correlation between the climate change occurred in the mid-Holocene - mostly the most rapid climate change, which requires a prompter adaptation - and the development of civilization, which is therefore an additional trigger for causing social breakdown

in the society, such as war, population pressure, deforestation, resource depletion, etc. (Weiss and Bradley, 2001; deMenocal, 2001; Giosan et al., 2012). See also the aforementioned Cycle of Climate and Civilization (see e.g. Gregori et al., 2000, and Gregori, 2002a).

Conclusion

A large amount of literature is available, and it is impossible to give here any exhaustive review. The palaeoclimate and archæoclimate records exploited by the Chinese scientists show a great variability in both space and time through the entire Chinese subcontinent, showing the likely crucial role of air-earth currents. That is, climate change cannot be a simple matter of dynamics of the atmosphere/ocean system. The primary driver seems to be in the deep Earth interior.

The exploitation of this kind of observational evidence strictly requires the contribution of several kinds of learned specialists, while we give here only the reported results. In general, only a partial reminder is here given, based on the more or less random hints that we occasionally found. Even the term “Ice Age” appears now much vague. Historically, the former evidence was concerned only with few episodes. Then, the great improvements in detecting and measuring proxy data gave evidence of large temperature fluctuations, on the centennial or millennial time scale, which in general are not always a global phenomenon and involve rather more or less restricted regions. The interested reader should therefore refer to the increasing literature and available database concerning every period of time of his concern.

As a summary, maybe three periods seem to have been the object of a comparatively greater concern: ~ 8200 *Cal years BP*, ~ 5200 *Cal years BP*, and ~ 4000 *Cal years BP*, and three cold periods of duration, respectively, ~ 8200 – 7000 *Cal years BP*, ~ 5800 – 4900 *Cal years BP*, and ~ 3300 – 2400 *Cal years BP*. A fourth period, ~ 450 – 430 *Cal years BP* is better known as Little Ice Age, which is, however, in the historical range.

“Climate” is not a simple topic and cannot be defined by either one proxy or index alone. Even the term “climatology” looks like a vague concept as it encloses almost the entire Earth’s science.

Climate change is certainly in progress, associated with the ongoing “Iceland” heartbeat of the Earth electrocardiogram. However, the manifestation is in general quite different at different sites.

As a final comment - which is of good attitude - the feeling appears naïve, claimed by several so-called “authoritative climatologists”, that the CO_2 increase is the certain anthropic main cause responsible for the present climate change (either global warming or other).

Certainly, the humans have a great responsibility in the pollution and destruction of several components of “climate”. However, it is just reductive and simplistic to refer only to one aspect - i.e. to CO_2 that, by the way, has now been proven to be irrelevant compared to the natural CO_2 exhalation from soil (Mearns, 2015a, and Gregori, 2020).

Acknowledgement

We express sincere gratitude to the late Professor Tang Maocang for his far-looking intuition, and for sending in sabbatical year Dong Wenjie and Gao Xiaoqing.

We also deeply thank Professor Antonino Zichichi, President of *World Laboratory*, for awarding a fellowship to Dong Wenjie and to Gao Xiaoqing, in the framework of a promotion of international cooperation between Italy and PRC.

These actions resulted essential for the achievement and progress of understanding of the present set of papers.

We also thank several scientists and colleagues who in different ways, along the years, contributed to the friendly discussions on several related items. It is impossible to list all of them.

Funding Information

G. P. Gregori retired since 2005. B. A. Leybourne is a semi-retired self-funded independent researcher. Dong Wenjie and to Gao Xiaoqing graduated and worked at the *Lanzhou Institute of Plateau Atmospheric Physics*, where Gao Xiaoqing is still active. Dong Wenjie had important commitments in Beijing, and at present is Professor and Dean, *School of Atmospheric Science, Sun Yat-sen University*, Zhuhai, Guangdong, (PRC), and Director of *Future Earth Global Secretariat Hub China* and Secretary-General of *FE Chinese National Committee*.

Author’s Contributions

This study derived from a long-lasting cooperation by all coauthors and resulted from the emergence of long-lasting thought and discussion, particularly during the two sabbatical years spent, at different times, in Rome by Dong Wenjie and by Gao Xiaoqing, sponsored by two fellowships awarded by *World Laboratory*, with President Prof. Antonino Zichichi, for promoting international cooperation.

Ethics

This article is original and contains unpublished material. Authors declare that there are not ethical issues and no conflict of interest that may arise after the publication of this manuscript.

References

- Abrantes, F.A., 2003. 340000 year continental climate record from tropical Africa-news from opal phytoliths from the equatorial Atlantic. *Earth and Planetary Science Letters*, 209: 165-179
- An, Chengbang, Feng Zhaodong, and L. Barton, 2006. Dry or humid? Mid-Holocene humidity changes in arid and semi-arid China, *Quaternary Science Reviews*, 25: 351-361; DOI:doi:10.1016/j.quascirev.2005.03.013
- An, Zhisheng et al., 1986 – Cited by Liu et al., (1996b). Missing information

- An, Zhisheng, 2000. The history and variability of the East Asian paleomonsoon climate. *Quaternary Science Reviews*, 19: 171-187
- An, Zhisheng, G. Kukla, and Liu Tunghsheng, 1989. Loess stratigraphy in Luochuan of China, *Quaternary Sci. (in Chinese)*, (2), 155-.
- An, Zhisheng, G. Kukla, S.C. Porter, and Jule Xiao, 1991. Late Quaternary dust flow on the Chinese Loess Plateau, *Catena*, 18 (2): 125-132; DOI:10. 1016/0341-8162(91)90012-M
- An, Zhisheng, Liu Tunghseng, Lu Yanchou, S.C. Porter, G. Kukla, Wu Xihao, Hua Yingming, 1990. The long-term paleomonsoon variation recorded by the loess-palaeosol sequence in Central China, *Quaternary International*, 7/8: 91-95; DOI:10.1016/1040-6182(90)90042-3
- An, Zhisheng, S.C. Porter, J.E. Kutzbach, Wu Xihao, Wang Suming, Liu Xiaodong, Li Xiaoqiang, and Zhou Weijian, 2000. Asynchronous Holocene optimum of the East Asian monsoon. *Quaternary Science Reviews* 19: 743-764
- An, Zhisheng, Wang Sumin, Wu Xihao, Chen Mingyang, Sun Donghuai, Liu Xiuming, Wang Fubao, Li Li, Sun Youbin, Zhou Weijian, Zhou Jie, Liu Xiaodong, Lu Huayu, Zhang Yunxiang, Dong Guangrong, and Qiang Xiaoke, 1999. Æolian evidence from the Chinese Loess Plateau: the onset of the Late Cenozoic Great Glaciation in the Northern Hemisphere and Qinghai-Xizang Plateau uplift forcing, *Science in China Series D-Earth Sciences*, 42 (3): 258-271
- Bard, E., F. Rostek, and C. Sonzogni, 1997a. Interhemispheric synchrony of the last deglaciation inferred from alkenone palaeothermometry. *Nature*, 385: 707-710
- Bar-Oz, G., L. Weissbrod, T. Erickson-Gini, Y. Tepper, D. Malkinson, M. Benzaquen, D. Langgut, Z.C. Dunseth, D.H. Butler, R. Shahack-Gross, J. Roskin, D. Fuks, E. Weiss, N. Marom, I. Ktalav, R. Blevis, I. Zohar, Y. Farhi, A. Filatova, Y. Gorin-Rosen, Xin Yan, and E. Boaretto, 2019. Ancient trash mounds unravel urban collapse a century before the end of Byzantine hegemony in the southern Levant. *Proceedings of the National Academy of Sciences*; DOI:10.1073/pnas.1900233116
- Bender, M., T. Sowers, M.-L. Dickson, J. Orchardo, P. Grootes, P.A. Mayewski, and D.A. Meese, 1994. Climate correlations between Greenland and Antarctica during the past 100000 years. *Nature*, 372: 663-666; DOI:10.1038/372663a0
- Berger, A., and M.F. Loutre, 1991. Insolation values for the climate of the last 10 million years. *Quaternary Science Reviews*, 10: 297-317
- Berger, A.L., 1978: Long-term variations of daily insolation and Quaternary climatic changes. *Journal of the Atmospheric Sciences*, 35: 2362-2367; DOI:10.1175/1520-0469(1978)035<2362:LTVODI>2.0.CO;2
- Bi, Fuzhi, Yuan Youshen, and Wen Qinglan, 1991. A study on periodicity of Holocene sea-level changes in China and future sea-level changes in the world, *Journal of Quaternary Science*, (01); DOI: cnki:ISSN:1001-7410.1991-01-005
- Blom, P., 2019. Nature's mutiny: how the Little Ice Age of the long seventeenth century transformed the West and shaped the present, *Liveright*; pp: 352
- Bloom, A.L., 1983. Sea level and coastal morphology of the United States through the late Wisconsin glacial maximum. In *Late-quaternary Environments of the United States*, Vol. 1 (1983), H.E. Wright, (ed.); Univ. of Minnesota Press, Minneapolis; pp: 215-229
- Blunier, T., and E.J. Brook, 2001. Timing of millennial-scale climate change in Antarctica and Greenland during the last glacial period. *Science*, 291: 109-112
- Blunier, T., J. Chappellaz, J. Schwander, B. Stauffer, T.F. Stocker, D. Raynaud, J. Jouzel, H.B. Clausen, C.U. Hammer, and S.J. Johnsen, 1998. Asynchrony of Antarctica and Greenland climate during the last glacial. *Nature*, 394: 739-743; DOI:10.1038/29447
- Bond, G., B. Kromer, J. Beer, R. Muscheler, M.N. Evans, W. Showers, S. Hoffmann, R. Lotti-Bond, I. Hajdas, and G. Bonani, 2001. Persistent solar influence on North Atlantic climate during the Holocene, *Science*, 294 (5549): 2130-2136; DOI:10.1126/science.1065680.
- Bond, G., W. Broecker, S. Johnsen, J. McManus, L. Labeyrie, J. Jouzel, and G. Bonani, 1993. Correlations between climate records from North Atlantic sediments and Greenland ice. *Nature*, 365: 143-147; DOI:10.1038/365143a0
- Bond, G., W. Showers, M. Cheseby, R. Lotti, P. Almasi, P. deMenocal, P. Priore, H. Cullen, I. Hajdas, and G. Bonani, 1997. A pervasive millennial-scale cycle in North Atlantic Holocene and glacial climates, *Science*, 278 (5341): 1257-1266; DOI:10.1126/science.278.5341.1257
- Broecker, W.S., 1998. Paleoocean circulation during the last deglaciation: A bipolar seesaw? *Paleoceanography*, 13 (2): 119-121; DOI:10.1029/97PA03707
- Broecker, W.S., 2003. Does the trigger for abrupt climate change reside in the ocean or in the atmosphere? *Science*, 300: 1519-1522
- Broecker, W.S., M. Andr e, W. Wolfli, H. Oeschger, G. Bonani, J. Kennett, and D. Peteet, 1988. The chronology of the last deglaciation: implications to the cause of the Younger Dryas Event. *Paleoceanography*, 3 (1): 1-19; DOI:10.1029/PA003i001p00001
- Brooks, C.E.P., 1926. *Climate through the Ages. A Study of the Climatic Factors and their Variations*, (the II rev. edition appeared in 1949), Ernest Benn, Ltd, and Dover Publ. Inc., New York; pp: 395
- Budd, W. F. 1969. The dynamics of ice masses. *Australian National Antarctic Research Expeditions scientific reports Series A(IV)*. Glaciology, Publ. No. 108
- Caillon, N., J.P. Severinghaus, J.I. Jouzel, J.-M. Barnola, Jiancheng Kang, and V.Y. Lipenkov, 2003. Timing of atmospheric CO₂ and Antarctic temperature changes across Termination III, *Science*, 299 (5613): 1728-1731; DOI:10.1126/science.1078758
- Carolin, S.A., R.T. Walker, C.C. Day, V. Ersek, R.A. Sloan, M.W. Dee, M. Talebian, and G.M. Henderson, 2019. Precise timing of abrupt increase in dust activity in the

- Middle East coincident with 4.2 ka social change, *Proceedings of the National Academy of Sciences*, 116 (1): 67-72; DOI:10.1073/pnas.1808103115
- Chen, Chentung A., Lan Hsinchi, Lou Jiannyuh, and Chen Yancheng, 2003. The dry Holocene megathermal in Inner Mongolia. *Palaeogeography, Palaeoclimatology, Palaeoecology*, 193: 181-200
- Chen, Fahu, Zhaodong Feng, and Jiawu Zhang, 2000. Loess particle size data indicative of stable winter monsoons during the last interglacial in the western part of the Chinese Loess Plateau, *Catena*, 39: 233-244
- Chen, Huizhong, Su Zhizhu, Ysng Ping, and Dong Guangrong, 2004b. Preliminary reconstruction of the desert and sandy land distributions in China since the last interglacial period, *Science in China Series D-Earth Sciences*, 47, Supp. I: 89-100; DOI:10.1360/04zd0010
- Chen, Jiyang, 1987. Preliminary research on the mid- and late-Holocene glacial fluctuations in Tianger Peak II Regions, Tianshan Mountains, *Journal of Glaciology and Geocryology*, (04); cnki:ISSN:1000-0240.0.1987-04-006
- Chen, M.Y., 1991. The evolution of Chinese æolian deposits and the global aridificator (in Chinese), *Journal of Quaternary Science*, 4: 361-371
- Chen, Shitao, Wang Yongjin, Kong Xinggong, Liu Dianbing, Cheng Hai, and R.L. Edwards, 2006b. A possible Younger Dryas-type event during Asian monsoonal Termination 3, *Science in China Series D-Earth Sciences*, 49 (9): 982-990; DOI:10.1007/s11430-006-0982-4
- Cheng, Hai, R.L. Edwards, W.S. Broecker, G.H. Denton, Kong Xinggong, Wang Yongjin, Zhang Rong, and Wang Xianfeng, 2009. Ice Age terminations, *Science*, 326 (5950): 248-252; DOI:10.1126/science.1177840
- Cheng, Hai, R.L. Edwards, Ashish Sinha, C. Spötl, Liang Yi, Shitao Chen, M. Kelly, Gayatri Kathayat, Xianfeng Wang, Xianglei Li, Xinggong Kong, Yongjin Wang, Youfeng Ning, and Haiwei Zhang, 2016. The Asian monsoon over the past 640,000 years and ice age terminations, *Nature*, 534: 640-646; DOI:10.1038/nature18591. Corrigendum Jan 2017
- Clark, P.U., A.S. Dyke, J.D. Shakun, A.E. Carlson, J. Clark, B. Wohlfarth, J.X. Mitrovica, S.W. Hostetler, and A. Marshall McCabe. 2009. The Last Glacial Maximum, *Science*, 325 (5941): 710-714; DOI:10.1126/science.1172873
- Clark, P.U., R.S. Webb, and L.D. Keigwin, (eds), 1999. *Mechanisms of Global Change at Millennial Time Scales. Geophysical Monograph, American Geophysical Union, Washington DC. 12; pp: 394*
- Cook, T., 2019. A 192,000-year record of northwest African fire history, *EOS, Transactions American Geophysical Union*, 100; DOI:10.1029/2019EO118155
- Cross, M., D. McGee, W.S. Broecker, J. Quade, J.D. Shakun, Hai Cheng, Yanbin Lu, and R. Lawrence Edwards, 2015. Great Basin hydrology, paleoclimate, and connections with the North Atlantic: a speleothem stable isotope and trace element record from Lehman Caves, NV, *Quaternary Science Reviews*, 127: 186-198; DOI:10.1016/j.quascirev.2015.06.016
- Cruz, F. W. Jr, S. J. Burns, I. Karmann, et al., 2005. Insolation-driven changes in atmospheric circulation over the past 116,000 years in subtropical Brazil. *Nature*, 434: 63-66; DOI:10.1038/nature03365
- Cui, Zhijiu, Wu Yongqiu, Liu Gengnian, Ge Daokai, Pang Qiqing, and Xu Qinghai, 1998. On Kunlun-Yellow river tectonic movement, *Science in China Series D-Earth Sciences*, 41 (6): 592-600
- Dansgaard, W., S.J. Johnsen, H.B. Clausen, D. Dahl-Jensen, N.S. Gundestrup, C.U. Hammer, C.S. Hvidberg, J.P. Steffensen, A.E. Sveinbjörnsdottir, J. Jouzel, and G. Bond, 1993. Evidence for general instability of past climate from a 250-ka ice-cores record, *Nature*, 364: 218-220
- Deckers, D.H., 2011. Warming up the atmosphere's heat engine: atmospheric energetics with higher greenhouse gas concentrations, *Berichte Erdsystemforsch., Reports of Earth System Science*, 85, pp: 121, PhD Thesis, International Max Planck Research School on Earth System Modelling, Max-Planck-Institut für Meteorologie, Hamburg
- Defleura, A.R., 2019. Impact of the last interglacial climate change on ecosystems and Neanderthals behavior at Baume Moula-Guercy, Ardèche, France, *Journal of Archaeological Science*, 104: 114-124; DOI:10.1016/j.jas.2019.01.002
- deMenocal, P.B., 2001. Cultural responses to climate change during the Late Holocene, *Science*, 292 (5517): 667-673; DOI:10.1126/science.1059287
- Ding, Zhongli, Ren Jianzhang, Liu Tunsheng, Sun, J. M., & Zhou, X. Q., 1996. Irregular millenary scale changes and mechanism of monsoon-desert system. *Science in China Series D-Earth Sciences*, 26 (5): 385-391
- Dong, Wenjie, and Maocang Tang, 1997. A numerical modelling study on the processes of uplift and planation of the Tibetan Plateau, *Science in China, Series D: Earth Sciences*, 40 (3): 246-252; DOI:10.1007/BF02877532
- Douglas, R.G., and F. Woodruff, 1981. Deep-sea benthic foraminifera. In *The sea*, vol. 7, *The oceanic lithosphere*, C. Emiliani (ed.), J. Wiley-Interscience, New York; pp: 1233-1328
- Dykoski, C.A., R.L. Edwards, H. Cheng, D. Yuan, Y. Cai, M. Zhang, Y. Lin, J. Qing, Z. An, and J. Revenaugh, 2005. A high-resolution, absolute-dated Holocene and deglacial Asian monsoon record from Dongge Cave, China. *Earth and Planetary Science Letters*, 233: 71-86
- Fan, Ronghe, and Yao Shangsen, 1982. Discussion on the formation and the trend of development of the perennial frost on Southern Qinghai-Northern Xizang (Tibet) Plateau, *Journal of Glaciology and Geocryology*, (01); DOI:cnki:ISSN:1000-0240.0.1982-01-004
- Farinotti, Daniel, Matthias Huss, Johannes J. Fürst, Johannes Landmann, Horst Machguth, Fabien Maussion, and Ankur Pandit, 2019. A consensus estimate for the ice thickness distribution of all glaciers on Earth, *Nature, Geoscience*, 12 (3): 168-173; DOI:10.1038/s41561-019-0300-3
- Feng, Song, Maocang Tang, and Dongmei Wang, 1998. New evidence for the Qinghai-Xizang (Tibet) Plateau as a pilot region of climatic fluctuation in China, *Chinese*

- Science Bulletin, 43 (20): 1745-1749; DOI:10.1007/BF02883978 [Chinese Science Bulletin, 43 (6): 633-636 (in Chinese)]
- Feng, Song, Yao Tandong, and Jiang Hao, 2001. Climate change in recent 600 years over TP. Plateau Meteorology, 20 (1): 105-108: 1051108 (in Chinese)
- Fischer, H., M. Wahlen, J. Smith, D. Mastroiani and B. Deck, 1999. Ice core records of atmospheric CO₂ around the last three glacial terminations. Science, 283: 1712-1714
- Frakes, L A., 1979. Climate through Geologic Time, Elsevier Scientific Publishing Co., Amsterdam; pp: 1-310
- Gao et al. (2004) missing information
- Gao, Guodong, and Lu Yurong, 1988. Climatology, China Meteorology Press, Beijing
- Gao, Jing, Tandong Yao, V. Masson-Delmotte, H.-, Steen-Larsen, and Weicai Wang, 2019. Collapsing glaciers threaten Asia's water supplies, Nature, 565, 19-21; DOI:10.1038/d41586-018-07838-4
- Gasse, F., M. Arnold, J.C. Fontes, M. Fort, E. Gibert, A. Huc, Li Bingyan, Li Yuanfang, Liu Qing, F. Mélières, E. Van Campo, Wang Fubao, and Zhang Qingsong, 1991. A 13,000-year climate record from western Tibet, Nature, 353: 742-745; DOI:10.1038/353742a0
- Ge, Quansheng, Wang Shaowu, Wen Xinyu, and Hao Zhixin, 2007. Climate change during the Holocene in China, China National Report on Meteorology and Atmospheric Sciences (2003-2006), Report No.11 [to IUGG General Assembly, Perugia], pp: 1-26
- Ge, Quansheng, Zheng Jingyun, Fang Xiuqi, Man Zhimin, Zhang Xueqin, and Wang Wei-Chyung, 2003. Temperature changes of winter-half-year in Eastern China during the past 2000 years. The Holocene, 13: 933-940
- Giosan, L., D.Q. Fuller, K. Nicoll, R. K. Flad, and P.C. Clift, (eds), 2012. Climates, Landscapes, and Civilizations, Geophysical Monograph, American Geophysical Union, Washington DC., 198; pp:1-226
- Gong, Gaofa, and S. Hameed, 1993. The relationship between temperature and wetness changes during recent 2000 years in China, China Meteorological Press, Beijing (in Chinese), pp: 70-77
- Gregori, G. P., B. A. Leybourne, and J. R. Wright, 2025d. Generalized Cowling theorem and the Cowling dynamo. In press in *New Concepts in Global Tectonics, Journal*
- Gregori, G. P., B. A. Leybourne, G. Paparo†, and M. Poscolieri, 2025a. The global Sun-Earth circuit. In press in *New Concepts in Global Tectonics, Journal*
- Gregori, G.P., 2002. Galaxy – Sun – Earth relations. The Origin of the Magnetic Field and of the Endogenous Energy of the Earth, with Implications for Volcanism, Geodynamics and Climate Control, and Related Items of Concern for Stars, Planets, Satellites, and Other Planetary Objects. A Discussion in a Prologue and Two Parts. Beiträge zur Geschichte der Geophysik und Kosmischen Physik, Band 3, Heft 3, pp. 471 [Available at <http://ncgtjournal.com/additional-resources.html>]
- Gregori, G.P., 2002a. History of science and the Cycle of Climate and Civilisation. The Deontology of a Science Historian. In Solar variability and geomagnetism, W. Schröder (ed.), Beiträge zur Geschichte der Geophysik und Kosmischen Physik, 3 (2), Science Edition, AKGGKP, Bremen-Roennebeck; pp: 250-257
- Gregori, G.P., 2020. Climate change, security, sensors. Acoustics, 2: 474-504; DOI:10.3390/acoustics2030026 [https://www.mdpi.com/2624-599X/2/3/26/html]
- Gregori, G.P., and B.A. Leybourne, 2021. An unprecedented challenge for humankind survival. Energy exploitation from the atmospheric electrical circuit, American Journal of Engineering and Applied Science, 14 (2): 258-291. DOI:10.3844/ajeassp.2021.258.291
- Gregori, G.P., and B.A. Leybourne, 2025a. Introduction – Air-earth currents, climate control, and the exploitation of the electrostatic energy of the atmosphere. In press in *New Concepts in Global Tectonics, Journal*
- Gregori, G.P., and B.A. Leybourne, 2025k. The global climate change perspective. The glaciers proxy, *New Concepts in Global Tectonics, Journal*, 13 (2): 270-335
- Gregori, G.P., and M.T. Hovland, 2025. Go for the anomaly – a golden strategy for discovery? Seepology & the origin and crucial role of the biosphere - Earth and planetary objects - Supercritical water and serpentinization. In press in *New Concepts in Global Tectonics, Journal*
- Gregori, G.P., B.A. Leybourne, and Gao Xiaoqing, 2025q. Atlas of the Joule heat released at the ALB, CMB and ICB during AD 1400 through present, *New Concepts in Global Tectonics, Journal*, 13 (3): 460-472
- Gregori, G.P., B.A. Leybourne, Dong Wenjie, and Gao Xiaoqing, 2025j. Topics in palaeoclimatology - The role of the biosphere for air-earth currents. In press in *New Concepts of Global Tectonics, Journal*
- Gregori, G.P., B.A. Leybourne, Dong Wenjie, and Gao Xiaoqing, 2025f. The Tang Maocang school. The uplift of Himalaya – shallow geotherms – palaeoclimate – endogenous heat. In press in *New Concepts in Global Tectonics, Journal*
- Gregori, G.P., B.A. Leybourne, Dong Wenjie, and Gao Xiaoqing, 2025l. Energy release from ALB, CMB and ICB and secular variation. II – Methods: the “principle of magnetic energy variation” & Joule heat on a spherical shell of currents *New Concepts in Global Tectonics, Journal*, 13 (3): 350-377
- Gregori, G.P., B.A. Leybourne, Dong Wenjie, and Gao Xiaoqing, 2025m. Energy release from ALB, CMB and ICB and secular variation. III – A physical analysis - Estimate of self-energies and radii & the LN law and related secular variation *New Concepts in Global Tectonics, Journal*, 13 (3): 378-409
- Gregori, G.P., B.A. Leybourne, Dong Wenjie, and Gao Xiaoqing, 2025n. Energy release from ALB, CMB and ICB and secular variation. IV – A physical analysis - The Poynting theorem and the estimate of s/σ , separating the roles of terms with different degree n , and a tentative physical explanation concerning the role of the “magpol” IC in the TD dynamo, *New Concepts in Global Tectonics, Journal*, 13, (3): 410-432

- Gregori, G.P., B.A. Leybourne, Dong Wenjie, and Gao Xiaoqing, 2025o. Energy release from *ALB*, *CMB* and *ICB* and secular variation. V – Results, *New Concepts in Global Tectonics, Journal*, 13 (3): 433-459
- Gregori, G.P., B.A. Leybourne, Dong Wenjie, and Gao Xiaoqing, 2025h. Shallow geotherms. In press in *New Concepts in Global Tectonics, Journal*
- Gregori, G.P., B.A. Leybourne, Dong Wenjie, and Gao Xiaoqing, 2025g. The timing of the uplift of Himalaya and the Third Pole. In press in *New Concepts in Global Tectonics, Journal*
- Gregori, G.P., B.A. Leybourne, F.T. Gizzi, Dong Wenjie, and Gao Xiaoqing, 2025k. Energy release from *ALB*, *CMB* and *ICB* and secular variation. I – The observational database, *New Concepts in Global Tectonics, Journal*, 13, (3): 341-349
- Gregori, G.P., M. Colacino, M.R. Valensise, and L.G. Gregori, 2000. Why a history of geophysics? In *Geschichte und Philosophie der Geophysik (History and Philosophy of Geophysics)*, W. Schröder (ed.) Beiträge zur Geschichte der Geophysik und Kosmischen Physik der DDG, 2, and Newsletter of IDCH-IAGA (42), W. Schröder, and AKGGKP (Arbeitskreis Geschichte der Geophysik und Kosmischen Physik der DDG), Bremen-Roenebeck and Potsdam; 112-122
- Grootes, P. M., M. Stuiver, J.W.C. White, S.J. Johnsen, and J. Jouzel, 1993. Comparison of oxygen isotope records from the GISP2 and GRIP Greenland ice cores. *Nature*, 366: 552-554
- Grootes, P.M., and M. Stuiver, 1997. Oxygen 18/16 variability in Greenland snow and ice with 10⁻³ to 10⁵-year time resolution, *Journal of Geophysical Research*, 102 (C12): 26,455–26,470; DOI:10.1029/97JC00880
- Guan Qingyu, Pan Baotian, Li Na, Li Qiong, Zhang Jundi, Gao Hongshan, and Liu Jia, 2010. A warming interval during the MIS 5a/4 transition in two high-resolution loess sections from China, *Journal of Asian Earth Sciences*, 38 (6): 255-261; DOI:10.1016/j.jseaeas.2010.02.004
- Guo, Dongxin, and Li Zuofu, 1981. Preliminary approach to the history and age of permafrost in Northeast China, *Journal of Glaciology and Geocryology*, (04); DOI:cnki:ISSN:1000-0240.0.1981-04-000
- Guo, Z.T., S.Z. Peng, Q.Z. Hao, X.H. Chen, and T.S. Liu, 1999. Late Tertiary development of aridification in northwestern China and its link with the Arctic ice-sheet formation and Tibetan uplifts (in Chinese), *Journal of Quaternary Science*, 6: 556-567
- Harrison, T.M., P. Copeland, W.S.F. Kidd, and, An Yin, 1992. Raising Tibet, *Science*, 255 (5052): 1663-1670; DOI:10.1126/science.255.5052.1663
- He, Yuanqing, Yao Tandong, Shen Yongping, Zhang Zhonglin, and Chen Tuo, 2003a. Climatic differences in China during the Holocene indicated by the various climatic proxy data from different parts of China. *Journal of Glaciology and Geocryology*, 25 (1): 11-18, (in Chinese)
- Hendy, I.L., J.P. Kennett, E.B. Roark, and B.L Ingram, 2002. Apparent synchronicity of submillennial scale climate events between Greenland and Santa Barbara Basin, California from 30-10 ka. *Quaternary Science Reviews*, 21 (10): 1167-1184; DOI:10.1016/S0277-3791(01)00138-X
- Herzschuh, U., H.J.B. Birks, Xingqi Liu, C. Kubatzki, and G. Lohmann, 2009. What caused the mid-Holocene forest decline on the eastern Tibet-Qinghai Plateau? *Global Ecology and Biogeography*, [9 pp.]; DOI:10.1111/j.1466-8238.2009.00501.x
- Higman, B., D.H. Shugar, C.P. Stark, G. Ekström, M.N. Koppes, P. Lynett, A. Dufresne, P.J. Haeussler, M. Geertsema, S. Gulick, A. Mattox, J.G. Venditti, M.A.L. Walton, N. McCall, E. Mckittrick, B. MacInnes, E.L. Bilderback, Hui Tang, M.J. Willis, B. Richmond, R.S. Reece, C. Larsen, B. Olson, J. Capra, A. Ayca, C. Bloom, H. Williams, D. Bonno, R. Weiss, A. Keen, V. Skanavis, and M. Loso, 2018. The 2015 landslide and tsunami in Taan Fiord, Alaska, *Scientific Reports*, 8: article no. 12993; DOI:10.1038/s41598-018-30475-w
- Hong, Jinkyu, Taejin Choi, Hirohiko Ishikawa, and Joon Kim, 2004. Turbulence structures in the near-neutral surface layer on the Tibetan Plateau, *Geophysical Research Letters*, 31 (15): L15106; DOI:10.1029/2004GL019935
- Hong, Yetang, H.B. Jiang, T.S. Liu, L.P. Zhou, J. Beer, H.D. Li, X.T. Leng, B. Hong, X.G. Qin, 2000. Response of climate to solar forcing recorded in a 6000-year δ¹⁸O time-series of Chinese peat cellulose, *The Holocene*, 10 (1): 1-7; DOI:10.1191/0959683006
- Hong, Yetang, Hong Bin, Lin Qinghua, Y. Shibata, M. Hirota, and X.T. Leng, 2005. Inverse phase oscillations between the East Asian and Indian Ocean summer monsoon during the last 12000 years and palaeo-El Nino. *Earth and Planetary Science Letters*, 231: 337-346
- Hori, M., T. Ishikawa, K. Nagaishi, Ke Lin, Bo-Shian Wang, Chen-Feng You, Chuan-Chou Shen, and A. Kano, 2013. Prior calcite precipitation and source mixing process influence Sr/Ca, Ba/Ca and 87Sr/86Sr of a stalagmite developed in southwestern Japan during 18.0–4.5ka, *Chemical Geology*, 347: 190-198; DOI:10.1016/j.chemgeo.2013.03.005
- Hou, Yandong, Hao Long, Ji Shen, and Lei Gao, 2021. Holocene lake-level fluctuations of Selin Co on the central Tibetan plateau: Regulated by monsoonal precipitation or meltwater? *Quaternary Science Reviews*, 261, 106919; DOI:10.1016/j.quascirev.2021.106919
- Hovan, S.A., D.K. Rea, N.G. Pisias, 1989. A direct link between the China loess and marine ¹⁸O records: Aeolian flux to the North Pacific, *Nature*, 340: 296-298
- Huang, Maohuan (Huang Mao-huan), and Yuan Jianmo (Yuan Chien-mo), 1965. The temperature regime of the surface snow and ice layer on No. 1 glacier of Urumchi river source, T'ien Shan (in Chinese). In *Researches on the glaciology and hydrology of Urumchi river source, T'ien Shan, Zhong-guo Ke-xue-yuan di-li Yan-jiu-suo Bing-chuan Dong-tu Yan-jiu-shi Bian-ji (Chung-kuo K'e-hsueh-yuan ti-li Yen-chiu-so Ping-ch'uan Tung-t'u Yen-chiu-shih Pien-chi)*, (eds). Published by K'e-hsueh Ch'u-pan-she, Peking; pp: 25- 30

- Huang, Maohuan, Wang Zhongxiang, and Ren Jiawen, 1982. On the temperature regime of continental type glaciers in China, *Journal of Glaciology*, 28 (98): 117-128; DOI:10.3189/S0022143000011837
- Indermühle, A., E. Monnin, B. Stauffer, T.F. Stocker, and M. Wahlen, 2000. Atmospheric CO₂ Concentration from 60 to 20 kyr BP from the Taylor Dome Ice Core, Antarctica, *Geophysical Research Letters*, 27 (5): 735–738
- Islam, Nabilah, 2019. Historical data on black carbon and melting glaciers in Tibet, glacierhub blog, issued 3 Jan 2019. Republished by Earthsky, issued 11 Jan 2019
- Jansen, J.H.F., A. Kuijpers, and S.R. Troelstra, 1986. A Mid-Brunhes climatic event: long-term changes in global atmosphere and ocean circulation. *Science*, 232: 619–622
- Jiang, Xinsheng, Pan Zhongxi, and Fu Qingping, 2001. Primary study on pattern of general circulation of atmosphere before uplift of the Tibetan Plateau in eastern Asia, *Science in China, Ser. D*, 44 (8): 680-688; DOI:10.1007/BF02907197
- Jin, Guiyun, and Liu Dongsheng, 2002. Mid-Holocene climate change in North China, and the effect on cultural development, *Chinese Science Bulletin*, 47 (5): 408-413; DOI:10.1360/02tb9095
- Jin, Xingchun, Zhou Zuyi, and Wang Pinxian, 1995. *Ocean Drilling Program and Earth Science in China (in Chinese)*, Tongji University Press, Shanghai; pp: 349
- Johnsen, S.J., D. Dahl-Jensen, N. Gundestrup, J.P. Steffensen, H.B. Clausen, H. Miller, V. Masson-Delmotte, A.E. Sveinbjörnsdóttir, and J. White, 2001. Oxygen isotope and palaeotemperature records from six Greenland ice-core stations: Camp Century, Dye-3, GRIP, GISP2, Renland and NorthGRIP. *Journal of Quaternary Science*, 16 (4): 299–307; DOI:10.1002/jqs.622
- Kang, Xingcheng, Zhang Qihua, L.J. Graumlich, and P. Sheppard, 2000. Reconstruction of A 1835 a past climate for Dulan, Qinghai province, using tree-ring, *Journal of Glaciology and Geocryology*, (01); DOI:cnki:ISSN:1000-0240.0.2000-01-015 [Advances in Earth Science, 15 (2): 215-221, (in Chinese)]
- Kiefer, T., M. Sarnthein, H. Elderfield, P.M. Grootes, and H. Erlenkeuser, 2006. Warmings in the far northwestern Pacific support pre-Clovis immigration to America during Heinrich event 1. *Geology*, 34 (3): 141-144; DOI:10.1130/G22200.1
- Klitgaard-Kristensen, D., H.P. Sejrup, H. Haflidason, S. Johnsen, and M. Spurk, 1998. A regional 8200 cal. a BP cooling event in northwest Europe, induced by final stages of the Laurentide ice-sheet deglaciation? *Journal of Quaternary Science*, 13: 165-169
- Kocha, A., C. Brierley, M.M. Maslin, and S.L. Lewis, 2019. Earth system impacts of the European arrival and Great Dying in the Americas after 1492, *Quaternary Science Reviews*, 207 (1): 13-36; DOI:10.1016/j.quascirev.2018.12.004
- Kornei, K., 2019a. Glacial census reveals ice thicknesses around the world, *EOS, Transactions American Geophysical Union*, 100; DOI:10.1029/2019EO116153
- Koutavas, A., J. Lynch-Stieglitz, T.M. Marchitto, Jr., and J.P. Sachs, 2002. El Niño-like pattern in ice age tropical Pacific sea surface temperature. *Science*, 297: 226-230; DOI:10.1126/science.1072376
- Kurosaki, Y., M. Shinoda, and M. Mikami, 2011. What caused a recent increase in dust outbreaks over East Asia? *Geophysical Research Letters*, 38: L11702; DOI:10.1029/2011GL047494
- Kutzbach, J.E. and P.J. Guetter, 1986. The influence of changing orbital parameters and surface boundary-conditions on climate simulations for the past 18000 years. *Journal of the Atmospheric Sciences*, 43 (16): 1726-1759
- Lachniet, M.S., R.F. Denniston, Y. Asmerom, and V.J. Polyak, 2014. Orbital control of western North America atmospheric circulation and climate over two glacial cycles. *Nature, Communications*, 5: 3805; DOI:10.1038/ncomms4805
- Lang, D.C., I.I. Bailey, P.A. Wilson, T.B. Chalk, G.L. Foster, and M. Gutjahr, 2016. Incursions of southern-sourced water into the deep North Atlantic during late Pliocene glacial intensification, *Nature Geoscience*, 9: 375–379; DOI:10.1038/ngeo2688
- Larson, R.L., and P. Olson, 1991. Mantle plumes control magnetic reversal frequency. *Earth and Planetary Science Letters*, 107: 437-447; DOI:10.1016/0012-821X(91)90091-U
- Li, Bin, Yuan Daoxian, Qin Jiaming, Lin Yushi, and Zhang Meiliang, 2000. Oxygen and carbon isotopic characteristics of rainwater, drip water and present speleothems in a cave in Guilin area, and their environmental meanings, *Science in China Series D-Earth Sciences*, 43 (3): 277-285; DOI:10.1007/BF02906823
- Li, Chaoliu, and Shichang Kang, 2006. Review of the studies on climate change since the last inter-glacial period on the Tibetan Plateau, *Journal of Geographical Sciences*, 16 (3): 337-345; DOI:10.1007/s11442-006-0309-6
- Li, Jijun, et al., 1995. Uplift of Qinghai-Xizang (Tibet) Plateau and Global Change, (in Chinese) Lanzhou Univ. Press, Lanzhou; pp: 207
- Li, Xiaoqiang, Zhou Xinying, Zhou Jie, J. Dodson, Zhang Hongbin, and Shang Xue, 2007. The earliest archaeological evidence of the broadening agriculture in China recorded at Xishanping site in Gansu Province, *Science in China Series D-Earth Sciences, Earth Sciences*, 50 (11): 1707-1714
- Li, Xingguo, Liu Guanglian, Xu Guoying, Li Fengchao, and Wang Fulin, 1982. Periglacial phenomena at the east open coal mine of Zhalianuoer in Inner Mongolia and their geochronology, *Journal of Glaciology and Geocryology*, (03); DOI:cnki:ISSN:1000-0240.0.1982-03-006
- Li, Yuanfang, Zhang Qingsong, Li Bingyuan, 1994a. Stracod fauna and environmental changes during the past 17000 years in the western Tibet. *Acta Geographica Sinica*, 49 (1): 46-54. (in Chinese)
- Lin and Wu, 1981. Missing information

- Lin Benhai et al., 1992 - Cited by Liu et al., (1996b). Missing information
- Lisiecki, L.E., and M.E. Raymo, 2005. A Pliocene-Pleistocene stack of 57 globally distributed benthic $\delta^{18}\text{O}$ records, *Paleoceanography*, 20, PA1003; DOI:10.1029/2004PA001071
- Liu, Dongshen, et al., 1985. *Loess and Environment*, Science Press, Beijing; pp: 251
- Liu, Dongsheng (Liu Tungsheng), An Zhisheng, Chen Mingyang, and Sun Donghuai, 1996b. A correlation between southern and northern hemispheres during the last 0.6 Ma, *Science in China Series D-Earth Sciences*, 39 (2): 113-120
- Liu, Guangxiu, Shi Yafeng, Shen Yongping, 1997. Holocene Megathermal environment in the TP. *Journal of Glaciology and Geocryology*, 19 (2): 114-123. (in Chinese)
- Liu, J. Y., Y. J. Chuo, Sergey Alexander Pulinetz, H. F. Tsai, and X. Zeng, 2002. A study on the TEC perturbations prior to the Rei-Li, Chi-Chi and Chia-Yi earthquakes. In *Seismo-electromagnetic Lithosphere-Atmosphere-Ionosphere Coupling*, M. Hayakawa and O.A. Molchanov (eds), TERRAPUB, Tokyo; pp: 297-301
- Liu, X. M. et al., 1988 – Cited by Liu et al., (1996b). Missing information
- Liu, Xiaodong, and Ma Zhuguo, 1996. An important cause leading to short-term climatic variation in China: the change in the surface albedo in TP. *Journal of Tropical Meteorology*, 12 (3): 240-245. (in Chinese)
- Liu, Xiaodong, and Tang Maocang, 1996. On the critical effecting height of the Tibetan Plateau on the atmosphere, *Plateau Meteorology*, 15 (2): 131- (in Chinese)
- Liu, Xiaodong, and Tang Maocang, 1997. On the critical height of the effect of the Tibetan Plateau on the atmosphere, *Proceedings of Qinghai-Xizang Plateau Project conference in 1995*. Science Press, Beijing (in press)
- Liu, Yu, An Zhisheng, H.W. Linderholm, Chen Deliang, Song Huiming, Cai Qiufang, Sun Junyan, and Tian Hua, 2009b. Annual temperatures during the last 2485 years in the mid-eastern Tibetan Plateau inferred from tree rings, *Science In China Series D-Earth Sciences, Earth Sciences*, 52 (3): 348-359
- Liu, Yu, An Zhisheng, Ma Haizhou, Cai Qiufang, Liu Zhengyu, J.K. Kutzbach, Shi Jiangfeng, Song Huiming, Sun Junyan, Yi Liang, Li Qiang, Yang Yinke, and Wang Lei, 2006g. Precipitation variation in the northeastern Tibetan Plateau recorded by the tree rings since 850 AD and its relevance to the Northern Hemisphere temperature, *Science In China Series D-Earth Sciences, Earth Sciences*, 49 (4): 408-420; DOI:10.1007/s11430-006-0408-3
- Lorenz, E.N., 1967. *The Nature and Theory of the General Circulation of the Atmosphere*, WMO (No. 218), World Meteorological Organization; pp: 161
- McDermott, F., D.P. Mattey, and C. Hawkesworth, 2001. Centennial-scale Holocene climate variability revealed by a high-resolution speleothem $\delta^{18}\text{O}$ record from SW Ireland, *Science*, 294: 1328-1331
- Mearns, E., 2015. CO₂ – the view from space, energy matters, Posted on January 26, 2015. [CO₂ . the View from Space Energy Matters.htm].
- Nichols, J.E., M. Walcott, R. Bradley, J. Pilcher, and Y. Huang, 2009a. Quantitative assessment of precipitation seasonality and summer surface wetness using ombrotrophic sediments from an Arctic Norwegian peatland, *Quaternary Research*, 72 (3): 443-451; DOI:doi:10.1016/j.yqres.2009.07.007
- Ninnemann, U.S., C.D. Charles, and D.A. Hodell, 1999. In *Mechanisms of Global Change at Millennial Time Scales*. Clark, Peter U., R.S. Webb, and L.D. Keigwin (eds), *Geophysical Monograph*, American Geophysical Union, Washington DC.; pp: 99-112
- North Greenland Ice Core Project* members, 2004. High-resolution record of Northern Hemisphere climate extending into the last interglacial period. *Nature*, 431: 147-151; DOI:10.1038/nature02805
- Overpeck, J., and J. Cole, 2008. Palaeoclimate: the rhythm of the rains, *Nature*, 451: 1061-1063; DOI:10.1038/4511061a
- Pahnke, K., R. Zahn, H. Elderfield, and M. Schulz, 2003. 340,000-Year centennial-scale marine record of southern hemisphere climatic oscillation. *Science*, 301: 948-952; DOI:10.1126/science.1084451
- Peltier, W.R., and L. Tarasov, 2005. Arctic freshwater forcing of the Younger Dryas cold reversal. *Nature*, 435: 662-665
- Peterson, L.C., G.H. Haug, K.A. Hughen, and U. Rohl, 2000. Rapid changes in the hydrologic cycle of the tropical Atlantic during the last glacial. *Science*, 290: 1947-1951
- Petit, J.R., J. Jouzel, D. Raynaud, N.I. Barkov, J.-M. Barnola, I. Basile, M. Bender, J. Chappellaz, M. Davis, G. Delaygue, M. Delmotte, V.M. Kotlyakov, M. Legrand, V.Y. Lipenkov, C. Lorius, L. Pépin, C. Ritz, E. Saltzman, and M. Stievenard, 1999. Climate and atmospheric history of the past 420,000 years from the Vostok ice core, Antarctica, *Nature*, 399: 429-436; DOI:10.1038/20859
- Pettet, D., 1995. Global Younger Dryas? *Quaternary Int.*, 28: 93-104
- Porter, S.C., 2007. Neoglaciation in the American Cordilleras. In *Encyclopedia of Quaternary Science, Glaciations*, II ed. Published by Elsevier in 2013; pp: 1133-1142
- Qin, Jiaming, Yuan Daoxian, Cheng Hai, Lin Yushi, Zhang Meiliang, Wang Fuxing, R.L. Edwards, Wang Hua, and Ran Jingcheng, 2005. The Y.D. and climate abrupt events in the early and middle Holocene: Stalagmite oxygen isotope record from Maolan, Guizhou, China, *Science in China, Series D, Earth Sciences*, 48 (4): 530-537; DOI:10.1360/02yd0461
- Qiu, Jane, 2008. Asian monsoon cycle disrupted by man-made climate change Chinese stalagmite reveals low rainfalls that may have brought down dynasties, *Nature, News*; DOI:10.1038/news.2008.1213

- Qiu, Shihua, and Cai Lianzhen, 1992. The age on the lowest boundary of Holocene by radiocarbon dating, *Journal of Quaternary Science*, (03); DOI:cnki:ISSN:1001-7410.0.1992-03-008
- Raina, V.K., 2009. Himalayan glaciers-Behaviour and climate change-A state-of-art review of glacial studies, glacial retreat and climate change, SPPI Reprint Series, Ministry of Environment & Forests, Government of India-G.B. Pant Institute of Himalayan Environment & Development, pp: 1-62
- Ramstein, G., F. Fluteau, J. Besse, and S. Jousseaume, 1997. Effect of orogeny, plate motion and land-sea distribution on Eurasian climate change over the past 30 million years, *Nature*, 386: 788-795; DOI:10.1038/386788a0
- Rea, D.K., 1994. The palaeoclimatic record provided by eolian deposition in the deep sea: the geologic history of wind, *Reviews of Geophysics*, 32: 159-195
- Rea, D.K., H. Snoeckx, and L.P. Joseph, 1998. Late Cenozoic eolian deposition in the North Pacific: Asian drying, Tibetan uplift, and cooling of the Northern Hemisphere, *Paleoceanography*, 13 (3): 215-224
- Ren, Jiawen (Jen Chia-wen), and Huang Maohuan (Huang Mao-huan), 1981. Analysis of heat transfer within glacial active layer (in Chinese). *Journal of Glaciology and Cryopedology*, 3 (3): 23-28
- Schreuder, L.T., E.C. Hopmans, I.S. Castañeda, E. Schefuß, S. Mulitza, J.S. Sinninghe Damsté, and S. Schouten, 2019. Late Quaternary biomass burning in Northwest Africa and interactions with climate, vegetation, and humans, *Paleoceanography and Paleoclimatology*, 34 (2): 153-163; DOI:10.1029/2018PA003467
- Schwander, J., T. Sowers, J.-M. Barnola, T. Blunier, A. Fuchs, and B. Malaizé, 1997. Age scale of the air in the summit ice: Implication for glacial-interglacial temperature change. *Journal of Geophysical Research*, 102 (D16): 19483-19494; DOI:10.1029/97JD01309
- Seki, O., R. Ishiwatari, and K. Matsumoto, 2002. Millennial climate oscillations in NE Pacific surface waters over the last 82 kyr: new evidence from alkenones. *Geophysical Research Letters*, 29: 5962-
- Shackleton, N.J., J. Le, A. Mix and M.A. Hall, 1992. Carbon isotope records from Pacific surface waters and atmospheric carbon dioxide, *Quaternary Science Reviews*, 11 (4): 387-400; DOI:10.1016/0277-3791(92)90021-Y
- Shakun, J.D., S.J. Burns, P.U. Clark, H. Cheng, and R.L. Edwards, 2011. Milankovitch-paced Termination II in a Nevada speleothem? *Geophysical Research Letters*, 38; DOI:10.1029/2011GL048560
- Shao, Xuemei, Huang Lei, Liu Hongbin, Liang Eryuan, Fang Xiuqi, and Wang Lili, 2005. Reconstruction of precipitation variation from tree rings in recent 1000 years in Delingha, Qinghai, *Science in China Series D-Earth Sciences*, Earth Sciences, 48 (7): 939-949
- Shao, Xuemei, Huang Lei, Liu Hongbin, Liang Eryuan, Fang Xiuqi, and Wang Lili, 2004. Reconstruction of precipitation variation from tree rings in recent 1000 years in Delingha, Qinghai, (in Chinese). *Science in China Series D-Earth Sciences*, 34 (2): 145-153
- Shi, Yafeng, (ed.), 1992. The climate and environment of China in the Megathermal of the Holocene, China Ocean Press (in Chinese); pp: 1-212
- Shi, Yafeng, and Zheng Benxing, 1997. Age and elevation of Tibetan Plateau entering into the cryosphere and its influence on neighboring areas, *Proceedings of Qinghai-Xizang Plateau Project conference in 1995*. Science Press, Beijing (in press)
- Shi, Yafeng, et al., 1992. Basic characteristics of climate and environment of China in the megathermal of the Holocene. In
- Shi, Yafeng, Kong Zhaochen, Wang Sumin, Tang Linyu, Wang Fubao, Yao Tandong, Zhao Xitao, Zhang Piyuan, and Shi Shaohua, 1992a. Climate fluctuation and vital events of Holocene in China. *Science in China, Series B (12)*: 1300-1308 (in Chinese)
- Shi, Yafeng, Kong Zhaozheng, Wang Sumin, Tang Linyu, Wang Fubao, Yao Tandong, Zhao Xitao, Zhang Peiyuan, and Shi Shaohua, 1993. Mid-Holocene climates and environments in China, *Global and Planetary Change*, 7 (1/3): 219-233; DOI:doi:10.1016/0921-8181(93)90052-P
- Shi, Yafeng, Liu Xiaodong, Li Bingyuan, and Yao Tandong, 1999a. The extremely strong summer monsoon during last 40-30 ka over TP and its relationship with precessional cycle. *Chinese Science Bulletin*, 44 (14): 1475-1480, (in Chinese)
- Shi, Yafeng, Tang Maocang, and Ma Yuzhen, 1999. Linkage between the second uplifting of the Qinghai-Xizang (Tibetan) Plateau and the initiation of the Asian monsoon system, *Science in China, Earth Sciences (Ser. D)*, 42 (3): 303-312; DOI:10.1007/BF02878967
- Shi, Yafeng, Zheng Benxing, Su Zhen, and Mu Yunzhi, 1984. Study of Quaternary glaciation in Mts. Tomur-Hantengri Area, Tien Shan, *Journal of Glaciology and Geocryology*, (02); DOI:cnki:ISSN:1000-0240.0.1984-02-001
- Smith, A., 2000. Terrestrial, planetary and interplanetary magnetic fields, *Astronomy & Geophysics*, 41 (3): 3.32-3.33
- Steponaitis, E., A. Andrews, D. McGee, J. Quade, Yu-Te Hsieh, W.S. Broecker, B.N. Shuman, S.J. Burns, and Hai Cheng, 2015. Mid-Holocene drying of the U.S. Great Basin recorded in Nevada speleothems, *Quaternary Science Reviews*, 127: 174-185; DOI:10.1016/j.quascirev.2015.04.011
- Stocker, T.F., 2000. Past and future reorganizations in the climate system, *Quaternary Science Reviews*, 19 (1/5): 301-319; DOI:10.1016/S0277-3791(99)00067-0
- Stuiver, M., and P.M. Grootes, 2000. GISP2 oxygen isotope ratios. *Quaternary Research*, 53: 277-284
- Stuiver, M., P.M. Grootes, and T.F. Braziunas, 1995. The GISP2 ¹⁸O climate record of the past 16,500 years and the role of the sun, ocean and volcanoes, *Quaternary Research*, 44: 341-354
- Stuiver, M., T.F. Braziunas, P.M. Grootes, and G.A. Zielinski, 1997. Is there evidence for solar forcing of climate in the GISP2 oxygen isotope record? *Quaternary Research*, 48 (3): 259-266; DOI:10.1006/qres.1997.1931

- Sun, Youbin, and An Zhisheng, 2002. Variation of the East Asian winter monsoon recorded by Chinese loess during the last four glacial-interglacial cycles. *Earth Science-Journal of China University of Geosciences (in Chinese)*, 27 (1): 19-24
- Sun, Youbin, and Zhisheng An, 2002a. History and variability of Asian interior aridity recorded by eolian flux in the Chinese Loess Plateau during the past 7 Ma. *Science in China Series D-Earth Sciences.*, 45 (5): 420-429; DOI:10.1360/02yd9044
- Tan, Ming, Liu Tungsheng, Hou Juzhi, Qin Xiaoguang, Zhang Hucai, and Li Tieying, 2003. Cyclic rapid warming on centennial-scale revealed by a 2650-year stalagmite record of warm season temperature. *Geophysical Research Letters*, 30 (12): ID 1617; DOI:10.1029/2003GL017352
- Tang, Lingyu, Caiming Shen, Kambiu Liu, and J.T. Overpeck, 2000a. Changes in South Asian monsoon: new high-resolution paleoclimatic records from Tibet, China. *Chinese Science Bulletin*, 45 (1): 87-91
- Tang, Lingyu, Shen Caiming, Kong Zhaochen, Wang Fubao, and Liu Kambiu, 1998a. Pollen evidence of climate during the last glacial maximum in eastern TP. *Journal of Glaciology and Geocryology*, 20 (2): 42-49, (in Chinese)
- Tang, Maocang, 1981. Estimation of some thermodynamic parameters over the Tibetan Plateau in summer. In *Proceedings of the Meteorology Meeting of the Tibetan Plateau in 1987 (in Chinese)*: 79-86, Beijing: Science Press
- Tang, Maocang, 1993. Progress in research on plateau monsoon, *Plateau Meteorology*, 12 (1): 95-101
- Tang, Maocang, 1997. Approach on the cause of climate abruption leaded by uplift of Tibetan Plateau, *Proceedings of Qinghai-Xizang Plateau Project conference in 1995*, (in press)
- Tang, Maocang, and Dong Wenjie, 1997a. Influences of seven Tibetan Plateau raising processes on climate and environment, *Plateau Meteorology*, 16 (1): 23-29
- Tang, Maocang, and E.R. Reiter, 1984. Plateau monsoons in the Northern Hemisphere, *Monthly Weather Review*, 112 (4): 617-
- Tang, Maocang, and Liu Xiaodong, 1995. A new mark for delimitation of Quaternary: stable appearance of plateau monsoon and its environmental results, *Quaternary Research (1)*: 82-88 (in Chinese)
- Tang, Maocang, and Liu Yanxiang, 2001. On causes and environmental consequences of the uplift of Qingghai-Xizang Plateau, *Quaternary Science*, (06); DOI:cnki:ISSN:1001-7410.0.2001-06-004
- Tang, Maocang, and Weidong Guo, 2000. The Great Ice Age cycles associated with the variation of the atmospheric heat engine efficiency, *Science in China (Ser. D)*: 43 (3): 286-292; DOI:10.1007/BF02906824
- Tang, Maocang, Gao Xiaoqing, and Dong Wenjie, 1995. A discussion on the cause on Earth great ice ages, *Atmospheric Information*, 2 (3): 1-10; also *Atmospheric Information*, 15 (3): 1-9
- Tarasov, P., Jin Guiyun, and Mayke Wagner, 2006. Mid-Holocene environmental and human dynamics in northeastern China reconstructed from pollen and archaeological data, *Palaeogeography, Palaeoclimatology, Palaeoecology*, 241 (2): 284-300; DOI:10.1016/j.palaeo.2006.03.038
- The Climate and Environment of China in the Megathermal of the Holocene, Shi, Yafeng, (ed.), China Ocean Press (in Chinese)
- Thompson, L.G., T. Yao, M.E. Davis, K.A. Henderson, E. Mosley-Thompson, P.-N. Lin, J. Beer, H.-A. Synal, J. Cole-Dai, and J.F. Bolzan, 1997. Tropical climate instability: the last Glacial Cycle from a Qinghai-Tibetan ice core, *Science*, 276 (5320): 1821-1825; DOI:10.1126/science.276.5320.1821
- Timmermann, A., and L. Menviel, 2009. What drives climate flip-flops? *Science*, 325 (5938): 273-274; DOI:10.1126/science.1177159
- Trenberth, K.E., and S.C. Chen, 1988. Planetary waves kinematically forced by Himalayan Orography, *Journal of the Atmospheric Sciences*, 45: 2934-
- Vidal, L., R.R. Schneider, O. Marchal, T. Bickert, T.F. Stocker, and G. Wefer, 1999. Link between the North and South Atlantic during the Heinrich events of the last glacial period. *Climate Dynamics*, 15, 909-919; DOI:10.1007/s003820050321
- Wang, K., 1990. Low-temperature event during the warm period of Holocene in China and its geological implication, *Journal of Quaternary Science*, (02); DOI: CNKI:SUN:DSJJ.0.1990-02-006
- Wang, Luejiang, M. Sarnthein, H. Erlenkeuser, P.M. Grootes, J.O. Grimalt, C. Pelejero, and G. Linck, 1999a. Holocene variations in Asian monsoon moisture: A bidecadal sediment record from the South China Sea. *Geophysical Research Letters*, 26: 2889-2892
- Wang, Qi, Pei-Zhen Zhang, J.T. Freymueller, R. Bilham, K.M. Larson, Xi'an Lai, Xinzhao You, Zhijun Niu, Jianchun Wu, Yanxin Li, Jingnan Liu, Zhiqiang Yang, Qizhi Chen, 2001. Present-day crustal deformation in China by Global Positioning System measurements, *Science*, 294 (5542): 574-577; DOI:10.1126/science.1063647
- Wang, Qi, Qiao Xuejun, Lan Qigui, Jeffrey Freymueller, Yang Shaomin, Xu Caijun, Yang Yonglin, You Xinzhao, Tan Kai, and Chen Gang, 2011a. Rupture of deep faults in the 2008 Wenchuan earthquake and uplift of the Longmen Shan, *Nature, Geoscience*, 4: 634-640; DOI:10.1038/ngeo1210
- Wang, Qiming, Zhigang Suo, and Xuanhe Zhao, 2012b. Bursting drops in solid dielectrics caused by high voltages, *Nature, Communications*, 3: 1157; DOI:10.1038/ncomms2178
- Wang, X., A. S. Auler, R. L. Edwards R L, Hai Cheng, P.S. Cristalli, P.L. Smart, D.A. Richards, and Chuan-Chou Shen, 2004a. Wet periods in northeastern Brazil over the past 210 kyr linked to distant climate anomalies. *Nature*, 432: 740-743; DOI:10.1038/nature03067
- Wang, Yongjin, Hai Cheng, R.L. Edwards, Xinggong Kong, Xiaohua Shao, Shitao Chen, Jiangyin Wu, Xiouyang Jiang, Xianfeng Wang, and Zhisheng An, 2008a. Millennial- and orbital-scale changes in the East

- Asian monsoon over the past 224,000 years, *Nature*, 451: 1090-1093; doi:10.1038/nature06692
- Wang, Yongjin, Hai Cheng, R.L. Edwards, Yaoqi He, Xingdong Kong, Zhisheng An, Jiangying Wu, Megan J. Kelly, C.A. Dykoski, and Xiangdong Li, 2005. The Holocene Asian monsoon: links to solar changes and North Atlantic climate, *Science*, 308 (5723): 854-857; DOI:10.1126/science.1106296
- Wei, Jiangfeng, and Wang Huijun, 2004. A possible role of solar radiation and ocean in the mid-Holocene East Asian monsoon climate. *Advances in Atmospheric Sciences*, 21 (1): 1-12
- Weisberger, M., 2019b. Ancient garbage heaps show fading Byzantine Empire was 'plagued' by disease and climate change, *Live Science*, issued Mar 25, 2019
- Weiss, H., and R.S. Bradley, 2001. What drives societal collapse?, *Science*, 291 (5504): 609-610; DOI:10.1126/science.1058775
- Wilson, R.M., 2016c. Asian monsoons and ice-age cycles, *Physocs Today, Physics Update*, issued Aug 1st, 2016
- Winograd, I.J., T.B. Coplen, J.M. Landwehr, A.C. Riggs, K.R. Ludwig, B.J. Szabo, P.T. Kolesar, and K.M. Revesz, 1992. Continuous 500,000-year climate record from vein calcite in Devils Hole, Nevada, *Science*, 258 (5080): 255-260; DOI:10.1126/science.258.5080.255
- Wu, G.X., and J.F. Wang, 1996. Comparison of the correlations of lower tropospheric circulation with tropical and extratropical sea surface temperature anomalies (in Chinese), *Acta Meteorologica Sinica*, 54 (4): 385-397
- Wu, Guangjian, Yao Tandong, Xu Baiqin, Li Zheng, Tian Lide, Duan Keqin, and Wen Linke, 2006. Grain size record of microparticles in the Muztagata ice core, *Science in China Series D-Earth Sciences, Earth Sciences*, 49 (1): 10-17; DOI:10.1007/s11430-004-5093-5
- Wu, Hong-Chun, 2004. Preliminary findings on perturbation of jet stream prior to earthquakes. *EOS, Transactions American Geophysical Union*, 85: T51B-0455
- Wu, Jiangying, Wang Yongjin, Cheng Hai, and L.R. Edwards, 2009. An exceptionally strengthened East Asian summer monsoon event between 19.9 and 17.1 ka BP recorded in a Hulu stalagmite, *Science in China Series D-Earth Sciences, Earth Sciences*, 52 (3): 360-368; DOI:10.1007/s11430-009-0031-1
- Wu, Xihao, and Zhisheng An, 1996. Loess-paleosol sequence on Loess Plateau and uplift of the Qinghai-Xizang Plateau, *Science in China, Ser. D*, 39 (2): 121-133
- Wunsch, C., 2003. Greenland-Antarctica phase relations and millennial time-scale climate fluctuations in the Greenland ice-cores. *Quaternary Science Reviews*, 22: 1631-1646
- Xia, ZhiFeng, Kong XingGong, Jiang XiuYang, and Cheng Hai, 2007. Precise dating of East-Asian-monsoon D/O events during 95-56 ka BP: based on stalagmite data from Shanbao cave at Shennongjia, China, *Science in China Series D-Earth Sciences, Earth Sciences*, 50 (2): 228-235; DOI:10.1007/s11430-007-2029-x
- Xie, Zichu (Hsieh Tzu-ch' u), 1980. Mass balance of glaciers and its relationship with characteristics of glaciers. *Journal of Glaciology and Cryopedology*, 2 (4): 1-10
- Xie, Youyu, 1985. Climatic condition in the formation and evolution of permafrost in Northeast China, *Journal of Glaciology and Geocryology*, (04); DOI:cnki:ISSN:1000-0240.0.1985-04-003
- Xu, Xiaobin, Wang Jian, and Zhu Jie, 2004. Study on glacial erosion surface of the southeast of Qinghai-Xizang Plateau using cosmogenic isotopes dating. *Scientia Geographica Sinica*, 24 (1): 101-104, (in Chinese)
- Yang, Bao, 2003. Climatic history of TP during the last 2000 years (in Chinese), *Advances in Earth Science*, 18 (2): 285-291
- Yang, Bao, A. Braeuning, and K. R. Johnson. 2002. General characteristics of temperature variation in China during the last two millennia. *Geophysical Research Letters*, 29 (9): 381-384
- Yang, Bao, B. Braeuning, and Shi Yafeng, 2003. Late Holocene temperature fluctuations on the Tibetan Plateau. *Quaternary Science Reviews*, 22, 2335-2344
- Yang, Bao, Shi Yafeng, and Zhou Qingbo, 2002a. Analyzing the effect of solar and volcanic activities on temperature variations in the Guliya ice core record and in the lower reaches of the Yangtze River over the last three centuries, *Journal of Glaciology and Geocryology*, (01); DOI:cnki:ISSN:1000-0240.0.2002-01-005
- Yang, Huaijen, and Chiu Shuchang, 1965. Quaternary glaciation and the postglacial climatic fluctuations in the region of upper Urumchi valley, Sinkiang, *Acta Geographica Sinica*, (03); DOI:cnki:ISSN:0375-5444.0.1965-03-001
- Yang, Zhihong, and Yao Tandong, 1997. Younger Dryas event recorded in Guliya ice core. *Chinese Science Bulletin*, 42 (18): 1975-1978, (in Chinese)
- Yao Tandong, 1995. Climate change since Little Ice Age from Guliya ice core (in Chinese). *Science in China Series D-Earth Sciences*, 25 (10): 1108-1114
- Yao Tandong, Liu Xiaodong, Wang Ninglian, and Shi Yafeng, 2000a. Amplitude of climatic changes in Qinghai-Tibet Plateau. *Chinese Science Bulletin*, 45 (1): 98-106 (in Chinese); 45 (13): 1236- 1243 (in English)
- Yao, Tandong, 1999. Abrupt climate change on the Tibetan Plateau during the last glacial, *Science in China, Series D*, 42 (4): 358-368
- Yao, Tandong, and Shi Yafeng, 1992. Climate change of the Holocene recorded in ice core of Dunde, Qilian Mountain, (in Chinese). In *The Climate and Environment of China in the Megathermal of the Holocene*, Shi, Yafeng, (ed.), China Ocean Press (in Chinese); pp: 206-211
- Yao, Tandong, and Yang Zhihong, 1994. Qinghai-Tibet Plateau temperature increase showed from ice core recodes, (in Chinese). *Chinese Science Bulletin*, 39 (5): 438- 441
- Yao, Tandong, Duan Keqin, Tian Lide et al., 2000. Record of Dasuopu ice core accumulated amount and the variation of Indian Monsoon during the last 400 years,

- (in Chinese). *Science in China, Series D*, 30 (6): 619-627
- Yao, Tandong, Jiao Keqin, Tian Lide, Li Zhongqin, Li Yuefang, Liu Jingshou, Huang Cuilan, Xie Chao, L.G. Thompson, and E.M. Thompson, 1995. Climatic and environmental records in Guliya Ice Cap, *Science in China. Series B, Chemistry, life sciences [Sci. China Ser. B]*, 38 (2): 228-237
- Yao, Tandong, L.G. Thompson, Shi Yafeng, Qin Dahe, Jiao Keqin, Yang Zhihong, Tian Lide, and E.M. Thompson, 1997. Climate variation since the last interglaciation recorded in the Guliya ice core, *Science in China, Series D-Earth Sciences*, 40 (6): 662-668; DOI:10.1007/BF02877697
- Yao, Tandong, L.G. Thompson, Shi Yafeng, et al., 1997a. Research on climate change since the last inter-glacial period from Guliya ice core, (in Chinese). *Science in China, Series D-Earth Sciences*, 27 (5): 447-452
- Yao, Tandong, Xu Baiqing, and Pu Jianchen, 2001. Climatic changes on orbital and sub-orbital time scale recorded by the Guliya ice core in Tibetan Plateau, *Science In China Series D-Earth Sciences, Suppl.*, 44, 360-368; DOI:10.1007/BF02912007
- Yao, Tandong, Yang Meixue, and Kang Xingcheng, 2001a. Comparative study of the climate changes in the past 2000 years by using ice core and the ring records, (in Chinese), *Journal of Quaternary Science*, 21 (6): 514-519; DOI:CNKI:SUN:DSJJ.0.2001-06-007
- Yao, Tandong, Yang Zhihong, Jiao Keqin, C. Huanh, and L. Tian, 1997b. A study of climate and environment in the past 2000 years based on ice cores, (in Chinese), *Earth Sciences Frontiers*, 4 (1/2): 95-100
- Yu, Ge, Bin Xue, Jian Liu, and Xing Chen, 2003. LGM lake records from China and an analysis of climate dynamics using a modelling approach, *Global and Planetary Change*, 38 (3/4): 223-256; DOI:doi:10.1016/S0921-8181(02)00257-6
- Yu, Kefu, Liu Dongsheng (Liu Tungsheng), Shen Chengde, Zhao Jianxin, Chen Tegu, Zhong Jinliang, Zhao Huanting, and Song Chaojing, 2002. High-frequency climatic oscillations recorded in a Holocene coral reef at Leizhou Peninsula, South China Sea, *Science in China Series D-Earth Sciences*, 45 (12): 1057-1067
- Yuan, Daoxian, Hai Cheng, R. Lawrence Edwards, Carolyn A. Dykoski, Megan J. Kelly, Meiliang Zhang, Jiaming Qing, Yushi Lin, Yongjin Wang, Jiangyin Wu, Jeffery A. Dorale, Zhisheng An, and Yanjun Cai, 2004. Timing, duration, and transitions of the last interglacial Asian monsoon. *Science*, 304 (5670): 575-578; DOI:10.1126/science.1091220
- Zeng, Qingcun, 1979. The mathematical and physical bases for numerical weather forecasting (in Chinese), vol. 1, Science Press, Beijing
- Zhang, Meiliang, Cheng Hai, Yuan Daoxian, Lin Yushi, Qin Jiaming, Wang Hua, Feng Yumei, Tu Lingling, and Zhang Huiling, 2004. High-resolution climate records from two stalagmites in Qixin Cave, southern Guizhou, and Heinrich events during the last glacial period, *Episodes*, 27 (2): 112-118
- Zhang, Pengxi; Zhang Baozhen; Qian Guimin, Li Haijun, and Xu Liming, 1994. The study of paleoclimatic parameter of Qinghai Lake since Holocene, *Journal of Quaternary Science*, (03) (in Chinese)
- Zhang, Qiang, and Zhu Cheng, 2000. Holocene climate variation in North bank of the Yangtze river, Nanjing, inferred from accumulation record from Lifeng profile, *Journal of Anhui Normal University (Natural Science)*, (03); DOI:cnki:ISSN:1001-2443.0.2000-03-009
- Zhao, Songling, Yu Hongjun, and Liu Jingpu, 1997. Origin, development and evolutionary model of shelf desertification environment in late stage of Upper Pleistocene, *Science in China Series D-Earth Sciences*, 40 (2): 207-214
- Zheng, Jingyun, Wang Weichyung, Ge Quansheng, Man Zhimin, and Zhang Piyuan, 2006a. Precipitation variability and extreme events in eastern China during the past 1500 years. *Terrestrial, Atmospheric and Oceanic Sciences*, 17: 579-592
- Zhou, Jiamao, Xuexi Tie, Baiqing Xu, Shuyu Zhao, Mo Wang, Guohui Li, Ting Zhang, Zhuji Zhao, Suixin Liu, Song Yang, Luyu Chang, and Junji Cao, 2018a. Black carbon (BC) in a northern Tibetan mountain: effect of Kuwait fires on glaciers, *Atmospheric Chemistry and Physics*, 18, 13673-13685; DOI:10.5194/acp-18-13673-2018
- Zhou, Weijian, Lu Xuefeng, Wu Zhengkun, Deng Lin, A.J.T. Jull, D. Donahue, and W. Beck, 2002. Peat record reflecting Holocene climatic change in zoige plateau and AMS radiocarbon dating. *Chinese Science Bulletin*, 47 (1): 66-70
- Zhou, Weijian, Zhisheng An, S.C. Porter, D. Donahue, and A.J.T. Jull, 1997. Correlation of climatic events between East Asia and Norwegian Sea during last deglaciation, *Science in China*, 40 (5): 496-501; DOI:10.1007/BF02877615
- Zhu, Liping, Wang Junbo, Chen Ling, Yang Jingrong, Li Bingyuan, Zhu Zhaoyu, K. Hirokyi, and P. Goran, 2004. 20,000-year environmental change reflected by multidisciplinary lake sediments in Chen Co, Southern Tibet, *Acta Geographica Sinica/Dili Xuebao*, 59 (4): 514-524 (in Chinese)
- Zubakov, V.A., and I.I. Bonenkova, 1990. *Global Paleoclimate of the Late Cenozoic*, Elsevier, Amsterdam

Acronyms

- AGCM - atmospheric general circulation model
 AHEE - atmospheric heat engine efficiency
 ALB - asthenosphere-lithosphere boundary
 AM - Asian monsoon
 AMOC - Atlantic meridional overturning circulation
 APE - available potential energy
 BA - Bølling Allerød period
 BC - black carbon
 BT2 - Brazil stalagmite
 CC3 - a stalagmite in southwestern Ireland
 D4 - a stalagmite in the Dongge cave in Libo, Guizhou, China

- DO - Dansgaard-Oeschger
 E - Mount Everest (8848 m)
 EASM - East-Asian-Summer monsoon
 EDC - *European Project for Ice Coring in Antarctica (EPICA)* has provided two records in East Antarctica, one at Dome C (EDC), and one in the Dronning Maud Land area (EDML).
 ENSO – El Niño Southern Oscillation
 FR – field reversal (geomagnetic)
 GCA - general circulation of the atmosphere
 GIA - great Ice Age
 GISP - *Greenland Ice Sheet Project*
 H - Heinrich’s event
 H82 – a stalagmite from the Nanjing Hulu cave
 HS - Heinrich stadial
 IRD - ice rafted debris
 ITS - Indus-Tsangbo suture
 K - Mount Kailas (6714 m)
 K2 - Mount Godwin-Austin (8611 m);
 LC-2 - speleothem from Lehman Caves, Nevada
 LGM - last glacial maximum
 LR04 - is an average of 57 globally distributed benthic $\delta^{18}O$ records reported in the scientific literature spanning 5.3 Ma (Lisiecki and Raymo, 2005)
 MBE - Mid-Brunhes Event
 MBT - Main Boundary thrust
 MCT - Main Central thrust
 MD – initials for sediment cores collected by the research vessel *Marion Dufresne II* named in honour of the 18th-century French explorer Marc-Joseph Marion du Fresne
 MIS - marine isotope stage or marine oxygen-isotope stage, sometimes called “*marine interglacial stage*” or “*oxygen isotope stage*” (OIS)
 MKT - Main Karakoram thrust
 MMT - Main Mantle thrust
 MSD - a stalagmite
 NAO - North Atlantic Ocean
 NB - Namche Barwa (7756 m)
 NH – Northern Hemisphere
 NHSI - NH summer insolation
 NP - Nanga Parbat (8126 m)
 NQTL - Nyainqentanghla Shan
 ODP - Ocean Drilling Program
 OIS - oxygen isotope stage; see MIS
 PCP - prior calcite precipitation, i.e. carbonate precipitation from infiltrating water before the water drips on a stalagmite
 RFI - radiative forcing increase
 RM - Ruoergai hole
 SB - Sanbao Cave, on the northern slope of Mt Shennongjia in central China (110° 26’E, 31° 40’N , elevation 1,900 m a.s.l.).
 SH – Southern Hemisphere
 SST – sea surface temperature
 STDS - Southern Tibetan detachment system
 T - Termination
 TD – tide-driven geodynamo
 TP - Tibet Plateau
 TQP - Tibet-Qinghai Plateau
 TrP - Third Pole”
 V21-146 - a sediment core in the North Pacific
 WAIS - a temperature proxy (West Antarctic Ice Sheet)
 WMI - weak monsoon interval
 WMO – *World Meteorological Organization*
 WMT – warm mud tectonics
 YD - Younger Dryas period
 YT – a stalagmite
 YXB – a stalagmite

Topics in palaeoclimatology

The role of the biosphere for air-earth currents

Giovanni Pietro Gregori¹, Bruce Allen Leybourne², Dong Wenjie³, Gao Xiaoqing⁴

¹ Former Senior Researcher at IDASC-Institute of Acoustics and Sensors O. M. Corbino (CNR), Rome, now merged with the INM-Institute of Marine Engineering "Section of Acoustics and Sensors O.M. Corbino"- (CNR Rome); and ISSO-International Seismic Safety Organization, Italy

² GeoPlasma Research Institute-(GeoPlasmaResearchInstitute.org), Aurora, CO 80014, USA

³ Professor and Dean, School of Atmospheric Science, Sun Yat-sen University, Zhuhai, Guangdong, (PRC), Director of Future Earth Global Secretariat Hub China and Secretary-General of FE Chinese National Committee

⁴ Northwest Institute of Eco-Environment and Resources, Chinese Academy of Sciences, 730000, Lanzhou, (PRC)

Corresponding Author: G. P. Gregori, IDASC-Istituto di Acustica e Sensoristica O. M. Corbino (CNR), Roma, now merged into IMM-Istituto per la Microelettronica e Microsistemi (CNR);
Email:
giovannipgregori38@gmail.com
leybourneb@iascc.org
dongwj3@mail.sysu.edu.cn
xqgao@lzb.ac.cn

Abstract: The present paper deals with a few highlights of palaeoclimatology, mostly concerned with the role of the biosphere. This is a complement to the discussion related to the topics treated in previous papers and dealing with the achievements of the school of the late Professor Tang Maocang. Soil exhalation is a leading component of air-earth currents. Tang Maocang and coworkers discussed – in addition to earthquake precursors and middle range meteorological forecasting - the implications for palaeoclimatology. The biosphere is an effective control driver of the energy exchanges between soil and atmosphere. We highlight several topics of such a general set of investigations with no presumption for completeness. We only give a reminder of items that help to emphasize the meaning and extent of the achievements of the Chinese school. In fact, it is impossible to give a synthesis of this entire scenario. The present reminder is only a partial illustration, because an encyclopedia would be insufficient for any exhaustive treatment. The topics that are here concisely (and partially) illustrated deal with: (i) the palaeocomposition of the atmosphere and the role of the biosphere, (ii) the palaeodensity of the atmosphere, (iii) the carbon cycle, (iv) desertification, (v) Sahel and a few other planetary-scale phenomena, (vi) the first human settlements in the Americas, (vii) the understanding of biogeochemical cycles, (viii) some items concerning the Chinese dynasties including a global perspective, (ix) the carbon, phosphorus, iron and nitrogen cycles, (x) the early interactions between Earth's atmosphere and oceans, and (xi) a more extensive discussion on the Sahel drought and planetary phenomena.

Keywords: palaeocomposition and palaeodensity of the atmosphere - role of the biosphere – desertification - Sahel drought and planetary phenomena – first human arrival in the Americas - cycles (carbon, phosphorus, iron, nitrogen, biogeochemical) - Chinese dynasties and global perspective - early interactions between atmosphere and oceans

Background – The present set of papers includes the coauthors Dong Wenjie and Gao Xiaoqing, who in the 1990s spent one sabbatical year each, at the *Istituto di Fisica dell'Atmosfera (CNR)* in Rome for cooperation with G.P. Gregori. Dong Wenjie and Gao Xiaoqing had a scholarship provided by of *World Laboratory*, with President Prof. Antonino Zichichi, who is warmly thanked for providing this opportunity. *World Laboratory*, with the support of the Italian government, strongly promoted cooperation between different countries. The content of the present papers strictly and exclusively relies on information that was exchanged during those two sabbatical years. The full responsibility is by G.P. Gregori and B.A. Leybourne, while Dong Wenjie and Gao Xiaoqing agreed to be included as coauthors. Dong Wenjie and Gao Xiaoqing - two really brilliant scientists and gentlemen - greatly contributed to the implementation of the present study, and we feel sincerely very grateful to them. We hope this is also a way to honor the recent passing away of Professor Tang Maocang.

Introduction

The present paper deals with a few highlights of palaeoclimatology, mostly concerned with the role of the biosphere.

This is a complement to the discussion related to the topics described in Gregori et al. (2025g, 2025h and 2025i) and dealing with achievements of the school of the late Professor Tang Maocang. The present best known approach in the western literature is focused on the role of atmospheric heating that propagates underground, and heats oceans, ice sheets, and soil. In contrast, the Tang's school is focused on the flow of endogenous heat - while searching for earthquake precursors and for middle-range meteorological forecasting.

Indeed, soil exhalation is a leading component of air-earth currents. Tang Maocang and coworkers also discuss the implications for palaeoclimatology. In this respect, the biosphere is an effective driver of the energy exchanges between soil and atmosphere. Hence, the role of the biosphere is an implicit concern in the discussion of these crucial items.

The present paper aims to highlight several topics of such a general facet of investigation, however with no presumption for completeness.

Every topic is not treated like a formal exhaustive review. Rather, we provide a reminder of items that help to emphasize the meaning and extent of the achievements of the Chinese school discussed in Gregori et al. (2025g, 2025h and 2025i). *For respect to the authors, we report the original statements – as far as permitted by copyright constraints.*

Owing to the great difficulty of these topics, it is impossible - or in any case premature - to attempt to give a synthesis of the entire scenario. Therefore, the discussion in the literature is generally restricted to several distinct topical groups of specialists, and - in general - different groups can hardly communicate with each other. The present reminder can therefore give only a partial illustration of this intricate and important realm of climatology.

An encyclopedia would be insufficient for any exhaustive illustration. The topics are here concisely (and partially) reported by distinguishing a few leading anthems. We first deal with the palaeocomposition of the atmosphere and the role of the biosphere. Then, the focus is on the palaeodensity of the atmosphere. The next topics are carbon cycle, and desertification. Sahel and a few other planetary-scale phenomena are discussed including the first human arrival in the Americas, altogether with the understanding of biogeochemical cycles. Then, we deal with some items concerned with the Chinese dynasties and with the global perspective. The next topics are the carbon, phosphorus, iron and nitrogen cycles, and the early interactions between Earth's atmosphere and oceans. The last topic is a more extensive discussion on the Sahel drought and planetary phenomena. A short conclusion ends our reminder.

The palaeocomposition of the atmosphere and the role of the biosphere

Every attempt is still premature for giving an exhaustive treatment of these topics. Only a few relevant items are here considered that, in some way, are pertinent for the present general discussion. Contrary to the general expectation, the conclusion will be found that the primary driver is the exhalation of endogenous energy that displays a large gradient in space and time. The biosphere is crucial, as it reacts in different ways through a control on the chemistry of the atmosphere, in terms of production and/or sequestration of O_2 , CO_2 and/or CH_4 . The greenhouse gases H_2O , CO_2 and CH_4 finally contribute to control climate temperature. However, at equal atmospheric concentration, CH_4 is a greenhouse gas that is 23 times more powerful than CO_2 , although with a shorter lifetime (Pappas, 2016). As far as the human impact is concerned, it is certainly relevant in several respects, although, compared to natural exhalation, the anthropic CO_2 plays a secondary - or maybe even a negligible - role (Mearns, 2015a and Gregori, 2020).

In general, several indications agree - and clearly suggest - that the biosphere is a leading component of the Earth's crust. The evidence derives from the huge percent of metamorphosed biomass. However, the combined role of vegetation and water seems to be crucial. Senar et al. (2018) call "*hydrologic connectivity*" this effect. They explain and highlight as follows their inference.

"The capacity of forest soils to store organic carbon is influenced by changing hydrologic connectivity. We hypothesized that hydrologic connectivity, the water-mediated transfer of matter and energy between different landscape positions, controls the partitioning between aquatic and atmospheric soil carbon fates. Results from a 5 year study of a northern hardwood forested catchment indicated that hydrologic connectivity affected both the magnitude and fate of carbon export. Atmospheric carbon export was the major export pathway from the catchment; its rate was regulated by topographic position (i.e., uplands, ecotones, and wetlands) but enhanced or suppressed through changes in soil moisture and hydrologic connectivity.

Wetter soil conditions reduced CO_2 flux from the ecotones and wetlands where microbial respiration was oxygen-limited, whereas drier soil conditions that decreased hydrologic connectivity increased CO_2 flux by relieving the oxygen limitation. In contrast, aquatic carbon export was a minor export pathway from the catchment and was driven by hydrologic connectivity, with less carbon export during relatively low discharge years. Past trends suggest a shift to a warmer climate [note that this is consistent with several other clear indications of an ongoing increase of the release of endogenous energy through the whole northern polar cap] and changes in the timing, duration, and intensity of hydrologic connectivity that are leading to an increase in annual atmospheric carbon export but a decrease in annual aquatic carbon export, despite the

intensification of autumn storms. The increase in atmospheric carbon export creates a positive feedback for climate warming that will further disrupt hydrologic connectivity and aquatic carbon export, with consequences for downstream streams and lakes.”

That is, the natural system relies on a very intricate combined role and feedback by the biosphere. In general, the result is a trend to balance and reduce extreme conditions.

Sidder (2018a) illustrates the Senar et al. (2018) study and states that “*from forested coastal wetlands to northern boreal forests, forests are considered essential cogs in the global carbon cycle. Generally, forests act as ‘sinks’ by absorbing more carbon from the atmosphere through photosynthesis than they release, but they still do emit a considerable amount of carbon dioxide. Much of this release happens through respiration by soil microbes. However, not all carbon lost by forests escapes to the atmosphere: a small but significant amount is exported into aquatic systems via dissolved organic carbon, which derives from soil material like plant litter and peat. Compared to atmospheric carbon export, aquatic export is small, but it is still considered a critical carbon flux. [That is, water mobility plays a fundamental role.] ... The flow of water between habitat types is closely tied to soil moisture, water table depth, and stream discharge.*

The research took place in the Turkey Lakes Watershed, an experimental watershed located approximately 60 km north of Sault Ste. Marie, Ontario, Canada. The researchers collected stream samples for 5 years to monitor dissolved organic carbon, and they monitored CO₂ emissions using flux chambers placed across habitat types. Other measurements included soil temperature, moisture, and organic carbon.

The results indicated that hydrologic connectivity between uplands, ecotones (regions of transition), and wetland habitats does indeed control the fate of carbon - both atmospheric and aquatic - in the northern hardwood forest; however, the study unexpectedly found that hydrological connectivity also dictates the magnitude of carbon exported from the ecosystem. In water-limited habitats, like uplands, the increase in soil water stimulated microbial activity and, subsequently, CO₂ released from respiration. In contrast, as wetlands and other water-saturated areas became hydrologically linked to the surrounding uplands, the increase in soil water tamped down the soil bacteria liveliness in the resulting anaerobic soils.

The study also found that hydrologically connected habitats resulted in an increase in aquatic transport of carbon. In other words, as more water entered the ecosystem, more carbon washed downstream into streams and lakes. The findings showed a distinct seasonal pattern, with increased aquatic transport during periods of high hydrologic connectivity, namely, spring snowmelts and fall storms ... “

However, the scenario during the early evolution of the Earth was even more intricate. The origin of atmospheric oxygen is well-known to have originated by photosynthetic bacteria. “*It has been suggested that a decrease in*

atmospheric CH₄ levels triggered the progressive rise of atmospheric oxygen, the so-called Great Oxidation Event (GOE), about ~ 2.4 Ga ago. Oxidative weathering of terrestrial sulphides, increased oceanic sulphate, and the ecological success of sulphate-reducing microorganisms over methanogens has been proposed as a possible cause for the CH₄ collapse, but this explanation is difficult to reconcile with the rock record” (Konhauser et al., 2009).

According to Godfrey and Flakowski (2009), “*organisms that produce oxygen through photosynthesis existed during the late Archaean Eon, about ~2,500 Ga ago, but controversial evidence suggests that they may have evolved several hundred million years earlier. Oxygen is expected to react with oceanic nitrogen, altering its redox state. The reaction leaves a signature in the isotopic composition of the nitrogen bound in organic matter.”*

They studied “*minimally altered shales from the Campbellrand - Malmani platform in South Africa. Between the Palaeoarchaean and ~ 2.670 Ga ago, the Δ¹⁵N values ... rose by about 0.2%.” They suggested “that coupled nitrification and denitrification drove the loss of fixed inorganic nitrogen, leading to nitrogen limitation, and concluded that the low levels of biologically available nitrogen limited the growth of oxygen-producing plankton, delaying the accumulation of oxygen in the atmosphere.” That is, the prime driver ought to be conceived in terms of an original insufficient nitrogen concentration.*

“A second increase in nitrogen isotopic composition around ~ 2.520 Ga ago implies instability of the N cycle with loss of fixed N. This evidence for available oxygen in the oceans occurs at least 200 Ma before geochemical indications of the presence of significant levels of atmospheric oxygen.”

These first peaks were later followed by other production peaks, eventually of smaller intensity, thus resulting into a very complicated trend. Frei et al. (2009) comment that “*geochemical data suggest that oxygenation of the Earth atmosphere occurred in two broad steps. The first rise in atmospheric oxygen is thought to have occurred between 2.45 – 2.2 Ga ago, leading to a significant increase in atmospheric oxygen concentrations and concomitant oxygenation of the shallow surface ocean. The second increase in atmospheric oxygen appears to have taken place in distinct stages during the late Neoproterozoic era (800 – 542 Ma ago), ultimately leading to oxygenation of the deep ocean 580 Ma ago, but details of the evolution of atmospheric oxygenation remain uncertain.”*

They used “*Cr stable isotopes from banded iron formations (BIFs) to track the presence of [Cr(VI)] in Precambrian oceans, providing a time-resolved picture of the oxygenation history of the Earth atmosphere-hydrosphere system. The geochemical behavior of Cr is highly sensitive to the redox state of the surface environment because oxidative weathering processes produce the oxidized hexavalent [Cr(VI)] form. Oxidation of reduced trivalent [Cr(III)] chromium on land is accompanied by an isotopic fractionation, leading to enrichment of the mobile hexavalent form in the heavier isotope. Our fractionated Cr isotope data indicate the*

accumulation of [Cr(VI)] in ocean surface waters 2.8 – 2.6 Ga ago - and a likely transient elevation in atmospheric and surface ocean oxygenation before the first great rise of oxygen 2.45 – 2.2 Ga ago (the GOE). In 1.88 Ga-old BIFs we find that Cr isotopes are not fractionated, indicating a decline in atmospheric oxygen.”

Therefore, Frei et al. (2009) conclude that their “findings suggest that the GOE did not lead to a unidirectional stepwise increase in atmospheric oxygen. In the late Neoproterozoic, we observe strong positive fractionations in Cr isotopes ($\delta^{53}\text{Cr}$ up to +0.49%), providing independent support for increased surface oxygenation at that time, which may have stimulated rapid evolution of macroscopic multicellular life.”

Other authors (Konhauser et al., 2009) claim that this GOE was associated with an abrupt reduction of Ni concentration in the oceans. According to sedimentological evidence - i.e. banded Fe formations preserving the history of Precambrian oceanic elemental abundance - the Ni concentration was originally ~ 400 times larger than at present. This favored the development of methanogenic organisms. Hence, the large amount of CH_4 that was thus produced forbade the development of oxygen formation, as oxygen reacted with CH_4 to produce CO_2 and water.

Konhauser et al. (2009) measured a decline in the molar Ni to Fe ratio corresponding to ~ 2.7 Ga ago. They attributed this to a reduced flux of Ni to the oceans, following a cooling of upper- mantle temperatures and a decreased eruption of Ni-rich ultramafic rocks at the time. They found that “dissolved Ni concentrations may have reached ~ 400 nM throughout much of the Archaean Eon, but dropped below ~ 200 nM by ~ 2.5 Ga ago and to modern day values (~ 9 nM) by ~ 550 Ma ago.”

“Ni is a key metal cofactor in several enzymes of methanogens and ... its decline would have stifled their activity in the ancient oceans and disrupted the supply of biogenic CH_4 .” This rapid decrease of the Ni availability ought to have caused a reduction of the development of methanogenic organisms. Meanwhile, the algae and other microorganisms, which produced oxygen, used other enzymes and did not need for Ni. “A decline in biogenic CH_4 production therefore could have occurred before increasing environmental oxygenation and not necessarily be related to it.”

If this interpretation is correct, the reduction of Ni availability should be justified by means of a suitable geodynamic mechanism, such as the aforementioned decreased eruption of Ni-rich ultramafic rocks. These geodynamic factors should however be checked. In addition, “the enzymatic reliance of methanogens on a diminishing supply of volcanic Ni links mantle evolution to the redox state of the atmosphere.”

Sekine et al. (2011) investigated the correlation of the GOE with the Palaeoproterozoic deglaciation. “Early Palaeoproterozoic (2.5 – 2.0 Ga ago) was a critical phase in Earth’s history, characterized by multiple severe glaciations and a rise in atmospheric O_2 (the GOE). Although glaciations occurred at the time of O_2 increase, the relationship between climatic and atmospheric

transitions remains poorly understood. Here we report high concentrations of the redox-sensitive element Os with high initial $^{187}\text{Os}/^{188}\text{Os}$ values in a sandstone-siltstone interval ... Together with the results of Re, Mo and S analyses of the sediments, we suggest that immediately after the second Palaeoproterozoic glaciation, atmospheric O_2 levels became sufficiently high to deliver radiogenic continental Os to shallow- marine environments, indicating the synchronicity of an episode of increasing O_2 and deglaciation. This result supports the hypothesis that climatic recovery from the glaciations acted to accelerate the GOE.”

A more recent investigation (Koehler et al., 2018) gives some additional inference. “... Incipient oxygenation of Earth’s surface environments before the GOE (~ 2.4 Ga) has been well-documented, but the nature of these redox changes, whether protracted or transient, is poorly understood. We present N isotope ratios, Se abundances, and Se isotope ratios from the Jeerinah Formation (~ 2.66 Ga; Fortescue Group, Western Australia) that represent (i) high-resolution evidence of transient surface ocean oxygenation ~ 260 Ma before the GOE, (ii) a possible muted pulse of oxidative continental weathering, and (iii) the oldest firm evidence for nitrification and denitrification metabolisms. These results, in concert with previous studies, highlight the variability in mechanisms and magnitudes of Neoproterozoic oxygen fluctuations.

... Many palaeoredox proxies indicate low-level and dynamic incipient oxygenation of Earth’s surface environments during the Neoproterozoic (2.8 – 2.5 Ga) before the GOE at ~ 2.4 Ga. The mode, tempo, and scale of these redox changes are poorly understood, because data from various locations and ages suggest both protracted and transient oxygenation. ... We find that both shallow and deep depositional facies in the Jeerinah Formation display episodes of positive primary $\delta^{15}\text{N}$ values ranging from +4 to +6 ‰, recording aerobic nitrogen cycling that requires free O_2 in the upper water column.

Moderate Se enrichments up to 5.4 ppm in the near-shore core may indicate coincident oxidative weathering of sulfide minerals on land, although not to the extent seen in the younger Mt. McRae Shale that records a well-documented ‘whiff’ of atmospheric oxygen at 2.5 Ga. Unlike the Mt. McRae Shale, Jeerinah Se isotopes do not show a significant excursion concurrent with the positive $\delta^{15}\text{N}$ values. Our data are thus most parsimoniously interpreted as evidence for transient surface ocean oxygenation lasting < 50 Ma, extending over hundreds of kilometers, and occurring well before the GOE. The nitrogen isotope data clearly record nitrification and denitrification, providing the oldest firm evidence for these microbial metabolisms.”

Ice cores contain samples of ancient atmosphere, and these samples can check models. Stolper et al. (2016) investigated this proxy in some ice cores from Greenland and Antarctica. They claim that the coevolution of life and Earth’s biogeochemical cycles is closely linked to the history of the partial pressures P_{O_2} of atmospheric O_2 . However, the reconstructions of past P_{O_2} are based on

models and proxies that often substantially disagree. They investigate ancient air trapped in ice that records P_{O_2} by means of O_2/N_2 ratios. They find a 7‰ decline of P_{O_2} during the past 800,000 years, implying that O_2 sinks were ~2% larger than sources. Note, however, that sources and sinks of O_2 are quite varied, and they basically poorly understood.

They comment that this finding is consistent with variations of the weathering fluxes and burial of organic carbon and pyrite, which were driven either by Neogene cooling or by an increase of Pleistocene erosion rates. In addition, they find that a silicate weathering feedback causes an efficient stabilization - on million-year time scales - of the average CO_2 partial pressures (P_{CO_2}) during declining P_{O_2} , being observed as a steady phenomenon in the 800,000 year record.

Concerning the “*silicate weathering feedback*” let us refer to Choi (2016i), who illustrates this study, also relying on an interview with Daniel Stolper. Choi (2016i) states that “*atmospheric O_2 levels are fundamentally linked to the evolution of life on Earth, as well as changes in geochemical cycles related to climate variations. As such, scientists have long sought to reconstruct how atmospheric O_2 levels fluctuated in the past, and what might control these shifts. However, models of past atmospheric O_2 levels often markedly disagree, differing by as much as ~20% of Earth’s atmosphere, which is O_2 ’s present-day concentration ... It is not even known if atmospheric O_2 levels varied or remained steady over the past 1 Ma. There was no consensus on whether the O_2 cycle before humankind began burning fossil fuels was in or out of balance and, if so, whether it was increasing or decreasing,* ...

... *O_2 sinks ... were about 1.7% larger than O_2 sources during this time ... There are two hypotheses that may help explain this O_2 decline over the past million years ... The first is that global erosion rates may have increased over the past few to tens of million years due to, among other things, the growth of glaciers - glaciers grind rock, thereby increasing erosion rates, ... Rising erosion rates would have exposed more pyrite and organic carbon to the atmosphere ... organic carbon consists of the remains of organisms, mostly land plants and aquatic photosynthetic microorganisms such as algæ. Previous research found that both pyrite and organic carbon can react with O_2 and remove it from the atmosphere. Alternatively, when the ocean cools, as it has done over the past 15 Ma, before fossil fuel burning, the solubility of O_2 in the ocean increases. That is, the oceans can store more O_2 at colder temperatures for a given concentration of O_2 in the atmosphere ... O_2 -dependent microbes in the ocean and in sediments can then become more active and consume this O_2 , leaving less of the element in the atmosphere ...*

... *These findings also reveal what might be a strange contradiction, because it could be assumed that atmospheric CO_2 levels should rise as O_2 levels fall ... However, previous research has found that atmospheric CO_2 levels have not, on average, changed over the past 800,000 years ... One way out of this conundrum is a well-known but relatively untested concept that suggests that on*

timescales longer than a few hundred thousand years, atmospheric CO_2 and Earth’s temperature are regulated via a ‘silicate weathering thermostat’, ...

Basically, increasing atmospheric CO_2 levels will boost the rates at which volcanic rocks wear down and their components wash into the seas, which can then go on to trap atmospheric CO_2 in ocean minerals. This means that one can have a change in atmospheric O_2 with no observable change in average CO_2 ... Importantly, this silicate weathering thermostat is one reason why Earth is thought to have remained habitable for billions of years despite changes in solar luminosity.”

Several aspects, however, still remain to be explained. In addition, a very recent finding envisages that O_2 is transported by the polar wind from the Earth to the Moon, when the Moon crosses inside the Earth’s magnetosphere. Terada and Hashimoto (2017) summarize their finding as follows.

“For five days of each lunar orbit, the Moon is shielded from solar wind bombardment by the Earth’s magnetosphere, which is filled with terrestrial ions. Although the possibility of the presence of terrestrial nitrogen and noble gases in lunar soil has been discussed based on their isotopic composition ..., complicated oxygen isotope fractionation in lunar metal ... (particularly the provenance of a ^{16}O -poor component) remains an enigma ...

Here, we report observations from the Japanese spacecraft KAGUYA of significant numbers of 1–10 keV O^+ ions, seen only when the Moon was in the Earth’s plasmashet. Considering the penetration depth into metal of O^+ ions with such energy, and the ^{16}O -poor mass-independent fractionation of the Earth’s upper atmosphere ..., we conclude that biogenic terrestrial oxygen has been transported to the Moon by the Earth wind (at least 2.6×10^4 ions $cm^{-2} sec^{-1}$) and implanted into the surface of the lunar regolith, at around tens of nanometres in depth ... We suggest the possibility that the Earth’s atmosphere of billions of years ago may be preserved on the present-day lunar surface.”

Wendel and Kumar (2017a) illustrate this study, reporting also about an interview with Kentaro Terada, and they comment as follows. “... *during every lunar orbit, the Moon passes through the plasmashet ... But do these particles - in particular, oxygen ions - make it to the lunar surface, and if so, how would we know? Thus far, it’s been an enigma ... After all, oxygen carried on the solar wind also arrives at the Moon after it orbits out of Earth’s magnetotail. ... Data from KAGUYA, which stopped collecting observations in 2010, revealed that during a few hours every month the orbiter was bombarded with oxygen ions reminiscent of a terrestrial origin. These moments corresponded to when the Moon orbited through Earth’s plasmashet.*

The researchers could fingerprint these ions because oxygen originating in the Sun is more often ‘multicharged’, meaning that more of its electrons get stripped away because of the Sun’s extreme heat ... The charge on these oxygen atoms might be +6, +7, or +8, whereas terrestrial oxygen generally loses only one electron ... However,

distinguishing old Earth oxygen, new Earth oxygen, and oxygen that arrived on the solar wind will be extremely tricky. We have no method of dating the exact time at which the sample reached the surface ... the authors expect that high-energy ions burrow into minerals in lunar soil. There's currently no way to tell whether one ion burrowed thousands of years ago or only yesterday. And although higher abundances of heavier oxygen arrive at the Moon from Earth, Earth delivers to the Moon all isotopes, so it's impossible right now to tell where an individual oxygen ion hailed from ... " Wendel and Kumar (2017a) also comment that, owing to this same mechanism, Phobos could keep a record of the ancient Martian atmosphere.

The palæodensity of the atmosphere

The palæodensity of the Earth's atmosphere very likely changed during Earth's history. Owing to the large variety of living forms, the biosphere is a potential important proxy suited to monitor these changes.

One likely possibility is provided by insects, or other small animals that were captured inside amber. They keep a record of their breathing apparatus: this can define an upper and a lower boundary for atmospheric density and composition derived from their assumed physiological requirement. Investigators do not seem, however, to have yet focused on this item, as researchers are rather mainly concerned with the time of appearance and with the evolution of species.

For instance, Schmidt et al. (2012) studied arthropods in amber since the Triassic Period, i.e. since ~ 230 Ma ago. They stress that "the occurrence of arthropods in amber exclusively from the Cretaceous and Cænozoic is widely regarded to be a result of the production and preservation of large amounts of tree resin beginning ~ 130 Ma ago.

Abundant 230 Ma -old amber from the Late Triassic (Carnian) of northeastern Italy has previously yielded myriad microorganisms."

They report "that it also preserves arthropods some 100 Ma older than the earliest prior records in amber ... [They found mites that] are the oldest definitive fossils of a group, the Eriophyoidea, which includes the gall mites and comprises at least 3,500 recent species, 97% of which feed on angiosperms and represents one of the most specialized lineages of phytophagous arthropods. Antiquity of the gall mites in much their extant form was unexpected, particularly with the Triassic species already having many of their present-day features (such as only two pairs of legs); further, it establishes conifer feeding as an ancestral trait. Feeding by the fossil mites may have contributed to the formation of the amber droplets, but we find that the abundance of amber during the Carnian (~ 230 Ma) is globally anomalous for the pre-Cretaceous and may, alternatively, be related to palæoclimate." They also claim that "further recovery of arthropods in Carnian-aged amber is promising and will have profound implications for understanding the evolution of terrestrial members of the most diverse phylum of organisms."

Geggel (2016c) informs about Delclòs et al. (2016), who report about three findings of mantis, discovered in modern-day Lebanon, Myanmar and Spain (Fig. 1). "All of them date to the Cretaceous period (145.5 – 65.5 Ma ago)." The Myanmar mantis is an incomplete adult (97 Ma old). The Spain mantis is an incomplete nymph (young insect) 105 Ma old. It is the first record of a Mesozoic mantis and it is "the most complete specimen of its species on record". Also, the Lebanon specimen is a nymph, 128 Ma old. It is "the oldest mantis species known in amber".

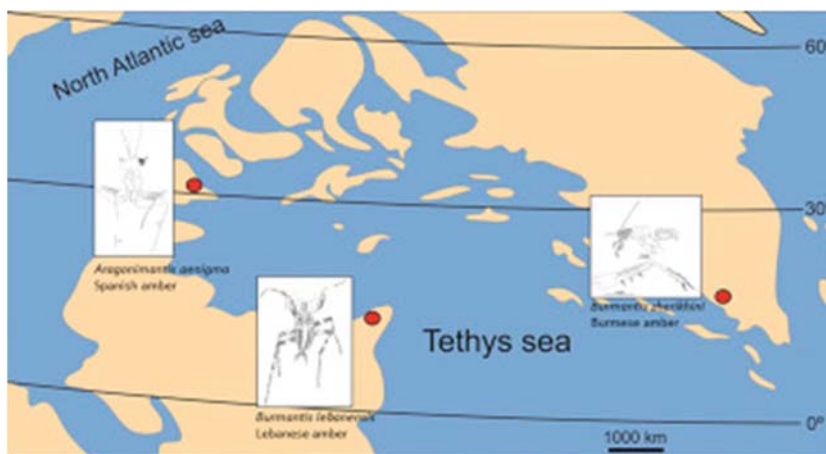


Fig. 1. "The three specimens were found in modern-day Lebanon, Myanmar and Spain. Credit: Group AMBARES." Figure and captions after Geggel (2016c). NASA copyright free policy.

A new finding, however, is claimed to be the best-preserved available specimen. It has been recently reported from Brazil (Weisberger, 2017c, who announces Hörnig et al., 2017). It is a "fossil embedded in a rock slab excavated from a site in northeastern Brazil, dating the mantis to ~ 110 Ma ago and identifying it as Santanmantis axelrodi ... [The site is named Crato Formation.] While the earliest mantids - another name for insects in the mantis family - can be traced to the Jurassic Period (199.6 – 145.5 Ma

ago), the Cretaceous Period (145.5 – 65.5 Ma ago) is when the group's diversity began to emerge ... The oldest example of insect sex dates to 165 Ma ago; the oldest known stick insect dates to 126 Ma ago; and a 46 Ma-old mosquito was preserved while still engorged with its final blood meal ... "

The fossil has a ~ 4 mm head, and wings ~ 164 mm long with "remarkably detailed vein patterns"(Fig. 2), although no reported feature seems relevant as a proxy

datum concerning the Earth's palaeoatmosphere. Compared to present mantises, this specimen shows greater raptorial facilities.

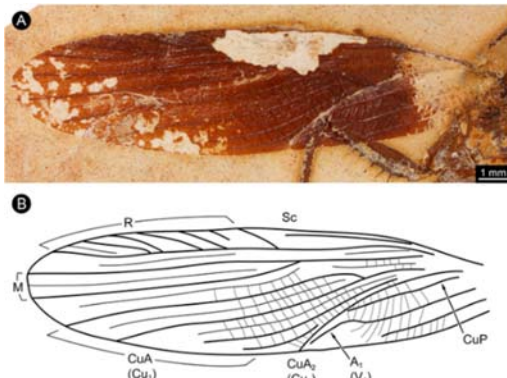


Fig. 2. “Details of wing of specimen MB.I.2068. (A) Close-up image of left wing. (B) Drawing of wing venation pattern ... “Figure and captions after Hörmig et al. (2017). With kind permission of PeerJ (granted through CC-BY 4.0 license).

Fossilized giant insects were however found (Welsh, 2012; Figs 3 and 4), and their information can be relevant for checking atmospheric density and composition. According to Welsh (2012), who announces Clapham and Karr (2012), “insects during the Permian era (~ 290 – 250 Ma ago) were huge compared with their counterparts today, boasting wingspans up to 70 cm across. The high levels of O_2 in the prehistoric atmosphere helped fuel their growth.¹ For comparison, the biggest modern winged insect is a dragonfly from the tropics, which has a wingspan of ~ 8 cm across.



Fig. 3. “A fossilized insect wing from the species *Stephanotypus schneideri* and it is about 300 Ma old. The wing is ~ 19 cm long, substantially smaller than the largest fossil insect (*Meganeuropis permiana*, ~ 33 cm). Superimposed on the fossil is a drawing of the largest Cænozoic insect (it's about 12 Ma old), *Epischna lucida*, which comes in at ~ 6.7 cm long, similar to modern insects. Credit: Wolfgang Zessin and Matthew Clapham.” Figure and captions after Welsh (2012). NASA copyright free policy.

To figure out why modern insects are no longer so big, the researchers compiled a database of wingspan measurements of 10,500 fossilized insects from the last 320 Ma of insect evolution. The authors found that during the first 150 Ma of insect evolution, the wingspans on these

insects mirrored levels of atmospheric O_2 ; the more O_2 in the atmosphere, the larger the insects the environment could support. These flying insects need lots of O_2 to support their flight muscles ... and since their breathing tubes are inefficient, they need high atmospheric O_2 levels to grow large. The more O_2 in the environment, the more muscle mass the insect can provide O_2 for and the larger the insect can be. Around 140 Ma ago, though, things changed. Insect wingspan stopped depending on O_2 levels and started dropping.



Fig. 4. “Fossil remains of *Meganeura Monyi*, a member of the extinct insect genus *Meganeura*. Their wingspans could reach 0.6 m. This specimen is housed at the Fossil at the Museum of Natural History in Toulouse. Image via Wikimedia Commons. [It was] “first described by researchers in Kansas in 1937 ... It's still considered one of the largest known insects that ever lived.” Figure and captions after Anonymous (2016ae). See also Cannell (2018). With CC BY-SA 4.0 Wikimedia Commons kind permission.

The researchers noticed that this change happened around the same time that birds first took to the skies. About 150 Ma ago, the ‘first bird’ *Archæopteryx* appeared, and 25 Ma later, the lineage had diversified greatly. Over time, the birds developed physical features that enabled quick flying and better maneuvering. As a result, they started eating the large insects, and competing with them for food sources ...

A second slump in insect size happened ~ 60 Ma ago, which the researchers think could be related to the evolution of bats, further increases in birds' aerial abilities, or to the mass extinction event that killed the dinosaurs.”

Clapham and Karr (2012) give a plot (not here shown) of “phanerozoic trends in insect wing lengths and atmospheric P_{O_2} (GEOCARBSULF model)” and claim that they “show - using a dataset of more than 10,500 fossil insect wing lengths - that size tracked atmospheric O_2 concentrations only for the first 150 Ma of insect evolution. The data are best explained by a model relating maximum size to atmospheric environmental O_2 concentration (P_{O_2}) until the end of the Jurassic, and then at constant sizes, independent of O_2 fluctuations, during the Cretaceous and, at a smaller size, the Cænozoic.

Maximum insect size decreased even as atmospheric P_{O_2} rose in the Early Cretaceous following the evolution

¹ “During the Carboniferous and Permian periods, Earth's air contained 31 – 35% O_2 , as compared to just 21% O_2 in the air today” (Anonymous, 2016ae).

and radiation of early birds, particularly as birds acquired adaptations that allowed more agile flight. A further decrease in maximum size during the Cænozoic may relate to the evolution of bats, the Cretaceous mass extinction, or further specialization of flying birds. The decoupling of insect size and atmospheric P_{O_2} coincident with the radiation of birds suggests that biotic interactions, such as predation and competition, superseded O_2 as the most important constraint on maximum body size of the largest insects.”

Geggel (2016d) reports about a 99 Ma old spider.

Daza et al. (2016) investigated the exceptionally preserved tropical amber entombed lizards that were found in Myanmar. They claim that “twelve specimens from the Albian-Cænomanian boundary of Myanmar (99 Ma) preserve fine details of soft tissue and osteology, and high-resolution X-ray computed tomography permits detailed comparisons to extant and extinct lizards” (Gekkota and Chamaleonida).

Geggel (2017b) reports about another 7 cm long lizard, probably it “was likely a gecko” that “lived in an area with a lot of rainfall and dated to the Neogene, a period that lasted from ~ 23 – 2.6 Ma ago.”

Another possible evidence of the changes of the palæodensity of the Earth’s atmosphere could be provided, perhaps, by the volume of dinosaur lungs,² hence by the oxygen refill for their blood. On the other hand, well-known and unsolved aspects remain of their physiology, in addition to the objective difficulty to estimate their lung volume.

Another indication could perhaps derive from the study of the flying capability of pterosaurs, the enigmatic extinct Mesozoic reptiles.³ They were the first vertebrates to evolve true flapping flight. This implied (Claessens et al., 2009) “a complex and physiologically demanding activity that required profound anatomical modifications, most notably of the forelimb, but which subsequently conferred great success in terms of clade longevity and diversity. Following a basal radiation in the Late Triassic, pterosaurs diversified into a wide variety of continental and marine ecosystems and remained successful aerial predators until the end of the Cretaceous, an interval of > 150 Ma.”

Some time ago engineers (seemingly unsuccessfully) attempted to implement some mechanical model of a flying pterosaur, i.e. of a mechanical flapping flying object, similarly to a bird. This topic is not pertinent for the present study. Some specific discussion is, however, available (Chatterjee and Templin, 2004). Various lines of evidence are strongly indicative of a highly efficient wing design, control, and flight capabilities. In contrast, the motion of Plesiosaurians through water has been successfully modelled by computer simulation, finding that their motion was by “flapping their two front flippers, much like penguins do today” (Geggel, 2015a, who announces Liu et al., 2015a).

The pterosaurs lived from ~ 225 Ma through ~ 65 Ma ago. They are believed to have spent much time in coastal areas, similarly to modern seabirds. Small and medium-size pterosaurs probably plunged diving - like modern pelicans – for food supply. Large pterodactyloids were probably active waders, maybe like surface riders during feeding, using their feet to propel with their wings folded sidewise. Chatterjee and Templin (2004) discuss the cases of 10 genera. Their estimated body mass ranged between ~ 0.015 kg to ~ 70 kg, and wingspans from ~ 0.4 m through ~ 10.4 m. However, in addition to engineering aspects, their flying capability also depended on physiological requirements.

Another concern (see also below) deals with the appearance of feathers, which occurred also on pterosaurs that did not fly. In fact, feathers experienced a slow evolution (see e.g. Byrd, 2016u; Edathikunnel, 2016; Geggel, 2015c, 2016e, 2018, 2018k; Imster, 2016g; Xing et al., 2016; Robitzski, 2017; ...). Also enigmatic dinosaurs have been found with a swan-like neck that could walk like a duck and swim like a penguin (Geggel, 2017f).

The finding of a “first giant” dinosaur - referred to an unexpected early epoch - provides with new hints for the evolution of gigantic animals. The study by Apaldetti et al. (2018) is illustrated by Geggel (2018d) who also relies on interviews with the authors. “... The newly identified bus-size beast - named *Ingentia prima*, which means ‘first giant’ in Latin - weighed up to 10 metric tons and measured up to 10 m long (Fig. 5). ... Palæontologists used to think that the first giant dinosaurs evolved during the early Jurassic period, which lasted from 199.6 Ma – 145.5 Ma ago ... *Ingentia prima* and other lessemsaurids (large dinosaurs from the late Triassic that all belong to the sauropod group), that the researchers studied, tell us that at least some dinosaurs were able to attain huge sizes during the latest part of the Triassic, before the extinction ...

... the lessemsaurids stood on bent legs, and they had bones that grew thicker in accelerated bursts, unlike their later cousins, which grew continuously throughout the year ... the lessemsaurids had long necks and tails ... The lessemsaurids did share one big feature with other long-necked sauropods: they had bird-like air sacs, respirator structures that may have helped keep the giant animals cool ... “

The animal class of dinosaurs is mysterious. For future reference, a detail can be highlighted that can be achieved by means of a fossil. Let us report the summary of Xing et al. (2016). “In the two decades since the discovery of feathered dinosaurs ... the range of plumage known from non-avian theropods has expanded significantly, confirming several features predicted by developmentally informed models of feather evolution ... However, 3D feather morphology and evolutionary patterns remain

reconstructions are much arbitrary and not reliable for this purpose.

³ A huge literature is available. For instance, some recent references are Geggel (2015b, 2017c), Pappas (2016c), Skibba (2016), Martin-Silverstone et al. (2016), ...

² According to an intuitive feeling derived from the popular reconstructions of dinosaurs in natural museum, one might conclude that they had comparably very small lungs. However, palæontologists warn that these

difficult to interpret, due to compression in sedimentary rocks ...

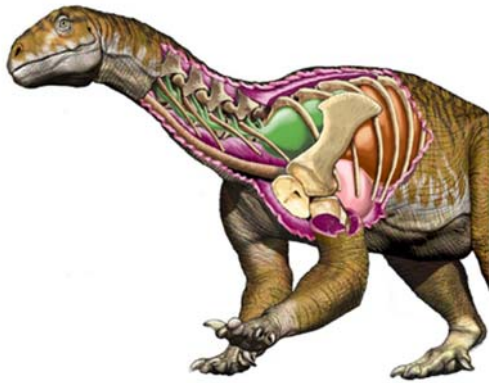


Fig. 5. “*Ingentia prima* lived during the late Triassic, from ~ 205 Ma – 210 Ma ago, in what is now Argentina. Note its avianlike respiratory system that has cervical air sacs (green) and its lungs (brown). Credit: Jorge A. González.” Figure and captions after Geggel (2018d). NASA copyright free policy.

Recent discoveries in Cretaceous amber from Canada, France, Japan, Lebanon, Myanmar, and the United States ... reveal much finer levels of structural detail, but taxonomic placement is uncertain because plumage is rarely associated with identifiable skeletal material ... Here we describe the feathered tail of a non-avian theropod preserved in mid-Cretaceous (~ 99 Ma) amber from Kachin State, Myanmar ..., with plumage structure that directly informs the evolutionary developmental pathway of feathers. This specimen provides an opportunity to document pristine feathers in direct association with a putative juvenile coelurosaur, preserving fine morphological details, including the spatial arrangement of follicles and feathers on the body, and micrometer-scale features of the plumage. Many feathers exhibit a short, slender rachis with alternating barbs and a uniform series of contiguous barbules, supporting the developmental hypothesis that barbs already possessed barbules when they fused to form the rachis ...

Beneath the feathers, carbonized soft tissues offer a glimpse of preservational potential and history for the inclusion; abundant Fe^{2+} suggests that vestiges of primary hemoglobin and ferritin remain trapped within the tail. The new finding highlights the unique preservation potential of amber for understanding the morphology and evolution of coelurosaurian integumentary structures.”

Xing et al. (2016) also show Fig. 6, which is also reported by Byrd (2016u). No detailed explanation is here given, and the interested reader ought to refer to Xing et al. (2016).

Fossils of flying birds are reported (see e.g. Edathikunnel, 2015a; Xing et al., 2016a; Weisberger, 2017d; ...), also having airplane-size (Cenizo et al., 2015; Geggel, 2016f). See here below Fig. 18 and the related discussion. The transition between dinosaurs and birds is reviewed by Brusatte et al. (2014). See also below some mentions dealing with the Archæopteryx.

Already 160 Ma ago mammals (or, more precisely, mammaliaforms that are Mesozoic forerunners to mammals) had developed some gliding capability, similar to present squirrels (see e.g. Geggel, 2017d, who announces Meng et al., 2017). However, independent of flight capabilities, the pulmonary system is poorly known that was required for flight.

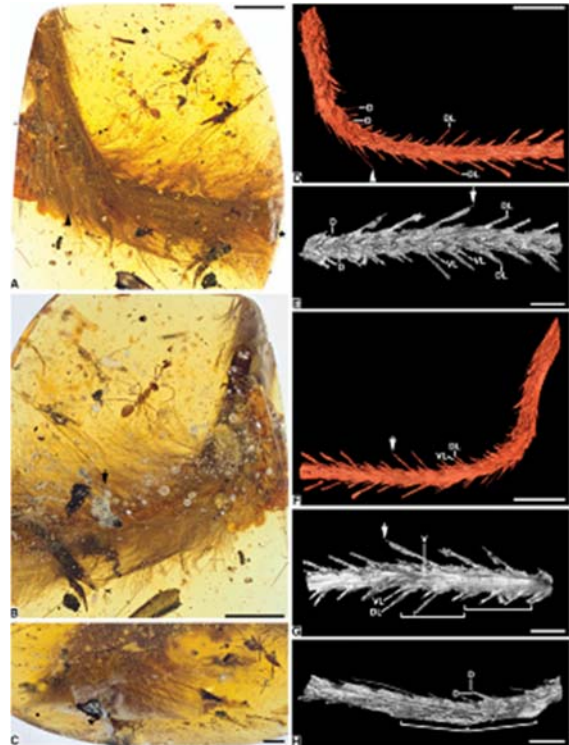


Fig. 6. Detailed picture of the tail of a non-avian theropod preserved in mid-Cretaceous (~ 99 Ma) amber from Kachin State, Myanmar. See text. Figure after Byrd (2016u). For description refer to Xing et al. (2016, 2016a, 2016b). Reproduced with kind permission of Nature Communications, (CC BY 4.0).

Claessens et al. (2009) “investigated the structure and function of the pterosaurian breathing apparatus through a broad scale comparative study of respiratory structure and function in living and extinct archosaurs, using computer-assisted tomographic (CT) scanning of pterosaur and bird skeletal remains, cineradiographic (X-ray film) studies of the skeletal breathing pump in extant birds and alligators, and study of skeletal structure in historic fossil specimens.” They analyzed bones of the rib cage of a pterosaur of the genera *Rhamphorrhynchus*, and found “various lines of skeletal evidence that indicate that pterosaurs had a highly effective flow-through respiratory system, capable of sustaining powered flight, predating the appearance of an analogous breathing system in birds by approximately ~ 70 Ma. Convergent evolution of gigantism in several Cretaceous pterosaur lineages was made possible through body density reduction by expansion of the pulmonary air sac system throughout the trunk and the distal limb girdle skeleton, highlighting the importance of respiratory adaptations in pterosaur evolution, and the dramatic effect of the release of physical constraints on morphological diversification and evolutionary radiation.”

Claessens et al. (2009) conclude that “the evidence for a lung-air sac system and a precisely controlled skeletal breathing pump supports a flow-through pulmonary ventilation model in pterosaurs, analogous to that of birds. The relatively high efficiency of flow-through ventilation was likely one of the key developments in pterosaur evolution, providing them with the respiratory and metabolic potential for active flapping flight and colonization of the Late Triassic skies. This interpretation is consistent with other lines of evidence supporting relatively high metabolic rates in pterosaurs, including the filamentous nature of the integument, a flight performance comparable to that of extant birds and bats and relatively large brain size. The expansion of a subcutaneous air sac system in the forelimb facilitated the evolution of gigantism in several derived pterodactyloid groups and resulted in the emergence of the largest flying vertebrates that ever existed.”

A more recent report deals with “exquisitely preserved lungs from 120 Ma ago” (Geggel, 2018h). The possibility to investigate lungs opens unexpected perspectives. “... Initially, scientists were excited to describe the specimen of *Archæorhynchus spathula*, a bird that lived about 120 Ma ago, because its fossil had exquisitely preserved feathers, including a unique pintail that isn't seen in any other Cretaceous bird, but is common in birds nowadays. A closer inspection, however, revealed that the bird's lungs had also fossilized, meaning the palæontologists had discovered the oldest 'informative' fossilized lung on record (more on that later) and the oldest fossilized lung ever seen in a bird fossil ... “

The fossil had been collected in China and it was found “at the Shandong Tianyu Museum of Nature, in Pingyi, where an avid fossil collector houses the thousands of bird fossils he's purchased over the decades. This is the fifth described *A. spathula* specimen - a toothless, pigeon-size bird - but it's by far the best preserved ... The finding reveals that the lung structures in early birds are similar to the lungs of modern birds ... This means that *A. spathula* likely had unidirectional airflow in its lungs - the air that flowed in was largely fresh and full of oxygen, unlike the air in mammals' lungs, which is mixed with both new and previously breathed air, meaning it has a lower oxygen content.



Fig. 7. Reconstruction of *P. sandersi* and comparison with *D. exulans* (Royal Albatross; 3 m average wingspan). Schematic and much simplified figure redrawn after a more complete figure shown by Ksepka (2014). Unpublished figure.

The last pelagornithids were contemporaries of *Homo habilis*. “A fossil species of pelagornithid bird exhibits the largest known avian wingspan. Pelagornithids are an extinct group of birds known for bony tooth-like beak projections, large size, and highly modified wing bones that raise many questions about their ecology. At 6.4 m, the

Lungs of birds are very different from our lungs and had much more complex structures ... They are kind of like a bag pipe, with an air management system (the air sacs) separated from the gas exchanger (the lung proper) which is preserved here.

Living crocodylians also have lungs with unidirectional airflow, and palæontologists considered it to be ancestral in early feathered dinosaurs ... An analysis of the tissue showed that it contained structures that resemble blood capillaries, which absorb oxygen to help power the highly energetic flight of birds ...

It's possible that this unique structure was unique to Ornithuromorpha, a clade (group) of ancient birds that survived the mass extinction about 66 Ma ago and includes today's living birds. Maybe this specialization was only in that clade and was one of the many factors that allowed their survival ... What's more, it appears that the fossilized lung was embedded in the birds ribs, just as bird lungs are today. Unlike human lungs, which expand with every breath, bird lungs are rigid, so they can easily inhale and exhale at the same time ...

... However, this specimen isn't the oldest lung on record. That honor goes to Spinolestes, an early Cretaceous mammal that has fossilized lungs about 5 Ma older than the newly analyzed bird. But those lung fossils didn't preserve any microstructure and don't provide much information about Spinolestes, other than that it likely had a muscular diaphragm ... “

That is, the evolution from reptiles through dinosaurs and birds involved relevant physiological aspects, related to the need for survival within the chancing “climate”. It is likely that palæontologists will get additional evidence suited to provide with some crucial indication on the palæoclimate. The challenge is open.

Ksepka (2014) investigated the flying capability of the largest ever existed seabird (Fig. 7), i.e. he studied a prehistoric family, the *Pelagornithida*, also called pelagornithids, pseudodontorns, bony-toothed birds, false-toothed birds or pseudotooth birds (see also Cenizo et al., 2015; Geggel, 2016f). Their fossils have been reported from all over the world, dating between the Late Palæocene and the Pliocene-Pleistocene boundary. They were the dominant seabirds during most of the Cænozoic.

wingspan of this species was approximately two times that of the living Royal Albatross.

Modeling of flight parameters in this species indicates that it was capable of highly efficient gliding and suggests that pelagornithids exploited a long-range marine soaring strategy similar, in some ways, to that of extant albatrosses” (Ksepka, 2014).

That is, the concern about the palæodensity of the atmosphere seemingly does not exist for birds. Ksepka (2014a) reviews the whole evolution of birds during their 150 *Ma* history.

For the sake of completeness, a nearly complete skeleton of “the largest winged dinosaur yet known” has been recently discovered in northeast China’s Liaoning province, including several details of its feathers (Edathikunnel, 2015c; referring to Lü and Brusatte, 2015). It has been named *Zhenyuanlong suni* and it is reported to date back to 125 *Ma* ago (Figs 8 and 9).



Fig. 8. “The holotype of the large-bodied, short-armed Liaoning dromaeosaurid *Zhenyuanlong suni* gen et. sp. nov. (JPM-0008).” Figure and captions after Lü and Brusatte (2015). Reproduced with kind permission of *Scientific Reports*, (CC BY 4.0).



Fig. 9. “Artists concept of largest winged dinosaur - *Zhenyuanlong suni* - by Zhao Chuang. Image via Science.” Figure and captions after Edathikunnel (2015c). Reproduced with kind permission of *Scientific Reports*, (CC BY 4.0).

A nearly complete specimen has been found of 1.6 *m* size, preserved with multiple layers of feathers along its arms and torso. It has been estimated to weigh over 20 *kg*.

Owing to its short forearms and dense bone structure, it is guessed that it could not fly. Being ~ 1.65 *m* long, it “was a little longer than a modern condor, but probably nearly twice as heavy. Yet unlike other feathered dinosaurs in its fossil family, it evolved complex quill-like feathers, typically found in modern birds” (Edathikunnel, 2015c). Therefore, some speculation remains about the real use of feathers, although, maybe, the atmosphere was much denser, as shown below, and in this case perhaps also *Zhenyuanlong suni* could fly.⁴ The world’s largest pterosaur jawbone has been recently discovered in Transylvania. See Geggel (2018f) who illustrates the study by Vremir et al. (2018). According to Geggel (2018f), in 1984 they found “... the fossilized jawbone at the junction of two creeks in the Hațeg Basin, near the village of Vălioara in Transylvania, Romania ... During the Cretaceous period, when this pterosaur was alive, Hațeg Basin was an island inhabited by dwarf dinosaurs, which were smaller than their counterparts on the mainland. Vremir unearthed the fossilized remains of one of these weird, stocky dinosaurs - a predator known as *Balaur bondoc* - in 2009 ... But Hațeg is also known for large pterosaurs, including *Hatzegopteryx*, which likely stood as tall as a giraffe, with a wingspan of up to 10.9 *m*. Another pterosaur from Hațeg, nicknamed *Dracula*, had an even larger wingspan of up to 12 *m*. ... We have a bunch of weird dinosaurs from Hațeg and a lack of really big carnivores, so the pterosaurs were basically tyrannosaur surrogates ... But just because the newly studied pterosaur ... has the largest jawbone ever found, it doesn’t necessarily mean it was the biggest pterosaur on record ... Rather, it probably had a wingspan of over 8 *m* and likely belonged to a family of pterosaurs known as the *Azhdarchids* ...”

Geggel (2018f) also shows Fig. 10 that summarizes the size of the different flying animals that are known to have occurred on the Earth.

Nudds and Dyke (2010) investigated the feathers of fossil birds⁵ and, specifically of *Archaeopteryx* and *Confuciusornis*. They had feathered wings and resembled present living birds, even though their flight capabilities are

⁴ As a personal reflection (GPG), a possible guess is that, maybe, feathers formerly represented a skin protection that later evolved as a feature suited to expand the wing surface, while keeping small the body weight. However, we are not palæontologists.

⁵ The oldest reported fossil of *Archaeopteryx* was found in Germany, the estimated date being ~ 152 *Ma* ago (Gannon, 2018a). The boundary between dinosaurs and birds is somewhat debated (Castro, 2018). However, according to the most recent findings, it seems that *Archaeopteryx* represents a stage of advanced evolution towards a bird. According to Kunderat et al. (2019), “From an initial isolated position as the oldest evolutionary prototype of a bird, *Archaeopteryx* has, as a result of recent fossil discoveries, become embedded in a rich phylogenetic context of both more and less

*crownward stem-group birds. This has prompted debate over whether *Archaeopteryx* is simply a convergently bird-like non-avian theropod ...*” Kunderat et al. (2019) analyzed a new specimen, younger than the previous specimens. Thus, they define a new species and conclude that the “innovations appear to be convergent on those of more crownward avialans, suggesting that Bavarian archaeopterygids independently acquired increasingly bird-like traits over time. Such mosaic evolution and iterative exploration of adaptive space may be typical for major functional transitions like the origin of flight.” Some relevant references are Christiansen and Bonde (2004), Erickson et al. (2009), Carney et al. (2012), Castro (2018), Voeten et al. (2018), ...

uncertain. The analysis of the rachises of their primary feathers envisages rachises much thinner and weaker than the rachises of modern birds. Therefore, these birds could not fly. Flight had been possible only if the primary feather rachises had a solid in cross-section, i.e. with the strongest structural configuration, and not hollow like in present birds. Therefore, if Archæopteryx and Confuciusornis were

flapping flyers, their feather structure was fundamentally different, compared to present birds. In the case that they were simple gliders, the flapping wing stroke appeared after the divergence of Confuciusornis, likely during the enantiornithine or ornithurine radiations. See better details on the original paper.

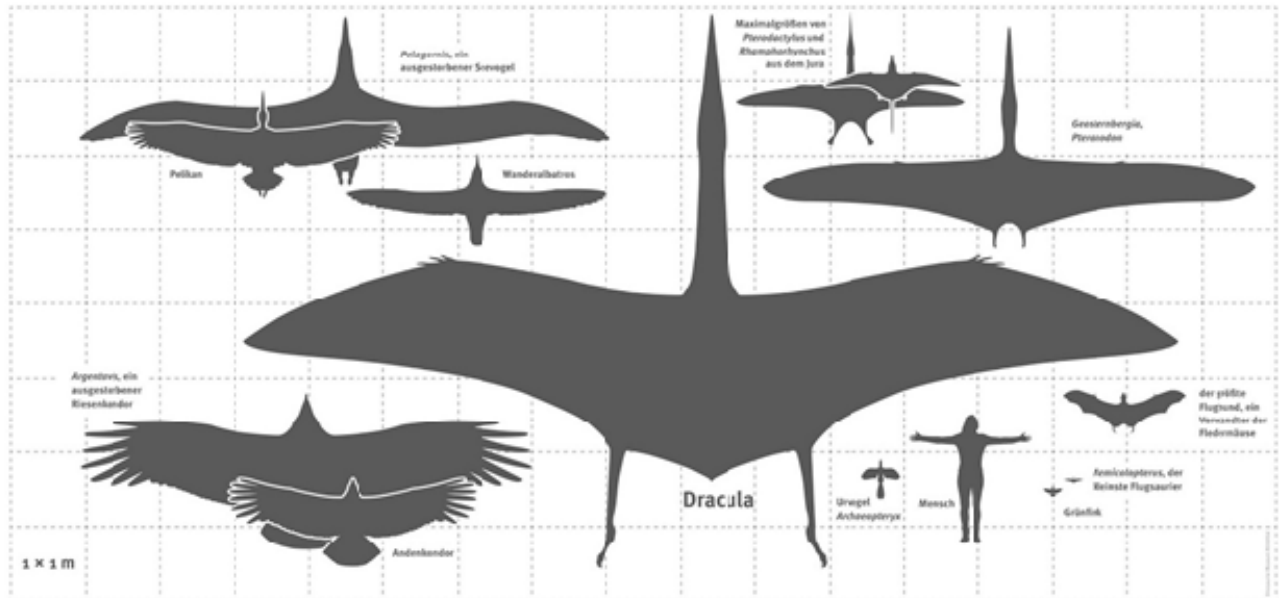


Fig. 10. “The newly studied specimen is slightly smaller than Dracula, shown here. Credit: Dinosaurier Museum.” Figure and captions after Geggel (2018f). NASA copyright free policy.

Hurrell (2014) attempts to use this information to support the expansionism hypothesis of the Earth. He computes the “values for gravity which would enable these birds to fly with weaker feathers ... based on the controversial theory that palaeogravity was less”. He assumes some equivalence with present birds, and he correspondingly scales their size and supposed weight. He first comments that “the conclusion that the feathers would be incapable of supporting the weight of the birds, as proposed by Nudds and Dyke, generated intense debate. Paul (2010) replied that the ‘total biology of the birds indicates that they could achieve flapping flight’ and suggested there might be errors in either the mass estimates of the birds or the shaft diameters of the feathers. Zheng et al. (2010) recognized that the innovative analysis offered important new insights into bird evolution. However, they believed that some recently collected data for Confuciusornis indicating thicker main shaft diameters, about twice those used in the original calculations, would mean that their conclusions would need to be further evaluated. But despite this they noted that ‘even our measurements are considerably smaller than the predicted rachis diameter of primary feathers with similar feather length in similarly sized extant birds’. Nudds and Dyke (2010a) responded to these two comments by agreeing that their model is of course dependent on the data fed into it, but calculating the maximum lift forces sustainable by a bird still provides a novel way of estimating the flight capabilities of ancient birds. Using the other values

suggested still indicated the birds were not capable of flapping flight and the feather’s strength was barely enough for gliding.”

Then, Hurrell (2014) claims that “Nudds and Dyke calculated the body mass of Archæopteryx and Confuciusornis respectively as 0.276 kg and 0.5 kg based on their size in relation to modern birds. They also estimated the downward force required so the feathers were ‘strong enough to sustain a force equal to their body weight’ as equivalent to a mass of 0.188 kg and 0.215 kg respectively in today’s gravity.”

He assumes that palaeogravity was less, and thus he can “calculate palaeogravity ... by assuming that ... in a reduced gravity the weight (mass × gravity) would be reduced to the appropriate level required for flight. So ancient gravity (g_a) can be calculated from

$$g_a = F_a/M_p \quad (1)$$

where F_a is taken as the maximum ancient force produced by the birds’ wings, and M_p is the mass of the bird.”

Thus, he evaluates $g_a = 0.68$ and $g_a = 0.43$ for Archæopteryx (i.e. 145 Ma ago) and Confuciusornis (i.e. 120 Ma ago), respectively. We recall that the Dirac’s hypothesis of a reduction of gravity vs. time has the appeal and fascination of “simplicity”, although no real support seems to have yet been found.

The flying capability of fossil birds can, however, have been improved by a denser atmosphere (Gregori, 2015a), as a larger Archimedean buoyancy force implied a smaller mechanical stress on feathers. In fact, the force applied to

feathers is proportional to gravity. However, the Archimedean buoyancy force is proportional to air density. Hence, if the aforementioned assumptions are reasonably akin to reality, the palæodensity of the Earth's atmosphere was, approximately respectively, $\sim 1/0.68 = 1.47$ and $\sim 1/0.43 = 2.33$ times the present density.

A more correct computation ought to consider, however, the volume V of a flying animal, including its feathers. However, V is not specified in the aforementioned papers, although it was approximately estimated in order to evaluate the weight of the bird. In fact, call ρ the density of the bird, and - referring to epoch t - call $\rho_A(t)$ the air density and $g(t)$ the gravity. In order to fly, the bird should satisfy either one of the following relations (present time is $t = 0$)

$$V \rho g(0) - V \rho_A(0) g(0) = V \rho g(t) - V \rho_A(t) g(t) \quad (2)$$

or, equivalently,

$$V g(0) [\rho - \rho_A(0)] = V g(t) [\rho - \rho_A(t)] \quad (3)$$

Hurrell (2014) assumes that air density was the same at every epoch. Hence, $g(t)$ had to change. In contrast, g can be assumed to be invariant in time, while $\rho_A(t)$ experienced a variation.

Note that these estimates ought to correspond to ~ 5.3 and ~ 4.4 Earth's heartbeats ago, respectively, (every heartbeat lasts 27.4 Ma; see Gregori and Leybourne, 2021). In addition, a depletion of a large fraction of the Earth's atmosphere - caused by the solar wind - ought to have occurred on the occasion of several geomagnetic field reversals (FRs). In fact, it is well-known that the solar wind exploits an effective spoiling action on every planetary object when the object is not protected by the shield of a magnetosphere. During every FR the Earth supposedly remained without magnetosphere for some time. The typical duration of a FR (maybe a few thousand years or less) and its progression (i.e. whether the field vanishes and re-grows, or rather it flips) are not clear. In addition, during every FR an excess production occurs of endogenous energy. Therefore, the density of the atmosphere varied depending on the competing balance between the spoiling action by the solar wind, and the increased soil exhalation. Hence, according to the aforementioned guessed inference, a large depletion of the Earth's atmosphere by the solar wind ought to have occurred on the occasion of several FRs that happened during about 5 Earth's heartbeats. In any case, in general one must expect that the palæodensity of the Earth's atmosphere changed in some seemingly erratic way depending on the timing of FRs. In addition, no reason requires that it varied according to any smooth or monotonic trend.

For instance, according to Som et al. (2016), 2.7 Ga ago - i.e. much earlier than the time when some dinosaurs and/or birds were flying - the air pressure was constrained to less than half of modern levels. They summarize as follows their conclusion. "How the Earth stayed warm several billion years ago when the Sun was considerably fainter is the long-standing problem of the 'faint young Sun paradox'. Because of negligible ... O_2 and only moderate CO_2 levels ... in the Archæan atmosphere, CH_4 has been invoked as an auxiliary greenhouse gas ... Alternatively, pressure

broadening in a thicker atmosphere with a N_2 partial pressure around 1.6 – 2.4 bar could have enhanced the greenhouse effect ...

But fossilized raindrop imprints indicate that air pressure 2.7 Ga ago was below twice modern levels and probably below 1.1 bar, precluding such pressure enhancement ... This result is supported by nitrogen and argon isotope studies of fluid inclusions in 3.0 – 3.5 Ga rocks ... Here, we calculate absolute Archæan barometric pressure using the size distribution of gas bubbles in basaltic lava flows that solidified at sea-level ~ 2.7 Ga in the Pilbara Craton, Australia. Our data indicate a surprisingly low surface atmospheric pressure of $P_{atm} = 0.23 \pm 0.23$ (2s) bar, and combined with previous studies suggests ~ 0.5 bar as an upper limit to late Archæan P_{atm} . The result implies that the thin atmosphere was rich in auxiliary greenhouse gases and that P_{atm} fluctuated over geologic time to a previously unrecognized extent."

Pease (2016) announces and illustrates this study and comments that "... very little is known about how thick Earth's ancient atmosphere once was. Now, a new study suggests that Earth's atmosphere 2.7 Ga ago was between a quarter to half as thick as it is today ...

Scientists have long assumed that Earth's ancient atmosphere had a stronger greenhouse than today's. That's because the Sun put out 20% less heat than it does today, and even with elevated levels of greenhouse gases, Earth would have struggled to keep global temperatures above freezing. A thicker atmosphere would have helped to compensate. But in recent research, this expected thickness hasn't been found: a 2012 study of fossilized raindrops, e.g., found that Earth's early atmosphere was as little as half as thick as it is today.

Now, the same team of scientists has come up with a more precise way of measuring early pressure: gas bubbles trapped in ancient lava. In what is now the Australian outback, basalt lavas poured out over thousands of square kilometers billions of years ago, hardening when they hit seawater ... the hot lava quickly cools and freezes, trapping the bubbles. By measuring the size of the bubbles at the top - which were pushing against the weight of the atmosphere - and comparing them with the smaller bubbles at the bottom - which were pushing against both the atmosphere and the weight of the rock itself - the team came up with a proxy for ancient air pressure ... The difficulty was finding lava that was both old enough and pristine enough to have retained a true record of the deep past ...

... some of the lavas ... had clearly reacted with ancient seawater, proving they had erupted at sea-level. After years of hunting, only three slabs from all this extent were adequate for the task. When they first eyeballed the bubbles, sitting around a campfire, the implications were immediately obvious ... They quickly saw from the size of bubbles exposed at the surface that the ancient atmosphere must have been much lower than previously assumed ...

The key was nitrogen. Today nitrogen dominates the atmosphere, making up 4/5 of our atmosphere; oxygen makes up the other fifth. At the time of the basalt eruptions, there was no free oxygen in the atmosphere - that didn't happen until cyanobacteria flooded the atmosphere with the

gas hundreds of millions of years later. So that absence would explain some of the difference between now and then, but not the 50% or more the bubbles reveal. The explanation for that has to involve a lack of nitrogen as well.

Although nitrogen appears to be extraordinarily inert, life today works hard to catch this biologically essential element using fixation. Bacteria and phytoplankton draw tens of millions of tons from the atmosphere every year. And each year, an equal amount is returned to the skies by a mixture of other biological and geological processes. Because the cycle is balanced, the net nitrogen in the atmosphere remains unchanged ... A high rate of removal, implying substantial biological fixation, without the balancing return would do. Last year, Buick published evidence that biological nitrogen fixation was already well established half a billion years before these Pilbara basalts erupted. He and Catling say that in the absence of oxygen, the return mechanism was weakened, so that for hundreds of millions of years, life steadily transformed the atmosphere by removing nitrogen. That impact was reversed only when life's better known transformation, the GOE, arrived ~ 2.4 Ga ago. The low nitrogen levels, however, close off a nitrogen-boosted greenhouse effect as one favored solution to the problem of keeping Earth warm when the young Sun was faint. Evidence has accumulated that levels of the known greenhouse gases, like CO₂ and CH₄, were inadequate to compensate for the low warmth of the early Sun.

Yet evidence of ancient liquid water makes it clear the planet had not chilled below freezing. In 2009, Colin Goldblatt ... proposed a way out. His calculations showed that in an atmosphere with double the nitrogen pressure, the effect of greenhouse gases could be amplified, producing enough warming to stop the planet freezing over. Goldblatt concedes that the new findings, if confirmed, kill that solution. With such little pressure, it's going to be very hard to account for the warm temperatures ... "The nitrogen cycle is discussed also below.

A specific, authoritative, previous, and related study (Levenspiel⁶ et al., 2000) tackles in a systematic way the problem of the palæodensity of the Earth's atmosphere. Some excerpts are here reported, although by changing some items concerned with the rejection of their model that relies on standard plate tectonics. However, plate tectonics is not a necessary requirement for their interpretation. In addition, some fundamental newly available evidence is included into the discussion in order to get an updated perspective. Levenspiel et al. (2000) remind about a previous study (Levenspiel, 2000) where it was shown that if the "mouse-to-elephant curve also applies to the flying creatures of the past, and if you also trust aerodynamic theory (which applies equally to flying insects, birds, and airplanes), then the giant flying creatures of the dinosaur age could only fly if the atmospheric pressure was much higher than it is now: at least 3.7 – 5.0 bar." This concept is better clarified in the following.

During 97% of the Earth's life before the age of dinosaurs, air pressure could display three possible trends. Taken for granted that these giant creatures could fly only with a substantially denser atmosphere, air density was either (i) formerly as it is at present, later increased, and subsequently it decreased anew to the original value that was equal to the present pressure, or (ii) it was constant and higher than at present, and later it decreased to its present value, or (iii) it was originally very large and it progressively decreased until reaching the present value.

In any case, owing to the erratic time sequence of FRs, maybe an oscillating trend is more likely. In either case, these flying animals became extinct when air density was insufficient for their flight and survival. Levenspiel et al. (2000) guess that - according to their feelings that, eventually, are not shared by the present study (see below) - the third possibility seems to be, perhaps, more reasonable, and discuss how this might have happened.

Consider that, during the whole Earth's history, at any epoch air density was determined by a fluctuating balance between (i) soil exhalation, which varied depending on the time-varying amount of endogenous energy production, and (ii) atmospheric spoiling by the solar wind during the time of absence of the magnetospheric shield (i.e. on the occasion of every FR and also during a large number of analogous case histories when a FR did not occur, i.e. during several so-called geomagnetic excursions). Concerning the Earth's original atmosphere, Levenspiel et al. (2000) claim that "geologists believe that most of the carbon on the young, hot Earth, > 4000 Ma, was in the form of gaseous CO₂, CO, and CH₄. With time, the CO and CH₄ reacted with oxide minerals and were transformed into CO₂. These reactions did not change the total amount of carbon in the atmosphere" [while the CO and CH₄ concentration eventually experienced comparably large variations, unlike the CO₂ reservoir that played the role of final long-term carbon storage.]

Our sister planet and nearest neighbor, Venus, has an atmosphere of 90 bar pressure, consisting of 96% CO₂ (CRC Handbook of Chemistry and Physics, 1986, p. F-129) ... Ronov measured the equivalent of at least 55 bar of CO₂ tied up as carbonates around the world (Hay, 1985), whereas Holland estimates that at least 70 bar of CO₂ is bound as carbonate materials (Holland, 1984). These carbonates had to come from the atmosphere, by way of the oceans, so we propose that, after the original oxidation of CH₄ and CO, Earth's early atmosphere was at very high pressure, up to 90 bar, and that it consisted primarily of CO₂."

Levenspiel et al. (2000) compare the Earth with Venus. They speculate that the birth of the Moon, stripped from the Earth's mass, ought to have caused a comparatively thinner, and more fragile, Earth's crust. Therefore, they guess that "Venus's thicker crust remained rigid and did not permit the mechanisms that removed the CO₂ from its bound state. In addition, because Venus is closer to the Sun and hotter than Earth, free liquid water cannot exist on it, whereas

⁶ Octave Levenspiel (1926-2017), Professor of chemical engineering at Oregon State University (OSU).

Earth has giant oceans that cover two-thirds of the planet. The oceans played an important secondary role in removing CO₂ from the atmosphere."

According to the viewpoint, which is here used, the origin of the Moon requires a different consideration, as the present preferred model appeals to a substantially different mechanism. The comparison ought to be made, rather, between Venus, Earth and Mars that have a roughly comparable mass, in decreasing order. It appears that inside the Earth a nuclear reactor was active during its first few Ga (Herndon, 2014, 2010). Then, the nuclear reactor exhausted. This seems to be the unique explanation suited to justify the well-known unexpected large ³He/ ⁴He ratio in basalt. Venus, which is slightly larger than the Earth, could still have an internal nuclear reactor, and this ought to explain a large endogenous energy release, hence its enormous surface temperature, its impressive topography, and its ongoing volcanism and presumable large soil exhalation. In any case, as mentioned above, the total mass of the atmosphere - hence the air density at ground - results from a balance between soil exhalation and the spoiling of the atmosphere by the solar wind - and Venus has no magnetosphere. As far as Mars is concerned, Mars has no magnetosphere, hence soil exhalation is promptly spoiled by the solar wind, as confirmed by space probe observations.

Concerning the dissolution of CO₂ in the oceans, Levenspiel et al. (2000) consider some chemical arguments. "At an atmospheric pressure of ~ 90 bar, a considerable amount of CO₂ would dissolve in the oceans. CO₂ dissolves in water according to the equilibrium relationship

$$[\text{Partial pressure of CO}_2 \text{ in the atmosphere}] = H \times [\text{Mol fraction of CO}_2 \text{ in H}_2\text{O}] \quad (4)$$

where *H* is the Henry's Law constant. *H* depends on temperature, but is ~ 876 – 1000 bar per unit Mol fraction of CO₂ (Hougen et al., 1954, p. 182; International Critical Tables, 1928, Vol. 3, p. 279). If we assume that Earth's oceans are 2 km deep, the values given above imply that at equilibrium, for each mole of CO₂ in the atmosphere, there is one mole of CO₂ dissolved in the ocean. So an atmosphere originally consisting of 90 bar of CO₂ would decrease to 45 bar of CO₂ by dissolution alone; however, another factor acts to lower the concentration of CO₂ in the atmosphere even further."

In fact, Levenspiel et al. (2000) stress that there is a reaction of CO₂ with subsoil minerals. They argue in terms of conventional plate tectonics, mantle convection etc. that cannot be shared by the rationale which is here used. More realistically, let us refer to the serpentinization process (Hovland and Gregori, 2025) by which water penetrates into cracks through dehydrated rocks; serpentinization occurs explosively, thus producing geogas and additional cracks, etc. hence additional soil exhalation. The resulting rehydrated rocks are then heated by endogenous heat and lose anew their water content, and are thus ready for new serpentinization, etc. Note that this is one of the three crucial "engines" for climate control (Gregori et al., 2025a). As far as the palæodensity of the atmosphere is concerned, this "engine" implies a permanent role in the carbon cycle, including a CO₂ exchange of soil with the atmosphere. These three "engines" are: serpentinization which is chemical, another "engine" is biological (i.e. the biosphere), and another is physical, being the tide-driven (TD) geodynamo (Fig. 11). See also Gregori and Hovland (2025).

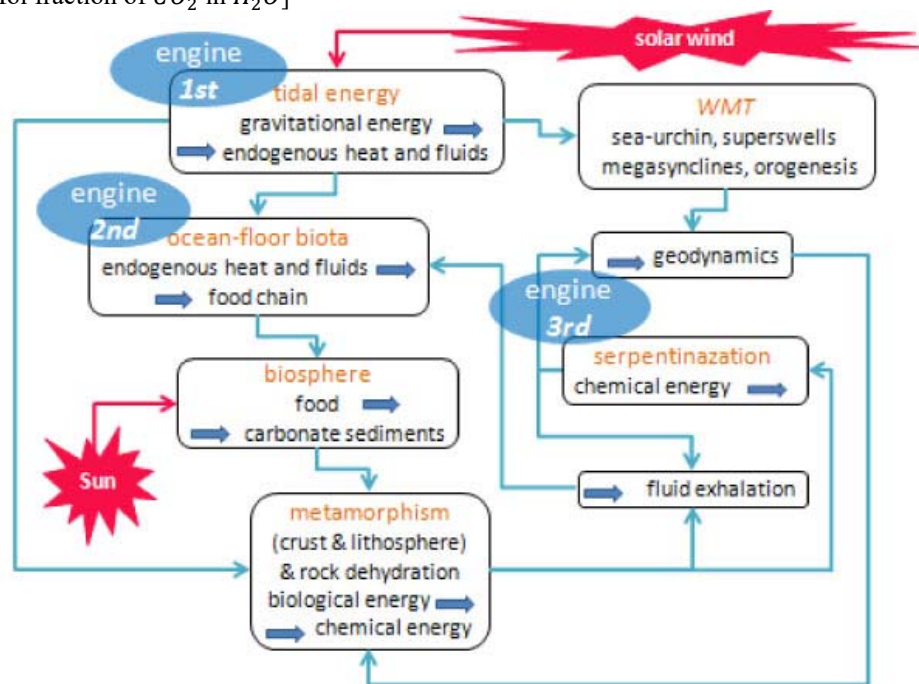


Fig. 11 - The leading drivers of "climate" are three engines. The Sun modulates, by means of the solar wind, the efficiency of the physical engine (i.e. the TD geodynamo). In addition, concerning the food-chain and the production of biomass, the solar irradiance amplifies the role of fluids and energy that are exhaled from soil. Biomass finally returns into ground in the form of organic sediments. After Gregori (2015b). With kind permission of *New Concepts in Global Tectonics*.

One fundamental related result is the “principle of preservation of life” (Ronov, 1982, and Budiko et al., 1985; Fig. 12). The exhalation of CO_2 , of CH_4 etc. from soil occurs through volcanism, but also through gentle fluid exhalation, and air-earth currents. This exhalation is the primary supply for the survival of the biosphere, and the biosphere later transports carbon into sediments and crust etc. That is, with no volcanism and with no soil exhalation, life extinguishes.

Levenspiel et al. (2000) finally guess “that the

concentration of CO_2 in the atmosphere decreased roughly linearly with time ... “ This conclusion may, or may not, be correct. However, this is not relevant for the following. They show Fig. 13 that can be adapted to the aforementioned serpentinization argument, although there is no need that “fresh oxides” are supplied by the mantle. Instead, “fresh oxides” ought to be considered the result of a shallow chemical explosive process.

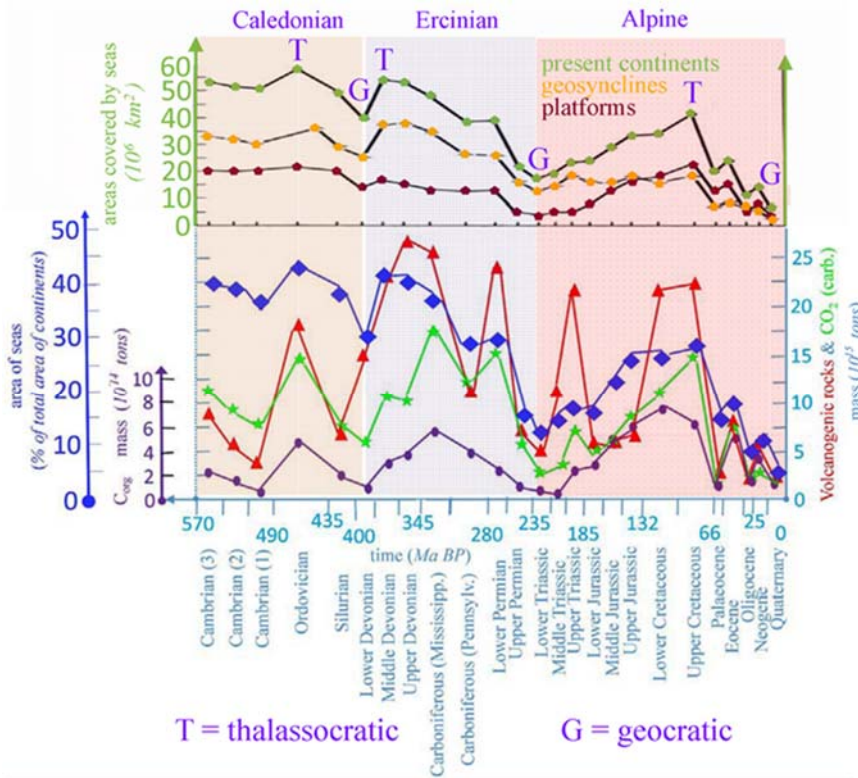


Fig. 12. Synthesis of the analysis reported by Ronov (1982) and Budyko et al. (1985), and here compiled on the basis of a few figures shown by Ronov and co-workers. Thalassocratic and geocratic mean an environmental setting dominated by prevailing seas, or continents, respectively. According to the WMT rationale, envisaged in the present study, the alternation of a varying amount of land vs. oceans depended either (i) on overthrust of lithospheric slabs and consequent varying elevation of platforms and orogens, or (ii) on a (presently unknown) variation of the total amount of water stored in the atmosphere, in ice sheets, or underground (down to the serpentosphere). Ronov (1982) and Budyko et al. (1985) claim that volcanism and soil exhalation of carbon compounds is the needed basic supply for the preservation of life. Unpublished figure.

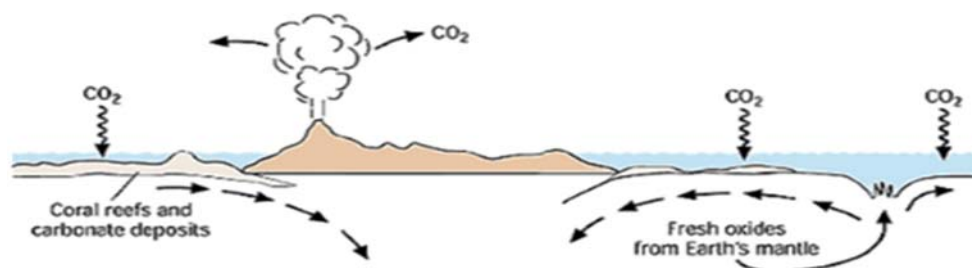


Fig. 13. CO_2 cycle through atmosphere and subsoil. After Levenspiel et al. (2000). *Chemical Innovations* is a “defunct ACS magazine for which we do not have any information in our file regarding the copyright status; therefore, we are unable to grant you permission” (according to the Office of Secretary & General Counsel of ACS). According to the web, this paper, however, is granted through “CC BY 4.0 licence by Inist-CNRS”.

The following statements by Levenspiel et al. (2000) are noteworthy.

“Today, vast deposits of sedimentary carbonate rocks are found on land and on ocean bottoms, $> 1,000,000 km^3$ throughout Earth’s crust. Above the continents, the CO_2 was taken up by rainwater and by groundwater. This CO_2 -rich water reacted with rocks to form bicarbonates, followed by transport to the ocean and precipitation as Ca

and Mg carbonates. In the ocean, dissolved CO_2 combined with the calcium hydroxide ($Ca[(OH)_2]$) to form deposits of chalk, or it was taken up by coral, mollusks, and other living creatures to form giant reefs. A study of the distribution through time of these deposits gives us clues to the history of CO_2 in the atmosphere.

A detailed analysis by Hay (1985) of the extensive measurements taken from around the world by Ronov and

Yareshevsky (1969) is summarized in Fig. 14. Hay's analysis shows that today the continents contain at least $2.82 \times 10^6 \text{ km}^3$ of limestone, which are the remains of deposits over the past 570 Ma that have not been washed to sea ... This is equivalent to a CO_2 atmospheric pressure of 38 bar. If we add the carbonates found on the ocean floor, the equivalent CO_2 atmospheric pressure rises to 55 bar. Integrating the values plotted in Fig. 15 gives the progressive depletion of CO_2 from the atmosphere (Fig. 14). Thus, CO_2 is recycled: 55 – 70 bar or more is accounted for on the surface of Earth (Hay, 1985; Holland, 1984), and ~ 30 bar is in the process of being recycled in the planet's interior.

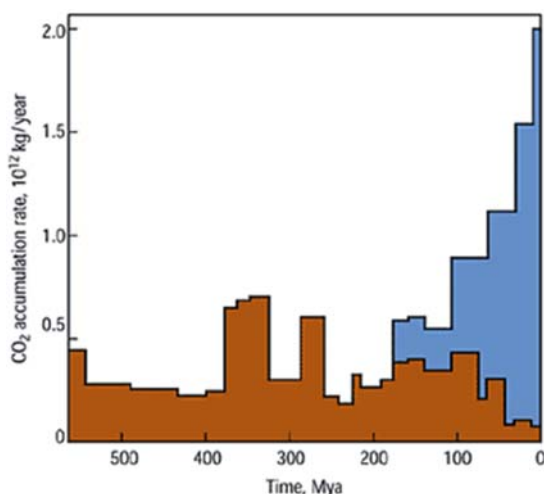


Fig. 14. "History of deposition of CO_2 as carbonates. The red area represents continental deposits ... The blue area represents ocean deposits ... " Figure and captions after Levenspiel et al. (2000). *Chemical Innovations* is a "defunct ACS magazine for which we do not have any information in our file regarding the copyright status; therefore, we are unable to grant you permission" (according to the Office of Secretary & General Counsel of ACS). According to the web, this paper, however, is granted through "CC BY 4.0 licence by Inist-CNRS".

Fig. 14 verifies the earlier statement that the present oceans are relatively young because they contain limestone not older than 200 Ma. On the other hand, the continental land masses are much older because, 100 – 65 Ma, the oceans and the atmosphere shared the free CO_2 equally. Consequently, the pressure of CO_2 in the atmosphere was ~ 8 – 10 bar in the age of the flying creatures (Fig. 15). The geological evidence is consistent with and lends support to the physiological and aerodynamic arguments (Levenspiel, 2000) that the atmospheric pressure was definitely higher in the age of dinosaurs than it is today. If you reject this argument and if you prefer to believe that the atmosphere was at 1 bar throughout Earth's history, how do you explain where the measured 55 – 70 bar of CO_2 in limestone and other carbonates came from?"

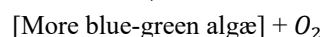
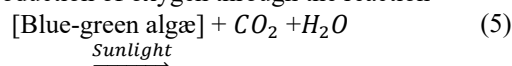
Levenspiel et al. (2000) also consider an "astronomical argument".

"From the viewpoint of the modern theory of stellar evolution, Sagan and Mullen discussed the 'faint early Sun' paradox, which asks why Earth's surface did not freeze in

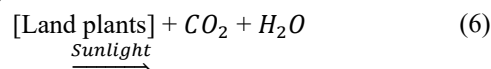
its early days, given a 25 – 40% lower solar luminosity at that time (Sagan and Mullen, 1972). These values represent the range of five estimates. With these lower luminosities, Earth's average temperature would have been somewhere between -5°C and -21°C instead of the present 13°C – 15°C . With frozen oceans covering our planet, how could life have established itself and thrived under these inhospitable conditions? One reasonable answer to this question is that CO_2 , the atmosphere's efficient greenhouse gas, was present at high concentration in those early times. Kasting and co-authors suggest a factor of 100 – 800 times as high as today, all at 1 bar (Kasting et al., 1984; Kasting, 1985); however, he did not consider the possibility of a higher total pressure of the atmosphere ... "

In addition, the role ought to be considered of the aforementioned nuclear reactor that ought to have existed during the early few Ga of the Earth's history. In any case, the Levenspiel's et al. (2000) discussion begins since the Earth's "primordial soup" when life is believed to have started. According to more recent evidence (Gregori and Hovland, 2025), nowadays microorganisms are observed on the deep ocean floors, where no sunlight is available. Their development is supplied by CH_4 exhalation. They are the beginning of the food web that later develops through the several life forms that are observed close to MORs (mid-ocean ridges) - and including also corals etc. at shallow layers. Subsequently, the living forms can progressively occupy shallower ocean layers, as they find supply from sunlight etc. That is, it appears that, at present, life is steadily regenerated on the ocean floors. See also Gregori et al. (2025w).

In any case, Levenspiel et al. (2000) remind about the earliest production of oxygen through the reaction



In addition, later "life came up with its most important invention, photosynthesis, and so learned to live off the abundant CO_2 of the atmosphere plus sunlight and thereby invade the land masses. Land plants evolved and lived by the reaction



During the Carboniferous period, 350 – 280 Ma ago, these plants proliferated widely, covering the land surfaces with lush forests of giant ferns, trees, and plants of all types. Because the atmosphere was rich in CO_2 , but very poor in O_2 , dead plant material did not decompose rapidly, so layer upon layer of it was laid down in thick blankets that would transform over time to coal.

It is estimated that each 1 m thickness of coal comes from the compression of a 10 – 20 m layer of dead organic matter (Stach et al., 1975, p. 18), so that today's 10 m thick coal seam represents an original 100 m of decayed material. Such a thick layer of decaying matter is something that we do not see anywhere today. Tropical forests today only support a very thin layer of decaying matter because of rapid oxidation. Thus, 100 m-thick layers can only occur

if the atmosphere discourages oxidation. This is additional strong evidence that the atmosphere in those distant times was rich in CO₂, but poor in oxygen.

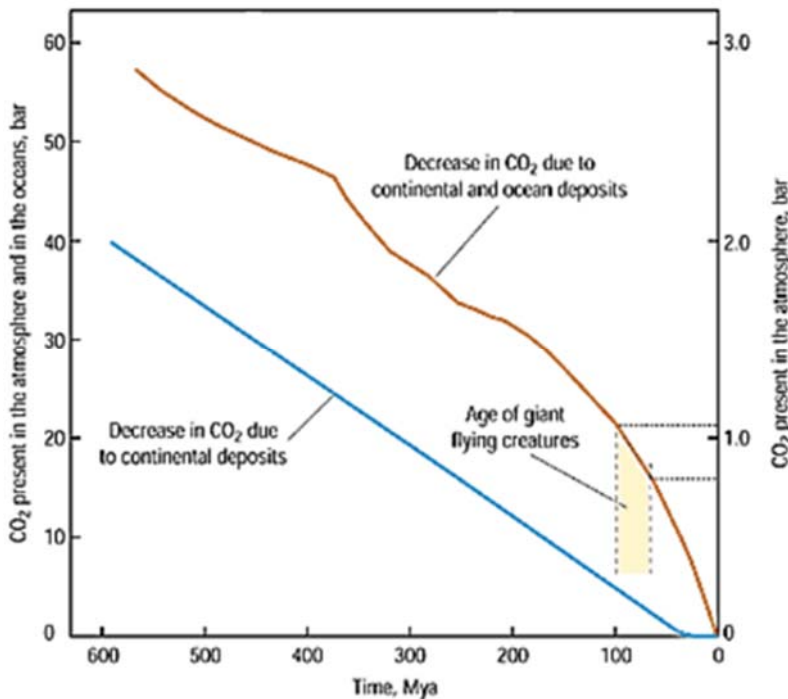


Fig. 15. “Progressive lowering of CO₂ pressure due to carbonate formation and deposition on Earth’s surface.” Figure and captions after Levenspiel et al. (2000). *Chemical Innovations* is a “defunct ACS magazine for which we do not have any information in our file regarding the copyright status; therefore, we are unable to grant you permission” (according to the Office of Secretary & General Counsel of ACS). According to the web, this paper, however, is granted through “CC BY 4.0 licence by Inst-CNRS”.

With time, the concentration of CO₂ steadily decreased, primarily because of the formation and deposition of limestone and other carbonaceous materials. CO₂ was also lost by photosynthesis followed by the deposition of carbonaceous substances such as coal, petroleum, peat, oil shale, and tar sands; however, this loss was quite minor. Calculations show that the deposit of what are now considered fuel reserves lowered the atmospheric CO₂ by << 1 bar . [Note the large time variation of CO₂ concentration in the atmosphere, depending on a balance between several different concurring mechanisms.] At the same time, the concentration of O₂ slowly rose. These two changes, the decrease in CO₂ and the rise in O₂, thinned the forests and the dead material began to be oxidized more rapidly, so that dense layers of dead organics were no longer deposited. Evidence of this change in atmospheric conditions is that we cannot find any massive coal deposits younger than 65 Ma the giant flying creatures [appeared] close to the end of the dinosaur age. It could be that these creatures died out as the total pressure of the atmosphere dropped below their sustainable level (Fig. 16).”

limestone caves were formed relatively recently indicates that the CO₂ concentration in the atmosphere was very high long ago, leading to the deposits of limestone, but became very low recently, allowing limestone to dissolve. ”

Levenspiel et al. (2000) also stress the relevance of the age and of the extension of limestone caves. “These caves are all relatively young, most of them < 100 Ma old, and were carved by running water, which dissolved the limestone ... Because of its high concentration in the atmosphere, CO₂ dissolved in rainwater and groundwater, and the reaction



was driven to the right. When the atmosphere becomes lean in CO₂, the reaction shifts to the left. The fact that the

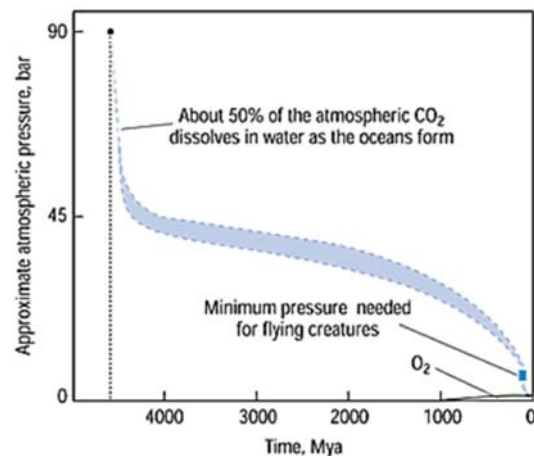


Fig. 16. “Earth’s proposed atmospheric history.” Figure and captions after Levenspiel et al. (2000). *Chemical Innovations* is a “defunct ACS Magazine for which we do not have any information in our file regarding the copyright status; therefore, we are unable to grant you permission” (according to the Office of Secretary & General Counsel of ACS). According to the web, this paper, however, is granted through “CC BY 4.0 licence by Inst-CNRS”.

The role of CO₂ density in air was investigated by checking crops in test fields where CO₂ was pumped. Other tests were carried out by investigating the vegetation that grows at the border of mud volcanic areas, depending on

the leading wind direction, etc. (see below for some detail). However, these studies can hardly be likened to the speculated dramatically larger CO_2 concentrations of the palaeo-atmosphere. In this respect, the present ongoing increase of atmospheric concentration of CO_2 expands the

green cover of the Earth. Fig. 17 shows this impressive datum. On the other hand, periods of prolonged and extended drought in some regions can produce the opposite effect. "Climate" is not a steady state at all.

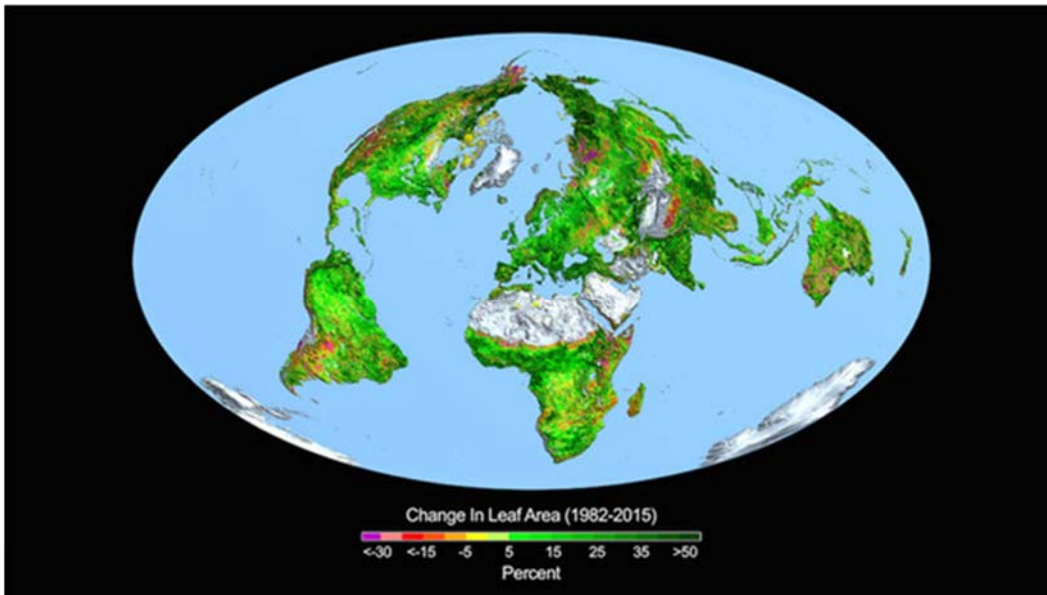


Fig. 17. "The surface area of the Earth covered by leafy green vegetation has increased dramatically over the last several decades, thanks to excess carbon emissions ... Credit: Boston University/ R. Myneni." Figure and captions after Ghose (2016d). NASA copyright free policy.

Levenspiel et al. (2000) recall Daniels et al. (1996), who have shown that "in high- CO_2 atmospheres and other hostile environments, life forms can take advantage of free energy in an amazing range of environments: above the boiling point and below the freezing point of water, in pressures as high as 300 bar, in oxygen-rich and oxygen-poor environments, and in the presence and absence of sunlight (Lutz et al., 1994; Adams and Kelly, 1995)." [See also Gregori et al. (2025w).]

Levenspiel et al. (2000) also remind about Des Marais (1985) who studied carbon exchange between mantle and crust, and "suggests that 3000 Ma, the atmosphere contained at least 100 times as much CO_2 (or 0.03 bar) as it does today." In addition, "Holland (1984) estimates that Earth's earliest atmosphere contained up to 20 bar of CO_2 and that ~ 10 bar could conceivably have persisted for several hundreds of millions of years (Walker, 1986). Many other such proposals have been put forth."

Levenspiel et al. (2000) remind about an astute experiment aimed to test how far a large CO_2 concentration affects plant development and survival. Their results look astonishing. "Pine and aspen trees grown at the University of Michigan's biological station at Pellston, were found to respond dramatically to elevated CO_2 levels. They grew 30% faster than normal trees at about double the normal CO_2 level (700 ppm) ...

However, to test our speculation we need to see if plants can survive, not at double today's CO_2 concentration, but at thousands of times higher. We put this proposal to the test by growing plants in 32 sealed containers (1 and 2 l plastic soda bottles containing weighed amounts of CO_2) at pressures from 2 to 10 bar. These conditions gave CO_2 partial pressures 3000 – 27,000 times greater than

normal, or 50 – 90% CO_2 . Of the species tested, *Taxodium*, *Metasequoia*, *Araucaria*, *Equisetum*, and *Sphagnum* grew best at these higher pressures; one specimen of *Taxodium* grew 7 cm over 2 years at 2 bar (50% CO_2). In general, however, plant growth was considerably slower than at 1 bar. Mosses, ferns, and flowering plants died within a month at these high CO_2 levels.

The poor growth observed in these experiments is most likely due to the buildup of product gases in the sealed containers, rather than high CO_2 pressure, and therefore these results could be flawed. We would expect that vigorous growth would be observed in a continually rejuvenated atmosphere. Although present-day plant life is probably not adapted to living at the very different atmospheres and pressures of the past, our preliminary experiments do suggest that a dense CO_2 atmosphere could have existed on early Earth without violating any known constraints on the planet's evolution."

A different concern deals with the nutrition potential of vegetation for the giant dinosaurs. In this respect, Gill et al. (2018) - which is also reviewed by Letzter (2018b) - claim that "a major uncertainty in estimating energy budgets and population densities of extinct animals is the carrying capacity of their ecosystems, constrained by net primary productivity (NPP) and its digestible energy content. The hypothesis that increases in NPP due to elevated atmospheric CO_2 contributed to the unparalleled size of the sauropods has recently been rejected, based on modern studies on herbivorous insects that imply a general, negative correlation of diet quality and increasing CO_2 . However, the nutritional value of plants grown under

elevated CO₂ levels might be very different for vertebrate megaherbivores than for insects.

Here we show plant species-specific responses in metabolizable energy and nitrogen content, equivalent to a two-fold variation in daily food intake estimates for a typical sauropod, for dinosaur food plant analogues grown under CO₂ concentrations spanning estimates for Mesozoic atmospheric concentrations. Our results potentially rebut the hypothesis that constraints on sauropod diet quality were driven by Mesozoic CO₂ concentration."

Independent of every more or less exotic speculation, it is well-known – and unanimously acknowledged - that during the whole Earth's history a dramatic substantial evolution occurred of the biosphere that must be considered in its broadest sense. All living forms afforded to survive only by adapting to their changing environment (see Gregori et al., 2025w). The total amount of CO₂ concentration in the atmosphere is therefore likely to have attained very high levels in the past, thus affecting the evolution, development and survival of the biosphere. In the final analysis, compared to other several unwanted and dangerous forms of pollution, the often complained anthropic production of CO₂ that contributes to increase its concentration in the atmosphere could well be a comparatively lesser hazard and a secondary driving factor for climate control.

In a subsequent paper (Levenspiel, 2006) the specific item of palæodensity of the atmosphere is studied in terms of two arguments, i.e. (i) aerodynamic capability to fly, and

(ii) physiology of blood circulation in a huge warm-blood animal. The Levenspiel (2006) paper is relevant for the present discussion. Note that all these arguments certainly rely on some speculation. In any case, a conspicuous amount of other observational evidence dealing with palæo-Earth relies on arguments that are even more speculative than the items that are thus considered. In any case, every conscience-driven scientist must take into serious account all possible hunches, while every attempt must always be avoided to conform to every "generally agreed" or self-claiming "well assessed" evidence.

We report here in detail a few relevant excerpts from Levenspiel (2006) as that paper was published on a journal that is outside the standard channels of geophysics.⁷

"... In the Cretaceous fossil record, we find flying creatures which have an estimated mass between 86 – 100 kg ... The Washington DC Museum of Natural History displays a full sized model of the quetzalcoatlus having a 13 – 15 m wingspan while a Texas find is estimated to have a wingspan of 15.5 m (Lawson, 1975). This is about half the wingspan of a Boeing 737 commercial airliner, see Fig. 18 ... Today, the world's target flying birds, the South American condor, the Australian kori bustard, and the largest European swan have wings span no more than 4 m. Considering the limitation of skeletal and muscle structure, physiologists and aerodynamicists (Smith, 1984; Schmidt-Nielsen, 1984) estimate that these birds which weigh up to 14.5 kg, represent the upper size limit of creatures that can support and propel themselves through air ... "



Fig. 18. "Wingspan of a quetzalcoatlus compared to today's largest bird and a Boeing 737 aircraft." Figure and captions after Levenspiel (2006). With kind permission of the Association of Chemical Engineers of Serbia. Chem. Industry and Chem. Eng. Quart. is "Open Access" licensed under CC BY 4.0.

⁷ In an "afterthoughts" section, Levenspiel (2006) reports the several times his paper was rebutted by several international best known scientific journals, during several years and after several attempts. Taken for granted that his quantitative computations - which are here enclosed - are even less speculative than several arguments that are typical in palæoclimatology, the reason of such a blind obstinate hostility, maybe, relies on the fact that the acceptance of the possibility of a substantial larger ancient atmospheric density implies that the CO₂ concentration could have been much larger than today. This is a real handicap for the most

fashionable today's speculation about the hazard represented by the increase of the atmospheric concentration of CO₂, which is claimed – like a "state truth" - to be caused by anthropic pollution. Hence, like it happened in several other disciplines (e.g. dealing with the plate tectonics controversy), all what is against a "generally agreed" belief or paradigm is to be considered as an "unreliable evidence" that is not representative of true phenomena. This feeling is evidently totally nonsensical - and dishonest like other tragic "state truth" of the 20th century.

Several *ad hoc* explanations were speculated and proposed aimed to justify the flight of prehistoric animals. No detail is here given. In any case, Levenspiel (2006) after reviewing the different proposals and related difficulties comments that “all these difficulties lead to improbable scenarios. To have survived and thrived for millions of years, these flyers had to be fast, efficient, and well adapted to their environment.” A few interesting quantitative checks can be carried out. “The power of resting warm-blooded creatures (in effect, their metabolic rate) is represented by the mouse-to-elephant curve (Schmidt-Nielsen, 1984), see Fig. 19, with its representative equation

$$\text{Power available} \propto M^{0.764} \quad (8)$$

where M is the creature's body mass.

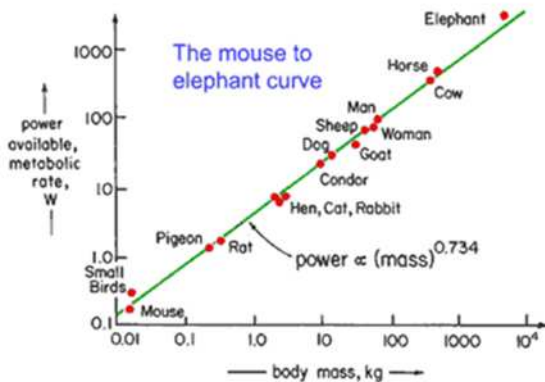


Fig. 19. “The ‘mouse-to-elephant’ curve shows that the power of a warm blooded animal is proportional to its mass to the 0.734 power, as given by equation (8).” Figure and captions after Levenspiel (2006). With kind permission of the Association of Chemical Engineers of Serbia. Chem. Industry and Chem. Eng. Quart. is “Open Access” licensed under CC BY 4.0.

Now the minimum power needed for the level flight of any creature was given by Renard (1889) over a century ago

$$\text{Power needed} \propto \frac{M^{3/2}}{\rho^{1/2} A^{1/2}} \quad (9)$$

where A is the wing area of the creature and ρ is the air density. [Differently stated, the power per unit muscle-mass is constant for every animal.] It was pointed out by von Kärman (1963)⁸ that this expression is essentially what is used today by aerodynamicists and aircraft designers to represent the power needed to keep an aircraft aloft, from Piper Cub to the largest of passenger planes.

If L represents the size of the flying creature, then for creatures of different size but of similar geometry

$$\begin{aligned} \text{Mass} & M \propto L^3 & (10) \\ \text{Wing area} & A \propto L^2 \end{aligned}$$

Replacing eq. (10) in eq. (9), we find that the power needed for a creature to fly is given by

$$\text{Power needed to fly} \propto \frac{M^{7/6}}{\rho^{1/2}} \quad (11)$$

This is shown in Fig. 20.

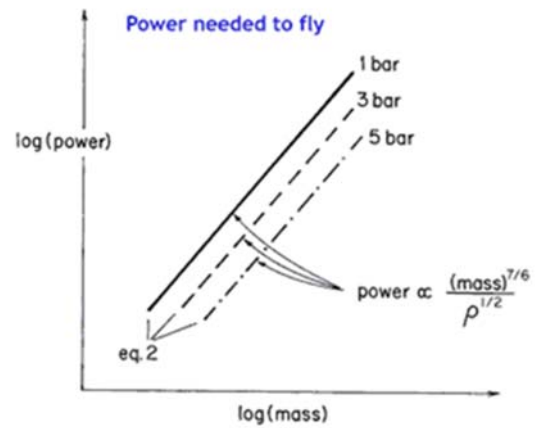


Fig. 20. “Aeronautics plus thermodynamics tell that the power needed to stay aloft depends on the creatures’ mass and the atmospheric density, as given by eq. (9).” Figure and captions after Levenspiel (2006). With kind permission of the Association of Chemical Engineers of Serbia. Chem. Industry and Chem. Eng. Quart. is “Open Access” licensed under CC BY 4.0.

Next compare the power needed to fly with the power available, see Fig. 21. This graph shows that there is always a maximum size above which no creature can fly. This limit today is the 4 m wingspan 14.5 kg bird. But how do we explain the existence of the 15 m wingspan, 86 – 100 kg quetzalcoatlus? Since the power needed is lower at higher atmospheric pressure, see eq. (9), let us propose that the atmosphere in the Cretaceous period was different from today's in that it was denser.

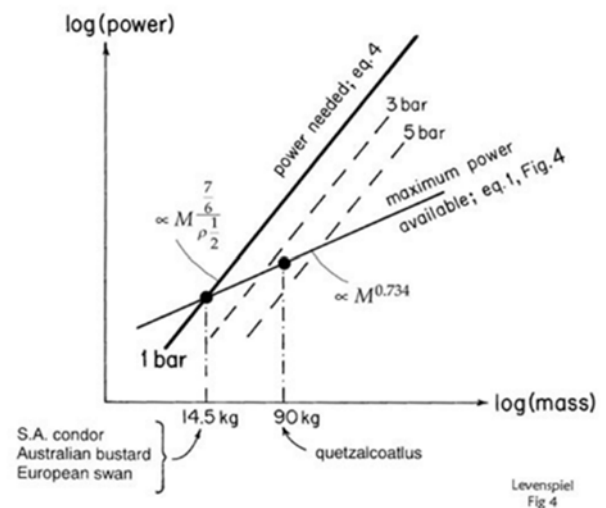


Fig. 21. “The maximum mass of today's flying birds is 14.5 kg. Heavier birds can fly in denser air.” Figure and captions after Levenspiel (2006). The mentioned equations are (8) and (11). With kind permission of the Association of Chemical Engineers of Serbia. Chem. Industry and Chem. Eng. Quart. is “Open Access” licensed under CC BY 4.0.

Comparing masses (86 – 100 kg vs. 14.5 kg) and assuming geometrical similarity, eq. (8) and eq. (11)

⁸ Theodore von Kärman (1881-1963).

combined leads us to conclude that the atmospheric pressure at the time of the quetzalcoatlus had to be about 3.2 – 4.8 bar. This is significantly greater than today's 1 bar. Graphically, we illustrate this conclusion in Fig. 21.

From a different point of view, from flight energetics, Figs 22 and 23 show the great flight diagram of Tennekes (1996) (quetzalcoatlus point added by me). These diagrams clearly show that the point for the pteranodon and the quetzalcoatlus are far from the correlation for all of today's birds, today's insects and today's airplanes. To bring these points to the correlation line would require having a significantly higher gas density.

We know of no other scenario which can account for and explain why the metabolic rate of these giant flyers differs from all other warm blooded flyers, and why the flight energetics of pterosaurs is not consistent with all other flyers - from the smallest of insects, to birds and aircraft, all the way to the Boeing 747 (see Fig. 22)."

The second item focused by Levenspiel (2006) deals with blood circulation in a tall animal like a dinosaur. No detail is here given. The heart of a large dinosaur has been estimated to weigh a few tons, even 5 tons, in order to pump blood up to a 10 m height or higher. Different hypotheses have thus been speculated. One thus can envisage several hearts along the neck. Others envisaged that the dinosaurs kept their neck almost horizontal, also upon considering the effort needed to lift such a huge mass. Another proposal was that the heart had to be located along the neck, etc.

These physiological and anatomic details are not of concern for the present discussion. Rather, Levenspiel (2006) discusses a siphon effect, i.e. atmospheric pressure lifts-up blood inside a siphon. Upon carrying out a simple computation, Levenspiel (2006) concludes that "when the atmospheric pressure is roughly over 2 bar these long necked creatures could exist. Then we tentatively conclude that the atmospheric pressure at the time of dinosaurs had to be higher than 1 bar or at least 2 bar. At these higher atmospheric pressures taller siphons would work - at 1 bar 7 m high; at 2 bar 14 m high, and so on."

Thus, Levenspiel (2006) finally states that "if you allow yourself to entertain the idea that a higher atmospheric pressure - say between 3 – 5 bar - could have existed in the time of the dinosaurs, it would resolve two of the anomalies that face us today, which are:

- how a dinosaur's heart could pump blood 7 or more meters upwards, without introducing the ideas of multiple hearts (as many as 5), giant hearts, and hearts located right under their chins, and
- how a giant flying quetzalcoatlus had the energy to stay airborne, something that biology and aerodynamics says is not possible in today's atmosphere.

All of this leads us to the next fascinating question - what was the atmospheric pressure before that time? Was it higher still? But this is another matter ... "

A more recent investigation by Aureliano et al. (2023) is illustrated on São Paulo Research Foundation (2023) that claims that " ... Macrocollum itaquii, which was discovered in the region of Agudo in the Rio Grande do Sul state of South Brazil and dates back 225 Ma, is the most ancient

dinosaur known to have structures referred to as air sacs. These bone cavities, which persist in present-day birds, enabled dinosaurs to capture more oxygen, keep their bodies cool, and withstand the harsh conditions of their era. They also helped some become giants: Tyrannosaurus rex and Brachiosaurus, for example.

'Air sacs made their bones less dense, allowing them to grow to more than 30 m in length,' said Tito Aureliano, first author of the article ... 'M. itaquii was the largest dinosaur of its time, with a length of about 3 m. A few million years before then, the largest dinosaurs were about 1 m long. Air sacs certainly facilitated this increase in size,' Aureliano added ...

'This was one of the first dinosaurs to walk the Earth, in the Triassic period,' she said. 'The air sac adaptation enabled it to grow and withstand the climate in this period and later, in the Jurassic and Cretaceous. Air sacs gave dinosaurs an evolutionary advantage over other groups, such as mammals, and they were able to diversify faster.'

In a previous study, the group showed that the earliest fossils found so far did not have air sacs, taking their absence as a sign that this trait evolved at least three times independently. M. itaquii was a biped, a sauropodomorph, and an ancestor of the giant quadrupeds with a small head, and a neck at least as long as the trunk.

Until air sacs were discovered in M. itaquii, these vertebral cavities were known to consist of either camerate or camellate tissue, the former referring to hollow spaces observed by microtomography, and the latter to spongy bone. According to the authors, in this case, they found 'internal pneumatic chambers', which are 'neither camerate nor camellate, but a new type of tissue with an intermediate texture'. They propose to call the new structures 'protocamerate', as they 'are not large enough to be considered camerae, but also present a camellate array internally'.

'The most widely held hypothesis until now was that the air sacs began as camerae and evolved into camellae. Our proposal, based on what we observed in this specimen, is that this other form existed first of all,' Aureliano said.

The vertebrae in which the air sacs were found also changed what was known about the evolution of these structures. Based on the fossils analyzed previously, other research groups proposed that air sacs first appeared in the abdominal region and did not appear in the cervical region until the early Jurassic (190 Ma ago), a long time after the period in which M. itaquii was alive. Here, however, the authors found clear evidence of air sacs in the cervical and dorsal regions, with no sign of the structures in the abdominal region.

'It's as if evolution had conducted different experiments until it arrived at the definitive system, in which air sacs run from the cervical region to the tail. It wasn't a linear process,' Aureliano said"

That is, it appears that the evolution either of large dinosaurs and/or of flying animals, until birds, was closely related to the adaptation (see Gregori et al., 2025w) to the changing atmospheric density and composition, through the development of air sacs.

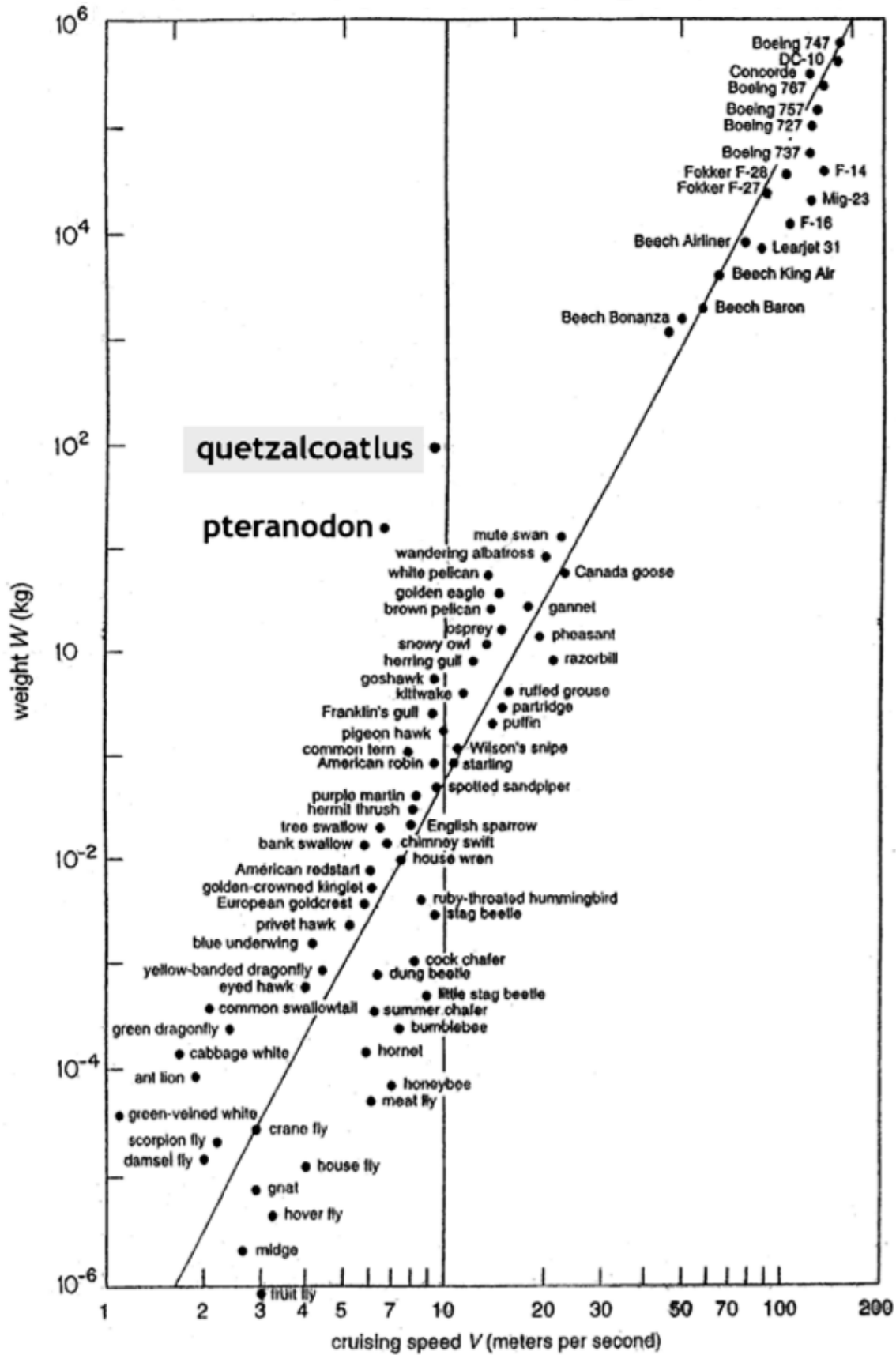


Fig. 22. "Prehistoric flyers do not correlate with today's birds, insects and aircraft." Figure and captions after Levenspiel (2006). With kind permission of the Association of Chemical Engineers of Serbia. Chem. Industry and Chem. Eng. Quart. is "Open Access" licensed under CC BY 4.0.

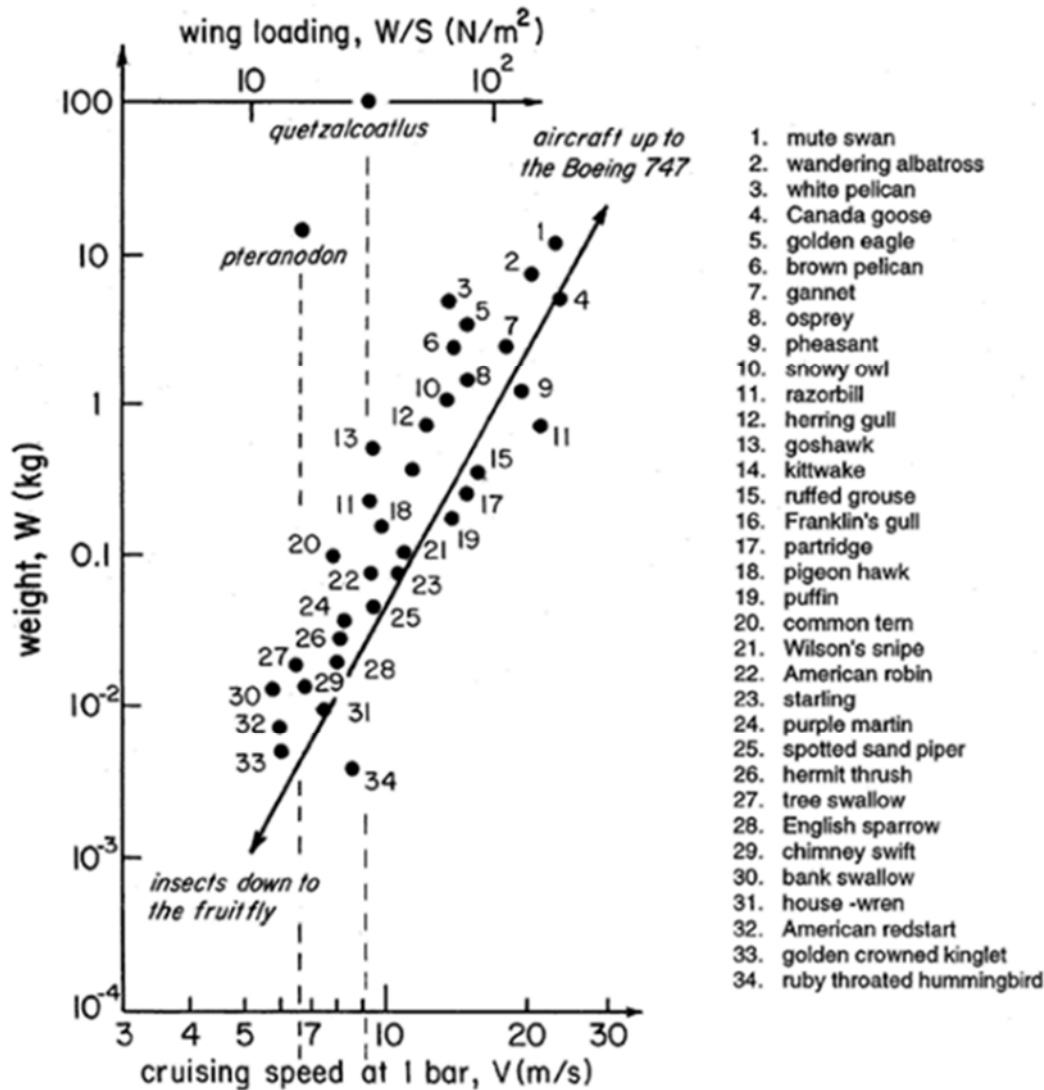


Fig. 23. “The bird section of Fig. 22.” Figure and captions after Levenspiel (2006). With kind permission of the Association of Chemical Engineers of Serbia. Chem. Industry and Chem. Eng. Quart. is “Open Access” licensed under CC BY 4.0.

As far as the role is concerned of gravity constant vs. air density variation [i.e. refer to (3)], it is nonsensical to be partisan either pro or con either one hypothesis or the other. Several independent hunches, however, seem to be in favor of a much denser ancient atmosphere. In any case, harder thinking, and more specific investigations, by means of several distinct approaches and techniques, are likely to be capable to provide with additional indicative constraint. In any case, it should be stressed that - compared to its potential heuristic capability - the use of the biosphere is still insufficiently exploited. The biosphere is an important source of proxy data for the study of the palæo-environment and of its drivers. The biosphere (including also humankind and its history) has always been - and it still is - a crucial component of the natural system and a key driver. The biosphere plays a twofold role, being both an active agent and a passive recorder. The cooperation of biologists and palæontologists, and also of historians (for the investigation of the Cycle of Climate and Civilization, see e.g. Gregori et al., 2000, and Gregori, 2002a), is strongly encouraged according to this viewpoint, in order to tackle

environmental studies from a joint perspective of Earth’s sciences.

The carbon cycle

A related fundamental and general topic deals with the carbon cycle, which involves *per se* a large number of different approaches. For instance, Fraterrigo et al. (2018) considers the role for tree mortality played by insect infestation that can enhance carbon stabilization. A table with a list of the masses of carbon in various reservoirs, including carbon fluxes to and from them, plus average $\delta^{13}\text{C}$, is given by Bowen (1991, p. 121).

Let us try to list just a few additional items, but this is not a complete list, and apologies are due for certainly forgetting about important items. In any case, this phenomenon was not steady, as the palæoclimatic evidence shows a very large scatter that can be compared to no smooth trends. This is shown by several figures displaying other palæoclimatic trends, or the evidence of the subtropical environment, which was found in the Arctic Ocean two heartbeats ago, i.e. $\sim 55 \text{ Ma}$ ago that we cannot

report in detail. In fact, note that the time sequence seems quite erratic of the FRs time series, envisaging a corresponding large scatter of climate.

In general, the palaeoclimatic information largely relies on entire sedimentology, which deals with records of processes associated with the role of the biosphere, including black shales and sapropels.

The past exhalation of CH_4 is a record of the changes of the local release of endogenous heat. It can be recorded by investigating CH_4 within foraminifera.⁹ For instance, Panieri et al. (2009) investigated “benthic foraminifera from seep carbonates and from enclosing non-seep marls present within Miocene formations in the Northern Apennines (Italy) ... as proxies of CH_4 seepage in the marine environment.” They found a “local influence of CO_2 produced by microbial anaerobic CH_4 oxidation on the benthic ecosystem” and that “each species represents a potential proxy for past seafloor CH_4 emissions.”

In addition, the role (at present time, rather than during some geological past) of the biosphere - as a proxy for monitoring the release of endogenous energy - is systematically investigated by the extensive and very general study by Judd and Hovland (2007). See Gregori and Hovland (2025) for details. This impressive study is likely to be a milestone in Earth’s sciences. An almost classic concern deals with corals and with their location depending on endogenous energy supply.

In this same respect, since a long time it is well-known that vegetation is a very important sink for CO_2 . The reaction of vegetation to different concentration of atmospheric CO_2 – and other gas exhalation from soil - is the object of specific studies. The mechanisms and the actual role of vegetation in the control of atmospheric chemistry are not yet understood (e.g. see Lelieveld et al., 2008; Marris, 2008), including the role of roots (see e.g. Barnett, 2008), or of insects (e.g. see Kurz et al., 2008), or of soil microbes and CH_4 (see e.g. Barnett, 2007), even by desert ecosystem, from shrubs to microscopic organisms living in the soil (see e.g. Newton, 2008). This item is reviewed and discussed by Robinson et al. (2007). A few excerpts are here reported.

“How high will the CO_2 concentration of the atmosphere ultimately rise if mankind continues to increase the use of coal, oil, and natural gas? ... The current rise is a non-equilibrium result of the rate of approach to equilibrium. One reservoir that would moderate the increase is especially important. Plant life provides a large sink for CO_2 . Using current knowledge about the increased growth rates of plants and assuming increased CO_2 release as compared to current emissions, it has been estimated that atmospheric CO_2 levels may rise to about 600 ppm before leveling off. At that level, CO_2 absorption by increased Earth biomass is able to absorb ~ 10 Gton C year⁻¹ (Idso, 1989). At present, this absorption is estimated to be ~ 3 Gton C year⁻¹ (Houghton, 2007) ...

As atmospheric CO_2 increases, plant growth rates increase. Also, leaves transpire less and lose less water as

CO_2 increases, so that plants are able to grow under drier conditions. Animal life, which depends upon plant life for food, increases proportionally. Figs 24, 25, 26, ... show examples of experimentally measured increases in the growth of plants. These examples are representative of a very large research literature on this subject (Kimball, 1983; Cure and Acock, 1986; Mortensen, 1987; Lawlor and Mitchell, 1991; Drake and Leadley, 1991; Gifford, 1992; Poorter, 1993).

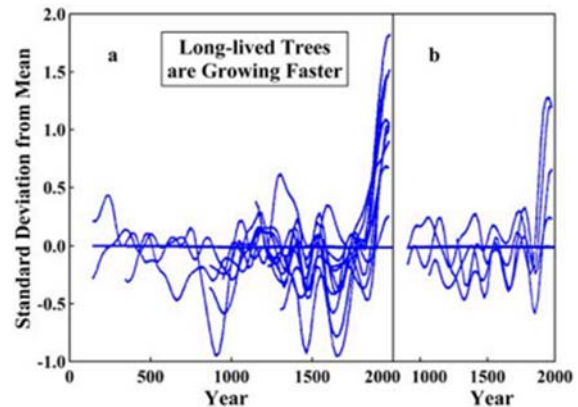


Fig. 24. “Standard deviation from the mean of tree ring widths for (a) bristlecone pine, limber pine, and fox tail pine in the Great Basin of California, Nevada, and Arizona and (b) bristlecone pine in Colorado (Graybill and Idso, 1993). Tree ring widths were averaged in 20 year segments and then normalized so that the means of prior tree growth were zero. The deviations from the means are shown in units of standard deviations of those means.” Figure and captions after Robinson et al. (2007). Reproduced with kind permission of the Association of American Physicians and Surgeon.

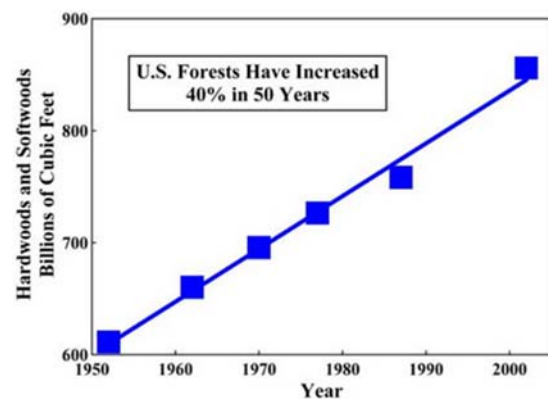


Fig. 25. “Inventories of standing hardwood and softwood timber in the United States compiled in Forest Resources of the United States, 2002, U.S. Department of Agriculture Forest Service (Waddell et al., 1987; Smith et al., 2002a). The linear trend cited in 1998 (Robinson et al., 1998) with an increase of 30% has continued. The increase is now 40%. The amount of U.S. timber is rising almost 1% year⁻¹.” Figure and captions after Robinson et al. (2007). Reproduced with kind permission of the Association of American Physicians and Surgeon.

⁹ See e.g. Hedley and Adams (1974, 1977, 1978), or Haslett (2002).

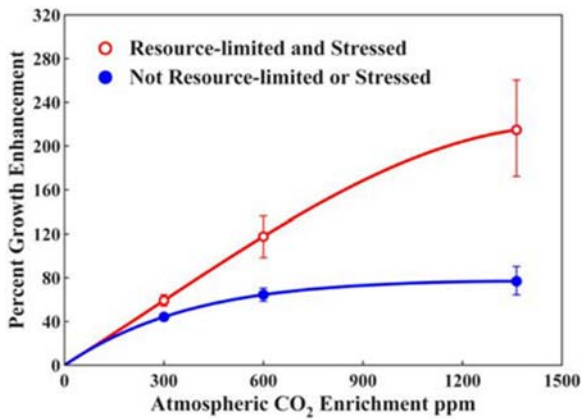


Fig. 26. “Summary data from 279 published experiments in which plants of all types were grown under paired stressed (open red circles) and unstressed (closed blue circles) conditions (Idso and Idso, 1974). There were 208, 50, and 21 sets at 300, 600, and an average of ~ 1350 ppm CO₂, respectively. The plant mixture in the 279 studies was slightly biased toward plant types that respond less to CO₂ fertilization than does the actual global mixture. Therefore, the figure underestimates the expected global response. CO₂ enrichment also allows plants to grow in drier regions, further increasing the response.” Figure and captions after Robinson et al. (2007). Reproduced with kind permission of the Association of American Physicians and Surgeon.

In this respect, according to the available estimates, Grace et al. (1995) report that the Amazonian rain forests increase the vegetation carbon by $\sim 1.1 \times 10^{-4} \text{ kg m}^{-2} \text{ year}^{-1} \text{ carbon}$, i.e. $\sim 5.5 \times 10^{-8} \text{ kg m}^{-2} \text{ year}^{-1} \text{ biomass}$. In addition, the response of trees to CO₂ fertilization is stronger than in other plants, even though - to some extent - all plants have a response. “The green revolution in agriculture has already benefitted from CO₂ fertilization, and benefits in the future will be even greater.” The effect also influences animal life in a proportional increase. This has been shown for 51 terrestrial ecosystems (McNaughton et al., 1989), and 22 aquatic ecosystems (Cyr and Face, 1993). In addition, Scheiner and Rey-Benayas (1994) carried out a study of 94 terrestrial ecosystems on all continents except Antarctica. They show that biodiversity, i.e. species richness, is correlated with productivity, i.e. with the total quantity of plant life per unit surface, more effectively than with any other parameter.

In fact, the life by both plants and animals requires atmospheric CO₂, as the unique source of carbon for protein, carbohydrate, fat, and other organic molecules. Plants are fertilized by atmospheric CO₂ from which they extract carbon, and animals get carbon from plants. The three most important substances for life survival are water, oxygen, and CO₂. With no atmospheric CO₂, life would not exist on Earth. This is the same as the “principle of preservation of life” by Ronov (1982), mentioned about Fig. 12.

These items are of interest for geophysicists and for agronomists. Laboratory research is in progress, and - from a macroscopic viewpoint - different man-made simulations result generally invasive, as the system is always affected by some unwanted perturbation. The best approach seems to be by comparing the growth and development of

vegetation on the borders of a mud lake, depending on the prevailing circulation of wind in that area (e.g. Pfanz et al., 2004). Vegetation is seen to increase its production with increasing availability of CO₂, and this can be used to investigate the role of CO₂ pollution. This phenomenon also reminds about the analogous study of coral location relative to the sites of exhalation of endogenous fluids (Gregori and Hovland, 2025 and references therein). In particular, marshes were found to be particularly important (Pelly, 2008), as wetlands are much effective for carbon storage. However, they also release CH₄, which - at equal concentration - is a greenhouse gas 23 times more potent than CO₂. (Pappas, 2016). The concern is therefore about whether the cooling effect of carbon storage prevails or not, compared to the global warming by CH₄ in wetlands. The present evidence shows that the greatest cooling occurs from saltwater marshes.

A USGS project captured “carbon by growing tules (a species of sedge also known as bulrushes) and cattails in wetlands created on abandoned farmland”. The result is that carbon was captured at an average of $\sim 3 \text{ kg m}^{-2} \text{ year}$ over the past 5 year. This datum should be compared with reforested agricultural land that captures carbon at a rate $\ll 0.1 \text{ kg m}^{-2} \text{ year}$. The mechanism is claimed to work as follows. Wetlands incorporate CO₂ into new plant growth. “When the plant material dies, near-constant water cover keeps oxygen out of the rich mud, slowing decomposition that would otherwise emit CO₂. Undisturbed wetlands are so effective at accreting carbon that their organic peat soils can be 20 m deep and 7000 – 10,000 years old ... The low-oxygen conditions that promote carbon storage also promote release of H₄ ...

Microbes prefer using oxygen to produce energy, but if they can't get oxygen, they can use other electron acceptors such as iron oxides, sulfate, and CO₂. When they use CO₂, they emit CH₄ ... Because the tiny traces of CH₄ gas from microbes are hard to measure, very few data are available on CH₄ releases from wetlands, ... The climate-warming potential of CH₄ very likely cancels out the climate-cooling potential of CO₂ storage for most North American freshwater wetlands. Because saltwater is high in sulfate, microbes in saltwater marshes don't have to use CO₂ as an electron acceptor, and therefore they produce negligible amounts of CH₄”

The conclusion is that “North American salt marshes sequester an average of $0.210 \text{ kg m}^{-2} \text{ year}$.” Moreover, “initial measurements suggest that these emissions may not cancel out the climate-cooling potential of the CO₂ storage.” Therefore, the target is to search for “ways to add nutrients to the wetlands and to make water levels fluctuate to maximize carbon storage while minimizing CH₄ emissions.”

In addition, also the formation of aerosols is controlled by the biosphere (Paulot et al., 2009), and aerosols can be condensation nuclei that favor atmospheric precipitations (see Gregori et al., 2025d). The biosphere also affects soil roughness, hence atmospheric circulation. Those authors claim that emissions of non-CH₄ hydrocarbon compounds to the atmosphere from the biosphere exceed those from anthropogenic activity. Upon considering a complicated

reaction with the hydroxyl radical OH they envisage an enormous flux injected into the atmosphere - nearly ~ 100 Terag carbon year⁻¹.

Also, the way of managing agriculture can play an important role. Dissolved organic carbon (DOC) exported from agricultural lands can affect watershed carbon budgets and aquatic ecosystem functions. Agricultural practices, and particularly enhanced drainage, can influence the amount of DOC exported from an area. This is a widespread and expanding feature in mid-western USA: buried tubes directly convey water out of soil.

Dalzell et al. (2011) compared fields that drained water at conventional rates (13 mm day^{-1}) with fields with intense drainage (51 mm day^{-1}). Intense drainage resulted to export 55% more DOC per year. The cause was twofold: increased water export and also increased DOC concentration. DOC export from drained fields depended strongly on precipitation rates. Thus, it varied considerably from year to year.

DOC concentration increased in stream networks in the drained watershed. In addition, they resulted to shift from microbial sources in farm field drainage to more terrestrially derived and higher molecular weight DOC at downstream sites. Mean DOC concentrations in drainage water were low, 1.62 and 1.87 mg l^{-1} for conventional and intense treatments. “*These results show that DOM [dissolved organic matter] compositional characteristics change with catchment area and that the relevant observation scale for DOM dynamics is likely to vary among watersheds. This study also demonstrates that land management practices can directly affect DOC via changes to water flow paths.*”

A synthesis of some major related items is given by Barr et al. (2014). “*What is the Coastal Carbon Cycle? [It] is the set of all biogeochemical processes and lateral aquatic fluxes of C that occurs within the coastal domain residing between the terrestrial system and the open ocean. The coastal C domain consists of subdomains of flooded or partially flooded ecosystems, such as tidal freshwater and brackish marshes, mangrove forests and salt marshes, seagrass meadows and the coastal ocean, and estuarine waters and tidal rivers, which form a broad, integrated ‘biogeochemical reactor’. Inputs of terrestrial C enter and are subsequently transformed within the biogeochemical reactor to other forms, including dissolved and particulate organic and inorganic C. Carbon that is not stored via burial in soils and sediments may exit the coastal ocean through CO_2 outgassing or export to the open ocean, with C import across these interfaces also possible.*”

They also briefly review this difficult topic. “*The coastal zone, despite occupying a small fraction of the Earth’s surface area, is an important component of the global carbon cycle. Coastal wetlands, including mangrove forests, tidal marshes, and seagrass meadows, compose a domain of large reservoirs of biomass and soil C (Fourqurean et al., 2012; Donato et al., 2011; Pendleton et al., 2012; Regnier et al., 2013; Bauer et al., 2013). These wetlands and their associated C reservoirs (2 – 25 petagrams C ; best estimate of 7 petagrams C)*

(Pendleton et al., 2012) provide numerous ecosystem services and serve as key links between land and ocean.

However, these coastal resources are in jeopardy from a variety of threats. Land-use change, nutrient pollution, urbanization, and climate change (e.g., sea-level rise) are affecting C cycling in the coastal zone, with the potential to alter exchanges of CO_2 with the atmosphere and therefore affect the longer-term stability and function of these and adjacent systems. While information regarding coastal C cycling is developing rapidly, variation within and among coastal ecosystems contributes to high uncertainties in component stocks and fluxes. For example, the issue of ‘missing C’ in mangrove forests persists (Maher et al., 2013). That is, the sum of C sinks, including C accumulation, soil respiration, burial, and export, is falling well short of net ecosystem productivity estimates ... “

The ocean is a major sink for CO_2 . Its acidification is increasing, i.e. its pH is decreasing. The chemistry of the ocean is fundamentally changed due to climate change, to the rise of atmospheric CO_2 , to the excess of nutrient inputs, and to pollution in several forms. The effects involve often the global scale. In addition, in some cases, the rates of change greatly exceed those in the historical and recent geological past. Major observed trends deal with a shift in the acid-base chemistry of seawater, with a reduction of subsurface oxygen both in coastal water and in the open ocean, and with a rise of coastal nitrogen levels and of a widespread increase in Hg and persistent organic pollutants (Doney, 2010).

Up to 30% of the C release from fossil-fuel combustion is absorbed by the ocean. Measurements of CO_2 and pH during the past two decades off the Hawai’ian shores have shown that the ocean is becoming more acid at a rate 30-100 times faster compared to the geological time scale. Other unwanted impacts deal (i) with limitation on precipitation of carbon carbonate, needed by several marine species for their shells and skeletons, and (ii) with hypoxia (the degradation of organic matter causes dangerous low levels of subsurface oxygen concentration, and it produces even more CO_2). In addition, the anthropic action has to be added to the natural seepage.

At present, a well-known great concern deals with anthropic CO_2 production. Asefi-Najafabady et al. (2014) (but, see also Anonymous, 2014I) developed a new system - which they call the Fossil Fuel Data Assimilation System (FFDAS) – to estimate CO_2 emissions from burning fossil fuels. “*The FFDAS uses information from satellite feeds, national fuel accounts and a new global database on power plants to create high-resolution planetary maps. These maps provide a scientific, independent assessment of the planet’s greenhouse gas emissions ... The research team combined information from space-based ‘nighttime lights’, a new population database, national statistics on fuel use, and a global database on power plants to create a CO_2 emissions map broken down by hour, year and region ... “ (Anonymous, 2014I).*

Refer to Asefi-Najafabady et al. (2014) for details on the computation method; $v2$ denotes their improved model, and $v1$ a previous model relying on as less complete database. Some results are shown in Figs 27 and 28. In

particular, Fig. 28 shows the relevant impact of a global economic crisis on the environment. That is, this economic crisis resulted to be an active experiment to test the anthropic effectiveness on the environment. Also, error bars

ought to be suitably indicated, and Fig. 29 shows the robustness of these maps. In any case, these maps rely on computed models.

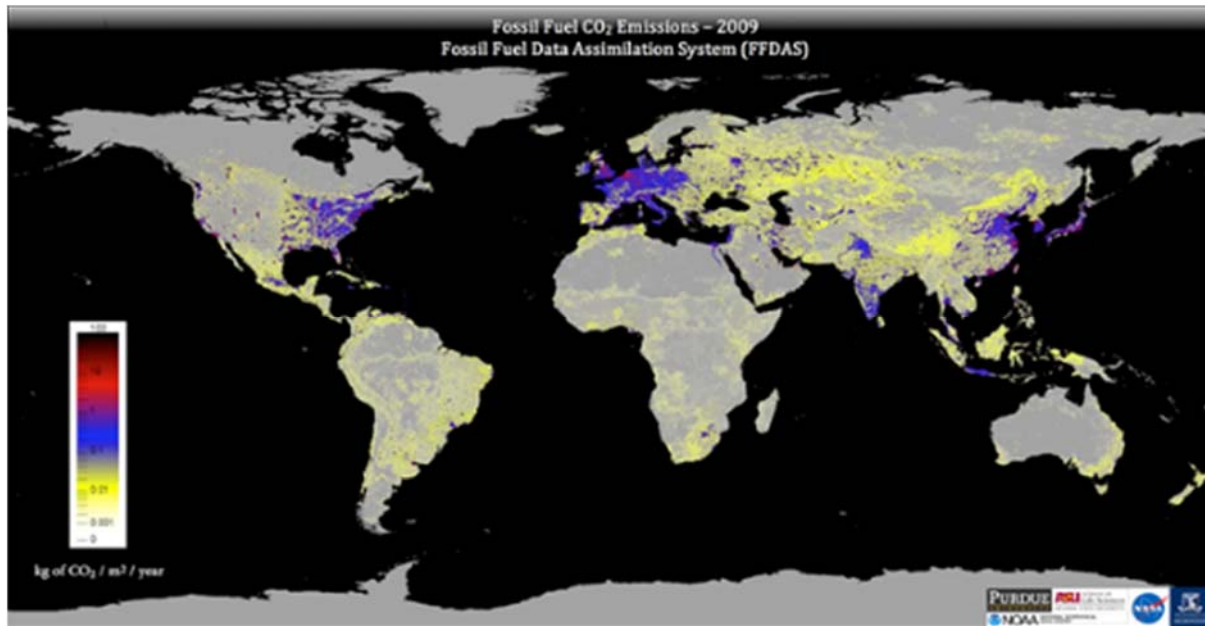


Fig. 27. “New map of 15 years of CO_2 emissions. Image credit: Gurney lab.” Scientific paper Asefi-Najafabady et al. (2014). Figure and captions after Anonymous (2014). With kind permission of Northern Arizona University and by NASA free copyright policy.

Ruddiman et al. (2016) investigated the role of humankind as a warming agent of the Earth through agriculture. The briefly summarize as follows their investigation.

“For more than a decade, scientists have argued about the warmth of the current interglaciation. Was the warmth of the preindustrial late Holocene natural in origin, the result of orbital changes that had not yet driven the system into a new glacial state? Or was it in considerable degree the result of humans intervening in the climate system through greenhouse gas emissions from early agriculture? Here we summarize new evidence that moves this debate forward by testing both hypotheses. By comparing late Holocene responses to those that occurred during previous interglaciations ... we assess whether the late Holocene responses look different (and thus anthropogenic) or similar (and thus natural). This comparison reveals anomalous (anthropogenic) signals ... we review palaeoecological and archaeological syntheses that provide ground truth evidence on early anthropogenic releases of greenhouse gases. The available data document large early anthropogenic emissions consistent with the anthropogenic ice core anomalies, but more information is needed to constrain their size. [Finally they] compare natural and anthropogenic interpretations of the $\delta^{13}C$ trend in ice core CO_2 .”

Summarizing, humankind certainly is an important driver in climate control, and CO_2 emissions are responsible for one anthropic action, even though it is very difficult to carry out any precise estimate of either the cause or of its effect. In addition, the natural spacetime variability

is poorly known of CO_2 soil emissions, also considering the global carbon cycle. In this respect, consider, however, the evidence provided by the NASA satellite OCO-2 that shows that anthropic CO_2 production is a tiny or almost negligible fraction of natural CO_2 exhalation from soil (see Mearns, 2015a and Gregori, 2020). There is urgent need to get a several-year monitoring data series in order to understand in better detail the actual role played by every different driver.

However, no other anthropic actions ought to be neglected, which might eventually originate some unwanted consequence that, maybe, could result to be worse than the “general” concern about CO_2 . On the other hand, every natural catastrophe is always a strict requirement of “climate” in order to ensure some balance aimed to seek natural equilibrium. The target of humankind is therefore to respect the needs of nature, and to avoid that people are located at the wrong site at some unsuitable instant of time. In any case, the worst anthropic pollution is caused by the severely destructive weapons, by which every military “victory” is a Pyrrhic victory. Since we cannot ban wars, *heavily destructive weapons (not only nuclear weapons) should be severely banned* (Gregori and Leybourne, 2025k).

Concerning CO_2 it is important to assess the evolution of CO_2 concentration in the environment on the geological time scale, in order to envisage trends in the CO_2 production of natural origin. Ocean sediments contain relevant information. The $\delta^{11}B$ composition appears to be a very effective proxy datum of past seawater pH . Hence, indirectly, the past CO_2 atmospheric concentration can be

inferred by measuring $\delta^{11}B$ inside sediments.

The following information mainly relies on Hönisch (2007).¹⁰

Other control factors had, however, to be suitably understood before using this proxy datum with sufficient confidence. Hönisch (2007) carried out laboratory and sediment experiments on the resulting boron isotopic composition of planktic foraminifers. Thus, a careful selection of the samples was found to be important. Finally they got “convincing evidence that surface seawater pH reflects variations in atmospheric P_{CO_2} across late Pleistocene glacial cycles ... A remarkable match between boron isotope estimates and the Vostok ice core bears this out and confirms that glacial surface ocean pH was ~ 0.2 units higher compared to interglacials.”

This is shown in Fig. 30.¹¹ Note the clear and remarkable sawtooth trend with tooth duration of different size, from main cycles, through lesser subcycle during every cycle. “... It has been suggested the ‘Mid-Pleistocene Transition’ (MPT) may be due to global cooling, possibly caused by a long-term decrease in atmospheric CO_2 concentrations. Direct evidence for such a decrease, however, has not yet been demonstrated ... Our data thus

do not support the hypothesis that a longterm P_{CO_2} decrease was the primary driver of the transition.”

Hönisch et al. (2009) report additional results (plot not here shown) that envisage that during the Mid-Pleistocene the leading period of Pleistocene glacial cycles varied from $\sim 40,000$ years to $\sim 100,000$ years, even though “for as yet unknown reasons.” According to the rationale of the present study, this depends on the timing of the release of endogenous energy that determines the shape and duration of one sawtooth.

Hönisch et al. (2009) plot the estimates of atmospheric P_{CO_2} from marine proxies, during the last 2.1 Ma, based on records at ODP site 668B (eastern equatorial Atlantic). They plot several proxies, and for details see the original paper. They comment that their estimates appear consistent with a close relation between global climate and atmospheric CO_2 concentration. However, no gradual decrease in interglacial P_{CO_2} is observed, and this fact does not support the suggestion that the main cause of the climate transition was the cause of a long-term drawdown of atmospheric CO_2 . In fact, according to the interpretation which is here given, the leading driver is the timing of the endogenous energy release, while CO_2 concentration is just a consequence, rather than a primary driver.

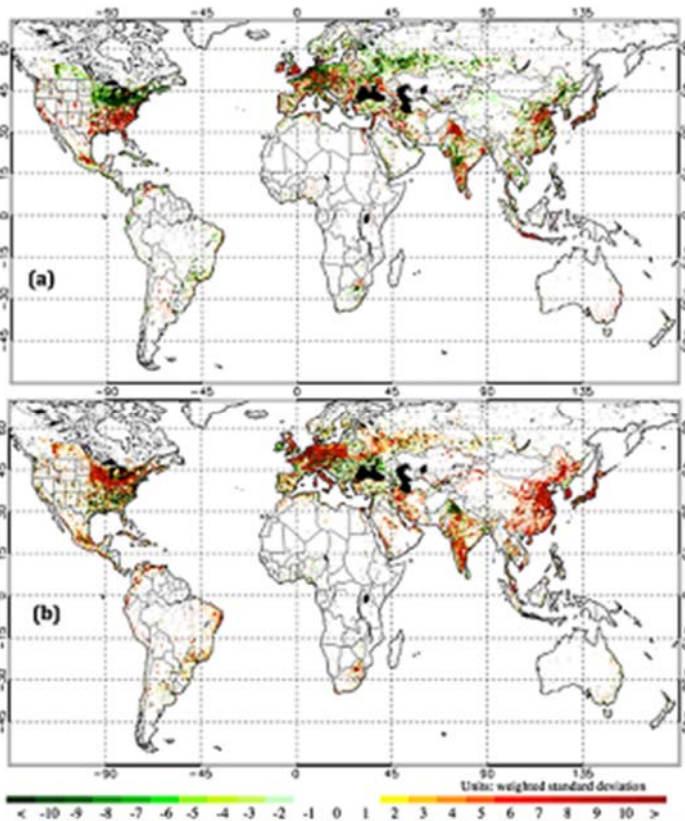


Fig. 28. “Annual FFDAS v2 fossil fuel CO_2 anomalies for 2 years before and after the Global Financial Crisis. Years (a) 2006 and (b) 2010. Units: weighted standard deviation ... “ Figure and captions after Asefi-Najafabady et al. (2014). AGU copyright free policy.

¹⁰ Bärbel Hönisch is of the school of Wallace Smith Broecker (1931-).

¹¹ p_{CO_2} means partial pressure of CO_2 . This symbol is frequent in the medical literature. P_{CO_2} is generally reported with the same meaning. To our knowledge, the distinction between P_{CO_2} and p_{CO_2} is not specified. Hönisch et al. (2008) use P_{CO_2} for ocean water and they

specify that it is an “aqueous” datum. They use p_{CO_2} for the atmosphere datum, while in other papers this is used also for ice core data. However, other authors use equivalent symbols, as it is here reported *passim*. Sometimes, some authors specify some different meaning, but no general agreement seems to exist. We use P_{CO_2} .

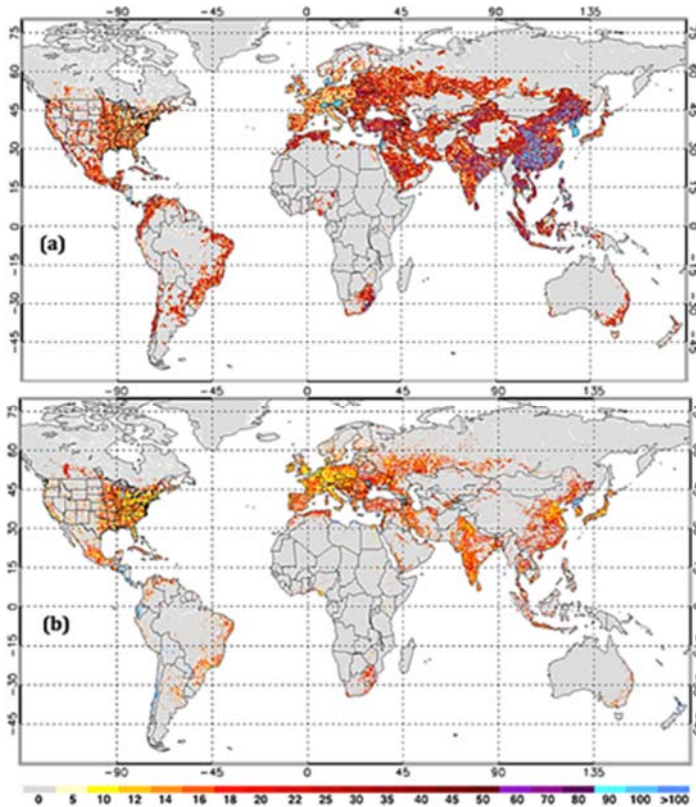


Fig. 29. “Posterior uncertainties associated with the total fossil fuel CO₂ emissions (expressed as percentage standard deviation). (a) FFDAS v1 at 0.25° for 2002. (b) FFDAS v2 at 0.1° for 2003. Year 2003 was used for FFDAS v2 results due to the fact that 2002 was an interpolated nighttime lights year.” Figure and captions after Asefi-Najafabady et al. (2014). AGU copyright free policy.

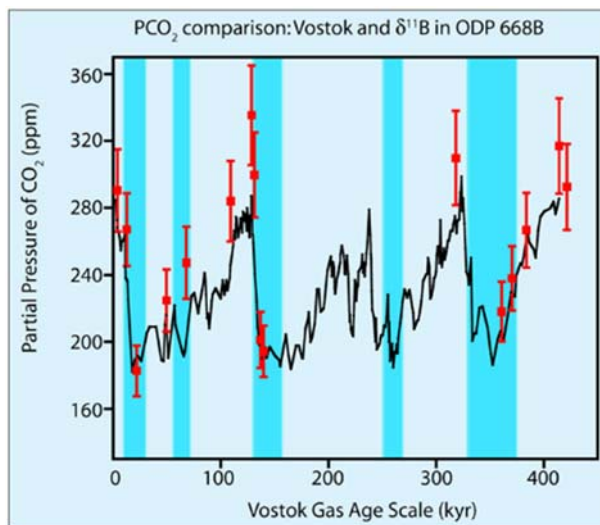


Fig. 30. Estimated aqueous P_{CO_2} in ocean water from $\delta^{11}B$ in planktic foraminifera (red squares), superposed on the Vostok ice core record (black line) for atmospheric P_{CO_2} . Blue bars indicate glacial intervals. After Hönlisch et al. (2008), modified from Hönlisch and Hemming (2005). Reproduced with kind permission of *Earth and Planetary Science Letters* (“Open Access” CC BY-4).

van de Wa et al. (2009), however, object their conclusion. They stress that Hönlisch et al. (2009) rely on the equilibrium sensitivity of present-day climate with respect to doubling CO₂ concentrations, and on the difference of temperature between the Last Glacial Maximum and preindustrial climate. Conversely, van de Wa et al. (2009) “believe that even a seemingly small decrease of 30 ppmv might have been sufficient to cause

the transition from ~ 40 ka to ~ 100 ka glacials.” They rely on the computation of the sensitivity based on the temperature derived by an ice sheet model constrained by marine benthic $\delta^{18}O$, which implicitly contains all (albedo) feedbacks. They find a sensitivity of ~ 0.15 K for a change of 1 ppmv in CO₂. Thus, during the *MPT*, they estimate in the *NH* (Northern Hemisphere) a long-term change of only ~ 4.5 °C. That is, a CO₂ change of 30 ppmv was sufficient to determine the observed climate change during the *MPT*. That is, the transient climate sensitivity of an Earth covered by conspicuous amounts of ice sheets seems to be much higher than what can be estimated by the current climate. The presumable cause is the more intense albedo feedback.

In this same respect, Pongratz et al. (2011) investigated the mitigation potential of reforestation. “Anthropogenic land cover change (ALCC) influences global mean temperatures via counteracting effects: CO₂ emissions contribute to global warming, while biogeophysical effects, in particular the increase in surface albedo, often impose a cooling influence. Previous studies of idealized, large-scale deforestation found that albedo cooling dominates over CO₂ warming in boreal regions, indicating that boreal reforestation is not an effective mitigation tool. Here we show the importance of past land use decisions in influencing the mitigation potential of reforestation on these lands.

In our simulations, CO₂ warming dominates over albedo cooling because past land use decisions resulted in the use of the most productive land with larger carbon stocks and less snow than on average. As a result past land use decisions extended CO₂ dominance to most agriculturally important regions in the world, suggesting

that in most places reversion of past land cover change could contribute to climate change mitigation. While the relative magnitude of CO₂ and albedo effects remains uncertain, the historical land use pattern is found to be biased towards stronger CO₂ and weaker albedo effects as compared to idealized large-scale deforestation.”

Much more generally, the crucial and extremely multifaceted role of the biosphere is the object of an ever increasing number of investigations. The number of papers on these items is rapidly expanding, and it is nonsensical to attempt here to give even a partial list. As already stressed, a basic limitation of the largest number of present studies - similarly to every standard discussion that relies only on geophysics and geochemistry - is an insufficient discussion of the role of the biosphere. At present, the state-of-the-art is certainly far from any kind of a possible attempt for a synthesis. A long time, and hard thinking, are still needed in order to fill such a gap. These items show the extreme difficulty of all studies that deal with the global carbon cycle, and with the role of the associated processes and mechanisms like climate drivers. Owing to brevity requirements, only a few more or less randomly selected studies are here mentioned.

Concerning the active role of vegetation on climate, another certainly impressive result was found by Professor Joseph Otterman (1925-). Otterman et al. (1990) showed that the average October rainfall in southern Israel steeply increased during the last quarter of the century. They correlated this effect with a difference in land usage. Indeed, a newly posed fence had been located at the border between Israel and Egypt across the Sinai Peninsula. Therefore, the goat herds no more could pasture on the Israel side, and some much elementary organisms (algæ, fungi, etc.) could flourish on the stones of that semi-arid area. Thus, an increased vegetation cover - which is dormant at the end of the dry summer season - decreased the typical high albedo of soil. This affected the surface radiation balance and modified the surface heat fluxes and the conditions for stability of the planetary boundary layer. A weaker inversion capping finally favored the penetration of rain-bearing convective clouds. These conditions are likely to occur in this area mainly during October.

Otterman et al. (1990) describe their findings as follows. *“The October rains (at the onset of the rainy season that extends to April) in southern Israel have steeply increased in the last quarter century relative to the prior two decades. A less pronounced, but appreciable, increase is noted for the rest of the rainy season. This apparent reversal of desertification is attributed here to land use changes. Afforestation, increased cultivation and limitations on grazing after the establishment of the State of Israel resulted in an increased vegetation cover over the inherently high-albedo soils in this region (an area of ~ 10⁴ km²). The changes are shown in a July 1985 Landsat image of the area.*

The increase in precipitation is specifically attributed to intensification of the dynamical processes of convection

and advection resulting from plant-induced enhancement of the day time sensible heat flux from the generally dry surface. This enhancement results both from the reduced surface albedo and the reduced soil heat flux (reduced day-to-night heat storage in the soil) in October when insolation is strong. Stronger daytime convection [i.e. stronger Cowling dynamo, hence more abundant precipitation] can lead to penetration of the inversions capping the planetary boundary layer (which are weaker in October than in summer) while strengthened advection (sea breeze) can provide moist air from the warm Mediterranean Sea. This suggested mechanism is consistent with previous studies showing that the autumn rains in southern Israel exhibit convective mesoscale characteristics [hence, associated to intense Cowling dynamo and increased precipitation] and occur predominantly in the daytime. However, other causes, such as a shift in the synoptic-scale circulation, cannot be ruled out at this stage.”

Consistently with this explanation, according to the viewpoint of the whole present discussion on air-earth currents, a few additional details can be considered, aimed to justify, in general, why some very elementary form of life can be capable of “attracting” rain-bearing clouds, thus improving life survival conditions. In fact, a few different drivers are to be taken into account.

One is the aforementioned Otterman’s “*intensification of the dynamical processes of convection and advection resulting from plant-induced enhancement of the day time sensible heat flux from the generally dry surface*”, which favors a strengthened sea breeze thus supplying moist air.

Another driver deals with an influence of the vegetation cover on ion generation by friction between air and soil. A very thin - even almost monomolecular - vegetation cover of soil can be crucial in changing “friction electricity” phenomena between soil and blowing air, leading to a substantial change of ion composition in air.¹²

Cosmic rays are another relevant cause for ionization (the so-called “Svensmark effect”, and a conspicuous literature is available).

Another driver is therefore the Cowling dynamo, which is always associated with every convective pattern inside an ionized medium. Then, ions are the primary starters for water condensation, while they are moved by the electric field through the water molecules which are neutral (Gregori et al., 2025d). Thus, a change of ion composition caused by a tiny vegetation cover can eventually result to be crucial in order to determine water precipitation.

Whatever the relative relevance of either one driver or the other, this statistically significant increase of the average October rainfall in southern Israel was also explained by means of other hypotheses. Several different models were computed. Alpert and Mandel (1986) appealed to a decrease both of wind variability and of the daily temperature amplitudes. They associated this phenomenon

¹² Concerning the role of the biosphere in the control of the “friction interaction” between air and soil, refer also the

investigations by Biello (2008), Christner et al. (2008) and Schiermeier (2008a).

to the operation of the *National Water Carrier* started in 1964.¹³

Branston and Schickendanz (1984) considered the influence of irrigation, and Segal et al. (1988) envisaged changes in atmospheric circulation when comparing irrigated and non-irrigated areas, or between the sea and nearby non-irrigated areas. They afforded to show details up to ~ 3 km size. This effect ought to be explained by means of temperature gradients.

Note that in this - like in every other - explanation the role can be considered of all aforementioned primary drivers. The difference between different interpretations relies rather on the way every driver is supposed to become operative.

Also other mechanisms were proposed (see details on Ben-Gai et al., 1993), including roughness increase deriving from anthropic action, or large scale or synoptic variations of pressure, or SST (sea surface temperature), or low tropospheric temperatures. This problem was the object of several subsequent investigations. Let us mention a few of them.

Ben-Gai et al. (1993, 1998) made a careful analysis of rainfall data of this entire area since the 1930s. They found statistically significant changes in the spatial rainfall distribution patterns in the southern, northern and central parts of the country. Considerable changes were found in October and November, at the beginning of the rainfall season, and an appreciable change in March, at the end of the rainfall season. In contrast, less clear inferences resulted from the historical series of temperature (Ben-Gai et al., 1999). The daily maximum and minimum temperatures during the second half of the 20th century revealed significant trends. Both the daily maximum and minimum temperature decreased during the cool season, and increased during the warm season. Conversely, they found almost no apparent annual trend, as the changes in winter and summer showed an opposite tendency.

The focus on the albedo change was the object of Ben-Gai et al. (1998a), who measured soil reflection by means of an airborne pyranometer. They showed large differences between the cultivated areas in southern Israel (as low as ~ 0.15), and the adjacent arid regions (up to ~ 0.35). In addition, a comparison between recent albedo map and the historical reconstructed maps since the 1930s showed that temporal changes in the surface albedo pattern occurred during the last decades.

Ben-Gai et al. (2001) also analyzed a long-term record (1964-1995) of radiosonde data from the central part of the south-east Mediterranean coastal plain. The target was the detection of possible temporal trends in moisture content and instability of the atmospheric boundary layer. They evidenced a clearly defined, statistically significant, increasing trend in the moisture content, mainly during summer in an area that had experienced drastic changes in land usage, urbanization, irrigation, forestation, etc.

All these findings are in agreement with the Otterman guess. However, the phenomenon cannot be simply reckoned only to local phenomena. Ben-Gai et al. (2001a) investigated the teleconnections - always during the second half of the 20th century - that are associated with changing patterns of temperature and pressure anomalies over Israel. They found relatively high - statistically significant - correlation coefficients (~ 0.8 – 0.9) between the North Atlantic Oscillation (*NAO*) index anomalies (a guessed mechanism is shown in Fig. 31) and either the smoothed (5 year running mean) cool season temperature or the surface pressure anomalies in Israel. The correlation was also investigated of the *NAO* index anomalies with a few other meteorological parameters, finding a relatively high positive correlation (~ 0.8). Therefore, the entire phenomenon has to be understood in the framework of planetary atmospheric circulation and radiation balance.

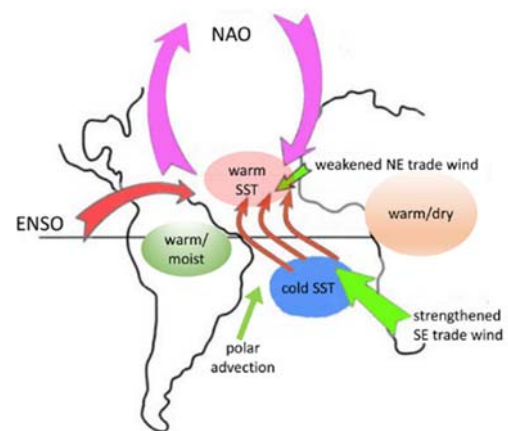


Fig. 31. “Map showing the possible remote forcing of Atlantic SST by El Niño events and the interaction with Mobile Polar Fronts, adapted from Martin et al. (1997) and Marshall et al. (2001).” Captions after Marchant and Hooghiemstra (2004). The figure has been redrawn by improving a figure after Marshall et al. (2001), reproduced with kind permission of *International Journal of Climatology*. The warm SST region is associated to low sea-level pressure, and the cold SST region to high sea-level pressure.

Note that this is a phenomenon other than the aforementioned Otterman’s et al. evidence dealing with a tiny vegetation layer. In fact, the *NAO* index refers to the general dynamics of atmospheric circulation that eventually also influence the convection pattern over Israel. The effect of vegetation is, rather, an amplification of the effects that ought to occur independently and depending on atmospheric dynamics alone.

A conspicuous amount of investigations is reported dealing with modeling of various features of Earth’s surface and their respective different influence of the atmosphere. These preliminary studies were fundamental for a correct interpretation of remote sensing measurements. Professor Joseph Otterman published several papers. Let us only

and it consists of giant pipes, open canals, tunnels, reservoirs, and large pumping stations.

¹³ The *National Water Carrier* of Israel is a large water project with the purpose to transfer water from the Sea of Galilee in the north of the country to the highly populated center and arid south. Its length is ~ 130 km

recall, like examples, only his more recent studies. The thermal-IR (longwave) emission from a vegetated terrain is generally anisotropic, i.e., the emission temperature varies with the view direction, and this depends on plant density and canopy architecture (Otterman et al., 1995). This can raise conspicuous errors. Also leaf orientation is a crucial factor (Otterman and Brakke, 1991; Otterman et al., 1992, 1995a), but also the vegetation density, and its vertical extension can be an important control factor, as it significantly increases the coefficient of turbulent heat transfer from the surface (Otterman and Chou, 1992).

In addition to flora, also fauna is important for climate control (e.g. kangaroo rats in southeastern Arizona; see Brown and Heske, 1990), and humankind is a particular component of “fauna”. The anthropic impact on weather and climate has been systematically treated by Cotton and Pielke (1995). The investigation can be carried out “bottom-up” at ground, but over limited areas. For instance, Douglas et al. (2006) investigated the impact on land-atmosphere of agricultural activity in India. They compared vapor fluxes (estimated evaporation and transpiration) from a pre-agricultural and from a contemporary land cover. They found conspicuous increases in mean annual vapor fluxes. Two thirds appear to be attributed to irrigation. “*The largest increases occurred where both cropland and irrigated lands were the predominant contemporary land uses.*”

The correct impact of vegetation on albedo still needs to be assessed in its varied forms and consequent Earth’s surface morphology. Zheng et al. (2014) report a careful investigation where they compare a desert area with some other regions with different kind of semi-arid land. They carried out field experiments “*on ground surface spectral broadband solar radiation (SR) and corresponding albedo ... at three man-made sites at Gobi desert and bare loess zones during three different intensive observational periods (IOP) from 2010 to 2013 in Gansu Province, respectively. The continuous and high temporal resolution records of ground surface SR are presented, including global (GR), ultraviolet (UV), visible (VIS), and near-IR radiation (NIR). The corresponding albedos are analyzed over three typical non-vegetated underlying surfaces in arid and semi-arid and semi-humid regions of northwestern China ...*”

The results show the variation trends of UV, VIS and NIR are coincident with the GR, and the irradiances are gradually decreasing throughout the IOP at each site; the energy ratios of VIS/GR are all approximately 40.2%, and the ratios of NIR/GR are all approximately 54.4% at the Gobi, desert and bare loess zones; the averaged albedos of the soil for VIS are 0.231, 0.211 and 0.142, for the NIR are 0.266, 0.252 and 0.255 over the Gobi, desert and bare loess land surfaces, respectively. The energy ratios of VIS/GR and NIR/GR are not 50% as prescribed for all of the soil color classes in most of land surface models (LSMs). The observational soil albedo values for NIR are not twice to that of the VIS as predicted in some LSMs for the underlying surface at the three sites. GR albedo is

determined by the energy ratios of SR/GR and SR albedos.”

A different investigation - that in some respect is more effective from the planetary perspective - can be carried out by satellite remote sensing. The presently available satellite data mostly rely on the *Advanced Spaceborne Thermal Emission and Reflection Radiometer (ASTER)* and the *Moderate Resolution Imaging Spectroradiometer (MODIS)* aboard the *NASA Earth Observing System (EOS) TERRA* satellite, which was launched in 1999. Ogawa and Schmugge (2004) estimated a broadband window emissivity from *ASTER* and *MODIS* data. They investigated several definitions of the broadband emissivity: the 8 – 13.5 μm integrated emissivity is the best index for the net longwave radiation under clear-sky conditions. Then, they searched for a method to estimate broadband emissivity at the continental scale. They also used emissivity’s measured in the laboratory. A range 0.85 – 0.96 was found of the broadband emissivity for desert area.

Lim et al. (2005) investigated, by means of the *MODIS* database, the sensitivity of surface climate change to land types. They restricted their analysis to the *NH*. Their leading idea was that the large-scale climate changes are due to greenhouse gases and atmospheric circulation, while regional surface processes associated with land types are of local character. They found that:

- “warming over barren areas is larger than most other land types;
- urban areas show large warming second only to barren areas;
- croplands with agricultural activity show a larger warming than natural broadleaf forests.

The overall assessment indicates surface warming is larger for areas that are barren, anthropogenically developed, or covered with needle-leaf forests. [That is, leaf vegetation is an important agent.]

Ogawa et al. (2008) investigated the spatial and temporal variations of surface emissivity, and specifically, the broadband emissivity (*BBE*; 8 – 13.5 μm). They considered several arid regions, and plotted the maps of 8 – 9 μm band emissivity of sparsely or non-vegetated desert areas. They found emissivity values between 0.66 – 0.96 caused by to the low emissivity at these wavelengths of quartz-rich sands. Therefore, they claim that the range of *BBE* is between 0.86 – 0.96.

However, some most relevant results seem to be reported by Jin and Dickinson (2010), who investigated the relations between surface skin temperature (T_{skin}), obtained by satellite, and surface air temperature (T_{air}) measured at ground, during the period 2001-2006. For T_{skin} they used *MODIS* observations and studied the diurnal, seasonal, and interannual variations of monthly skin temperature at 0.050 latitude/longitude grid over global land surface. For the T_{air} database they used the *Global Historical Climatological Network (GHCN)*.¹⁴

¹⁴ <http://www.ncdc.noaa.gov/temp-and-precip/ghcn-gridded-temp.html>, and Peterson et al. (1997, 1998), or Free et al. (2004), created from observations at 2 m

above ground, at the observation sites of the *World Meteorological Organization (WMO)*.

Then, they also combined these measurements with other MODIS based variables. They found that skin temperature variations appear “to be closely related to vegetation cover, albedo, and soil moisture, but differing from surface 2 m T_{air} in terms of both physical meaning and magnitude.” They distinguished between 16 different classes of Earth’s surface cover. Figs 32 and 33 show the total temperature variation during the 6 year period spanned by observations.

Fig. 33 relies on an observational database that, compared to the satellite monitoring of Fig. 32, is much more sparse and incomplete. However, the details of Fig. 33 are consistent with the satellite information. Hence, let us focus on Fig. 32 alone. Concerning the physical interpretation, the increase of endogenous heat released underneath the whole Arctic cap is most evident feature,

consistently with other inferences related to the tetrahedron vertex under the North Pole (Gregori and Leybourne, 2021). The polar regions are essentially poorly affected by anthropic heating. Hence, there is no doubt about the leading driver, i.e. by natural soil exhalation.

In contrast, a substantial increase is observed in USA and Canada. Maybe, one should correlate this map with the interannual variation of the total energy consumption, i.e. mean consumption per inhabitant times the local population density. In this respect, for comparison purpose, note the absence of any analogous effect in western Europe - except at most some small isolated “heat islands” that are probably associated with the comparatively more industrialized areas.

MODIS Terra Day time Tskin Diff (2006.01–2001.01) (K)

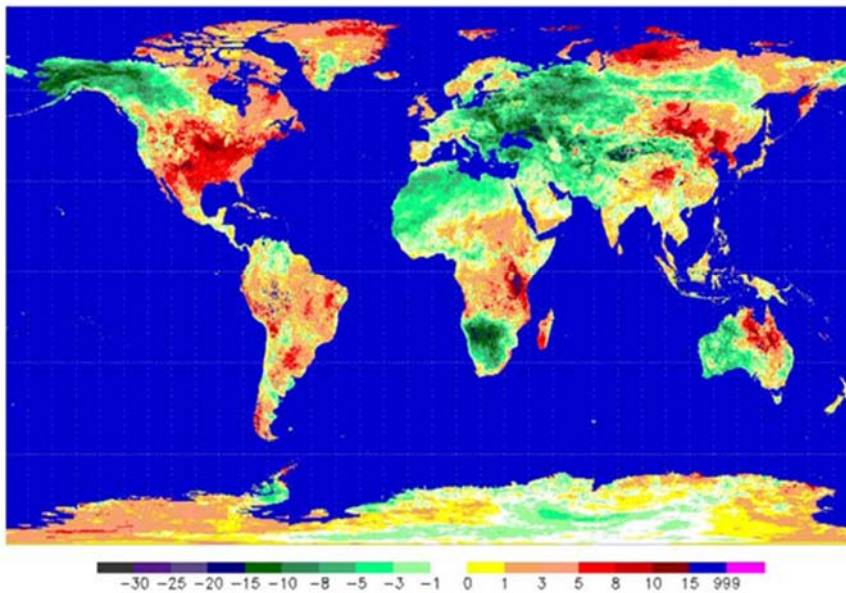


Fig. 32. Inter-annual variability for skin temperature T_{skin} , at 0.05° latitude/longitude resolution. After Jin and Dickinson (2010). Kind permission granted through © IOP Publishing Ltd., CC BY-NC-SA, and authors permission.

GHCN Tair Anomalies Diff (2006.01–2001.01) (C)

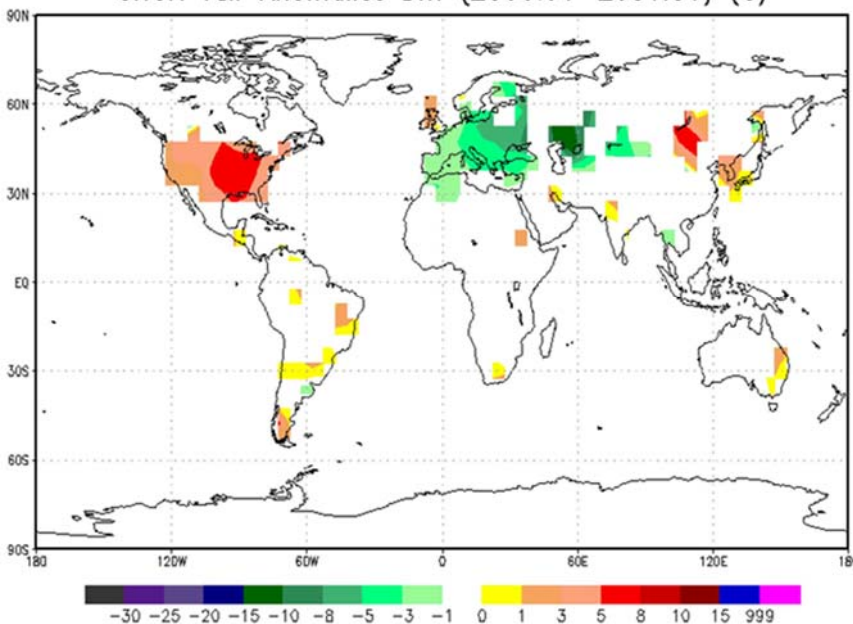


Fig. 33. Inter-annual variability for 2 m surface air temperature T_{air} , based on monthly mean from GHCN. After Jin and Dickinson (2010). Kind permission granted through © IOP Publishing Ltd., CC BY-NC-SA, and authors permission.

Also note the Himalaya region, which is well-known to be characterized by a large geothermal flux originated (i) by friction due to geodynamic overthrust, and also (ii) by Joule heat on the ALB (asthenosphere-lithosphere boundary) that is amplified by the telluric currents channeled from other regions on the planetary scale (see Fig. 1 of Gregori et al., 2025q). A different concern deals with northeastern China, Korea, and with their respective bordering regions in southern Siberia. A possible explanation can be in terms of friction heat. In fact, a wildfire “flash” is located in this region (Gregori and Leybourne, 2025i), and it ought to be associated with the region where the violent earthquakes are triggered that stroke the Beijing area in the past.

A different mechanism has to be considered dealing with the observed increase in Kenya/Tanzania, and more generally through whole central Africa, including Madagascar. This is very likely to be the effect of the “plume” of the quatrefoil pattern (see Gregori et al., 2025a, Gregori and Leybourne, 2021), i.e. a phenomenon roughly correlated with the DUPAL anomaly (see Gregori et al., 2025a, Appendix) of the isotopic chemism of basalt. In fact, in this respect, a significant comparison can be made with the seasonal maps of atmospheric CO₂ concentration monitored by the satellite OCO-2 (see Mearns, 2015a; Gregori, 2020).

The maximum in Africa is a very clear evidence, which is roughly correlated with the DUPAL anomaly, while everywhere on the planetary scale the role of anthropic CO₂ is surprisingly found to be secondary, or maybe even almost negligible. That is, some regions in Fig. 32 can be associated with some anthropic and more or less extended “heat islands”. Conversely, other regions, such as the

northern polar cap, or central Africa or also Brazil (where the SAA could be an effective primary cause), clearly seem to be explained only in terms of endogenous origin. In addition, note that the large temperature in USA and Canada in Fig. 32 - temperature that, as mentioned above, seems likely to be of anthropic origin - has no equivalent in the OCO-2 seasonal maps, except maybe only in the winter map. This means that humankind certainly is a relevant source of heat injected into the atmosphere, although this temperature increase is not related to the anthropic CO₂ production. That is, the CO₂ concentration is increasing worldwide, while the human contribution is a negligible fraction of the effect. However, the increase of some mean global temperature is originated by several drivers, including anthropic activity. On the other hand, the anthropic CO₂ plays a definitely secondary role in this whole phenomenon.

A similar concern, referring to the relative maxima in Fig. 32, deals with several locations through South America or also with northeastern Australia. No certain inference, however, can be assessed as long as no crustal-stress monitoring is available through these huge regions.

As far as Antarctica is concerned, the environment is substantially complicated (i) by the role of glaciers, (ii) by the amplification caused by changes of albedo, and (iii) by the warming originated by changes of the temperature of ocean water. Hence, it seems impossible to interpret Fig. 32 concerning Antarctica, until additional climatic and/or crustal parameters are available.

Figs 34 and 35 show intriguing relations between T_{skin} and albedo, either like global average, or across Greenland, along 70°N.

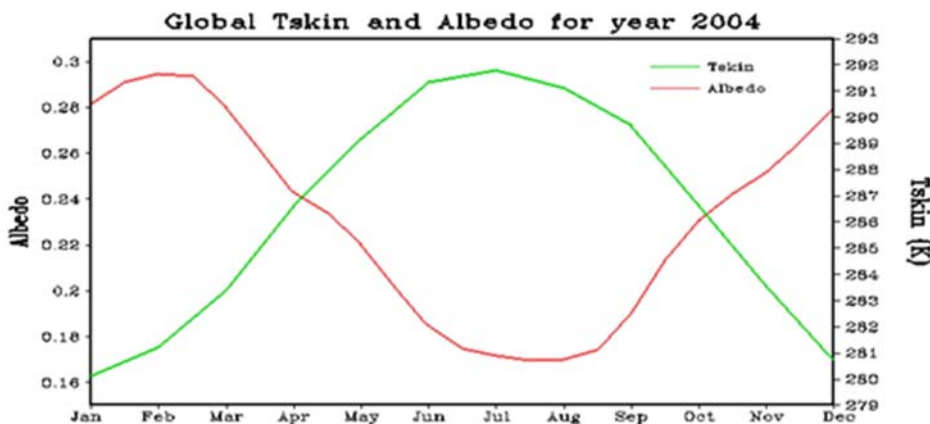


Fig. 34. Global averaged T_{skin} vs. surface albedo for months of the year 2004. The T_{skin} and albedo observations are from MODIS TERRA measurements. After Jin and Dickinson (2010). Kind permission granted through © IOP Publishing Ltd., CC BY-NC-SA, and authors permission.

Remote sensing by satellite of these key climatic features is the object of a great effort and rapidly evolving improvement. It is impossible to mention here all most recent achievements. Several movies, with one frame every month and every one dealing with one satellite-monitored parameter, are being provided by the Earth Observatory by NASA, and maybe also by some other institutions, and they will certainly provide intriguing proofs dealing with the climatic drivers that have been here envisaged.

The purpose of the present study is to give no exhaustive review of the most recent achievements, as this would be

impossible. Rather, the scope is to focus on the basic processes and mechanisms, and on the way they can be eventually monitored at a level of some given spatial and temporal detail. That is, the present discussion aims to be some kind of “tutorial” reminder for the reader who wants to understand the ever increasing and large amount of available literature on these challenging topics.

Summarizing - independent of eventual additional suggested primary drivers - perhaps no final conclusive assessment is yet available. Several effects altogether contribute to drive rainfall. However, as far as the present

study is concerned, the importance is evident of the role of the biosphere in controlling the energy balance of the air-soil interaction, and its implication on air-earth currents and on water condensation and precipitation. An exhaustive and satisfactory understanding is perhaps beyond human reach. No model that relies on one effect alone - i.e. suited for fitting the requirements for “simplicity” by human mind - can give a full explanation of all observations. In any case, treating this problem by means of physics and chemistry alone, by neglecting the leading role of the biosphere, appears to be definitely unrealistic.

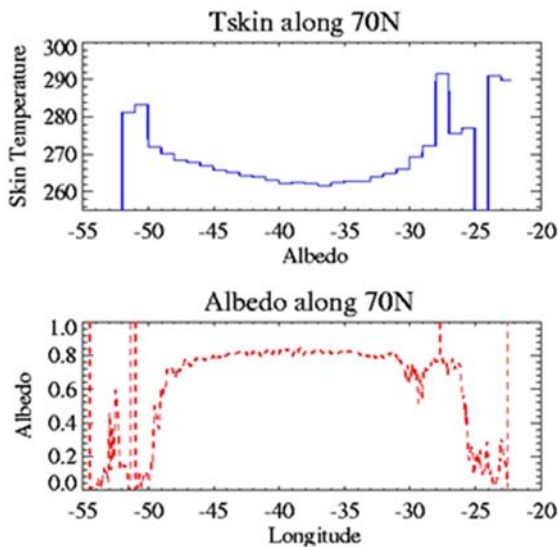


Fig. 35. MODIS albedo and skin temperature T_{skin} for Greenland along $70^{\circ}N$. After Jin and Dickinson (2010). Kind permission granted through © IOP Publishing Ltd., CC BY-NCSA, and authors permission.

A closely related item is the concern about the climatic impact of dams. They are of concern also when their associated hazard is considered, which can be even enhanced by their climatic impact. Hossain et al. (2009) briefly summarize the state-of-the art. The following information is borrowed after their paper. The *International Commission on Large Dams (ICLD)* defines “large” a dam when it is $> 15\text{ m}$ tall. In USA there are $\sim 75,000$ dams. According to the *World Commission on Dams (WCD)*, since the 1930s at least $\sim 45,000$ dams were built worldwide. Dams favor irrigation possibilities, and also a denser urbanization in downstream regions, due to the reduced flood hazard, and to increased availability of hydropower. Hence, they cause changes in the large-scale land usage and land cover (*LULC*). Since they modify the vertical profile of temperature and humidity, they are believed to enhance atmospheric instability, hence air-earth currents and rainfall. In fact, consider the associated effect of the Cowling dynamo. The atmospheric instability “is usually characterized by convective available potential energy (CAPE). The significant changes in LULC that large dams invariably trigger, combined with the greater availability of atmospheric moisture through evaporation from open-water bodies and irrigated land, can result in a similar change in land use surface fluxes of heat and moisture. Thus, under certain circumstances, dams and

reservoirs can be considered as ‘enhancers’ of CAPE, which in turn may induce more precipitation.” Hossain et al. (2009) envisage that the effect is expected mostly on extreme precipitations, with consequent implications for dam security.

Let us only report a few flashes from their discussion. “Eltahir (1989) analyzed data on swamps in southern Sudan to demonstrate that a wet year usually favored increased precipitation the following year through increased evaporation from the expanded open-water surfaces. Conversely, Pielke et al. (1999) have shown that the draining of swamps can result in decreased precipitation through a negative feedback mechanism ...”

“A word of caution: atmospheric model-based studies of precipitation recycling remain somewhat controversial (Ruiz-Barradas and Nigam, 2005). [In fact, the role of the Cowling dynamo as a primary cause of precipitation is an original mechanisms proposed by the present study.] Further, other factors may be involved, such as global climate change, effects of aerosols and urbanization, etc. However, not enough is known about these other factors or the extent to which they influence the patterns observed in the vicinity of dams. Thus, more research is needed on all fronts, including dam induced extreme precipitation.”

The statement that “a wet year usually favored increased precipitation the following year” reminds about the long-range climatic forecast by the Tang’s school (see Gregori et al., 2025h). That is, a spacetime change of geothermal flux through a given region, combined with water availability for an eventual increased evaporation, can - altogether with air dynamics and Cowling dynamo - contribute to originate a final significant change of water condensation and precipitation. That is, a greater amount of water (or vegetation) on the Earth’s surface seems very likely to increase the probability of precipitation. In the final analysis, this occurs through alteration of the convective pattern that determines a more effective role of the Cowling dynamo at different scales in spacetime. Biosphere, humankind, land usage and changes of territory by alteration of the natural hydrologic cycle, are all crucial factors that influence climate by a substantial amount. When considering urbanization, different effects are to be taken into account, such as the heat island effect in the atmosphere, or the time delay introduced in the water cycle and in its associated energy balance due to the injection of warm water in the environment.

Summarizing, it is likely that a reasonable understanding of climate phenomena and of climate evolution strictly requires taking into account the crucial role of the biosphere as an active agent that affects the natural system. This is likely to be one very important frontier of climate science in the next future. Present Earth’s sciences still appear to be in a very preliminary stage. Much harder thinking is required before attaining substantial advances in our comprehensive understanding of “climate”.

Desertification

This entire item and concern also leads to the whole great debate about desertification, which is the most direct

and evident result of the - both passive and active - relationship between environment and biosphere. Desertification is a concern for several areas of the world (UNEP, 1992). However, it is impossible to define one unique average datum, either for “climate temperature”, or for “glacier retreat”, or for “desertification”, etc. An entire encyclopedia could hardly focus on all related items. Also, humankind is a fundamental part of the biosphere. This whole huge item is identified with “environmental anthropology” (see the Cycle of Climate and Civilization; see e.g. Gregori et al., 2000, and Gregori, 2002a).

Another intriguing planetary-scale evidence was found¹⁵ by Vautard et al. (2010), who summarize their findings as follows. “Surface winds have declined in China, the Netherlands, the Czech Republic, the United States and Australia over the past few decades ... The precise cause of the stilling is uncertain. Here, we analyze the extent and potential cause of changes in surface wind speeds over the northern mid-latitudes between 1979 and 2008, using data from 822 surface weather stations. We show that surface wind speeds have declined by 5 – 15% over almost all continental areas in the northern mid-latitudes, and that strong winds have slowed faster than weak winds. In contrast, upper-air winds calculated from sea-level pressure gradients, and winds from weather reanalyses, exhibited no such trend. Changes in atmospheric circulation that are captured by reanalysis data explain 10 – 50% of the surface wind slowdown. In addition, mesoscale model simulations suggest that an increase in surface roughness - the magnitude of which is estimated from increases in biomass and land-use change in Eurasia - could explain between 25% and 60% of the stilling. Moreover, regions of pronounced stilling generally coincided with regions where biomass has increased over the past 30 years, supporting the role of vegetation increases in wind slowdown.”

The decline of wind speed (10 m above ground) produces a reduction of evaporation, hence of water content in the atmosphere. After carrying out climate model

simulations, those authors guess that the main cause has been an increase in topographical surface roughness, due to a surge in vegetation growth. This was a possible consequence of the increase of atmospheric CO_2 concentration. The unicity of the atmosphere/ocean system must be considered. A few features appear consistent with this explanation as follows.

The phenomenon is observed in the *NH*, where it can be seemingly tracked back to 1960. A smaller effect, or even an increase of wind speed, was measured in areas that experienced no significant increase of vegetation cover. At the same time, Vautard et al. (2010) claim that the planetary circulation changes associated with global warming do not seem to be responsible for their findings. In addition, the effect does not occur at 50 – 100 m, where surface roughness certainly plays a less relevant influence. Summarizing, even though several features, processes and mechanisms have still to be clarified and suitably modeled and understood, the biosphere certainly is a crucial and leading driver in “climate” phenomena.

Sahel and a few planetary phenomena. Understanding biogeochemical cycles

Let us take for granted (i) that it is impossible to define a “global” climate, (ii) that reference must be made to climatic variations that involve limited regions, and (iii) that different regions can eventually experience climate changes opposite to one another. It is also well-known that either one polar cap experienced very large – and mutually non-synchronous - climate variations on the time scale of several 10^7 years due to the North Pole vertex of the tetrahedron (see Gregori and Leybourne, 2021).

Sahara is a very interesting natural laboratory (Fig. 36) that on the time scale of several 10^2 years experienced violent climate changes (see below), and the real role played by humankind in these processes has yet to be suitably ascertained. Sahara is the largest desert in the world, $\sim 7 - 9 \times 10^6$ km², or roughly 1/3 the African continent.



Fig. 36. Sahara and Sahel. Credit: NASA's MODIS instrument. NASA copyright free policy.

¹⁵ See also *Physics Today*, 63, (12), 25-26, 2010.

Africa is also the site where the earliest archaeological evidence has been found - in Morocco - dealing with the modern humans. This is reported by Choi (2017a), who illustrates two studies published in the June 8th, 2017 issue of *Nature*. “The new analyses revealed that all of the fossils recovered from the site came from at least five individuals - three adults, one adolescent and one 7 – 8 year old child ... Those individuals date back about 285,000 – 350,000 years - much older than 40,000 years” [which was the previous date of the earliest appearance of humans developed at a comparable stage (Neanderthal)]. Choi (2017a) reports an interview with Jean-Jacques Hublin, a palaeoanthropologist at the *Max Planck Institute for Evolutionary Anthropology*. “One ‘green Sahara’ period may have occurred between about 300,000 – 330,000 years ago’, *Hublin said*. ‘This means grasslands over the Sahara, rivers, huge lakes, like those in Germany, in size, fauna such as elephants and zebra. All over a geographic domain that is absolutely gigantic - the Sahara is the size of the United States’, *Hublin said*. ‘These periods happened again and again, probably playing a role in what we think were episodes of connection and exchanges between different populations of *H. sapiens*’.”

Although different compared to Sahara, Sahel is a related case history, as its dramatic climate change occurred - and is presently occurring - on the time scale of a few 10^2 years. It is therefore the natural “laboratory” that can be comparatively more easily tackled and investigated by means of both prehistorical information and historical instrumental data series, and even by satellite remote sensing during Space Age. However, before dealing with Sahel, let us stress that Sahel is not the unique prehistorical and historical natural “laboratory”.

For instance, a well-known case history is the Easter Island, a “microcosm” devastated by anthropic deforestation. In addition, another interesting case history deals with the Silk Road. Unfortunately, however, its investigation is a typical study of environmental anthropology that - to our knowledge - at present was never tackled. Rather, it is a concern for the realm of traditional historians. There is need for a joint cooperation (see e.g. Gregori et al., 2000, and Gregori, 2002a) between enlightened specialists in history, prehistory, geophysics, geochemistry, sedimentology, geology, natural sciences, agronomy, etc. (note that climatology is not in the list, as the definition of “climatology” is excessively vague and it includes several disciplines).

The Silk Road is the way through which - since prehistorical times - an intense east/west connection always existed. A conspicuous documentations is available concerning the classical ancient Roman times (e.g. Innes Miller, 1969; De Romanis, 1996), including epic crossing on rafts from the Sunda archipelago through Madagascar and southern Africa, and then transport of goods until the Mediterranean area, etc. A long and intriguing historical development (e.g. Uhlig, 1986; Boulnois, 1992) occurred in the wide region of the Silk Road, in the Tarim Basin (or Altishahr in Uyghur, which means “six cities”), located between the Tian Shan Mountains and the Kunlun

Mountains on the edge of the Qinghai-Tibet Plateau (TP), with the large Taklamakan (or Taklimakan or Teklimakan) desert inside it (Figs 37, 38, and Fig. 10 of Gregori and Leybourne, 2025k). At present, the Silk Road is considered a tourist resource (e.g. Bonavia et al., 1992). See Gregori et al. (2025f) for some names and locations.



Fig. 37. “The Tarim Basin, seen in this August 2011 image taken by NASA’s TERRA satellite, lies in the westernmost part of China and is home to the Taklimakan Desert, the hottest, driest and biggest desert in the country. Credit: NASA.” Figure and captions after Thompson (2015). NASA copyright free policy.



Fig. 38. “A vast alluvial fan in the Xinjiang province of China. The right side is the active part of the fan, and appears blue from water currently flowing in the many small streams. The image was acquired on May 2, 2002. Image credit: NASA / GSFC / METI / ERSDAC / JAROS / US-Japan ASTER Science Team.” Figure and captions after Romero (2017). NASA copyright free policy. Also, in Byrd (2017t) who specifies that it refers to the Taklamakan Desert.

During the first millennium AD, western Europe was experiencing an often painful or dramatic transition from the fall of the Roman Empire to Middle Age. It is likely that at that time the best life quality was enjoyed along the Silk Road that was a comparatively happy world, with a flourishing economy and a multi-religious seemingly peaceful cohabitation, between followers of Mazdaism (or

Zoroastrianism), Hinduism, Buddhism, Nestorianism (Christians), etc. However, roughly beginning in the 8th century AD, at the time of the Muslim penetration, a deterioration of the environment occurred: (i) climate changed, maybe due to destruction of irrigation plants, etc. and (ii) a period of religious conflicts was started that severely impacted the environment. A large amount of archaeological research has still to be exploited. Owing to the uncomfortable regions to be explored and to the sand cover of several ancient ruins - and often upon considering the hostility of the local inhabitants – satellite images are a very helpful tool. For instance, Choi (2018a) illustrates the results presented by Li et al. (2017). They report about ancient irrigation system, of > 1,700 years ago, that archaeologists found in the foothills of Xinjiang, China. Quoting Choi (2018a), the location is “*a region dubbed Mohuchahangoukou, or MGK, which gets a seasonal trickle of snowmelt and rainfall from the Mohuchahan River ... Initial excavations at the site confirmed the presence of farmhouses and graves that radiocarbon dating and other methods suggest likely date back to the 3rd or 4th century AD ... This ancient farming community was likely built by local herding groups that sought to add crops such as millet, barley, wheat and perhaps grapes to their diet ...*

... this ancient, well-preserved irrigation system helped people grow crops in one of the world’s driest climates. The area at the edge of the Taklamakan Desert historically receives < 6.6 cm of rainfall annually, or about one-fifth of the water typically deemed necessary to cultivate even the most drought-tolerant strains of wheat and millet ... The area is drier than the Kalahari in southern Africa, the Gobi Desert in Central Asia and the American Southwest, but not as dry as the Atacama Desert in Chile or the Sahara Desert in northern Africa ... The most likely scenario is that this irrigation technology came from the West ...

... Prior work suggested that so-called agropastoral communities, which practiced both farming and herding along mountain ranges in ancient Central Asia, may have spread crops throughout a region that scientists call the Inner Asian Mountain Corridor. This giant exchange network may have spanned much of the Eurasian continent, bringing ancient nomadic groups together as they moved herds to seasonal pastures, and perhaps spreading irrigation techniques as well ... irrigation systems similar to MGK’s have also been found at the Geokysur river delta oasis in southeast Turkmenistan dating to about 3000 BC and further west at the Tepe Gaz Tavila settlement in Iran dating to about 5000 BC. The researchers added that an irrigation system nearly identical to MGK’s is seen at the Wadi Faynan farming community, which was established in a desert environment in southern Jordan during the latter part of the Bronze Age (2500 – 900 BC) and includes boulder-constructed canals, cisterns and field boundaries ... “

A comparably more interesting time span is, say, between Alexandre the Great (see e.g. Ghose, 2017e) - or Alexander III of Macedon (356 BC - 323 BC) and his

expedition when in 326 BC he invaded India - until the epoch of the great navigators (see e.g. Lawler, 2017, and Ghose, 2017f). During this time span, commerce was safer through the ocean, better than along the Earth route due to bandits and lack of local rulers etc. That is, the comparative role should be ascertained of natural and anthropic factors in the decay of this “happy” world. Humankind can be either an active or a passive agent, or both. It is premature to make any statement. A long multidisciplinary study of archaeology and environmental anthropology - and hard thinking - is required, before getting any final inference.

Also the archaeology of Arabia has to be investigated - and the time span ranges much earlier than Biblical times (see e.g. Kessler, 2011; Jarus, 2017b; Kennedy, 2017; and Letzter, 2018), but the archaeology through whole central and northern Eurasia is still to be investigated (e.g. Jarus, 2016a; ...).

Concerning the Sahel case history, the dramatic morphology of severe droughts in Africa are shown e.g. in Figs 39 and 40 (shown also in Gregori and Leybourne, 2025j).

Let us therefore consider Sahel, which in any case is one of the most relevant and most investigated case histories. It has been suggested (Celant, 1995;¹⁶ see also Gregori and Gregori, 1998) that one major component of the problem is related to the human legal convention about state borders. Namely, Sahel is a band, ~ 300 – 800 km wide, which is extended longitudinally across entire Africa, between the Atlantic Ocean through the Red Sea.

During past centuries and millennia, owing to natural causes, this band always moved in latitude, fluctuating northward/southward. No state border existed, and large human migrations were a generally accepted and usual occurrence. It was therefore more important being the owner of a camel, than of some land. Its inhabitants always migrated with Sahel’s displacement. In contrast, at present, if this belt crosses one state border while it drifts in latitude, a former simple migration phenomenon - which was a natural occurrence - becomes a serious concern of refugees.

However, also natural causes certainly have a relevant responsibility in the Sahel crisis. In addition, during past millennia a demographic self-quenching process was active, by which the local density of inhabitants per unit area never exceeded the upper threshold needed in order to ensure the local survival. These self-quenching factors - that at present, maybe excessively optimistically, are presumed no more to exist - were (i) mortality (due to lack of medicine), and (ii) the slave trade (which implied genocides, or violent deportation of entire ethnical groups, by the winners of *ad hoc* triggered wars). The Sahel inhabitants eventually had a flourishing economy, based on trades across Sahara (either of slaves or of other goods). In the final analysis, the phenomenon is the same as what occurs inside every colony of biological organisms, whenever their density per unit surface exceeds the survival threshold.

¹⁶ Attilio Celant is Dean of the Faculty of Economy of the University “La Sapienza” in Rome.

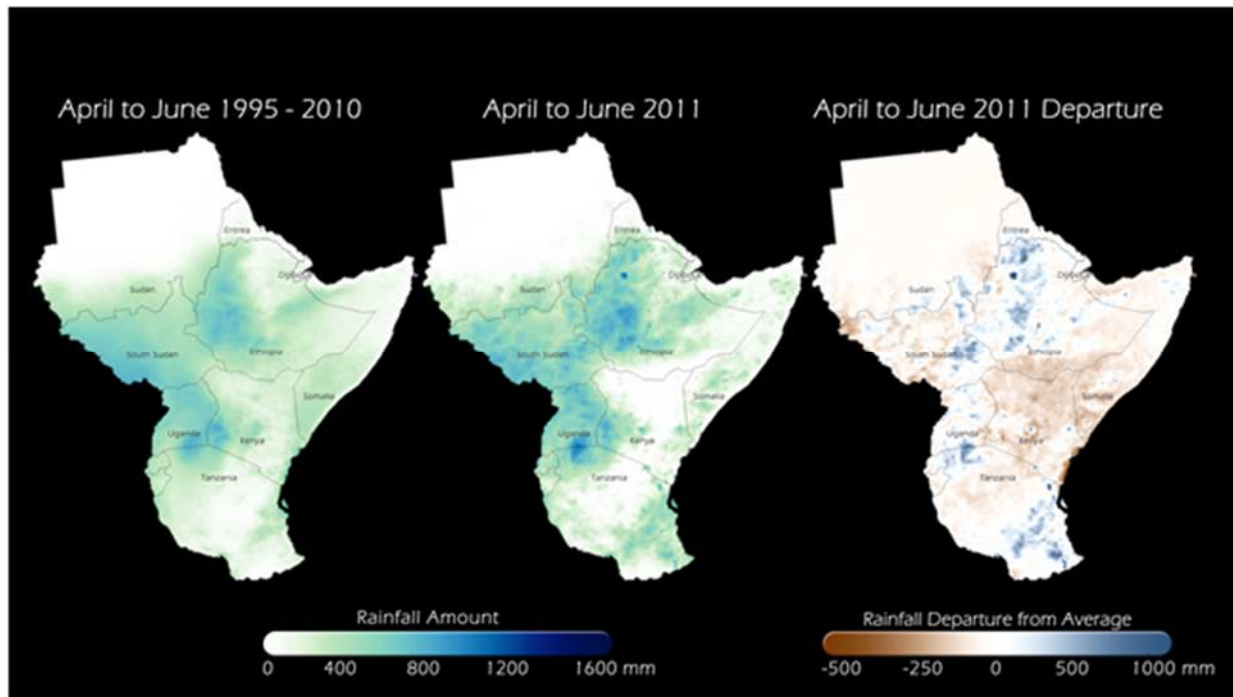


Fig. 39. “Measuring Somalia’s lack of rainfall. Prolonged drought in the Horn of Africa along with political turmoil has created a dire situation in Somalia. The Horn receives the majority of its precipitation during two wet seasons: one in the fall and another in the spring. The spring rains are especially critical, as the water is needed to last throughout the brutal sub-Saharan summer. This past year has been especially dry. Both wet seasons have failed to produce the rainfalls necessary to sustain crops and livestock, leading to widespread food shortages and famine. In many areas around the world, even the U.S., rain gauge data can be sparse. Nevertheless, accurate rainfall estimates are needed for weather models and hazard warnings, so NOAA has developed techniques to augment rainfall measurements by including IR and microwave data from geostationary and polar-orbiting satellites. Besides aiding forecasts in the U.S., these estimate techniques have proven very useful for detecting possible famines in Africa, and the data is widely used by the U.N., the World Meteorological Organization, and USAID. Shown here are plots of the average spring wet season (April through June) rainfall since 1995, the total rainfall during the wet season this past year (April through June 2011), and how the past season compared to the long-term average. Drier than normal conditions (brown colors) can be seen in the image on the far right throughout much of Somalia, Ethiopia, Kenya, The Republic of Tanzania, Uganda, and the newly-formed South Sudan.” Credit: NOAA. Figure and captions after Anonymous (2012d). NOAA and NASA copyright free policy.

That is, independent of the geophysical and geochemical aspects, the impact of the biosphere - and humankind is just a part of it - is likely to be an important and critical control factor. Differently stated, the role of environmental anthropology (Gregori and Gregori, 1999, 1999a) has been fundamental as a concurrent driver for most relevant final climate changes. If we want to avoid phenomena that remind about the ancient slave trade and deportations, these populations must be practically helped in order to solve their eventual huge survival problems. Note that, in this respect, the well-known dramatic present problem of huge migrations from Africa to Europe is just a matter of environmental anthropology, including its critical socio-political, economic, and humanitarian implications. In addition, no easy “recipe” can solve this tremendous problem.

Humankind has always been - and presently still is - one of the most active components of the biosphere, including the present concern about the different forms of pollution. In any case, the most important anthropic pollution is just the steady increase of demographic expansion (which implies a progressive occupation of the Earth’s surface and

destruction of biodiversity), and the steady increase of energy consumption per inhabitant. These are unavoidable drivers – and their management is a difficult challenge. However, even more important – and more easily manageable – is the violent pollution caused by destructive weapons used in several conflicts that impact the environment with global consequences that require a very long time for recovery. Destructive weapons should be firmly banned. They cannot be justified by any reason.

Nevertheless, it is understating to simplify the problem by claiming that the Sahel climatic crises - like the Sahara desertification - can be explained only by means of anthropic action. Instead, several natural causes converge altogether and are then combined with humankind impact. The problem is very complicated and its understanding is still substantially uncertain.¹⁷ The early discussion emphasized the role of human overexploitation, such as overgrazing (e.g. Hiernaux, 1992), overcultivation and the cutting of trees, while the discussion more recently has become more balanced in terms of invoking both human and natural causes as well as the dynamic linkage between

¹⁷For a general discussion refer e.g. to Demuth (2006), or Leblanc et al. (2008).

them. The dramatic intensity and rapidity of this phenomenon is shown e.g. by Lake Chad (Fig. 41).

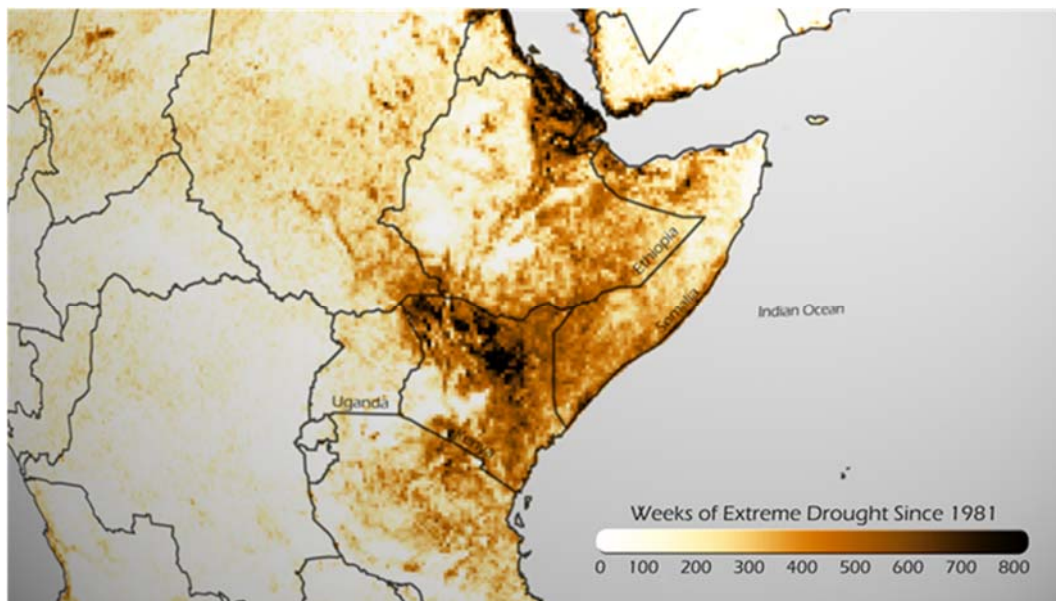


Fig. 40. “Africa’s extremely prolonged drought. The Horn of Africa - the peninsula loosely comprised of Somalia, Ethiopia, Eritrea, and Djibouti - has been experiencing seemingly unrelenting droughts for decades. Parts of Somalia are plagued with widespread famine due to crop failures, and the U.N. is now involved in airlifting food and aid to the region. Data from NOAA’s satellites has been used by organizations such as the U.N. and USAID to monitor global drought conditions. Satellites can detect drought conditions by measuring either soil moisture or the impacts on vegetation ‘greenness’. The droughts are then classified in terms of their intensity: abnormally dry, moderate, severe, extreme and exceptional. However, these terms do not consider the length of the drought impact on an area. For example, Texas is currently also experiencing an exceptional, albeit seasonal, drought. With the launch of NOAA-7, the precursor to today’s NOAA-19 and the future JPSS satellites, there have been continuous global measurements of vegetation and drought since 1981. In that time, the Horn of Africa has been under drought conditions classified as extreme for up to 800 weeks (~ 15 years), and many other weeks were classified as abnormally dry, severe, or even exceptional. In comparison, small parts of Texas have had extreme droughts for about 300 weeks in that same time period. There is not much improvement expected in the Horn of Africa – another reason for great concern. Shown here is a plot of the number of weeks that the Horn has experienced extreme drought conditions since data archives began in November 1981. Extreme droughts are identified as areas with a vegetation health index value from 6-15. Vegetation health indices are derived from the normalized difference vegetation index (NDVI) - the most commonly used satellite dataset for assessing global vegetation condition.” Credit: NOAA. Figure and captions after Anonymous (2012e) [<http://www.nvnl.noaa.gov/MediaDetail.php?MediaID=789&MediaTypeID=1>]. NOAA and NASA copyright free policy.

The famines in this large area - caused by any kind of environmental change either by droughts or by severe seasons etc. - are an important historical information recorded by chroniclers everywhere. That is, in any case humankind is a very effective proxy datum. For instance, the case history of northern Nigeria is discussed by Tarhule and Woo (1997), who give a geophysical definition of “famine” as follows: “the most disruptive famines occurred when the cumulative deficit of rainfall fell below 1.3 times the standard deviation of long-term mean annual rainfall for a particular place.” More recently - in semiarid regions - the ratio, called rain-use efficiency (RUE), of the annual net primary production to precipitation has been used as an index of desertification, although its significance is debated (Hein and de Ridder, 2006; Prince et al., 2007).

Sahara contains several dried lakes (Figs 42, 43, and 44). Its climatic evolution during the last few millennia is shown in Fig. 45, and some climatic information, which however is only indicative, is given in Table 1, which is an expansion of a table shown by Sansoni (1994, p. 11) by including some information after Le Quellec (2006 and 2013). The different phases eventually overlap one another, and migrations occurred on the occasion of arid periods, etc.

A more recent and more precise information is shown in Figs 46 and 47 borrowed after the tutorial report by deMenocal and Tierney (2012). An extensive discussion of the archaeological evidence is made by Le Quellec (2006), and his Figs 1, 2 and 4 are synthesized in a unique Fig. 48. The starting hypothesis is the search for a correlation with Milanković.

The modeled solar luminosity is plotted, expressed as the difference (%) with respect to the average over 90,000 years (after Perry and Hsü, 2000). Warm periods in the NH correspond to humid phases in Sahara - and the European Glacial Ages correspond to Sahara Arids. Other plotted parameters are: the Holocene palaeolakes number (after Petit-Maire, 2002), the sea-level variations (after Ters, 1987), the Jerma Playa level (after Mattingly, 2003), and the number of ¹⁴C dates in anthropic levels of the Akākūs shelters (after Cremaschi and Zerboni, 2003). The Holocene Climatic Optimum coincides with the maximum occupancy rate of the Akākūs shelters and with the introduction of the first potteries in Sahara.

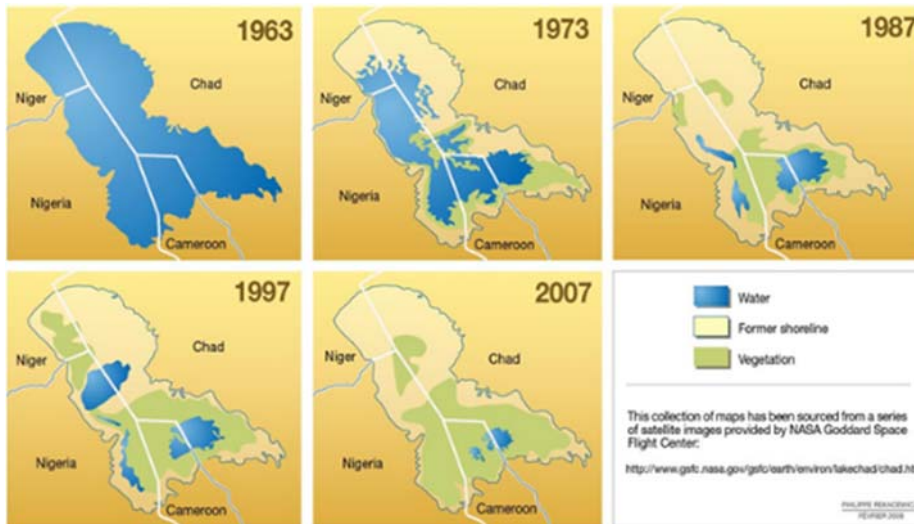


Fig. 41. Collection of maps derived from a series of satellite images provided by *NASA GSFC*. Credit Philippe Rekacewicz, February 2008. After <https://library.ecc-platform.org/conflicts/lake-chadafrica-local-conflicts-over-survival-resources>. *NASA* copyright free policy.

Table 1. Schematic table of the periods of cave art in Sahara

| Period | Current name | Tentative dates (±) | Environment | Comments |
|----------------------------------|---|---------------------|--|---|
| Recent | - Berber phase nomad populations | | Desert with oases | The camel is introduced from nearby eastern countries in the first millennium BC |
| (<i>M.E.</i> = Mixed Economy) | - Camelin phase Tuareg | 2,800 BP | | |
| Chariot and trade | - Horse or Garamantian phase | | flourishing oases in arid zone | Mediterranean population; merchants with two-horsed chariots and horses; commanders of mercenary troops |
| (<i>M.E.</i> = Mixed Economy) | | | | |
| hiatus | | ? | arid episode | |
| Pastoral (<i>PA</i>) | - Bovidian phases | | Savanna with swampy zones being drained | Immigrations from North, West and South. white-skin and negroid-skin cowboys. Different populations |
| Late Hunters (<i>L.H.</i>) | - Anecdotic phase of Hunters - late Gatherers | 8,000 BP | | |
| hiatus | | | arid episode | |
| Gatherers of spontaneous fruits | - Round Head phases | | Lakes and flourishing vegetation. Maximum extension of Central-African Lakes | The bow appears. Negroid population; practice of fishing and fruit gathering; widespread use of hallucinogens |
| (<i>E.G.</i> = Early Gatherers) | | | | |
| | - Persisting Bubalus phases | 11,000 BP | | |
| brief | | ? | arid | |

| | | | |
|----------------------|------------------------|--|--|
| hiatus | | episode | |
| Early Hunters (E.H.) | - Early Bubalus phases | ? | Prairie and savanna with water pools |
| | | | Hunters of large-sized fauna. They do not know bow and arrow |
| hiatus | | ? | arid episode |
| Aterian | - Middle Stone Age or | 20,000 BP through 145,000 BP - Middle Palaeolithic | stone tool industry |

Legend: The dating techniques are discussed in detail by Le Quellec (2013).
 (‡) - See also Figs 45, 48 and 49, and respective captions.

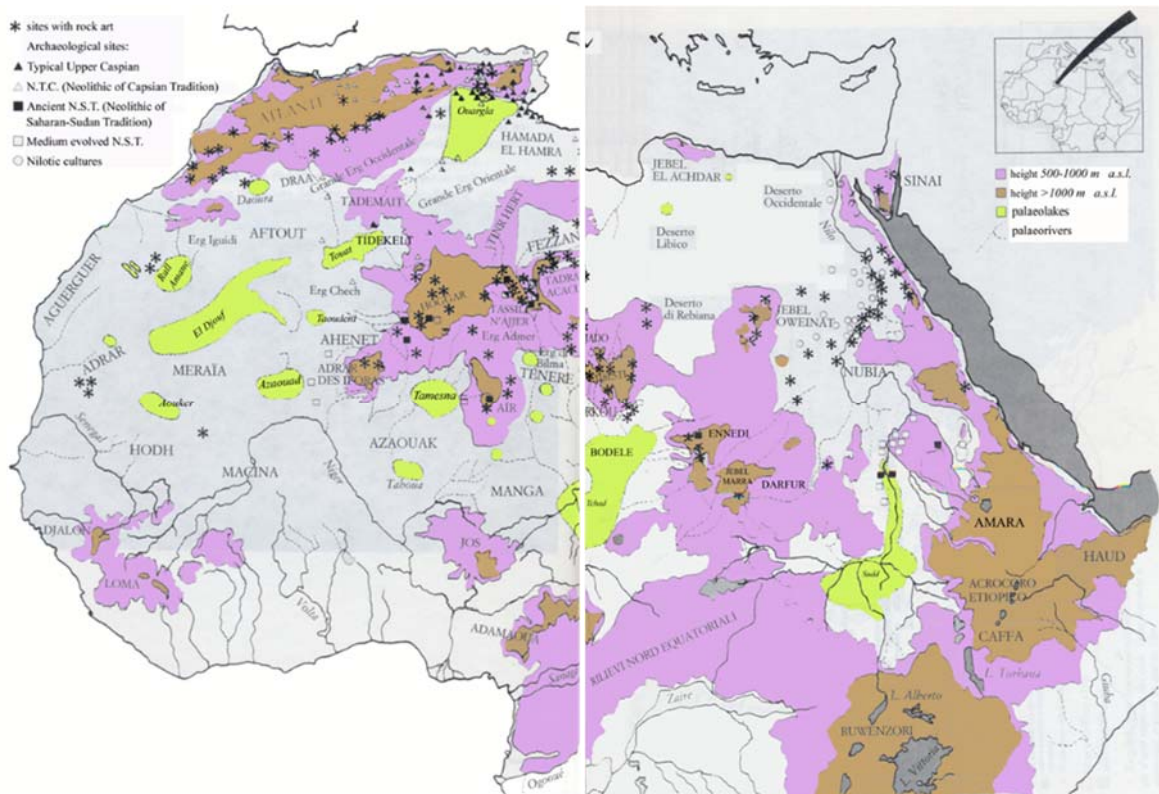


Fig. 42. Indicative map of North Africa showing the main archaeological and cave-art sites. Some indication is also added of environmental information (palaeo-lakes and palaeo-rivers). Redrawn and adapted, with added colors, after Sansoni (1994). Reproduced with kind permission of *Jaca Book*.

Jean-Loïc Le Quellec kindly provided the updated Fig. 49, after Le Quellec (2013). Dating archaeological relics is very difficult, unless some biological indicators can be used and ¹⁴C techniques can be applied. See Le Quellec (2013). The Akâkûs shelters refer to a particularly rich array of prehistoric rock art in the Akâkûs (or Acacus) mountains. They are also called Tadrart Akâkûs, as Tadrart means mountain in the Tamahaq language, the native language of the area. They are located in the desert of western Libya, east of Ghat, and stretch north from the Algerian border.

The Jerma Playa refers to Garama/Jerma (or Djerma), the Garamantian capital, located ~ 160 km SW of Sabha, in Wadi al-Hayat, South-Western Libya. It was the capital city of the ancient Berber Garamantian Kingdom of Fazzân, Libya's first indigenous empire. The Garamantes had

control over a wide area, spanning the entire region from Tibesti to Akâcû including the enigmatic Messaks and Wadi Metkhandoush. Pliny placed them 12 days, and Herodotus 10 days, journey from the Awjilas (in Latin Augilæ) in the interior of Libya. They occupied the most habitable region of the Sahara: Wadi al-Hayat (Wadi Al-Agial), Wadi Ashati (Sciati), and the oases from Murzuk to Zuila. Its origin ranges back into the earliest prehistory, and Jerma was still an important trade center in the classical times of the Roman Empire. Impressive ruins survive to the devastating destruction by the violent thermal environmental gradient of the desert, including several flat-topped burial pyramids.

Le Quellec (2006) briefly synthesizes as follows the cultural responses to climate changes. "Herders appeared

only after the Mid-Holocene Arid Period, ~ 6000 BP, and created petroglyphs and painting glorifying, above all, their domestic bovids. When the Saharan climate seriously deteriorated during the Post-Neolithic Arid Period, cattle farming declined in favor of ovicaprid farming, and the later replaced the former around ~ 4000 BP. The great African fauna disappeared once for all, palm trees appeared ~ 3000 BP, and the dromedary was introduced around the beginning of the Christian era. Since then, the Saharan landscape did not change significantly.”

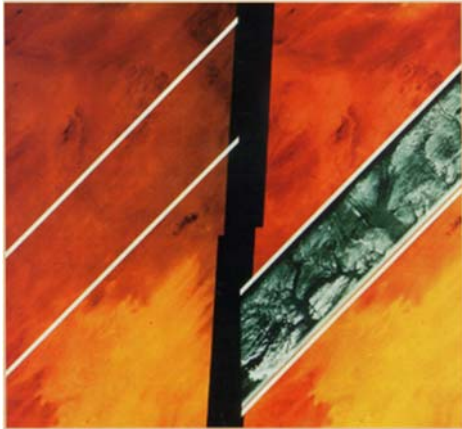


Fig. 43. Landsat image of part of eastern Sahara, from 920 km altitude. Also a strip is shown of the same area observed by the Space Shuttle Imaging Radar, where palaeochannels of rivers can be recognized beneath the desert sand. After IGCP (1997). Permission granted through IGCP “Fair Dealing” and/or “Fair Use” licence.



Fig. 44. Evidence of palaeo-lakes in present Sahara (Mali). These lakes formed during a warm and wet period, ~ 8,500 – 4,400 years ago. Image provided by N. Petit-Maire for IGCP (1997). Permission granted through IGCP “Fair Dealing” and/or “Fair Use” licence.

A few major cold periods are indicated in Fig. 48: the last two European Glaciations, denoted as Dryas II and Dryas III, the mid-Holocene Arid (~ 6900 BP), the ~ 4000 BP event (~ 4400 – 3800 BP), and the Little Ice Age (~ AD 1280 – 1680). In addition, note the large Holocene warming occurred roughly between ~ 11000 – 9000 years BP that led to the so-called Holocene Climatic Optimum, roughly spanning the time interval between ~ 9000 – 5000 years B.

Le Quellec (2006) conclude and claim that “without trying to link systematically all significant events in the history of mankind to climatic events, and without going as far as to say that ‘climate makes history’ (Hsü, 2000), some important human adaptations (Fig. 48) must have been regionally induced by shifts as important as the rapid warm-up which began at the Pleistocene/Holocene time boundary around ~ 10,000 BP, as the Mid-Holocene Arid Period which dominated the Saharan climate around ~ 6900 BP, or as the ‘4000 BP Event’ which lasted from ~ 4000–3800 BP and which corresponds to the Post-Neolithic Arid Period in the Sahara ... “

Much more specific details are given by Le Quellec (2006). However, these items are not of direct concern for the present discussion and are not here reported.

A remarkable new study addresses milk properties as a dating tool. Dunne et al. (2012) synthesize as follows their investigation as conclusions. “In the prehistoric green Sahara of Holocene North Africa - in contrast to the Neolithic of Europe and Eurasia - a reliance on cattle, sheep and goats emerged as a stable and widespread way of life, long before the first evidence for domesticated plants or settled village farming communities (Gifford-Gonzalez and Hanotte, 2011; Marshall and Hildebrand, 2002; di Lernia, 2002). The remarkable rock art found widely across the region depicts cattle herding among early Saharan pastoral groups, and includes rare scenes of milking; however, these images can rarely be reliably dated (di Lernia and Gallinaro, 2010).

Although the faunal evidence provides further confirmation of the importance of cattle and other domesticates (Gautier, 2002), the scarcity of cattle bones makes it impossible to ascertain herd structures via kill-off patterns ... [therefore it is impossible to ascertain] “whether dairying was practiced. Because pottery production begins early in northern Africa (Huysecom et al., 2009) the potential exists to investigate diet and subsistence practices using molecular and isotopic analyses of absorbed food residues (Evershed, 2008). This approach has been successful in determining the chronology of dairying beginning in the ‘Fertile Crescent’ of the Near East and its spread across Europe (Evershed et al., 2008; Copley et al., 2003; Dudd and Evershed, 1998; Craig et al., 2005).”

They report unquestionable chemical evidence. They rely on the analysis of the major alkanolic acids of milk fat, in terms of $\delta^{13}\text{C}$ and $\Delta^{13}\text{C}$ values. These are indicators of dairying practices in the prehistoric Saharan African society during the 5th millennium BC. They use a database referred to modern ruminant animal fats found in Africa. Thus, they get confirmation of the importance of “lifetime products”, such as, e.g., milk, in early Saharan pastoralism. This supports the evidence for the evolutionary context concerning the emergence of lactase persistence in Africa. These findings are clearly suggestive of extensive processing of dairy products in pottery vessels during the Middle Pastoral period (approximately 5200 – 3800 BC) through the Libyan Sahara. That is, this confirms that milk was an important part in the diet of these prehistoric pastoral societies.

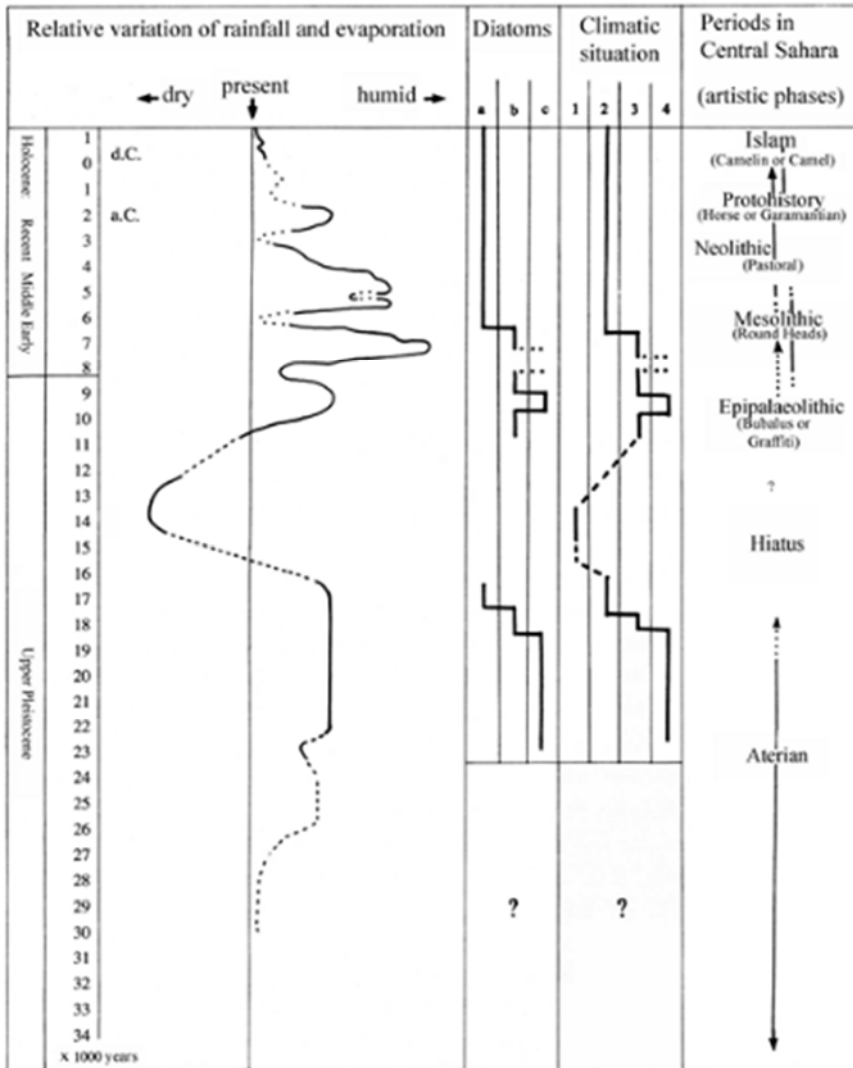


Fig. 45. "Palaeoclimatic evolution of the Tchad basin (around 14°N). Table of variation of rain/evaporation ratio related to the evolution of lacustrine diatoms (A= tropical diatoms; B=cold water diatoms associated with diatoms of high and middle latitude and to rarer tropical diatoms; C= diatoms of high and middle latitude) and to the changes of atmospheric circulation [reconstruction hypothesis: 1) hyper-arid phase; 2) tropical climate phase with rare and decreasing penetration of polar air. Seasonal and stormy rain. 3) humid phase with regular penetration of polar air. Rain precipitation distributed during the year. 4) hyper-humid phase]. The results of observations carried out in the Tchad basin are indicative of a wider palaeoclimatic phenomenon of central-southern Sahara (re-handling after Servant and Servant-Vildary, 1980, including their chronological indications obtained by non-calibrated ¹⁴C). The last column proposes the corresponding cultures and their associated cave-art phases in central Sahara (the timing of Epipalaeolithic and of Bubalus phase are only tentative)." Figure and captions after Sansoni (1994). Reproduced with kind permission of Jaca Book.

"The findings are notable for three other reasons: (1) they confirm that domesticated cattle, used as part of a dairying economy, were present in North Africa during the 5th millennium BC, thus supporting the idea of an earlier ingress into the central Sahara (Gifford-Gonzalez and Hanotte, 2011; Marshall and Hildebrand, 2002; di Lernia, 2002) and suggesting a local process of pastoral development, based on the exploitation of secondary products; (2) the finding of dairy fat residues in pottery is consistent with milk being processed, thereby providing an explanation of how, in spite of lactose intolerance, milk products could be consumed by these people with the practice being adopted quickly; (3) they are consistent with the finding of the -213910*T allele, associated with the lactase persistence (LP) trait in Europeans, across some Central African groups such as the Fulbe from northern Cameroon (Mulcare et al., 2004), supporting arguments for some movement of people, together with their cattle, from the Near East into eastern Africa in the Early to Middle Holocene; and (4) they provide a context for understanding the origins and spread of other, independently arising LP-

associated gene variants in sub-Saharan Africa (Itan et al., 2010)."

Maybe, the most impressive heritage of ancient Saharan civilizations is the mysterious and incredible engineering skill of the ancient Egyptians who built their wonderful temples.

Also, other presently desert areas give similar information. For instance, archaeological evidence is available from Arabia. Breeze et al. (2017) report about an investigation that they briefly summarize and claim that significant records of human occupations in southwest Asia are found in mid-latitude dune fields, as they reflect the human response to climate changes. In this respect, the Nefud desert of northern Saudi Arabia, which is currently arid, was episodically wetter in the past. Several examples are found of human-environment interactions and population movements in this desert belt. Breeze et al. (2017) report the results of interdisciplinary surveys in the western Nefud, with reference to palaeolake deposits mapped by means of satellite imagery.

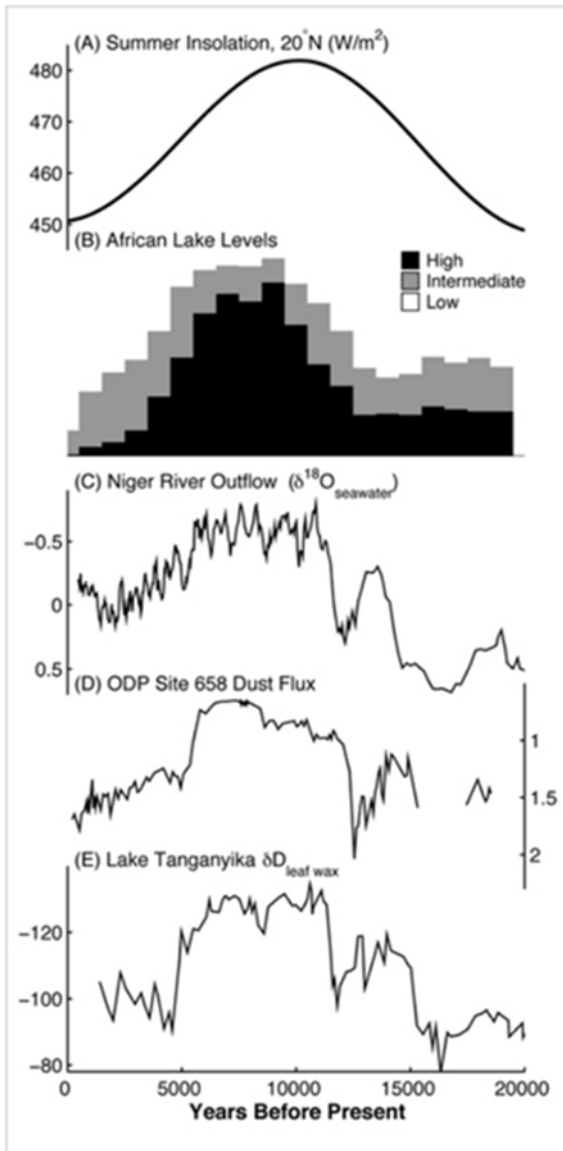


Fig. 46. “(a) Change in seasonal (summer) insolation for North Africa (20°N) and palaeoclimate records of the AHP: (b) African lake level status ... (c) Niger River outflow inferred from $\delta^{18}\text{O}$ seawater ... ; (d) ODP Site 658 dust flux ... ; (e) Lake Tanganyika δD of leaf waxes (δD wax ...),” Figure and captions after deMenocal and Tierney (2012). With kind permission of Peter B. DeMenocal.

Thousands of discrete palaeolakes and palaeowetlands represent a valuable palaeoenvironmental record, to be correlated with numerous archaeological and palaeontological information. According to geomorphological investigations, it is likely that several other deposits are still buried. They identified 46 prehistoric archaeological sites, associated with freshwater deposits, referred to the range between the Lower Palaeolithic and the pre-Islamic Holocene. The Lower Palaeolithic sites are found close to raw material sources near the Nefud fringe,

despite the deeper presence in the dune field of freshwater and fauna. However, a broader extension was found of Middle Palaeolithic occupations, while the early Holocene humans occupied, at least periodically, areas deep in the desert.

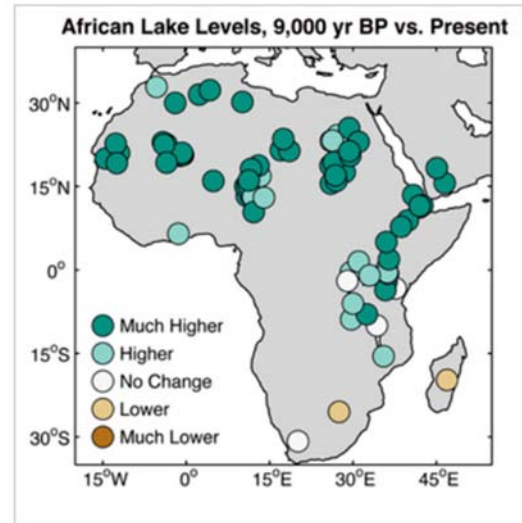


Fig. 47. “Distribution map of reconstructed lake levels across Africa, 9,000 years ago relative to today ... “ Figure and captions after deMenocal and Tierney (2012). With kind permission of Peter B. DeMenocal.

Breeze et al. (2017) report about the first records, in this dune field, of Neolithic sites. They found substantial hearth complexes deep within the dunes, which are potential indication of and increased mobility during this period. Around the dune fringes, and Late Holocene sites were found with stone structures.

Breeze et al. (2017) concludes that, owing to the high density of depressions where wetlands flourish, during wet periods of the Pleistocene and Holocene - according to the western Nefud evidence - the northern Arabia had a greater water availability than other regions of northern Arabia. The relevant frequency of lakes or marshes is likely to have facilitated a widespread human occupation through this whole region.

A large amount of archaeological research is still lacking. For instance, Jarus (2017) informs about 400 mysterious ancient stone structures discovered in Saudi Arabia. But one should also remind about the information concerning the Biblical and Quranic figure of the Queen of Sheba. Her visit to King Solomon is a tale that had extensive Jewish, Islamic, and Ethiopian elaborations. It is the topic of most widespread cycles of legends in the Orient.¹⁸

For completeness sake, consider that - upon referring to historical times - much more recent though extremely interesting data can be found. The literature is very large, although it is outside the general framework of the present study. For instance, concerning the environmental change in Jordan occurred ~ 2,000 years ago, see Corbett et al. (2016), also illustrated by Jarus (2016).

¹⁸ See e.g. Blau (1905, p. 235-236), Jacobs (1905, p. 408b-409a), Ullendorff (1991, p. 1219-1220), Beeston, (1995, p. 663-665), Jamme (2003, p. 450-451), and Tobi (2007,

p. 765). See also “Solomon”, *Encyclopaedia Judaica*, 18 (2nd ed.), Gale, p. 755-763.

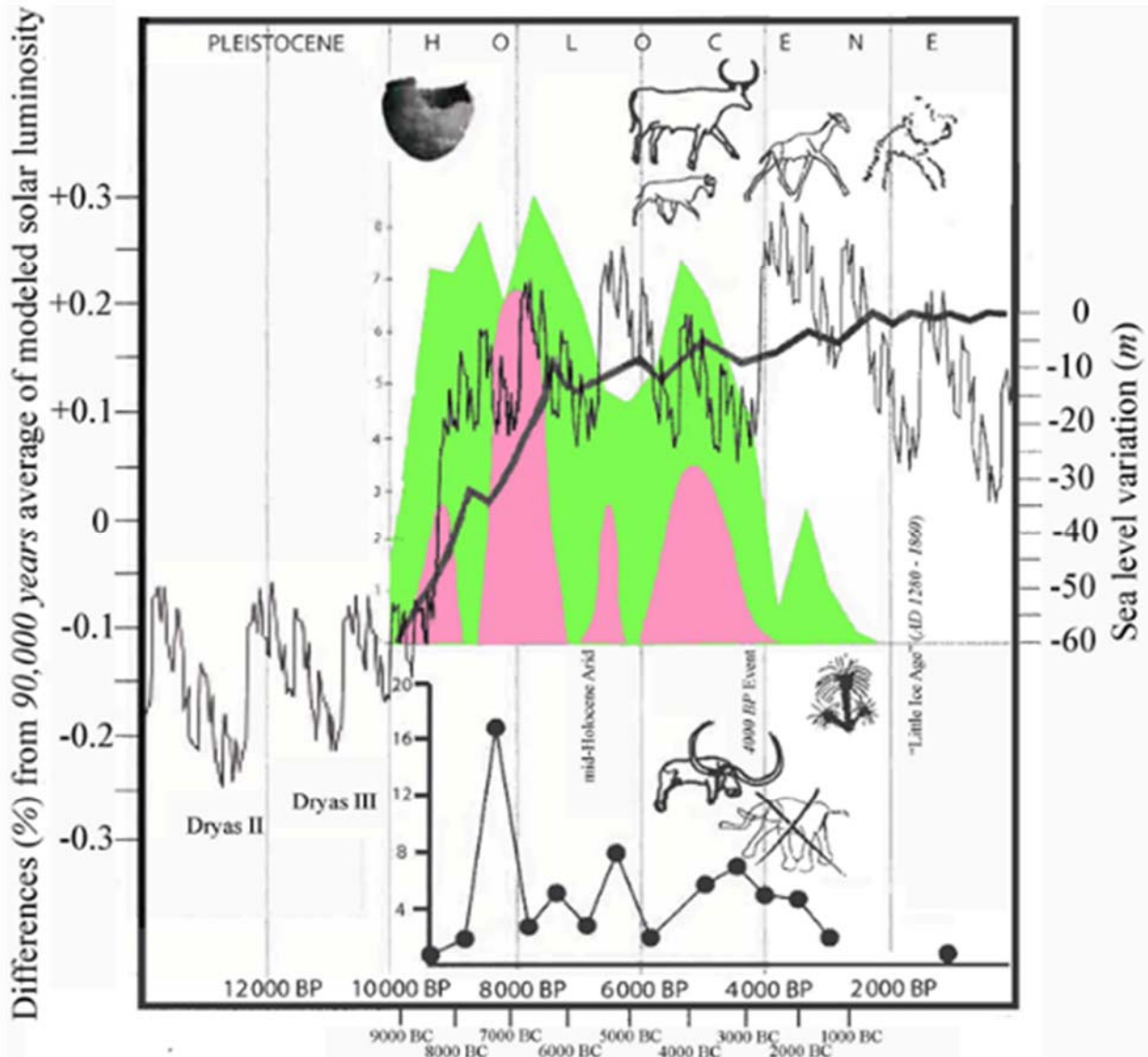


Fig. 48. The climatic history of Sahara. Redrawn upon combining information borrowed after three figures of Le Quellec (2006). See text. The thin very-scattered line (with left-hand scale) refers to the difference in modelled solar-output (luminosity) from Perry and Hsu (2000, Fig. 2, modified) for the NH from 14.000 BP to 2000 AD. Warm-up periods in the NH correspond to humid phases in the Sahara, and European Glacial Ages correspond to Saharan Arids. The plot also compares the aforementioned luminosity difference with (i) Holocene palaeolakes number (from Petit-Maire, 2002, page 74) [light-green plot, scale-range 0 – 9, expressed as difference-number from total for 10,000 years], (ii) sea-level variations (from Ters, 1987) [thick black line, right-hand scale], (iii) Jerma Playa level (from Mattingly, 2003) [pink patches], and (iv) the number of ¹⁴C dates in anthropic levels of the Akâkûs shelters (from Cremaschi and Zerboni, 2003) [lowest plot, with black circles connected by straight line and scale-range 0 – 20]. The various symbols show the time of first appearance either of potteries, or of palm trees in Fazzân (or Fazzân, or Fezzan, Lybia), or information related to various kinds of animals [first domestic bovids in Sahara; first ovicaprids in Central Sahara; generalization of ovicaprid farming; latest fossils of Great Bubalus; disappearance of great fauna; introduction of the dromedary in Sahara, indicated by the icon at the top-right corner]. Various animal distributions vs. time are discussed and plotted in Le Quellec (2006 and 2013). The Holocene Climatic Optimum coincides with the maximum occupancy rate of the Akâkûs shelters and with the introduction of the first potteries in the Sahara. See also Table 1. Reproduced with kind permission of Jean-Loïc Le Quellec.

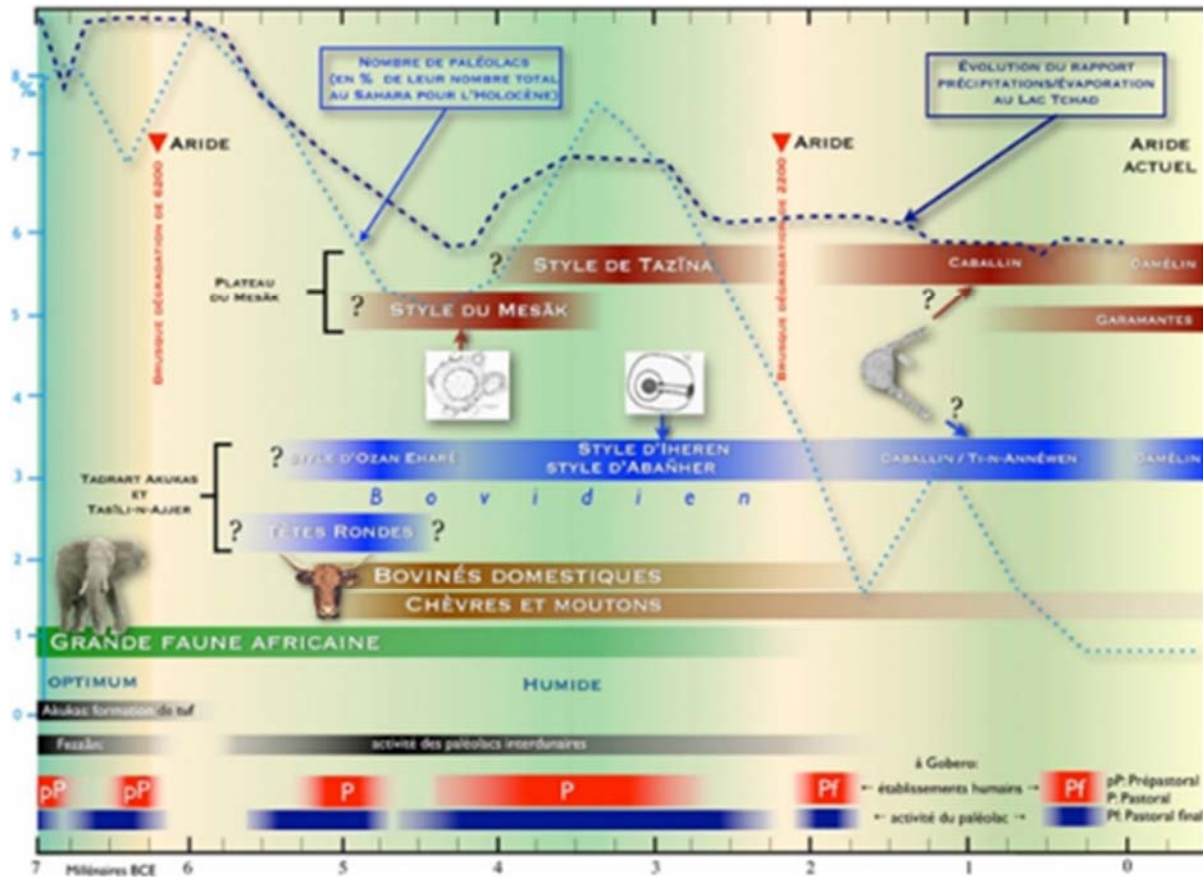


Fig. 49. “The dotted line indicates the number of palaeolakes observed in every period - as a percentage of their total over the entire Holocene (from Petit-Maire, 2002, page 74; Petit-Maire, 2012, page 105). The dashed line shows the variation in the precipitation / evaporation ratio for Lake Chad (from Servant, 1983, fig. 22 and Zerboni, 2008, fig. 13). The period of formation of tuff in the Akukas (after Cremaschi et al., 2010), that of the activity of the interdune lakes in Fezzān (ibid.) and that of Gobero lake in Niger (after Giraudi and Mercuri, 2013, fig. 9.2) are shown at the bottom of the table. The data on Gobero’s human settlements are taken from Giraudi (2013, fig. 6.11, where the names ‘Pre-pastoral’, ‘Pastoral’ and ‘Pastoral final’ are those used by the authors). The arid phases following the abrupt peyorations of 6200 BC and 2200 BC form the two terms of the period during which domestic cattle were massively represented on rock images, notably in the style of Mesāk and the various styles usually grouped together under the term ‘Bovidian’. The large African fauna declined as the climate deteriorated, and the people of the Sahara devoted themselves to raising cattle as long as the environment allowed. When climatic conditions worsened, they developed goat farming because sheep and goats (which multiply in Iheren style) are better suited to the harsh environments in which they now had to live. After the start of the common era, the dromedary, possibly arriving in central Sahara around the 5th century, enabled the people of central Sahara to retain control of the desert until the upheavals of the last centuries.” (Our translation from the French original.) Note the “monuments en corbeille”(monuments in basket; ~ 4,600 BC - 3,800 BC), at present over 360 reported case histories, associated to stela belonging to the Style de Mesāk and probably related to some kind of “cattle worship”, and indicated in the figure related to the Plateau du Mesāk. Also note the “monuments `a couloir” (hallway monuments; ~ 3,300 BC - 2,700 BC), at present 973 monuments are known, associated to 152 cave painting sites in Style d’Iheren, and indicated in the figure associated with Tadrar Akukas et Tasāli-n-Ajjer. In addition, also note another kind of lithic monuments, i.e. the “monuments `a antennes en <<V>>” (monuments with antennas in <<V>>; ~ 2,000 BC - 1,200 BC) associated with caballine style paintings, and widespread over a large region. All these features denote a developed culture, which is certainly associated to astronomical myth and knowledge, even though the archæastronomical investigations are still to be exploited (see e.g. Le Quellec, 2019). Figure and captions after Le Quellec (2013). With kind permission of Jean-Loïc Le Quellec. *Préhistoires Méditerranéennes* is an “Open Access” journal.

First human arrival in the Americas

For comparison purpose, also other regions are interesting that were less affected by the anthropic impact, such as the Americas, where the humans arrived in comparably much later time (see e.g. Dixon, 1993, including relics of mastodon hunting). The environmental changes in these areas are therefore almost exclusively determined by natural drivers. In this respect, however,

according to a recent finding, the humans may have occupied North America 100,000 years earlier than thought (Pultarova, 2017). In fact, Holen et al. (2017) investigated a 130,000 year -old archaeological site in southern California and describe their findings as follows.

“The earliest dispersal of humans into North America is a contentious subject, and proposed early sites are required to meet the following criteria for acceptance: (1) archaeological evidence is found in a clearly defined and undisturbed geologic context; (2) age is determined by

reliable radiometric dating; (3) multiple lines of evidence from interdisciplinary studies provide consistent results; and (4) unquestionable artifacts are found in primary context ... Here we describe the Cerutti Mastodon (CM) site, an archaeological site from the early late Pleistocene epoch, where in situ hammer-stones and stone anvils occur in spatio-temporal association with fragmentary remains of a single mastodon (*Mammuth americanum*). The CM site contains spiral-fractured bone and molar fragments, indicating that breakage occurred while fresh. Several of these fragments also preserve evidence of percussion. The occurrence and distribution of bone, molar and stone refits suggest that breakage occurred at the site of burial.

Five large cobbles (hammer-stones and anvils) in the CM bone bed display use-wear and impact marks, and are hydraulically anomalous relative to the low-energy context of the enclosing sandy silt stratum. $^{230}\text{Th}/\text{U}$ radiometric analysis of multiple bone specimens using diffusion-adsorption-decay dating models indicates a burial date of 130.7 ± 9.4 Ka ago. These findings confirm the presence of an unidentified species of *Homo* at the CM site during the last interglacial period (MIS 5e; early late Pleistocene), indicating that humans with manual dexterity and the experiential knowledge to use hammer-stones and anvils processed mastodon limb bones for marrow extraction and/or raw material for tool production. Systematic proboscidean bone reduction, evident at the CM site, fits within a broader pattern of Palaeolithic bone percussion technology in Africa ..., Eurasia ... and North America ... The CM site is, to our knowledge, the oldest in situ, well-documented archaeological site in North America and, as such, substantially revises the timing of arrival of *Homo* into the Americas."

The way is debated through which the first humans reached North America (see Fig. 50).¹⁹ According to Pedersen et al. (2016) (or see Ghose, 2016e; or McGowan, 2016), "during the LGM (last glacial maximum), continental ice sheets isolated Beringia (northeast Siberia and northwest North America) from unglaciated North America. By around 15 – 14 Cal ka BP (calibrated radiocarbon years before present), glacial retreat opened an approximately 1,500 km long corridor between the ice sheets. It remains unclear when plants and animals colonized this corridor and it became biologically viable for human migration. We obtained radiocarbon dates, pollen, microfossils and metagenomic DNA from lake sediment cores in a bottleneck portion of the corridor. We find evidence of steppe vegetation, bison and mammoth by approximately 12.6 Cal ka BP, followed by open forest, with evidence of moose and elk at about 11.5 Cal ka BP, and boreal forest approximately 10 Ca ka BP. Our findings reveal that the first Americans, whether Clovis or earlier groups in unglaciated North America before 12.6 Cal ka BP, are unlikely to have travelled by this route into the Americas. However, later groups may have used this north-south passageway."

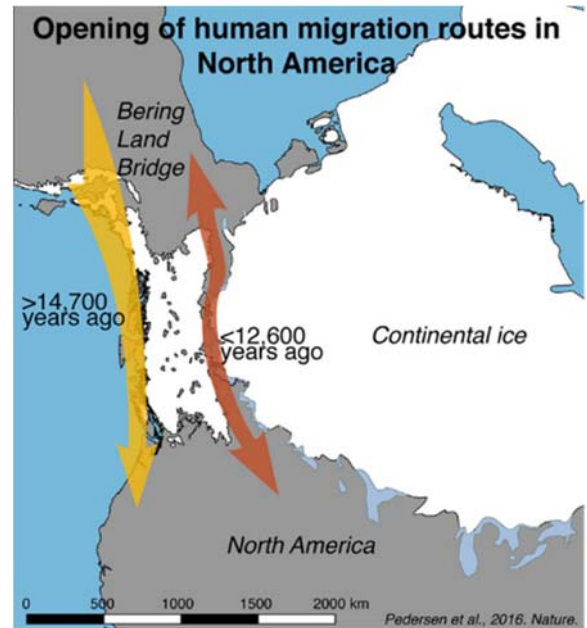


Fig. 50. "Map outlining the opening of the human migration routes in North America ... Image via Mikkel Winther Pedersen." Figure and captions after McGowan (2016). With kind permission of Deborah Byrd, EarthSky.org.

However, a recent finding of pre-Clovis projectile points changed the date guessed for the earliest Americans, according to Waters et al. (2018) that is illustrated by Geggel (2018i) as follows. "Archaeologists have unearthed what are potentially the oldest weapons ever found in North America: eleven spear-points dating to about 15,500 years ago ... If the discovery, located about 64 km NW of Austin, Texas, can be verified, it could strengthen the argument that people settled the Americas earlier than previously thought. But not all experts are convinced by the evidence, with some saying the dating techniques used are unconventional. The stone-made spear-points, each measuring up to 10 cm long, are so old they predate the Clovis people ...

...Who were the first Americans? ...Most researchers agree that the first Americans left northwest Asia and southern Siberia between 25,000 – 20,000 years ago and then traveled to the area of the now-submerged Bering Strait land bridge. But scientists disagree on how long they stayed in this region, known as Beringia, and which route people took from there - e.g. whether ancient people traveled inland or along the coast. ... For decades, researchers believed the first inhabitants of North America were part of the Clovis culture, which lasted from 13,000 – 12,700 years ago. But archaeological evidence suggests that people made it all the way to Monte Verde, Chile, at least 14,500 years ago, and there are other, more controversial sites in the Americas, that suggest they were peopled even earlier.

Almost all of these pre-Clovis sites have some stone tools, but the Texas site – the Debra L. Friedkin site, named for the family that owns the land - also has weapons that

¹⁹ An authoritative review of the available information is given by Dixon (1993).

were clearly made by pre-Clovis people ... The pointy spears were discovered beneath a layer that held projectile points made by the Clovis and Folsom peoples. (The Folsom people followed the Clovis culture ...) ... It's no surprise that so many cultures lived in this spot, since it had fresh water year-round ... The pre-Clovis layer holds about 100,000 artifacts, including 328 tools and 12 complete and fragmentary projectile points ... The soil around the newfound weapons dates to between 13,500 –

15,500 years ago ... the team ... used optically stimulated luminescence (OSL), which reveals how long ago quartz grains in the surrounding sediment were exposed to sunlight. ... the dating of these artifacts would be strengthened if the researchers relied on more than just OSL But Waters thinks the findings help paint a nuanced picture of the first Americans ... “

Geggel (2019) illustrates a map (Fig. 51) by “Jeffrey Bond, who studies the geology of ice age sediments at the Yukon Geological Survey in Canada”.



Fig. 51. “This newly designed map shows how Beringia - which includes the famous ice age land bridge - looked about 18,000 years ago. Credit: Bond, J. D. 2019. Paleodrainage map of Beringia. Yukon Geological Survey, Open File 2019-2.” Figure and captions after Geggel (2019). NASA copyright free policy.

Geggel (2019) comments that “... the Bering Land Bridge persisted for thousands of years, from about 30,000 years ago to 16,000 years ago, according to global sea-level estimates, ... The drop at 30,000 years ago was very rapid with the build up of ice sheets over North America ... for most of the time from about 30,000 – 18,000 years ago, the land bridge was nearly 1,000 km wide in the north-south direction ... At 18,000 years ago, Beringia was a relatively cold and dry place, with little tree cover. But it was still speckled with rivers and streams. Bond’s map shows that it likely had a number of large lakes. ‘Grasslands, shrubs and tundra-like conditions would have prevailed in many places’, Bond said. These environments helped megafauna - animals heavier than 45 kg - thrive, including the woolly mammoth, Beringian lion, short-faced bear, grizzly bear, muskox, steppe bison, American scimitar cat, caribou, Yukon horse, saiga antelope, gray wolf and giant beaver, according to the Yukon Beringia Interpretive Centre.

This vast, open region allowed megafauna and early humans to live off the land ... However, it’s still a mystery exactly when humans began crossing the land bridge. Genetic studies show that the first humans to cross became genetically isolated from people in East Asia between about 25,000 – 20,000 years ago. And archaeological evidence shows that people reached the Yukon at least 14,000 years ago, Bond said. But it’s still unclear how long it took the

first Americans to cross the bridge and what route they took. The fact that this land bridge was repeatedly exposed and flooded and exposed and flooded over the past 3 Ma is really interesting because Beringia, at its largest extent, was really a high latitude continental landscape ... “

A careful genetic investigation is reported by Posth et al. (2018) who synthesize their inference by means of their graphical abstract in Fig. 52. They explain their study as follows. “We report genome-wide ancient DNA from 49 individuals forming four parallel time transects in Belize, Brazil, the Central Andes, and the Southern Cone, each dating to at least ~ 9,000 years ago. The common ancestral population radiated rapidly from just one of the two early branches that contributed to Native Americans today.

We document two previously unappreciated streams of gene flow between North and South America. One affected the Central Andes by ~ 4,200 years ago, while the other explains an affinity between the oldest North American genome associated with the Clovis culture and the oldest Central and South Americans from Chile, Brazil, and Belize. However, this was not the primary source for later South Americans, as the other ancient individuals derive from lineages without specific affinity to the Clovis associated genome, suggesting a population replacement that began at least 9,000 years ago and was followed by substantial population continuity in multiple regions.”

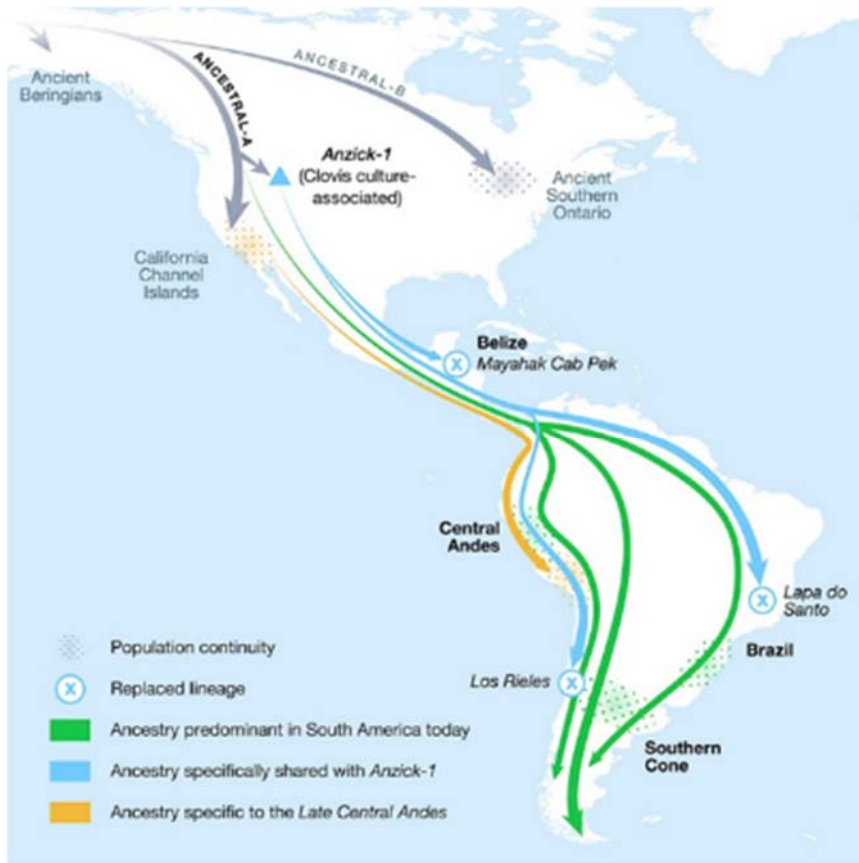


Fig. 52. “According to a new ancient DNA analysis, prehistoric people from different populations made their way across the Americas thousands of years ago. Credit: Michelle O’Reilly; Posth et al. (2018).” Figure and captions after Geggel (2018j). Reproduced with kind permission of Cell (“Open Access”).

Geggel (2018j) illustrates their investigation and gives some detail. “... People genetically linked to the Clovis culture ... made it down to South America as far back as 11,000 years ago. Then they mysteriously vanished around 9,000 years ago ... findings ... suggest that this population turnover happened across the entire continent of South America ...

... Previous research suggests that the first Americans diverged genetically from their Siberian and East Asian ancestors almost 25,000 years ago. These people traveled across the Bering Strait Land Bridge and eventually split into distinct North and South American populations. By about 13,000 years ago, people of the Clovis culture, known for its use of distinctive, pointy stone tools, swept across North America. Meanwhile, people were living as far south as Monte Verde, Chile by least 14,500 years ago ... findings showed that DNA associated with the North American Clovis culture was found in people from Chile, Brazil and Belize, but only between about 11,000 – 9,000 years ago ...

... A key discovery was that a Clovis culture-associated individual from North America dating to around 12,800 years ago shares distinctive ancestry with the oldest Chilean, Brazilian and Belizean individuals ... Curiously, around 9,000 years ago, the Clovis lineage disappears ... Even today, there is no Clovis-associated DNA found in modern South Americans ... This suggests that a continent-wide population replacement happened at that time ...

Following this mysterious disappearance, there is a surprising amount of genetic continuity between people who lived 9,000 years ago and those living today in multiple South American regions ... The ... study also revealed a surprising connection between ancient people living in California’s Channel Islands and the southern Peruvian Andes at least 4,200 years ago. It appears that these two geographically distant groups have a shared ancestry ...

It’s unlikely that people living in the Channel Islands actually traveled south to Peru ... Rather, it’s possible that these groups’ ancestors sallied forth thousands of years earlier, with some ending up in the Channel Islands and others in South America. But those genes didn’t become common in Peru until much later, around 4,200 years ago, when the population may have exploded ... There is archaeological evidence that the population in the Central Andes area greatly expanded after around 5,000 years ago ... The approximately 11 000 year-old individual from the Chile site of Los Rieles was the oldest in the study ... “

Human migration is a difficult topic of investigation. A modeling was carried out by Timmermann and Friedrich (2016), also illustrated by Choi (2016j) who shows, as an example, Fig. 53.

Timmermann and Friedrich (2016) appeal to Milanković and briefly summarize their investigation as follows. “On the basis of fossil and archaeological data it has been hypothesized that the exodus of Homo Sapiens out of Africa and into Eurasia between ~ 50 – 120 ka ago occurred in several orbitally paced migration episodes ...

Crossing vegetated pluvial corridors from northeastern Africa into the Arabian Peninsula and the Levant and expanding further into Eurasia, Australia and the Americas, early *Homo Sapiens* experienced massive time-

varying climate and sea-level conditions on a variety of timescales. Hitherto it has remained difficult to quantify the effect of glacial- and millennial-scale climate variability on early human dispersal and evolution.

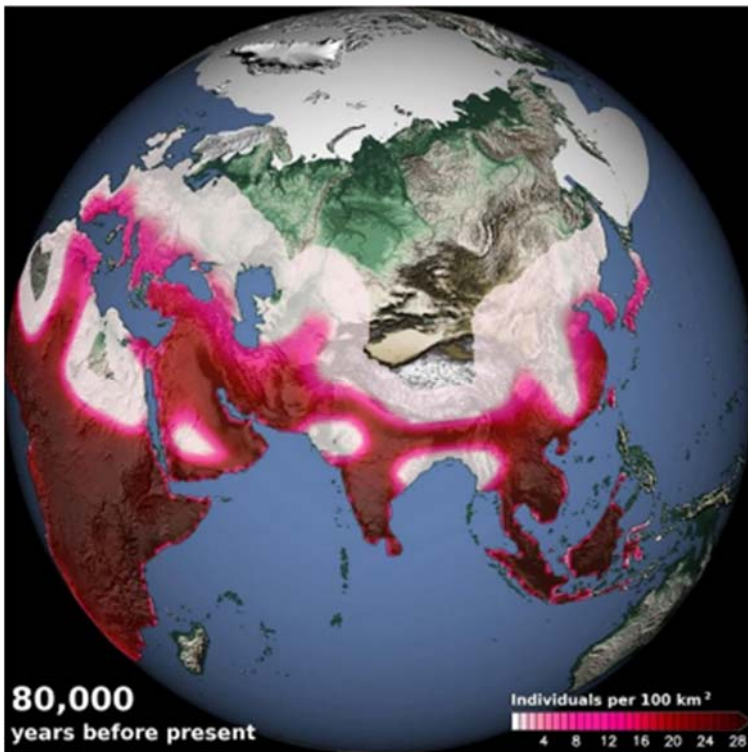


Fig. 53. “A computer model simulated human density 80,000 years ago, showing the arrival of humans in eastern China and southern Europe as well as migrations out of Africa along vegetated paths in Sinai and the Arabian Peninsula. Credit: Tobias Friedrich.” Figure and captions after Choi (2016j). NASA copyright free policy.

Here we present results from a numerical human dispersal model, which is forced by spatiotemporal estimates of climate and sea-level changes over the past 125 ka. The model simulates the overall dispersal of *Homo sapiens* in close agreement with archaeological and fossil data and features prominent glacial migration waves across the Arabian Peninsula and the Levant region around 106 – 94 ka, 89 – 73 ka, 59 – 47 ka and 45 – 29 ka ago. The findings document that orbital-scale global climate swings played a key role in shaping Late Pleistocene global population distributions, whereas millennial-scale abrupt climate changes, associated with Dansgaard-Oeschger events, had a more limited regional effect.”

In addition, the western USA deserts were relatively wet up until ~ 8,200 years ago (see e.g. Anonymous, 2015bb; Chu, 2015a). In fact, Steponaitis et al. (2015) summarize as follows their investigation on stalagmites.

Dramatic changes in Great Basin water balance during the last 25 ka are shown by lake level records, even though the timing and pace is poorly documented of Holocene drying in the region. Steponaitis et al. (2015) studied stable isotope and trace metal data from two speleothems of the Lehman Caves, NV, dealing with a well-dated information of hydroclimate in the Great Basin during the latest

Pleistocene to mid-Holocene. The time span is 16.4 – 3.8 ka, including a hiatus from 15.0 – 12.7 ka. They claim that “Mg/Ca and $\delta^{13}\text{C}$ covary throughout the records, consistent with control by the extent of degassing and prior calcite precipitation²⁰ (PCP)”. In fact, measurements of modern cave and soil waters, both support the primary control on drip-water trace-element composition by PCP. Therefore, Steponaitis et al. (2015) infer that Mg/Ca and $\delta^{13}\text{C}$ reflect the infiltration rates, and higher values are indicative of drier periods. Thus, both Mg/Ca and $\delta^{13}\text{C}$ show a wet period during 12.7 – 8.2 ka, at the beginning of the record, which preceded a pronounced drying after 8.2 ka.

Steponaitis et al. (2015) stress that the mid-Holocene drying is confirmed by the evidence around the western U. S., also by a new compilation of the lake-level records in the Great Basin. Specifically, the collapse of the Laurentide ice sheet over Hudson Bay corresponded to this drying and may have been triggered by the winter storm track that drifted northward due to ice sheet retreat. We note that this event may have been related to a change of the local endogenous heat release that caused the ice sheet retreat.

Steponaitis et al. (2015) comment that, however, the alternative hypothesis cannot be excluded that a connection existed between wet early Holocene conditions and the

stalagmite”, according to Hori et al. (2013) who report about an investigation on stalagmites in Japan.

²⁰ Concerning the prior calcite precipitation (PCP) definition, it is “carbonate precipitation from infiltrating water before the water drips on a

equatorial Pacific SST. In any case, Steponaitis et al. (2015) conclude that their results “suggest that Great Basin water balance in the early Holocene was driven by factors other than orbital changes.”

The role of climate as a critical driver is also debated when dealing with a comparably recent historical time. For instance, it is guessed that the decay of the Maya civilization occurred at the end of a prolonged period of drought, according to the finding by Hoggarth et al. (2016) who identified three major intervals of drought between AD 820 – 1100, with two waves at AD 850 – 925 and AD 1000 – 1050.

The recent historical period is even more intricate. According to Graham (2019) who reports *BBC*, “epidemics brought by European settlers killed such a huge number of indigenous Americans that there was a drop in CO₂ in the atmosphere, cooling the climate. Regrowth of forests on depopulated land caused around half of the drop in carbon that has been observed in Antarctic ice cores, and contributed to the ‘Little Ice Age’ of the 1600s. Researchers estimate that colonization led to the deaths of 56 million of the estimated 60 million inhabitants of North and South America between 1492 and 1600.”

That is, the humans and the microorganism responsible for epidemics are altogether a unique biological system that interacts with “climate”. In general, this occurs in some unpredictable way.

For instance, it is often stated that the cruel Genghis Khan (c. 1162-1227) conquered Eurasia and got rid of the several robbers who plundered and killed travelers. The new “order” permitted the development of travels, and the Marco Polo (1254-1324) travels are the best known case histories. It is claimed that the more frequent travels favored the widespread of epidemics between western and eastern world.

Chinese dynasties

Also, the Chinese dynasties were probably affected by severe drought periods. For instance, Tan et al. (2015) used ancient cave inscriptions to infer the anthropic record of severe droughts, to be compared with other proxies. This is an example of how humans were direct recorders of climate data. Tan et al. (2015) synthesize as follows their results, and show, among others, Figs 54 and 55, where *DY1* denotes a stalagmite from the Dayu cave.

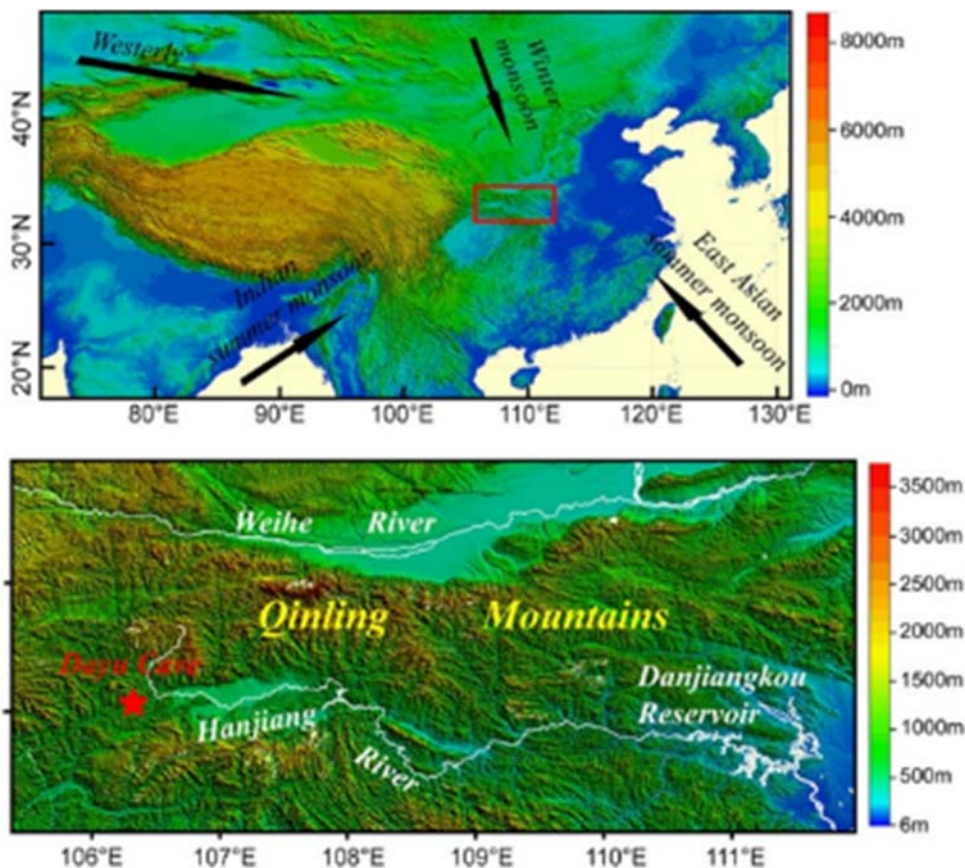


Fig. 54. “Location of Dayu Cave. The upper panel is an overview topographic map showing the study region (red rectangle). Black arrows denote the directions of the East Asian summer monsoon, Indian summer monsoon, East Asian winter monsoon, and Westerly, which affect the climate in China. The lower panel is an enlarged map showing the location of Dayu Cave (33° 08'N , 106° 18'E , 870 m asl) in southern Qinling Mountains. The Hanjiang and Weihe River, as well as the Danjiangkou Reservoir are also shown ... “ Figure and captions after Tan et al. (2015). Reproduced with kind permission of *Scientific Reports*, (CC BY 4.0).

“The collapse of some pre-historical and historical cultures, including Chinese dynasties were presumably linked to widespread droughts, on the basis of synchronicities of societal crises and proxy-based climate events. Here, we present a comparison of ancient inscriptions in Dayu Cave from Qinling Mountains, central China, which described accurate times and detailed

impacts of seven drought events during the period of AD 1520 – 1920, with high-resolution speleothem records from the same cave. The comparable results provide unique and robust tests on relationships among speleothem $\delta^{18}O$ changes, drought events, and societal unrest. With direct historical evidences, our results suggest that droughts and even modest events interrupting otherwise wet intervals can

cause serious social crises. Modeling results of speleothem $\delta^{18}\text{O}$ series suggest that future precipitation in central China may be below the average of the past 500 years. As Qinling Mountain is the main recharge area of two large water transfer projects and habitats of many endangered species, it is imperative to explore an adaptive strategy for the decline in precipitation and/or drought events.”

A later synthesis is given by Liu et al. (2018) who illustrate their study as follows. “... The $\delta^{18}\text{O}$ records from Chinese cave deposits can be used as an indicator for Asian summer monsoon (ASM) variability, which is closely related to changes of North Atlantic climates and shifts of the ITCZ (Intertropical Convection Zone). In this study, a comparison of $\delta^{18}\text{O}$ records from different caves in China revealed that the ASM declined rapidly at the onset of the Heinrich events in the last glacial period but gradually at the onset of Bond events in the Holocene. This indicates that the volume of freshwater inputs into the North Atlantic during the Heinrich events was large, and the southerly movement of the ITCZ was exceptionally significant. As an atmospheric bridge linking bipolar climate changes, different expressions in ASM variations in the last glacial and the Holocene should be considered when correlating northern and southern hemispheric climate changes.”

More in detail, Liu et al. (2018) specify that “detailed ASM variability across Heinrich stadials (HSs) 5 to 2 was reconstructed from four stalagmite $\delta^{18}\text{O}$ records in central and southern China. For the last glacial period, these speleothem records, combined with previous cave records, reveal a rapid ASM decline at the onset of each HS. During this time, ASM intensity decreases immediately to the weakest level within approximately 50 years, which is followed by a gradual intensification in the mid-HS. Typically, this process of ASM weakening is synchronous with peak ice-rafted debris deposition and large freshwater outbursts into the North Atlantic, implying a tight link between the two. During the Holocene, however, a relatively gradual ASM decrease occurred at the start of the Bond events. Comparatively, the ASM decrease during the Bond events is generally accomplished within 110 years, and the weakest ASM occurs near the end. This difference implicates a further southward displacement of the ITCZ and a stronger impact from the AMOC on the ASM in the early HS. Moreover, contrasting expressions of the ASM during HSs and Bond events suggest that a fixed phase relationship during bipolar climate changes cannot be expected.”

The global perspective

Phenomena, however, are not simple. For instance, even the popular notion is being questioned that 10th century Norse people colonized Greenland because of a period of unusually warm weather. In fact, Young et al. (2015) claim that “the climatic mechanisms driving the shift from the Medieval Warm Period (MWP) to the Little Ice Age (LIA) in the North Atlantic region are debated. We use cosmogenic ^{10}Be dating to develop a moraine chronology with century-scale resolution over the last millennium and

show that alpine glaciers in Baffin Island and western Greenland were at or near their maximum LIA configurations during the proposed general timing of the MWP. Complimentary palaeoclimate proxy data suggest that the western North Atlantic region remained cool, whereas the eastern North Atlantic region was comparatively warmer during the MWP - a dipole pattern compatible with a persistent positive phase of the NAO.

These results demonstrate that over the last millennium, glaciers approached their eventual LIA maxima before what is considered the classic LIA in the NH. Furthermore, a relatively cool western North Atlantic region during the MWP has implications for understanding Norse migration patterns during the MWP. Our results, paired with other regional climate records, point to non-climatic factors as contributing to the Norse exodus from the western North Atlantic region.”

Rush et al. (2023), which is illustrated by University of Leeds (2023), investigated a core from Scotland's Ythan Estuary and suggest that a melting ice sheet was the likely trigger of a major climate-change 8,200 years ago. This coincided with a significant cooling in North Atlantic and in Northern Europe. A change occurred of a major system of ocean currents (AMOC). They guess that the influx of a massive amount of freshwater into the salt-water of the North Atlantic caused the break down of AMOC. According to University of Leeds (2023), “... The analysis of the core samples provides further evidence that there were at least two major sources of freshwater that drained into the North Atlantic, causing the changes to the AMOC, and not a single source as previously thought. The view held by many scientists was that the freshwater had come from a giant lake - Lake Agassiz-Ojibway, which was the size of the Black Sea and was situated near what is now northern Ontario - which had drained into the ocean.

Dr. Rush said: ‘we have shown, that although huge, the lake was not large enough to account for all that water going into the ocean and causing the sea-level rise that we observed.’ Instead, Dr Rush and his colleagues believe the melting of the Hudson Bay Ice Saddle which covered much of eastern Canada and the north-eastern United States provided the injection of vast quantities of water that was reflected in the core samples....

Temperatures in the North Atlantic and Europe dropped by between 1.5°C and 5°C and lasted for about 200 years, with other regions experiencing above-average warming. Levels of rainfall also increased in Europe, while other parts of the world, such as parts of Africa, experienced drier conditions and extended periods of drought ...”

We point out that these events seemingly derived from a large release of endogenous energy beneath the northern polar cap - it does not matter whether this event originated melting of the ice cover in the Hudson Bay and North America, or in Greenland. Endogenous heat is the likely trigger for these phenomena.

In general climate must be considered as a unique response by the whole Earth system. The events that occur in every given region affect all other areas of the planet, including the role of humankind, which is a driver like

every other component of the system. Therefore, e.g., agriculture and irrigation have relevant effects on the planetary scale, due to a much faster erosion, but also to water injection in the atmosphere.

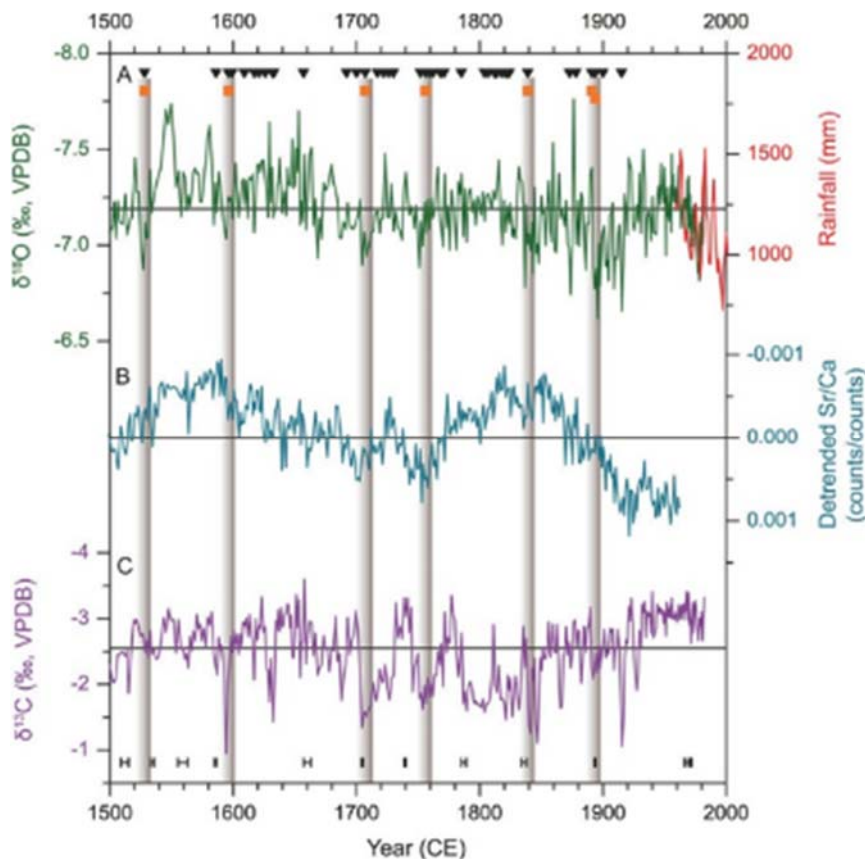


Fig. 55. “Comparison of drought events recorded in the inscriptions with speleothem $\delta^{18}\text{O}$, $\delta^{13}\text{C}$ and Sr/Ca records in Dayu Cave during the last 500 years. The black triangles indicate 70 visits recorded in the cave, with some occurred in the same year. The orange squares indicate seven historical drought events occurred in AD 1528, 1596, 1707, 1756, 1839, 1891 and 1894, respectively. (A) $\delta^{18}\text{O}$ record of DY1 (dark green). The red line represents annual rainfall amount record from the Ningqiang meteorological station, 38 km south of Dayu Cave, during the period 1957–2000, with a 3 year moving average. (B) Detrended Sr/Ca record of DY1 (light blue); (C) $\delta^{13}\text{C}$ record of DY1 (purple). Black vertical bars show locations of ^{230}Th dates, with errors of $\pm 0.4 - \pm 4$ years. The straight lines in panel (A) and (C) indicate the average $\delta^{18}\text{O}$ (-7.19 ‰) and $\delta^{13}\text{C}$ (-2.54 ‰) values of the entire series, respectively.” Figure and captions after Tan et al. (2015). Reproduced with kind permission of Scientific Reports, (CC BY 4.0).

For instance, de Vrese et al. (2016) investigated the present role of irrigation in Asia on the control of rainfall in Africa. They synthesize their investigation as follows. “Irrigation is not only vital for global food security but also constitutes an anthropogenic land use change, known to have strong effects on local hydrological and energy cycles. Using the Max Planck Institute for Meteorology’s Earth System Model, we show that related impacts are not confined regionally but that possibly as much as 40% of the present-day precipitation in some of the arid regions in Eastern Africa are related to irrigation-based agriculture in Asia. Irrigation in South Asia also substantially influences the climate throughout Southeast Asia and China via the advection of water vapor and by altering the Asian monsoon. The simulated impact of irrigation on remote regions is sensitive to the magnitude of the irrigation-induced moisture flux. Therefore, it is likely that a future extension or decline of irrigated areas due to increasing food demand or declining fresh water resources will also affect precipitation and temperatures in remote regions.”

That is, the demographic expansion is a critical driver for planetary climate, with either positive or unwanted consequences. However, also extinctions implied a climate change, due to a different kind of fauna that changed the biosphere impact on the whole system. For instance, Bakker et al. (2016) investigated the impact of megafauna

extinctions on woody vegetation. They summarize as follows their inference. “Until recently in Earth history, very large herbivores (mammoths, ground sloths, diprotodons, and many others) occurred in most of the world’s terrestrial ecosystems, but the majority have gone extinct as part of the late-Quaternary extinctions. How has this large-scale removal of large herbivores affected landscape structure and ecosystem functioning? In this review, we combine palaeo-data with information from modern enclosure experiments to assess the impact of large herbivores (and their disappearance) on woody species, landscape structure, and ecosystem functions. In modern landscapes characterized by intense herbivory, woody plants can persist by defending themselves or by association with defended species, can persist by growing in places that are physically inaccessible to herbivores, or can persist where high predator activity limits foraging by herbivores. At the landscape scale, different herbivore densities and assemblages may result in dynamic gradients in woody cover.

The late-Quaternary extinctions were natural experiments in large-herbivore removal; the palaeoecological record shows evidence of widespread changes in community composition and ecosystem structure and function, consistent with modern enclosure experiments. We propose a conceptual framework that

describes the impact of large herbivores on woody plant abundance mediated by herbivore diversity and density, predicting that herbivore suppression of woody plants is strongest where herbivore diversity is high. We conclude that the decline of large herbivores induces major alterations in landscape structure and ecosystem functions.”

In addition, an important anthropic impact on climate resulted from the reduction of forest cover due to expansion of agriculture and of use of territory. This item was investigated by Kaplan et al. (2016), who also showed the series of self-explanatory Figs 56 through 60 that are here reported upon consideration of their synthetic and clear

information. Note the acronym *PFT* for plant functional type, and *APFT* for average *PFT*. For brevity purpose the details of the model (explained in Pfeiffer et al., 2013) are here omitted. The model is denoted as *LPJmL*, or *Lund-Potsdam-Jena managed Land* model that is described as follows by the website of the *Postdam Institute for Climate Impact Research*. “The *LPJmL* model has been developed from *LPJ*, a Dynamic Global Vegetation Model (DGVM), which was designed to simulate the global terrestrial carbon cycle and the response of carbon and vegetation patterns under climate change. As carbon and water cycles are intimately linked, it was quickly extended to also simulate the terrestrial water cycle ...”

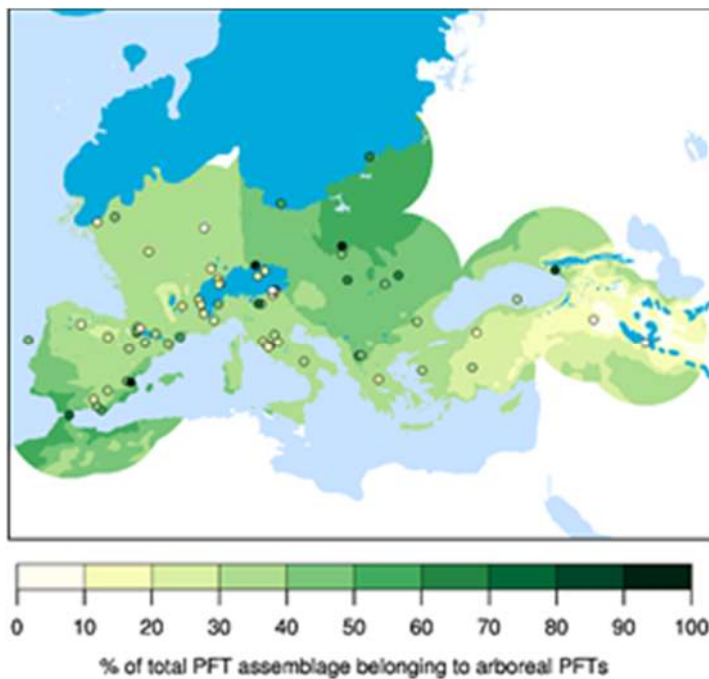


Fig. 56. “Pollen-based reconstructed tree cover at LGM. Estimated tree cover at LGM (APFT%), calculated as percent sum of all PFT scores belonging to arboreal PFTs. The tree cover surface is based on the 3D interpolation of PFT scores from individual fossil pollen sites (circles) ... “Figure and captions after Kaplan et al. (2016). With kind permission of *PLoS ONE* (“Open Access”).

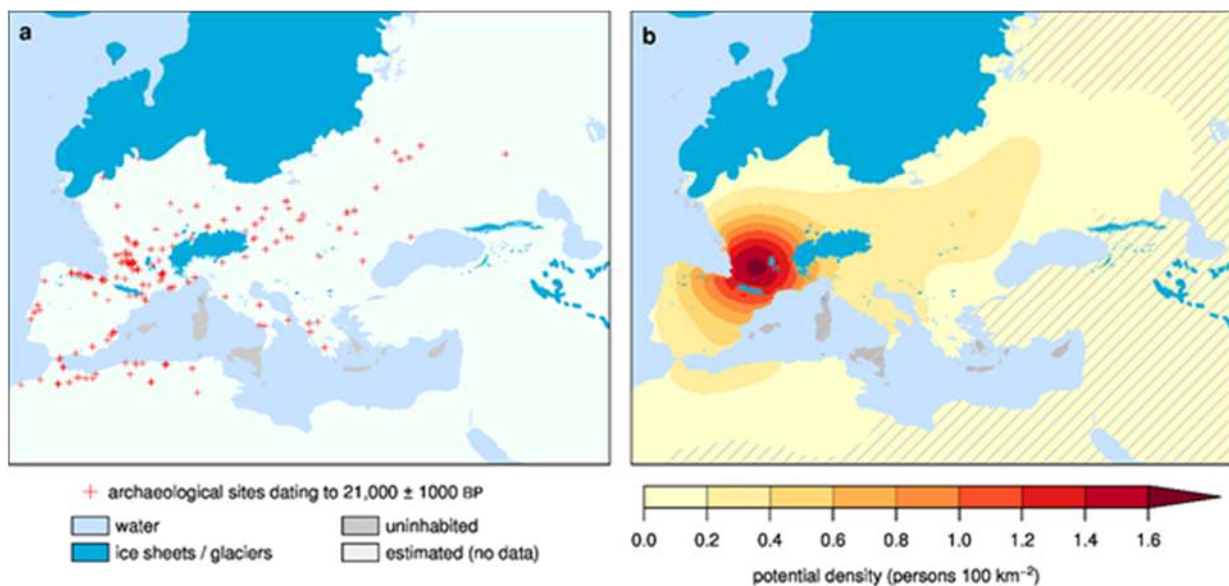


Fig. 57. “Archaeological evidence for human population in LGM Europe. (A) Distribution of archaeological sites dating to LGM ... (B) estimated baseline population density using kernel interpolation ... “ Figure and captions after Kaplan et al. (2016). With kind permission of *PLoS ONE* (“Open Access”).

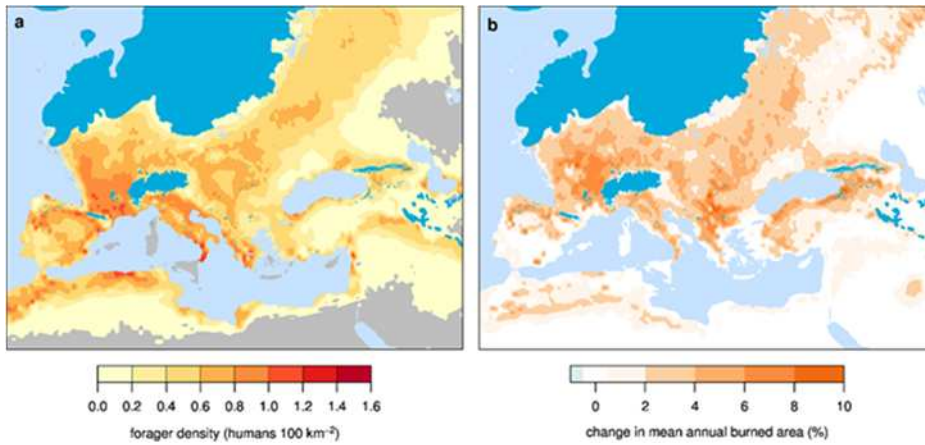


Fig. 58. “Forager population density and human induced fire at LGM. (A) Forager population density, and (B) the change in mean annual burned area ... “ Figure and captions after Kaplan et al. (2016). With kind permission of PLoS ONE (“Open Access”).

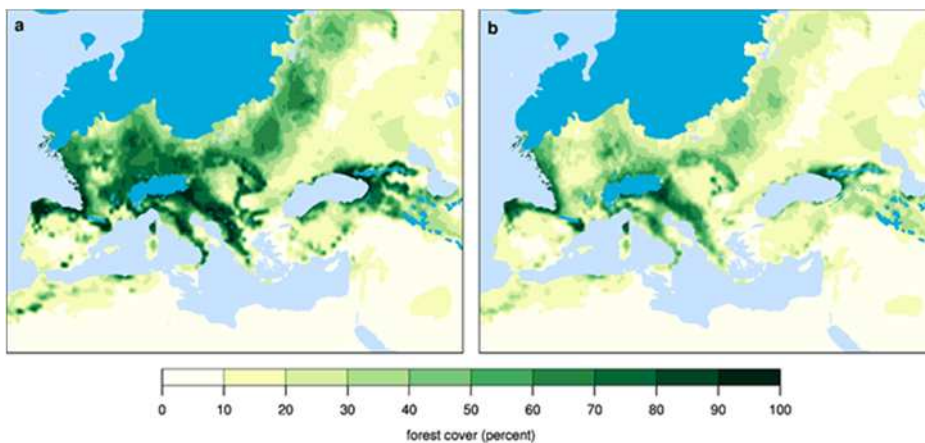


Fig. 59. “Influence of anthropogenic burning on tree cover in LGM Europe. (A) Tree cover simulated without and (B) with human burning ... “ Figure and captions after Kaplan et al. (2016). With kind permission of PLoS ONE (“Open Access”).

Kaplan et al. (2016) state that “reconstructions of the vegetation of Europe during the LGM are an enigma. Pollen-based analyses have suggested that Europe was largely covered by steppe and tundra, and forests persisted only in small refugia. Climate-vegetation model simulations on the other hand have consistently suggested that broad areas of Europe would have been suitable for forest, even in the depths of the last glaciation. Here we reconcile models with data by demonstrating that the highly mobile groups of hunter-gatherers that inhabited Europe at the LGM could have substantially reduced forest cover through the ignition of wildfires. Similar to hunter-gatherers of the more recent past, Upper Palaeolithic humans were masters of the use of fire, and preferred inhabiting semi-open landscapes to facilitate foraging, hunting and travel. Incorporating human agency into a dynamic vegetation-fire model and simulating forest cover shows that even small increases in wildfire frequency over natural background levels resulted in large changes in the forested area of Europe, in part because trees were already stressed by low atmospheric CO₂ concentrations and the cold, dry, and highly variable climate ... “

That is, wildfires, whether anthropic-ondiced, or natural, are an important factor for the control of clime (see Gregori and Leybourne, 2025i).

Summarizing, concerning Sahara and Sahel, in general it appears that there is a great need for investigating the sedimentary history of the dried lakes of Sahara that can certainly give some very useful and interesting information

on the palæo- and archao-climatology of entire Earth. These case histories are particularly interesting due to the overlapping of climate changes of natural origin with an increasing anthropic impact. That is, these regions are effective laboratories for the investigation of environmental anthropology and of the concrete role of the humans in the climate change. This also proves the importance of the shallow geotherms of the Tang Maocang school that monitor the geothermal exhalation as a critical impact to the “climate” system. In addition, it appears that “climate” is a very complicated system, and it cannot be simply reduced to the result of one “simple” process alone. Several concurrent drivers contribute to determine its extremely complicated morphology, and the anthropic impact is just one of the several “natural” causes. The anthropic impact cannot be conceived either as the unique driver, or a negligible impact factor,

Fig. 61 shows the Sahel rainfall index that was defined in 1996 by Todd Mitchell, of the *University of Washington, Joint Institute for the Study of the Atmosphere and Ocean (JISAO)*. The averaging region (20° – 8°N , 20°W – 10°E) is based on a study by Janowiak (1988), who evaluated the “rotated” principal component analysis of average African rainfall during June through September. The index is an average that is standardized such that the mean and standard deviation of the series are 0 and 1, respectively, for the entire period of every given plot. Extended wet periods were thus found in 1905-1909 and 1950-1969 and extended dry periods in 1910-1914 and

1970-1997. From 1990 until present rainfall returned to levels slightly below the 1898-1993 average, but year-to-year variability was high. This anomalous trend raised a great concern and debate about its interpretation. The problem is presently unsolved. No details can be here entered, and the literature is very large. The recent greening of Sahel is raising several discussions (e.g. Olsson et al., 2005; Olsson, 2008), including the impact on - and/or the feedback from - vegetation and the humans (e.g. Herrmann et al., 2005; Seaquist et al., 2008).

Olsson (2008) shortly reminds about this item as follows. “The first and the most well-known mechanism was proposed in the mid 1970s by Otterman and Charney and often referred to the ‘Charney hypothesis’, by which albedo increases, due to overgrazing and cultivation, leads to a general cooling of the land surface and thereby reductions of evapotranspiration and of surface air convergence, leading to reductions of cloudiness and rainfall. This chain of effects was hypothesized to cause a positive feedback loop responsible for the persistent drought in the Sahel. Model studies using the Goddard Institute for Space Studies (GISS) general circulation model (GCM) suggested that albedo changes from 14% to 35% over all continents’ desert areas would sharply reduce clouds and rainfall. These results were, however, contested by Ripley, claiming that the model did not adequately treat the role of

evapotranspiration in regulating surface temperature and also that the albedo changes assumed were much larger than might be supported by observations. According to Ripley, regions with higher albedo are generally hotter than their surroundings due to the lower rate of evapotranspiration, a conclusion supported by a study using the NCAR GCM. The Otterman-Charney mechanism was further questioned based on studies in the Sonoran Desert in Mexico, claiming that denuding the soil may have completely opposite thermal and climatic effects. More recently, a number of modeling studies have concluded that vegetation changes play a significant role in the rainfall variability of the Sahel but so far a convincing explanatory mechanism is elusive ... “ Different studies considered vegetation dynamics, desertification, coupled ocean-land climate models, but no general agreement was found and the actual mechanism that controls rain in Sahel is not clear. A somewhat better relation was found with SST anomalies.

“The observed trend has also been subject to studies aimed at quantifying the role of the Sahel in the global tropical carbon balance. By using a mechanistic vegetation model it was possible to quantify the net amount of carbon being accumulated in the Sahel region as a result of the increasing greenness. Over the period 1983-1999, the Sahel accumulated on average $\sim 8.4 \text{ g C m}^{-2} \text{ year}^{-1}$, and aggregated over the entire region $\sim 50 \text{ Mtons C year}^{-1}$.”

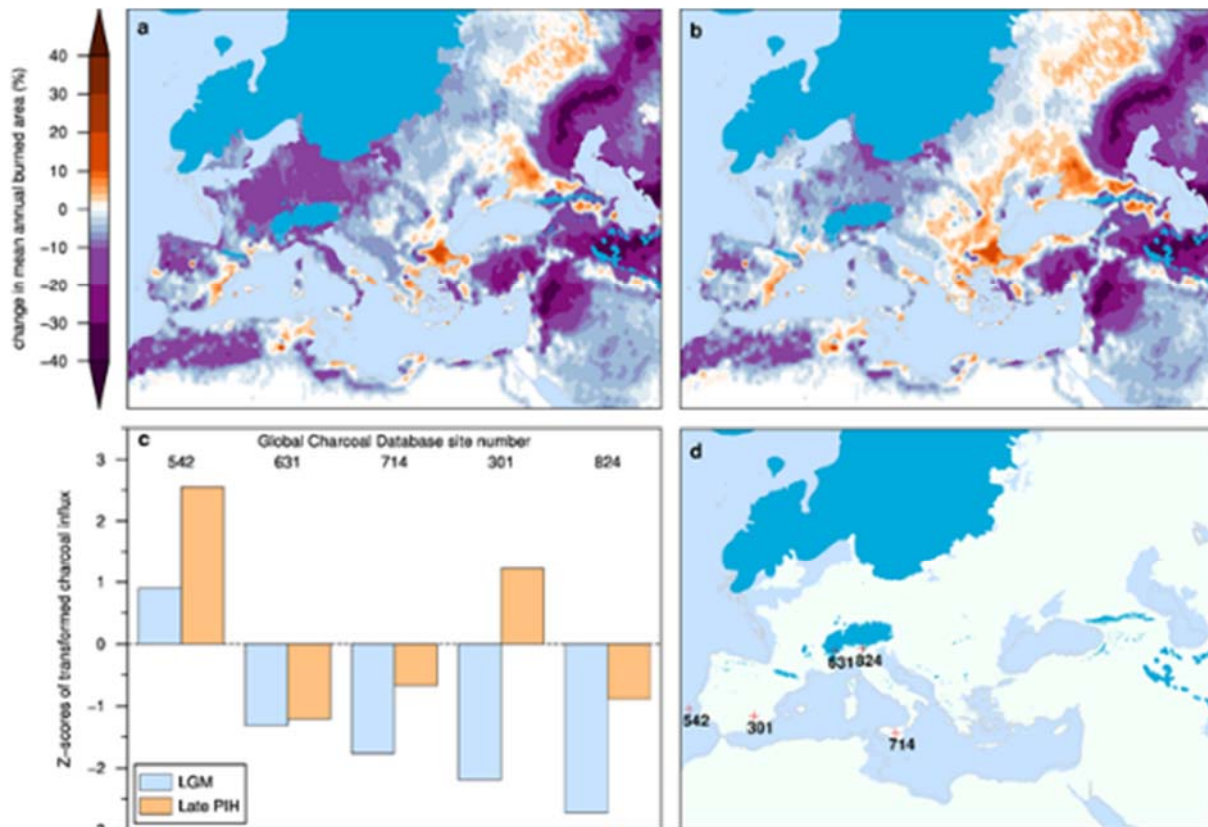


Fig. 60. “Change in burned area fraction between LGM and the Preindustrial Holocene (PIH). Difference in mean annual burned area fraction between LGM and the late PIH (AD 1770) in (A) the LPJ ensemble mean simulation without human burning, and in (B) the LPJ ensemble mean scenario including human burning. Panel (C) shows relative charcoal accumulation at the LGM and late PIH (AD 1650 ± 200 year) at the five Global Charcoal Database sites (D) containing lake and marine sediment microcharcoal dating to LGM ... At all charcoal sites the charcoal influx is smaller in samples dated to LGM compared to the PIH. The gray outline is the LGM coastline.” Figure and captions after Kaplan et al. (2016). With kind permission of PLoS ONE (“Open Access”).

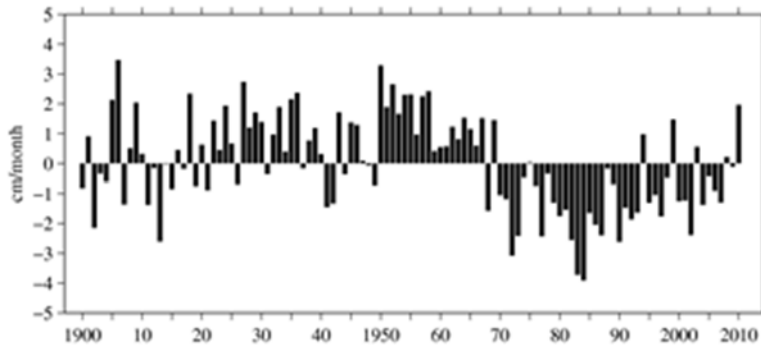


Fig. 61. Standardized Sahel rainfall index (see text), for 1900 - Oct 2008. Reproduced with permission. Credit: Todd Mitchell, NASA, Joint Institute for the Study of the Atmosphere and Ocean (JISAO). NASA copyright free policy.

Nicholson (2017) is a recent and authoritative review that summarizes her findings as follows. “Because of recent droughts and evidence of disastrous, long-term climatic change, the region has become a major focus of meteorological research. This review covers six relevant topics: climatic regionalization, seasonal cycle, intraseasonal variability, interannual variability, recent trends, and seasonal forecasting. What emerges is a markedly different view of the factors modulating rainfall, the dynamics associated with the seasons, and the character of teleconnections within the region and the interrelationships between the various rainy seasons. Some of the most important points are the following.

(1) - The paradigm of two rainy seasons resulting from the biannual equatorial passage of the ITCZ is inadequate.

(2) - The ‘long rains’ should not be treated as a single season, as character, causal factors, and teleconnections are markedly different in each month.

(3) - The ‘long rains’ have been declining continuously in recent decades.

(4) - The Madden-Julian Oscillation (MJO) has emerged as a factor in interannual and intraseasonal variability, but the relative strength of Pacific and Indian Ocean anomalies plays a major role in the downward trend.

(5) - Factors governing the ‘short rains’ are nonstationary.

(6) - Droughts have become longer and more intense and tend to continue across rainy seasons, and their causes are not adequately understood.

(7) - Atmospheric variables provide more reliable seasonal forecasts than the factors traditionally considered in forecast models, such as SSTs and ENSO.”

The interview is noteworthy to Sharon E. Nicholson, reported by Nicholson (2017a) that better clarifies a few main items. “Does the annual migration of the ITCZ affect rainfall over eastern Africa?

No, it does not. The ITCZ is best developed over the ocean. Such a convergence zone is evident over northern Africa, but it lies well north of eastern Africa throughout the year. Over the equatorial regions of Africa, a seasonal migration of the tropical rainfall zone is evident, producing the seasonal cycle in eastern Africa. However, it is not manifested as a low-level zone of wind convergence. The factors enhancing rainfall during the two main rainy seasons, and producing aridity during the other seasons, are much more complex and not yet completely understood.

What kind of extreme climate events does the region experience?

Eastern Africa faces some of the most extreme climatic events in the world. This includes not only devastating droughts, but also extreme flood conditions, sometimes within the same year. The most extreme flood occurred in 1961; Lake Victoria rose several meters and November rainfall in northern Kenya was several times the annual mean. In contrast, during the 2010-2011 drought rainfall was at least 50-75% below the long-term mean in Kenya, southern Somalia, and southern Ethiopia. Yet, high rainfall in November 2009, January 2010, and November 2011 produced flood situations.

Has the occurrence of extreme climate events changed over recent years?

Extreme climatic events in eastern Africa have increased in both frequency and severity in recent years. Droughts have become longer and more intense, and they now tend to continue across rainy seasons. They also appear to be affecting both the northern areas, where rainfall occurs primarily in the boreal summer, and the equatorial regions, with two rainy seasons during the boreal spring and autumn. At the same time, interannual variability has increased, producing unusually strong floods in the region. Overall, however, there is a general increasing tendency in the rains of the boreal autumn (the ‘short rains’), but a decline in the rains of the boreal spring (the main, ‘long rains’ season).

What are the main drivers of year to year rainfall variability and extreme events?

The main drivers are distinct for the three rainy seasons (summer, ‘long rains’, ‘short rains’). In the summer rainfall region (northeastern area), El Niño plays a major role in the summer rainfall region, but low- and mid-level westerly flow, a strong Somali Jet, and a strong Tropical Easterly Jet also enhance rainfall.

The main factor in the ‘short rains’ is the intensity of the Walker cell in the central equatorial Indian Ocean, an atmospheric circulation system which in turn has some association to both the ENSO and the Indian Ocean Zonal Mode. The drivers of the ‘long rains’ have been less definitely established, but the MJO and the relative temperature of the tropical Pacific and Indian Oceans appear to be very important.

How can prediction of climate variability be improved?

Predictability is already high for the ‘short rains’. For the ‘long rains’ it could be improved by considering each

month of the season separately and by producing individual forecasts for smaller sectors within eastern Africa. Further improvement can also be achieved by taking atmospheric variables (as opposed to SST and other surface variables) into consideration in forecast models.

Where is additional research needed to improve understanding in this field?

A major unresolved question is the factors producing drought during the 'short rains' season. Four factors have been shown to act jointly to produce the major flood events. However, droughts are usually associated with a single factor. In roughly half of the drought years, none of the four factors played a role. Overall the primary drivers change over time, so that another unresolved question is what produces these shifts in control. A related question is why the coupling of the 'short rains' to large-scale factors marked decreased after 1982. Further research is also needed to better understand the processes that produce the seasonal cycle of rainfall in eastern Africa."

Summarizing, the primary drivers and mechanism are not understood that control drought or flood in different areas in Africa. It is therefore reasonable to compare these frustrating difficulties with the achievement of the Tang's school in China illustrated in Gregori et al. (2025f, 2025g, 2025h and 2025i). That is, maybe, the spacetime variation of endogenous heat release from African soil ought to play the crucial role in the control of these extreme meteorological phenomena. Consider, however, that - compared to the Tibet Plateau - the endogenous energy release in Africa is substantially different.

In fact, stable cratons ought not to be the source of friction heat, in contrast to regions of intense overthrust such as underneath the Tibet Plateau. On the other hand, the DUPAL anomaly ought to be responsible for the formation of diamond-bearing kimberlites that ought to be real "aborted" volcanoes that are "plugged" by a heavy craton (see Gregori et al., 2025a, Appendix). On the other hand, in these areas it is reasonable to expect in any case the occurrence of some eventual large gradient of geothermal release that varies both in space and time. In addition, consider that the Afar triangle and the large gravity anomaly in Zaïre ought to be the source of conspicuous heat injection into the atmosphere. Indeed, they seem to be the origin of the tropical storms that, when they reach the Gulf of Mexico, are eventually transformed into devastating hurricanes (see Gregori and Leybourne, 2025j and Figs 39 and 40). In addition, consider the Oklo nuclear reactor in Gabon (see Schirber, 2004, and Moskowitz, 2011), or the CVL (Cameroon Volcanic Line, see Fig. 14 of Gregori et al., 2025a), including the Lake Nyos and Lake Monoun. Lake Nyos is well-known for the dramatic CO₂ eruption (see Gregori et al., 2025a). An additional crucial role is played by the quatrefoil pattern (see Gregori et al., 2025a, Gregori and Leybourne, 2021), shown by the DUPAL anomaly, but also correlated with the atmospheric CO₂ concentration (Mearns, 2015a, Gregori, 2020).

Certainly, Africa is a large and much varied continent. Therefore, it is likely that one or several time-varying sources of endogenous heat release can be active. If this guess is correct, as long as no monitoring exists of the

endogenous energy input in the atmosphere, it is impossible to get rid of the Sahel droughts and/or of floods in other regions. The problem needs therefore for some relevant additional monitoring, discussion, hard thinking, and modeling.

The reader, who is interested in the details of the present remarkable Nicholson's attempt aimed to explain observations, ought to refer to the long and exhaustive authoritative discussion by Nicholson (2017). Only Figs 62 through 65 are here shown.

Fig. 62 shows the conventional distinction of phenomena, adopted by Nicholson (2017). Note that, unlike the equatorial or southern sector, the summer rainfall or northern sector is likely to be influenced by the anomalous geothermal feature of the Afar triangle. Fig. 63 shows the rationale of the Nicholson's attempt, where, however, the role of the geothermal flow is not considered, while Fig. 64 gives some indication on the kind of different observed rainfall regime and seasonal variation in different areas. Fig. 64 justifies - by means of the available observations - the schematic distinction expressed in Fig. 62, while Fig. 65 explains why, compared to Ethiopia, Somalia is meteorologically much different.

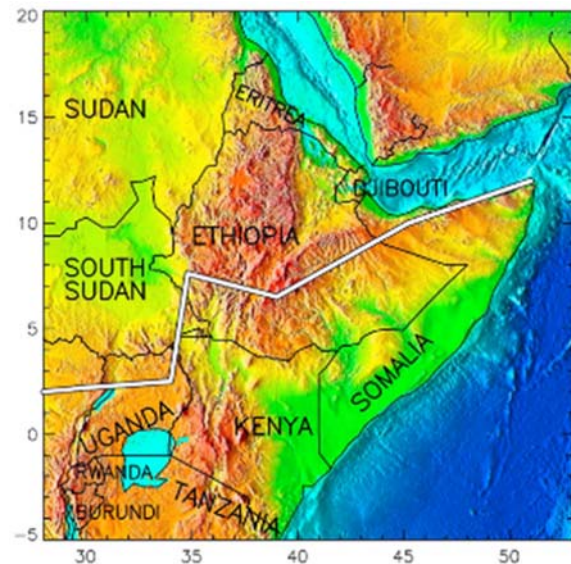


Fig. 62. "Location of equatorial (southern sector) and summer rainfall (northern sector) regions superimposed upon schematic of East African topography." Figure and captions after Nicholson (2017). AGU copyright free policy.

Independent of the explanation of this phenomenon, note that this peculiar feature of Fig. 65, i.e. of the meteorology of equatorial Indian Ocean vs. equatorial Africa, is related to the reason by which the aforementioned tropical storms - that cross through the Atlantic Ocean until the Gulf of Mexico - are originated from the Afar triangle, rather than further eastward on the Indian Ocean (see Gregori and Leybourne, 2025j). In this same respect, consider the anomalous behavior of the ITCZ over Africa, which is reported in the aforementioned abstract of Nicholson (2017). The meteorological circulation over Africa is peculiar and - even though we are not meteorologists - maybe its real drivers are to be found in the

jeopardized phenomena of soil exhalation of endogenous fluids that inject energy into the atmosphere. An array of shallow geotherm recorders in the meteorological station could be very useful.

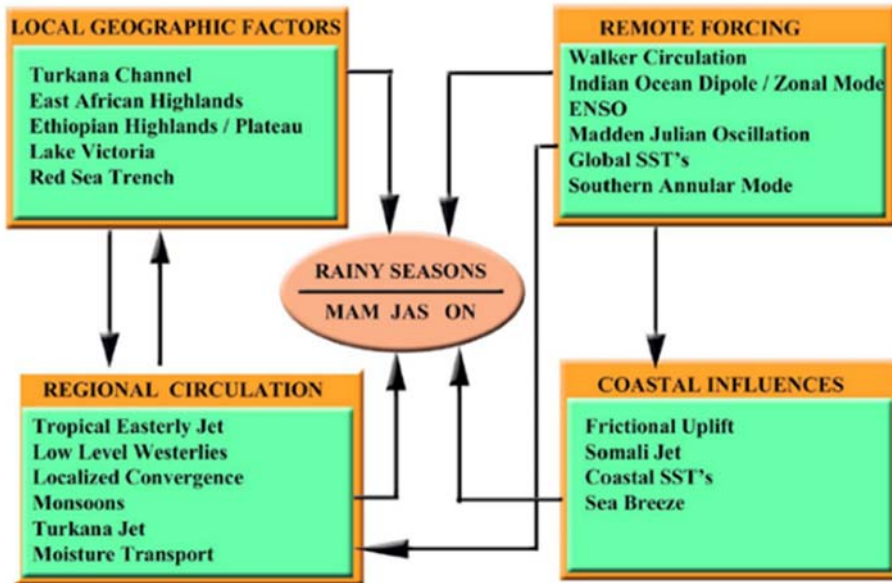


Fig. 63. “Schematic showing the factors influencing the three rainy seasons (MAM, i.e. March, April, May; JAS, i.e. July, August, September; and ON, i.e. October, November) of eastern Africa and the interrelationships among the factors.” Figure and captions after Nicholson (2017). AGU copyright free policy.

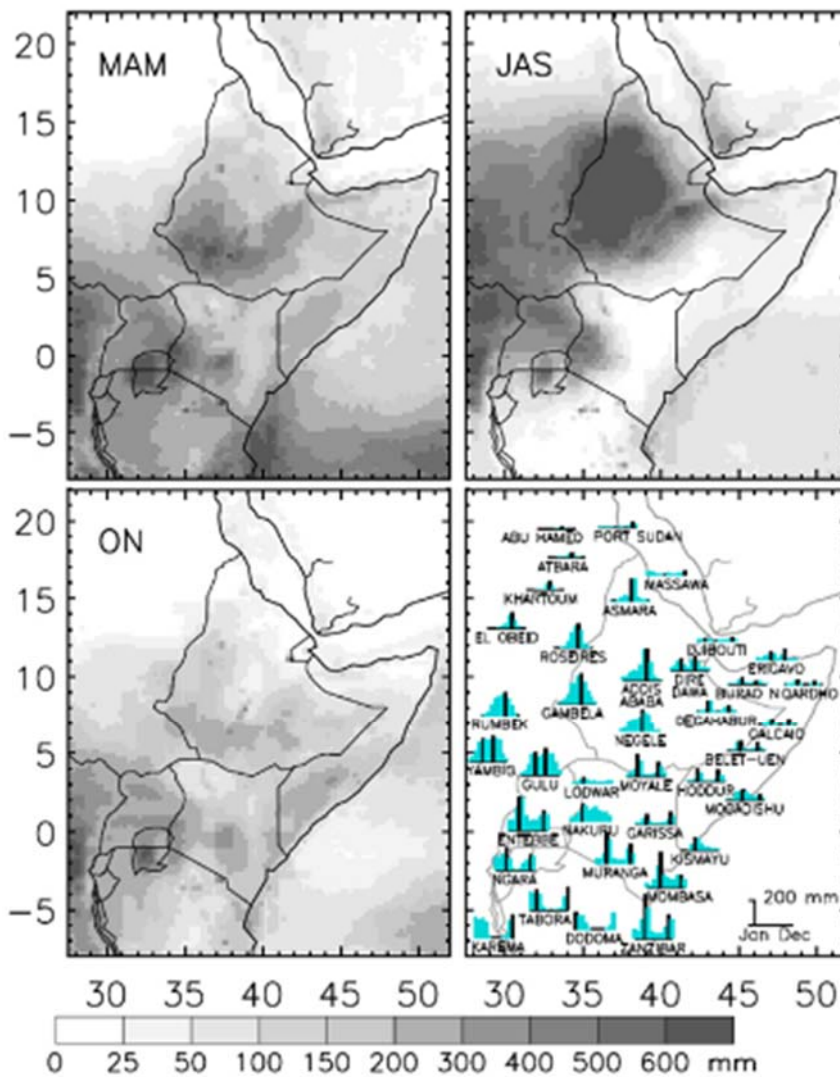


Fig. 64. “Mean rainfall in the three rainy seasons (March to May, July to September, and October–November) and schematic of the seasonal cycle at select stations. Seasonal rainfall is the total for the season, in millimeters. Black vertical lines/lines at each station indicate the month or months of maximum rainfall at the indicated stations.” Figure and captions after Nicholson (2017). AGU copyright free policy.

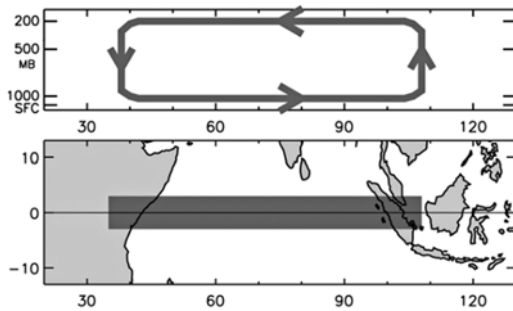


Fig. 65. “Schematic of the zonal circulation cell over the Indian Ocean during October-November. The shaded box in the bottom diagram shows the approximate geographical location of this cell.” Figure and captions after Nicholson (2017). AGU copyright free policy.

Concerning the role of agriculture in the global carbon cycle, for comparison purpose, Brown et al. (2010) refers to continental USA and report the following estimates. “Soils account for the largest location of terrestrial carbon (C) and thus are critically important in determining global C cycle dynamics. In North America, conversion of native prairies to agriculture over the past 150 years released 30 – 50% of soil organic carbon (SOC) stores (Mann, 1986). Improved cultural practices could recover much of this SOC, storing it in biomass and soil and thereby sequestering billions of tons of atmospheric CO₂. These practices involve increasing C inputs into soil (e.g. through crop rotation, higher biomass crops, and perennial crops) and decreasing losses (e.g. through reduced tillage intensity) (Janzen et al., 1998; Lal et al., 2003; Smith et al., 2007) ... Prairie soils account for 27% of the conterminous U.S. land surface and 31 – 39% of SOC stocks. These soils account for roughly 38% of U.S. croplands and roughly 37% of U.S. grasslands, hosting agricultural ‘breadbaskets’ in the central U.S. Thus, the management of these soils is important for carbon fluxes in the U.S ...

The carbon, phosphorus, iron and nitrogen cycles

The role of vegetation in the carbon cycle is related – among other drivers - to water requirement (e.g. Goldman et al., 2008; Holbrook and Zwieniecki, 2008). That is, a correct use of agriculture can imply a positive feedback concerning the challenge of the global carbon cycle, while every other biogeochemical cycle implies a different concern.

As far as the carbon cycle is concerned, a gauge - for the planetary-scale integral of the role of vegetation - can be expressed by means of the “terrestrial NPP” (Zhao and Running, 2010), which is a measure of the amount of atmospheric carbon that is fixed - and accumulated as biomass - by plants. Zhao and Running (2010) remind about previous studies that showed that climate constraints were relaxing when temperature and solar radiation increased, thus allowing for an upward trend of NPP during 1982 through 1999.

Zhao and Running (2010) claim that the decade 2000-2009 was the warmest since the beginning of instrumental measurements. This could imply a continue increase of NPP. In contrast, they find estimates that are suggestive of a reduction of 0.55 petagrams of C in the global NPP. On the other hand, there is an opposite trend in the two hemispheres. In fact, large-scale droughts imply a reduced regional NPP. Thus, a drying trend in the Southern Hemisphere (SH) showed a decreased NPP in that area, and an increased NPP in the NH. “A continued decline in NPP would not only weaken the terrestrial carbon sink, but it would also intensify future competition between food demand and proposed biofuel production.”

Food production, altogether with demographic increase, dramatically enters into play for the concern about carbon cycle. For instance, according to Pelletier and Tyedmers (2010), “food systems - in particular, livestock production - are key drivers of environmental change.” Pelletier and Tyedmers (2010) “compare the contributions of the global livestock sector in 2000 with estimated contributions of this sector in 2050 to three important environmental concerns: climate change, reactive nitrogen mobilization, and appropriation of plant biomass at planetary scales. Because environmental sustainability ultimately requires that human activities as a whole respect critical thresholds in each of these domains, we quantify the extent to which current and future livestock production contributes to published estimates of sustainability thresholds at projected production levels and under several alternative endpoint scenarios intended to illustrate the potential range of impacts associated with dietary choice ... “

According to Fiala (2009), the zootechnics related production is responsible for 18% of the total greenhouse gas production, being second only to energy production (21%), while all other sources play a comparably smaller role (agriculture is 5th with 12%).

As far as phosphorus (P) is concerned, its cycle is going soon to face a crisis, due to the large consumption compared to the available reservoir (Vaccari, 2009), with a most serious consequence on food supply. Phosphorus is generally thought to be a biolimiting nutrient of primary productivity in the oceans. There is some concern about the northern regions of the Florida Everglades, because years of agricultural and urban runoff have resulted into an excessive production of P. Hence, very large constructed wetlands, known as Storm-water Treatment Areas (STAs), have been built with the purpose to strip P from runoff before the water enters the protected Everglades areas. The STA project relies on large areas (cells) of submerged aquatic vegetation (SAV) to absorb P as the final stage of treatment. The SAV cells as responsible for the treatment of 85% of the whole STA project.

Juston and DeBusk (2011) studied the inflows, outflows, and background P levels by means of long-term measurements in one of these SAV cells. They found that no more P removal occurs when the total P levels in the cells reaches $\sim 15 \mu\text{g l}^{-1}$. The mean environmental concentration was $\sim 16 \mu\text{g l}^{-1}$ (13 – 17, with 90% bounds). “Background P concentrations of 7 and $\sim 6 \mu\text{g l}^{-1}$ were identified for dissolved organic and

particulate P fractions in the data pool, respectively ... “They envisage the possibility of “tangible risks for exceeding proposed annual discharge criteria from the STAs in the range of $\sim 16 - 20 \mu\text{g l}^{-1}$.”

The concern about P contribution by aerosols has been investigated in detail in the Mediterranean region. Longo et al. (2014) summarize the problem as follows. “Biological productivity in many ocean regions is controlled by the availability of the nutrient P. In the Mediterranean Sea, aerosol deposition is a key source of P and understanding its composition is critical for determining its potential bioavailability. Aerosol P was investigated in European and North African air masses using P near-edge X-ray fluorescence spectroscopy (P-NEXFS). These air masses are the main source of aerosol deposition to the Mediterranean Sea. We show that European aerosols are a significant source of soluble P to the Mediterranean Sea. European aerosols deliver on average 3.5 times more soluble P than North African aerosols and furthermore are dominated by organic P compounds. The ultimate source of organic P does not stem from common primary emission sources. Rather, P associated with bacteria best explains the presence of organic P in Mediterranean aerosols.” That is, the biosphere is a fundamental driver in the P cycle, and this is crucial for bioavailability, and for food production.

In addition, P is important in regulating the redox state of the ocean-atmosphere system. According to Planavsky et al. (2010c), P concentrations appear to have been elevated in Precambrian oceans. Planavsky et al. (2010) estimate the evolution through time of the marine phosphate reservoir, by means of the ratio of P to Fe in iron-oxide-rich sedimentary rocks. By this, they can track dissolved phosphate concentrations, if the dissolved silica concentration of sea water is estimated. “The data suggest that phosphate concentrations have been relatively constant over the Phanerozoic Eon, the past 542 Ma ... In contrast, phosphate concentrations seem to have been elevated in Precambrian oceans. Specifically, there is a peak in P-to-Fe ratios in Neoproterozoic Fe formations dating from $\sim 750 - 635$ Ma ago, indicating unusually high dissolved phosphate concentrations in the aftermath of widespread, low-latitude ‘snowball Earth’ glaciations. An enhanced postglacial phosphate flux would have caused high rates of primary productivity and organic carbon burial and a transition to more oxidizing conditions in the ocean and atmosphere. The snowball Earth glaciations and Neoproterozoic oxidation are both suggested as triggers for the evolution and radiation of metazoans.” They conclude and “propose that these two factors are intimately linked; a glacially induced nutrient surplus could have led to an increase in atmospheric oxygen, paving the way for the rise of metazoan life.”²¹

This leads to consider also the Fe cycle, which is thus one important facet of metallogenesis, closely interwoven

with the action of the biosphere. Jickells et al. (2005) review the problem, considering Fe-containing soil dust, transported from land through the atmosphere to the oceans, thus affecting ocean biogeochemistry. They also identify the critical uncertainties.

Bekker et al. (2010) envisage that Precambrian sedimentary successions show the most common occurrence of Fe formations. According to a general agreement, the secular changes in the style of their deposition are likely to be connected to the environmental and geochemical evolution of Earth, even though several aspects are to be explained. Two types of Precambrian Fe formations are related to their depositional setting. “Algoma-type Fe formations are interlayered with stratigraphically linked to sub marine-emplaced volcanic rocks in greenstone belts and, in some cases, with volcanogenic massive sulfide (VMS) deposits. In contrast, larger Superior-type Fe formations are developed in passive-margin sedimentary rock successions and generally lack direct relationships with volcanic rocks.” A former distinction relied on these two types of Fe-formation, and was later contended by investigations, even though Bekker et al. (2010) claim that this distinction is a valid first approximation.

“Texturally, Fe formations were also divided into two groups. BIF is dominant in Archaean to earliest Palaeoproterozoic successions, whereas granular Fe formation (GIF) is much more common in Palaeoproterozoic successions.” Bekker et al. (2010) stress that over 20 years ago the secular changes were identified in the style of Fe-formation deposition, which appear related to diverse environmental changes. On the other hand, according to geochronologic investigations, the episodic nature was found of the deposition of giant Fe formations, as they appear coeval, and genetically related, to the emplacement of large igneous provinces (LIPs).

“Superior-type Fe formation first appeared at ~ 2.6 Ga, when construction of large continents changed the heat flux at the CMB [core-mantle boundary]. From ~ 2.6 Ga to ~ 2.4 Ga, global mafic magmatism culminated in the deposition of giant Superior-type BIF in South Africa, Australia, Brazil, Russia, and Ukraine. The younger BIFs in this age range were deposited during the early stage of a shift from reducing to oxidizing conditions in the ocean-atmosphere system.

Counterintuitively, enhanced magmatism at 2.50 – 2.45 Ga may have triggered atmospheric oxidation.” The GOE implied a rise of atmospheric oxygen at ~ 2.4 Ga, and GIF is correspondingly abundant in the rock record, while before the GOE, BIF were predominant. In general, however, at ~ 1.85 Ga, the Fe formations disappeared, and later reappeared at the end of the Neoproterozoic, being related, again, to intense magmatic activity - and, in this case, to also global glaciations, which was the so-called Snowball Earth events.

²¹ The “snowball Earth” hypothesis, which supposes a nearly or entirely frozen hypothesis, is still controversial (e.g. Walker, 2003 and Macdougall, 2006).

By the Phanerozoic, the marine Fe deposition is found in local settings, associated to closed to semiclosed basins, characterized by intensive volcanic and hydrothermal activity that was extensive – such as, e.g., in back-arc basins. Ironstones are found to be correlated with periods of intense magmatic activity and ocean anoxia.

“Late Palaeoproterozoic Fe formations and Palaeozoic ironstones were deposited at the redoxcline where biological and nonbiological oxidation occurred. In contrast, older Fe formations were deposited in anoxic oceans, where ferrous Fe oxidation by anoxygenic photosynthetic bacteria was likely an important process.” Bekker et al. (2010) claim that the conditions necessary for deposition of Fe formation were determined both by endogenic and exogenic factors. Specifically, they mention “mantle plume” events - i.e. a large, anomalous increase of the release of endogenous energy – responsible for the occurrence of LIPs and also an increase of the spreading rates of MORs, with larger growth rates of oceanic plateaus, all phenomena that were associated to a greater hydrothermal flux on the ocean floors. This flux was controlled by oceanic and atmospheric redox states. In fact, if the oceanic oxidation state was overwhelmed by the hydrothermal flux, Fe moved and was deposited far away from hydrothermal vents. Conversely, if the hydrothermal flux did not afford to overwhelm the oceanic redox state, Fe was deposited close to the hydrothermal vents, generally as oxides or sulfides. In contrast, Mn was more mobile.

Bekker et al. (2010) *“conclude that occurrences of BIF, GIF, Phanerozoic ironstones, and exhalites surrounding VMS systems record a complex interplay involving mantle heat, tectonics, and surface redox conditions throughout Earth history, in which mantle heat unidirectionally declined and the surface oxidation state mainly unidirectionally increased, accompanied by superimposed shorter term fluctuations.”*

Tang et al. (2018) investigated the geochemical and mineralogical implications of Fe supply from deep Earth in magma. Their paper is specialized and it is more simply illustrated as follows by Specktor (2018b) who reports also some interviews. *“For decades, scientists have pegged the case of the missing Fe on a process involving volcanoes, and a mineral called magnetite that sponges up Fe from molten magma pools deep underground. Now, Tang et al. (2018) points the finger at a new culprit for Earth’s missing Fe. The true thief is not magnetite ... but a sparkly mineral we all know and love: garnet ... The accepted wisdom is that magnetite pulls Fe from the magma melt before the melt rises and gets erupted out at continental volcano arcs ... Fe depletion is most pronounced at continental arcs, where the crust is thick, and much less so in island arcs, where the crust is thin ... If magnetite was sucking up Fe, then, you would expect magnetite to be more plentiful where the continental crust was thicker, and Fe depletion correspondingly greater. But the thickness of the crust doesn’t correlate with levels of magnetite.*

But garnet abundance, the authors said, does correlate with crust thickness. Almandine - an Fe -rich variety of garnet - forms best under high-pressure, high-temperature conditions. Conditions like these are common below the

land-based volcanoes that form at continental margins, when dense oceanic crust slides beneath continental crust. With garnet more plentiful below such volcano chains – known as continental arcs - and Fe less plentiful there, the researchers saw a correlation worth studying further ... in studies like these scientists tend to rely on the ancient rocks that have already been spewed out by past volcanic eruptions. Rocks like these are known as xenoliths, and can reside up to 80 km below the Earth before being ripped apart and scattered in a volcanic eruption. These rocks provide researchers with a direct window into the deep parts of the continental arc ... In the new study, Lee and several students embarked on an excursion to collect xenoliths from southern Arizona, which were spewed by an ancient volcano millions of years ago. Analysis of the xenoliths showed that these rocks formed below a continental arc, and were indeed laden with garnet.

To further test the correlation, the researchers spent several months examining xenolith records in the Max Planck Institute’s GEOROC database, which contains comprehensive information on volcanic rocks collected all over the world. They found that, true to their hypothesis, magma that included more fragments of garnet were also more Fe depleted ... So, is garnet the great Fe thief lurking in Earth’s crust? ... “

The more specialized Tang et al. (2018) summary is as follows. *“The two most important magmatic differentiation series on Earth are the Fe-enriching tholeiitic series, which dominates the oceanic crust and island arcs, and the Fe-depleting calc-alkaline series, which dominates the continental crust and continental arcs. It is well-known that calc-alkaline magmas are more oxidized when they erupt and are preferentially found in regions of thick crust, but why these quantities should be related remains unexplained. We use the redox-sensitive behavior of europium (Eu) in deep-seated, plagioclase-free arc cumulates to directly constrain the redox evolution of arc magmas at depth. Primitive arc cumulates have negative Eu anomalies, which, in the absence of plagioclase, can only be explained by Eu being partly reduced. We show that primitive arc magmas begin with low oxygen fugacities, similar to that of MORBs (MOR basalt), but increase in oxygen fugacity by over two orders of magnitude during magmatic differentiation. This intracrustal oxidation is attended by Fe depletion coupled with fractionation of Fe-rich garnet. We conclude that garnet fractionation, owing to its preference for ferrous over ferric Fe, results in simultaneous oxidation and Fe depletion of the magma. Favored at high pressure and water content, garnet fractionation explains the correlation between crustal thickness, oxygen fugacity, and the calc-alkaline character of arc magmas.”*

Also, the metallogenesis of rare earth elements (REE) is involved. Planavsky et al. (2010a) remark that, in the early Precambrian, both ocean and atmosphere were largely anoxic. Thus, the Fe cycle was much different than today's, and sedimentary deposits extremely Fe-rich - i.e., Fe formations - are the most conspicuous signature of this peculiar Fe cycle. A usual approach for understanding the origin of Fe formations - and the associated ancient ocean

chemistry – relied on *REE* systematics. On the other hand, several earlier *REE* studies of Fe formations were biased by analytical limitations and sampling from severely altered units leading to ambiguous conclusions.

Planavsky et al. (2010a) analyzed the Fe formation samples from 18 units, corresponding to a time range ~ 3.0 – 1.8 Ga, thus achieving a reevaluation of Precambrian Fe formations, depositional mechanisms, and significance. They observed many temporal trends in the *REE* and Y dataset, which reveal changes in marine redox conditions. “In general, Archæan Fe formations do not display significant shale-normalized negative Ce anomalies, and only Fe formations younger than 1.9 Ga display prominent positive Ce anomalies.” A peculiar feature deals with Y/Ho ratios and shale-normalized light to heavy *REE* ratios (*LREE/HREE*), which are low and high, respectively, in ~ 1.9 Ga and younger Fe formations, while these elements are not found in their Archæan counterparts. A varying *REE* cycling in the water column seems responsible for these relevant differences between Palæoproterozoic vs. Archæan *REE* + Y patterns. These observations are analogous to present observations of modern redox-stratified basins.

Thus, concerning the late Palæoproterozoic, it is inferred that the *REE* + Y patterns in Fe formations are indicative of a transport - of metal and Ce oxides - across the redoxcline from oxic shallow seawater to deeper anoxic waters. “Oxide dissolution - mainly of Mn oxides - in an anoxic water column lowers the dissolved Y/Ho ratio, raises the *LREE/HREE* ratio, and increases the concentration of Ce relative to the neighboring *REE* (La and Pr).” Therefore, the Fe oxides that precipitate at or near the chemocline are characterized by these *REE* features and are indicative of this oxide transport.

Conversely, concerning Archæan Fe formations, they show no *REE* + Y patterns suggestive of oxide transport, and this denotes that no distinct Mn redoxcline existed before to the rise of atmospheric oxygen during the early Palæoproterozoic. Additional evidence – which supports reducing conditions in shallow-water environments of the Archæan ocean - derives from missing negative Ce anomalies in *REE* data inside carbonates that are deposited on shallow-water Archæan carbonate platforms, and that are observed in layers beneath Fe formations.

Planavsky et al. (2010a) conclude that their evidence does not support the classical models that explain the deposition of Archæan Fe formations in terms of oxidation by free oxygen at or above a redoxcline. In contrast, they support evidence that these Fe formations are more likely to derive from an oxidative mechanism associated to metabolic Fe oxidation. They comment that the Fe distribution in Archæan oceans “could have been controlled by microbial Fe uptake”, better than by the oxidative potential in shallow- marine environments.

In general, all chemical cycles in the environment are a difficult and intricate topic. For instance, the nitrogen (N) cycle is poorly understood, even though N is one of the primary constituents of the biosphere. A recent study (Mattews et al. 2023, illustrated by University of Manchester, 2023) provides unprecedented evidence.

Mattews et al. (2023) synthesize their findings as follows. “Reduced N plays a fundamental role in ocean biogeochemistry, yet marine-reduced organic N (ON) species are poorly characterized as is their role in the global N cycle. Our observations suggest that biologically rich ocean environments are a significant source of urea to the atmosphere and that the atmosphere is likely to provide a fast transport route for the redistribution of reduced N across the seawater surface and as such have implications for marine productivity. Our findings show that the global marine burden of urea is significant which necessitates a revision of the atmospheric N cycle.”

In fact, they stress that reduced N is central to global biogeochemistry. However, large uncertainties persist concerning source and cycling. They rely on observations of gas-phase urea ($CO(NH_2)_2$) in the atmosphere by airborne high-resolution mass spectrometer over the North Atlantic Ocean. Urea is ubiquitous in the lower troposphere in the summer, autumn, and winter, while it was not detected in the spring. The ocean seems to be the primary emission source, even though the understanding of mechanisms requires additional investigation. Long-range transport of biomass-burning plumes are also responsible for urea transport. Therefore, airborne transfer of urea between nutrient-rich and -poor parts of the ocean can readily impact ecosystems and oceanic uptake of CO_2 . The entire N cycle plays therefore a central role in climate control.

The early interactions between Earth’s atmosphere and oceans

Important implications are therefore concerned with the early interactions between Earth’s atmosphere and oceans. According to Lyons et al. (2010) “recent studies are challenging the simple notion of unfailingly Fe -rich (ferruginous) conditions in the anoxic Archæan ocean that gave way to either an oxic or euxinic (anoxic and sulfidic) deep ocean throughout the Proterozoic. There is now convincing evidence for euxinic conditions in the late Archæan, prior to the GOE - with and without the driving force of incipient atmospheric oxygenation and associated weathering reactions that supplied sulfate to the ocean.

Emerging from this work is also a clear view of ocean stratification in the latest Archæan, with Fe domination in the deeper ocean and indications of at least episodic sulfide at mid depths and oxic surface waters. We assert that such conditions also prevailed throughout the Proterozoic beneath an atmosphere with oxygen at concentrations still well below the present level and support this assertion with a growing data set spanning the Proterozoic. As a corollary, accumulations of dissolved sulfide in the waters were controlled by locally high fluxes of organic matter and/or sulfate delivery, both favored along the ocean Margin.

The possibility of a persistently Fe-rich deep ocean, but a far patchier record of banded Fe formations, supports the view that almost all BIFs are anomalous sedimentary deposits linked to increased or local hydrothermal activity. Low sulfate conditions, as fingerprinted by the abundance

of isotopically heavy pyrite, were maintained throughout the Proterozoic by still widespread euxinia and associated copious pyrite burial. Nevertheless, a model for a pervasively ferruginous deep ocean over much if not all of the Proterozoic, coeval with frequent euxinia concentrated along the ocean margin including restricted basins, demands that we reevaluate our estimates for past availability of bioessential trace metals. This stratified ocean model, e.g., does a better job of explaining the Mo properties of Proterozoic seawater compared to previous models that assumed global euxinia.²²

Also, anomalous trends are sporadically detected. For instance, Planavsky et al. (2010b) investigated the carbonates deposited ~ 2.3 – 2.1 Ga ago that display²³ “markedly positive carbon isotope values, commonly reaching +10 ‰ and peaking above +20 ‰. If these values capture the primary composition of marine dissolved inorganic carbon, this event, referred to as the Lomagundi excursion, represents the most severe and long-lived perturbation to the Earth’s global carbon cycle and likely reflects greatly enhanced organic carbon burial. However, these carbon isotope values have also been attributed to widespread diagenetic carbonate formation associated with methanogenesis. These two models have profoundly different implications for the evolution of the carbon cycle and Earth’s oxygenation.” They overview the sedimentological and geochemical data and “point toward a marine (non-diagenetic) origin of the Lomagundi positive carbon isotope values.”

They stress that “the carbon and sulfur cycles are linked on both global and local scales”. Hence, they “focus on using records of coeval seawater or porewater sulfate to help distinguish between the two models. Coupled carbon and carbonate-associated sulfate (CAS) sulfur isotope data for samples from Lomagundi-aged carbonate platforms point to enhanced primary productivity rather than carbonate precipitation in the methanic zone as the underlying mechanism for this excursion. CAS concentrations in Lomagundi-aged carbonates typically range from 50 to 500 ppm, within the range of typical ancient marine carbonates and consistent with a sulfate-rich system.

Since porewater sulfate is typically depleted via bacterial sulfate reduction before the onset of methanogenesis, and given that CAS concentrations track ambient sulfate levels at the time of carbonate precipitation, our high concentrations argue against carbonate formation in the methanic zone. We have found a narrow range of only moderate ³⁴S-enrichments ($\delta^{34}S_{ave} = +14$ ‰) in CAS of Lomagundi-aged carbonates, which is also inconsistent with carbonate precipitation in the methanic zone. Furthermore, CAS $\delta^{34}S_{ave}$ values closely match those from coeval sulfate evaporites, suggesting that the

carbonates record primary seawater signals and that C – S isotope systematics can be used to track the global C and S cycles.”

In this same respect, drought and peatlands play a crucial role in the sulfur cycle, in combination with Hg cycling. Coleman Wasik et al. (2015) carried out a devoted investigation. Only their abstract is here reported.

“A series of severe droughts during the course of a long-term, atmospheric sulfate-deposition experiment in a boreal peatland in northern Minnesota created a unique opportunity to study how methylmercury (MeHg) production responds to drying and rewetting events in peatlands under variable levels of sulfate loading. Peat oxidation during extended dry periods mobilized sulfate, MeHg, and total mercury (Hg_T) to peatland pore waters during rewetting events. Pore water sulfate concentrations were inversely related to antecedent moisture conditions and proportional to past and current levels of atmospheric sulfate deposition.

Severe drying events caused oxidative release of MeHg to pore waters and resulted in increased net MeHg production likely because available sulfate stimulated the activity of sulfate-reducing bacteria, an important group of Hg-methylating bacteria in peatlands. Rewetting events led to increased MeHg concentrations across the peatland, but concentrations were highest in peat receiving elevated atmospheric sulfate deposition. Dissolved Hg_T concentrations also increased in peatland pore waters following drought but were not affected by sulfate loading and did not appear to be directly controlled by dissolved organic carbon mobilization to peatland pore waters.

Peatlands are often considered to be sinks for sulfate and Hg_T in the landscape and sources of MeHg. Hydrologic fluctuations not only serve to release previously sequestered sulfate and Hg_T from peatlands but may also increase the strength of peatlands as sources of MeHg to downstream aquatic systems, particularly in regions that have experienced elevated levels of atmospheric sulfate deposition.”

Strellich (2015), while illustrating Coleman Wasik et al. (2015) claim that “wetlands of all types play a key role in the biogeochemical cycling of elements. In peatlands, decaying vegetation forms a spongy, acidic habitat for hungry microbes that process substances like mercury and sulfur. A group of microbes known as sulfate-reducing bacteria uses sulfate deposited from the atmosphere to metabolize organic material. These microbes make peatlands an efficient sink for atmospheric sulfate. Microbes and other organisms also take in Hg from their surroundings. As a side effect of their normal metabolic processes, sulfate-reducing bacteria convert inorganic Hg into the organic compound MeHg. Methylmercury acts as a neurotoxin in humans and wildlife, and it is biomagnified

standard.” The carbon isotope ratio ($\delta^{13}C$) is commonly used to investigate plant materials in ancient ecosystems, e.g., in order to reconstruct a long-term record of C_{enozoic} $\delta^{13}C_{CO_2}$ (Tippie et al., 2010).

²² Euxinia, or euxinic conditions, are defined when water is both anoxic and sulfidic, i.e., there is no oxygen (O₂) and a raised level of free hydrogen sulfide (H₂S).

²³ According to Kendall (2004a), “carbon stable isotope ratios are reported relative to the PDB (for Pee Dee Belemnite) or the equivalent VPDB (Vienna PDB)

- meaning it becomes more concentrated as it travels up the food chain, from alga to fish to top predators, including humans.

Drought conditions can effectively transform peat bogs from sulfate sinks to sources by oxidizing the peat deposits and mobilizing the sulfate that they had previously sequestered. The released sulfate can then stimulate microbial populations, producing more MeHg that can make its way into downstream aquatic environments. Projected changes in climate, including an increase of droughts and less frequent, more intense rain events, imply that this phenomenon may make peat bogs into larger sources of MeHg to downstream water resources and ecosystems ... “

Concerning Coleman Wasik et al. (2015), “between 2000-2008 the scientists experimentally manipulated the amount of sulfate falling on a small peat bog in northern Minnesota and monitored how variations in water levels and sulfate input affected the release of MeHg. Two severe droughts that occurred during the study period provided a unique opportunity for the researchers to measure the environmental response as it unfolded. The study results revealed that drought conditions increased the production of MeHg in peatlands and its subsequent release into the food chain. When water returned to drought-affected peatlands it prompted the release of previously sequestered sulfate, increasing the overall power of peat bogs as MeHg sources. Perhaps unsurprisingly, these effects were amplified in areas where atmospheric sulfate deposition had been experimentally elevated to begin with ... “

The concern about MeHg is not only of academic interest. “Why do marine animals in the western Arctic have higher Hg levels than those in the east? The trend is seen throughout the food web, from the tiny zooplankton that drift along ocean currents to large mammals like polar bears. It matters because Hg is a contaminant of global concern and communities in the North rely on the ocean for food. Mercury can cause reproductive problems in some animals, severe neurological damage in people and hamper the development of infants” (Wang, 2018).

Wang et al. (2018) carried out an extensive investigation through the Arctic polar cap. “Decades of Hg observations in marine biota from across the Canadian Arctic show generally higher concentrations in the west than in the east. Various hypotheses have attributed this longitudinal biotic Hg gradient to regional differences in atmospheric or terrestrial inputs of inorganic Hg, but it is MeHg that accumulates and biomagnifies in marine biota. Here, we present high-resolution vertical profiles of total Hg and MeHg in seawater along a transect from the Canada Basin, across the Canadian Arctic Archipelago (CAA) and Baffin Bay, and into the Labrador Sea. Total Hg concentrations are lower in the western Arctic, opposing the biotic Hg distributions. In contrast, MeHg exhibits a distinctive subsurface maximum at shallow depths of 100 – 300 m, with its peak concentration decreasing eastwards. As this subsurface MeHg maximum lies within the habitat of zooplankton and other lower trophic-level biota, biological uptake of subsurface MeHg and subsequent biomagnification readily explains the biotic Hg

concentration gradient. Understanding the risk of MeHg to the Arctic marine ecosystem and Indigenous Peoples will thus require an elucidation of the processes that generate and maintain this subsurface MeHg maximum.” [That is, the non-understood role of the biosphere is crucial.]

All these items are the object of a large and steadily increasing number of studies and literature. *American Academy of Microbiology and American Geophysical Union* (2016) is a short report that summarizes the state-of-the-art. No review can be here given, rather only a few hints in order to highlight the great complexity of the problem, and the inextricable link between biosphere and geosphere, with much difficult geochemical and isotopic implications. In any case, the evolution of the biosphere on the geological time scale has been - and presently is - an essential driver in Earth’s history.

Sahel drought and planetary-scale phenomena

Upon referring anew to the Sahel drought, it seems to be controlled by planetary-scale phenomena. A clear hunch is derived from geological evidence. Mulitza et al. (2008) reconstructed the history of aeolian and fluvial sedimentation on the continental slope off Senegal during the past 57,000 years. They showed “that abrupt onsets of arid conditions in the West African Sahel were linked to cold North Atlantic SSTs during times of reduced meridional overturning circulation associated with Heinrich Stadials.” Owing to the present lack of understanding of this important and dramatic phenomenon, and owing to the relevance of this investigation, it is worthwhile to describe it in some detail.

They introduce their study by stressing the crucial role of water availability in the control of Sahel’s droughts. “Historical records suggest that Sahel droughts result from changes in the large-scale distribution of SST (e.g., Lamb, 1978; Folland et al., 1986) which (among other factors) is influenced by the heat transport due to the Atlantic meridional overturning circulation (AMOC) (Newell and Hsiung, 1987). The contribution of the AMOC to the long-term variability of Sahel precipitation has not yet been demonstrated. Since the AMOC underwent substantial variations during the late Quaternary (Mc Manus et al., 2004), high-resolution sediment records from ocean margin settings offer the opportunity to study the response of continental climate to changes in ocean circulation.

The continental slope off Northern Senegal is an ideal site to study the history of Sahel drought, because it records the varying input of aeolian dust and fluvial sediments from the adjacent African continent (Koopmann, 1981; Sarnthein et al., 1981) (Fig. 66). Dust with particle sizes up to 200 µm (Stuut et al., 2005) is mobilized in the Sahel and the western Sahara (Grousset et al., 1998; Jullien et al., 2007) and transported offshore mainly by continental trade winds and the Saharan Air Layer (Prospero and Carlson, 1981). Recent ship-based dust samples collected off Senegal and Mauritania between 13 – 20°N indicate that 44 – 83% of the dust is deposited at grain sizes larger than 10 µm (Stuut et al., 2005). By contrast, 95% of the terrigenous sediments delivered by the Senegal River have

grain sizes below 10 μm (Gac and Kane, 1986). The Fe/K ratio of atmospheric dust samples (Stuut et al., 2005) shows a close relation to precipitation, with values around ~ 2.01 ($\sim 28^\circ\text{N} - 14^\circ\text{N}$, $n = 7$, $SD = 0.41$) in the Sahel-Saharan area and values around ~ 3.88 ($\sim 6^\circ\text{N} - 7^\circ\text{S}$, $n = 11$, $SD = 0.41$) in the tropics ... This increase in Fe/K ratios toward the tropics reflects the increasing amount of dust derived from deeply chemically weathered terrains (Moreno et al., 2006) with relatively high concentrations of Fe and Al in comparison to the more mobile K.

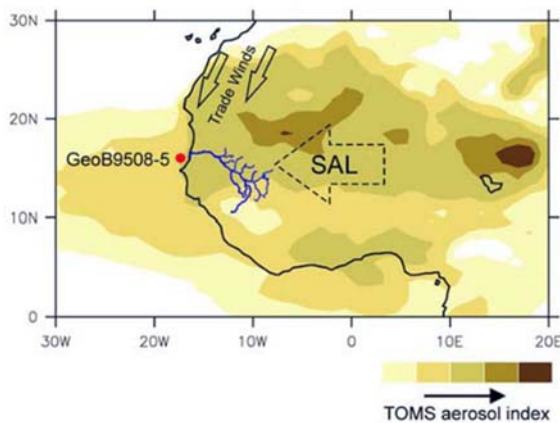


Fig. 66. "Position of gravity core GeoB9508-5 (red dot) close to the mouth of the Senegal River (blue) and Total Ozone Mapping Spectrometer (on Nimbus 7) (TOMS) averaged aerosol concentrations for the years 1997-2005 highlighting the Sahara-Sahel Dust Corridor (TOMS data are available at <http://toms.gsfc.nasa.gov/>). Arrows indicate principal wind directions of trade winds and Saharan air layer (SAL)." Figure and captions after Mulitza et al. (2008). AGU copyright free policy.

The material transported with the Senegal River also has a very distinct geochemical signature ... Compared to the chemical composition of atmospheric dust in the Sahel (Orange et al., 1993; Stuut et al., 2005), suspended sediments in the Senegal River show significantly higher Fe/K and Al/Si ratios (Gac and Kane, 1986). The Senegal River mainly drains the western part of Guinea. Sediment input from the Senegal River is highly dependent on the total water discharge and mainly occurs during the rainy summer season (Kattan et al., 1987) ... the most recent multidecadal Sahel drought has been associated with an increase in dust mobilization and export over the Atlantic (Prospero and Lamb, 2003) and a decrease in Senegal River discharge by more than 50% with respect to the long-term mean (Kattan et al., 1987). They analyzed "a 57 ka long record of terrigenous sedimentation from the continental slope off Senegal, westward of the Senegal River mouth." They synthesize their observations as follows.

"The age model of the core indicates an age at the base of the core of ~ 57 ka and mean sedimentation rates of ~ 17 cm ka^{-1} . Between $\sim 57 - 15$ ka BP, the benthic $\delta^{18}\text{O}$ record is characterized by a series of events with relatively low benthic $\delta^{18}\text{O}$ values (Fig. 67). It has been previously shown (Shackleton et al., 2000) that these events coincide with warm temperatures over Antarctica, the so-called

Antarctic Isotope maxima (AIM) (EPICA, 2006) (Figs 68d and 68e), and are probably due to a combination of ice volume and deep-water temperature changes that occur synchronously with temperature changes over Antarctica.

The Holocene section of this core contains only small amounts of coarse-grained dust (Fig. 67b). Al/Si and Fe/K ratios are highest in the mid-Holocene, when the values are very close to the modern composition of Senegal River suspension (Fig. 68 ...). Both ratios decrease gradually toward the present.

The glacial section of the down-core record of GeoB9508-5 is characterized by a series of abrupt increases in grain size associated with decreases of Al/Si and Fe/K ratios starting at about 49, 41, 31, 26, 19 and 13 ka BP (Figs 67 and 68). These events coincide with the most prominent AIMs 1, 2, 8, 12 and their NH counterparts, the Heinrich Stadials 1-5 and the Younger Dryas. During the Heinrich Stadials both low Al/Si and Fe/K ratios and the low amount of fine material ($< 20\%$) are consistent with the deposition of atmospheric dust and indicate a reduced contribution from Senegal River suspension. Generally, the amount of fine material ($< 10 \mu\text{m}$) is highly correlated ($R^2 = 0.9$ when interpolated to 500 year intervals) with Al/Si ratios."

They implemented a complicated model computation and concluded that "variations in the composition of the terrigenous material indicate that Sahel megadroughts occurred during Heinrich Stadials and were associated with cold North Atlantic SST during times of reduced meridional overturning circulation ... [They studied] the physics behind the changes in West African hydrology by means of... a fully coupled climate model ... results suggest that North Atlantic SST and West African rainfall are linked through shifts in the positions of the monsoon trough and the mid-tropospheric African Easterly Jet ... it seems likely that the future of precipitation in the Sahel will strongly depend on the behavior of the AMOC and its influence on the spatial structure of global warming."

However, for the purposes of the present study their physical discussion looks relevant, concerning their clear findings and inferences, although it is unavoidably based on a careful modeling for its interpretation.

"Today terrigenous sediments deposited on the continental slope of Senegal mainly stem from atmospheric dust and river input. These transport processes signify two different precipitation regimes: dust input mainly occurs during dry conditions whereas river input occurs when precipitation is high in the drainage basin of the Senegal River. Since our core is located at the boundary between both regimes, it reflects the relative proportions of fluvial and aeolian sediments and should be a sensitive recorder of Sahel precipitation. This interpretation is consistent with the general decrease of Al/Si and Fe/K ratios during the late Holocene along with a gradual drying trend over North Africa in response to weakening insolation forcing (e.g., Kröpelin et al., 2008).

The salient feature in gravity core GeoB9508-5 is series of abrupt increases in grain size associated with decreased Al/Si and Fe/K ratios.

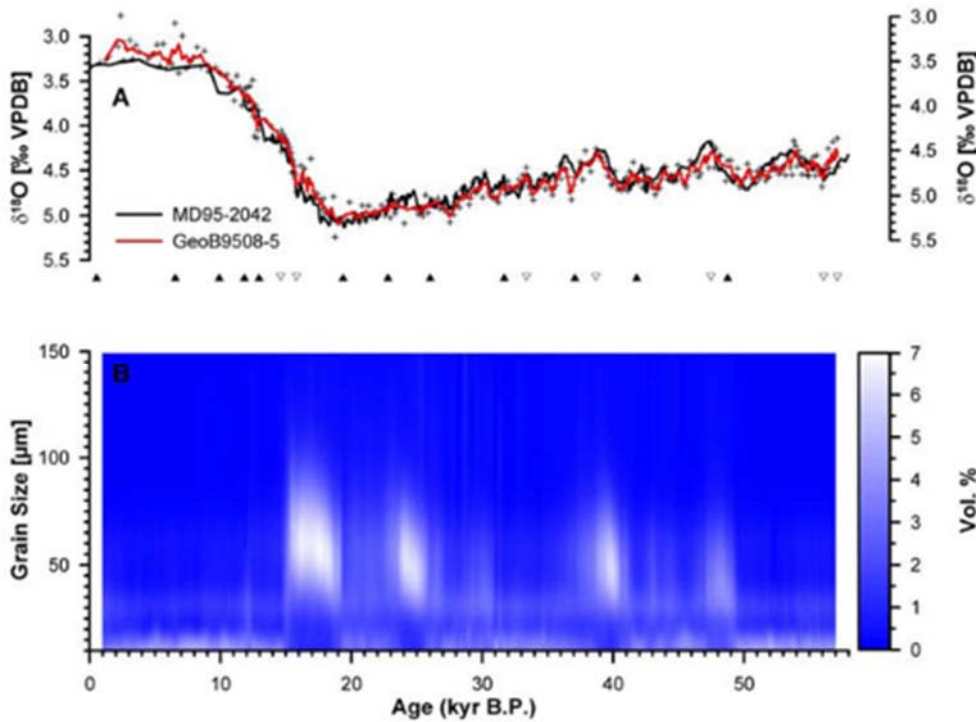


Fig. 67. “(a) Benthic $\delta^{18}O$ record of cores GeoB9508-5 (this paper) and MD95-2042 (Shackleton et al., 2004). (b) Grain size distribution in core GeoB9508-5 (this paper). Filled triangles indicate Accelerator Mass Spectrometer radiocarbon datings, and open triangles indicate age points derived by correlation with the benthic $\delta^{18}O$ record of core MD95-2042. The red curve is a three-point running mean of the benthic $\delta^{18}O$ data (crosses).” Figure and captions after Mulitza et al. (2008). AGU copyright free policy.

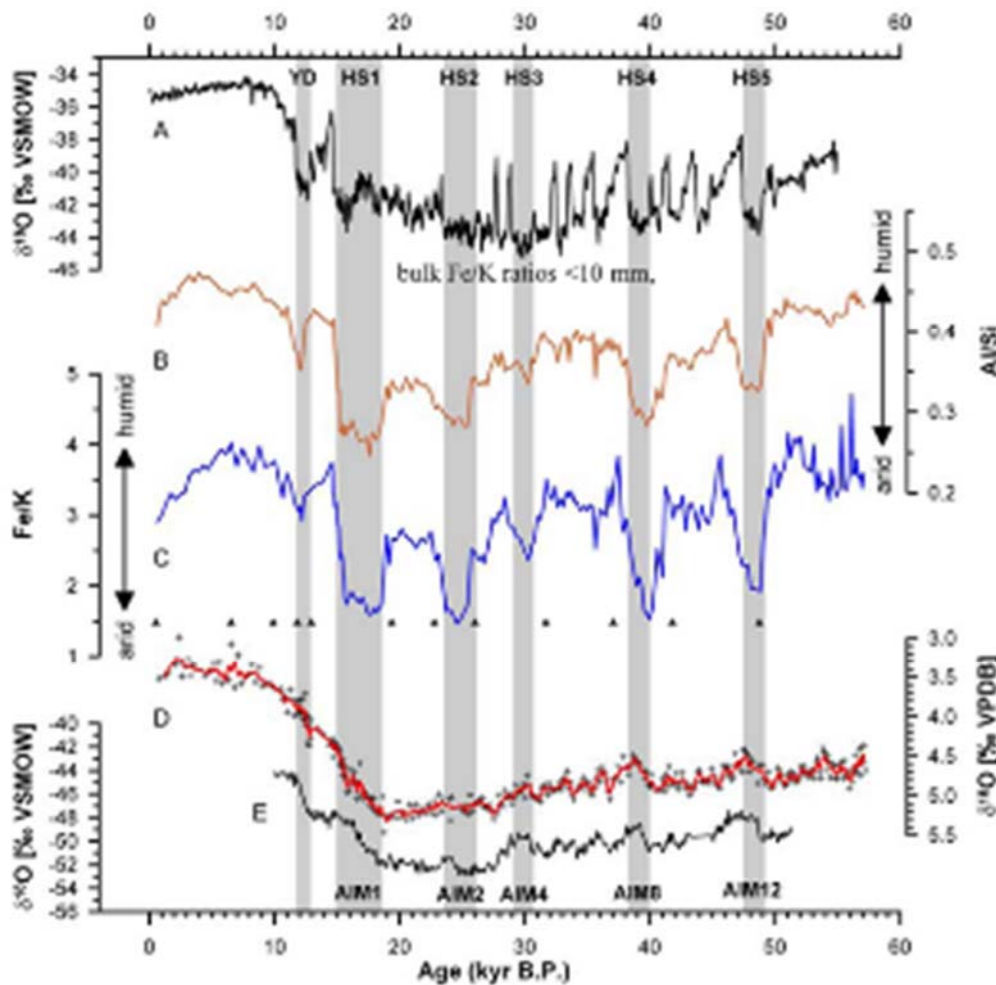


Fig. 68. “Comparison of sedimentary records of core GeoB9508-5 with (a) $\delta^{18}O$ of Greenland (North Greenland Ice core Project) and (e) Antarctic (EPICA Dronning Maud Land) ice cores vs. time (EPICA, 2006). (b) Bulk Al/Si ratios, (c) and (d) oxygen isotope record of benthic foraminifera in core GeoB9508-5. Gray bars indicate the approximate occurrence of Dansgaard-Oeschger Stadials associated with Heinrich events [i.e., HS] and the Younger Dryas (YD) in the NH and the corresponding Antarctic Isotope maxima in the SH.” Figure and captions after Mulitza et al. (2008). AGU copyright free policy.

These events must be interpreted as periods with much lower sediment discharge from the Senegal River together with an increase in atmospheric dust input as a consequence of drought. Geomorphological evidence for a much drier climate in much of northern Senegal is given for the most recent multimillennial period of drought, occurring between ~ 19 – 15 ka BP at the onset of the last deglaciation. During this time much of Senegal was covered by the so-called Ogolian Dunes (Michel, 1973).

The presence of these dunes as far south as 14°N suggests a southward shift of the corresponding climate zone by 4° – 5° and provides additional evidence for aridity in the West African Sahel. Further evidence for aridity in the Sahel, at least during the Younger Dryas, comes from several lake records (Gasse and van Campo, 1994; Gasse, 2000).

Within the accuracy of the age model the repeated and abrupt initiation of dry Sahel climates occurs synchronously with the coldest SST in the northeastern Atlantic during the past 60 ka (de Abreu et al., 2003). These extremely cold SST only occur during Dansgaard-Oeschger Stadials associated with ice rafting (Heinrich) events in the NH. The longest drought with an approximate duration of ~ 4 ka occurs at the onset of the last deglaciation together with Heinrich Stadial 1 in the North Atlantic (Sarnthein et al., 2001) and a pronounced warming (AIM 1) of the same duration over Antarctica (EPICA, 2006) (Fig. 68e).

It is generally accepted (EPICA, 2006) that the antiphasing of temperatures over Greenland and Antarctica is due to reductions in the AMOC with a decrease of the heat export from the South Atlantic to the North Atlantic and a subsequent cooling of much of the North Atlantic surface. Hence, our data strongly suggest a relation between the strength of the AMOC and SST in the North Atlantic on the one hand and Sahel precipitation on the other hand. Previous studies (e.g., Street-Perrott and Perrott, 1990; Mulitza and Rühlemann, 2000; Chiang and Koutavas, 2004; Dahl et al., 2005; A. C. Itambi et al., 2009) interpreted drought in the tropics by a southward shift of the ITCZ. Our [model] experiments indeed suggest a southward shift of the ITCZ (i.e., monsoon trough) during AMOC slowdown by a few degrees latitude over West Africa.

It is however problematic to explain the widespread nature of drought exclusively with an ITCZ shift. Today, the ITCZ seems to be effectively independent of the system that produces most of the rainfall. The tropical rain-belt (which is often confused with the ITCZ) is in fact produced by a deep core of ascent lying between the axes of the African Easterly Jet (AEJ) and the Tropical Easterly Jet (TEJ), some ten degrees of latitude south of the ITCZ (Nicholson and Grist, 2003). Interestingly, a southward shift of the ITCZ has been rejected as a cause of the multidecadal Sahel drought during the second part of the last century (Citeau et al., 1989).

Also, a southward shift of the ITCZ as the sole reason for drought would require increased precipitation to the south of the present-day ITCZ. Such a pattern would be in disagreement with late Quaternary palaeolimnological

records from Lake Bosumtwi (~ 6°N), Ghana, which indicate dry conditions at the Guinean coast during millennial-scale periods of reduced AMOC (Peck et al., 2004; Shanahan et al., 2006). Likewise, palaeoceanographic records off Nigeria (~ 3°N) (Weldeab et al., 2007), Congo (~ 6°S) (Schefuß et al., 2005) and Angola (~ 12°S) (Dupont et al., 2008) do not show indications of increased precipitation during Heinrich Stadials.

The simulated drying in our water hosing experiment is not restricted to the Sahel. Rather, it affects the entire West African region including the Guinea coast ... in agreement with the palaeoclimatic evidence, but in contrast to the simulation of Dahl et al. (2005). For this reason, the proposed mechanism which involves an intensified moisture export by the midlevel AEJ is a reasonable explanation for the observed precipitation pattern. It must be noted that our model setup includes a comprehensive land surface component with sophisticated soil-vegetation biogeophysics and hydrology (Bonan et al., 2002; Oleson et al., 2004), but fixed vegetation. An interactive vegetation cover would likely worsen the simulation of the present monsoon climatology. Prescribing the vegetation provides for a more reliable simulation of the climatology, although potentially important feedbacks are excluded in the water-hosing experiment. Even though vegetation-climate feedbacks could conceivably act to amplify the response of Sahel precipitation to a remotely forced perturbation (Charney, 1975; Zeng et al., 1999), there is no obvious reason why the basic dynamical mechanisms of Sahel drying deduced from our CGCM [coupled general circulation model] water-hosing experiment should be affected fundamentally by vegetation dynamics (cf. Hales et al., 2006).

We also note that the assumption of a strong positive vegetation-precipitation feedback over northern Africa has recently been challenged (Levis et al., 2004; Liu et al., 2007b, 2006; Wang et al., 2008). Essentially, the same holds for dust radiative feedbacks (Yoshioka et al., 2007). Excluding vegetation and dust feedbacks, our approach can be considered as a 'maximum simplicity model' to simulate a physically consistent mechanism of Sahel drying in response to a weakening of the AMOC. In the present study, no attempts have been made to simulate and perturb a glacial climate state. Simulations of glacial West African climate can hardly be validated. Moreover, it has recently been shown that the simulation of glacial African rainfall is mostly model dependent (Braconnot et al., 2007). Within the framework of the Palaeoclimate Modeling Intercomparison Project PMIP-2, simulations of the Last Glacial Maximum with five different CGCMs yielded summer Sahelian rainfall anomalies ranging between -42% and +16% depending on the model. We therefore suspect that trustworthy simulations of the glacial West African monsoon dynamics are currently not available. As a note of caution, however, we emphasize again that varying boundary conditions (i.e., ice sheet distribution, orbital parameters, atmospheric composition) through Marine Isotope Stages 2 and 3 have not been taken into account in our modeling study."

An analogous extensive and important related study was carried out by Tjallingii et al. (2008). Only a few highlights are here reported, but the interested reader ought to refer to the original paper. Let us report first their abstract. The migration of prehistoric humans was severely controlled by the northwest African hydrological balance during the Pleistocene (Kuper and Kröpelin, 2006). In addition, it is thought that the hydrological balance also played an important role in global teleconnection mechanisms, during both Dansgaard-Oeschger and Heinrich events (Broecker, 2003). On the other hand, the largest part of high-resolution African climate records do not refer to millennial-scale climate changes during the last glacial-interglacial cycle (Kuper and Kröpelin, 2006; Gasse, 2000; Street-Perrott and Perrott, 1990; deMenocal et al., 2000), or in any case they lack an accurate chronology (Zhao et al., 2006).

Tjallingii et al. (2008) study siliciclastic marine sediments collected off the coast of Mauritania. They analyze grain-size and reconstruct changes in northwest African humidity during the past 120,000 years. Then, they consider the simulations of palæohumidity – according to a coupled atmosphere-ocean-vegetation model referring to the period 1984-2003, provided by the *International Research Institute for Climatic Prediction* (<http://iri.ldeo.colombia.edu>). Their final figure (not here shown) shows a map of the mean values, for boreal winter and summer, of precipitation rates, and of surface wind direction and strength, through the northeastern Atlantic.

A simplified map is here shown (Fig. 69) to show the location of the sediment cores *GeoB7920-2* offshore Mauritania (yellow star) and *MD95 2042* offshore Spain (red circle), of the *North Greenland Ice core Project* (NGRIP) ice core (white circle) and of the two grid boxes (Sahara box and Sahel box) that are considered by the CLIMBER-2 model that they used.

Tjallingii et al. (2008) claim that they found a good agreement with the model indicating “the reoccurrence of precession-forced humid periods during the last interglacial period similar to the Holocene African Humid Period.” They “suggest that millennial-scale arid events are associated with a reduction of the North AMOC and that millennial-scale humid events are linked to a regional increase of winter rainfall over the coastal regions of northwest Africa.”

They specify that the CLIMBER-2 model “is a global atmosphere-ocean-vegetation (AOV) model of intermediate complexity ... The rather coarse geographic resolution of CLIMBER-2 covers northern Africa by three grid boxes corresponding to the Sahara, the Sahel and tropical northern Africa ...” The purpose of the two simulations was to focus on the “response of the North African precipitation and vegetation cover to low-latitude insolation variations and high-latitude Heinrich events....”

The AOV-IC simulation describes the long-term climate variations over multiple precessional cycles by using external forcing of orbital-induced insolation, prescribed variations in atmospheric CO₂ concentrations and prescribed inland ice variations derived from global sea-level variations (Claussen et al., 2006). The AOV-IC-f simulation describes millennial-scale climate variations

between 60 – 20 ka BP. In contrast to AOV-IC, AOV-IC-f includes an additional freshwater forcing in the North Atlantic to simulate Heinrich events (triggered every 7.5 ka) and Dansgaard-Oeschger events (Arz et al., 2003) ...” However, they remark that the timing of the simulated Heinrich events is included *a priori*, not predicted, and the events are not synchronous with real Heinrich events. In addition, they warn that “owing to the geographic coarseness of CLIMBER-2, these simulations are considered more a test of concept rather than a detailed prediction.”

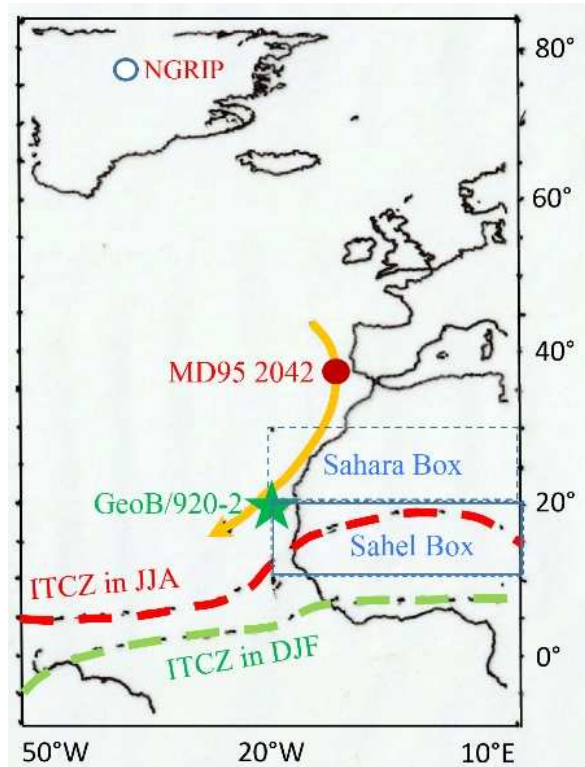


Fig. 69. Location of the *North Greenland Ice core Project* (NGRIP) ice core (white circle), of the sediment core *GeoB7920-2* offshore Mauritania (green star) and of the sediment core *MD95 2042* offshore Spain (red circle). The two grid boxes are shown of the CLIMBER-2 model used by Tjallingii et al. (2008). The North Atlantic eastern boundary current (orange arrow) and the position of the ITCZ (dotted line) are also shown, in two seasons (summer red; winter light green). Simplified figure based on a much more detailed figure after Tjallingii et al. (2008). See text. Unpublished figure.

Tjallingii et al. (2008) also show a plot (not here shown) that compares the simulations according to the AOV-IC model of both the vegetation cover and the annual mean daily precipitation (mm day⁻¹) computed either in the Sahara grid box (20° – 30°N) or in the Sahel grid box (10° – 20°N). In addition, the plot shows the time variation of the continental humidity index recorded in core *GeoB7920*.

Precipitations, according to the AOV-IC model display dominant precession-forced variations in both the Saharan and the Sahel regions, and are associated to increasing strength of monsoons, and to a northward ITCZ drift during

precession maxima (Claussen et al., 1999; Renssen et al., 2006).

In the Sahara region, abrupt (relative to orbital forcing) large-scale northward expansion of the Saharan grassland are observed correlated with these precession-forced variations that are likely to be caused by a nonlinear biogeophysical feedback (Claussen et al., 1999; Renssen et al., 2006; Liu et al., 2007b). These precession-forced humid periods agree with the humid periods during *MIS5* (*Marine Isotope Stage 5*; roughly ~105-95 ka BP; see Figs 31 and 32 of Gregori et al., 2025i) and the Holocene in core *GeoB7920*.

In any case, according to both evidence of simulation models and of proxy data, the Saharan vegetation expands and retreats much faster than the variations of orbital forcing, consistently with the evidence derived from the Holocene *AHP* (*African Humid Period*) (deMenocal et al., 2000; Weldeab et al., 2007). Therefore, humid period gives a test for the nonlinear response of both climate and vegetation. In addition, Tjallingii et al. (2008) find that, according to the *AOV-IC* Sahara simulation, no relevant precession-forced humid periods occurred during the last glacial period. In addition, they claim that the expansion of the *NH* ice caps, originating a colder and drier climate - in combination with a weaker precessional forcing during the last glacial - were such as to prevent the influence on the Sahara by the African monsoons. Similar dry conditions are observed in the humidity record of *GeoB7920*, both during the maximum glacial conditions of *MIS4* (roughly ~ 75 – 57 ka BP) and *MIS2* (roughly ~ 25 – 12 ka BP).

In another plot, not here shown, Tjallingii et al. (2008) compare the time variation of the continental humidity index of core *GeoB7920* with the model-data referring to the northern Africa humidity and vegetation cover from 65 to 15 ka ago. *AOV-IC-f* is the model simulation of the vegetation cover and the annual mean daily precipitation (mm day^{-1}) both in the Sahara grid box ($20^\circ - 30^\circ\text{N}$) and in the Sahel grid box ($10^\circ - 20^\circ\text{N}$). A trigger by North Atlantic freshwater pulses occurred every ~7.5 ka. They also show the North Atlantic ice rafted debris events (Marchal et al., 2002; Bard et al., 2000)."

Both the *AOV-IC-f* model and proxy data are suggestive of "millennial-scale dry events in response to freshwater pulses in the North Atlantic. Although the Heinrich event-like freshwater perturbations of the *AOV-IC-f* simulation were prescribed every 7.5 ka, the corresponding dry events in the Sahel region are strikingly similar to the dry events seen during H6, H5 and H1, and to a lesser extent H4 and H3 in the humidity record of *GeoB 7920-2* ..." Therefore, dry events on the millennial-scale in *GeoB 7920-2* seem to be the response to freshwater pulses into the North Atlantic, although an abrupt millennial-scale humid event during *MIS3* (roughly ~ 58 – 25 ka ago) is not found in both *AOV-IC* and *AOV-IC-f* simulations.

Both model simulations and proxy data are suggestive of an orbital-forced strengthening of the African monsoon during *MIS5*, resulting into an expansion of the Saharan vegetation cover, which is comparable to the Holocene *AHP*. These findings agree with the hydrological balance of tropical western African, seemingly depending on moisture

transport from the eastern equatorial Atlantic (Schefuß et al., 2003; Weldeab et al., 2007). In fact, the dominant process in model simulations is moisture transport from the tropical and subtropical Atlantic. "However, North African pollen and plant macrofossil data (Jolly et al., 1998) and the *aeolian dust record in the northern Red Sea region* (Arz et al., 2003) suggest that moisture transport from the North Atlantic and Mediterranean Sea into Africa's Mediterranean regions cannot be neglected." On the other hand, it is unfortunate that the *CLIMBER-2* simulations cannot assess the amount of moisture transport from Mediterranean to Africa.

In any case, both *AOV-IC-f* simulation and proxy data clearly envisage that high-latitude Heinrich events are a forcing agent for the millennial-scale dry events on the northern African continent. This agrees and supports the inference of previous studies (Gasse, 2000; Street-Perrott and Perrott, 1990; Zhao et al., 2006; Adegbe et al., 2003; deMenocal et al., 2000a). "However, generally dry conditions over the North African continent during periods of stronger glaciation probably resulted in a weaker expression of H3 and H4, and the absence of H2 in the humidity record of *GeoB7620-2*. In the model, the Heinrich event forcing is transmitted through large-scale changes in the North Atlantic overturning circulation (Claussen et al., 2003) ... which is supported by the $\delta^{13}\text{C}$ record of *GeoB7920-2* ..."

As an alternative mechanism, other authors (Street-Perrott and Perrott, 1990; Zhao et al., 2006; deMenocal et al., 2000a; Chapman et al., 2000; Bard, 2002) suggested a transmission of cold North Atlantic *SST* to lower latitudes, caused by the eastern boundary current. However, according to both model simulation and proxy data, the millennial-scale dry events are strongly suggestive of a decoupling between climate change on the millennial-scale in the northern high-latitude and low-latitude African monsoon forced by the precession. This supports the humidity reconstructions of the northwest African subtropics (Gasse, 2000; Street-Perrott and Perrott, 1990; Adegbe et al., 2003; deMenocal et al., 2000a).

On the other hand, concerning the differences between West African tropical humidity records (Schefuß et al., 2003; Adegbe et al., 2003), no consensus seems to exist dealing with the occurrence of millennial-scale climate variations in the African tropics, being the possible different response of distinct humidity proxy to different regional influences.

A remarkable agreement is found between the millennial-scale humid events displayed by the humidity record of *GeoB7920-2* during *MIS3*, and the millennial-scale humid events recorded in the western Mediterranean (Allen et al., 1999; Combourieu Nebout et al., 2002; Moreno et al., 2005). The explanation of these humid events was given in terms of a southward drift of the mid-latitude wind systems combined with an increase of the influence of North Atlantic winter precipitation (Allen et al., 1999; Combourieu Nebout et al., 2002; Moreno et al., 2005). The coarse scale used by the *CLIMBER-2* model cannot simulate these humid events in the *AOV-IC-f* model. However, the general scenario is supported by, and agrees

with, a decoupling of the low-latitude African monsoon during MIS3 and the millennial-scale climate change at northern high-latitude (Gasse, 2000; Street-Perrott and Perrott, 1990; Weldeab et al., 2007; Adegbe et al., 2003). In addition, two model-predicted events are supported by proxy data, i.e. (i) a largely vegetated Sahara, and (ii) an abrupt expansion and retreat of Saharan grassland vegetation during isotope stages 5a (roughly ~ 87 – 75 ka ago) and 5c (roughly ~ 120 – 103 ka ago). Moreover, both model and proxy data indicate that high-latitude Heinrich events are responsible for millennial-scale dry periods in North Africa. On the other hand, the *GeoB7920-2* records indicate millennial-scale humid events during MIS3 that cannot be reproduced by the *CLIMBER-2* simulations.

Skonieczny et al. (2015) investigated the palaeohydrology of western Africa. Their findings are a remarkable synthesis of previous investigations, and are closely pertinent to the present discussion of the global space and time variations of air-earth currents. They show Figs 70 through 73 that, in several respects, are self-explanatory. They use the *SAR* images from the *Japanese Advanced Land Observing Satellite/PALSAR*. No extensive details are here given. Refer, rather, to the original paper, where also the rich previous references are given that – in contrast - owing to brevity purpose are here omitted. We report here only some brief excerpts from their paper and discussion.

Skonieczny et al. (2015) state that “the Sahara experienced several humid episodes during the late Quaternary, associated with the development of vast fluvial networks and enhanced freshwater delivery to the surrounding ocean margins.” They refer specifically to marine sediments recorded offshore Western Sahara associated to palaeoriver deposition. The geomorphological data monitored by orbital radar satellite imagery shows the

location of a wide buried palaeodrainage network on the Mauritanian coast.

Hence, relying on information provided by the literature, they “propose that reactivation of this major palaeoriver during past humid periods contributed to the delivery of sediments to the Tropical Atlantic margin.” This is a way to interpret the marine sediments offshore Western Sahara, with a substantial improvement of our understanding of the palaeohydrological history of the Sahara.

During the last few million years, insolation changes, which were forced astronomically, drove the monsoon dynamics and the periodical onset of humid episodes in North Africa. This implied, during some periods of time, the “greening” of the Sahara and the expansion of savannah throughout most of the desert.

These are the aforementioned African humid periods (*AHPs*), which were caused by a great transformation of the hydrological cycle over North Africa and were associated with the intensification of the African summer monsoon, as a consequence of an increase of insolation and the subsequent northward migration of the *ITCZ*. Let us stress that Skonieczny et al. (2015) do not consider any possible role associated to a time varying input by air-earth currents, and soil exhalation of endogenous energy.

Thus, important fluvial networks were developed in the Sahara area, due to a variation of the position of this rain belt, implying and enhancement of freshwater delivery to the oceans (Fig. 70). In fact, marine sediment records from the Mediterranean and Atlantic margins are signatures of monsoon variability in northern Africa that occurred since the middle of the Pleistocene. The best documentation of past *AHPs* is probably given by the organic-rich sediment layers (*sapropels*) in the Eastern Mediterranean basin, related to periods of enhanced discharge from the Nile River, which date back to the Pliocene.

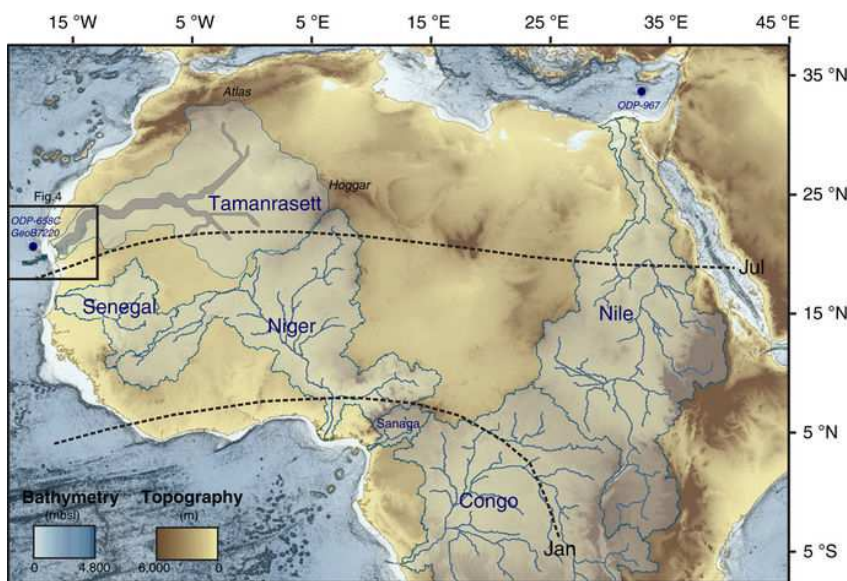


Fig. 70. “Hydrological context of Africa. Map of the main rivers of the Mediterranean, West African Tropical and Equatorial margins and associated watersheds. The present-day active Nile, Senegal, Niger, Sanaga and Congo rivers watersheds are drawn in light blue (adapted from the USGS HydroSHEDS database). The outlines and the main course of the Tamanrasett palaeowatershed ... are drawn in blue and grey, respectively. The newly identified Tamanrasett palaeodrainage ... as well as Cap Timiris Canyon ... (Fig. 73) are drawn in dark blue. January and July present-day ITCZ positions (dotted lines) as well as GeoB7920 core, ODP658 and ODP967 sites used in Fig. 71 are also plotted.” Figure and captions after Skonieczny et al. (2015). Reproduced with kind permission of Nature Communications, (CC BY 4.0).

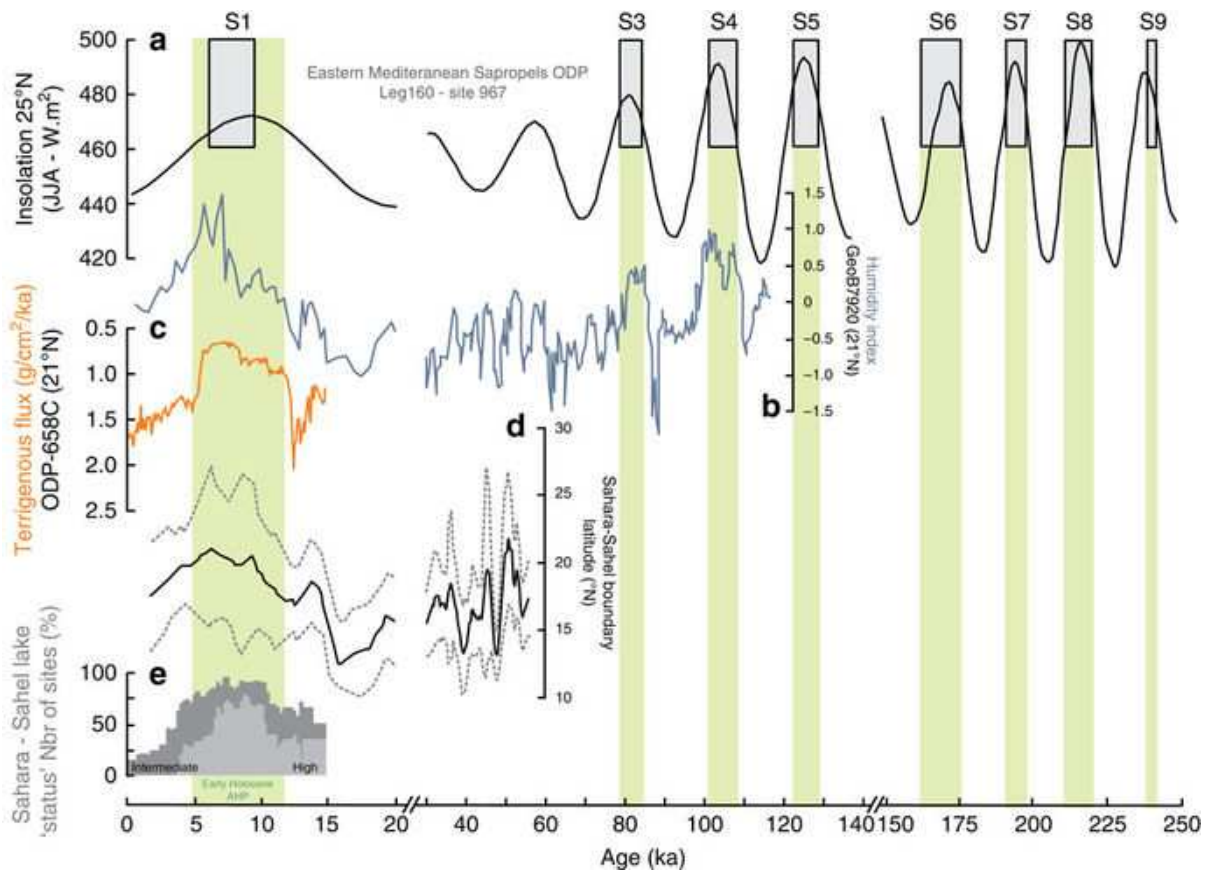


Fig. 71. "Compilation of North Africa palaeoclimate records for the last known period of activity of the Timiris Canyon. (a) Sapropels record from core ODP Leg 160 ... together with summer insolation (June, July and August) at 25°N The AHPs identified using the sapropels1 (except for the early Holocene AHP) are highlighted in green. (b) Continental humidity index from grainsize measurements of core GeoB7920 (... 20.75°N; 18.58°W), (c) Terrigenous Flux ... of ODP658 site (20.75°N; 18.58°W), (d) the estimated latitudinal position of the sedimentary Sahara/Sahel boundary ... (black line) with its uncertainty (grey dashed lines). (e) Lake level status in East and North African basins ... " Figure and captions after Skonieczny et al. (2015). Reproduced with kind permission of Nature Communications, (CC BY 4.0).

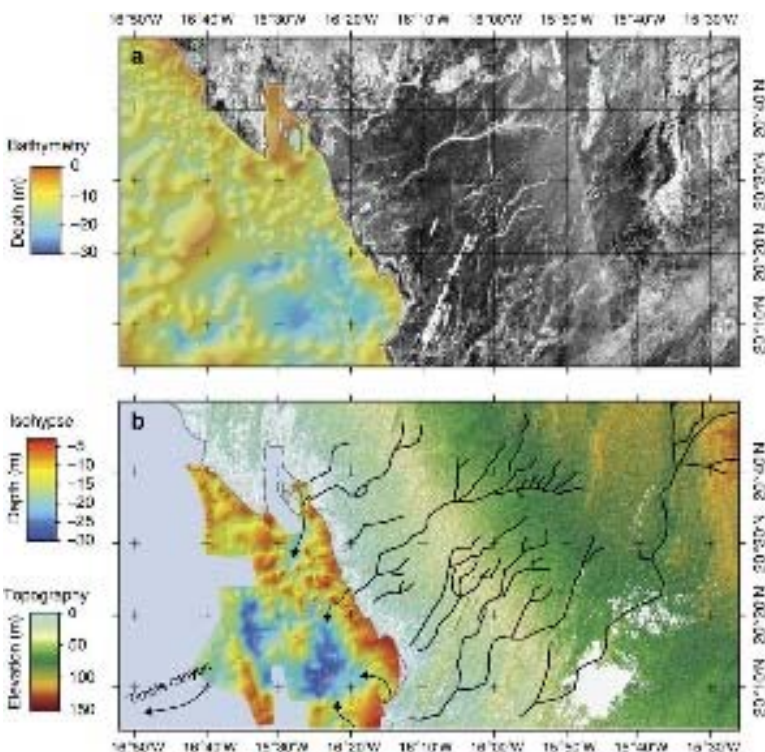


Fig. 72. "Coastal section of the Tamanrasset palaeoriver. (a) PALSAR radar observation of the coastal part of the Mauritania. The scale of grey corresponds to the back-scattering power. (b) Coastal part of the Tamanrasset palaeodrainage (black) identified in the PALSAR image. Isohypse map of the bedrock roof showing the presence of palaeovalleys (arrows) of the Arguin Basin ... " Figure and captions after Skonieczny et al. (2015). Reproduced with kind permission of Nature Communications, (CC BY 4.0).

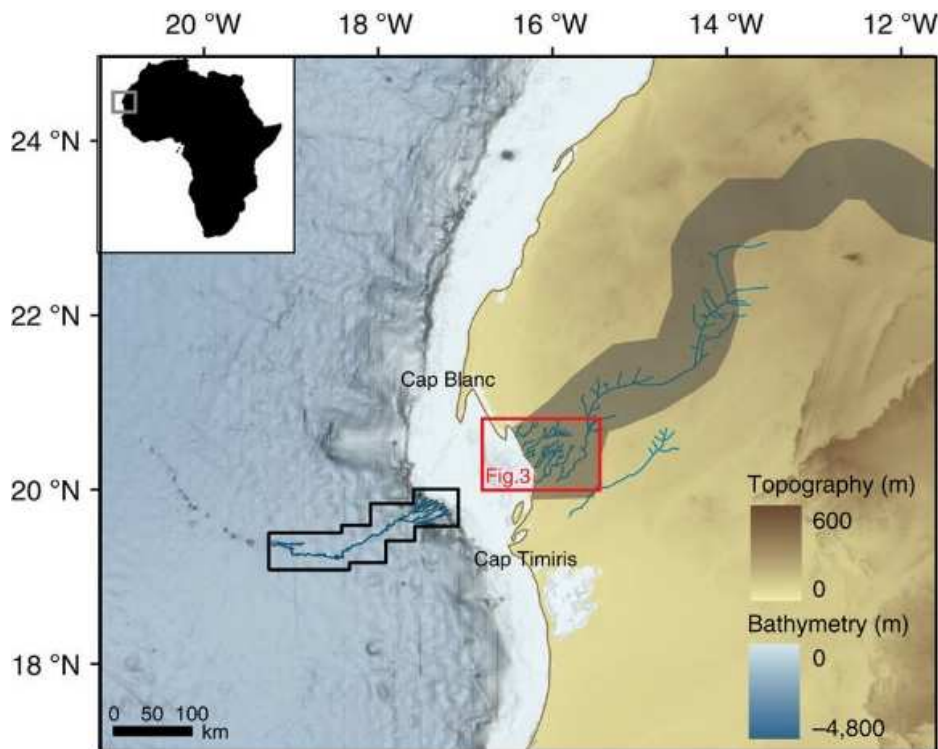


Fig. 73. "Continuity of the Tamanrasett River – Cap Timiris giant system. Complete identified Tamanrasett palæodrainage (blue), Tamanrasett River water valley as suggested by the STN ... (dark grey band), Cap Timiris Canyon pathway ... (dark blue) mapped on the GEBCO bathymetry." Figure and captions after Skonieczny et al. (2015). Reproduced with kind permission of *Nature Communications*, (CC BY 4.0).

In fact, biological proxies are available during the entire Phanerozoic. The evidence is inside sedimentary layers particularly rich in organic carbon. These information deal either with the geological past, and this is identified with "black shales" and with "sapropels". The "black shales" were first studied and are better known, while the so-called "sapropels" are a more recent concern. Even if their interpretation is somewhat controversial, they provide intriguing evidence. Their distinction is related to the time of their deposition. "Black shale" is the name of several comparatively common kinds of sedimentary rocks that look dark because they are rich in unoxidized carbon. They are the most common sedimentary rock.

The Late Cænozoic "sapropels" of the Mediterranean basin have been extensively studied (see the review by Cramp and O'Sullivan, 1999; or Passier et al., 2001), and are considered near-modern analogs of ancient black shale.

Compared to the Cænozoic or Mesozoic black shales, far less is generally known about the black shales of the Palæozoic. The exact mode of their origin is controversial. They appear thinly laminated, exceptionally rich in organic matter (~ 5% or more carbon content) and sulfide (mainly iron sulfide, usually pyrite), with unusual concentrations of some trace elements (*U*, *V*, *Cu*, *Ni*). They contain some rare fossil organisms, either replaced by pyrite or preserved as a film of graphite. When their thin lamina cannot be recognized, they are denoted as mudstones, made of particles < 1/16 mm size. In addition, siltstones are rocks with similar particle sizes but with less clay.

Shales can be typically found in some Palæozoic and Mesozoic strata, and were deposited in anoxic and reducing environments, such as in stagnant water columns or in very slow moving water, e.g. in lakes, lagoons, flood plains, river deltas, off the sandy beaches, and also on continental

shelves, in relatively deep and quiet water. In fact, some geologists hold that they formed at depth where a stable stratification of lighter, fresher water occurred, overlying and sealing off from the atmosphere a more saline, stagnant layer. Other authors envisage that the stagnant conditions occurred in shallow seas or in lagoons. Black shales denote periods of anomalous expansion of the biosphere, which were certainly related to anomalous atmospheric concentrations of CO_2 , consistently with the aforementioned Ronov' "principle of preservation of life".

Also "oil shales" are specifically reported. Significant amounts of shale oil and combustible gas can be extracted from them. Their potential amount is therefore normally quoted in terms of profitable extraction of shale oil and combustible gas or for burning as a fuel. Their age can be from Cambrian to Tertiary, and they range from small occurrences to enormous size that occupy thousands of square kilometers.

"Sapropels" - their name derives from ancient Greek "sapro" (putrefaction) and "pelos" (mud) - are analogous to black shales, but they allow for a comparably better temporal resolution. This term is used in marine geology to describe dark colored, fine-grained sediments that are rich in amorphous organic matter. For a review refer to Kemp (1996, 2003), Camp and O'Sullivan (1999) and Rohling and Thunell (1999), including their correlations with other palæoclimatic indicators.

Formerly, two separate communities studied black shales and sapropels. However, since Meyers and Negri (2003) and Negri et al. (2006), they joined their studies (e.g., Meyers, 2006, 2006a). With Negri et al. (2009, 2009a) also the Palæozoic Era was included, thus spanning altogether a deep time interval (291 Ma).

Upon making reference to Skonieczny et al. (2015), “*the most recent AHP, during the early Holocene, spans from ~ 11,700 – 5,000 years BP ... and is well recorded in a number of marine sedimentary archives from the Gulf of Guinea to the Northeastern Tropical Atlantic Ocean, the Mediterranean margin and the east of Africa ... Recently, a spectacular 400 km-long submarine channel system, the Cap Timiris Canyon, has been discovered on the western Sahara margin off Mauritania ... (Fig. 70) ...*”

That is, the Cap Timiris Canyon was linked to a major past river system. Skonieczny et al. (2015) used a *Simulated Topological Network (STN)* and mapped potential flow pathways based on a digital elevation model and inferred the location of a large river system in Western Sahara, upon considering the probable water sources in the Hoggar Highlands and the southern Atlas mountains in Algeria (Fig. 70). “*This so-called Tamanrasett River valley has been described as a possible vast ancient hydrographic system that would rank 12th at present among the top 50 largest drainage basins worldwide ... Although a putative link between the Tamanrasett palæoriver and the Cap Timiris Canyon has been already suggested previously ... direct evidence of any fluvial activity and of a connection to the canyon has never been found on the continent.*”

Skonieczny et al. (2015) relied on remote sensing monitoring by satellite, and identified “*a large palæodrainage network on the arid Mauritanian coast, shallowly buried at present under æolian sediments.*” They found also consistent information in the literature, and conclude that in agreement with other geomorphological and sedimentary evidence “*a major river system was indeed reactivated during some of the humid periods of the last 245 ka*”. Skonieczny et al. (2015) used the *Phased Array type L-band Synthetic Aperture Radar (PALSAR)*, which is one of the Japanese *ALOS* remote-sensing instruments. In particular, the L-band (1.2 GHz) can penetrate meters of low electrical loss material, such as æolian sand. Thus, it affords, in arid areas, to probe the first meters of subsurface geological features. They compared the records with the *STN*, and mapped geomorphological features buried under shallow æolian deposits.

In the coastal Mauritania area (Fig. 72a) they found geomorphological evidence of “*a palæodrainage system located in the Arguin Bay, between Cap Blanc and Cap Timiris (Figs 72b and 73)*” i.e. a palæoriver bed ~ 520 km long. “*Interestingly, it overlaps remarkably well with the coastal section of the course of the Tamanrasett River inferred from the STN (... Fig. 73). The reconstruction of the complete palæodrainage was not possible using the PALSAR because of the presence of thick sand dunes ... However, the branch of the palæodrainage network identified ... represents a fifth of the total length of the Tamanrasett fossil River highlighted by the STN ...*” In addition, they found that “*the course of the palæoriver is perfectly aligned with palæovalleys identified in the Arguin Basin ... (Fig. 72b), as well as with the proximal tributaries of the submarine Cap Timiris Canyon system (Fig. 73) ...*”

The discussion by Skonieczny et al. (2015) looks particularly pertinent for the present concern about air-earth

currents (several quotations are here skipped, and the reader ought to refer to the original paper).

“*Previous studies, focused on the morphology and the seismic structures of the Cap Timiris Canyon, have suggested that it may have been active for at least the last 245 ka ... during periods of lower sea-level stand, including during past humid phases of the West African tropical climate ... The only well-documented humid phase in the region is the early Holocene AHP, which is characterized by a strong summer insolation (Fig. 71) driving the ITCZ and the associated precipitations to higher latitudes than at the present. At that time, equatorial lakes reached their highest level (Fig. 71) and the present-day Saharan desert was the location of extensive vegetation, animal life and human settlements ... A recent geochemical study of marine records located off West Africa has estimated a position of the Sahara/Sahel boundary in this area to be ~ 21°N (±30) during the early Holocene AHP ... (Fig. 71). Because the identified branch of the Tamanrasett River lies at 20 – 23°N (Fig. 73), enhanced precipitations in the western Sahara region during this AHP could have fed most of the now buried palæodrainage system identified in this study. This hypothesis would be coherent with a recent seismic investigation of the Arguin Basin, which indicates the presence of wadi deltas in the inner part of the basin dated from 8.7 – 6.5 ka ... , implying significant runoff at that time. In addition, evidence that fluvial sediments were deposited in the Arguin Basin during the mid-Holocene between 11 – 6.5 ka ... supports the idea that the Tamanrasett River, at least its coastal part, was active during the last AHP and that it delivered river-borne sediments to the Arguin Basin at that time.*”

Also, sedimentary records from the Eastern Mediterranean Sea off the Nile River are suggestive of evidence of nine distinct sapropel layers during the last 245 ka, all of them corresponding to precession-driven summer insolation maxima (Fig. 71). In addition, these sapropel evidence, and the inferred corresponding *AHPs* are found to be synchronous with the aforementioned grain-size humidity index maxima, which are recorded on the West African margin in the fine fluvial deposits off Mauritania, with reference to the available period of time, i.e. the last 120 ka (Fig. 71). “*This correlation suggests that Nile floods and Tamanrasett River runoffs were synchronous during the AHPs of the last 120 ka.*”

Skonieczny et al. (2015) comment that no sedimentological evidence is presently available of fluvial deposits off Mauritania referring to the earlier period. If one assumes the synchronous behavior of humid phases in Eastern and Western sides of the Sahara hold during the 120 – 245 ka time period of activity of the Cap Timiris canyon, one infers “*as many as nine potential periods of runoff for the Tamanrasett River during the last 245 ka.*”

Skonieczny et al. (2015) note, however, comparing different *AHPs*, the span probably varied of the reactivated Tamanrasett River section and tributaries, depending on the extent of the northward migration of the *ITCZ* and associated rain belt.

For instance, it has been guessed that the Sahara vegetation was even more humid during the *MIS5e* (i.e., < 125 ka ago), and a wooded grassland predominated throughout Sahara. That is, during *MIS5e* the *ITCZ* rain belt position seemingly reached even higher latitudes, compared to the Holocene climatic optimum. This triggered the largest and northernmost reactivation of the Tamanrasset Basin. This evidence envisages that at those times the river-borne material deposited off Mauritania during the early Holocene *AHP*, and previous humid phases (e.g., *MIS5*), are likely to represent the contribution of the Tamanrasset River to the Tropical Atlantic margin.

“Overall, the identification of the palæodrainage system in the Arguin Bay area is very coherent with the hydrological landscape of Western Sahara, especially during the most recent AHPs. The testimony of a fluvial activity on the Mauritanian coast during recent humid periods provides the missing link between the development of lakes over Algeria and Mauritania ... fluvial evidence in Algeria ... and riverine signals recorded in the Arguin Basin ... and in marine sediments off Mauritania at that times ... This finding has also major implications for the interpretation of the terrigenous signals recorded during humid periods in marine sediments of the Northeastern Atlantic Tropical Ocean. A marine sediment record often used in the literature as a regional reference for the recent climatic evolution of the West Sahara is the one obtained at the ODP658C site (Fig. 70). This record documents a drastic reduction in terrigenous fluxes - assumed to be entirely of æolian origin - during the early Holocene AHP ... (Fig. 71), and has been used frequently over recent years to illustrate the abruptness of the Saharan environmental response to past insolation changes. The fact that a fraction of the terrigenous material deposited at this site possibly derived from the Tamanrasset River would imply that the dust contribution might have been even lower than inferred during the early Holocene AHP ... Our findings therefore support the hypothesis of a major drop in æolian inputs to the Northeastern Tropical Atlantic at that time, reinforcing the idea that the Saharan environment responds nonlinearly to gradual insolation and hydrological changes ...”

The emphasis ought to be on the great interannual variability that cannot be included in any model that displays some smooth trend. In fact, from a physical viewpoint, one should consider e.g. the role of the “Kenya hotspot” that is found to generate the formation of atmospheric perturbations that are the “seeds” for the tropical storms (see Gregori and Leybourne, 2025j and Figs 39 and 40). When a drought occurs in northern Kenya, rain precipitations is increased over Sahel. Kenya is also close to the region of the origin of desert dust. Also note in Figs 17 and 18 of Gregori et al. (2025g) the large perturbation of the *ITCZ* that seems originated just by the “Kenya hotspot”.

Hence, the erratic behavior of the Kenya hotspot - linked to the Southeast Indian Ridge (*SEIR*) (<https://www.iiisci.org/journal/sci/FullText.asp?var=&id=ZA424OY20>) - is a primary global circuit linked to these perturbations, and it is a primary driver co-responsible for the hurricanes in the Gulf of Mexico, and also for rain across central and western Africa. That is, no regular trend

vs. time is observed in the hurricane phenomenon. In general, there is a link to the 11 year solar cycle ascension/descension phases, which is also related to *ENSO*, but the link appears very erratic due to how much of this energy from solar activity affects the Earth, through e.m. induction into the *TD* dynamo. In any case, no regular trend can be observed in the climate of Africa. The role is always crucial of the time varying release of endogenous energy and the solar modulation through the “internal way”.

As far as the instrumental data are concerned dealing with the last several decades, Thomas and Nigam (2018), analyze the 20th century trends in seasonal temperature and precipitation over the African continent by means of observational datasets and historical climate simulations. They warn, however, that, owing to the agricultural economy of the continent, a seasonal perspective is better suited than an annual-average treatment, as seasonal hydroclimate variations are a leading control factor for agriculture. *“Examination of linear trends in seasonal surface air temperature (SAT) shows that heat stress has increased in several regions, including Sudan and northern Africa where the largest SAT trends occur in the warm season. Broadly speaking, the northern continent has warmed more than the southern one in all seasons.”* [This seems to be consistent with the several evidences linked to the approaching solar minimum that envisage an ongoing increase of endogenous heat from the northern polar cap, which is a vertex of the tetrahedron (Gregori and Leybourne, 2021).]

They conclude and claim that *“precipitation trends are varied but notable declining trends are found in the countries along the Gulf of Guinea, especially in the source region of the Niger River in West Africa, and in the Congo River basin. Rainfall over the African Great Lakes - one of the largest freshwater repositories - has, however, increased. It is shown that the Sahara desert has expanded significantly over the 20th century, by 11% – 18% depending on the season, and by 10% when defined using annual rainfall. The expansion rate is sensitively dependent on the analysis period in view of the multidecadal periods of desert expansion (including from the drying of the Sahel in the 1950s-1980s) and contraction in the 1902-2013 record, and the stability of the rain gauge network. The desert expanded southward in summer, reflecting retreat of the northern edge of the Sahel rainfall belt, and to the north in winter, indicating potential impact of the widening of the tropics.”*

Thomas and Nigam (2018) investigate the possible mechanisms, also by means climate simulations and comparison of the 20th century hydroclimate trends. However, *“modeling regional hydroclimate change over the African continent remains challenging, warranting caution in the development of adaptation and mitigation strategies.”*

In any case, it appears that the Sahel climate is part of the planetary climate system, where teleconnection plays a fundamental role, and it is impossible to reckon a regional climate trend to any one specific local primary driver because the driver is solar “internal way” e.m. induction related. The conspicuous palæoclimatic variations are

clearly indicative of the great complication of the system and of its several forms of feedback. The local biosphere, including the anthropic action, always enters into play by some more or less relevant, either direct or indirect, amount. A wise environmental management can certainly mitigate the unwanted climatic aspects, or the hazard of natural catastrophes. However, the natural trend in the background may be mitigated, though not changed.

Formal correlation analysis was carried out by several authors, between the West African climate and either one of the best known planetary circulation indices - such as e.g. ENSO, the Arctic Oscillation (AO), the North Atlantic Oscillation (NAO), the Pacific-North American pattern (PNA), the Quasi-Biannual Oscillation (QBO), the accumulated cyclone energy (ACE) (see Gregori and Leybourne, 2025j) or SST anomalies in various oceanic areas. However, the evidence appears much contradictory, the system is not stationary, and the results depend on the time interval of analysis. For instance, see Nicholson et al. (2000), Klotzbach and Gray (2004), and Fink et al. (2010), and references therein. The system is not linear. Neither it relies only on one degree of freedom (*d.o.f.*), while formal correlation analysis makes sense only for linear systems. The sunspot cycle has some regularities, but the energy impacting Earth's orbit from this cycle is not, as the leading role must be considered played by e.m. induction in the TD-dynamo, with control on the time-delayed release of endogenous energy.

Lyon and DeWitt (2012) attempted to investigate the teleconnection on the planetary scale of climatic anomalies. They introduce the problem as follows. "The failure of consecutive rainy seasons in East Africa presents a major climatic shock to the region, as witnessed by the resulting humanitarian crisis in 2011 (FEWS NET, 2011; United Nations Organization for the Coordination of Humanitarian Affairs, 2011).

While the East African short rains (the terms 'short rains' and 'long rains' are used to broadly describe a typically bimodal rainfall season across East Africa; the seasonal cycle of rainfall has notable regional variations and differing terms to describe them) have been studied

extensively, exhibiting a robust relationship with ENSO on the seasonal to interannual time scale (Mason and Goddard, 2001), climate scientists have focused considerably less attention on the long rains season. Attempts to link interannual variability of the long rains to large scale climate patterns such as ENSO and tropical Atlantic or Indian Ocean SSTs have met with limited success (Camberlin and Philippon, 2002; Indeje et al., 2000) or revealed relationships that only apply to the early, or late, stages of the season (Camberlin and Philippon, 2002; Camberlin and Okoola, 2003). On longer timescales, total precipitation received during the long rains season has been reported to be in decline in recent decades (e.g., Williams and Funk, 2011). This decline has been attributed to a contemporaneous, upward trend in SSTs in the south-central Indian Ocean and west Pacific Ocean. The suggested physical link is that increasing SSTs in this region favor a local enhancement of precipitation with the resultant latent heating altering regional wind and moisture flux patterns, ultimately reducing long rains precipitation in East Africa (Williams and Funk, 2011; Funk et al., 2008).

Recent rainfall and SST changes. An intriguing aspect of the failure of the long rains in 2011 is the associated large-scale, anomalous precipitation pattern (departure of March-May (MAM) 2011 rainfall from a 1979-2009 base period average ... Janowiak and Xie, 1999). Below-average rainfall in East Africa was accompanied by drier than average conditions across much of southwest Asia, the central and southern Indian Ocean and the west-central tropical Pacific. Precipitation was concurrently well above average in the western tropical Pacific and in a zonally elongated band extending across the northern Indian Ocean from the west Pacific westward to the Arabian Sea. Was this precipitation pattern a singular event, associated only with the most recent long rains failure?"

They implemented a detailed study and made reference to different models and data sets. No details are here reported, and only Fig. 74 is shown, which is one detail of a more complicated original figure. Data are somewhat unreliable before global satellite coverage as noted in Fig. 74 by the increased detail after late 1970's.

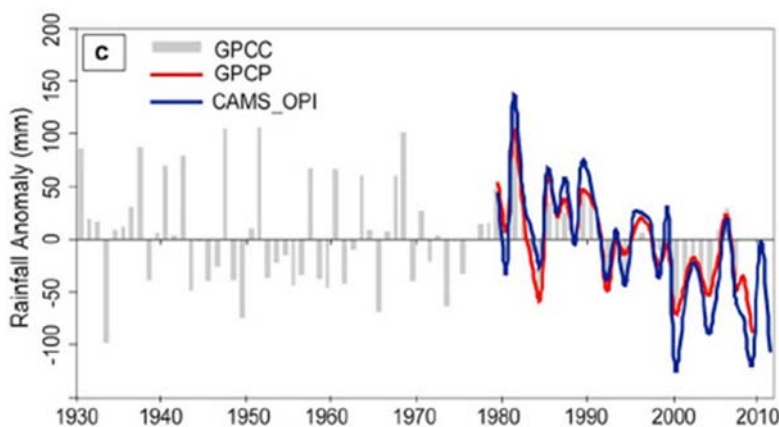


Fig. 74. "Time series of MAM precipitation departures from a 1979-2010 base period average (mm) averaged across land areas of East Africa (10°S - 12°N , 30°E - 52°E) from GPCC (Rudolf and Rubel, 2005), GPCP (Huffman et al., 2009), and CAMS-OPI (Janowiak and Xie, 1999)." Figure (simplified) and captions after Lyon and DeWitt (2012). AGU copyright free policy.

They conclude that their "analysis leads us to conclude that an abrupt decline in the East African long rains occurred around 1999 and it has been associated with a

recurrent, anomalous large-scale precipitation pattern during boreal spring since that time. While previous work has shown a strong connection between Indian Ocean SSTs

and variability in the East African short rains (e.g., Goddard and Graham, 1999), the long rains decline appears to be primarily forced by large scale SST changes mainly in the tropical Pacific (with abrupt changes in ocean temperatures in other regions near this time also observed; e.g., Cantin et al., 2010). The observed shift in Pacific SSTs in the late 1990s does not appear to be closely related to previously identified patterns of decadal variability in the basin and is not explained simply by changes ENSO behavior (e.g., Merrifield, 2011). What caused the shift is a currently unresolved question. [Let us stress this statement.] Our analysis does not preclude decadal variability or the influence of anthropogenic forcing.

Interestingly, the recent tendency for a cool eastern, and warm western, tropical Pacific is consistent with observational studies of global SST trends (Cane et al., 1997; Compo and Sardeshmukh, 2010; Williams and Funk, 2010) and somewhat reminiscent of theoretical studies of an ocean thermocline control on SST under anthropogenic forcing (Clement et al., 1996). It is noteworthy that over roughly the past three decades the difference in SST trends between observations and coupled model runs which include anthropogenic forcing is an ocean state reminiscent of La Niña. The climate models generate too much warming in the eastern Pacific in response to anthropogenic forcing (Hoerling et al., 2010; Cane et al., 1997; Clement et al., 1996) weakening the Pacific branch of the atmospheric Walker circulation (Vecchi and Soden, 2007). While some observational evidence suggests the Walker circulation has shown some signs of weakening over the past century (Vecchi et al., 2006), the results here and of Merrifield (2011) suggest that, at least over the last decade or so, the Walker circulation may have intensified, or at least been modified... “

That is, also upon looking at phenomena from the viewpoint of planetary-scale teleconnection, no clear inference seems evident. Concerning the Walker circulation, refer to Gregori et al. (2025g) for a propædeutic introductory science of the phenomena related to ENSO.

Conclusion

Summarizing, according to the general rationale of the whole present study, one must consider the huge variations of solar activity experienced by the Earth, and the spacetime changes of the release of endogenous heat in different parts of the world. These are air-earth currents that significantly affect the planetary oceanic and atmospheric large-scale circulation, thus producing - regionally and locally - eventual unexpected and seemingly erratic climate changes. These phenomena therefore cannot be explained in the frameworks of investigations referring to simple regional or even continental scale size or dealing only with a concern about the dynamics of the atmosphere/ocean system. These phenomena involve the crucial role of the planetary circulation pattern of Earth's fluids (ocean and atmosphere), as a response to the crucial trigger deriving from the “internal way” (Gregori et al., 2025a) of solar-terrestrial relations. However, since the input by the “internal way” is typically characterized by conspicuous

spacetime gradients that, at present, are still poorly known, the real predictability is very poor of these anomalous events.

The understanding and modeling of such a planetary-scale phenomenon requires a preliminary achievement of a reasonable way to monitor the spacetime variations of endogenous heat release. It is certain that the biosphere, including the anthropic impact, can amplify or reduce some unwanted natural trends, or in some way it can “dump” the system. The understanding of these very complicated and competing mechanisms is essential in order to be able to envisage - in every given case history of some unwanted concern - the most suitable actions that ought to mitigate or to recover from devastating climate changes. For instance, the real role played by humankind ought to be assessed, in the process that determined the desertification of Sahara. It is very likely that the anthropic impact alone had to be combined with natural causes. However, what anthropic action ought now to be implemented in order to attempt to recover from this very bad climatic condition? Would this be feasible?

In any case, it is just nonsensical to claim that anthropic pollution is - or is not - responsible for these climatic catastrophes and for the ongoing “climate change”.

Acknowledgement

We express sincere gratitude to the late Professor Tang Maocang for his far-looking intuition, and for sending in sabbatical year Dong Wenjie and Gao Xiaoqing. We also deeply thank Professor Antonino Zichichi, President of *World Laboratory*, for awarding a fellowship to Dong Wenjie and to Gao Xiaoqing, in the framework of a promotion of international cooperation between Italy and PRC. These actions resulted essential for the achievement and progress of understanding of the present set of papers. We also thank several scientists and colleagues who in different ways, along the years, contributed to the friendly discussions on several related items. It is impossible to list all of them.

Funding Information

G. P. Gregori retired since 2005. B. A. Leybourne is a semi-retired self-funded independent researcher. Dong Wenjie and to Gao Xiaoqing graduated and worked at the *Lanzhou Institute of Plateau Atmospheric Physics*, where Gao Xiaoqing is still active. Dong Wenjie had important commitments in Beijing, and at present as Professor and Dean, *School of Atmospheric Science, Sun Yat-sen University, Zhuhai, Guangdong, (PRC)*, and Director of *Future Earth Global Secretariat Hub China* and Secretary-General of *FE Chinese National Committee*.

Author's Contributions

This study derived from a long-lasting cooperation by all coauthors and from the emergence of long-lasting thought and discussion, particularly during the sabbatical years spent by Dong Wenjie and by Gao Xiaoqing.

Ethics

This article is original and contains unpublished material. Authors declare that there are not ethical issues and no conflict of interest that may arise after the publication of this manuscript.

References

- Adams, M. W., and R.M. Kelly, 1995. Enzymes from microorganisms in extreme environments. *Chemical Engineering News*, 73 (51): 32-42
- Adegbe, A. T., R. R. Schneider, U. Rohl, and G. Wefer, 2003. Glacial millennial-scale fluctuations in central African precipitation recorded in terrigenous sediment supply and freshwater signals offshore Cameroon. *Palaeogeography, Palaeoclimatology, Palaeoecology*, 197: 323–333
- Allen, J.R.M., U. Brandt, A. Brauer, H.-W. Hubberten, B. Huntley, J. Keller, M. Kraml, A. Mackensen, J. Mingram, Jörg F.W. Negendank, N.R. Nowaczyk, H. Oberhänsli, W.A. Watts, S. Wulf, and B. Zolitschka, 1999. Rapid environmental changes in southern Europe during the last glacial period. *Nature*, 400: 740–743; DOI:10.1038/23432
- Alpert, P., and M. Mandel, 1986. Wind variability – An indicator for a mesoclimatic change in Israel, *Journal of Applied Meteorology and Climatology*, 25: 1568-1576
- American Academy of Microbiology and American Geophysical Union*, 2016. Report on a Colloquium on Microbes and Climate Change, held in Washington, DC, in March 2016: 22 pp
- Anonymous*, 2012d. African rainfall estimates from NOAA Climate Prediction Center, NOAA/ National Weather Service, Center for Weather and Climate Prediction, Climate Prediction Center, National Weather Service, Environmental Visualization Laboratory
- Anonymous*, 2012e. Global Vegetation Mapping Data from NOAA Satellites, NOAA/ National Weather Service, Center for Weather and Climate Prediction, Climate Prediction Center, National Weather Service, Environmental Visualization Laboratory
- Anonymous*, 2014l. New map of 15 years of CO2 emissions, EarthSky, issued September 17, 2014
- Anonymous*, 2015bb. US deserts wet until 8,200 years ago, EarthSky, issued August 3, 2015
- Anonymous*, 2016ae. Why were prehistoric insects so huge? EarthSky, issued December 5, 2016
- Apaldetti, C., R.N. Martínez, I.A. Cerda, D. Pol, and O. Alcober, 2018. An early trend towards gigantism in Triassic sauropodomorph dinosaurs, *Nature Ecology & Evolution*; DOI:10.1038/s41559-018-0599-y
- Arz, H.W., F. Lamy, J. Pätzold, P.J. Müller, and M. Prins, 2003. Mediterranean moisture source for an early-Holocene humid period in the Northern Red Sea. *Science*, 300: 118–121
- Asefi-Najafabady, S., P.J. Rayner, K.R. Gurney, A. McRobert, Y. Song, K. Coltin, J. Huang, C. Elvidge, and K. Baugh, 2014. A multiyear, global gridded fossil fuel CO2 emission data product: Evaluation and analysis of results, *Journal of Geophysical Research, Atmospheres*, 119 (17): 10,213–10,231; DOI:10.1002/2013JD021296
- Aureliano, T., A.M. Ghilardi, R.T. Müller, L. Kerber, M.A. Fernandes, F. Ricardi-Branco and M.J. Wedel, 2023. The origin of an invasive air sac system in sauropodomorph dinosaurs”, *The Anatomical Record*; DOI:10.1002/ar.25209
- Bakker, E.S., J.L. Gill, C.N. Johnson, F.W.M. Vera, Christopher J. Sandom, G.P. Asner, and J.-C. Svenning, 2016. Combining paleo-data and modern exclosure experiments to assess the impact of megafauna extinctions on woody vegetation, *Proceedings of the National Academy of Sciences*, 113 (4): 847–855; DOI:10.1073/pnas.1502545112
- Bard, E., 2002. Climate shock: abrupt changes over millennial time scale. *Physocs Today*, 55: 32-38
- Bard, E., F. Rostek, J.-L. Turon, and S. Gendreau, 2000. Hydrological impact of Heinrich Events in the subtropical Northeast Atlantic, *Science*, 289 (5483): 1321-1324.; DOI:10.1126/science.289.5483.1321
- Barnett, A., 2007. Sizing up the sink, *Nature*, Publ. online: 12 Dec 2007; DOI:10.1038/climate.2007.76; reporting *Global Biogeochemical Cycles*, 21: GB4013 (2007)
- Barnett, A., 2008. The root problem, *Nature*, Publ. online: 4 Feb 2008; DOI:10.1038/climate.2008.10; reporting *Science*; DOI:10.1126/science.1151382 (2008)
- Barr, J.G., T.G. Troxler, and R.G. Najjar, 2014. Understanding coastal carbon cycling by linking top-down and bottom-up approaches, *EOS, Transactions of the American Geophysical Union*, 95 (35): 315-316
- Bauer, J.E., W.-J. Cai, P.A. Raymond, T.S. Bianchi, C.S. Hopkinson, and P.A.G. Regnier, 2013. The changing carbon cycle of the coastal ocean, *Nature*, 504: 61–70
- Beeston, A.F.L., 1995. Saba, *The Encyclopaedia of Islam*, 8 (2nd ed.), Brill.
- Bekker, A., J.F. Slack, N. Planavsky, B. Krape, A. Hofmann, K.O. Konhauser, and O.J. Rouxel, 2010. Iron formation: the sedimentary product of a complex interplay among mantle, tectonic, oceanic, and biospheric processes, *Economic Geology*, 105 (3): 467-508; DOI:10.2113/gsecongeo.105.3.467
- Ben-Gai, T., A. Bitan, A. Manes, and P. Alpert, 1993. Long-term change in October rainfall patterns in southern Israel, *Theoretical and Applied Climatology*, 46: 209-217
- Ben-Gai, T., A. Bitan, A. Manes, and P. Alpert, 2001. Climatic variations in the moisture and instability patterns of the atmospheric boundary layer on the east Mediterranean coastal plain of Israel, *Boundary-Layer Meteorology*, 100 (2): 363-371; DOI:10.1023/A:1018952406156
- Ben-Gai, T., A. Bitan, A. Manes, P. Alpert, and A. Israeli, 1998a. Aircraft measurements of surface albedo in relation to climatic changes in southern Israel, *Theoretical and Applied Climatology*, 61 (3/4): 207-215; DOI:10.1007/s007040050065
- Ben-Gai, T., A. Bitan, A. Manes, P. Alpert, and S. Rubin, 1998. Spatial and temporal changes in rainfall frequency distribution patterns in Israel, *Theoretical and Applied*

- Climatology, 61 (3-4): 177-190; DOI:10.1007/s007040050062
- Ben-Gai, T., A. Bitan, A. Manes, P. Alpert, and S. Rubin, 1999. Temporal and spatial trends of temperature patterns in Israel, *Theoretical and Applied Climatology*, 64 (3-4): 163-177; DOI:10.1007/s007040050120
- Ben-Gai, T., A. Bitan, A. Manes, P. Alpert, and Y. Kushnir, 2001a. Temperature and surface pressure anomalies in Israel and the North Atlantic Oscillation, *Theoretical and Applied Climatology*, 69 (3-4): 171-177; DOI:10.1007/s007040170023
- Biello, D., 2008. Do microbes make snow? *Scientific American*, 298, February 28th: pp. 6
- Blau, L., 1905. Sheba, Queen of. In *Jewish Encyclopedia*, I. Singer (ed.), Funk and Wagnall, vol. 11: 235–236
- Bonan, G.B., K.W. Oleson, M. Vertenstein, S. Levis, X. Zeng, Y. Dai, R.E. Dickinson, and Z.-L. Yang, 2002. The land surface climatology of the community land model coupled to the NCAR community climate model, *Journal of Climate*, 15: 3123-3149; DOI:10.1175/1520-0442(2002)015<3123:TLSCOT>2.0.CO;2
- Bonavia, J., S. Jessup, and E. Juanteguy, 1992. *The Silk Road from Xi'an to Kashgar*, Odyssey, Hong Kong; pp.: 1-320
- Boulnois, L., 1992. *La Route de la Soie*, Luce Boulnois et les Editions Olizane, Genève. Italian translation, published by Rusconi Libri, Milano; pp.: 1-316
- Bowen, R., 1991. *Isotopes and Climate*. Elsevier Applied Science, London and New York; pp.: 1-483
- Braconnot, P., B. Otto-Bliessner, S. Harrison, S. Joussaume, J.-Y. Peterchmitt, A. Abe-Ouchi, M. Crucifix, E. Driesschaert, Th. Fichefet, C. D. Hewitt, M. Kageyama, A. Kitoh, M.-F. Loutre, O. Marti, U. Merkel, G. Ramstein, P. Valdes, L. Weber, Y. Yu, and Y. Zhao, 2007. Results of PMIP2 coupled simulations of the mid-Holocene and Last Glacial Maximum-Part 2: Feedbacks with emphasis on the location of the ITCZ and mid- and high latitudes heat budget, *Climate of the Past*, 3: 279-296
- Branston, A.G., and P.T. Schickendanz, 1984. The effect of irrigation on warm season precipitation in the southern great plains, *Journal of Applied Meteorology and Climatology*, 23: 865-888
- Breeze, P.S., H.S. Groucutt, N. A. Drake, J. Louys, E.M.L. Scerri, S.J. Armitage, I.S. A. Zalmout, A.M. Memesh, M.A. Haptari, S.A. Soubhi, A.H. Matari, M. Zahir, A. Al-Omari, A.M. Alsharekh, M.D. Petraglia, 2017. Prehistory and palaeoenvironments of the western Nefud Desert, Saudi Arabia, *Archaeological Research in Asia*, 10: 1-16; DOI:10.1016/j.ara.2017.02.002
- Broecker, W.S., 2003. Does the trigger for abrupt climate change reside in the ocean or in the atmosphere? *Science*, 300: 1519-1522
- Brown, D.J., E.R. Hunt Jr., R.C. Izaurralde, K.H. Paustian, C.W. Rice, B.L. Schumaker, and T.O. West, 2010. Soil organic carbon change monitored over large areas, *EOS, Transactions of the American Geophysical Union*, 91 (47): 441-442
- Brown, J.H., and E.J. Heske, 1990. Control of a desert-grassland by a keystone rodent guild, *Science*, 250: 1705-1707
- Brusatte, S.L., G.T. Lloyd, S.C. Wang, and M.A. Norell, 2014. Gradual assembly of avian body plan culminated in rapid rates of evolution across the dinosaur-bird transition, *Current Biology*, 24 (20): 2386–2392. DOI:10.1016/j.cub.2014.08.034
- Budyko, M.I., A.B. Ronov, and A.L. Yanshin, 1985. *Istoriya atmosfery (in Russian)*. Gidrometeoizdat. English translation, *History of the Earth's atmosphere*. Published in 1987 by Springer-Verlag, Berlin, etc.; pp.:139
- Byrd, D., 2016u. *Rare Glimpse of Feathered Dinosaur Tail*, EarthSky, issued December 13, 2016
- Byrd, D., 2017t. *Intense storms batter Saturn moon Titan*, EarthSky, issued October 14, 2017
- Camberlin, P., and N. Philippon, 2002. The East African March-May rainy season: associated atmospheric dynamics and predictability over the 1968–97 period, *Journal of Climate*, 15: 1002–1019; DOI:10.1175/1520-0442(2002)015<1002:TEAMMR>2.0.CO;2
- Camberlin, P., and R.E. Okoola, 2003. The onset and cessation of the “long rains” in eastern Africa and their interannual variability, *Theoretical and Applied Climatology*, 75: 43–54
- Camp, A., and G. O'Sullivan, 1999. Neogene sapropels in the Mediterranean: a review, *Marine Geology*, 153: 11-28
- Cane, M.A., A.C. Clement, A. Kaplan, Y. Kushnir, D. Pozdnyakov, R. Seager, S.E. Zebiak, and R. Murtugudde, 1997. Twentieth-century sea surface temperature trends, *Science*, 275 (5302): 957–960; DOI:10.1126/science.275.5302.957
- Cannell, A.E.R., 2018. The engineering of the giant dragonflies of the Permian: revised body mass, power, air supply, thermoregulation and the role of air density, *Journal of Experimental Biology*, 221: jeb185405; DOI:10.1242/jeb.185405
- Cannell, A.E.R., 2018. The engineering of the giant dragonflies of the Permian: revised body mass, power, air supply, thermoregulation and the role of air density, *Journal of Experimental Biology*, 221: jeb185405; DOI:10.1242/jeb.185405
- Cantin, N.E., A.L. Cohen, K.B. Karnauskas, A.M. Tarrant, and D.C. McCorkle, 2010. Ocean warming slows coral growth in the central Red Sea, *Science*, 329: 322–325; DOI:10.1126/science.1190182
- Carney, R.M., Jakob Vinther, Matthew D. Shawkey, Liliana D'Alba, and Jörg Ackermann, 2012. New evidence on the colour and nature of the isolated *Archaeopteryx* feather, *Nature Communications*, 3: Article number: 637; DOI:10.1038/ncomms1642
- Castro, J., 2018. *Archaeopteryx: the transitional fossil*, Live Science, issued March 14, 2018
- Celant, A., (ed.), 1995. *Sahel. Geografia di una Sconfitta*. Pacini editore, Ospedaletto (Pisa); pp.: 1-239
- Cenizo, M., C. Acosta Hospitaleche, and M. Reguero, 2015. Diversity of pseudo-toothed birds (Pelagornithidae) from the Eocene of Antarctica, *Journal of Paleontology*, 89 (5): 870-881. DOI:10.1017/jpa.2015.48

- Chapman, M.R., N.J. Shackleton, and J.-C. Duplessy, 2000. Sea surface temperature variability during the last glacial-interglacial cycle: assessing the magnitude and pattern of climate change in the North Atlantic. *Palaeogeography, Palaeoclimatology, Palaeoecology*, 157: 1–25
- Charney, J.G., 1975. Dynamics of deserts and drought in Sahel, *Quarterly Journal of the Royal Meteorological Society*, 101: 193–202; DOI:10.1002/qj.49710142802
- Chatterjee, S., and R.J. Templin, (eds) 2004. Posture, locomotion, and paleoecology of pterosaurs, *Geological Society of America, Special Paper*, (376): 1–64
- Chiang, J.C.H., and A. Koutavas, 2004. Climate change - Tropical flip-flop connections, *Nature*, 432: 684–685; DOI:10.1038/432684a
- Choi, C.Q., 2016i. Earth's atmospheric oxygen levels continue long slide, *Live Science*, issued September 22, 2016
- Choi, C.Q., 2016j. Earth wobbles may have driven ancient humans out of Africa, *Live Science*, issued September 21, 2016
- Choi, C.Q., 2017a. Oldest fossils of our species push back origin of modern humans, *Live Science*, issued June 7, 2017
- Choi, C.Q., 2018a. Silk Road travelers' ancient knowledge may have irrigated desert, *Live Science*, issued January 12, 2018
- Christensen, T.R., T. Johansson, H.J. Akerman, M. Mastepanov, N. Malmer, T. Friborg, P. Crill, and B.H. Svensson, 2004. Thawing sub-arctic permafrost: effects on vegetation and methane emissions, *Geophysical Research Letters*, 31: L04501; DOI:10.1029/2003GL018680
- Christner, B.C., C.E. Morris, C.M. Foreman, Rongman Cai, and D.C. Sands, 2008. Ubiquity of biological ice nucleators in snowfall, *Science*, 319 (5867): 1214–; DOI:10.1126/science.1149757
- Chu, J., 2015a. Stalagmites pinpoint drying of American West, *MIT News*, issued July 27, 2015
- Citeau, J., L. Finaud, J.P. Cammas, and H. Demarcq, 1989. Questions relative to ITCZ migrations over the tropical Atlantic Ocean, sea surface temperature and Senegal River runoff, *Meteorology and Atmospheric Physics*, 41: 181–190; DOI:10.1007/BF01026109
- Claessens, L.P.A.M., P.M. O'Connor, and D.M. Unwin, 2009. Respiratory evolution facilitated the origin of pterosaur flight and aerial gigantism, *PLoS ONE*, 4 (2): e4497. DOI:10.1371/journal.pone.0004497
- Clapham, M.E., and J.A. Karr, 2012. Environmental and biotic controls on the evolutionary history of insect body size, *Proceedings of the National Academy of Sciences*, 109 (27): 10,927–10,930; DOI:10.1073/pnas.1204026109
- Claussen, M., A. Ganopolski, V. Brovkin, F.W. Gerstengarbe, and P. Werner, 2003. Simulated global-scale response of the climate system to Dansgaard/Oeschger and Heinrich events. *Climate Dynamics*, 21: 361–370
- Claussen, M., C. Kubatzki, V. Brovkin, A. Ganopolski, P. Hoelzmann, and H.-J. Pachur, 1999. Simulation of an abrupt change in Saharan vegetation in the mid-Holocene. *Geophysical Research Letters*, 26 (14): 2037–2040
- Claussen, M., J. Fohlmeister, A. Ganopolski, and V. Brovkin, 2006. Vegetation dynamics amplifies precessional forcing. *Geophysical Research Letters*, 33: L09709
- Clement, A.C., R. Seager, M.A. Cane, and S.E. Zebiak, 1996. An ocean dynamical thermostat, *Journal of Climate*, 9: 2190–2196; DOI:10.1175/1520-0442(1996)009<2190:AODT>2.0.CO;2
- Coleman Wasik, J.K., D.R. Engstrom, C.P.J. Mitchell, E.B. Swain, B.A. Monson, S.J. Balogh, J.D. Jeremiason, B.A. Branfireun, R.K. Kolka, and J.E. Almendinger, 2015. The effects of hydrologic fluctuation and sulfate regeneration on mercury cycling in an experimental peatland, *Journal of Geophysical Research-Biogeosciences*, 120 (9): 1697–1715; DOI:10.1002/2015JG002993
- Combouret N., N., J.L. Turon, R. Zahn, L. Capotondi, L. Londeix, and K. Pahnke, 2002. Enhanced aridity and atmospheric high-pressure stability over the western Mediterranean during the North Atlantic cold events of the past 50 kyr. *Geology*, 30 (10): 863–866; DOI:10.1130/0091-7613(2002)030<0863:EAAHP>2.0.CO;2
- Compo, G.P., and P.D. Sardeshmukh, 2010. Removing ENSO-related variations from the climate record, *Journal of Climate*, 23: 1957–1978; DOI:10.1175/2009JCLI2735.1
- Copley, M.S., R. Berstan, S.N. Dudd, G. Docherty, A.J. Mukherjee, V. Straker, S. Payne, and R.P. Evershed, 2003. Direct chemical evidence for widespread dairying in prehistoric Britain. *Proceedings of the National Academy of Sciences*, 100 (4): 1524–1529; DOI:10.1073/pnas.0335955100
- Corbett, G.J., D.R. Keller, B.A. Porter and C.P. Shelton, 2016. Archaeology in Jordan, 2014 and 2015 seasons, *American Journal of Archaeology*, 120 (4): 631–672; DOI:10.3764/aja.120.4.0631
- Cotton, W.R., and R.A. Pielke, 1995. *Human Impacts on Weather and Climate*, Cambridge Univ. Press; pp.: 1–288
- Craig, O.E., J. Chapman, C. Heron, L.H. Willis, L. Bartosiewicz, G. Taylor, A. Whittle, and M. Collins, 2005. Did the first farmers of central and eastern Europe produce dairy foods? *Antiquity*, 79 (306): 882–894
- CRC Handbook of Chemistry and Physics*, 1986. 66th ed., Chemical Rubber Company, Cleveland; pp.: 1–2363
- Cremaschi, M., A. Zerboni, C. Spötl, and F. Feletti, 2010. The calcareous tufa in the Tadrart Acacus Mt. (SW Fezzan, Libya): An early Holocene palaeoclimate archive in the central Sahara, *Palaeogeography, Palaeoclimatology, Palaeoecology*, 287 (1/4): 81–94; DOI:10.1016/j.palaeo.2010.01.019
- Cremaschi, M., and A. Zerboni, 2003. Wet and dry. Proxies for Holocene climate reconstruction in Central Sahara. The case study of the Acacus and surrounding ergs. Sahara Workshop, 12–13 June 2003, Univrsoty of East Anglia, Norwich

- Cure, J.D., and B. Acock, 1986. Crop responses to carbon dioxide doubling: a literature survey. *Agricultural and Forest Meteorology*, 38 (1/3): 127-145; DOI:10.1016/0168-1923(86)90054-7
- Cyr, H., and M.L. Face, 1993. Magnitude and patterns of herbivory in aquatic and terrestrial ecosystems, *Nature*, 361: 148-150; DOI:10.1038/361148a0
- Dahl, K., A.J. Broccoli, and R.J. Stouffer, 2005. Assessing the role of North Atlantic freshwater forcing in millennial scale climate variability: A tropical Atlantic perspective, *Climate Dynamics*, 24: 325-346; DOI:10.1007/s00382-004-0499-5
- Dalzell, B.J., J.Y. King, D.J. Mulla, J.C. Finlay, and G.R. Sands, 2011. Influence of subsurface drainage on quantity and quality of dissolved organic matter export from agricultural landscapes, *Journal of Geophysical Research*, 116; G02023; DOI:10.1029/2010JG001540
- Daniels, L.R.M., J.J. Gurney, and B. Harte, 1996. A crustal mineral in a mantle diamond. *Nature*, 379 (6561): 153-156
- Daza, J.D., E.L. Stanley, P. Wagner, A.M. Bauer, and D.A. Grimaldi, 2016. Mid-Cretaceous amber fossils illuminate the past diversity of tropical lizards, *Science Advances*, 2 (3): e1501080; DOI:10.1126/sciadv.1501080
- de Abreu, L., N.J. Shackleton, J. Schöfeld, M. Hall, and M. Chapman, 2003. Millennial scale oceanic climate variability off the Western Iberian margin during the last two glacial periods, *Marine Geology*, 196: 1-20; DOI:10.1016/S0025-3227(03)00046-X
- De Romanis, F., 1996. *Cassia, Cinnamomo, Ossidiana. Uomini e Mercè tra Oceano Indiano e Mediterraneo*, "Lerma" di Bretschneider, Roma; pp.: 1-324 + 20 plates
- de Vrese, P., S. Hagemann, and M. Claussen, 2016. Asian irrigation, African rain: Remote impacts of irrigation, *Geophysical Research Letters*, 43: 3737-3745; DOI:10.1002/2016GL068146
- Delclòs, X., E. Peñalver, A. Arillo, M.S. Engel, A. Nel, D. Azar, and A. Ross, 2016. New mantises (Insecta: Mantodea) in Cretaceous ambers from Lebanon, Spain, and Myanmar, *Cretaceous Research*, 60: 91-108; DOI:10.1016/j.cretres.2015.11.001
- deMenocal, P., J. Ortiz, T. Guilderson, and M. Sarnthein, 2000. Coherent high- and low-latitude climate variability during the Holocene warm period, *Science*, 288 (5474): 2198-2202; DOI:10.1126/science.288.5474.2198
- deMenocal, P.B., and J.E. Tierney, 2012. Green Sahara: African humid periods paced by Earth's orbital changes, *Nature Education Knowledge*, 3 (10): 12-17
- deMenocal, P.B., J. Ortiz, T. Guilderson, and M. Sarnthein, 2000a. Coherent high- and low-latitude climate variability during the Holocene Warm Period. *Science*, 288: 2198-2202
- Demuth, S., 2006. *Climate Variability and Change - Hydrological Impacts*, IAHS; pp.: 1-707
- Des Marais, D.J., 1985. Carbon exchange between the mantle and the crust, and its effect upon the atmosphere: today compared with Archean time. In *The Carbon Cycle and Atmospheric CO₂: Natural Variations Archean to present*, E.T. Sundquist, and W.S. Broecker, (eds), *Geophysical Monograph Series*, 32, American Geophysical Union: Washington, DC; pp.: 602-611
- di Lernia, S., 2002. Dry climatic events and cultural trajectories: adjusting Middle Holocene Pastoral economy of the Libyan Sahara. In *Droughts, Food and Culture: Ecological Change and Food Security in Africa's Later Prehistory*, F.A. Hassan (ed.) Springer; pp.: 225-250
- di Lernia, S., and M. Gallinaro, 2010. The date and context of Neolithic rock art in the Sahara: engravings and ceremonial monuments from Messak Settafet (south-west Libya). *Antiquity*, 84:954-975
- Dixon, E.J., 1993. *Quest for the Origins of the First Americans*, University of New Mexico Press, Albuquerque; pp.: 1-154
- Donato, D.C., J.B. Kauffman, D. Murdiyarsa, S. Kurnianto, M. Stidham, and M. Anninen, 2011. Mangroves among the most carbon-rich forests in the tropics, *Nature Geoscience*, 4: 293-297
- Doney, S.C., 2010. The growing human footprint on coastal and open-ocean biogeochemistry, *Science*, 328 (5985): 1512-1516; DOI:10.1126/science.1185198
- Douglas, E.M., D. Niyogi, S. Frolking, J.B. Yeluripati, R.A. Pielke Sr., N. Niyogi, C.J. Vörösmarty, and U.C. Mohanty, 2006. Changes in moisture and energy fluxes due to agricultural land use and irrigation in the Indian Monsoon Belt, *Geophysical Research Letters*, 33: L14403[5 pp.]; DOI:10.1029/2006GL026550
- Drake, B.G., and P.W. Leadley, 1991. Canopy photosynthesis of crops and native plant communities exposed to long-term elevated CO₂. *Plant, Cell & Environment*, 14 (8): 853-860; DOI:10.1111/j.1365-3040.1991.tb01448.x
- Dudd, S.N., and R.P. Evershed, 1998. Direct demonstration of milk as an element of archaeological economies. *Science*, 282: 1478-1481
- Dunne, J., R.P. Evershed, M. Salque, L. Cramp, S. Bruni, K. Ryan, S. Biagetti, and S. di Lernia, 2012. First dairying in green Saharan Africa in the fifth millennium BC, *Nature*, 486: 390-394; DOI:10.1038/nature11186
- Dupont, L.M., H. Behling, and J.H. Kim, 2008. Thirty thousand years of vegetation development and climate change in Angola (Ocean Drilling Program Site 1078), *Climate of the Past*, 4: 111-147
- Edathikunnel, T., 2015a. First-of-its-kind bird fossil found in Brazil, *EarthSky*, issued Jun 9, 2015
- Edathikunnel, T., 2015c. Largest dinosaur with birdlike wings and feathers, *EarthSky*, issued Jul 29, 2015
- Edathikunnel, T., 2016. China's new feathered Mud Dragon dino, *EarthSky*, issued Nov 15, 2016.
- Eltahir, E.A.B., 1989. A feedback mechanism in annual rainfall in central Sudan, *Journal of Hydrology*, 110: 323-334
- EPICA community members*, 2006. One-to-one coupling of glacial climate variability in Greenland and Antarctica, *Nature*, 444: 195-198; DOI:10.1038/nature05301
- Erickson, G.M., O.W.M. Rauhut, Zhonghe Zhou, A.H. Turner, B.D. Inouye, Dongyu Hu, and M.A. Norell, 2009. Was dinosaurian physiology inherited by birds?

- Reconciling slow growth in Archaeopteryx, PLOS; DOI:10.1371/journal.pone.0007390
- Evershed, R.P., 2008. Organic residue analysis in archaeology: the archaeological biomarker revolution. *Archaeometry*, 50: 895–924
- Evershed, R.P., S. Payne, A.G. Sherratt, M.S. Copley, J. Coolidge, D. Urem-Kotsu, K. Kotsakis, M. Özdoğan, A.E. Özdoğan, O. Nieuwenhuys, P.M., M.G. Akkermans, D. Bailey, R.-R. Andeescu, S. Campbell, S. Farid, I. Hodder, N. Yalman, M. Özbaşaran, E. Bıçakçı, Y. Garfinkel, T. Levy, and M.M. Burton, 2008. Earliest date for milk use in the Near East and southeastern Europe linked to cattle herding. *Nature*, 455: 528–531
- FEWS NET, 2011. Past year one of the driest on record in the eastern Horn, Famine Early Warning System Network Report, June 14, 2011, U.S. Agency for International Development, Washington, D.C.
- Fiala, N., 2009. The greenhouse hamburger. *Scientific American*, 300, February: 72-75
- Fink, A.H., J.M. Schrage, and S. Kotthaus, 2010. On the potential causes of the nonstationary correlations between West African precipitation and Atlantic hurricane activity. *Journal of Climate*, 23: 5437-5456; DOI:10.1175/2010JCLI3356.1
- Folland, C.K., T.N. Palmer, and D.E. Parker, 1986. Sahel rainfall and worldwide sea temperatures, 1901-1985, *Nature*, 320: 602-607; DOI:10.1038/320602a0
- Fourqurean, J.W., C.M. Duarte, H. Kennedy, N. Marbà, M. Holmer, M.A. Mateo, E.T. Apostolaki, A. Kendrick, D. Krause-Jensen, K.J. McGlathery, and O. Serrano, 2012. Seagrass ecosystems as a globally significant carbon stock, *Nature Geoscience*, 5: 505–509; DOI:10.1038/ngeo1477
- Fraterriago, J.M., K. Ream, and J.D. Knoepp, 2018. Tree mortality from insect infestation enhances carbon stabilization in Southern Appalachian forest soils, *Journal of Geophysical Research Biogeosci.*, 123 (7): 2121-2134; DOI:10.1029/2018JG004431
- Free, M., J.K. Angell, I. Durre, J. Lanzante, T.C. Peterson and D.J. Seidel, 2004: Using first differences to reduce inhomogeneity in radiosonde temperature datasets, *Journal of Climate*, 21: 4171-4179
- Frei, R., C. Gaucher, S.W. Poulton, and D.E. Canfield, 2009. Fluctuations in Precambrian atmospheric oxygenation recorded by chromium isotopes, *Nature*, 461: 250-253; DOI:10.1038/nature08266
- Funk, Ch., M.D. Dettinger, J.C. Michaelsen, J.P. Verdin, M.E. Brown, M. Barlow, and A. Hoell, 2008. Warming of the Indian Ocean threatens eastern and southern African food security but could be mitigated by agricultural development, *Proceedings of the National Academy of Sciences*, 105 (32): 11,081–11,086; DOI:10.1073/pnas.0708196105
- Gac, J.Y., and A. Kane, 1986. Le fleuve Sénégal: I. Bilan hydrologique et flux continentaux de matières particulières à l'embouchure, *Sciences Géologiques. Bulletin*, 39: 99-130
- Gannon, M., 2018a. Oldest fossil of 'missing link' dinosaur discovered in Germany, *Live Science*, issued Jan 30, 2018
- Gasse, F., 2000. Hydrological changes in the African tropics since the Last Glacial Maximum, *Quaternary Science Reviews*, 19: 189-211; DOI:10.1016/S0277-3791(99)00061-X
- Gasse, F., and E. van Campo, 1994. Abrupt postglacial climate events in West Asia and North Africa monsoon domains, *Earth and Planetary Science Letters*, 126: 435-456; DOI:10.1016/0012-821X(94)90123-6
- Gautier, A., 2002. The evidence for the earliest livestock in North Africa: or adventures with large bovids, ovicaprids, dogs and pigs. In *Droughts, Food and Culture: Ecological Change and Food Security in Africa's Later Prehistory*, F.A. Hassan (ed.) Springer; pp.: 195–208
- Geggel, L., 2015a. Ancient marine reptiles flew through the water, *Live Science*, issued December 18, 2015
- Geggel, L., 2015b. Giant pterosaur sported 110 teeth (and 4 wicked fangs), *Live Science*, issued October 26, 2015
- Geggel, L., 2015c. Rare dinosaur find: fossil covered in feathers, skin, *Live Science*, issued November 5, 2015
- Geggel, L., 2016c. Sticky amber preserved dinosaur-age insects for millions of years, *Live Science*, issued January 8, 2016
- Geggel, L., 2016d. 99-million-year-old spider mummy sported horned fangs, *Live Science*, issued July 8, 2016
- Geggel, L., 2016e. Mummified, 99-million-year-old wings caught in amber, *Live Science*, issued June 28, 2016
- Geggel, L., 2016f. Airplane-size seabird flew above Antarctica 50 million years ago, *Live Science*, issued Jun 14, 2016
- Geggel, L., 2017b. Frozen in time: ancient, long-fingered lizard trapped in amber, *Live Science*, issued September 11, 2017
- Geggel, L., 2017c. Truck- and plane-size pterosaurs once flew over dinosaurs, *Live Science*, issued August 29, 2017
- Geggel, L., 2017d. First 'winged' mammals lived alongside dinosaurs 160 million years ago, *Live Science*, issued August 9, 2017
- Geggel, L., 2017f. This dinosaur fossil was so bizarre, scientists thought it was fake, *Live Science*, issued December 7, 2017
- Geggel, L., 2018. Little 'Rainbow' dinosaur discovered by farmer in China, *Live Science*, issued January 15, 2018
- Geggel, L., 2018d. Discovery of 'First Giant' dinosaur is a huge evolutionary finding, *Live Science*, issued July 10, 2018
- Geggel, L., 2018f. World's largest pterosaur jawbone discovered in Transylvania, *Live Science*, issued May 25, 2018
- Geggel, L., 2018h. Exquisitely preserved lungs from 120 million years ago stun scientists studying early bird, *Live Science*, issued October 19, 2018.
- Geggel, L., 2018i. Controversial spearpoints could rewrite the story of the first Americans, *Live Science*, issued October 25, 2018
- Geggel, L., 2018j. Who were the 1st Americans? 11,000-year-old DNA reveals clues, *Live Science*, issued November 8, 2018

- Geggel, L., 2018k. It's official: those flying reptiles called pterosaurs were covered in fluffy feathers, *Live Science*, issued December 17, 2018
- Geggel, L., 2019. Humans crossed the Bering land bridge to people the Americas. Here's what it looked like 18,000 years ago, *Live Science*, issued February 15, 2019
- Ghose, T., 2016d. Earth gets greener as globe gets hotter, *Live Science*, issued April 27, 2016
- Ghose, T., 2016e. First Americans took coastal route to get to North America, *Live Science*, issued August 10, 2016
- Ghose, T., 2017e. Lost city of Alexander the Great unearthed in Kurdish Iraq, *Live Science*, issued September 28, 2017
- Ghose, T., 2017f. Spy satellites reveal ancient lost empires in Afghanistan, *Live Science*, issued December 14, 2017
- Gifford, R.M., 1992. Interaction of carbon dioxide with growth-limiting environmental factors in vegetation productivity: implications for the global carbon cycle, *Advances in Bioclimatology* 1, 1: 24-58
- Gifford-Gonzalez, D., and O. Hanotte, 2011. Domesticating animals in Africa: implications of genetic and archaeological findings. *Journal of World Prehistory*, 24: 1-23
- Gill, F.L., J. Hummel, A.R. Sharifi, A.P. Lee, and B.H. Lomax, 2018. Diets of giants: the nutritional value of sauropod diet during the Mesozoic, *Palaeontology*; DOI:10.1111/pala.12385
- Giraudi, C., 2013. Late Upper Pleistocene and Holocene stratigraphy of the palaeolakes in the Gobero Basin. In *Gobero: the no-Return Frontier. Archaeology and Landscape at the Saharo-Sahelian Borderland*, E.A.A. Garcea, (ed.); pp.: 67-80
- Giraudi, C., and A.M. Mercuri, 2013. Early to Middle Holocene environmental variations in the Gobero Basin. In *Gobero: the no-Return Frontier. Archaeology and Landscape at the Saharo-Sahelian Borderland*, E.A.A. Garcea, (ed.); pp.: 114-126
- Goddard, L., and N.E. Graham, 1999. The importance of the Indian Ocean for simulating precipitation anomalies over eastern and southern Africa, *Journal of Geophysical Research*, 104: 19,099-19,116; DOI:10.1029/1999JD900326
- Godfrey, L.V., and P.G. Falkowski, 2009. The cycling and redox state of nitrogen in the Archaean ocean, *Nature Geoscience*, 2: 725 - 729; DOI:10.1038/ngeo633
- Goldman, T., J. Roy, N.M. Holbrook, M. Zwieniecki, 2008. Water in trees, *Physics Today*, 61 (8): 10-; DOI:10.1063/1.2970949
- Grace, J., J. Lloyd, J. McIntyre, A.C. Miranda, P.Meir, H.S. Miranda, C. Nobre, J. Moncrieff, J. Massheder, Y. Mahli, I. Wright, and J. Gash, 1995. Carbon dioxide uptake by an undisturbed tropical rain forest in southwest Amazonia, 1992 to 1993, *Science*, 270, (5237): 778-780
- Graham, F., 2019. Daily briefing: American colonization contributed to the Little Ice Age, *Nature*, Briefing, issued 4 February 2019
- Graybill, D.A., and S.B. Idso, 1993. Detecting the aerial fertilization effect of atmospheric CO₂ enrichment in tree-ring chronologies. *Global Biogeochemical Cycles*, 7 (1): 81-95
- Gregori, G. P., B. A. Leybourne, G. Paparo†, and M. Poscolieri, 2025a. The global Sun-Earth circuit. In press in *New Concepts in Global Tectonics, Journal*
- Gregori, G. P., M. T. Hovland, B. A. Leybourne, S. Pellis, V. Straser, B. G. Gregori, G. M. Gregori, and A. R. Simonelli, 2025w. Air-earth currents and a universal "law": filamentary and spiral structures - Repetitiveness, fractality, golden ratio, fine-structure constant, antifragility and "statistics" - The origin of life, *New Concepts in Global Tectonics, Journal*, 3, (1): 106-225
- Gregori, G.P., 2002a. History of science and the Cycle of Climate and Civilisation. The deontology of a science historian. In W. Schröder (ed.), *Solar variability and geomagnetism*, Beiträge zur Geschichte der Geophysik und Kosmischen Physik, 3 (2), Science Edition, AKGGKP, Bremen-Roennebeck; pp.: 250-257
- Gregori, G.P., 2015a. Comment on Stephen W. Hurrell: A new method to calculate paleogravity using fossil feathers, *New Concepts in Global Tectonics, Journal*, 3 (1): 68-70
- Gregori, G.P., 2020. Climate change, security, sensors. *Acoustics*, 2: 474-504; DOI:10.3390/acoustics2030026.[https://www.mdpi.com/2624-599X/2/3/26/htm]
- Gregori, G.P., and B.A. Leybourne, 2021. An unprecedented challenge for humankind survival. Energy exploitation from the atmospheric electrical circuit, *American Journal of Engineering and Applied Science*, 14 (2): 258-291; DOI:10.3844/ajeassp.2021.258.291
- Gregori, G.P., and B.A. Leybourne, 2025i. Wildfires from the Banda Sea through Beijing and through Karakoram. *New Concepts in Global Tectonics, Journal*, 13, (6): 854-887
- Gregori, G.P., and B.A. Leybourne, 2025j. The energy supply to hurricanes. *New Concepts in Global Tectonics, Journal*, 13 (5): 731-786
- Gregori, G.P., and B.A. Leybourne, 2025k. The global climate change perspective. The glaciers proxy, *New Concepts in Global Tectonics, Journal*, 13 (2): 270-335
- Gregori, G.P., and L.G. Gregori, 1998. Solar-terrestrial relations. A reminder. *Acta Geodaetica et Geophysica Hungarica*, 33 (2/4): 391-459; DOI:10.1007/BF03325551
- Gregori, G.P., and L.G. Gregori, 1999. Prehistory of geophysics, anthropology, and archaeoastronomy. In W. Schröder, (ed.), *Physics and Geophysics (A Compilation with Special Historical Case Studies)*, History Commission of the German Geophysical Society, Mitteilungen des Arbeitskreises Geschichte der Geophysik der DGG, 18, Jahrgang (1999), Heft 1-3, Science Edition/DGG, Bremen; pp.: 246-267
- Gregori, G.P., and M.T. Hovland, 2025. Go for the anomaly - a golden strategy for discovery? Seepology & the origin and crucial role of the biosphere - Earth and planetary objects - Supercritical water and

- serpentinization. In press in *New Concepts in Global Tectonics, Journal*
- Gregori, G.P., B.A. Leybourne, and G. Paparo†, 2025b. Introduction – Anomalous lesser air-earth phenomena. In press in *New Concepts in Global Tectonics, Journal*
- Gregori, G.P., B.A. Leybourne, and Gao Xiaoqing, 2025q. Atlas of the Joule heat released at the *ALB, CMB* and *ICB* during AD 1400 through present, *New Concepts in Global Tectonics, Journal*, 13, (3): 460-472
- Gregori, G.P., B.A. Leybourne, and J. R. Wright, 2025d. Generalized Cowling theorem and the Cowling dynamo. In press in *New Concepts in Global Tectonics, Journal*
- Gregori, G.P., B.A. Leybourne, Dong Wenjie, and Gao Xiaoqing, 2025f. The Tang Maocang school. The uplift of Himalaya – shallow geotherms – palaeoclimate – endogenous heat. In press in *New Concepts in Global Tectonics, Journal*
- Gregori, G.P., B.A. Leybourne, Dong Wenjie, and Gao Xiaoqing, 2025i. Palaeo- and archaeo-climate in the Chinese subcontinent. In press in *New Concepts in Global Tectonics, Journal*
- Gregori, G.P., B.A. Leybourne, Dong Wenjie, and Gao Xiaoqing, 2025g. The timing of the uplift of Himalaya and the Third Pole. In press in *New Concepts in Global Tectonics, Journal*
- Gregori, G.P., B.A. Leybourne, Dong Wenjie, and Gao Xiaoqing, 2025h. Shallow geotherms. In press in *New Concepts in Global Tectonics, Journal*
- Gregori, G.P., M. Colacino, M.R. Valensise, and L.G. Gregori, 2000. Why a history of geophysics? In W. Schröder (ed.), *Geschichte und Philosophie der Geophysik (History and Philosophy of Geophysics)*, Beiträge zur Geschichte der Geophysik und Kosmischen Physik der DDG, 2, and Newsletter of IDCH-IAGA (42), W. Schröder, and AKGGKP (Arbeitskreis Geschichte der Geophysik und Kosmischen Physik der DDG), Bremen-Roennebeck and Potsdam; pp.: 112-122
- Gregori, L.G., and G.P. Gregori, 1999a. The consciousness of time and the conquest of space. The dawn of civilisation, anthropology, and archaeoastronomy. *Annals of the New York Academy of Sciences*, 879: 158-163
- Grousset, F.E., M. Parra, A. Bory, P. Martinez, P. Bertrand, G. Shimmield, and R.M. Ellam, 1998. Saharan wind regimes traced by the Sr-Nd isotopic composition of subtropical Atlantic sediments: Last Glacial Maximum vs. today, *Quaternary Science Reviews*, 17: 395-409; DOI:10.1016/S0277-3791(97)00048-6
- Hales, K., J.D. Neelin, and N. Zeng, 2006. Interaction of vegetation and atmospheric dynamical mechanisms in the mid-Holocene African monsoon, *Journal of Climate*, 19: 4105-4120; DOI:10.1175/JCLI3833.1
- Haslett, S., 2002. *Quaternary Environmental Micropalaeontology*, Hodder Arnold; pp.: 1-288
- Hay, W.W., 1985. Potential errors in estimates of carbonate rock accumulating through geologic time. In *The Carbon Cycle and Atmospheric CO₂: Natural Variations Archean to present*, E.T. Sundquist, and W.S. Broecker, (eds), *Geophysical Monograph Series*, 32, American Geophysical Union: Washington, DC; pp.: 573–583
- Hedley, R.H., and C.G. Adams, (eds), 1974, 1977, 1978. *Foraminifera*, Vol. I, 276 pp., Vol. II, 265 pp., Vol. III, 290 pp., Academic Press, London, etc.
- Hein, L., and N. de Ridder, 2006. Desertification in the Sahel: a reinterpretation. *Global Change Biology*, 12: 751-758
- Herndon, J.M., 2010. Inseparability of science history and discovery, *History of Geophysics and Space Science*, 1: 25-41
- Herndon, J.M., 2014. Terracentric nuclear fission georeactor: background, basis, feasibility, structure, evidence and geophysical implications, *Current Science*, 106 (4): 528-541
- Herrmann, S.M., A. Anyamba, and C.J. Tucker, 2005. Recent trends in vegetation dynamics in the African Sahel and their relationship to climate, *Global Environmental Change*, 15: 394–404
- Hiernaux, P., 1992. The Crisis of Sahelian Pastoralism: Ecological or Economic? *International Livestock Centre for Africa (ILCA)*, Addis Ababa (Ethiopia); pp.: 1-15
- Hoerling, M.P., J. Eischeid, and J. Perlwitz, 2010. Regional precipitation trends: distinguishing natural variability from anthropogenic forcing, *Journal of Climate*, 23: 2131–2145; DOI:10.1175/2009JCLI3420.1
- Hoggarth, J.A., S.F.M. Breitenbach, B.J. Culleton, C.E. Ebert, M.A. Masson, and D.J. Kennett, 2016. The political collapse of Chichén Itzá in climatic and cultural context, *Global and Planetary Change*, 138: 25–42; DOI:10.1016/j.gloplacha.2015.12.007
- Holbrook, N.M., and M.A. Zwieniecki, 2008. Transporting water to the tops of trees, *Physics Today*, 61 (1): 76-77
- Holen, S.R., T.A. Deméré, D.C. Fisher, R. Fullagar, J.B. Paces, G.T. Jefferson, J.M. Beeton, R.A. Cerutti, A.N. Rountrey, L. Vesceraand, and K.A. Holen, 2017. A 130,000-year-old archaeological site in southern California, USA, *Nature*, 544: 479–483; DOI:10.1038/nature22065.
- Holland, H.D., 1984. *The chemical evolution of the atmosphere and oceans*, Princeton University Press, Princeton; pp.: 1-598
- Hönisch, B., and N.G. Hemming, 2005. Surface ocean pH response to variations in pCO₂ through two full glacial cycles, *Earth and Planetary Science Letters*, 236 (1/2): 305-314; DOI:10.1016/j.epsl.2005.04.027
- Hönisch, B., 2007. Pleistocene records of marine carbonate chemistry. Invited talk given at the Crafoord Prize Symposium, Lund, on 26 April 2007, in honour of Crafoord Laureates 2006
- Hönisch, B., J. Yu, and N.G. Hemming, 2008. Pleistocene records of marine carbonate chemistry, *PAGES (Past Global Changes) News*, 16 (1): 11-12
- Hönisch, B., N.G. Hemming, D. Archer, M. Siddall, and J.F. McManus, 2009. Atmospheric carbon dioxide concentration across the Mid-Pleistocene transition, *Science*, 324 (5934), 1551-1554; DOI:10.1126/science.1171477
- Hori, M., T. Ishikawa, K. Nagaishi, Ke Lin, Bo-Shian Wang, Chen-Feng You, Chuan-Chou Shen, and A. Kano, 2013. Prior calcite precipitation and source mixing process influence Sr/Ca, Ba/Ca and 87Sr/86Sr of

- a stalagmite developed in southwestern Japan during 18.0–4.5ka, *Chemical Geology*, 347: 190-198; DOI:10.1016/j.chemgeo.2013.03.005
- Hornafius, JS., D. Quigley, and B.P. Luyendyk, 1999. The world's most spectacular marine hydrocarbon seeps (Coal Oil Point, Santa Barbara Channel, California): quantification of emissions, *Journal of Geophysical Research*, 104 (C9): 20703-
- Hörnig, M.K., J.T. Haug, and C. Haug, 2017. An exceptionally preserved 110 million years old praying mantis provides new insights into the predatory behaviour of early mantodeans. *Peer J.*, 5: e3605; DOI:10.7717/peerj.3605
- Hossain, F., I. Jeyachandran, and R. Pielke Sr., 2009. Have large dams altered extreme precipitation patterns? *EOS, Transactions of the American Geophysical Union*, 90 (48): 453-454
- Hougen, O.A., K.M. Watson, and R.A. Ragatz, 1954. *Chemical process principles*, Part 1, 2nd ed.; John Wiley, New York; pp.: 1-525
- Houghton, R.A., 2007. Balancing the global carbon budget. *Annual Review of Earth and Planetary Sciences*, 35: 313-347; DOI:10.1146/annurev.earth.35.031306.140057
- Hsü, K.J., 2000. *Klima macht Geschichte. Menschheitsgeschichte als Abbild der Klimaentwicklung*. Orell Füssli, Zürich; pp.: 1-334
- Huffman, G.J., R.F. Adler, D.T. Bolvin, and G. Gu, 2009. Improving the global precipitation record: GPCP Version 2.1, *Geophysical Research Letters*, 36: L17808; doi; 10.1029/2009GL040000
- Hurrell, S.W., 2014. A new method to calculate paleogravity using fossil feathers, *New Concepts in Global Tectonics, Journal*, 2(3): 29-34
- Huysecom, E., M. Rasse, L. Lespez, K. Neumann, A. Fahmy, A. Ballouche, S. Ozainne, M. Magetti, C. Tribolo, S. Soriano, 2009. The emergence of pottery in Africa during the tenth millennium cal BC: new evidence from Ounjougou (Mali). *Antiquity*, 83: 905–917
- Idso, K E., and S. Idso, 1974. *Agricultural and Forest Meteorology*, 69: 153-203
- Idso, S.B., 1989. *Carbon Dioxide and Global Change: Earth in Transition*, IBR Press; pp.: 1-292
- IGCP, 1997. *Geoscience in the service of society. The International Geological Correlation Programme (IGCP)*, booklet prepared by UNESCO; pp.: 1-16
- Imster, E., 2016g. Giant flightless bird roamed Arctic 50 million years ago, *EarthSky*, issued February 18, 2016
- Indeje, M., F.H.M. Semazzi, and L.J. Ogallo, 2000. ENSO signals in East African rainfall seasons, *International Journal of Climatology*, 20: 19–46; DOI:10.1002/(SICI)1097-0088(200001)20:1<19::AID-JOC449>3.0.CO;2-0
- Innes Miller, J., 1969. *The Spice Trade of the Roman Empire, 29 B.C. to A.D. 641*; pp.:1-294., Clarendon Press. Italian translation published in 1974 by Giulio Einaudi Editore, Torino; pp.: 1-312
- International Critical Tables*, 1928. McGraw-Hill, New York.
- Itambi, A.C., T. von Dobeneck, S. Mulitza, T. Bickert, and D. Heslop, 2009. Millennial-scale northwest African droughts related to Heinrich events and Dansgaard-Oeschger cycles: evidence in marine sediments from offshore Senegal, *Paleoceanography*, 24: PA1205 [16 pp.]; DOI:10.1029/2007PA001570
- Itan, Y., B.L. Jones, C.J. Ingram, D.M. Swallow, and M.G. Thomas, 2010. A worldwide correlation of lactase persistence phenotype and genotypes. *BMC Evolutionary Biology*, 10: 36
- Jacobs, J., 1905. Riddle. In *Jewish Encyclopedia*, I. Singer (ed.), Funk and Wagnall, vol. 10: 408b–409a
- Jamme, A., 2003. Saba (Sheba), *New Catholic Encyclopedia*, 12 (2nd ed.), Gale, pp.: 450–451
- Janowiak, J.E., 1988. An investigation of interannual rainfall variability in Africa. *Journal of Climate*, 1: 240-255
- Janowiak, J.E., and P. Xie, 1999. CAMS-OPI: A global satellite-rain gauge merged product for real-time precipitation monitoring applications, *Journal of Climate*, 12: 3335–3342; DOI:10.1175/1520-0442(1999)012<3335:COAGSR>2.0.CO;2
- Janzen, H.H., C.A. Campbell, R.C. Izaurralde, B.H. Ellert, N. Juma, W.B. McGill and R P. Zentner, 1998. Management effects on soil C storage on the Canadian prairies, *Soil and Tillage Research*, 47 (3/4): 181-195; DOI:10.1016/S0167-1987(98)00105-6
- Jarus, O., 2016. Ancient inscriptions show life once flourished in Jordan's 'Black Desert', *Live Science*, issued November 21, 2016.
- Jarus, O., 2016a. Built by the Huns? Ancient stone monuments discovered along Caspian, *Live Science*, issued November 14, 2016
- Jarus, O., 2017. 400 mysterious ancient stone structures discovered in Saudi Arabia, *Live Science*, issued Oct ober17, 2017
- Jarus, O., 2017b. Spectacular images reveal mysterious stone structures in Saudi Arabia, *Live Science*, issued November 12, 2017
- Jickells, T.D., Z.S. An, K.K. Andersen, A.R. Baker, G. Bergametti, N. Brooks, J.J. Cao, P.W. Boyd, R.A. Duce, K.A. Hunter, H. Kawahata, N. Kubilay, J. la Roche, P.S. Liss, N. Mahowald, J.M. Prospero, A.J. Ridgwell, I. Tegen, and R. Torres, 2005. Global iron connections between desert dust, ocean biogeochemistry, and climate, *Science*, 308, (5718): 67-71; DOI:10.1126/science.1105959
- Jin, M., and R.E. Dickinson, 2010. Land surface skin temperature climatology: benefitting from the strengths of satellite observations, *Environmental Research Letters*, 5 (4)
- Jolly, D., S.P. Harrison, B. Damnati, and R. Bonnefille, 1998. Simulated climate and biomes of Africa during the late quaternary: comparison with pollen and lake status data. *Quaternary Science Reviews*, 17: 629–657
- Judd, A.G., and M. Hovland, 2007. *Submarine fluid flow, the impact on geology, biology, and the marine environment*. Cambridge University Press; pp.: 475
- Jullien, E., F. Grousset, B. Malaizé, J. Duprat, M.F. Sanchez-Goni, F. Eynaud, K. Charlier, R. Schneider, A.

- Bory, V. Bout, and J.A. Flores, 2007. Low-latitude “dusty events” vs. highlatitude “icy Heinrich events”, *Quaternary Research*, 68: 379-386; DOI:10.1016/j.yqres.2007.07.007
- Juston, J.M., and T.A. DeBusk, 2011. Evidence and implications of the background phosphorus concentration of submerged aquatic vegetation wetlands in Stormwater Treatment Areas for Everglades restoration, *Water Resources Research*, 47: W01511; DOI:10.1029/2010WR009294
- Kaplan, J.O., M. Pfeiffer, J.C.A. Kolen, and B.S. Davis, 2016. Large scale anthropogenic reduction of forest cover in Last Glacial Maximum Europe. *PLoS ONE*, 11, (11): e0166726; DOI:10.1371/journal.pone.0166726
- Kasting, J.F., 1985. Photochemical consequences of enhanced CO₂ levels in Earth’s early atmosphere. In *The Carbon Cycle and Atmospheric CO₂: Natural Variations Archaean to present*, E.T. Sundquist, and W.S. Broecker, (eds), *Geophysical Monograph Series*, 32, American Geophysical Union: Washington, DC; pp.: 612–622
- Kasting, J.F., J.B. Pollack, and D. Crisp, 1984. Effects of high CO₂ levels on surface temperature and atmospheric oxidation state of the early Earth. *Journal of Atmospheric Chemistry*, 1 (4): 403-428
- Kattan, Z., J.Y. Gac, and J.L. Probst, 1987. Suspended sediment load and mechanical erosion in the Senegal Basin-Estimation of the surface runoff concentration and relative contributions of channel and slope erosion, *Journal of Hydrology Amsterdam*, 92: 59-76; DOI:10.1016/0022-1694(87)90089-8
- Kemp, A.E.S., (ed.), 1996. *Palaeoclimatology and palaeoceanography from laminated sediments*, Geological Society of London, Special Publication, (116): 1-272
- Kemp, A.E.S., 2003. Evidence for abrupt climate changes in annually laminated marine sediments, *Philosophical Transactions of the Royal Society of London*, 361A, (1810), 1851-1870; DOI:10.1098/rsta.2003.1247.
- Kendall, C., 2004a. Resources on Isotopes. *Fundamentals of Stable Isotope Geochemistry*, A brief review prepared for USGS
- Kennedy, D., 2017. Aerial images may unlock enigma of ancient stone structures in Saudi Arabia, *Live Science*, issued November 12, 2017
- Kessler, R., 2011. Thousands of tombs in Saudi desert spotted from space, *LiveScience*, issued February 15, 2011
- Kimball, B.A., 1983. Carbon dioxide and agricultural yield: an assemblage and analysis of 430 prior observations, *Agronomy Journal* 75 (5): 779-788; DOI:10.2134/agronj1983.00021962007500050014x
- Klotzbach, P.J., and W.M. Gray, 2004: Updated 6–11-month prediction of Atlantic basin seasonal hurricane activity. *Weather Forecasting*, 19: 917-934; DOI:10.1175/1520-0434(2004)019<0917:UMPOAB>2.0.CO;2
- Koehler, M.C., R. Buick, M.A. Kipp, E.E. Stüeken, and J. Zaluski, 2018. Transient surface ocean oxygenation recorded in the ~2.66-Ga Jeerinah Formation, Australia, *Proceedings of the National Academy of Sciences*, 201720820; DOI:10.1073/pnas.1720820115
- Konhauser, K.O., E. Pecoits, S.V. Lalonde, D. Papineau, E.G. Nisbet, M.E. Barley, N.T. Arndt, K. Zahnle, and B.S. Kamber, 2009. Oceanic nickel depletion and a methanogen famine before the Great Oxidation Event, *Nature*, 458: 750-753; DOI:10.1038/nature07858
- Koopmann, B., 1981. Sedimentation von Saharastaub im subtropischen Nordatlantik während der letzten 25.000 Jahre, *Meteor Forschungsergebnisse. Reihe C: Geologie und Geophysik*, 35: 23-59
- Kröpelin, S., D. Verschuren, A.M. Lézine, H. Eggermont, C. Cocquyt, P. Francus, J.-P. Cazet, M. Fagot, B. Rumes, J.M. Russell, F. Darius, D.J. Conley, M. Schuster, H. von Suchodoletz, and D.R. Engstrom, 2008. Climate-driven ecosystem succession in the Sahara: the past 6000 years, *Science*, 320, (5877), 765-768; DOI:10.1126/science.1154913. See also, 320, (5877): 765-768; DOI:10.1126/science.1163483
- Ksepka, D.T., 2014. Flight performance of the largest volant bird, *Proceedings of the National Academy of Sciences*, 111 (29): 10624–10629; DOI:10.1073/pnas.1320297111
- Ksepka, D.T., 2014a. Flights of fancy in avian evolution, *American Scientist*, 102 (1), 36; DOI:10.1511/2014.106.36
- Kundrát, M., J. Nudds, B.P. Kear, Junchang Lü, and Per Ahlberg, 2019. The first specimen of *Archaeopteryx* from the Upper Jurassic Mörnsheim formation of Germany, *Historical Biology*, 31 (1): 3-63; DOI:10.1080/08912963.2018.1518443
- Kuper, R., and S. Kröpelin, 2006. Climate-controlled Holocene occupation in the Sahara: motor of Africa’s evolution. *Science*, 313: 803–807
- Kurz, W.A., C.C. Dymond, G. Stinson, G.J. Rampley, E.T. Neilson, A.L. Carroll, T. Ebata, and L. Safranyik, 2008. Mountain pine beetle and forest carbon feedback to climate change, *Nature*, 452: 987-990; DOI:10.1038/nature06777
- Lal, R., R.F. Follett, and J.M. Kimble, 2003. Achieving soil carbon sequestration in the United States: a challenge to the policy makers, *Soil Science*, 168 (12): 827-845
- Lamb, P.J., 1978. Large-scale tropical Atlantic surface circulation patterns associated with sub-Saharan weather anomalies, *Tellus*, 30: 240-251
- Lawler, A., 2017. Spy satellites are revealing Afghanistan’s lost empires, *Science News*, issued December 13, 2017
- Lawlor, D.W., and R.A.C. Mitchell, 1991. The effects of increasing CO₂ on crop photosynthesis and productivity: a review of field studies, *Plant, Cell & Environment*, 14 (8): 807-818; DOI:10.1111/j.1365-3040.1991.tb01444.x
- Lawson, D.A., 1975. Pterosaur from the Latest Cretaceous of West Texas: discovery of the largest flying creature, *Science*, 187 (4180): 947-948; DOI:10.1126/science.187.4180.947
- Le Quellec, J.-L., 2006. Rock art and cultural responses to climatic changes in the central Sahara during the Holocene. In *Exploring the Mind of Ancient Man -*

- Festschrift to Robert G. Bednarik, P. Chenna Reddy, (ed.), Research India Press, New Delhi; pp.: 173-188
- Le Quellec, J.-L., 2013. Périodisation et chronologie des images rupestres du Sahara central, *Préhistoires Méditerranéennes* [<http://journals.openedition.org/pm/715>], 4
- Le Quellec, J.-L., 2019. Égypte, Afrique, Sahara: arts rupestres et mythologies. *Archéo-Nil*, 29 : 81-100
- Leblanc, M.J., G. Favreau, S. Massuel, S.O. Tweed, M. Loireau, and B. Cappelare, 2008. Land clearance and hydrological change in the Sahel: SW Niger, *Global and Planetary Change*, 61: 135-150
- Lielieveld, J., T.M. Butler, J.N. Crowley, T.J. Dillon, H. Fischer, L. Ganzeveld, H. Harder, M.G. Lawrence, M. Martinez, D. Taraborrelli, and J. Williams, 2008. Atmospheric oxidation capacity sustained by a tropical forest, *Nature*, 452: 737-740; DOI:10.1038/nature06870
- Letzter, R., 2018. Who created these strange, ancient sculptures hidden in the Saudi desert? *Live Science*, issued February 20, 2018
- Letzter, R., 2018b. Scientists may have wildly underestimated the giant dinosaurs of the ancient world, *Live Science*, issued July 17, 2018
- Levenspiel, O., 2000. DEPARTMENTS-Learning from the past-Earth's early atmosphere. *Chemical Innovation*, 30(5): 47-51
- Levenspiel, O., 2006. Atmospheric pressure at the time of dinosaurs, *Chemical Industry and Chemical Engineering Quarterly*, 12(2): 116-122; *Chemical Engineering Department, Oregon State University, Scientific Paper 591.044:596.19"63"*
- Levenspiel, O., T.J. Fitzgerald, and D. Pettit, 2000. Earth's atmosphere before the age of dinosaurs, *Chemical Innovation*, 30(12): 50-55
- Levis, S., G.B. Bonan, and C. Bonfils, 2004. Soil feedback drives the mid-Holocene North African monsoon northward in fully coupled CCSM2 simulations with a dynamic vegetation model, *Climate Dynamics*, 23: 791-802; DOI:10.1007/s00382-004-0477-y
- Li, W.Y., M. André, Y.V. Khotyaintsev, A. Vaivads, S.A. Fuselier, D.B. Graham, S. Toledo-Redondo, B. Lavraud, D.L. Turner, C. Norgren, B.B. Tang, C. Wang, P.A. Lindqvist, D.T. Young, M. Chandler, B. Giles, C. Pollock, R. Ergun, C.T. Russell, R. Torbert, T. Moore, and J. Burch, 2017. Cold ionospheric ions in the magnetic reconnection outflow region. *Journal of Geophysical Research, Space Phys.*, 122: 10,194-10,202; DOI:10.1002/2017JA024287
- Lim, Young-Kwon, Ming Cai, E. Kalnay, and Liming Zhou, 2005. Observational evidence of sensitivity of surface climate changes to land types and urbanization, *Geophysical Research Letters*, 32: L22712 [4 pp.]; DOI:10.1029/2005GL024267
- Lisiecki, L.E., and M.E. Raymo, 2005. A Pliocene-Pleistocene stack of 57 globally distributed benthic $\delta^{18}\text{O}$ records, *Paleoceanography*, 20: PA1003; DOI:10.1029/2004PA001071
- Liu, Dianbing, Yongjin Wang, Hai Cheng, R.L. Edwards, Xinggong Kong, Shitao Chen, and Shushuang Liu, 2018. Contrasting patterns in abrupt Asian summer monsoon changes in the last glacial period and the Holocene, *Paleoceanography and Paleoclimatology*, 33 (2), 214-226; DOI:10.1002/2017PA003294
- Liu, Shiqiu, A.S. Smith, Yuting Gu, Jie Tan, C.K. Liu, and G. Turk, 2015a. Computer simulations imply forelimb-dominated underwater flight in plesiosaurs. *PLOS Computational Biology*, 11 (12): e1004605; DOI:10.1371/journal.pcbi.1004605
- Liu, Z., Yi Wang, R. Gallimore, F. Gasse, T. Johnson, P. deMenocal, J. Adkins, M. Notaro, I.C. Prentice, J. Kutzbach, R. Jacob, P. Behling, Lihua Wang, E. Ong, 2007b. Simulating the transient evolution and abrupt change of Northern Africa atmosphere-ocean-terrestrial ecosystem in the Holocene, *Quaternary Science Reviews*, 26 (13-14): 1818-1837; DOI:10.1016/j.quascirev.2007.03.002
- Liu, Z.Y., Y. Wang, R. Gallimore, M. Notaro, and I.C. Prentice, 2006. On the cause of abrupt vegetation collapse in North Africa during the Holocene: Climate variability vs. vegetation feedback, *Geophysical Research Letters*, 33: L22709; DOI:10.1029/2006GL028062
- Longo, A.F., E.D. Ingall, J.M. Diaz, M. Oakes, L.E. King, A. Nenes, N. Mihalopoulos, K. Violaki, A. Avila, C.R. Benitez-Nelson, J. Brandes, I. McNulty, and D.J. Vine, 2014. P-NEXFS analysis of aerosol phosphorus delivered to the Mediterranean Sea, *Geophysical Research Letters*, 41 (11): 4043-4049; DOI:10.1002/2014GL060555
- Lü, Junchang, and S.L. Brusatte, 2015. A large, short-armed, winged dromaeosaurid (Dinosauria: Theropoda) from the Early Cretaceous of China and its implications for feather evolution, *Scientific Reports*, 5 (11775); DOI:10.1038/srep11775
- Lutz, R.A., T.M. Shank, D.J. Fornari, R.M. Haymon, M.D. Lilley, K.L. Von Damm, and D. Desbruyeres, 1994. Rapid growth at deep-sea vents, *Nature*, 371: 663-664
- Lyon, B., and D.G. DeWitt, 2012. A recent and abrupt decline in the East African long rains, *Geophysical Research Letters*, 39 (2): L02702 [5 pp.]; DOI:10.1029/2011GL050337
- Lyons, T.W., A.D. Anbar, A. Bekker, B. Kendall, C. Li, G.D. Love, P. McGoldrick, N.J. Planavsky, R. Raiswell, C.T. Reinhard, and C. Scott, 2010. New view of the old ocean: a prevalence of deep iron and marginalized sulfide from the late Archean through the Proterozoic, abstract 238-1, 2010 GSA Denver Ann. Meet. (31 October-3 November, 2010)
- MacDonald, G.M., D.W. Beilman, K.V. Kremenetski, Y. Sheng, L.C. Smith, and A.A. Velichko, 2006. Rapid early development of the circumarctic peatlands and atmospheric CH_4 and CO_2 variations, *Science*, 314 (5797): 285-288; DOI:10.1126/science.1131722
- Maher, D.T., I.R. Santos, L. Golsby-Smith, J. Gleeson, and B.D. Eyre, 2013. Groundwater-derived dissolved inorganic and organic carbon exports from a mangrove tidal creek: the missing mangrove carbon sink? *Limnology and Oceanography*, 58: 475 - 488
- Mann, L.K., 1986. Changes in soil carbon storage after cultivation, *Soil Science*, 142 (5): 279-288

- Marchal, O.I. Cacho, T.F. Stocker, J.O. Grimalt, E. Calvo, B. Martrat, N. Shackleton, M. Vautravers, E. Cortijo, S. van Kreveland, C. Andersson, N. Koç, M. Chapman, L. Scaffi, J.-C. Duplessy, M. Sarnthein, J.-L. Turon, J. Duprat, and E. Jansen, 2002. Apparent long-term cooling of the sea surface in the northeast Atlantic and Mediterranean during the Holocene, *Journal of Quaternary Science*, 21 (4/6): 455-483
- Marchant, R., and H. Hooghiemstra, 2004. Rapid environmental change in African and South American tropics around 4000 years before present: a review, *Earth-Science Reviews*, 66: 217–260; DOI:10.1016/j.earscirev.2004.01.003
- Marris, E., 2008. Old forests capture plenty of carbon. Planting a new tree may be a less effective way to sequester carbon than saving an old tree from the axe. *Nature*, Publ. online 10 September 2008; DOI:10.1038/news.2008.1092
- Marshall, F., and E. Hildebrand, 2002. Cattle before crops: the beginnings of food production in Africa. *Journal of World Prehistory*, 16: 99–143
- Marshall, J., Y. Kushnir, D. Battisiti, P. Chang, A. Czaja, R. Dickson, J. Hurrell, M. McCartney, R. Saravanan, and M. Visbeck, 2001. North Atlantic variability: phenomena, impacts and mechanisms. *International Journal of Climatology*, 21: 1863-1898
- Martin, L., J. Bertaux, T. Correge, M.-P. Ledru, P. Mourguiart, A. Sifeddine, F. Soubiès, D. Wirmann, K. Suguio, and B. Turcq, 1997. Astronomical forcing of contrasting rainfall changes in tropical South America between 12,400 and 8800 cal yr BP. *Quaternary Research*, 47: 117–122
- Martin-Silverstone, E., M.P. Witton, V.M. Arbour, and P.J. Currie, 2016. A small azhdarchoid pterosaur from the latest Cretaceous, the age of flying giants, *Royal Society Open Science*, 3: 160333; DOI:10.1098/rsos.160333
- Matthews, E., T.J. Bannan, M.A.H. Khan, D.E. Shallcross, H. Stark, E.C. Browne, A.T. Archibald, A. Mehra, S.J.-B. Bauguitte, C. Reed, N.M. Thamban, Huihui Wu, P. Barker, J. Lee, L.J. Carpenter, Mingxi Yang, T.G. Bell, G. Allen, J.T. Jayne, C.J. Percival, G. McFiggans, M. Gallagher, and H. Coe, 2023. Airborne observations over the North Atlantic Ocean reveal the importance of gas-phase urea in the atmosphere, *Proceedings of the National Academy of Sciences*; DOI:10.1073/pnas.2218127120
- Mattingly, D.J. (ed.), 2003. *The archaeology of Fazzân. Volume 1, Synthesis. The Department of Antiquities / The Society of Libyan Studies, Tripoli/London [Volume 2: Site Gazetteer, Pottery and other Survey Finds, 2007, ed. by David J. Mattingly]*
- McGowan, S., 2016. How did humans first reach America? *EarthSky*, issued August 18, 2016
- McManus, J.F., R. Francois, J.-M. Gherardi, L.D. Keigwin, and S. Brown-Leger, 2004. Collapse and rapid resumption of Atlantic meridional circulation linked to deglacial climate changes, *Nature*, 428: 834-837; DOI:10.1038/nature02494
- McNaughton, S.J., M. Oesterhold, D.A. Frank, and K.J. Williams, 1989. Ecosystem-level patterns of primary productivity and herbivory in terrestrial habitats, *Nature*, 341: 142-144
- Mearns, E., 2015a. CO2 – the view from space, energy matters, Posted on October 13, 2015. [CO2 – the View from Space _ Energy Matters.htm]
- Meng, Qing-Jin, D.M. Grossnickle, Di Liu, Yu-Guang Zhang, A.I. Neander, Qiang Ji, and Zhe-Xi Luo, 2017. New gliding mammaliaforms from the Jurassic, *Nature*, 548: 291–296; DOI:10.1038/nature23476
- Merrifield, M.A., 2011. A shift in western tropical Pacific sea level trends during the 1990s, *Journal of Climate*, 24: 4126–4138; DOI:10.1175/2011JCLI3932.1
- Meyers, P.A., 2006. Mediterranean sapropels near-modern analogs for deposition of organic-carbon-rich Mesozoic-Paleozoic black shales, AGU Fall Meeting 2006, abstract #PP41A-1182 (code 2006AGUFMPP41A1182M)
- Meyers, P.A., 2006a. Paleoclimatic and paleoclimatic similarities between Mediterranean sapropels and Cretaceous black shales. *Palaeogeography, Palaeoclimatology, Palaeoecology*, 235: 305–320
- Meyers, P.A., and A. Negri, 2003. Paleoclimatic and paleoceanographic records in Mediterranean sapropels and Mesozoic black shales. *Palaeogeography, Palaeoclimatology, Palaeoecology*, 190, Spec. Issue : 1–480
- Michel, P., 1973. Les bassins des fleuves Sénégal et Gambie. Étude Géomorphologique, *Mémoires ORSTOM 63*, Paris, France
- Moreno, A., I. Cacho, M. Canals, J.O. Grimalt, M.F. Sanchez-Goni, N. Shackleton, and F.J. Sierro, 2005. Links between marine and atmospheric processes oscillating on a millennial time-scale: A multi-proxy study of the last 50000 yr from the Alboran Sea (western Mediterranean Sea), *Quaternary Science Reviews*, 24: 1623–1636
- Moreno, T., X. Querol, S. Castillo, A. Alastuey, E. Cuevas, L. Herrmann, M. Mounkaila, J. Elvira, and W. Gibbons, 2006. Geochemical variations in aeolian mineral particles from the Sahara-Sahel Dust Corridor, *Chemosphere*, 65: 261-270; DOI:10.1016/j.chemosphere.2006.02.052
- Mortensen, L.M., 1987. CO₂ enrichment in greenhouses. Crop responses, *Scientia Horticulturae*, 33 (1/2): 1–25
- Moskowitz, C., 2011. Could natural nuclear reactors have boosted life on this and other planets? *Space.com* (in cooperation with *Astrobiology Magazine*), issued 01 December 2011; 04:42 PM ET
- Mulcare, C.A., M.E. Weale, A.L. Jones, B. Connell, D. Zeitlyn, A. Tarekegn, D.M. Swallow, N. Bradman, and M.G. Thomas, 2004. The T Allele of a Single-Nucleotide Polymorphism 13.9 kb Upstream of the Lactase Gene (LCT) (C–13.9kbT) Does Not Predict or Cause the Lactase-Persistence Phenotype in Africans, *American Journal of Human Genetics*, 74 (6): 1102–1110; DOI:10.1086/421050
- Mulitza, S., and C. Rühlemann, 2000. African monsoonal precipitation modulated by interhemispheric temperature gradients, *Quaternary Research*, 53: 270-274; DOI:10.1006/qres.1999.2110

- Mulitza, S., M. Prange, J.-B. Stuut, M. Zabel, T. von Dobeneck, A. C. Itambi, J. Nizou, M. Schulz, and G. Wefer, 2008. Sahel megadroughts triggered by glacial slowdowns of Atlantic meridional overturning, *Paleoceanography*, 23: PA4206 [11 pp.]; DOI:10.1029/2008PA001637
- Negri, A., A. Ferretti, T. Wagner, and P.A. Meyers, 2009. Organic-carbon-rich sediments through the Phanerozoic: processes, progress, and perspectives, *Palaeogeography, Palaeoclimatology, Palaeoecology*, 273: 213–217
- Negri, A., A. Ferretti, T. Wagner, and P.A. Meyers, 2009a. Phanerozoic organic-carbon-rich marine sediments: overview and future research challenges, *Palaeogeography, Palaeoclimatology, Palaeoecology*, 273: 218–227
- Negri, A., T. Wagner, and P.A. Meyers, 2006. Causes and consequences of marine organic carbon burial through time. *Palaeogeography, Palaeoclimatology, Palaeoecology*, 235: 1–320
- Newell, R.E., and J. Hsiung, 1987. Factors controlling free air and ocean temperature of the last 30 years and extrapolation to the past. In *Abrupt Climatic Change: Evidence and Implications*, W.H. Berger and L.D. Labeyrie, (eds), . Reidel Publ., NATO ASI Series, Dordrecht; pp.: 67–87
- Newton, A., 2008. Sandy storehouse, *Nature*, Publ. online: 17 Apr 2008; DOI:10.1038/climate.2008.34; reporting *Global Change Biology*; DOI:10.1111/j.1365-2486.2008.01593.x (2008)
- Nicholson, S.E., 2017. Climate and climatic variability of rainfall over eastern Africa, *Reviews of Geophysics*; DOI:10.1002/2016RG000544
- Nicholson, S.E., 2017a. Short Rains and Long Rains, *EOS, Transactions of the American Geophysical Union, Editors' Vox*, issued 25 July 2017
- Nicholson, S.E., and J.P. Grist, 2003. The seasonal evolution of the atmospheric circulation over West Africa and equatorial Africa, *Journal of Climate*, 16: 1013-1030; DOI:10.1175/1520-0442(2003)016<1013:TSEOTA>2.0.CO;2
- Nicholson, S.E., B. Some, B. Kone, 2000. An analysis of recent rainfall conditions in West Africa, including the rainy seasons of the 1997 El Niño and the 1998 La Niña years. *Journal of Climate*, 13: 2628-2640; DOI:10.1175/1520-0442(2000)013<2628:AAORRC>2.0.CO;2
- Nudds, R.L. and G.J. Dyke, 2010a. Response to comments on “Narrow Primary Feather Rachises in *Confuciusornis* and *Archaeopteryx* suggest poor flight ability”. *Science*, 330 (6002): 320-320; DOI:10.1126/science.1193474
- Nudds, R.L., and G.J. Dyke, 2010. Narrow primary feather rachises in *Confuciusornis* and *Archaeopteryx* suggest poor flight ability. *Science*, 328(5980): 887-889. DOI:10.1126/science.1188895
- Ogawa, K., and T. Schmugge, 2004. Mapping surface broadband emissivity of the Sahara desert using ASTER and MODIS data, *Earth Interactions*, 8 (7): 1-14
- Ogawa, K., T. Schmugge, and S. Rokugawa, 2008. Estimating broadband emissivity of arid regions and its seasonal variations using thermal infrared remote sensing, *Geoscience and Remote Sensing, IEEE Transactions* , 46, (2): 334-343; DOI:10.1109/TGRS.2007.913213
- Oleson, K.W., Y. Dai, G. Bonan, M. Bosilovich, R. Dickinson, P. Dirmeyer, F. Hoffman, P. Houser, S. Levis, G.-Y. Niu, P. Thornton, M. Vertenstein, Z.-L. Yang, X. Zeng, 2004. Technical description of the Community Land Model (CLM), NCAR/TN-461+STR, National Center for Atmospheric Research, Boulder, Colo.; pp.: 1-174
- Olsson, L., L. Eklundh, and J. Ardö, 2005. A recent greening of the Sahel-trends, patterns and potential causes, *Journal of Arid Environments*, 63: 556-566
- Olsson, Lennart, 2008. Greening of the Sahel [Mryka Hall-Beyer (Topic Editor)]. In *Encyclopedia of Earth*. Ed. by J. Cutler Cleveland. [First published January 30, 2008; Last revised July 23, 2008]. <http://www.eoearth.org/article/Greening_of_the_Sahe>
- Orange, D.L., J.Y. Gac, and M.I. Diallo, 1993. Geochemical assessment of atmospheric deposition including Harmattan dust in continental West Africa. In *Tracers in hydrology*, N.E. Peters, E. Hoehn., Ch. Leibundgut, N. Tase, and D.E. Walling, (eds), IAHS Publications, 215; pp.: 303-312
- Otterman, J., A. Manes, S. Rubin, Pinhas Alpert, and D. Starr, 1990. An increase of yearly rain in southern Israel following land use change? *Boundary-Layer Meteorology*, 53 (4), 333-351; DOI:10.1007/BF02186093
- Otterman, J., and Ming-Dah Chou, 1992. Simulation of desert-scrub growth: a forcing to warmer and more pluvial climate, *Advances in Atmospheric Sciences*, 9 (4): 441-450; DOI:10.1007/BF02677076
- Otterman, J., and T.W. Brakke, 1991. Dense canopy albedo as a function of illumination direction: dependence on structure and leaf transmittance, *Theoretical and Applied Climatology*, 43 (1/2): 3-16; DOI:10.1007/BF00865038
- Otterman, J., J. Susskind, T. Brakke, D. Kimes, R. Pielke, and T.J. Lee, 1995. Inferring the thermal-infrared hemispheric emission from a sparsely-vegetated surface by directional measurements, *Boundary-Layer Meteorology*, 74 (1/2): 163-180; DOI:10.1007/BF00715715
- Otterman, J., T. Brakke, and J. Smith, 1995a. Effects of leaf-transmittance versus leaf-reflectance on bidirectional scattering from canopy/soil surface: An analytical study, *Remote Sensing of Environment*, 54 (1): 49-60
- Otterman, J., T.W. Brakke, and J. Susskind, 1992. A model for inferring canopy and underlying soil temperatures from multi-directional measurements, *Boundary-Layer Meteorology*, 61 (1/2): 81-97; DOI:10.1007/BF02033996
- Panieri, G., A. Camerlenghi, S. Conti, G.A. Pini, and I. Cacho, 2009. Methane seepages recorded in benthic foraminifera from Miocene seep carbonates, Northern Apennines (Italy), *Palaeogeography,*

- Palaeoclimatology, Palaeoecology, 284 (3-4): 271-282; DOI:10.1016/j.palaeo.2009.10.006
- Pappas, S., 2016. 500 'Champagne' methane seeps discovered off Pacific coast, Live Science issued October 20, 2016
- Pappas, S., 2016c. New pterosaur species with intact skull uncovered in Patagonia, Live Science, issued August 30, 2016
- Passier, H.F., G.J. de Lange, M.J. Dekkers, 2001. Magnetic properties and geochemistry of the active oxidation front and the youngest sapropel in the eastern Mediterranean Sea, *Geophysical Journal International*, 145 (3): 604-614; DOI:10.1046/j.0956-540X.2001.01394.x
- Paul, G.S., 2010. Comment on "Narrow Primary Feather Rachises in Confuciusornis and Archaeopteryx suggest poor flight ability". *Science*, 330 (6002): 320-320
- Paulot, F., J.D. Crouse, H.G. Kjaergaard, A. Kürten, J.M. St. Clair, J.H. Seinfeld, and P.O. Wennberg, 2009. Unexpected epoxide formation in the gas-phase photooxidation of isoprene, *Science*, 325 (5941): 730-733; DOI:10.1126/science.1172910
- Pease, R., 2016. Earth's ancient atmosphere was half as thick as it is today, *Science News*, issued May. 9, 2016; DOI:10.1126/science.aaf9981
- Peck, J.A., R.R. Green, T. Shanahan, J.W. King, J.T. Overpeck, and C.A. Scholz, 2004. A magnetic mineral record of Late Quaternary tropical climate variability from Lake Bosumtwi, Ghana, *Palaeogeography, Palaeoclimatology, Palaeoecology*, 215: 37-57
- Pedersen, M.W., A. Ruter, C. Schweger, H. Friebe, R.A. Staff, K.K. Kjeldsen, M.L.Z. Mendoza, A.B. Beaudoin, C. Zutter, N.K. Larsen, B.A. Potter, R. Nielsen, R.A. Rainville, L. Orlando, D.J. Meltzer, K.H. Kjær, and E. Willerslev, 2016. Postglacial viability and colonization in North America's ice-free corridor, *Nature*, 537: 45-49; DOI:10.1038/nature19085
- Pelletier, N., and P. Tyedmers, 2010. Livestock production and the global environment: Consume less or produce better? *Proceedings of the National Academy of Sciences*, 107 (43): 18237-18238 ; DOI:10.1073/pnas.1012541107
- Pelly, J., 2008. Can wetland restoration cool the planet? *Environmental Science & Technology*:10.1021/es802790q
- Pendleton, L., D.C. Donato, B.C. Murray, S. Crooks, W.A. Jenkins, S. Sifleet, C. Craft, J.W. Fourqurean, J.B. Kauffman, N. Marbà, P. Megonigal, E. Pidgeon, D. Herr, D. Gordon, A. Baldera, 2012. Estimating global "blue carbon" emissions from conversion and degradation of vegetated coastal ecosystems, *PLoS ONE*, 7 (9): e43542; DOI:10.1371/journal.pone.0043542
- Perry, C.A., and K.J. Hsü, 2000. Geophysical, archaeological, and historical evidence support a solar-output model for climate change, *Proceedings of the National Academy of Sciences*, 97 (23): 12,433-12,438
- Peterson, T.C. and R.S. Vose, 1997. An overview of the Global Historical Climatology Network temperature data base, *Bulletin of the American Meteorological Society*, 78: 2837-2849
- Peterson, T.C., T.R. Karl, P.F. Jamason, R. Knight, and D.R. Easterling, 1998: The first difference method: maximizing station density for the calculation of long-term global temperature change. *Journal of Geophysical Research, Atmospheres*, 103 (D20): 25967-25974
- Petit-Maire, N., 2002. Sahara: sous le Sable ... des Lacs : un Voyage dans le Temps, CNRS Editions, Paris ; pp.: 1-127
- Pfanz, H., D. Vodnik, Ch. Wittman, G. Aschan, and Antonio Raschi, 2004. Plants and geothermal CO₂ exhalations-Survival in and adaptation to a high CO₂ environment. *Progress in Botany*, 65: 499-538
- Pfeiffer, M., A. Spessa, and J.O. Kaplan, 2013. A model for global biomass burning in preindustrial time: LPJ-LMfire (v1.0). *Geoscientific Model Development*, 6 (3): 643-85; DOI:10.5194/gmd-6-643-2013
- Pielke, R.A., R.L. Walko, L.T. Steyaert, P.L. Vidale, G.E. Liston, W.A. Lyons, and T.N. Chase, 1999. The influence of anthropogenic landscape changes on weather in south Florida, *Monthly Weather Review*, 127: 1663-1673
- Pierret, M.C., N. Clauer, D. Bosch, G. Blanc, and C. France-Lanord, 2001. Chemical and isotopic (87Sr/86Sr, δ18O, δD) constraints on the formation of Red Sea brines. *Geochimica et Cosmochimica Acta*, 65: 1259-1275
- Pilkington, M., and A.R. Hildebrand, 2000. Three-dimensional magnetic imaging of the Chicxulub crater, *Journal of Geophysical Research*, 105: 23,479-23,491
- Pirajno, F., 2009. *Hydrothermal processes and mineral systems*. Springer, Berlin;pp.: 1250
- Pizzarello, S., Yongsong Huang, L. Becker, R.J. Poreda, R.A. Nieman, G. Cooper, and M. Williams, 2001. The organic content of the Tagish Lake meteorite, *Science*, 293 (5538): 2236-2239; DOI:10.1126/science.1062614
- Pla-Garcia, J., S.C.R. Rafkin, Ö. Karatekin, and E. Gloesener, 2019. Comparing MSL Curiosity Rover TLS-SAM Methane - Measurements with Mars regional atmospheric - Modeling system atmospheric transport experiments, *Journal of Geophysical Research, Planets*, 124 (8): 2141-2167; DOI:10.1029/2018JE005824
- Planavsky, N., A. Bekker, O.J. Rouxel, B. Kamber, A. Hofmann, A. Knudsen, and T.W. Lyons, 2010a. Rare earth element and yttrium compositions of Archean and Paleoproterozoic Fe formations revisited: new perspectives on the significance and mechanisms of deposition, *Geochimica et Cosmochimica Acta*, 74 (22): 6387-6405; DOI:10.1016/j.gca.2010.07.021
- Planavsky, N., T.W. Lyons, and .Bekker, 2010b. A non-diagenetic origin of the Lomagundi positive carbon isotope excursion, abstract 161-13, 2010 GSA Denver Annual Meeting (31 October-3 November, 2010)
- Planavsky, N.J., O.J. Rouxel, A. Bekker, S.V. Lalonde, K.O. Konhauser, C.T. Reinhard, and T.W. Lyons, 2010. The evolution of the marine phosphate reservoir, *Nature*, 467: 1088-1090; DOI:10.1038/nature09485
- Planavsky, N.J., S. Lalonde, K. Konhauser, and T.W. Lyons, 2010c. Nutrient limitation in the Precambrian,

- Astrobiology Scientific Conference 2010: Evolution and Life: Surviving Catastrophes and Extremes on Earth and Beyond, held April 26-20, 2010 in League City, Texas. LPI Contribution No. 1538; p: 5523
- Pongratz, J., C.H. Reick, T. Raddatz, K. Caldeira, and M. Claussen, 2011. Past land use decisions have increased mitigation potential of reforestation, *Geophysical Research Letters*, 38: L15701 [5 pp.]; DOI:10.1029/2011GL047848
- Poorter, H., 1993. Interspecific variation in the growth response of plants to an elevated ambient CO₂ concentration, *Vegetatio*, 104/105, (1): 77-97; DOI:10.1007/BF00048146
- Posth, C., N. Nakatsuka, I. Lazaridis, P. Skoglund, S. Mallick, T.C. Lamnidis, N. Rohland, K.Nägele, N. Adamski, E. Bertolini, N. Broomandkoshbacht, A. Cooper, B.J. Culleton, T. Ferraz, M. Ferry, A. Furtwängler, W. Haak, K. Harkins, T.K. Harper, T. Hünemeier, A.M. Lawson, B. Llamas, M. Michel, E. Nelson, J. Oppenheimer, N. Patterson, S. Schiffels, J. Sedig, K. Stewardson, S. Talamo, Chuan-Chao Wang, J.-J. Hublin, M. Hubbe, K. Harvati, A. Nuevo Delaunay, J. Beier, M. Francken, P. Kaulicke, H. Reyes-Centeno, K. Rademaker, W.R. Trask, M. Robinson, S.M. Gutierrez, K.M. Prufer, D.C. Salazar-García, E.N. Chim, L. Müller P. Gomes, M.L. Alves, A. Liryo, M. Inglez, R.E. Oliveira, D.V. Bernardo, A. Barioni, V. Wesolowski, N.A. Scheifler, M.A. Rivera, C.R. Plens, P.G. Messineo, L. Figuti, D. Corach, C. Scabuzzo, S. Eggers, P. DeBlasis, M. Reindel, C. Méndez, G. Politis, E. Tomasto-Cagigao, D.J. Kennett, A. Strauss, L. Fehren-Schmitz, J. Krause, and D. Reich, 2018. Reconstructing the deep population history of Central and South America, *Cell*, 175 (5): 1185-1197.E22; DOI:10.1016/j.cell.2018.10.027
- Prince, S.D., K.J. Wessels, C.J. Tucker, and S.E. Nicholson, 2007. Desertification in the Sahel: a reinterpretation of a reinterpretation, *Global Change Biology*, 13: 1308-1313; DOI:10.1111/j.1365-2486.2007.01356.x
- Prospero, J.M., and P.J. Lamb, 2003. African droughts and dust transport to the Caribbean: Climate change implications, *Science*, 302: 1024-1027; DOI:10.1126/science.1089915
- Prospero, J.M., and T.N. Carlson, 1981. Saharan air outbreaks over the tropical North Atlantic, *Pure and Applied Geophysics*, 119: 677-691; DOI:10.1007/BF00878167
- Pultarova, T., 2017. Humans may haveo North America 100,000 years earlier than thought, *Live Science*, issued April 26, 2017
- Regnier, P., P. Friedlingstein, P. Ciais, F.T. Mackenzie, N. Gruber, I.A. Janssens, G.G. Laruelle, R. Lauerwald, . Luysaert, A.J. Andersson, S. Arndt, C. Arnosti, A.V. Borges, A.W. Dale, A. Gallego-Sala, Y. Goddérís, N. Goossens, J. Hartmann, C. Heinze, T. Ilyina, F. Joos, D.E. LaRowe, J. Leifeld, F.J.R. Meysman, G. Munhoven, P.A. Raymond, R. Spahni, P. Suntharalingam, and M. Thullner, 2013. Anthropogenic perturbation of the carbon fluxes from land to ocean, *Nature Geoscience*, 6: 597-607; DOI:10.1038/ngeo1830
- Renard, C., 1889. Nouvelles expériences sur la résistance de l'air, *l'Aeronaute*, 22: 73; quoted by von Kármán (1963).
- Renssen, H., V. Brovkin, T. Fichefet, and H. Goosse, 2006. Simulation of the Holocene climate evolution in Northern Africa: the termination of the African Humid Period. *Quaternary International*, 150: 95-102
- Robinson, A.B., N.E. Robinson, and W. Soon, 2007. Environmental effects of increased atmospheric carbon dioxide, *Journal of the American Physicians and Surgeons*, 12: 79-90
- Robinson, A.B., S.L. Baliunas, W. Soon, and Z.W. Robinson, 1998. Environmental effects of increased atmospheric carbon dioxide, *Journal of the American Physicians and Surgeons*, 3: 171-178
- Robitzski, D., 2017. Feathered Jurassic Dinosaurs were Fierce and ... Fluffy? *Live Science*, issued November 29, 2017
- Rohling, E.J., and R.C. Thunell, 1999. Editorial-Five decades of Mediterranean palaeoclimate and sapropel studies, *Marine Geology*, 153: 7-10
- Romero, J., 2017. Have we seen evidence of Titan's catastrophic methane downpours? *Science news*, issued January 9, 2017
- Ronov, A.B., 1982. The Earth's sedimentary shell. Quantitative patterns of its structure, compositions and evolution. The 20th V. I. Vernadskiy Lecture. *International Geology Review*, 24 (11/12): 1313-1388. Translated from the Russian edition of 1980 (Izd-vo Nauka, Moscow, pp.:80). Reprinted in 1983 by the American Geological Institute as a monograph, pp.: 80
- Ronov, A.B., and A.A. Yareshevsky, 1969. Chemical composition of the Earth's crust. In *The Earth's Crust and Upper Mantle*, P.J. Hart, (ed.), *Geophysical Monograph Series*, 13, American Geophysical Union: Washington, DC.: pp.: 37-57
- Ruddiman, W.F., D.Q. Fuller, J.E. Kutzbach, P.C. Tzedakis, J.O. Kaplan, E.C. Ellis, S.J. Vavrus, C.N. Roberts, R. Fyfe, F. He, C. Lemmen, and J. Woodbridge, 2016. Late Holocene climate: natural or anthropogenic? *Reviews of Geophysics*, 54: 93-118; DOI:10.1002/2015RG000503
- Rudolf, B., and F. Rubel, 2005. Global precipitation. In *Observed Global Climate, Landolt-Börnstein: Numerical Data and Functional Relationships in Science and Technology - New Series*, ed. by M. Hantel, Springer, Berlin; pp.: 11.1-11.53
- Ruiz-Barradas, A., and S. Nigam, 2005. Warm season rainfall variability over the U.S. Great Plains in observations, NCEP and ERA-40 reanalyses, and NCAR and NASA atmospheric model simulations, *Journal of Climate*, 18 (11): 1808-1830
- Rush, G., E. Garrett, M.D. Bateman, G.R. Bigg, F.D. Hibbert, D.E. Smith and W.R. Gehrels, 2023. The magnitude and source of meltwater forcing of the 8.2 ka climate event constrained by relative sea-level data from eastern Scotland, *Quaternary Science Advances*. DOI: 10.1016/j.qsa.2023.100119

- Sagan, C., and G. Mullen, 1972. Earth and Mars: evolution of atmospheres and surface temperatures, *Science*, 177, (4043): 52–56; DOI:10.1126/science.177.4043.52
- Sansoni, U., 1994. *Le più Antiche Pitture del Sahara. L'Arte delle Teste Rotonde*, Jaca Book, Milano; pp.:1-325
- São Paulo Research Foundation*, 2023. Missing link discovered: new research sheds light on how dinosaurs became giants, *SciTechDaily*, issued September 12, 2023
- Sarnthein, M., G. Tetzlaff, B. Koopmann, K. Wolter, and U. Pflaumann, 1981. Glacial and interglacial wind regimes over the eastern subtropical Atlantic and north-west Africa, *Nature*, 293: 193-196; DOI:10.1038/293193a0
- Sarnthein, M., K. Statterger, D. Dreger, H. Erlernkeuser, P. Grootes, B. Haupt, S. Jung, T. Kiefer, W. Kuhnt, U. Pflaumann, C. Schäfer-Neth, H. Schulz, M. Schulz, D. Seidov, J. Simstich, S. van Kreveld, E. Vogelsang, A. Völker, and M. Weinelt, 2001. Fundamental modes and abrupt changes in North Atlantic circulation and climate over the last 60 ky-Concepts, reconstruction, and numerical modelling. In *The Northern North Atlantic: a Changing Environment*, P. Schäfer, W. Ritzrau, M. Schlüter, and J. Thiede, (eds), Springer, Berlin; pp.: 365-410
- Schefuß, E., S. Schouten, and R.R. Schneider, 2005. Climatic controls on central African hydrology during the past 20,000 years, *Nature*, 437: 1003-1006; DOI:10.1038/nature03945
- Schefuß, E., S. Schouten, J.H.F. Jansen, and J.S. Sinninghe Damsté, 2003. African vegetation controlled by tropical sea surface temperatures in the mid-Pleistocene period. *Nature*, 422: 418–421
- Scheiner, S.M., and J.M. Rey-Benayas, 1994. Global patterns of plant diversity, *Evolutionary Ecology*, 8 (4): 331-347; DOI:10.1007/BF01238186
- Schiermeier, Q., 2008a. Sediment cores reveal Antarctica's warmer past-ANDRILL project discovers that life at the pole wasn't so chilly 16 million years ago, *Nature News*, 453, 13 (24 April 2008); DOI:10.1038/453013a
- Schirber, M., 2004. Natural nuclear reaction powered ancient geyser, *Live Science*, issued 09 November 2004; 04:00 AM ET; <http://www.Live Science.com/75-natural-nuclear-reaction-powered-ancient-geyser.html>
- Schmidt, A.R., S. Jancke, E.E. Lindquist, E. Ragazzi, G. Roghi, P.C. Nascimbene, K. Schmidt, T. Wappler, and D.A. Grimaldi, 2012. Arthropods in amber from the Triassic Period, *Proceedings of the National Academy of Sciences*, 109 (37): 14796–14801, DOI:10.1073/pnas.1208464109; published ahead of print August 27, 2012, DOI:10.1073/pnas.1208464109
- Schmidt-Nielsen, K., 1984. *Scaling: why is Animal Size so Important?* Cambridge University Press; pp.: 1-241
- Sequist, J.W., T. Hickler, L. Eklundh, J. Ardö, and B.W. Heumann, 2008. Disentangling the effects of climate and people on Sahel vegetation dynamics, *Biogeosciences Discussions*, 5: 3045–3067
- Segal, M., R. Avissar, M.C. McCumber, and R.A. Pielke, 1988. Evaluation of vegetation effects on the generation and modification of mesoscale circulations, *Journal of the Atmospheric Sciences*, 45: 2268-2292
- Sekine, Y., K. Suzuki, R. Senda, K. T. Goto, E. Tajika, R. Tada, K. Goto, S. Yamamoto, N. Ohkouchi, N.O. Ogawa, and T. Maruoka, 2011. Osmium evidence for synchronicity between a rise in atmospheric oxygen and Palaeoproterozoic deglaciation, *Nature, Communications*, 2: article n. 502; DOI:10.1038/ncomms1507
- Senar, O.E., K.L. Webster, and I.F. Creed, 2018. Catchment-scale shifts in the magnitude and partitioning of carbon export in response to changing hydrologic connectivity in a northern hardwood forest, *Journal of Geophysical Research, Biogeosciences*, 123 (8): 2337-2352; DOI:10.1029/2018JG004468
- Servant, M., 1983. Séquences Continentales et Variations Climatiques et Évolution du Bassin du Tchad au Cénozoïque Supérieur, Orstom, (Travaux et documents; 159) Paris; pp.: 1-573
- Servant, M., and S. Servant-Vildary, 1980. L'environnement quaternaire du bassin du Tscad. In *The Sahara and the Nile: Quaternary Environments and Prehistoric Occupation in Northern Africa*, M.A.J. Williams and H. Faure, (eds), A.A. Balkema, Rotterdam; pp.: 133-163
- Shackleton, N.J., M.A. Hall, and E. Vincent, 2000. Phase relationships between millennial-scale events 64,000–24,000 years ago, *Paleoceanography*, 15: 565-569; DOI:10.1029/2000PA000513
- Shackleton, N.J., R.G. Fairbanks, T.-C. Chiu, and F. Parrenin, 2004. Absolute calibration of the Greenland time scale: implications for Antarctic time scales and for $\delta^{14}\text{C}$, *Quaternary Science Reviews*, 23: 1513-1522; DOI:10.1016/j.quascirev.2004.03.006
- Shanahan, T.M., J.T. Overpeck, C.W. Wheeler, J.W. Beck, J.S. Pigati, M.R. Talbot, C.A. Scholz, J. Peck, and J.W. King, 2006. Paleoclimatic variations in West Africa from a record of late Pleistocene and Holocene lake level stands of Lake Bosumtwi, Ghana, *Palaeogeography, Palaeoclimatology, Palaeoecology*, 242: 287-302; DOI:10.1016/j.palaeo.2006.06.007
- Sidder, A., 2018a. Hydrology dictates fate of carbon from northern hardwood forests, *EOS, Transactions of the American Geophysical Union*, 99; DOI:10.1029/2018EO105537
- Skibba, R., 2016. Tiny pterosaur claims new perch on reptile family tree, *Nature, News*, issued 31 August 2016; DOI:10.1038/nature.2016.20507
- Skonieczny, C., P. Paillou, A. Bory, G. Bayon, L. Biscara, X. Crosta, F. Eynaud, B. Malaizé, M. Revel, N. Aleman, J. -P. Barusseau, R. Vernet, S. Lopez, and F. Grousset, 2015. African humid periods triggered the reactivation of a large river system in Western Sahara, *Nature Communications*, 6: Article number 8751; DOI:10.1038/ncomms9751
- Smith, J.M., 1984. *Mathematical ideas in biology*, Chap. 1, Cambridge University Press
- Smith, P., D. Martino, Zucong Cai, D. Gwary, H. Janzen, P. Kumar, B. McCarl, S. Ogle, F. O'Mara, C. Rice, B. Scholes, and O. Sirotenko, 2007. *Agriculture. In*

- Mitigation of Climate Change: Working Group III Contribution to the Fourth Assessment Report of the IPCC, Cambridge University Press; pp.: 497-540
- Smith, W.B., P D. Miles, J.S. Vissage, and S.A. Pugh, 2002a. Forest Resources of the United States, U.S. Forest Service and Department of Agriculture
- Som, S.M., R. Buick, J.W. Hagadorn, T.S. Blake, J.M. Perreault, J.P. Harnmeijer, and D.C. Catling, 2016. Earth's air pressure 2.7 billion years ago constrained to less than half of modern levels, *Nature Geoscience*, 9: 448–451; DOI:10.1038/ngeo2713
- Specktor, B., 2018b. Something is sucking iron out of Earth's crust, and scientists think they know what, *Live Science*, issued May 18, 2018
- Stach, E., M.-T. Machowski, M. Teichmüller, G.H. Taylor, D. Chandra, and R. Teichmüller, 1975. *Coal Petrology*, 2nd ed. (3rd ed.), Gebrüder Borntraeger, Berlin; pp.: 1-535
- Steponaitis, E., A. Andrews, D. McGee, J. Quade, Yu-Te Hsieh, W.S. Broecker, B.N. Shuman, S.J. Burns, and Hai Cheng, 2015. Mid-Holocene drying of the U.S. Great Basin recorded in Nevada speleothems, *Journal of Quaternary Science*, 127: 174-185; DOI:10.1016/j.quascirev.2015.04.011
- Stolper, D.A., M.L. Bender, G B. Dreyfus, Y. Yan, and J.A. Higgins, 2016. A Pleistocene ice core record of atmospheric O₂ concentrations, *Science*, 353 (6306): 1427-1430; DOI:10.1126/science.aaf5445
- Street-Perrott, F.A., and R A. Perrott, 1990. Abrupt climate fluctuations in the tropics: the influence of Atlantic Ocean circulation, *Nature*, 343: 607–612; DOI:10.1038/343607a0
- Streich, L., 2015. Drought changes how peat bogs cycle mercury and sulfur, *EOS, Transactions of the American Geophysical Union*, 96; DOI:10.1029/2015EO039121
- Stuut, J.B., M. Zabel, V. Ratmeyer, P. Helmke, E. Schefuß, G. Lavik, and R. Schneider, 2005. Provenance of present-day eolian dust collected off NW Africa, *Journal of Geophysical Research*, 110; D04202; DOI:10.1029/2004JD005161
- Tan, Liangcheng, Yanjun Cai, Zhisheng An, Hai Cheng, Chuan-Chou Shen, S.F.M. Breitenbach, Yongli Gao, R.L. Edwards, Haiwei Zhang, and Yajuan Du, 2015. A Chinese cave links climate change, social impacts, and human adaptation over the last 500 years, *Scientific Reports*, 5: 12284; DOI:10.1038/srep12284
- Tang, Ming, M. Erdman, G. Eldridge, and Cin-Ty A. Lee, 2018. The redox “filter” beneath magmatic orogens and the formation of continental crust, *Science Advances*, 4 (5): eaar4444; DOI:10.1126/sciadv.aar4444
- Tarhule, A., and Ming-Ko Woo, 1997. Towards an interpretation of historical droughts in northern Nigeria, *Climate Change*, 37: 601-616
- Tennekes, H., 1996. *The simple science of flight – from insects to Jumbo*, MIT Press; pp.: 1-152
- Terada, A., and T. Hashimoto, 2017. Variety and sustainability of volcanic lakes: response to subaqueous thermal activity predicted by a numerical model, *Journal of Geophysical Research Solid Earth*, 122: 6108–6130; DOI:10.1002/2017JB014387
- Ters, M., 1987. Variations in Holocene sea level on the French Atlantic coast and their climatic significance. In *Climate-History, Periodicity, and Predictability*, M.R. Rampino, J.E. Sanders, W.S. Newman, and L.K. Königsson, (eds), Van Nostrand Reinhold, New York; pp.: 204–336
- Thomas, N., and S. Nigam, 2018. Twentieth-century climate change over Africa: seasonal hydroclimate trends and Sahara desert expansion, *Journal of Climate*, 31: 3349-3372; DOI:10.1175/JCLI-D-17-0187.1
- Thompson, A., 2015. Underground desert aquifers could hold missing carbon, *Climate Central*, issued August 10, 2015
- Timmermann, A., and T. Friedrich, 2016. Late Pleistocene climate drivers of early human migration, *Nature*, 538: 92–95; DOI:10.1038/nature19365
- Tipple, B.J., S.R. Meyers, and M. Pagani, 2010. Carbon isotope ratio of Cenozoic CO₂: a comparative evaluation of available geochemical proxies, *Paleoceanography*, 25: PA3202 [11 pp.]; DOI:10.1029/2009PA001851
- Tjallingii, R., M. Claussen, J.-B.W. Stuut, J. Fohlmeister, A. Jahn, T. Bickert, F. Lamy, and U. Röhl, 2008. Coherent high- and low-latitude control of the northwest African hydrological balance, *Nature Geoscience*, 1: 670-675; DOI:10.1038/ngeo289
- Tobi, Y., 2007. *Queen of Sheba*, Encyclopaedia Judaica, 16 (2nd ed.), Gale
- Uhlig, H., 1986. *Die Seidenstrasse. Antike Weltkultur zwischen China und Rom*, Gustav Lübke Verlag, Bergisch Gladbach. Italian translation published in 1991 by Garzanti; pp.: 1-294
- Ullendorff, E., 1991. *Bilḳīs*, The Encyclopaedia of Islam, 2 (2nd ed.), Brill
- UNEP, 1992. *World Atlas of Desertification*, Edward Arnold, London; pp.: 1-69
- United Nations Organization for the Coordination of Humanitarian Affairs, 2011. *Eastern Africa Drought Humanitarian Report*, 4, 15 July, New York, NY
- University of Leeds, 2023. *Unlocking ancient climate secrets – Melting ice likely triggered climate change over 8,000 years ago*, SciTechDaily, issued September 16, 2023
- University of Manchester, 2023. *Profound consequences for the climate – Scientists discover urea in the atmosphere*, SciTechDaily, issued September 2, 2023
- Vaccari, D.A., 2009. Phosphorus famine: the threat to our food supply, *Scientific American*, 300, June: 54-59
- van de Wa, S., W. Roderik, and R. Bintanja, 2009. Changes in temperature, ice, and CO₂ during the Mid-Pleistocene Transition, *Science*, Published online 18 September 2009
- Vautard, R., J. Cattiaux, P.I. Yiou, J.-N. Thépaut, and P. Ciais, 2010. Northern Hemisphere atmospheric stilling partly attributed to an increase in surface roughness, *Nature Geosciences*, 3: 756–761; DOI:10.1038/ngeo979
- Vecchi, G.A., and B.J. Soden, 2007. Global warming and the weakening of the tropical circulation, *Journal of Climate*, 20: 4316–4340; DOI:10.1175/JCLI4258.1

- Vecchi, G.A., B.J. Soden, A.T. Wittenberg, I.M. Held, A. Leetmaa, and M.J. Harrison, 2006. Weakening of the tropical Pacific atmospheric circulation due to anthropogenic forcing, *Nature*, 441: 73–76; DOI:10.1038/nature04744
- Voeten, D.F.A.E., J. Cubo, E., de Margerie, M. Röper, V. Beyrand, S. Bureš, P. Tafforeau, and S. Sanchez, 2018. Wing bone geometry reveals active flight in *Archaeopteryx*, *Nature Communications*, 9, Article number 923; DOI:10.1038/s41467-018-03296-8
- von Kármán, T., 1963. *Aerodynamics, Selected Topics in Light of their Historical Development*, McGraw Hill, 1963. New publication in 2004 by Courier Corp.; pp.: 1-203
- Vremir, M., G. Dyke, Z. Csiki-Sava, D. Grigorescu, and E. Buffetaut, 2018. Partial mandible of a giant pterosaur from the uppermost Cretaceous (Maastrichtian) of the Hateg Basin, Romania, *Lethaia*, 51 (4): 493-503; DOI:10.1111/let.12268
- Waddell, K.L., D.D. Oswald, and D.S. Powell, 1987. *Forest Statistics of the United States*, U.S. Forest Service and Department of Agriculture.
- Walker, G., 2003. *Snowball Earth*, Crown Publishing Group; pp.: 269
- Walker, J.C.G., 1986. Carbon dioxide on the early Earth, *Origins of life and evolution of the biosphere*, 16: 117–127
- Wang, F., 2018. How we solved an Arctic mercury mystery, *The Conversation*, issued October 18, 2018
- Wang, Kang, K.M. Munson, A. Beaupré-Laperrière, A. Mucci, R.W. Macdonald, and Feiyue Wang, 2018. Subsurface seawater methylmercury maximum explains biotic mercury concentrations in the Canadian Arctic, *Scientific Reports*, 8: article no. 14465; DOI:10.1038/s41598-018-32760-0
- Waters, M.R., J.L. Keene, S.L. Forman, E.R. Prewitt, D.L. Carlson, and J.E. Wiederhold, 2018. Pre-Clovis projectile points at the Debra L. Friedkin site, Texas - Implications for the Late Pleistocene peopling of the Americas, *Science Advances*, 4 (10): eaat4505; DOI:10.1126/sciadv.aat4505
- Weisberger, M., 2017c. Eat, pray, fossilize? Praying mantis fossil Is 110 million years old, *Live Science*, issued August 3, 2017
- Weisberger, M., 2017d. 66 Million years ago, Bird-like Dinosaurs Laid Blue-green Eggs, *Live Science*, issued August 31, 2017
- Weldeab, S., D.W. Lea, R.R. Schneider, and N. Andersen, 2007. 155,000 years of West African monsoon and ocean thermal evolution, *Science*, 316: 1303-1307; DOI: 10.1126/science.1140461
- Welsh, J., 2012. Giant insects shrunk as birds entered prehistoric skies, *Live Science*, issued June 4, 2012
- Wendel, J.A., and M. Kumar, 2017a. Biogenic oxygen on the Moon could hold secrets to Earth's past, *EOS, Transactions of the American Geophysical Union*, 98; DOI:10.1029/2017EO066979
- Williams, A.P., and C. Funk, 2010. A westward extension of the tropical Pacific warm pool leads to March through June drying in Kenya and Ethiopia, *US Geological Survey Open-File Report*, 2010–1199: 7 pp
- Williams, A.P., and C. Funk, 2011. Westward extension of the warm pool leads to a westward extension of the Walker circulation, drying eastern Africa, *Climate Dynamics*, 37 (11/12): 2417-2435; DOI:10.1007/s00382-010-0984-y
- Xing, L., J.K. O'Connor, R.C. McKellar, L.M. Chiappe, Kuowei Tseng, Gang Li, and Ming Bai, 2016a. A mid-Cretaceous enantiornithine (Aves) hatchling preserved in Burmese amber with unusual plumage Author links open overlay panel, *Gondwana Research*, 49: 264-277. DOI:10.1016/j.gr.2017.06.001
- Xing, L., R.C. McKellar, Min Wang, Ming Bai, J.K. O'Connor, M.J. Benton, Jianping Zhang, Yan Wang, Kuowei Tseng, M.G. Lockley, Gang Li, Weiwei Zhang, and Xing Xu, 2016. Mummified precocial bird wings in mid-Cretaceous Burmese amber, *Nature, Communications*, 7: 2089. DOI:10.1038/ncomms12089
- Xing, Lida, R.C. McKellar, Xing Xu, Gang Li, Ming Bai, W.S. Persons IV, T. Miyashita, M.J. Benton, Jianping Zhang, A.P. Wolfe, Qiru Yi, Kuowei Tseng, Hao Ran, P.J. Currie, 2016b. A feathered dinosaur tail with primitive plumage trapped in Mid-Cretaceous amber, *Current Biology*, 26 (24): 3352-3360; DOI:10.1016/j.cub.2016.10.008, (Open archive)
- Yoshioka, M., N.M. Mahowald, A.J. Conley, W.D. Collins, D.W. Fillmore, C.S. Zender, and D.B. Coleman, 2007. Impact of desert dust radiative forcing on Sahel precipitation: relative importance of dust compared to sea surface temperature variations, vegetation changes, and greenhouse gas warming, *Journal of Climate*, 20: 1445-1467; DOI:10.1175/JCLI4056.1
- Young, N.E., A.D. Schweinsberg, J.P. Briner, and J.M. Schaefer, 2015. Glacier maxima in Baffin Bay during the Medieval Warm Period coeval with Norse settlement, *Science Advances*, 1 (11): e1500806; DOI:10.1126/sciadv.1500806
- Zeng, N., J.D. Neelin, K.-M. Lau, and C. . Tucker, 1999. Enhancement of interdecadal climate variability in the Sahel by vegetation interaction, *Science*, 286: 1537-1540; DOI:10.1126/science.286.5444.1537
- Zerboni, A., 2008. Holocene rock varnish on the Messak plateau (Libyan Sahara): Chronology of weathering processes, *Geomorphology*, 102: 640-651
- Zhao, M., J.L. Mercer, G. Eglinton, M.J. Higginson, and C.-Y. Huang, 2006. Comparative molecular biomarker assessment of phytoplankton paleoproductivity for the last 160 kyr off Cap Blanc, NW Africa. *Organic Geochemistry*, 37: 72–97
- Zhao, Maosheng, and S.W. Running, 2010. Drought-induced reduction in global terrestrial net primary production from 2000 through 2009, *Science*, 329 (5994): 940-943; DOI:10.1126/science.1192666
- Zheng, Xiaoting, X. Xu, Z. Zhou, D. Miao, and F. Zhang, 2010. Comment on “Narrow primary feather rachises in *Confuciusornis* and *Archaeopteryx* suggest poor flight ability”. *Science*, 330 (6002): 320
- Zheng, Zhiyuan, Wenjie Dong, Zhenchao Li, Wei Zhao, Shanshan Hu, Xiaodong Yan, Jiaqi Zhao, and Zhigang

Wei, 2014. Observational study of surface spectral radiation and corresponding albedo over Gobi, desert and bare loess surfaces in northwestern China, *Journal of Geophysical Research, Atmospheres*, 120 (3): 883-896; DOI:10.1002/2014JD022516

IOP – Institute of Physics
ITCZ – Intertropical Convection Zone
JAS - July, August, September
JISAO - Joint Institute for the Study of the Atmosphere and Ocean (University of Washington).
JPSS - Joint Polar Satellite System
KAGUYA - Japanese spacecraft
L.H. - Late Hunters
LGM - last glacial maximum
LIA - Little Ice Age
LIP - large igneous province
LP - lactase persistence
LPJ - Lund-Potsdam-Jena
LPJmL model - Lund-Potsdam-Jena managed Land model
LREE –light REE
LREE/HREE ratio
LSM - land surface model
LULC - land usage and land cover
M.E. - mixed economy
MAM - March, April, May
MGK - Mohuchahangoukou
MIS - marine isotope stage or marine oxygen-isotope stage, sometimes called “marine interglacial stage” or “oxygen isotope stage” (*OIS*)
MJO - Madden-Julian Oscillation
MODIS - Moderate Resolution Imaging Spectroradiometer aboard the *NASA Earth Observing System (EOS) TERRA* satellite,
MOR – mid-ocean ridge
MORB – MOR basalt
MPT - Mid-Pleistocene transition
MWP - Medieval Warm Period
NAO - North Atlantic Ocean
NCAR GCM - National Center for Atmospheric Research - global coupled model
NDVI - normalized difference vegetation index
NGRIP - North Greenland Ice core Project
NH – Northern Hemisphere
NIR - near-IR radiation
NIR/GR –near IR radiation / global radiation
NPP - net primary production
ODP - Ocean Drilling Program
ON - October, November
ON - organic nitrogen
OSL - optically stimulated luminescence
PA - Pastoral
PALSAR - Japanese Advanced Land Observing Satellite, aboard *ALOS*
PCP - prior calcite precipitation, i.e. carbonate precipitation from infiltrating water before the water drips on a stalagmite
PDB - Pee Dee Belemnite
PFT - plant functional type
PIH - Preindustrial Holocene
PMIP-2 - Palaeoclimate Modeling Intercomparison Project
PNA - Pacific-North American pattern
P-NEXFS - P near-edge X-ray fluorescence spectroscopy
QBO - Quasi-Biannual Oscillation
REE - rare earth element
RUE - rain-use efficiency
SAA –South Atlantic Anomaly or South American Anomaly (geomagnetic)
SAL - Saharan air layer
SAR – synthetic aperture radar
SAT - surface air temperature
SAV - submerged aquatic vegetation
SH – Southern Hemisphere
SOC - soil organic carbon

Acronyms

ACE - accumulated cyclone energy
ACS – American Chemical Society
AEJ - African Easterly Jet
AHP - African Humid Period]
AIM - Antarctic Isotope maxima
ALB – asthenosphere-lithosphere boundary
ALCC - anthropogenic land cover change
ALOS –Japanese Earth-Observation satellite
AMOC - Atlantic meridional overturning circulation
AO - Arctic oscillation
AOV -atmosphere-ocean-vegetation
AOV-IC model simulation
AOV-IC-f simulation
APFT - average PFT.
ASM - Asian summer monsoon
ASTER - Advanced Spaceborne Thermal Emission and Reflection Radiometer
BBC – British Broadcasting Corporation
BBE - broadband emissivity
BIF - banded iron formations
CAA - Canadian Arctic Archipelago
CAMS-OPI - a Global Satellite – Rain Gauge Merged Product
CAPE - convective available potential energy
CAS - carbonate-associated sulfate
CGCM - coupled general circulation model
CLIMBER-2 - simulations
CM -Cerutti Mastodon
CMB – core-mntle boundary
CVL - Cameroon Volcanic Line
d.o.f. - degree of freedom (
DGVM - Dynamic Global Vegetation Model
DNA - deoxyribonucleic acid
DOC - dissolved organic carbon
DOM - dissolved organic matter
DUPAL – Dupré-Allègre anomaly
DY1 - a stalagmite from the Dayu cave
E.G. - Early Gatherers
E.H. - Early Hunters
ENSO – El Niño Southern Oscillation
EPICA - European Project for Ice Coring in Antarctica, Dronning Maud Land area (*EDML*) ice cores
FFDAS - Fossil Fuel Data Assimilation System
FR – field reversal (geomagnetic)
GCM - general circulation model
GEBCO – General Bathymetric Chart of the Oceans
GEOROC - Max Planck Institute’s database
GHCN - Global Historical Climatological Network
GIF - granular Fe formation
GISS - Goddard Institute for Space Studies
GOE - Great Oxidation Event
GPCC - Global Precipitation Climatology Center
GPCP - Global Precipitation Climatology Project
GR - global radiation
HREE – heavy REE
HS - Heinrich stadial
ICLD - International Commission on Large Dams
IGCP - International Geoscience Programme
IOP - intensive observational periods

SR - solar radiation
SR/GR –solar radiation / global radiation
SST – sea surface temperature
STA - Storm-water Treatment Areas project
STN - Simulated Topological Network
TD – tide-driven (geodynamo)
TEJ - Tropical Easterly Jet
TERRA - NASA satellite Earth Observing System (EOS)
TOMS - Total Ozone Mapping Spectrometer (onboard Nimbus 7)
TP – Tibet Plateau
USAID - United States Agency for International Development
USGS – United States Geological Survey
UV - ultraviolet radiation
VIS - visible radiation
VIS/GR – visible radiation / global radiation
VMS - volcanogenic massive sulfide
VPDB - Vienna PDB standard
WCD - World Commission on Dams
WMO – World Meteorological Organization
WMT – warm mud tectonics
YD - Younger Dryas period

ABOUT THE NCGT JOURNAL

The NCGT Newsletter , the predecessor of the NCGT Journal , was begun as a result of discussions at the symposium “Alternative Theories to Plate Tectonics ” held at the 30th International Geological Congress in Beijing in August 1996 . The name is taken from an earlier symposium held in association with the 28th International Geological Congress in Washington , D. C. in 1989 . The first issue of the NCGT Newsletter was December 1996 . The NCGT Newsletter changed its name in 2013 to the NCGT Journal . Aims of the NCGT Journal include:

1. Providing an international forum for the open exchange of new ideas and approaches in the fields of geology, geophysics, solar and planetary physics, cosmology, climatology, oceanography, electric universe, and other fields that affect or are closely related to physical processes occurring on Earth from its core to the top of its atmosphere.
2. Forming an organizational focus for creative ideas not fitting readily within the scope of dominant tectonic models.
3. Forming the basis for the reproduction and publication of such work, especially where there has been censorship or discrimination.